United Arab Emirates University
Scholarworks@UAEU

Accounting Dissertations | Accounting

11-2016

Chiral Separation and Quantitation of KHAT Designer Drug- Synthetic Cathinones- In Urine And Plasma

Rashed Humaid Khalfan Bin Huzaim

Follow this and additional works at: https://scholarworks.uaeu.ac.ae/account_dissertations

Part of the Biology Commons

Recommended Citation

Khalfan Bin Huzaim, Rashed Humaid, "Chiral Separation and Quantitation of KHAT Designer Drug- Synthetic Cathinones- In Urine And Plasma" (2016). *Accounting Dissertations*. 20.
https://scholarworks.uaeu.ac.ae/account_dissertations/20

This Dissertation is brought to you for free and open access by the Accounting at Scholarworks@UAEU. It has been accepted for inclusion in Accounting Dissertations by an authorized administrator of Scholarworks@UAEU. For more information, please contact fadl.musa@uaeu.ac.ae.

United Arab Emirates University

College of Science

CHIRAL SEPARATION AND QUANTITATION OF KHAT DESIGNER DRUG – SYNTHETIC CATHINONES – IN URINE AND PLASMA

Rashed Humaid Ahmad Khalfan Bin Huzaim

This dissertation is submitted in partial fulfilment of the requirements for the degree of Doctor of Philosophy

Under the Supervision of Dr. Mohammed Almeetani

November 2016

Declaration of Original Work

I, Rashed Humaid Ahmad Khalfan Bin Huzaim, the undersigned, a graduate student at the United Arab Emirates University (UAEU), and the author of this dissertation entitled "*Chiral Separation and Quantitation of Khat Designer Drug – Synthetic Cathinones– in Urine and Plasma*", hereby, solemnly declare that this dissertation is my own original research work that has been done and prepared by me under the supervision of Dr. Mohammed Almeetani, in the College of Science at UAEU. This work has not previously been presented or published, or formed the basis for the award of any academic degree, diploma or a similar title at this or any other university. Any materials borrowed from other sources (whether published or unpublished) and relied upon or included in my dissertation have been properly cited and acknowledged in accordance with appropriate academic conventions. I further declare that there is no potential conflict of interest with respect to the research, data collection, authorship, presentation and/or publication of this dissertation.

Student's Signature: _____ Date: 7/12/2016

Approval of the Doctorate Dissertation

This Doctorate Dissertation is approved by the following Examining Committee Members:

1) Advisor (Committee Chair): Dr. Mohammed A. Almeetani
   Title: Associate Professor
   Department of Chemistry
   College of Science
   Signature _____ Date 10/11/2016

2) Member: Dr. Syed Salman Ashraf
   Title: Professor
   Department of Chemistry
   College of Science
   Signature Salman Ashraf Date 10/11/2016

3) Member: Dr. Murat Ahmad Oz
   Title: Professor
   Department of of Pharmacology and Therapeutics
   College of College of Medicine and Health Sciences
   Signature _____ Date 10/11/2016

4) Member (External Examiner): Dr. Franco Basile
   Title: Associate Professor
   Department of Chemistry
   Institution: University of Wyoming, Laramie, USA
   Signature _____ Date 10/11/2016

This Doctorate Dissertation is accepted by:

Dean of the College of Science: Professor Ahmed Murad

Signature 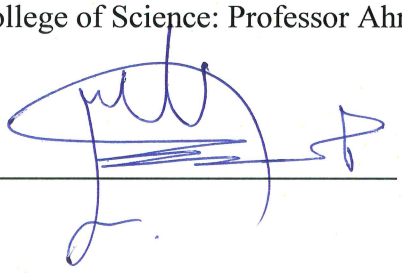 Date 15/12/2016

Dean of the College of the Graduate Studies: Professor Nagi T. Wakim

Signature 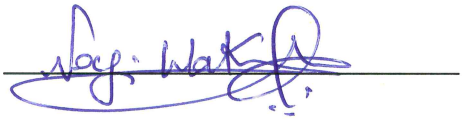 Date 20/12/2016

Copy 8 of 25

Copyright © 2016 Rashed Humaid Ahmad Khalfan Bin Huzaim
All Rights Reserved

Advisory Committee

1) Advisor: Dr. Mohammed AbdulRuhman Almeetani

Title: Associate Professor

Department of Chemistry

College of Science

2) Co-advisor: Prof. Muhammad Abdul Rauf

Title: Professor

Department of Chemistry

College of Science

3) Co-advisor: Dr. Soleiman Hisaindee

Title: Associate Professor

Department of Chemistry

College of Science

Abstract

This dissertation is concerned with the latest class of the new designer drugs (NDDs) which overruns the world in the last few years as “legal high” drugs, under the name of bath salts or synthetic cathinones. Bath salts are a group of central nervous system stimulants that consists mainly of synthetic cathinone derivatives. In nature, cathinone (β-keto amphetamine) exists in the leaves of the *Catha edulis* plant which can be found easily in the region of northeast Africa and the Arabian Peninsula. All synthetic cathinone derivatives contain a chiral center and most probably sold out as a racemic mixture. Commonly, one of the enantiomers will have greater psychological effect in human biological system than the other one. Therefore it’s important to distinguish between synthetic cathinone enantiomers. Enantiomeric separation and determination of these NDD’s may give information about the source of these synthetic drugs and the raw materials that were used in the synthesis process and also facilitates the drug tracking.

The main objective of this dissertation is to develop and validate sensitive and selective analytical methods that use direct and indirect chiral separation and quantitation for synthetic cathinones in real biological samples using chromatography coupled with mass spectrometer detector (MSD) and Diode Array detector (DAD).

The study goals were achieved successfully by developing and validation of three different methods for chiral separation and quantitation for 65 compounds of synthetic cathinones. Enantiomer quantitation in urine and plasma were performed and reported for the first time in this study; also it’s the first time to report the chiral

separation of tertiary amine cathinones where we were able to separate 19 out 22 of them.

Keywords: Chiral separation, quantitation, enantiomers, derivatization, Cathinones, bath salts, method validation, chiral column.

Title and Abstract (in Arabic)

الفصل الانطباقي والتحليل الكمي لعقاقير القات المصنع – الكاثينونات المصنعة – في عينات البوم والدم

الملخص

تختص هذه الأطروحة بأحدث فئة من العقاقير الجديدة المعروفة بالمخدرات المصنعة الحديثة (New Designer Drugs) التي طغت على العالم في السنوات القليلة الماضية كعقاقير مخدرة يسمح باستخدامها من ناحية قانونية تحت اسم "أملاح الاستحمام" (Bath salts) أو الكاثينونات الاصطناعية (Synthetic Cathinones). أملاح الاستحمام هي مجموعة من منشطات الجهاز العصبي المركزي و تتكون أساساً من مركبات الكاثينونات الاصطناعية. في الطبيعة توجد مادة الكاثينون (Cathinone) في أوراق نبات القات التي يمكن العثور عليها بسهولة في منطقة شمال أفريقيا و شبه الجزيرة العربية. جميع مركبات الكاثينونات الاصطناعية تحتوي على مركز انطباقي (Chiral center) و أغلب الظن أنها بيعت من قبل المروجين على شكل مزيج راسيمي (Racemic mixture). غالباً، إحدى المقابلات الضوئية (Enantiomer) تكون لديها قدرة أكبر على التأثير النفسي في النظام البيولوجي البشري من المقابلات الضوئية الأخرى، و بالتالي فإنه من المهم أن نميز بين المقابلات الضوئية للكاثينونات الاصطناعية. إن فصل المقابلات الضوئية للمخدرات المصنعة الحديثة قد يعطي معلومات حول مصدر هذه المخدرات الاصطناعية والمواد الخام التي استخدمت في عملية الاصطناع (Synthesis) وأيضا يسهل عملية تتبع مصادر هذه المخدرات.

الهدف الرئيسي من هذه الرسالة هو استحداث وتحقق علمي من طرق تحليل تسمح بشكل مباشر و غير مباشر بالفصل الانطباقي و التحليل الكمي للكاثينونات الاصطناعية في العينات البيولوجية الحقيقية باستخدام جهاز الكروماتوغرافيا موصولا بجهاز مطياف الكتلة (GC-MS) و جهاز الصمام الثنائي الكاشف (HPLC – UV).

تحققت أهداف هذه الدراسة بنجاح من خلال الاستحداث و التحقق العلمي من ثلاث طرق مختلفة للفصل الانطباقي و تحليل 65 مركبا للكاثينونات الاصطناعية. و قد أجري التحليل الكمي للمقابلات الضوئية لعينات البول و البلازما لهذا النوع من المركبات للمرة الأولى من

خلال هذه الدراسة كما أنها المرة الأولى التي يتم مناقشة الفصل الانطباقي بعمق للكاثينونات ذات الأمين الثالثي (Tertiary amine) حيث قمنا بفصل 19 من أصل 22 مركب.

مفاهيم البحث الرئيسية: الفصل الانطباقي، التحليل الكمي، المقابلات الضوئية، اشتقاق، كاثينون، أملاح الاستحمام، التحقق العلمي من أسلوب، عمود فصل انطباقي.

Acknowledgements

First and foremost, my thanks and all praise go to Allah (SWT) without Whom this life is nonexistent and absolutely meaningless. I thank Him for giving me the ability and patience to persevere through this process and I ask for His Guidance in becoming someone who continually seeks useful knowledge and delivers it to others.

My deepest gratitude is to advisor, Dr. Mohammed A. Almeetani. who has been the driving force behind my motivation and the guidance in in research to recover when my steps faltered. Also I would like to express my sincere gratitude to co-advisors, Prof. Muhammad Abdul Rauf and Dr. Soleiman Hisaindee for their assistance, good humour and infinite patience throughout my PhD.

I am particularly grateful to the research participants who took time to share their experiences, and for the valuable insights they contributed; Dr. John Graham for performing DFT studies for the inclusion reaction between PAH and β-CD, Dr. Na'il Saleh for his help on spectrofluorometric analysis for PAH, Mr. Mu'ath Mousa for development of sensitive HPLC-FLD method for the analysis of PAH in urine samples and Mr. Anas Alaidaros for his great efforts, patient and assistance in validation and development of GC-NCI-MS method for synthetic cathinones analysis.

I would like to express my special thanks to Dubai Police for giving me this opportunity and sincere support and help throughout the duration of my study where they provided me with all chemicals and instruments needed in my research. Also I would like to extend my appreciation to Col. Ahmad Mattar Almeheiri, Col. Khalid Alsumaiti, Dr. Foad Tarbah, Dr. Saif Eldin Khalil, Capt. Adnan Lenjawi, 1st Lt.

Nawaf Almansoori, Mr. Faisal Altunaiji, Ms. Fayzah Bin Tamim and Ms. Ibtisam Alabdooli for facilitating all researches procedures in Dubai Police Forensic Laboratory.

My thank also for all faculty member in Chemistry department at UAEU for their support and valued knowledge that I learn from them.

I wish to thank various people for their valuable technical support on the instruments; Eng. Annasamy Sankar, Eng. Baban Mahekar, Mr. Bassam Alhindawi and Eng. Partha Sarathi.

I want to appreciate as well as all my collegeagues for their encoungmnet; Dr. Ismail Alhaty, Dr. Abdulwahed Alsamadi, Dr. Abdultawab Ms. Lina Alkaabi, Ms. Afra Albloushi, Mrs Shaikha Alniyadi, Mrs. Khawla Alshamsi, Mrs. Heba AbuKhousa.

Finally, special deep appreciation is given to my family for providing me with unfailing support and encouragement that lead to this accomplishment.

Dedication

To my beloved family

Table of Contents

Title……....i
Declaration of Original Work ii
Copyright iii
Advisory Committee iv
Approval of the Doctorate Dissertation v
Abstract vii
Title and Abstract (in Arabic) ix
Acknowledgements xi
Dedication xiii
Table of Contents xiv
List of Tables xvii
List of Figures xx
List of Schemes xxii
Chapter 1: Introduction 1
1.1 Cathinone 1
1.1.1 Cathinone in nature (Khat) 1
1.1.2 Khat components and stability of active material 1
1.1.3 Cathinone and amphetamine 3
1.2 Legality of khat 3
1.3 New designer drug (NDD) 5
1.3.1 Bath salt (synthetic cathinones) 5
1.3.2 Methcathinone 6
1.3.2.1 Methcathinone synthesis 7
1.3.3 Synthetic cathinone abuse 9
1.3.4 Legality of synthetic cathinone 10
1.4 Effect of cathinones in dopamine system 14
1.5 Synthetic cathinones and chirality 16
1.5.1 What are chiral compounds? 16
1.5.2 Importance of chiral separation in synthetic cathinones 18
1.5.3 Principles of chiral separation 18
1.5.3.1 Indirect chiral separation methods 20
1.5.3.1.1 Chiral derivatizating agent (CDA) 20
1.5.3.1.2 Gas Chromatography in cathinone chiral separation.....21
1.5.3.2 Direct chiral separation methods.....23
1.5.3.2.1 High performance liquid chromatography in cathinone chiral separation.....24
1.5.3.2.2 Capillary electrophoresis in cathinone chiral separation.....26
1.5.4 Quantitative analysis of synthetic cathinones.....29
1.6 Objectives of the study.....44

Chapter 2: A validated gas chromatography mass spectrometry method for simultaneous determination of cathinone related drugs enantiomers in urine and plasma 45
2.1 Introduction 45
2.2 Experimental 49
2.2.1 Chromatographic conditions 49
2.2.2 Chemicals and reagents 49
2.2.3 Sample preparation 50
2.2.3.1 Samples 50
2.2.3.2 Urine and plasma spiking and solid phase extraction 50
2.2.3.3 Derivatization step 51
2.3 Results 52
2.4 Discussion 62
2.5 Conclusion 65

Chapter 3: Development and validation of an analytical methodology for the simultaneous quantitative determination of synthetic cathinones in urine and plasma using GC-NCI-MS 66
3.1 Introduction 66
3.2 Experimental 70
3.2.1 Chromatographic conditions 70
3.2.2 Chemicals and reagents 72
3.2.3 Sample preparation 73
3.2.3.1 Samples 73
3.2.3.2 Solid phase extraction (SPE) of spiked urine and plasma samples 73
3.2.3.3 Derivatization step 73
3.3 Results 74
3.4 Discussion 86
3.5 Conclusion 89

Chapter 4: Development and validation of an HPLC method for the determination of synthetic cathinones “bath salts” enantiomers in human samples 90
4.1 Introduction 90
4.2 Materials and methods 92
4.2.1 Chromatographic condition 92
4.2.2 Chemicals 92
4.2.3 Sample preparation 93
4.2.3.1 Samples 93
4.2.3.2 Urine and plasma spiking and SPE 93
4.3 Results 93
4.4 Discussion 106
4.5 Conclusion 109

Chapter 5: Determination of p-aminohippuric acid with β-Cyclodextrin sensitized fluorescence spectrometry 110
5.1 Introduction 110
5.2 Experimental 112
5.3 Results 115
5.4 Discussion 134

5.5 Conclusion 138

Chapter 6: Conclusion.....139
6.1 Recommendations.....145

References.....146

Appendix A: Gas chromatogram, mass spectrum and calibration plots of 31 synthetic cathinones that analyzed in chapter 2.....159
Appendix B: Gas chromatogram, mass spectrum and calibration plots of 37 synthetic cathinones that analyzed in chapter 3.....203
Appendix C: Liquid chromatogram of 65 Synthetic cathinones analyzed by HPLC-DAD using cellulose/amylose column (chapter 4).....253

List of Tables

Table 1: List of selected countries where khat is treated as controlled substance. 4

Table 2: Updated list of Bath Salts (Synthetic cathinones) identified by GCMS and published by the General's Bureau of Criminal Investigation. 11

Table 3: List of controlled synthetic cathinones in UAE. 12

Table 4: Common neuropsychiatric and physical effects of synthetic cathinones. ... 15

Table 5: Comparison between indirect and direct methods of chiral separation. 20

Table 6: Analysis of synthetic cathinones in biological materials using GC–MS. 30

Table 7: Analysis of synthetic cathinones in biological materials using HPLC–MS. 31

Table 8: List of the 31 cathinone related compounds and their synonyms, in addition to the retention times of the separated two diasterioisomers for each compound analyzed on GC-MS using SIM mode. 54

Table 9: Results for twelve cathinone related compounds spiked in urine including linearity coefficient, R^2 values, Limits of detection and limits of quantitations for the two enantiomers of each compound. 58

Table 10: Results for twelve cathinone related compounds spiked in plasma including linearity coefficient, R^2 values, Limits of detection and limits of quantitations for the two enantiomers of each compound. 58

Table 11: Inter-day and intraday reproducibility results in terms of coefficient of variance (CV) for twelve cathinone related compounds spiked in urine for the two enantiomers of each compound. 59

Table 12: Inter-day and intraday reproducibility results in terms of coefficient of variance for twelve cathinone related compounds spiked in plasma for the two enantiomers of each compound. 60

Table 13: Recovery measurements expressed in percent errors for three different concentrations of the cathinone related compounds spiked in urine matrix. 61

Table 14: Recovery measurements expressed in percent errors for three different concentrations of the cathinone related compounds spiked in plasma matrix. 61

Table 15: Time segments table with selected ions used in SIM mode for the analysis of cathinones mixture. 72

Table 16: List of the 36 cathinone related compounds and their synonyms, in addition to the retention times of the separated two diasterioisomers for each compound analyzed on GC-MS using SIM mode. 75

Table 17: Results for fourteen cathinone related compounds spiked in urine including linearity coefficient, R^2 values, limit of detection and limit of quantitations for the two enantiomers of each compound. 80

Table 18: Results for fourteen cathinone related compounds spiked in plasma including linearity coefficient, R^2 values, limit of detection and limit of quantitations for the two enantiomers of each compound. 81

Table 19: Interday and intraday reproducibility results in terms of coefficient of variance for fourteen cathinone related compounds spiked in urine at three different concentration levels for the two enantiomers of each compound. 82

Table 20: Interday and intraday reproducibility results in terms of coefficient of variance for fourteen cathinone related compounds spiked in plasma at three different concentration levels for the two enantiomers of each compound. 83

Table 21: Recovery measurements expressed in percent errors for three different concentrations of the cathinone related compounds spiked in urine matrix. 84

Table 22: Recovery measurements expressed in percent errors for three different concentrations of the cathinone related compounds spiked in plasma matrix. 85

Table 23: List of the 22 tertiary amine cathinone related compounds and their synonyms, in addition to the retention times, resolutions (Rs) and selectivity factor (α) of the separated two diasterioisomers for each compound analyzed on HPLC-UV by DMP cellulose column. 95

Table 24: List of the 22 tertiary amine cathinone related compounds and their synonyms, in addition to the retention times, resolution and selectivity factor of the separated two diasterioisomers for each compound analyzed on HPLC-UV by AS-H Amylose column. 96

Table 25: List of the 43 primary and secondary amine cathinone related compounds and their synonyms, in addition to the retention times, resolutions (Rs) and selectivity factor (α) of the separated two diasterioisomers for each compound analyzed on HPLC-UV by DMP cellulose column. 97

Table 26: List of the 43 primary and secondary amine cathinone related compounds and their synonyms, in addition to the retention times, resolution (Rs) and selectivity factor (α) of the separated two diasterioisomers for each compound analyzed on HPLC-UV by AS-H Amylose column. 99

Table 27: Results for three cathinone related compounds spiked in plasma including linearity coefficient, R^2 values, Limits of detection and limits of quantitations for the two enantiomers of each compound. 103

Table 28: Results for three cathinone related compounds spiked in urine including linearity coefficient, R^2 values, Limits of detection and limits of quantitations for the two enantiomers of each compound. 103

Table 29: Inter-day and intraday reproducibility results in terms of coefficient of variance for three cathinone related compounds spiked in plasma for the two enantiomers of each compound. 104

Table 30: Inter-day and intraday reproducibility results in terms of coefficient of variance for three cathinone related compounds spiked in urine for the two enantiomers of each compound. 104

Table 31: Recovery measurements expressed in percent errors for three different concentrations of the cathinone related compounds spiked in plasma matrix……...105

Table 32: Recovery measurements expressed in percent errors for three different concentrations of the cathinone related compounds spiked in urine matrix……...105

List of Figures

Figure 1: Gas chromatogram for separation of the Rand S enantiomers of methedrone drug in methanol after derivatization with L-TPC in the presence of nikethamide internal standard. 53

Figure 2: Total ion chromatogram (TIC) of the simultaneous chiral separation of 12 cathinones related compounds. All compounds were spiked in urine and separated as L-TPC derivatives. 55

Figure 3: Total ion chromatogram (TIC) of the simultaneous chiral separation of 12 cathinones related compounds. All compounds were spiked in plasma and separated as L-TPC derivatives. 56

Figure 4: Calibration graphs of the two separated enantiomers of the methdrone compound in (a & b) urine, and (c & d) in plasma. Calibration ranges was 10-200 ppm. 57

Figure 5: Gas chromatogram for separation of the R and S enantiomers of Nor-mephedrone drug in ethyl acetate after derivatization with L-TPC..... 74

Figure 6: Total ion chromatogram (TIC) of the simultaneous chiral separation of 14 synthetic cathinone compounds spiked in urine and separated as L-TPC derivatives. 77

Figure 7: Total ion chromatogram (TIC) of the simultaneous chiral separation of 14 synthetic cathinone compounds spiked in plasma and separated as L-TPC derivatives. 77

Figure 8: Calibration graphs of the two separated enantiomers of the Nor-mephedrone compound in (a & b) plasma, and (c & d) in urine. Calibration ranges was 1-100 ppb. 79

Figure 9: Liquid chromatogram for separation of the R and S enantiomers of 50 ppm of dimethylone drug using: a) on DMP cellulose column and (b) AS-H Amylose column. 94

Figure 10: Total ion chromatogram (TIC) of the simultaneous chiral separation of 4'-methyl-α-PPP, Dimethylone and 4'-MeO-α-PPP in urine sample by HPLC-UV system..... 100

Figure 11: Total ion chromatogram (TIC) of the simultaneous chiral separation of 4'-methyl-α-PPP, Dimethylone and 4'-MeO-α-PPP in plasma sample by HPLC-UV system..... 101

Figure 12: Calibration graphs of the two separated enantiomers of the 4-Methoxy-a-PPP compound in (a & b) urine, and (c & d) in plasma. Calibration ranges was 5-250 ppm. 102

Figure 13: UV-visible absorption spectra of 10 mM β-CD aqueous solution. 115

Figure 14: UV-visible absorption spectra of 20 µM PAH in (a) water and (b) β-CD aqueous solution 5.5 µM at pH 4.06. (P-aminohipparic acid structure is shown at the top)..... 116

Figure 15: Fluorescence spectra of 100 µM of PAH in (a) water (pH 3.1 and (b) hexane. 117

Figure 16: a) Fluorescence spectra of PAH in aqueous solution at concentrations of 0.1,1 and 10 uM, b) fluorescence spectra of PAH at concentrations of 0.1,1 and 10 uM in 5.53 mM β-CD solution. 118

Figure 17: Fluorescence spectra of 15 mM β-CD solution at excitation of 275 nm.119

Figure 18: Fluorescence spectra of deionized water at excitation of 275 nm. 119

Figure 19: Titration of 10uM PAH and (0 – 5.53mM) of: (A) α-CD, (B) γ-CD and (C) β-CD at pH 6.8. 121

Figure 20: Titration of 10uM PAH and (0 - 5.53) mM β-CD at: (a) acidic, (b) basic and (c) neutral solutions. 123

Figure 21: NMR spectra of β-CD (10 mM), PAH (0.5 mM) and mixture of (0.5 mM PAH and 10mM β-CD), all solutions were prepared in D2O Solvent. 129

Figure 22: Calibration curve of (0.05 – 100 µM) PAH in aqueous solution containing 15mM β-CD. 130

Figure 23: HPLC –FLD chromatograms for 10uM PAH in the presence of different concentrations of β-CD; Mobile phase is 90% 0.1 M acetic acid in water, 10% Acetonitrile. 131

Figure 24: Calibration curves of PAH (Conc. Range 0.025-500 µM) at different concentrations of β-CD in the mobile phase. 132

Figure 25: Calibration curves of the HPLC –FLD data of PAH after extraction from urine sample matrix in the presence of 15 mM β-CD in the mobile phase. 133

List of Schemes

Scheme 1: Summary of different classes of alkaloids in khat leaves. 2

Scheme 2: Chemical structures of cathinone and amphetamine. 3

Scheme 3: Chemical structures of Synthetic Cathinones derived from Methcathinone 8

Scheme 4: α-methoxy-α-(trifluoromethyl)phenylacetic acid (MTPA) structure. 22

Scheme 5: (S)-(−)-N-(trifluoroacetyl)pyrrolidine-2-carbonyl chloride (L-TPC) structure. 22

Scheme 6: Synthetic cathinones group 1. 33

Scheme 7: Synthetic cathinones group 2. 37

Scheme 8: Synthetic cathinones group 3. 38

Scheme 9: Synthetic cathinones group 4. 38

Scheme 10: Synthetic cathinones group 5. 41

Scheme 11: Structure of (S)-(–)-N- (trifluoroacetyl)pyrrolidine-2-carbonyl chloride (L-TPC). 46

Scheme 12: Structures of synthetic cathinones that were analyzed quantitatively. ... 48

Scheme 13: Derivatization reaction between Cathinone and L-TPC. 52

Scheme 14: Structures of tertiary amine synthetic cathinones that analyzed quantitatively. 70

Scheme 15: Structures of tertiary amine synthetic cathinone derivatives that analyzed quantitatively. 91

Scheme 16 Structures of cathinone and PAH. 112

Scheme 17: Optimized gas-phase structure for two PAH molecules inside β-CD cavity. 125

Scheme 18: Optimized gas-phase structure for interaction of PAH and β-CD with PAH outside β-CD cavity. 126

Scheme 19: Optimized gas-phase structure for interaction of PAH and β-CD with PAH inside β-CD cavity. 127

Scheme 20: Solid phase extraction (SPE) of spiked urine and plasma samples. 252

Scheme 21: Derivatization step of synthetic cathinones by L-TPC..... 252

Chapter 1: Introduction

1.1 Cathinone

1.1.1 Cathinone in nature (Khat)

Khat, *Catha edulis Forsk*, is an ever popular flowering shrub that can be found growing naturally or cultivated in the south east Africa and in the southern west part of Arabian Peninsula (Krikorian 1984). Khat chewing habit has persisted through this part of the world for centuries. Naming of khat plants varied with its origin: tchat is used in Ethiopia, qat is used inYemen (Alem, Kebede et al. 1999), qaad/jaad is used in Somalia (Elmi 1983), miraa is used in Kenya (Patel 2000), mairungi is used in Uganda (Ihunwo, Kayanja et al. 2004), Muhulo is used in Tanzania and Hagigat is used in Israel (Bentur, Bloom-Krasik et al. 2008). Abyssinian tea or Arabian tea is another name for the dried leaves of khat. However, khat is the most common name for this herbal stimulant (Alem, Kebede et al. 1999). Classification of khat can be as follows [Family: Celastraceae, genus: Catha, and Species C. edulis] (Nordal 1980).

1.1.2 Khat components and stability of active material

Regarding materials and components of *Catha edulis*, it was found that khat leaves contain different chemicals such as: amino acids, trace amount of vitamins, alkaloids and some metal elements such as: calcium, iron and manganese (Feyissa and Kelly 2008). From a forensic point of view, scientists and researchers focus on the alkaloids of khat which play the main role in the stimulation effect of this plant. Scheme 1 shows different classes of alkaloids in khat leaves.

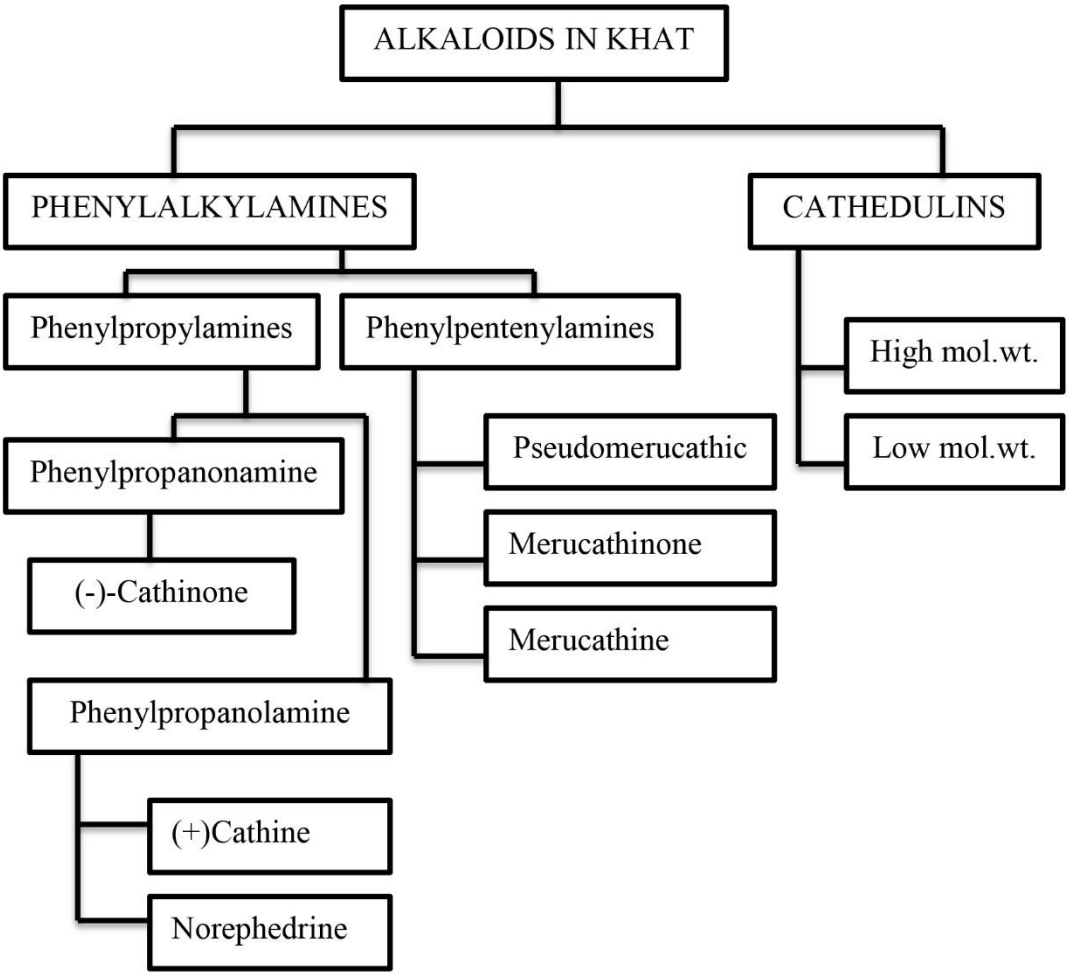

Scheme 1: Summary of different classes of alkaloids in khat leaves

Of all the alkaloids classes that are shown in the above figure, (-) Cathinone is known to be the major active constituent in khat leaves which can be in concentration range of 0.74 ± 0.40 mg per gram of khat leaf expressed as mean ± SD (Dimba, Gjertsen et al. 2004).

It was noticed that khat was cultivated and consumed at the same place or region. The reason for this was the fragility of active compounds in khat which were affected strongly by sunlight and heat which caused the degradation process. Degradation of active materials in khat leaves such as (-) Cathinone produces new

compounds that have less effect in the central nervous system of the human biological system (Banjaw, Fendt et al. 2005).

1.1.3 Cathinone and amphetamine

Cathinone can be classified as psychoactive phenethylalkylamine alkaloid that is present in khat plants. It has similar chemical structure to a very well-known abused drug called "amphetamine". The only difference in structure between cathinone and amphetamine is the β-keto group of cathinone which leads to different metabolism pathway in biological system and causes different effects (Hassan, Gunaid et al. 2007).

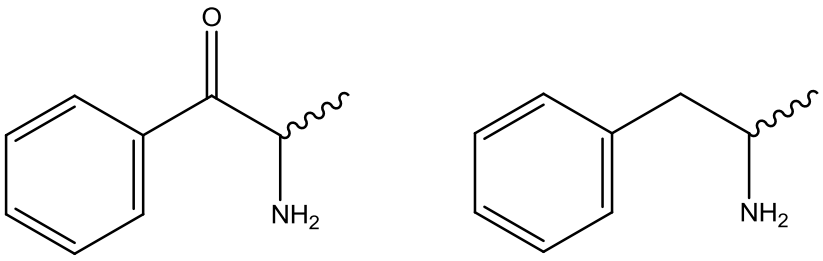

Cathinone **Amphetamine**

Scheme 2: Chemical structures of cathinone and amphetamine

1.2 Legality of khat

United Nations Convention on Psychotropic Substances (UNCP) banned Cathinone, a stimulant that occurs naturally in khat, as a Schedule I substance (By update of 1986, Cathinone was added to the list now). In addition, all international lists of controlled substances have listed Khat as an illegal substance, however, there is a variation from country to country about the legality of this herbal stimulant. Moreover, cathinone in khat degrades to cathine after an oxidization reaction that happened within 48–72 hr. The formed stimulant, i.e. cathine, after degradation had less potency and is thus listed as a Schedule III drug in the 1971 UN Convention.

Government of United Kingdom and Netherlands found that the use of khat make the users more violent than non-users which means that there is a relationship between the green plant and an organized crime (Armstrong 2008). There is some proof about khat use can cause health related problems such as: insomnia, gastrointestinal problems, and cardiovascular events and other harmful effect. As a result of that, khat had been treated as a controlled substance in all parts of the world, including China, the United Kingdom, and the Netherlands as shown in table 1.

Table 1: List of selected countries where khat is treated as controlled substance

Year	**Country**
1971	Saudi Arabia
1981	New Zealand
1986	Germany
1986	Australia
1988	Jordan
1989	Norway
1989	Sweden
1990	France
1993	Denmark
1993	Finland
1993	United States
1993	Ireland
1995	Tanzania
1995	United Arab Emirates
1996	Switzerland
1997	Canada
1999	Belgium
2005	Poland
2005	Italy
2012	Rwanda
2013	Netherlands
2014	China
2014	United Kingdom

1.3 New designer drug (NDD)

The psychostimulant herbal drug is chewed by addictors to extract the active material from green leaves. Approximately, 80 to 90% of the active material such as cathinone, cathine and norephedrine were extracted during green leaves chewing (Toennes and Kauert 2002). On other parts of the world, especially in developed countries, addiction of cathinone takes place but with a new generation of modified cathinones. Although governments established a number of regulations and laws that prevent sale, distribution, and consumption of the well-known abusive drug, clandestine labs played a dirty game by creating new psychoactive drugs that are not yet included in government's laws which give the abusers a good chance to use and consume these kinds of drugs under the shield of legality.

New designer drug (NDD) or Novel Psychoactive Drug (NPD) is a common name that describes the new generation of abused drug that overrun the whole world recently, which obligate governments to look for quick solution to prevent NDD from destroying their countries and societies.

1.3.1 Bath salt (synthetic cathinones)

In this study, we focused on one class of NDD called synthetic cathinones. Synthetic cathinones are known in US as "bath salt" and the reason for giving cathinones this name is just to mask these kinds of drugs. The illicit manufacturers mainly used this term in order to circumvent the Federal Analog Act which will give them kind of legality in market. ''Bath salts'' are not sold as tablets or capsules, but it was mainly in the form of fragrance-free, white, yellowish or brown crystals or powder. In United States the street price of bath salt is approximately $25–35 per

half gram package (Adebamiro and Perazella 2012). ‘‘Not for human consumption’’, a kind of warning written by suppliers on the product and sadly it is the only good thing that they did for consumers. Strangely, ingredients list indicates that there is no presence of psychoactive compounds even safety information is not provided (Zawilska and Wojcieszak 2013). This attitude causes a serious threat for usage of synthetic cathinones that can cause calamity for users. A good question can be raised, how do the clandestine chemist synthesize cathinone and who is the first scientist to synthesis it?

1.3.2 Methcathinone

N-methyl analogue of cathinone, methcathinone (ephedrone), was first synthesized in 1928 by Germans and French (Hyde, Browning et al. 1928). In the 1950s, Parke-Davis pharmaceutical company in US was planning to market methcathinone as an appetite suppressant and an antidepressant which was followed by a grant that funded the production process in 1957. Human testing of the new drug stopped due to adverse reactions of it in biological systems. Unfortunately, a student in University of Michigan who was working at Parke-Davis found his way to business through the illegal manufacturing process of methcathinone in 1989 after finding documents to explain the synthetic procedure of ephedrone (Bailey, Hernandez Martin et al. 1995). Due to the growing risk of methcathinone and its rapid spread in the world, methcathinone had been placed in Schedule I of the United Nations Controlled Substance Act in 1992 by the Drug Enforcement Administration (DEA) (Sikk and Taba 2015).

1.3.2.1 Methcathinone synthesis

Scientist considered methcathinone as the first “synthetic cathinone” which was found to be at least as potent as methamphetamine, the well-known stimulant (Glennon, Martin et al. 1995). The most common way in methcathinone synthesis is to use ephedrine or pseudoephedrine as precursors since they are easy to find as over-the-counter drugs and can produce methcathinone by a very simple reaction. Oxidation reaction of ephedrine can produce methcathinone while methamphetamine is the product of reduction reaction of ephedrine. In fact, reductive path of ephedrine is much more complicated. Potassium permanganate is used in the oxidation reaction of ephedrine in Russia and the Eastern Europe, followed by almost no refinement, unlike United States where they used sodium dichromates as an oxidant agent followed by a number of cleanup steps (Sikk and Taba 2015). Most of the synthetic cathinones have been derived from methcathinone as shown in Scheme 3.

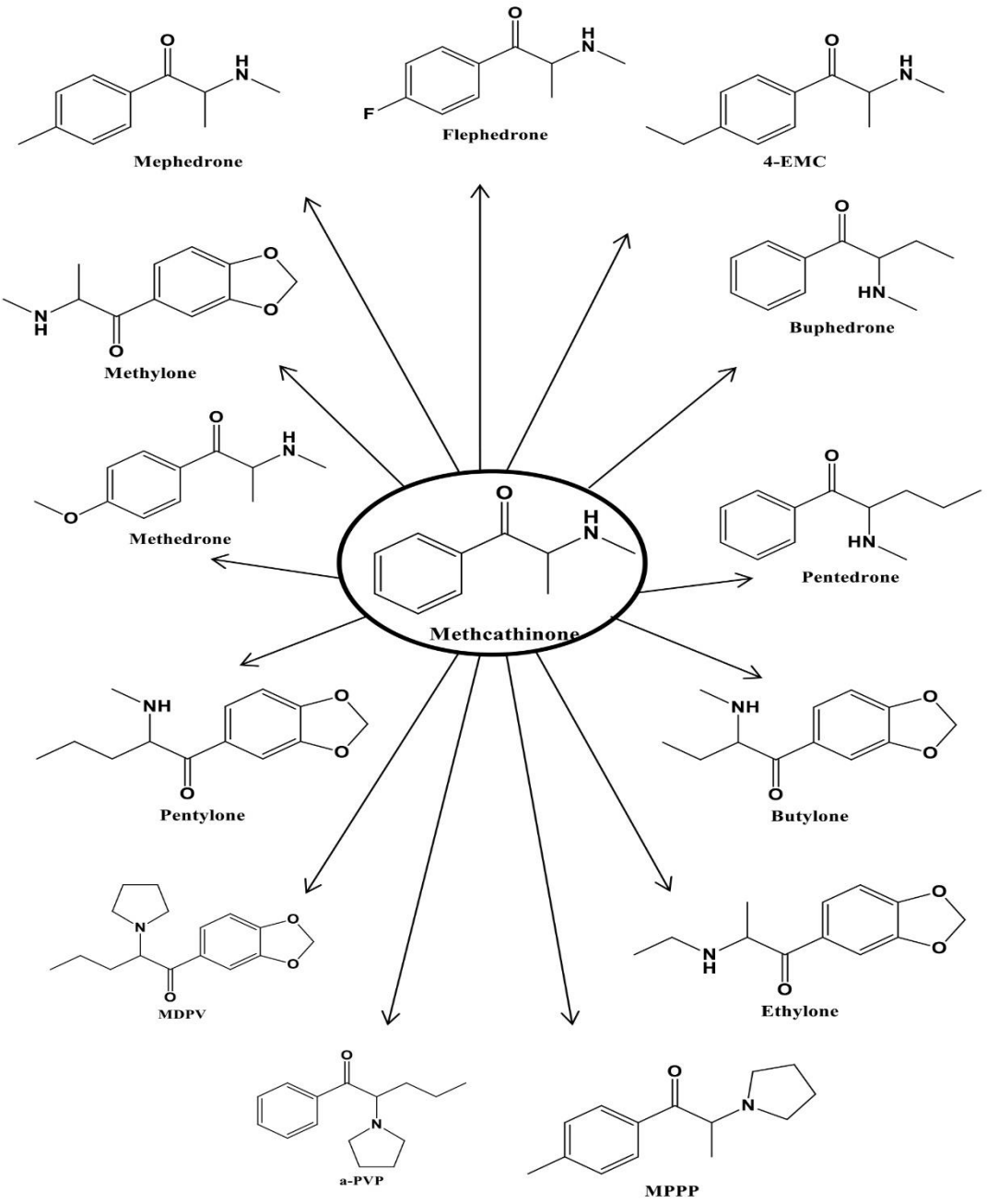

Scheme 3: Chemical structures of Synthetic Cathinones derived from Methcathinone

1.3.3 Synthetic cathinone abuse

Synthesis of some synthetic cathinones have been known for a long time ago, but only recently abused. It was noticed that some of synthetic cathinones had a higher popularity in terms of abused such as: 4-methylmethcathinone (mephedrone), 3,4-methylenedioxymethcathinone (methylone), and 3,4-methylenedioxyprovalerone (MDPV) (German, Fleckenstein et al. 2014). Although synthetic cathinones have been discovered long time ago, abusers ignored them until the use of cathinones by addictors as a legal alternative to 3,4-Methylenedioxymethamphetamine (MDMA) on internet drug websites in 2003 (Morris 2010) and within few years, cathinone-derivatives became prevalent within the United Kingdom. In Europe, mephedrone is the most common synthetic cathinone that was abused, while MDPV and methylone was widely abused in US (German, Fleckenstein et al. 2014). Most frequently, abused techniques of these compounds varied between: snorting, which can cause nasal irritation that obligates many abusers to smoke bath salts, consuming them orally, or by injecting themselves intravenously or intramuscularly (Kavanagh, O'Brien et al. 2013). Bath salt can be distributed through: street-level sellers, head shops, smoke shops, adult book stores, gas stations and internet within US, Europe and worldwide. It was found that most of the synthetic cathinones are synthesized in China and South East Asian countries (German, Fleckenstein et al. 2014). Methedrone abused spread over 28 European countries at the period between 2007 up to 2010 (EMCfDaD 2011). In 2009, UK National Poisons Information Service recorded no enquiry regarding cathinone toxicity and within one year the number jumped rapidly to over 600 reports in 2010 (James, Adams et al. 2011). As a result of that, mephedrone became the third most commonly abused drug in the UK by the

end of 2010. In school and college/university approximately 20% of individuals, ages between 14 to 20, are the most affected layer of society in UK by the mephedrone (Dargan, Albert et al. 2010). Within the same period of time in US, National Forensic Laboratory Information System (NFLIS) reported an increase in synthetic cathinone drug enquiries from 34 in 2009 to 628 in 2010 (Forrester 2012). For example, MDPV was reported as the fifth and methylone as the eleventh most common drug that can cause hallucinations within the US as reported by NFLIS in 2011. Moreover, calls that have been received by poison control center regarding exposure of bath salt increased from 304 in 2010 to 6136 in 2012 (German, Fleckenstein et al. 2014).

1.3.4 Legality of synthetic cathinone

Due to the growing risk of the synthetic cathinones, US Drug Enforcement Administration (DEA) took an important decision on prohibiting some of central nervous system stimulant drugs and schedule them in the law tables and consider them as illegal substances in 2010 (Banks, Worst et al. 2014).

Table 2: Updated list of Bath Salts (Synthetic cathinones) identified by GCMS and published by the General's Bureau of Criminal Investigation

#	Name	Synonyms	Legality
1	Cathinone	-	DEA Schedule I
2	Ethcathinone	-	DEA Schedule I
3	Mephedrone	-	DEA Schedule I
4	4-methylethcathinone	(4-MEC)	DEA Schedule I
5	4-fluoromethcathinone	(4-FMC)	DEA Schedule I
6	Buphedrone	-	DEA Schedule I
7	Pentedrone	-	DEA Schedule I
8	Methylone	-	DEA Schedule I
9	Butylone	-	DEA Schedule I
10	Pentylone	-	DEA Schedule I
11	Ethylone	-	DEA Schedule I
12	3,4-Methylenedioxy-α-pyrrolidinopropiophenone	(MDPPP)	DEA Schedule I
13	3,4-Methylenedioxy-α-pyrrolidinobutiophenone	(MDPBP)	DEA Schedule I
14	3,4-Methylenedioxypyrovalerone	(MDPV)	DEA Schedule I
15	α-Pyrrolidinovalerophenone	(Alpha-PVP)	DEA Schedule I
16	α-Pyrrolidinobutiophenone	(Alpha-PBP)	DEA Schedule I
17	α-Pyrrolidinopropiophenone	(Alpha-PPP)	DEA Schedule I
18	1-(4-methylphenyl)-2-(pyrrolidinyl)-1-propanone	(MPPP)	DEA Schedule I

Identification of novel bath salts including their chemical structures and names have been done by the Ohio Attorney General's Bureau of Criminal

Investigation. Not all the agents listed in table 2 have been scheduled by DEA; moreover pharmacological tests are not carried out yet for all of them in controlled human or animal studies.

In United Arab Emirates, some of synthetic cathinones have been scheduled in December 2015 as shown in Table 3.

Table 3: List of controlled synthetic cathinones in UAE

#	IUPAC name	Compound name	Synonyms
1	1-phenyl-2-(1-pyrrolidinyl)-1-heptanone	α-Pyrrolidinopentiophenone	α-PVP
2	1-phenyl-2-(1-pyrrolidinyl)-1-propanone	α-Pyrrolidinopropiophenone	α-PPP
3	2-(methylamino)-1-phenyl-1-butanone	Buphedrone	MABP
4	1-(1,3-benzodioxol-5-yl)-2-(dimethylamino)-1-butanone	Dibutylone /bk-DMBDB	-
5	2-(dimethylamino)-1-phenyl-1-propanone	Metamfepramone	N,N-DMC
6	1-(3,4-dimethylphenyl)-2-(ethylamino)propan-1-one	3,4-Dimethylethcathinone	3,4-DMEC
7	1-(3,4-dimethylphenyl)-2-(methylamino)-1-propanone	3,4-Dimethylmethcathinone	3,4-DMMC
8	1-(1,3-benzodioxol-5-yl)-2-(dimethylamino)-1-propanone	Dimethylone / bk-MDDMA	-
9	2-(ethylamino)-1-phenyl-1-propanone	Ethcathinone	-
10	2-(dimethylamino)-1-(4-ethylphenyl)propan-1-one	4-ethyl-N,N-Dimethylcathinone	4-ethyl-N,N-DMC
11	2-(ethylamino)-1-(4-ethylphenyl)propan-1-one	4-Ethylethcathinone	4-EEC
12	1-(4-ethylphenyl)-2-(methylamino)propan-1-one	4-Ethylmethcathinone	4-EMC
13	1-(benzo[d][1,3]dioxol-5-yl)-2-(ethylamino)propan-1-one	Ethylone /bk-MDEA	MDEC
14	1-(1,3-benzodioxol-5-yl)-2-(ethylamino)-1-butanone	Eutylone / bk-EBDB	-
15	2-(ethylamino)-1-(4-fluorophenyl)propan-1-one	4-Fluoroethcathinone	4-FEC
16	1-amino-1-(4-fluorophenyl)propan-2-one	4-Fluoroisocathinone	4-FIC

#	IUPAC name	Compound name	Synonyms
17	1-(1,3-benzodioxol-5-yl)-2-(1-pyrrolidinyl)-1-propanone	3,4-Methylenedioxy-α-Pyrrolidinopropiophenone	3,4-MDPPP
18	2-(methylamino)-1-(4-methylphenyl)-1-butanone	4-Methylbuphedrone	4-methyl BP
19	1-(1,3-benzodioxol-5-yl)-2-(1-pyrrolidinyl)-1-butanone	3,4-Methylenedioxy-α-Pyrrolidinobutiophenone	3,4-MDPBP
20	1-(4-methylphenyl)-2-(1-pyrrolidinyl)-1-butanone	4-methyl-α-Pyrrolidinobutiophenone	4-methyl PBP
21	2-(pyrrolidin-1-yl)-1-(p-tolyl)hexan-1-one	4'-methyl-α-Pyrrolidinohexanophenone	MPHP
22	1-(4-methoxyphenyl)-2-(pyrrolidin-1-yl)propan-1-one	4'-methoxy-α-Pyrrolidinopropiophenone	4'-MeOPPP
23	2-(ethylamino)-1-phenylbutan-1-one	N-Ethylbuphedrone	NEB
24	1-(1,3-benzodioxol-5-yl)-2-(methylamino)-1-butanone	Butylone / bk-MBDB	-
25	1-(1,3-benzodioxol-5-yl)-2-(1-pyrrolidinyl)-1-pentanone	3,4-Methylenedioxy Pyrovalerone	3,4-MDPV
26	2-(methylamino)-1-(4-methylphenyl)-1-propanone	Mephedrone	4-MMC
27	1-(4-fluorophenyl)-2-(methylamino)propan-1-one	4-Fluoromethcathinone	4-FMC
28	1-(4-methoxyphenyl)-2-(methylamino)-1-propanone	Methedrone	PMMC
29	1-(1,3-benzodioxol-5-yl)-2-(methylamino)-1-propanone	Methylone / bk-MDMA	-
30	2-(methylamino)-1-phenyl-1-pentanone	Pentedrone	-
31	1-(1,3-benzodioxol-5-yl)-2-(methylamino)-1-pentanone	Pentylone	-
32	1-(3-fluorophenyl)-2-(methylamino)propan-1-one	3-Fluoromethcathinone	3-FMC
33	2-(ethylamino)-1-(4-methylphenyl)-1-propanone	4-Methylethcathinone	4-MEC

However, the cat-and-mouse game seems to continue between lawmakers and clandestine laboratories, with continuous synthesis of new designer stimulants that will replace those outlawed psychoactive drugs (German, Fleckenstein et al. 2014).

1.4 Effect of cathinones in dopamine system

The synthetic cathinones, induce profound behavioral changes in dopamine system, probably through the central monoamine systems where the actions take place. Dopaminergic pathways are neural pathways in the brain that carry the neurotransmitter dopamine from one region to another. It can be divided into four major dopaminergic pathways: the nigrostriatal, mesolimbic, mesocortical, and tuberoinfundibular pathways (Björklund and Dunnett 2007). Motor control that is carried out by the central nervous system is associated with the nigrostriatal pathway, which is responsible to organization of the musculoskeletal system that will lead to produce coordinated activities and skillful movements (DeLong 1990). Reward system of the brain is another name of the mesolimbic pathway which is responsible for pleasure or the events that is usually associated with pleasure in human being like having sex and food in terms of rewards (Di Chiara 1998). Cognition, motivation, and emotional response are corresponded to the mesocortical pathway (Floresco and Magyar 2006). The secretion influences of hormone prolactin which counteracts the sexual arousal effect of dopamine is associated with tuberoinfundibular pathway (Porter, Kedzierski et al. 1990).

All four dopamine pathways in the brain will be affected by any drug that can affect dopamine levels such as synthetic cathinones. The effect of these drugs is based on the following mechanisms: both stimulating the dopamine releasing, and also an inhibition of reuptake process where the excess dopamine in the synaptic cleft will be reabsorbed (den Hollander 2015). As a result of increasing levels of dopamine, the action on dopamine receptors of post-synaptic neurons will increase, leading to activation of the dopaminergic pathways.

As synthetic cathinones are classified as stimulation-induced drugs, they are strongly responsible for alerting the dopaminergic pathways but at different rate for each pathway. Symptoms of twitching, restlessness, and repetitive motion can be produced as a result of nigrostriatal pathway stimulation (DeLong 1990). Stimulation of mesolimbic pathway produces pleasure, euphoria, dysphoria, hallucinations and psychotic behavior (Di Chiara 1998). Depression, fear, and anxiety are symptoms of mesocortical pathway stimulation produces (Floresco and Magyar 2006). Increase in sexual desire can occur when dopamine in the tuberoinfundibular pathway inhibits the release of prolactin from the pituitary gland (Porter, Kedzierski et al. 1990). Table 4 shows some of the physical and neuropsychiatric effect of bath salt in humans.

Table 4: Common neuropsychiatric and physical effects of synthetic cathinones

	Desirable	**Adverse**
Physical	Alertness Analgesic effects Increased energy Stimulation	Cerebral edema Diaphoresis Hyperreflexia Hyperthermia Jaw tension Muscle spasms Mydriasis Myocardial infarction Respiratory distress Seizures Tachycardic
Neuropsychiatric	Creativity Empathy Euphoria Sociability Productivity Mental clarity Sexual arousal Sharpened awareness	Aggression Agitation Combative behavior Dysphoria Hallucinations Insomnia Paranoia Psychosis Suicidal thoughts

In fact, this is a very short and general explanation about stimulant effect in dopamine system. More information and details about neuropharmacology of bath salt, is available in the literature (Miotto, Striebel et al. 2013, Zawilska and Wojcieszak 2013, Banks, Worst et al. 2014, German, Fleckenstein et al. 2014, Vouga, Gregg et al. 2015).

1.5 Synthetic cathinones and chirality

All cathinone derivatives have chiral center at their α-carbon where the carbon atom is attached to four different groups' schemes (6 – 10). Asymmetric carbon center in cathinones leads to the presence of cathinones as a racemic mixture of two optical isomers.

1.5.1 What are chiral compounds?

Unique three-dimensional shape molecule with an asymmetric carbon center describes special kind of molecules called chiral molecules. The origin of chiral as a term is from Greek language since they use it as a meaning ‘‘hand.’’ Although chiral molecules are mirror image of each other, they are different in their ‘‘handedness’’ so they cannot be superimposable. In Greek enantios, meaning ‘‘opposite’’ and this was the reason for naming chiral molecules as ‘‘enantiomers,’’. In the example of human hand, left and right hand are enantiomers since they are mirror images, ‘‘right’’ glove cannot be worn on a left hand. The arrangement of fingers and thumb in three dimensions makes a left hand and a right hand somehow different from each other. Enantiomers of chiral compounds exist as rectus (R) - and sinister (S) - or dextro(D) and levorotary (L) according to their ability to rotate plan polarized light. If the mixture of enantiomers contain the same concentration of each enantiomer, it

can be called a ‘‘racemate.’’Although the carbon frameworks of the two enantiomers align, the position of the functional groups is different at the chiral center. Complete alignment of the two molecules without breaking bonds is impossible (Li and Haynie 2006).

Since human biological system is chiral, dextro (D) and levorotary (L) enantiomers have different pharmacological effects in human being. For instance, in food industry, L - limonene gives a smell of lemons, while D - limonene gives a smell of oranges. The reason as to why enantiomers are not acting in the same identical way in the biological context is the difference in three-dimensional structure where sometimes one of the enantiomers is much suitable than the other for a precise interaction with a biological molecule, such as a receptor, enzyme, etc (Li and Haynie 2006).

Chiral specificity of the biological system is very high. The interaction and metabolism pathway with each racemic drug is different which will produce different pharmacological activity and potencies in living organisms. The desired therapeutic activities can be produced by one isomer, while the other may be considered as an inactive compound or can create undesirable side effects (Li and Haynie 2006).

1.5.2 Importance of chiral separation in synthetic cathinones

Synthetic cathinones have limited toxicological and pharmacological data due to their novelty (Mohr, Pilaj et al. 2012). However, few synthetic cathinones have been studied stereochemically in biological systems. For instance, it was found that R-(+) enantiomer of methcathinone and R-(-) enantiomer of amphetamine, show less stimulating effects than their S-(-) - and the S-(+) - antipodes (Glennon, Martin et al. 1995, Jirovský, Lemr et al. 1998, Rasmussen, Olsen et al. 2006). Therefore, enantioseparations of new class of cathinone derivatives may lead to preparative methods that are capable to separate racemic mixture enantiomers, which can be used easily in pharmacological studies. The second importance of chiral separation methods is to indicate the synthesis pathway, which can determine the starting materials used for synthesis. Drug trafficking will facilitate finding the origin lab of synthesis by the information that can be provided after chiral analysis of the targeted analytes. Chiral separation of new designer drugs could show the ratio between enantiomers which will help investigators to know the conditions and the chemicals that were used in clandestine labs (Jirovský, Lemr et al. 1998).

1.5.3 Principles of chiral separation

In the past 20 years, enantioseparation of molecules containing asymmetric chiral centers has attracted the attention of pharmaceutical industry. Chiral separations can be achieved by one of the following strategies: an indirect method, based on the reactions of chiral compounds with a chiral derivatizing agent (CDA) and separation of the diastereomeric derivatives on an achiral normal stationary phase. Second strategy of chiral separation is based on direct separation method, where the diastereoisomers can be formed on an immobilized chiral stationary phase

(CSP), or with a chiral macromolecule selector in a mobile phase with an achiral stationary phase (Ilisz, Berkecz et al. 2008). Table 5 shows the advantages and disadvantages of each technique.

Table 5: Comparison between indirect and direct methods of chiral separation

Indirect method	**Direct method**
Advantages 1. Good chromatographic properties of derivatives 2. Good chromophoric or fluorophoric properties of the regent (enhanced sensitivity can be achieved) 3. Low cost of achiral columns 4. Method development is simple 5. Selectivity can be increased (better separation is often achieved than with a direct method) 6. Possibility of appropriate selection of the elution sequence and the elution sequence predictable Disadvantages 1. The purity of the CDA is critical 2. The molar absorptivity of the diastereomers may differ 3. Possibility of racemization 4. Possibility of kinetic resolution 5. The excess of regent and side products may interfere with the separation 6. Preparative application is restricted 7. Derivatization may be time-consuming	Advantages 1. The purity of the chiral selector is not critical 2. Similar molar absorptivities of enantiomers 3. Absence of racemization and kinetic resolution 4. Racemates without functional groups are separable 5. Preparative applications are available 6. Change of temperature may be favorable 7. Simple preparation of analytes and simple chromatographic runs Disadvantages 1. The theoretical plate number of the CSP is small 2. Slow kinetics of desorption 3. The elution sequence is not clear 4. No universal column exists 5. CSPs are very sensitive to chromatographic conditions (rather difficult and lengthy method development) 6. High cost of critical columns

1.5.3.1 Indirect chiral separation methods

1.5.3.1.1 Chiral derivatizating agent (CDA)

Enantiomers can be derivatized through the use of homochiral reagents that lead to the formation of diastereoisomers which are separable on achiral columns. Achiral stationary phase cannot distinguish between enantiomers yet it interacts with the formed diastereoisomers in different way which leads to variation of retention times. Chiral derivatization was the first commonly used method in the analysis of

chiral drugs (Ilisz, Berkecz et al. 2008). The most critical points for this technique to succeed is the availability of the derivatizable group in the targeted analyte and the high purity of the homochiral reagent. For instance, in case of synthetic cathinones, tertiary amines cathinones will be excluded from this strategy since they do not contain a derivatizable site unlike primary and secondary amines cathinones which can be derivatized easily by the removal of acidic hydrogen of amine and the formation of new amide bond between analyte and the CDAs.

Due to the development of new chiral chromatographic techniques, enantioseparations based on covalent chiral derivatization became unpreferable to some extent, however, CDAs are still frequently used in GC and HPLC systems. The reasons for this are the ability to use achiral columns, the availability of large number of homochiral derivatizing reagents that have well-known reactions to produce diastereoisomers with well separated peaks of high resolution.

1.5.3.1.2 Gas chromatography in cathinone chiral separation

GC in combination with MS detection was one of the most popular techniques for chiral analysis which can be carried out directly on chiral stationary phases (CSPs) or indirectly using achiral stationary phases after performing chiral derivatization using pure reagents that form diastereoisomers (Jirovský, Lemr et al. 1998, Tao and Zeng 2002). Indirect analysis of enantiomers was preferable for GCMS users due to many reasons that were mentioned before.

(R)-(+)-α-methoxy-α-(trifluoromethyl)phenylacetic acid (MTPA) has been used for cathinone chiral separation which was considered as the most active derivatives of the alkaloids in Khat using Gas chromatographic-Mass spectrometric system (LeBelle, Lauriault et al. 1993). Another method was developed using the

same CDA (MTPA) for the simultaneous analysis of eight compounds that were structurally similar to cathinones (Wang, Lewis et al. 2005).

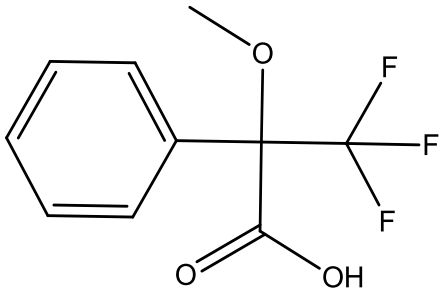

Scheme 4: α-methoxy-α-(trifluoromethyl)phenylacetic acid (MTPA) structure

Another CDA called (S)-(−)-N-(trifluoroacetyl)pyrrolidine-2-carbonyl chloride (L-TPC) was used to achieve chiral separation. L-TPC had many advantages, including effectiveness of derivatization reaction, commercial availability and good resolution of products (Wang, Wang et al. 2005).

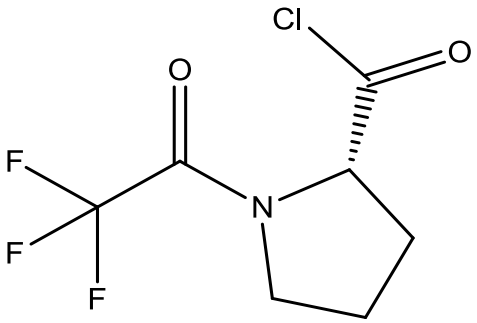

Scheme 5: (S)-(−)-N-(trifluoroacetyl)pyrrolidine-2-carbonyl chloride (L-TPC) structure

Recently, Stefan Mohr et al. (Mohr, Weiß et al. 2012) used L-TPC for chiral analysis of new synthetic cathinones and amphetamines with GCMS. The indirect chiral separation using L-TPC as CDA was successful to separate 19 of cathinone derivatives into their diastereoisomers on a common achiral stationary phase column. In 2015, the same group performed an enantioseparation for a new group of synthetic

cathinone derivatives where they were able to separate 4 out of 10 cathinone related drugs in that study indirectly on GCMS after performing derivatization reaction with L-TPC (Weiss, Mohr et al. 2015). Taschwer et al. were able to analyze and characterize a novel psychoactive drug called 4-chloromethcathinone (clephedrone) which was available by different online suppliers (Taschwer, Weiß et al. 2014). Clephedrone chiral separation was carried out indirectly also by GCMS system after derivatization step with L-TPC. Although efficient derivatization reactions between targeted analytes and CDA attracted chemists, the need for direct chiral techniques is growing, especially in order to save analysis time.

1.5.3.2 Direct chiral separation methods

Direct separation of enantiomers can be carried out by introducing a suitable optically active moiety into the system. Chiral selectors can be added to the mobile phase of HPLC system, or it can be added to background electrolyte of CE; alternatively it can be attached on a solid stationary phase of capillary (TesaŘOvÁ and Armstrong 1998). Separation mechanism of enantiomers using chiral stationary phases (CSPs) was based on one of the following three principles: host-guest inclusion interactions with chiral selectors such as cyclodextrin (CD) derivatives, hydrogen bonding on analyte chiral center, and coordination on chiral metal complexes (Schurig 2002). Direct chiral separation can be achieved also in GC by using chiral capillary column, however, to the best of our knowledge no one has used this technique in synthetic cathinones chiral separation. Therefore, the focus of this dissertation will be on the direct enantioseparation of synthetic cathinones using HPLC with CSPs which has earned a lot of interest lately.

1.5.3.2.1 High performance liquid chromatography in cathinone chiral separation

In HPLC (LC), five groups of chiral stationary phases can be used to facilitate the chiral separation such as: cyclodextrins, proteins, cellulose/amylose, small molecules and macrocyclic glycopeptides. They can be either bonded to silica or used as an active selector in mobile phases. Formation of diastereomeric adsorbates leads to high selectivity of CSPs in chiral separation of targeted analyte (Herraez-Hernandez, Campıns-Falcó et al. 2002).

A simple UHPLC-PDA method using achiral column with added (2-Hydroxypropyl)-beta-cyclodextrin (HP-β-CD) in the mobile phase has been developed for the successful analysis of 24 designer phenethylamines and cathinone derivatives (Li and Lurie 2015). Taschwer et al. were able to provide a chiral separation of a set of 6 amphetamine and 25 cathinone derivatives through the use of HPLC-UV where sulfated β-cyclodextrin was used as an additive in mobile phase (TASCHWER, SEIDL et al. 2014).

CHIRALPAK AS-H™ Column is a chiral column that contains amylose as a CSP. It was used by Mohr et al. for enantioseparation of synthetic cathinones. It showed its ability to separate 19 out of 24 cathinone enantiomers in normal phase (Mohr, Taschwer et al. 2012). 1-(3,4-dimethoxyphenyl)-2-(ethylamino)pentan-1-one (DL-4662), one of the recently abused synthetic cathinone which was separated enantiomerically using amylose CSP (Weiss, Taschwer et al. 2015). Perera et al. were interested in developing chiral method for the separation of mephedrone and related cathinones using different kind of chiral columns on HPLC-UV system. They tried different CSPs while varying the composition of the mobile phase from reverse

to normal phase in order to build a persuasive comparison between the different kinds of CSP (Perera, Abraham et al. 2012). Padivitage et al. have developed a method that used cyclofructan based (LARIHC) and cyclobond I 2000 RSP in HPLC chiral analysis for a group of illicit drugs and cathinone was one of them. They were able to separate 14 out of 20 racemic compounds, with 7 compounds baseline resolved and 7 partially separated (Padivitage, Dodbiba et al. 2014). Zhang et al. have studied six CSPs with different structural features and their ability to perform separation of enantiomers for a group of drugs and one of them was cathinone. The immobilized chiral stationary phases were amylose based in 4 columns (CHIRALPAK IA, ID, IE and IF) and cellulose based in two columns (CHIRALPAK IB and IC). Furthermore, the study covered the effects of mobile phase composition, mobile phase additives and the effect of sample solvents on the chiral separation. They found that the best resolution and selectivity factors for cathinone enantiomers can be achieved by using CHIRALPAK IB column with hexane/ethanol/TFA/TEA 80/20/0.1/0.05 as a mobile phase (Zhang, Franco et al. 2012). Comparisons between four different CSPs column in normal (NPLC) and reverse phase (RPLC) of HPLC-UV system were carried out for seven synthetic cathinones by Albals et al. (Albals, Vander Heyden et al. 2016). The analysis were done by using 4 polysaccharide-based chiral stationary phases (CSPs): cellulose tris(3,5-dimethylphenylcarbamate) (ODRH), amylose tris(3,5-dimethylphenylcarbamate)(ADH), amylose tris(5-chloro-2-methylphenylcarbamate) (LA2), and cellulose tris(4-chloro-3-methylphenylcarbamate) (LC4). According to their findings, ADH and LC4 showed the highest success rate after applying them to each compound. However the comparison between normal and reverse phase

revealed that RPLC showed higher number of the separated compounds (Albals, Vander Heyden et al. 2015).

Recently, an impressive paper talking about using chiral ion-exchange type stationary phases to separate selected synthetic cathinones has been published (Wolrab, Frühauf et al. 2016). They used three different kind of CSP: chiral strong cation exchanger c-SCX (CSP 1), chiral zwitterion ion exchanger [Chiralpak ZWIX (+)] (CSP 2) and the new synthesized naphthalene-based chiral SCX (CSP 3). Based on the separation of cathinones, the chromatographic performance was compared for the three CSPs. They found that the best chromatographic performance was shown by CSP 1 which has the smallest selector unit. It was able to separate 14 compounds of the synthetic cathinones (Wolrab, Frühauf et al. 2016).

Although HPLC chiral methods show their stability and ability to perform chiral separation, the use of high amount of chiral selector in mobile phase and long analysis time in some methods obligate researchers to look for smart alternatives.

1.5.3.2.2 Capillary electrophoresis in cathinone chiral separation

Over the past decade, CE has been widely used as a chiral separation technique and can be considered as an alternative or complementary technique to HPLC in pharmacological science and industry. Variety of enantioseparation techniques that were successfully applied in HPLC have shifted to CE. In 1985 Gassmann, Kuo, and Zare were successful to perform chiral separation by CE for the first time (Gallo 1983). CE as a separation technique expressed a valued advantage such as greater efficiency, simplifies method development by the possibility of combining a large number of chiral selectors, consumption of small amounts of solvents and chiral selector, short analysis time, low total cost, and environment

saving. Impurities with poor chromophores will not be an issue in CE system, since the use of low-UV wavelength (e.g.,200 nm) will not permit impurities to be observed. It is known that CE is suitable for chargable compounds which facilitate the separation of polar compounds for which chromatographic methods were inadequate for separation (Li and Haynie 2006).

Recently, chiral analysis of synthetic cathinone derivatives became a popular topic and a hot area of CE method development. Several CE methods utilized cyclodextrin derivatives as a chiral selector in the buffer of the CE system (Mohr, Pilaj et al. 2012, Merola, Fu et al. 2014, Taschwer, Hofer et al. 2014, Taschwer, Weiß et al. 2014, Li and Lurie 2015, Moini and Rollman 2015). Most of the developed methods for chiral separation have used diode array detector (DAD) which were successfully applied for the detection of new designer cathinones. Few publications used tandem mass spectrometry (MS) as detector coupled with CE (Merola, Fu et al. 2014, Švidrnoch, Lněníčková et al. 2014, Moini and Rollman 2015) due to the very low signal that was usually observed. In order to overcome this issue, a sheathless CE interface has been used in order to allow coupling of ESI-MS with CE in a single dynamic process within the same device to analyze various derivatives of cathinone (Moini and Rollman 2015).

Enantiomeric separation into their optical diastereoisomers in CE is due to a set of interactions that occur between chiral selector in the buffer and analytes. As mentioned earlier, cyclodextrin derivatives are the most commonly used chiral selectors. Different kind of cyclodextrins have been used in chiral separation of synthetic cathinones such as: 2-hydroxypropyl-β-cyclodextrin (HP-β-CD)(Mohr, Pilaj et al. 2012, Li and Lurie 2015), native β-cyclodextrin (β-CD)(Mohr, Pilaj et al.

2012, Merola, Fu et al. 2014), highly sulfated- γ -cyclodextrin (HS- γ -CD)(Merola, Fu et al. 2014, Moini and Rollman 2015), highly sulfated-β-cyclodextrin (HS-β-CD)(Mohr, Pilaj et al. 2012, Taschwer, Weiß et al. 2014), carboxymethyl-β-CD(Mohr, Pilaj et al. 2012), native γ- cyclodextrin (γ-CD)(Mohr, Pilaj et al. 2012) and sulfobutylether β –cyclodextrin (SBE-CD)(Taschwer, Hofer et al. 2014). Mohr et al. have studied the separation ability and suitability for most of the cyclodextrin derivatives mentioned above (Mohr, Pilaj et al. 2012). They have chosen 3 out of 19 cathinones as a model to validate their method by studying the effect of different types of CDs, pH of buffer solution and the effect of CD concentration. According to their findings, HS-β-CD was the best chiral selector for synthetic cathinones chiral analysis in terms of separation resolution and selectivity factor(Mohr, Pilaj et al. 2012).

On the other hand, some researchers investigated the use of another chiral selectors in CE for cathinones enantioseparation such as amylose tris(5-chloro-2-methylphenylcarbamate) which can be considered as a polysaccharide-based chiral stationary phase and interestingly, it was the first time this kind of CSP was used in the analysis of cathinones by CE system (Aturki, Schmid et al. 2014). Experimental parameters such as mobile phase composition, organic modifiers, pH of mobile phase buffer, separation voltage and capillary temperature have been studied and optimized to obtain an efficient and rapid chiral CE method that were capable to separate the studied 10 cathinone derivatives by using amylose CSP (Aturki, Schmid et al. 2014).

1.5.4 Quantitative analysis of synthetic cathinones

In the forensic field, qualitative analysis of illicit drugs is important in order to provide the right identification of the abused drug composition. Moreover, lawyers need to know the dosage of illicit drugs in biological sample of the abusers which can be estimated by performing quantitative analysis for the targeted analytes.

Determination of bath salt designer drugs qualitatively and quantitatively is one persistent need which puts great responsibility on scientists. Recently, the number of publications that discussed synthetic cathinones quantitative analysis has grown up quickly, which reflects the high interest of researchers to study and analyze these kinds of stimulants and narcotics. In the previous section, a lot of work reported in the literature showed qualitative studies on the new designer drugs. It can be noticed easily that the number of developed methods for cathinones chiral analysis using capillary electrophoresis (CE) systems is higher than chromatographic methods. However, HPLC and GC were preferable for quantitative analysis of synthetic cathinones since they are one of the most separation techniques that used in many laboratories around the world.

Several quantitative methods have been developed in gas chromatography coupled with mass spectrometry (GC-MS) to analyze the biological samples that contain cathinones, some of them are shown in table 6.

Table 6: Analysis of synthetic cathinones in biological materials using GC–MS

Targets	Samples	Purification	Derivatization	LOD (ppb)	Linear range (ppb)	References
MDPV, metabolites	Urine	SPE	Methyl, acetyl, trimethylsilyl	-	-	(Meyer, Du et al. 2010)
MDPV, metabolites	Cellular fraction, Urine	LLE	Trimethylsilyl	2	10–2,000	(Strano-Rossi, Cadwallader et al. 2010)
Mephedrone, MDPV	Blood, urine	LLE	-	-	-	(Spiller, Ryan et al. 2011)
MDPV	Urine	LLE	Heptafluorobutyryl	10	20–2,000	(Ojanperä, Heikman et al. 2011)
Methylone	Blood	LLE	Heptafluorobutyryl	50	100–2,000	(Pearson, Hargraves et al. 2012)
α-PVP, pyrovalerone (PV), MDPV	Blood	SPME	-	0.5 (PV, PVP), 1.0 (MDPV)	1–200	(Saito, Namera et al. 2013)
MDPV, α -PVP, α –PBP	Blood	LLE	-	1	2–2,000	(Namera, Urabe et al. 2013)
MDPV	Blood, tissue, urine	SPE	-	-	10–2,000	(Wyman, Lavins et al. 2013)
MDPV	Blood, urine	LLE	-	-	-	(Wright, Cline-Parhamovich et al. 2013)
3,4-DMMC, metabolites	Urine	LLE	Trifluoroacetyl	-	-	(Shima, Katagi et al. 2013)
16 Synthetic cathinones	Urine	LLE	Trifluoroacetyl	-	-	(Uralets, Rana et al. 2014)
a-PVP, metabolites	Urine	LLE	Trimethylsilyl	-	-	(Shima, Katagi et al. 2014)

Table 7 shows a set of methods used for quantitation of cathinone related drugs in urine, blood, hair and other biological samples by high performance liquid chromatography coupled with mass spectrometry (HPLC-MS).

Table 7: Analysis of synthetic cathinones in biological materials using HPLC–MS

Targets	Samples	Purification	LOD (ppb)	Linear range (ppb)	References
MDPV, metabolites	Urine	SPE	-	-	(Meyer, Du et al. 2010)
MDPV, metabolites	Cellular fraction, urine	LLE	-	-	(Strano- Rossi, Cadwallader et al. 2010)
MDPV	Serum	SPE	3	10–500	(Kriikku, Wilhelm et al. 2011)
Mephedrone	Plasma	LLE	39	78–10,000	(Maskell, De Paoli et al. 2011)
9 Cathinones	Blood	PP	0.5–3	10–400	(Sørensen 2011)
7 Cathinones	Hair	LLE	10–50 pg/mg	-	(Rust, Baumgartner et al. 2012)
Butylone	Blood, liver	SPE	25 (blood)	50–2,000 (blood)	(Rojek, Kłys et al. 2012)
4-MEC	Blood, urine	LLE	0.96 (blood), 0.68 (urine)	10–1,000	(Gil, Adamowicz et al. 2013)
MDPV, α-PVP, α-PBP	Hair	LLE	0.02 ng/10-mm	0.05–50 ng/ 10-mm	(Namera, Urabe et al. 2013)
Mephedrone	Blood	PP	0.08	1–100	(Adamowicz, Tokarczyk et al. 2013)
MDPV, mephedrone	Blood, plasma, urine	SPE	2	5–2,000	(Johnson and Botch-Jones 2013)
Mephedrone	Blood, urine	LLE	1 (blood), 2 (urine)	20–2,000	(Cosbey, Peters et al. 2013)
10 Cathinones	Blood, other specimens	LLE	-	5–200	(Marinetti and Antonides 2013)

Targets	Samples	Purification	LOD (ppb)	Linear range (ppb)	References
MDPV	Hair	SPE	2.0 pg/mg	2–3,000 pg/mg	(Wyman, Lavins et al. 2013)
MDPV	Blood	PP	0.5	5–500	(Adamowicz, Gil et al. 2013)
Buphedrone	Blood	PP	0.3	1–1,000	(Zuba, Adamowicz et al. 2013)
3,4-DMMC, metabolites	Urine	PP	-	10–5,000	(Shima, Katagi et al. 2013)
MDPV, metabolites	Plasma	PP	0.1	0.25–1,000	(Anizan, Ellefsen et al. 2014)
α-PBP	Blood, urine, tissues	QuEChERS	0.05 (blood, urine), 0.1 (tissues)	8.6–4,280	(Wurita, Hasegawa et al. 2014)
Targets	Samples	Purification	LOD (ppb)	Linear range (ppb)	References
3,4-DMMC, metabolites	Blood, urine	QuEChERS	1.03 (blood), 1.37 (urine)	5–400	(Usui, Aramaki et al. 2014)
MDPV metabolittes	Urine	PP, LLE, SPE	-	-	(Bertol, Mari et al. 2014)
α-PVP, metabolites	Urine	PP	-	10–10,000	(Shima, Katagi et al. 2014)
PV9	Blood, urine	QuEChERS	0.05	10–1,000	(Hasegawa, Wurita et al. 2014)

Capillary electrophoresis (CE) has also been used for quantitative analysis of cathinones, but less than chromatographic techniques. A total of 12 cathinone analogs were separated optically and quantified as a racemic mixture of pure sample by Gustavo et al. using CE coupled with TOF-MS and UV. Only 18 minutes were enough to separate all analytes, where ten compounds were chiraly separated using β-CD in the CE-UV mode in addition to two additional cathinones which separated using HS-γ-CD in the MS mode. Limit of detection was found to be 1.0 ng/mL.

Samples of seized drugs were used as an application of the developed method (Merola, Fu et al. 2014). Micellar electrokinetic chromatography (MEKC) is a modified separation technique from CE and utilized for synthetic cathinones separation. Martin et al. used MEKC with tandem mass spectrometry to develop a method for selective separation, identification and determination of 12 synthetic cathinones in urine sample. Linearity in the concentration range of 10–5000 ppb was achieved by the developed method and detection limits were in the range of 10–78 ppb (Švidrnoch, Lněníčková et al. 2014). They were able to validate their developed method and analyze a spiked urine sample using a MEKC-MS-MS system.

Most of the synthetic cathinones are sold as a mixture of the optical enantiomers with one of the mixed enantiomers showing a stronger central nervous system (CNS) stimulatory activity than the other (Mohr, Taschwer et al. 2012). Field of cathinones chiral separation is growing up rapidly in parallel with the quantitative analysis of cathinones as a racemic mixture and strangely, to the best of our knowledge there is no study focusing on the quantitation of each enantiomer of cathinone derivatives. “Chiral quantitation” for synthetic cathinones will be carried out for the first time in this thesis by using chromatographic techniques. Schemes 6 - 10 show the structures of the studied synthetic cathinones in this thesis.

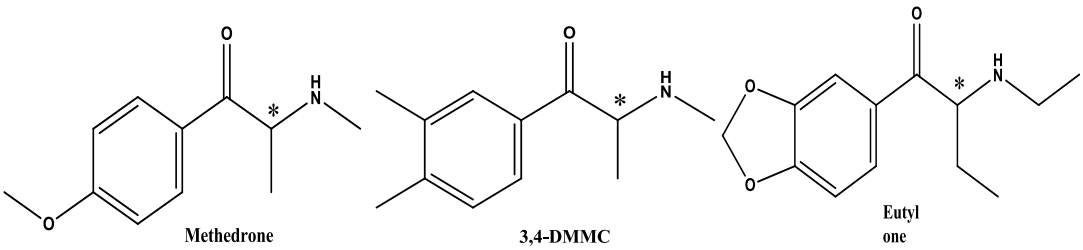

Scheme 6: Synthetic cathinones group 1

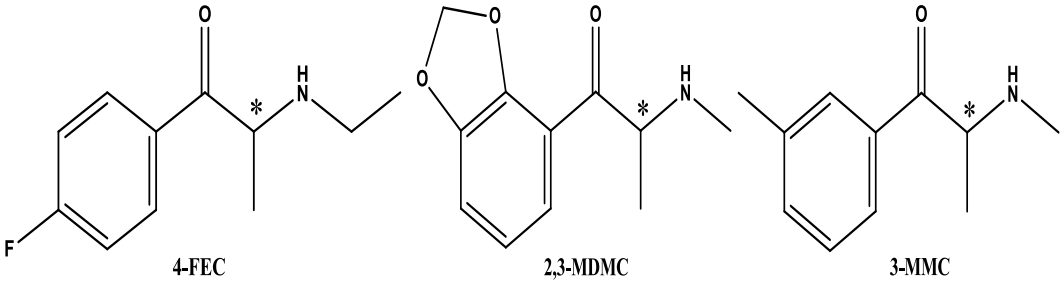

4-FEC 2,3-MDMC 3-MMC

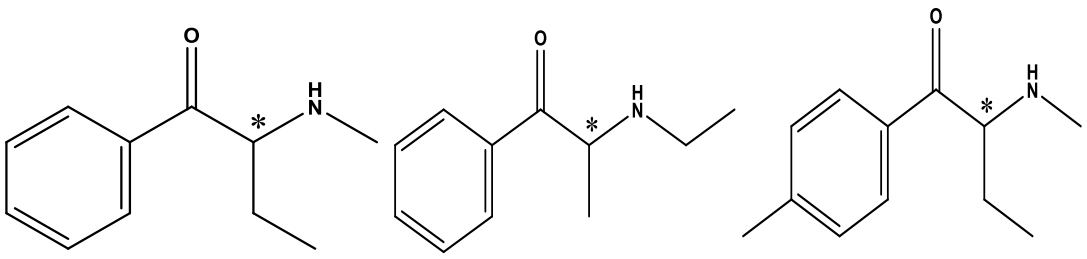

Buphedrone Ethcathinone 4-Methylbuphedrone

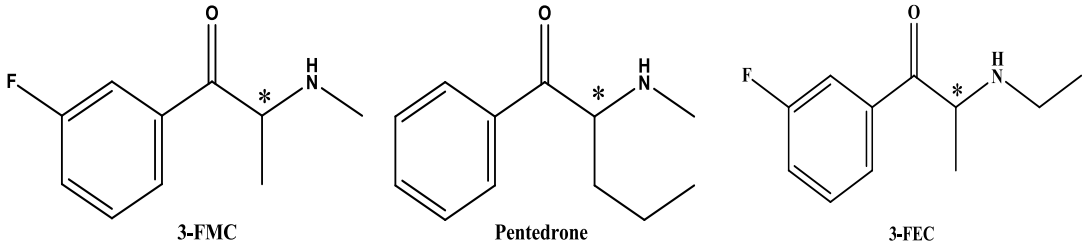

3-FMC Pentedrone 3-FEC

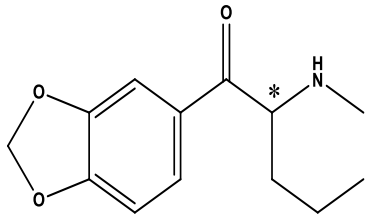

Pentylone

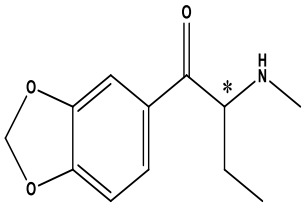

Butylone

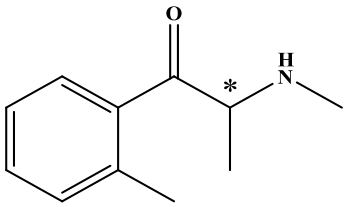

2-MeOMC

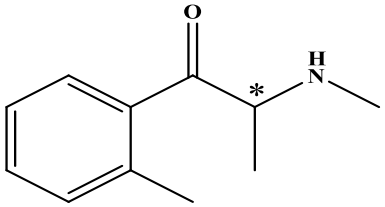

2-MMC

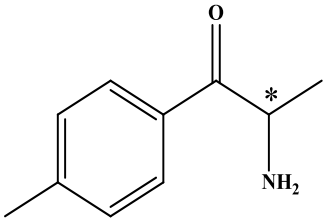

Nor-mephedrone

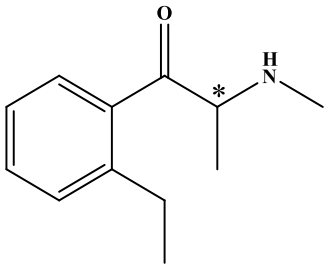

2-EMC

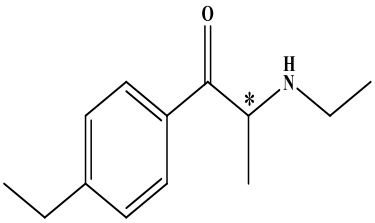

4-EEC

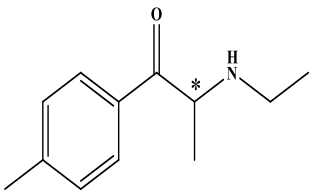

4-MEC

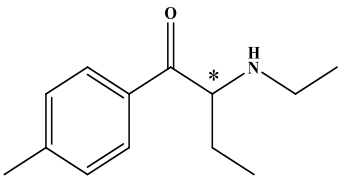

4-Methyl-a-ethylaminobutiophenone

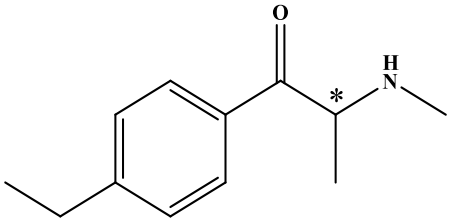

4-EMC

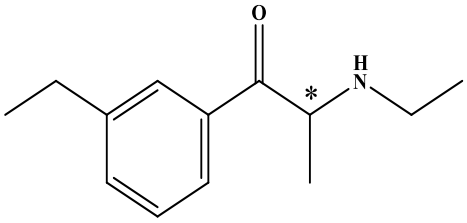

3-EEC

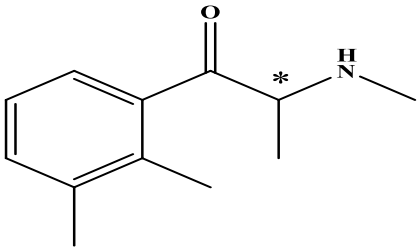

2,3-DMMC

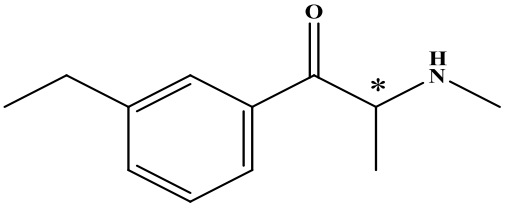

3-EMC

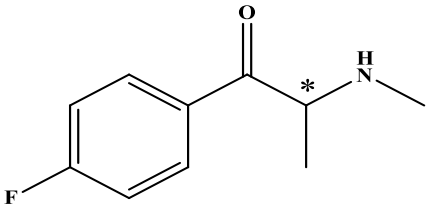

4-FMC

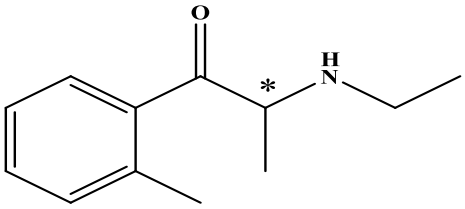

2-MEC

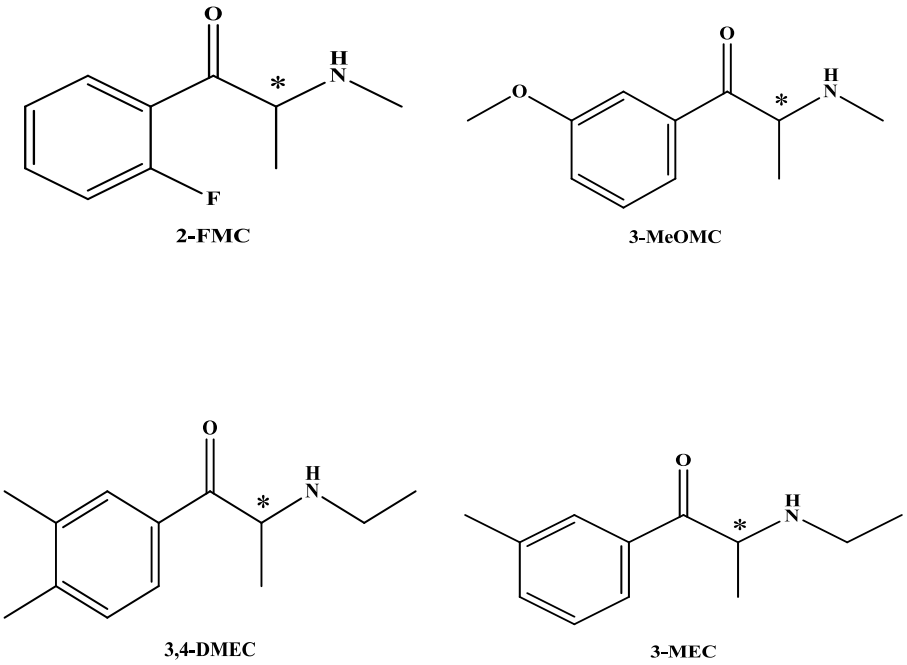

Scheme 7: Synthetic cathinones group 2

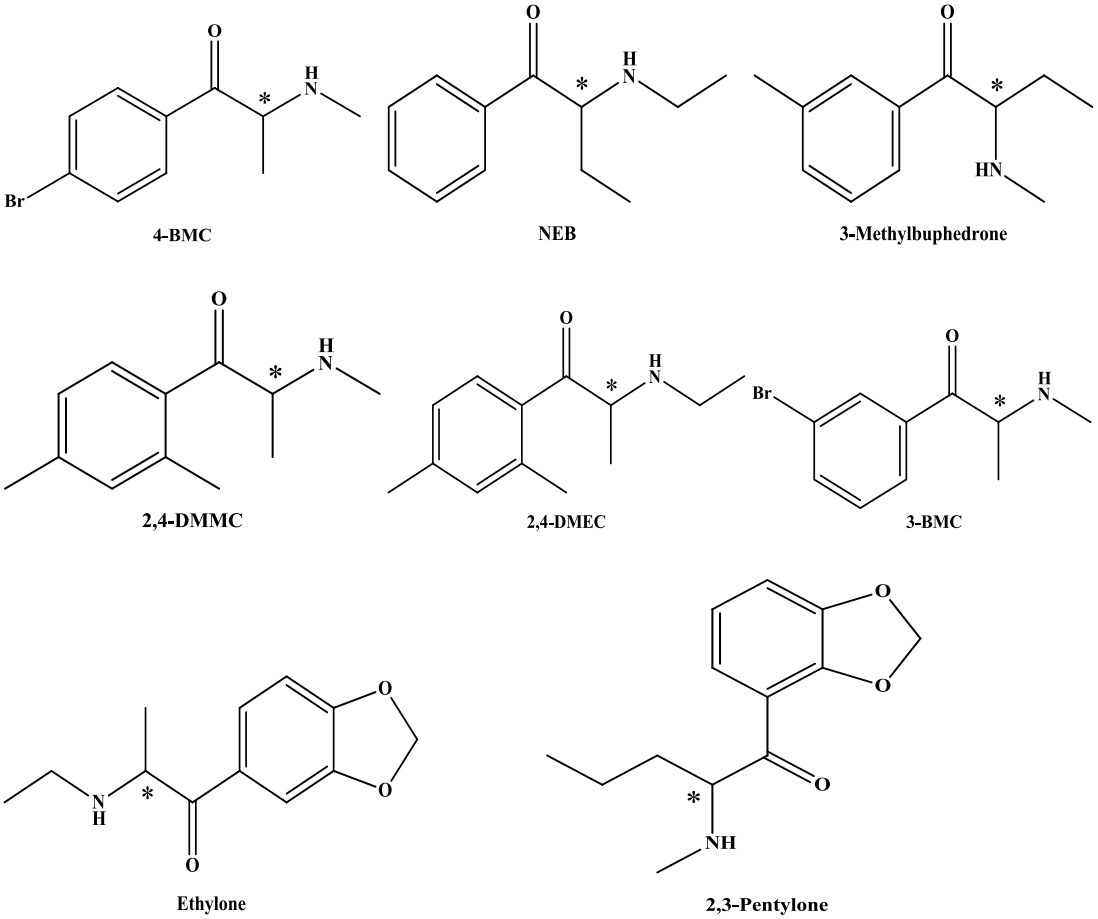

Scheme 8: Synthetic cathinones group 3

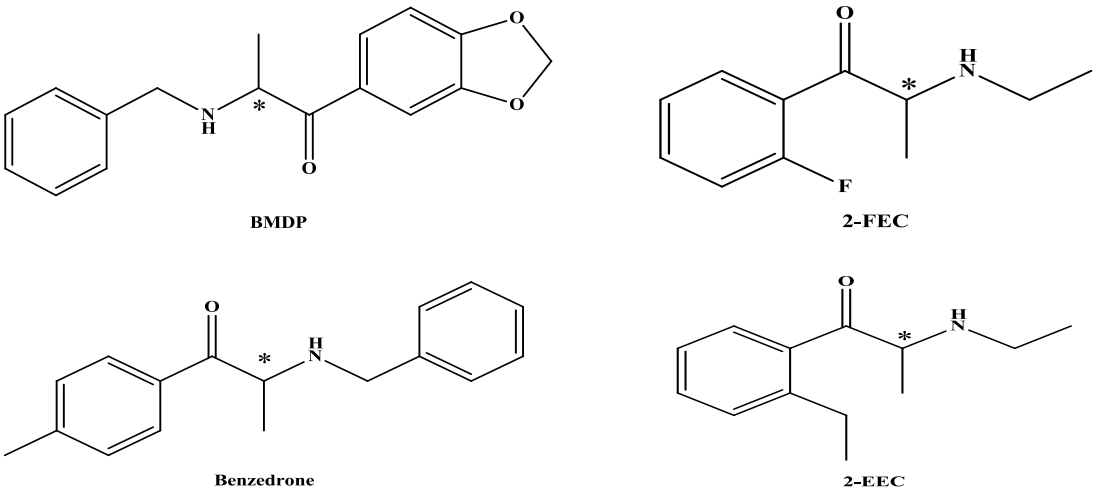

Scheme 9: Synthetic cathinones group 4

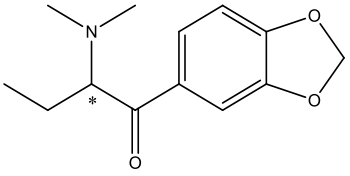

Dibutylone

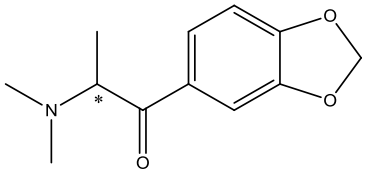

Dimethylone

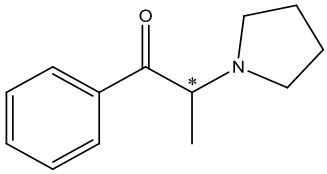

a-PPP

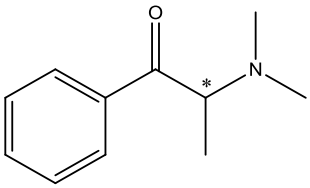

N,N-DMC

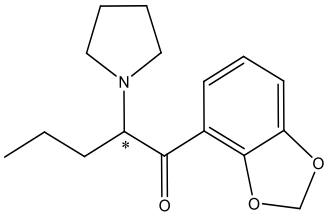

2,3-MDPV

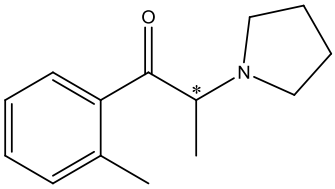

2-methyl-a-PPP

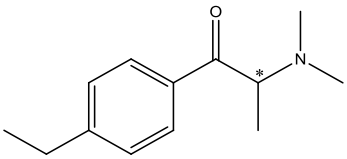

4-ethyl-N,N-DMC

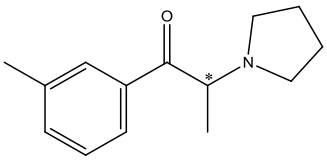

3-methyl-a-PPP

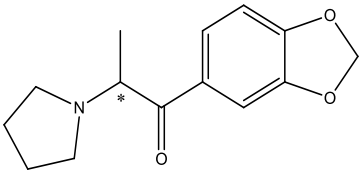

3,4-MD-a-PPP

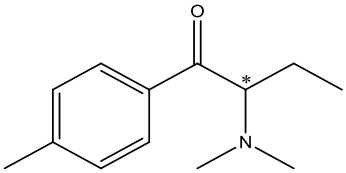

4-methyl-N-methylbuphedrone

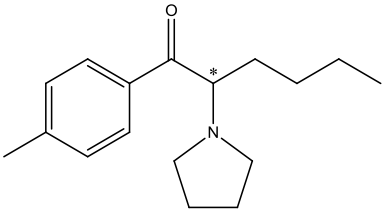

4'-methyl-a-PHP

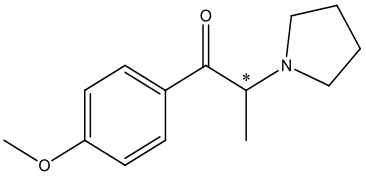

4'-MeO-a-PPP

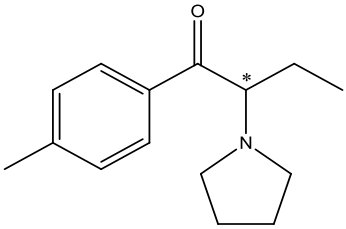

4-methyl PBP

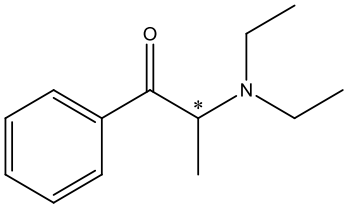

Diethylcathinone

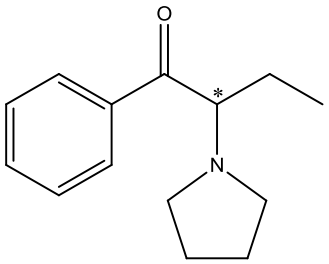

a-PBP

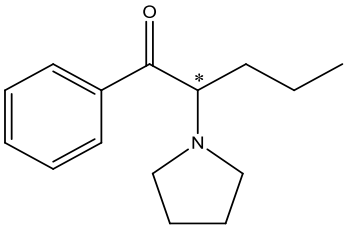

a-PVP

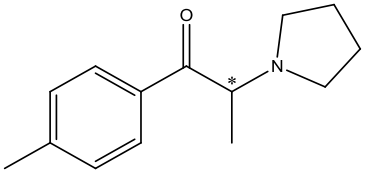

4'-methyl-a-PPP

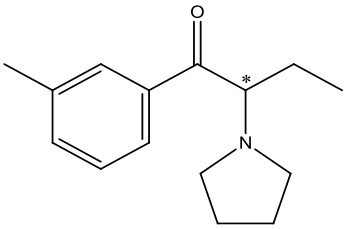

3-methyl PBP

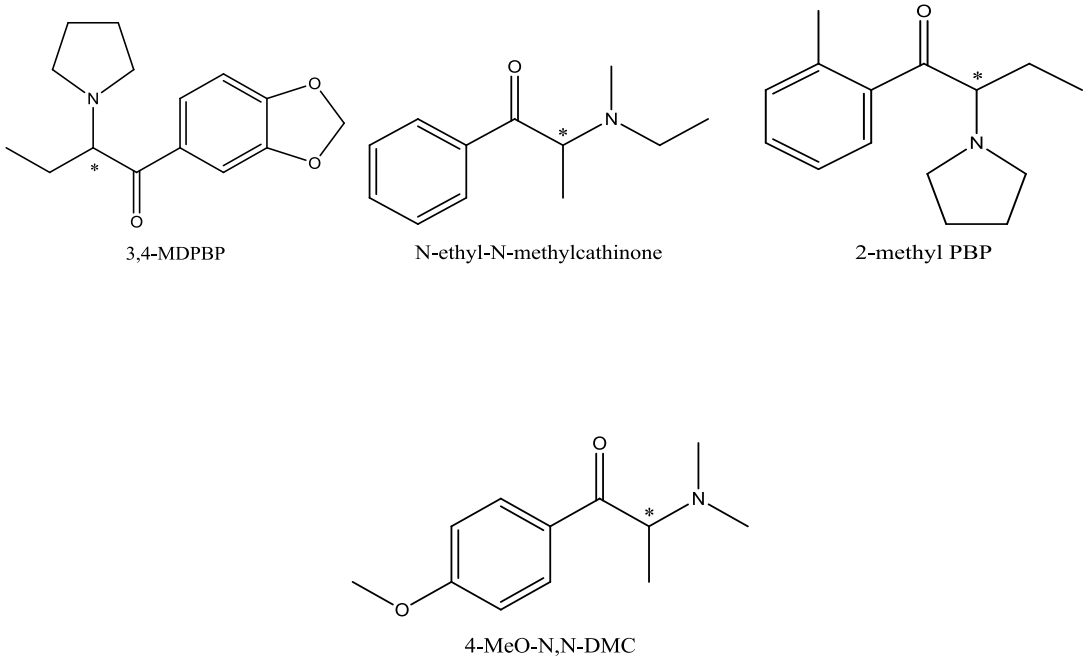

Scheme 10: Synthetic cathinones group 5

The work represented in this dissertation describes research into the development of methodology for the analysis of synthetic cathinones using gas chromatography mass spectrometry and liquid chromatography coupled to UV-Vis and fluorescence detections. Chapter 2 describes the GCMS analysis using electron ionization of thirty one synthetic cathinones after derivatization with chiral agent, L-TPC. Quantitative analysis of twelve synthetic cathinones in plasma and urine samples was conducted and the method was validated.

Chapter 3 describes the GC-MS analysis using negative chemical ionization of thirty-seven synthetic cathinoines who were converted into their diastereoisomers after a reaction with L-TPC chiral reagent. Quantitative analysis of fourteen racemic mixtures of these synthetic cathinones in urine and plasma was conducted as well as method validation.

Chapter 4 describes the HPLC-UV analysis of 65 synthetic cathinones using chiral HPLC column. Two chiral columns were examined to separate synthetic cathinones that have tertiary amine functional group in their structure. Around twenty of these compounds were successfully separated into their enantiomers on Astec Cellulose DMP chiral column and their separation is reported for the first time. Moreover, quantitative analysis of a mixture of three compounds was reported.

Chapter 5 describes the study of the inclusion reaction between cyclodextrins as a host molecule and synthetic cathinones as a guest molecule; however, these kinds of experiments may need a large amount of the synthetic cathinones which is considered as an expensive and hard to get chemical. Therefore an alternative compound, para aminohipparic acid (PAH) has been chosen in this study as a simulant due to the similarity in chemical structure of this compound to cathinone

derivatives. A sensitive method was developed using two techniques, namely spectrofluorometry and liquid chromatography with fluorescence detection. Fluorescence signals were enhanced with the addition of β-CD in aqueous solutions. The experimental conditions that gave the best results were investigated in terms of cyclodextrin cavity size, concentration of PAH, concentration of cyclodextin, and pH effects. The interaction between PAH and cyclodextrin was investigated and considered as a host – guest inclusion which was evident by mass spectrometry and DFT calculations and found to be with 1:2 (host-guest) stoichiometry. A calibration curve was established from the spectrofluorometric data in the concentration range 0.05 -100 μM and the detection limit was determined to be 0.015 μM. HPLC with fluorescence detection was investigated in the presence of β-CD in the mobile phase, during which the effect of concentration of β-CD in the mobile phase was also monitored.

Finally, Chapter 6 describes the conclusion of the research work in this dissertation and future research recommendations.

1.6 Objectives of the study

- To perform chiral separation and quantitation of primary and secondary amine of synthetic cathinone derivatives on GC-EI-MS after derivatization reaction with chiral derivatizing agent called L-TPC.
- To develop a sensitive and selective validated method for chiral quantitation of synthetic cathinones through a new GC-NCI-MS method and resolution enhancement by using slow heating rate in GC oven and the use of Ultra inert column.
- To develope and validate a sensitive and selective method for detection and quantitation of the enantiomers of tertiary amine synthetic cathinone compounds using HPLC-UV/VIS with two different chiral columns in order to perform chiral separation for the targeted racemic mixtures.

Chapter 2: A validated gas chromatography mass spectrometry method for simultaneous determination of cathinone related drugs enantiomers in urine and plasma

2.1 Introduction

In 1980, Khat was classified by the World Health Organization as a drug of abuse that can produce mild to moderate psychological dependence (Feyissa and Kelly 2008). It contains amphetamine-like stimulant alkaloids namely, cathinone and cathine (German, Fleckenstein et al. 2014), (see scheme 2 for the cathinone structure). In recent years, New Designer Drugs (NDDs) have been developed as derivatives of prohibited substances in clandestine laboratories and find their way to the illegal market. Different disguised names of these designer drugs have been marketed as “plant-growth fertilizers”, “bath-salts” and “spices” to sell them illegally on the black market (Boulanger-Gobeil, St-Onge et al. 2012, Wolrab, Frühauf et al. 2016).

All of the cathinone and amphetamine like drugs possess a chiral center which means that they can exist as a racemic mixture of enantiomers that have different potency rate in biological system as mentioned in chapter one. Unfortunately, drug dealers may distribute their substances as pure R or S-enantiomers, which can increase the risk of overdose and prove lethal (Mohr, Pilaj et al. 2012). Recently, L-TPC has been used for chiral separation of cathinone related drugs on GC-MS (Mohr, Weiß et al. 2012, Weiss, Mohr et al. 2015).

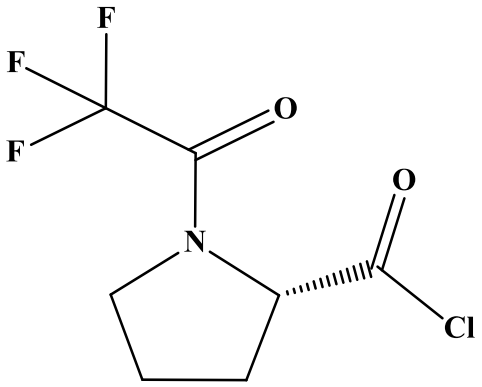

Scheme 11: Structure of (S)-(–)-N- (trifluoroacetyl)pyrrolidine-2-carbonyl chloride (L-TPC)

In this work, a GC-MS method, using electron ionization and selected ion monitoring (SIM) mode, has been developed to analyze 31 cathinone related compounds as diastereoisomers. Moreover, 18 of these compounds have been separated into their enantiomers for the first time. Quantitative analysis of spiked urine and plasma has been conducted simultaneously for a mixture of 12 cathinone related drugs; Scheme 12 shows the chemical structure of the 12 compounds. The method validation has been performed in spiked plasma and urine samples.

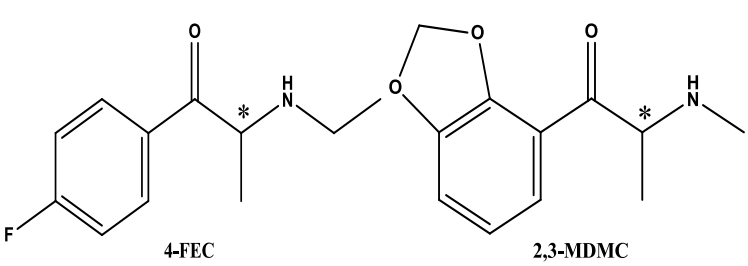

4-FEC 2,3-MDMC 3-MMC

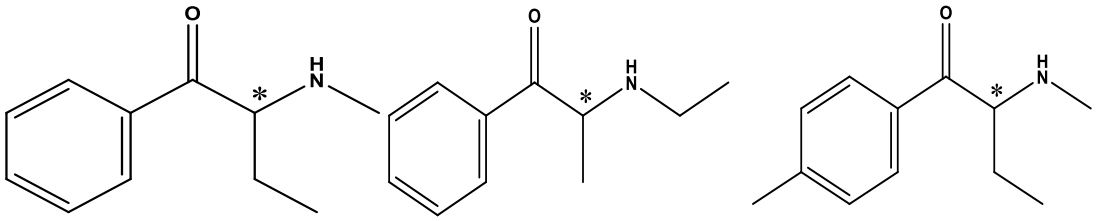

Buphedrone Ethcathinone 4-Methylbuphedrone

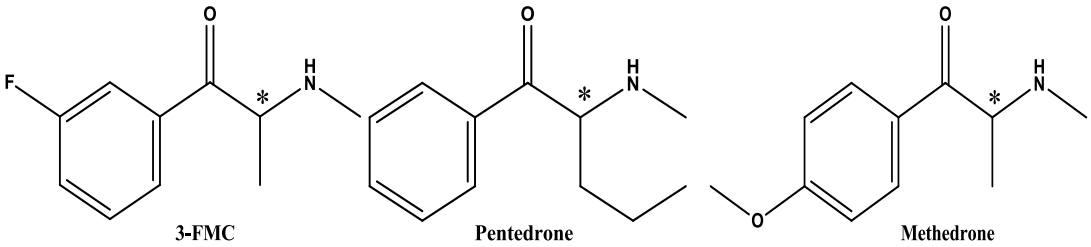

3-FMC Pentedrone Methedrone

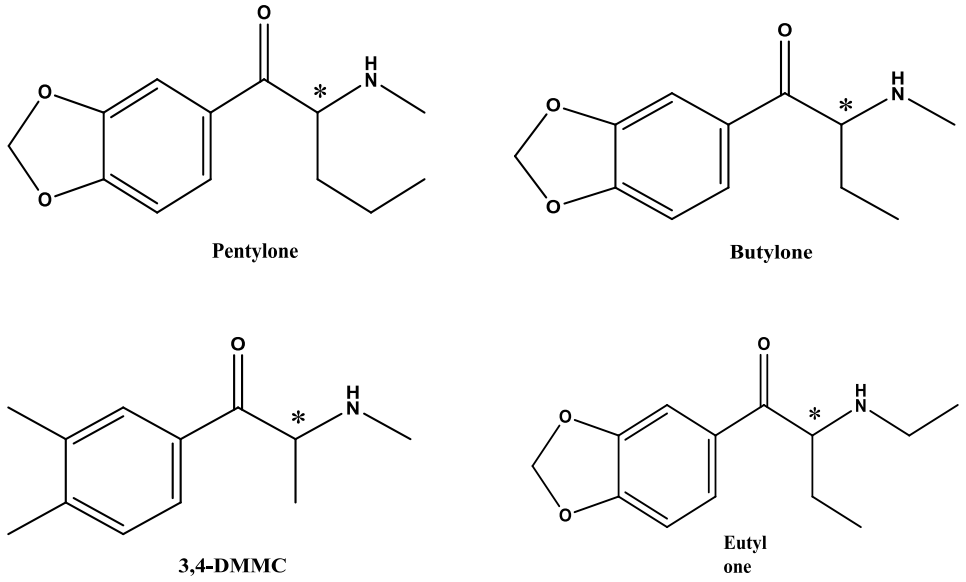

Scheme 12: Structures of synthetic cathinones that were analyzed quantitatively

2.2 Experimental

2.2.1 Chromatographic conditions

Chromatographic separation was performed on an Agilent (Waldbronn, Germany) HP 6890 GC coupled to an Agilent (Waldbronn, Germany) HP 5973 mass selective detector. A commercially available 60 m capillary column consisting of (5%-Phenyl)-methylpolysiloxane, with 0.25 mm inner diameter and a 0.25 µm film thickness was used as stationary phase. Helium was used as carrier gas at a constant flow rate of 1.2 mL/min. Injection of 2 µL of sample solution was performed automatically with a split ratio of 21:1. The injector and GC–MS interface temperature were set at 250 and 280 º C, respectively. Data collection was performed in Selected Ion Monitoring (SIM) mode with the following selected fragments: 58, 106, 166 and 251, and starting 10 min after injection (i.e., filament delay). The column temperature program was as follows: starting at 160 º C and hold for 5 min, followed by heating to 250 º C with a heating rate of 5ºC/min. The final temperature was held at 250ºC for 22 min.

2.2.2 Chemicals and reagents

All chemicals were of analytical grade. Ethylacetate, acetic acid, methanol, 2-propanol, ammonium hydroxide, dichloromethane ,0.1 M solution of (S)-(−)-N-(trifluoroacetyl)pyrrolidine-2-carbonyl chloride (L-TPC) with an enantiomer excess (ee) of 97% (according to supplier's specification) in dichloromethane, anhydrous sodium sulfate, sodium phosphate and nikethamide were obtained from Sigma–Aldrich Chemicals (St. Louis, MO, USA). Potassium carbonate was obtained from VWR (Darmstadt, Germany). Doubly deionized water was obtained from ultra-pure

Millipore system (MS, USA). All chemicals shown in Table 8 were purchased from Cayman chemicals (Michigan, USA). The cathinone related drugs were supplied as racoimic mixtures of R and S enantiomers.

2.2.3 Sample preparation

2.2.3.1 Samples

This investigation conforms to the UAE community guidelines for the use of humans in experiments. The Human Ethics committee at the Dubai police approved this study. Blood and urine samples were collected by Dubai police with the consent of the subjects.

2.2.3.2 Urine and plasma spiking and solid phase extraction

Solid phase extraction (SPE) was carried out using "Zymark rapid trace" SPE workstation (Artisan Technology Group, IL, USA) and the column was 200MG clean screen CSDAU203 from FluoroChem, (Hadfield, UK). Urine samples were diluted in 1:1 ratio with doubly deionized water. 3 mL of diluted urine was spiked with certain concentration of cathinones derivative and 50 ppm of internal standard (IS) (nikethamide) in addition to 1 mL of 0.1M phosphate buffer (pH 6.0). For plasma samples spiking, 1 mL of plasma was spiked with certain concentration of cathinone derivative, and 50 ppm of IS in addition to 3 mL of 0.1M phosphate buffer (pH 6.0). Samples were shaken well for 30 s. For SPE cartridge conditioning, 3 mL of methanol and the same volume of deionized water were used with 1 mL of 0.1 M phosphate buffer. After that the spiked urine or plasma sample was loaded to the cartridge and later on the cartridge was sequentially washed with 3 mL of methanol, 3 mL of deionized water and 1 mL 0.1M acetic acid. The column was left for 5 min

drying. Finally, 3 mL of the eluate, which is made of a mixture of dichloromethane, isopropanol and ammonium hydroxide with a relative ratio of (78:20:2), was collected and evaporated to dryness under nitrogen gas stream.

2.2.3.3 Derivatization step

For pure sample and spiked sample analysis, an evaporation step was needed before derivatization reaction can take place. After evaporation was done, 100 µL of deionized water was transferred into a glass test tube together with 125 µL of a saturated aqueous solution of potassium carbonate, 1.5 mL of ethylacetate and 12.5 µL of L-TPC. For the analysis of spiked urine and plasma samples, 50 µL of L-TPC was used. The mixture was covered and stirred for 10 min at room temperature. Afterwards, the upper layer was transferred to a new test tube and dried over anhydrous sodium sulfate. The dried solution was evaporated under a soft nitrogen stream to ensure that it is free from water. The remaining L-TPC-derivative was reconstituted in certain amount of ethylacetate – depending on concentration, e.g. a volume of 0.1 mL and 1.0 mL were used to obtain final concentration of 100 ppm and 10 ppm, respectively, prior to injection in GC–MS instrument.

2.3 Results

The basic idea of developing the analytical method for cathinone related drugs was to convert the two enantiomers of each one of these analytes into two diastereomers after reaction with pure chiral derivatization reagent, L-TPC (Scheme 13).

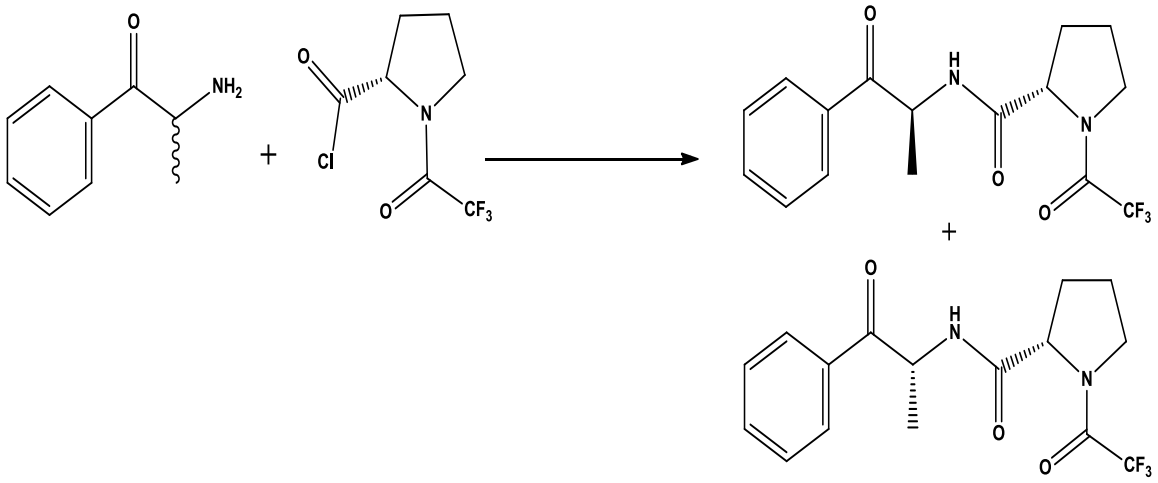

Scheme 13: Derivatization reaction between Cathinone and L-TPC

The resulting diastereomers can be separated due to their different chemical and physical properties on a common stationary phase column. The derivatization reagent, L-TPC, reacts with analytes that have primary or secondary amine group in the presence of sodium carbonate that causes the amidation between the acid chloride and the amine group. Figure 1 shows the gas chromatogram for separation of R and S enantiomers of methedrone drug after derivatization with L-TPC in the presence of nikethamide as an internal standard.

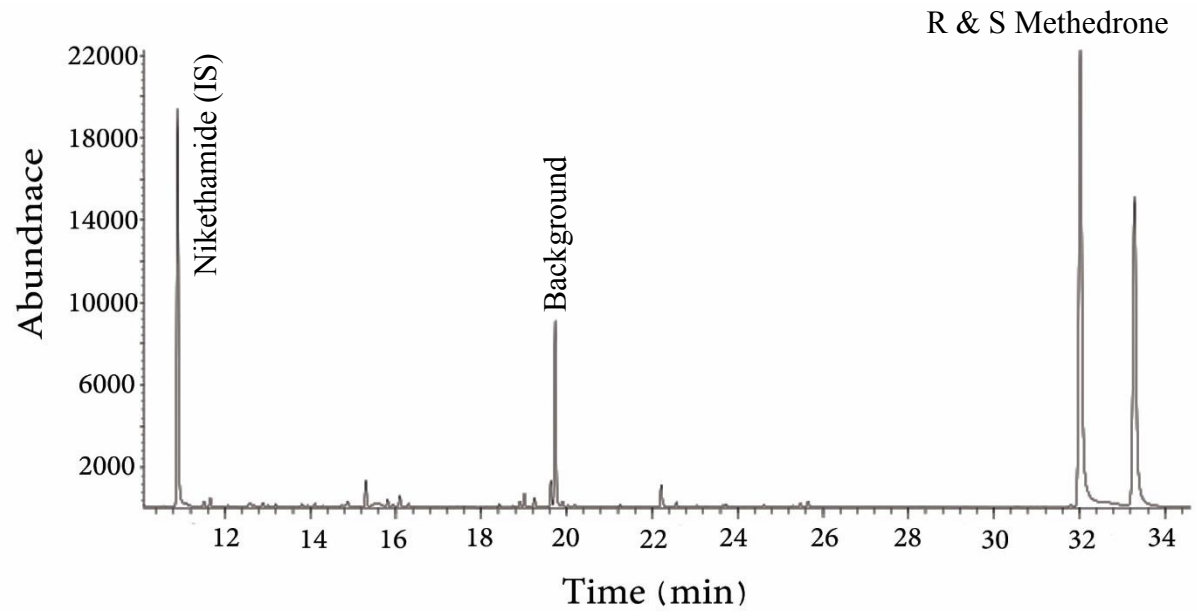

Figure 1: Gas chromatogram for separation of the Rand S enantiomers of methedrone drug in methanol after derivatization with L-TPC in the presence of nikethamide internal standard

Moreover, Table 8 shows the retention time of the separated enantiomers for the 31 cathinone related compounds. All the tested compounds contain at least one primary or secondary amine in their chemical structures. Each one of these compounds was prepared in methanol and was analyzed individually on GC-MS using SIM mode, after going through the derivatization step. Among the 31 compounds under study, twelve of these cathinone related compounds were tested in plasma and urine matrices. They were selected based on significant differences in the retention times of the two isomers as reported in Table 8.

Table 8: List of the 31 cathinone related compounds and their synonyms, in addition to the retention times of the separated two diasterioisomers for each compound analyzed on GC-MS using SIM mode

	Name	Abbreviation	Time (min)		Resolution	Selectivity Factor (α)
			t_{R1}	t_{R2}		
1	4-Methylbuphedrone	-	28.7	29.22	4.72	1.026
2	Pentylone	-	41.81	42.41	2.69	1.018
3	Methedrone	-	32.09	33.36	8.92	1.055
4	4-Methyl-α-ethylaminobutiophenone	-	29.2	29.62	3.24	1.021
5	Nor-mephedrone	-	26.15	27.5	14.89	1.079
6	Pentedrone	-	27.76	27.86	1.04	1.005
7	Ethcathinone	-	25.85	26.23	3.65	1.023
8	Butylone	-	38.6	39.59	5.22	1.033
9	Buphedrone	-	26.37	26.48	1.19	1.006
10	2-Methoxymethcathinone	2-MeOMC	28.73	29.41	5.81	1.034
11	4-Fluoromethcathinone	4-FMC	24.47	24.64	2.13	1.011
12	2-Methylethcathinone	2-MEC	27.08	27.82	5.08	1.041
13	2-Fluoromethcathinone	2-FMC	24.66	25.21	4.11	1.035
14	2-Ethylmethcathinone	2-EMC	27.78	28.47	5.39	1.037
15	2,3-Dimethylmethcathinone	2,3-DMMC	29.3	30.32	7.92	1.050
16	4-Fluoroethcathinone	4-FEC	25.05	25.28	2.45	1.014
17	4-Ethylmethcathinone	4-EMC	29.82	30.75	7.47	1.045
18	4-Ethylethcathinone	4-EEC	30.68	31.59	6.80	1.042
19	3-Methylmethcathinone	3-MMC	27.02	27.41	3.90	1.022
20	3-Methylethcathinone	3-MEC	27.69	28.13	3.71	1.024
21	3-Fluoromethcathinone	3-FMC	24.55	24.66	1.34	1.007
22	3-Ethylmethcathinone	3-EMC	28.98	29.4	3.67	1.021
23	3-Ethylethcathinone	3-EEC	29.7	30.17	3.91	1.023
24	3,4-Dimethylmethcathinone	3,4-DMMC	30.6	31.54	8.04	1.044
25	2-Methylmethcathinone	2-MMC	26.35	26.93	4.47	1.033
26	4-Methylethcathinone	4-MEC	28.1	28.87	6.73	1.040
27	3,4-Dimethylethcathinone	3,4-DMEC	31.42	32.34	7.39	1.041
28	3-Fluoroethcathinone	3-FEC	25.2	25.34	1.42	1.009
29	2,3-Methelendioxymethcathinone	2,3-MDMC	33.85	35.15	8.07	1.052
30	3-Methoxymethcathinone	3-MeOMC	30.45	30.71	2.01	1.012
31	Eutylone	-	39.46	40.11	3.47	1.021

Figure 2 shows the GC total ion chromatogram of these compounds after being spiked in urine. It was possible to see a good separation of the mixture components with good peak resolution for most of them.

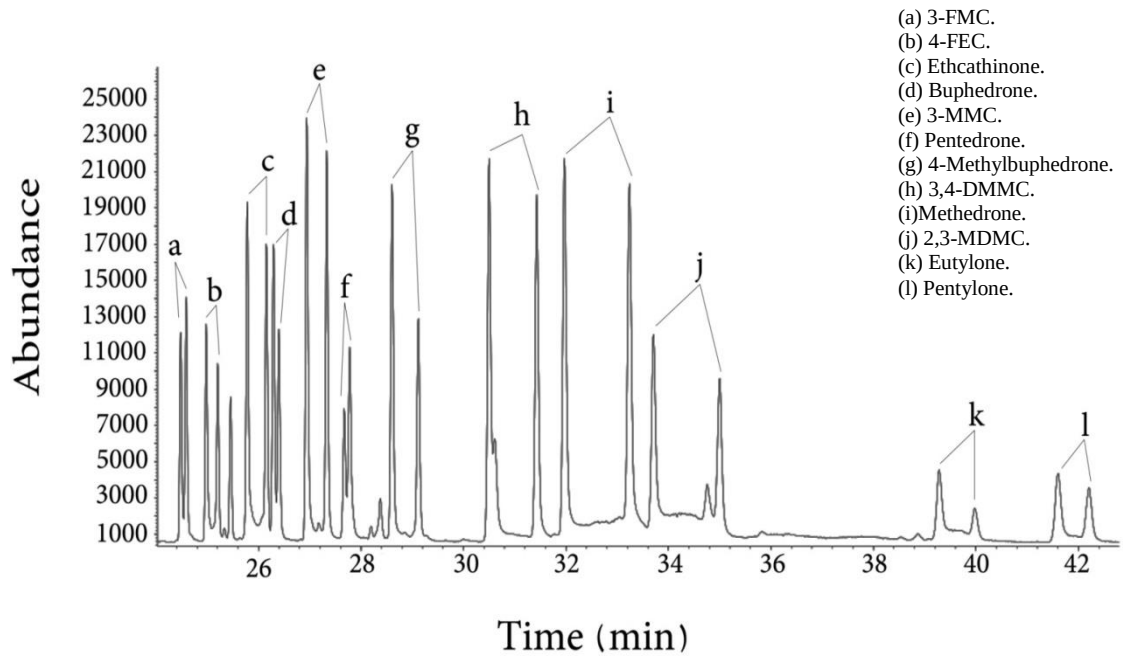

Figure 2: Total ion chromatogram (TIC) of the simultaneous chiral separation of 12 cathinones related compounds. All compounds were spiked in urine and separated as L-TPC derivatives

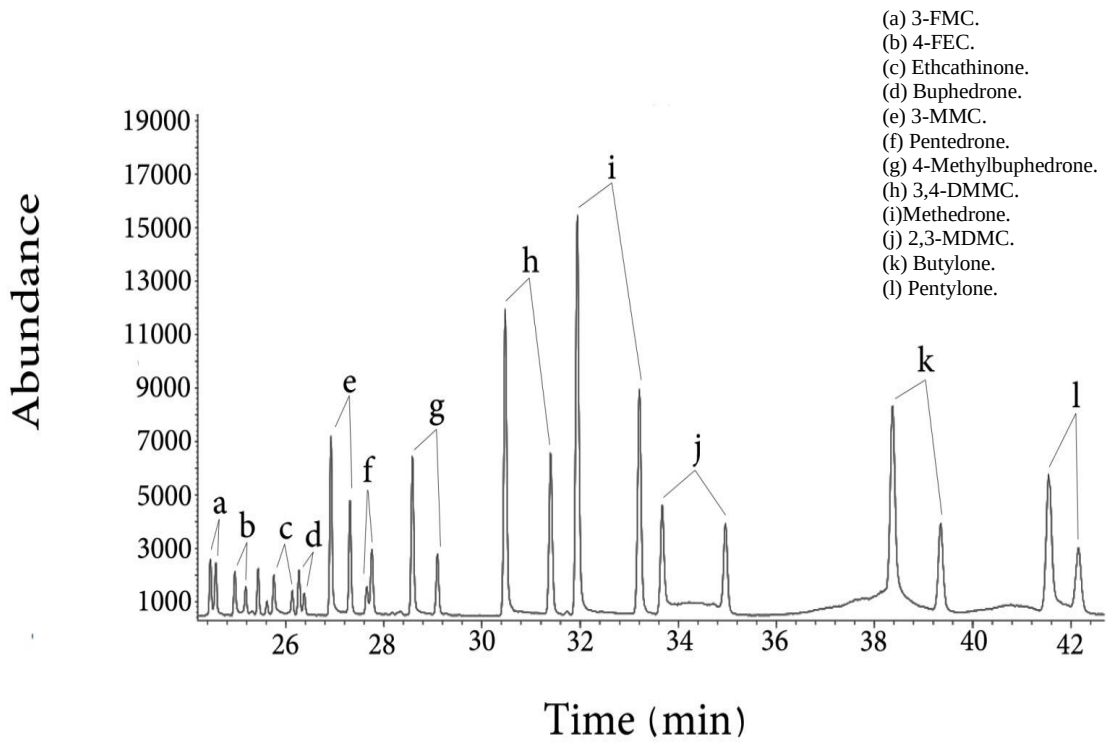

Figure 3: Total ion chromatogram (TIC) of the simultaneous chiral separation of 12 cathinones related compounds. All compounds were spiked in plasma and separated as L-TPC derivatives

Figure 3 shows the total ion chromatogram of the same twelve cathinone related compounds spiked in plasma. It was observed that the enantiomers were separated nicely with good peak resolution since R_s had a value higher than 1.5 for most of the separated compounds. To the best of our knowledge, this is the first example in the literature that demonstrates the separation of 12 pairs of cathinone enantiomers in a single analysis and in complex matrices such as urine and plasma.

Method validation was performed on these 12 tested compounds spiked in urine and plasma. The calibration curve linearity, limit of detection (LOD), limit of quantitation (LOQ), spike recovery in addition to inter-day and intra-day reproducibility were collected and are summarized in Tables 9-14.

The calibration graphs for the 12 enantiomer pairs of cathinone derivatives were established and found to be linear within the tested range of 10 to 200 μg/mL in urine and in plasma with mean regression coefficients (R^2; n = 3) of 0.99 or higher. Figure 4 shows the calibration graph of the two methedrone enantiomers in plasma and urine.

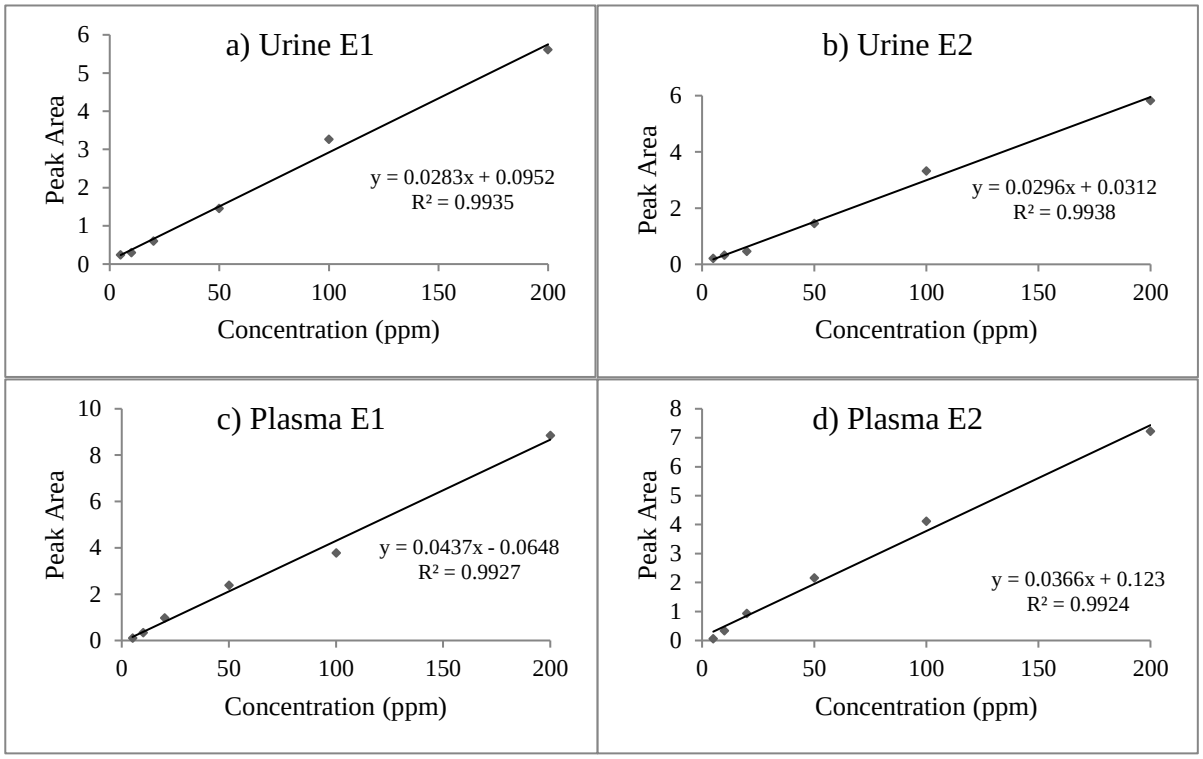

Figure 4: Calibration graphs of the two separated enantiomers of the methdrone compound in (a & b) urine, and (c & d) in plasma. Calibration ranges was 10-200 ppm

The regression coefficients and the limit of detection (LOD) and limit of quantitation (LOQ) values for the two enantiomers of each one of these compounds in urine and plasma are reported in Tables 9 and 10 respectively.

Table 9: Results for twelve cathinone related compounds spiked in urine including linearity coefficient, R^2 values, Limits of detection and limits of quantitations for the two enantiomers of each compound

		R^2		LOQ (ppm)		LOD (ppm)	
		E1	E2	E1	E2	E1	E2
1	Methedrone	0.9954	0.9976	1.80	2.02	0.59	0.67
2	Pentylone	0.9989	0.9966	2.14	1.92	0.71	0.63
3	4M-buphedrone	0.9940	0.9986	1.33	1.25	0.44	0.41
4	Ethcathinone	0.9954	0.9937	0.64	0.66	0.21	0.22
5	Pentedrone	0.9907	0.9954	1.41	1.44	0.47	0.47
6	4-FEC	0.9949	0.9957	0.67	0.67	0.22	0.22
7	3-MMC	0.9943	0.9985	0.26	0.26	0.08	0.09
8	3-FMC	0.9904	0.9925	0.29	0.23	0.10	0.08
9	3,4-DMMC	0.9965	0.9979	0.31	0.32	0.10	0.11
10	2,3-MDMC	0.9940	0.9917	0.24	0.23	0.08	0.08
11	Eutylone	0.9988	0.9976	1.31	1.32	0.43	0.44
12	Buphedrone	0.9952	0.9969	0.33	0.29	0.11	0.10

Table 10: Results for twelve cathinone related compounds spiked in plasma including linearity coefficient, R^2 values, Limits of detection and limits of quantitations for the two enantiomers of each compound

		R^2		LOQ (ppm)		LOD(ppm)	
		E1	E2	E1	E2	E1	E2
1	Methedrone	0.9927	0.9924	1.13	1.37	0.37	0.45
2	Pentylone	0.9913	0.9973	0.81	1.00	0.27	0.33
3	4M-buphedrone	0.9945	0.9985	1.21	2.15	0.40	0.71
4	Ethcathinone	0.9968	0.9927	3.13	4.01	1.03	1.32
5	pentedrone	0.9904	0.9984	4.03	2.46	1.33	0.81
6	4-FEC	0.9972	0.9939	1.37	1.52	0.45	0.50
7	3-MMC	0.9926	0.9983	0.50	0.52	0.16	0.17
8	3-FMC	0.9962	0.9925	2.20	2.09	0.73	0.69
9	3,4-DMMC	0.9986	0.9987	0.45	0.55	0.15	0.18
10	2,3-MDMC	0.9918	0.9946	0.82	0.91	0.27	0.30
11	Eutylone	0.9967	0.9906	0.97	1.22	0.32	0.40
12	Buphedrone	0.9940	0.9971	0.85	1.13	0.28	0.37

The accuracy and reproducibility of the method were evaluated as well in urine and plasma matrices. Tables 11 and 12 show the interday and intraday

reproducibilities of these 12 cathinone related compounds in urine and plasma matrices, respectively. Three different concentrations have been measured for each enantiomer of these compounds.

Table 11: Inter-day and intraday reproducibility results in terms of coefficient of variance (CV) for twelve cathinone related compounds spiked in urine at three different concentration levels for the two enantiomers of each compound

		%CV intraday						%CV interday					
		20 ppm		100 ppm		200 ppm		20 ppm		100 ppm		200 ppm	
		E1	E1	E2	E1	E2	E1	E1	E1	E2	E1	E2	E1
1	Methedrone	0.31	2.04	2.86	3.05	1.50	4.13	5.39	11.27	4.68	6.29	2.78	3.91
2	Pentylone	0.88	4.07	4.54	4.30	4.81	1.31	9.75	4.18	6.03	4.30	3.64	3.45
3	4Methyl-buphedrone	0.84	1.73	3.04	4.34	4.23	0.28	3.56	8.74	5.30	4.34	4.71	5.64
4	Ethcathinone	1.07	3.79	2.16	3.95	5.06	3.15	3.90	9.91	1.49	3.95	4.36	2.77
5	pentedrone	2.26	1.43	3.86	3.09	2.29	3.67	11.07	2.94	6.21	3.09	5.44	4.74
6	4-FEC	1.23	0.91	2.04	2.27	3.66	1.59	5.61	11.87	2.31	2.27	3.72	4.98
7	3-MMC	0.61	1.95	2.75	6.70	3.88	3.60	5.16	6.94	4.00	6.70	4.40	2.68
8	3-FMC	1.47	10.49	0.59	2.62	2.18	2.84	3.99	14.62	6.54	2.62	1.59	2.00
9	3,4-DMMC	2.26	1.08	4.09	3.06	1.09	1.53	6.30	9.16	6.14	3.06	2.32	2.77
10	2,3-MDMC	5.42	2.57	3.52	2.16	5.32	2.00	6.75	7.40	5.37	2.16	3.49	1.43
11	Eutylone	3.18	2.76	5.71	5.42	3.68	2.65	4.79	8.96	3.86	5.42	4.65	3.72
12	Buphedrone	1.19	1.22	3.68	3.70	5.60	4.92	5.50	12.31	3.92	3.70	4.44	3.90

Table 12: Inter-day and intraday reproducibility results in terms of coefficient of variance for twelve cathinone related compounds spiked in plasma at three different concentration levels for the two enantiomers of each compound

		%CV intraday						%CV interday					
		20 ppm		100 ppm		200 ppm		20 ppm		100 ppm		200 ppm	
		E1	E1	E2	E1	E2	E1	E1	E1	E2	E1	E2	E1
1	Methedrone	2.44	2.95	0.39	1.67	2.91	3.06	7.92	3.90	10.90	6.30	9.56	6.27
2	Pentylone	2.98	0.58	0.80	0.99	1.86	3.48	13.20	8.92	4.88	13.01	5.80	4.58
3	4Methyl-buphedrone	1.45	1.30	1.38	3.65	3.01	5.29	5.91	4.94	10.85	6.57	10.25	7.89
4	Ethcathinone	4.30	7.57	12.48	12.26	6.46	8.77	5.77	8.97	11.21	14.42	4.66	7.75
5	pentedrone	1.35	0.48	6.20	2.20	4.70	3.21	5.77	3.06	12.27	1.97	6.64	9.59
6	4-FEC	0.88	2.92	8.48	10.00	2.34	3.33	5.29	12.18	6.83	6.52	6.47	2.67
7	3-MMC	1.53	1.92	6.39	8.48	5.06	9.23	3.96	6.82	9.42	13.33	12.01	12.04
8	3-FMC	6.18	4.37	0.57	1.40	6.03	3.91	7.23	5.39	0.97	1.50	7.50	11.69
9	3,4-DMMC	1.03	2.11	1.59	3.03	2.21	4.27	2.23	3.56	10.62	6.91	9.30	7.51
10	2,3-MDMC	3.40	5.30	1.70	0.28	4.17	2.66	13.66	14.19	6.69	6.50	7.42	6.22
11	Eutylone	1.62	3.21	2.59	2.01	1.73	3.20	12.12	3.33	11.24	10.72	7.35	5.37
12	Buphedrone	2.21	5.30	7.77	9.18	2.04	3.71	2.46	9.81	5.27	12.69	8.18	5.70

Moreover, the recovery measurements have been conducted by spiking 20, 100 and 200 ppm of these compounds in urine and plasma matrices and evaluated by calculating the percent error. Tables 13 and 14 summarize the recovery measurements for the enantiomers of the 12 cathinone compounds at three different concentrations.

Table 13: Recovery measurements expressed in percent errors for three different concentrations of the cathinone related compounds spiked in urine matrix.

		Error %					
		20 ppm		100 ppm		200 ppm	
		E1	E2	E1	E2	E1	E2
1	Methedrone	2.24	1.20	7.76	7.15	2.33	1.58
2	Pentylone	4.69	13.26	2.97	5.09	0.23	0.36
3	4M-buphedrone	9.98	0.45	5.51	5.35	2.24	1.21
4	Ethcathinone	4.56	9.91	9.88	11.85	2.38	2.43
5	pentedrone	5.87	17.72	14.01	15.14	3.10	3.30
6	4-FEC	7.00	16.11	10.62	9.43	2.35	1.84
7	3-MMC	2.93	0.51	10.23	4.06	2.69	0.45
8	3-FMC	4.76	5.31	11.00	7.31	3.41	0.45
9	3,4-DMMC	1.82	0.17	5.82	6.32	1.96	1.10
10	2,3-MDMC	8.77	8.87	11.52	13.37	2.52	3.16
11	Eutylone	8.11	9.13	4.02	4.32	1.14	0.30
12	Buphedrone	4.69	12.12	9.00	7.50	2.44	1.26

Table 14: Recovery measurements expressed in percent errors for three different concentrations of the cathinone related compounds spiked in plasma matrix.

		Error %					
		20 ppm		100 ppm		200 ppm	
		E1	E2	E1	E2	E1	E2
1	Methedrone	18.51	10.36	11.90	9.11	2.08	2.90
2	Pentylone	5.13	13.00	3.74	1.49	2.25	0.36
3	4M-buphedrone	7.82	3.64	1.46	0.91	0.80	0.41
4	Ethcathinone	4.80	12.06	2.81	9.09	0.16	0.99
5	pentedrone	8.86	3.56	14.64	1.92	3.20	1.00
6	4-FEC	7.81	6.40	2.67	4.26	0.17	0.25
7	3-MMC	6.08	3.37	3.79	3.21	0.48	0.13
8	3-FMC	4.05	0.49	4.49	9.54	1.79	2.96
9	3,4-DMMC	16.67	2.88	3.25	4.02	0.70	1.24
10	2,3-MDMC	23.71	13.90	9.79	9.05	2.04	2.44
11	Eutylone	0.21	4.48	7.73	7.87	1.38	0.48
12	Buphedrone	9.50	34.40	3.94	1.65	0.25	0.67

2.4 Discussion

L –TPC is one of the known chiral derivatizing agents (CDA) that can interact easily with primary and secondary amine of cathinone related drugs. It can react with the enantiomers and produces two corresponding diastereomers. The enantioseparation was possible due to the difference of stereochemistry and stability of the formed diastereoisomers on achiral stationary phase which led to different resolution of products (Toyo'oka 2002, Płotka, Biziuk et al. 2011). The separation of enantiomers on achiral stationary phase is difficult since they have the same physical and chemical properties, by contrast, diastereoisomers have a different physical and chemical properties (i.e., different boiling point, solubility) which lead to variation on the interaction of these diastereoisomers with the achiral stationary phases. All cathinone related compounds in Table 8 have been derivatized by L–TPC where each one of them has formed a unique product after interacting with the derivatizing agent. Thirty-one racemic mixtures of cathinone derivatives have been separated as their diastereoisomers, as shown in the example of methedrone in Figure 1. Eighteen of them have been separated for the first time. Moreover, the enantioseparations that were obtained showed that the peak areas of some enantiomers were not equal and the reason of that according to Mohr (Mohr, Weiß et al. 2012) is due to racemization of L-TPC during the derivatization reaction, kinetic resolution of the two enantiomers and the difference in diastereoisomers yields as a result of keto-enol tautomerization of the analytes. Interestingly, it was possible to separate 12 of these cathinone derivatives simultaneously in one chromatogram after spiking them in urine and plasma samples since they have a different retention times in the new developed method, unlike Mohr method where overlapped between many of the

cathinone derivatives were observed. Calibration curves of 12 selected cathinone derivatives in urine and plasma were constructed based on the diastereoisomers peak areas for the following concentrations: 5, 10, 20, 50, 100, 200 ppm. Figure 4 shows the calibration graphs for methedrone enantiomers in plasma and urine sample matrices. One can see a good linearity of the four calibration lines in addition to high correlation coefficient (R^2) values. In all these calibration measurements, nikethamide (50 ppm) was added to each sample in the quantitation step as an internal standard, due to its similar structure to cathinones and good stability. The R^2 values of the constructed calibration curves for both enantiomers of 12 selected cathinone drivatives \ have been measured in spiked samples where most of them showed R^2 value higher than 0.99 in most cases as shown in Tables 9 and 10. Moreover, the Limits of Detection (LOD) and Limits of Quantitation (LOQ) for these enantiomers were calculated according to the IUPAC Method and reported in the Tables 9 and 10. The LOD in urine was in the range of 0.1 -0.7 ppm and in plasma it was in the range of 0.17 -1.33 ppm. The LOQ in urine was in the range of 0.29 - 2.14 ppm and in plasma it was in the range of 0.50 - 4.01 ppm.

The inter day and intraday reproducibility measurements of the twelve cathinone related compounds in urine and plasma were evaluated and reported at three different concentration levels in Tables 11 and 12. It was observed that the method has good reproducibility and repeatability, since most of the coefficients of variance values were below 5 % in both urine and plasma matrices for measurements done on the same day or at two different days. Spiked urine samples were more reproducible than spiked plasma due to the competition between analyte and blood interferences unlike spiked urine samples where the dilution with deionized water took place.

Efficiency of solid phase extraction (SPE) and its effect on the method recovery has been studied by percent error calculations for the spiked mixture of the 12 cathinone related compounds in plasma and urine samples at the following concentration levels: 20, 100 and 200 ppm. Most of the values in recovery studies were within the acceptable range except some of them in spiked plasma sample. The reason is due to the inefficiency in the extraction method for plasma sample which were probably because of the presence of proteins and other interferences that can cause difficulty in solid phase extraction process (Prabu and Suriyaprakash 2012). However, the spiked urine samples gave much better recovery results since they were diluted with deionized water twice.

2.5 Conclusion

It was possible to develop a sensitive and selective method for detection and quantitation of cathinone related compounds using GC-MS after indirect chiral derivatization with (S)-(–)-N- (trifluoroacetyl) pyrrolidine-2-carbonyl chloride (L-TPC). Thirty-one compounds of synthetic cathinones were separated as their optical enantiomers successfully using a 60m HP5-MS capillary column. Nikethamide was used as an internal standard in cathinones quantitation which has similar chemical structure to cathinones and showed good stability. Twelve cathinone derivatives were separated in one chromatogram simultaneously after spiking in urine and plasma sample. Calibration curves of twelve selected cathinone derivatives in urine were constructed including the following concentrations: 5, 10, 20, 50, 100, 200 ppm. Method validation in terms of recoveries, reproducibilities, linearities, LOD, and LOQ for all the tested compounds was also done. It was found that the LOD's of the 12 cathinone derivatives in urine was in the range of 0.1 -0.7 ppm and in plasma it was in the range of 0.17 -1.33 ppm. The LOQ's in urine was in the range of 0.29 - 2.14 ppm and in plasma it was in the range of 0.50 - 4.01 ppm.

Chapter 3: Development and validation of an analytical methodology for the simultaneous quantitative determination of synthetic cathinones in urine and plasma using GC-NCI-MS

3.1 Introduction

From the beginning of the new century till now, governments and forensic science specialists are suffering from a nightmare called new designer drugs (NDDs) such as synthetic cathinones which comprise a risk in society that is growing up day by day. In nature, cathinone (β-keto amphetamine) exists in the leaves of the *Catha edulis* plant which can be found easily in the region of northeast Africa and the Arabian Peninsula (Banks, Worst et al. 2014). However, scientists have synthesized cathinone in laboratory when the Germans and the French chemists reported the synthesis of methcathinone for the first time in late 1920's as mentioned in chapter one (Sikk and Taba 2015).

During the 1930's and 1940's, methcathinone was available in pharmacological markets as an appetite suppressant and antidepressant medicine (Glennon, Martin et al. 1995). Methcathinone abuse spread to USA in 1991 and as a result of that it was included in UN Convention on Psychotropic Substances (DeRuiter, Hayes et al. 1994).

In the meantime, drug dealers were looking for new strategies to sell their products and they found it by the "legal high" drugs (NDD) which contain at least one chemical substance that has similar biological effects as of illegal drugs. For instance, "Explosion" is the trade name of the synthetic cathinone methylone, which emerged for sale in Japan and Netherlands via the Internet in 2004 (Bossong, Van Dijk et al. 2005). In 2007, 4-methylmethcathinone (mephedrone) became one of the most commonly abused drugs in Europe (Bossong, Van Dijk et al. 2005). Thus,

concerns about the abuse of legal highs drugs especially cathinone related derivatives grew up in Europe which gave rise to ban of cathinone derivatives in April 2010 by the UK government and by the European Monitoring Centre for Drugs and Drug Addiction (EMCDDA) (Dargan, Sedefov et al. 2011). Despite all the actions taken by legal authorities, an intensive attention by drug dealers have been put on the synthesis of new generations of synthetic cathinone derivatives.

In order to obviate the abuse risks of these psychoactive stimulants, focused studies should be carried out on the neuropharmacological properties for each enantiomer of these active compounds. As a result of that, enantioseparation of chiral synthetic cathinones became an attractive and promised field of research where the use of major separation techniques took place such as: Gas Chromatography (GC) (Mohr, Weiß et al. 2012, Weiss, Mohr et al. 2015), High Performance Liquid Chromatography (HPLC) (Mohr, Taschwer et al. 2012, Padivitage, Dodbiba et al. 2014, TASCHWER, SEIDL et al. 2014, Li and Lurie 2015, Weiss, Taschwer et al. 2015, Wolrab, Frühauf et al. 2016) and Capillary Electrophoresis (CE) (Fanali 2000, Mohr, Pilaj et al. 2012, Aturki, Schmid et al. 2014, Merola, Fu et al. 2014, Taschwer, Hofer et al. 2014, Taschwer, Weiß et al. 2014, Li and Lurie 2015, Moini and Rollman 2015).

In the literature, only two papers have discussed the chiral separation of L-TPC cathinone derivatives by using GC-EI-MS (Mohr, Weiß et al. 2012, Weiss, Mohr et al. 2015). Electron Iionization (EI) is the most preferable ionization source in GC/MS which provides characteristic and reproducible mass spectrum for each compound. EI is considered as a harsh ionization technique which provides mass spectra that are crowded with fragments and for some compounds (e.g., primary

alcohol) the molecular ion peak is absent (Li, Gan et al. 2015). Recently, a short communication on the analysis of twenty nine synthetic cathinones in GC – MS/MS with positive chemical ionization mode (PCI) has been reported (Waters, Ikematsu et al. 2016). However, no quantitative assessment was given for these compounds in biological fluids. Unlike EI source, determination of molecular weight and structure elucidation can be carried out through the use of chemical ionization source coupled with tandem mass spectrometry (Waters, Ikematsu et al. 2016). Furthermore, when the investigated compounds are electronegative moieties, the use of negative chemical ionization (NCI) mode can dramatically improve the detection sensitivity of the targeted compounds (Wu, Lin et al. 2008). There are no literature reports that discuss the use of negative chemical ionization mode in GC – MS to analyze synthetic cathinones.

In this work, a sensitive and selective GC-NCI-MS method has been developed to analyze thirty-six synthetic cathinone compounds after their conversion into diastereoisomers through the derivatization reaction with L-TPC. Quantitative analysis of spiked urine and plasma samples were conducted for fourteen of these synthetic cathinones (see scheme 14) which were run in one mixture simultaneously. The method validation was performed in spiked biological samples.

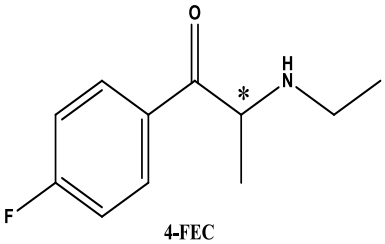

4-FEC

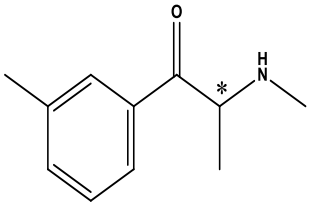

3-MMC

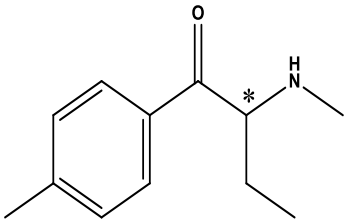

4-Methylbuphedrone

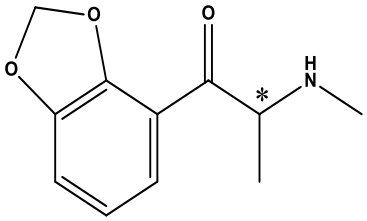

2,3-MDMC

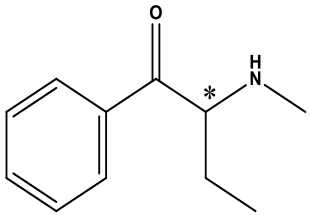

Buphedrone

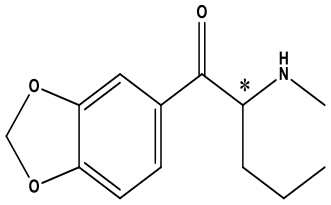

Pentylone

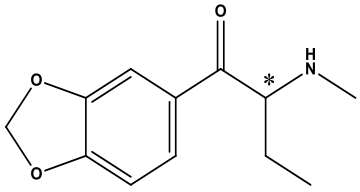

Butylone

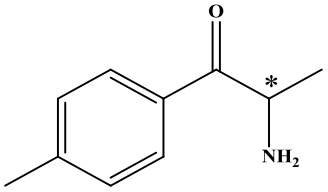

Nor-mephedrone

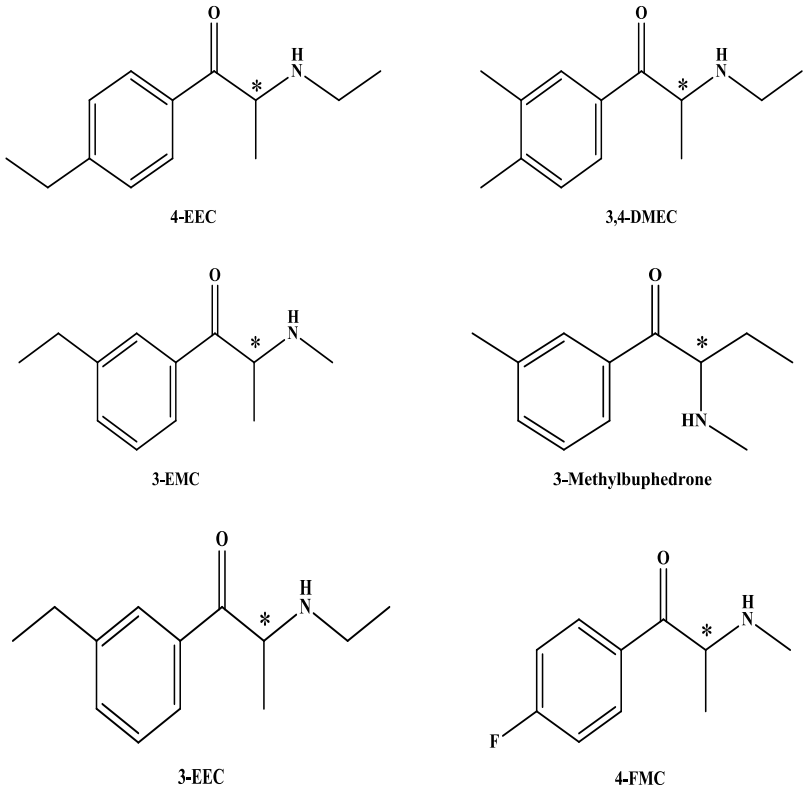

Scheme 14: Structures of tertiary amine synthetic cathinones that analyzed quantitatively

3.2 Experimental

3.2.1 Chromatographic conditions

Chromatographic separation was performed on an Agilent 7890A GC coupled to an Agilent HP 7000 Triple Quad mass selective detector. A commercially available 60 m Ultra inert capillary column consisting of (5%-Phenyl)-methylpolysiloxane, with 0.25 mm inner diameter and a 0.25 µm film thickness was used as stationary phase. Chemical ionization (CI) with methane gas (40%, 2.0 ml/min) was employed in the negative ion mode at a voltage of 70 eV. Helium was used as carrier gas at a constant flow rate of 0.8 ml/min. Injection of 3 µl of sample solution was performed automatically in splitless mode. The injector and GC–MS

interface temperature were set at 250 and 280 ◦C, respectively. Data collection was performed in Selected Ion Monitoring (SIM) mode with the selected fragments as shown in Table 15 starting at 30 min after injection. The column temperature program was as follows: starting at 160 ◦C held for 5 min, followed by subsequent heating to 260 ºC at a heating rate of 2 ºC /min. The final temperature was held at 260 ºC for 10 min.

Table 15: Time segments table with selected ions used in SIM mode for the analysis of cathinones mixture

Compound Name	Abbreviation	Time	m/z
(+)-Cathinone	-	39.00-41.00	189, 209, 342
4-Fluoromethcathinone	4-FMC	41.00-42.50	153, 223, 374
4-Fluoroethcathinone	4-FEC	42.50-44.70	167, 237, 388
Nor-Mephedrone	-	44.70-45.06	189, 209, 356
Buphedrone 3-Methylmethcathinone	- 3-MMC	45.06-47.13	153, 223, 370
Nor-Mephedrone	-	47.13-48.00	189, 209, 356
3-Mehtylbuphedrone 4-Methylbuphedrone 3-Ethylmethcathinone	- - 3-EMC	48.00-50.15	153, 223, 384
3-Ethylethcathinone 4-Ethylethcathinone 3,4-Dimethylethcathinone	3-EEC 4-EEC 3,4-DMEC	50.15-54.00	167, 237, 398
2,3-Methelendioxymethcathinone	2,3-MDMC	54.00-59.00	153, 223, 400
Butylone	-	59.00-62.00	153, 223, 414
Pentylone	-	62.00-65.00	156, 223, 428

3.2.2 Chemicals and reagents

All chemicals were of analytical grade. Ethylacetate, acetic acid, methanol, 2-propanol, ammonium hydroxide, dichloromethane, 0.1 M solution of (S)-(−)-N-(trifluoroacetyl) pyrrolidine-2-carbonyl chloride (L-TPC) with an enantiomer excess (ee) of 97% (according to supplier's specification) in methylene chloride, anhydrous sodium sulfate and sodium phosphate were obtained from Sigma–Aldrich Chemicals (St. Louis, MO, USA). Potassium carbonate was obtained from VWR (Darmstadt, Germany). Doubly deionized water was obtained from ultra-pure Millipore system

(MS, USA). All chemicals shown in Table 16 were purchased from Cayman chemicals (Michigan, USA), and were provided as racemic mixtures for individual cathinones.

3.2.3 Sample preparation

3.2.3.1 Samples

This investigation conforms to the UAE community guidelines for the use of humans in experiments. The Human Ethics committee at the Dubai police approved this study. Blood and urine samples were collected by Dubai police with the consent of the subjects.

3.2.3.2 Solid phase extraction (SPE) of spiked urine and plasma samples

SPE was carried out for the spiked urine and plasma samples as shown in extraction steps of section 2.2.3.2.

3.2.3.3 Derivatization step

Derivatization steps were carried out for the pure and spiked samples as shown in section 2.2.3.3.

3.3 Results

The indirect chiral separation method that has been developed is based on the conversion of synthetic cathinones to L-TPC derivatives. A normal (or achiral) stationary phase column has been used for the separation of the resulting diastereomers due to their different chemical and physical properties. The primary and secondary amine cathinones react with the derivatization reagent L-TPC in the presence of sodium carbonate, the amidation reaction occurs between the acid chloride in L-TPC and the amine group of the target analytes. The gas chromatogram in Figure 5 shows the separation of the (R) and (S) enantiomers of Nor-mephedrone drug after derivatization with L-TPC.

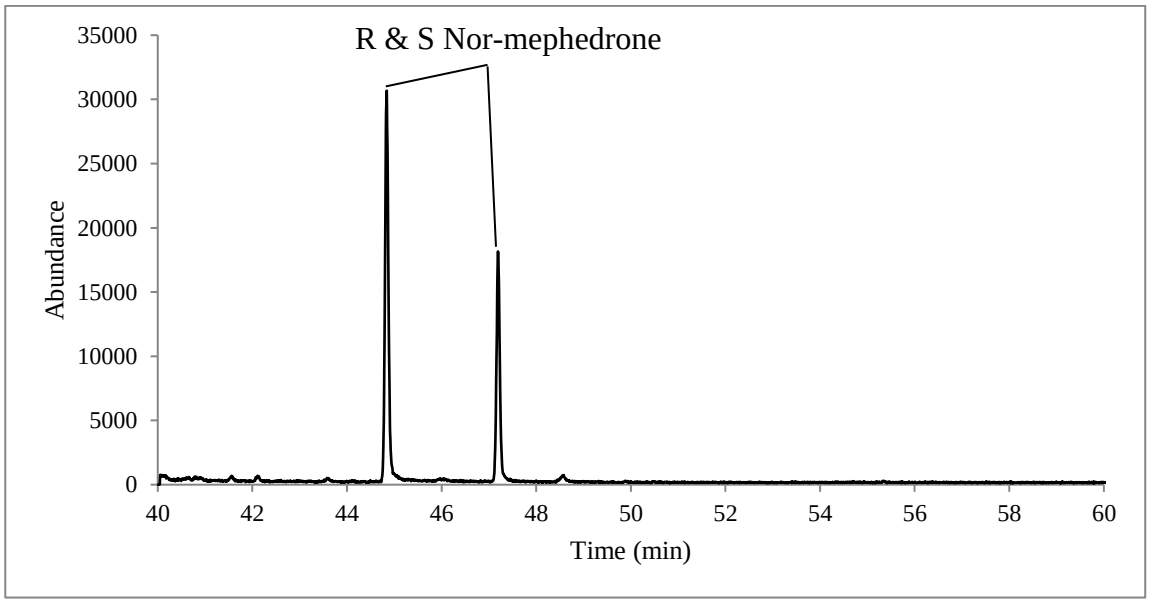

Figure 5: Gas chromatogram for separation of the R and S enantiomers of Nor-mephedrone drug in ethyl acetate after derivatization with L-TPC

Table 16 shows the retention times, resolution, and selectivity factors of the separated enantiomers of all the studied synthetic cathinones. All compounds in

Table 16 were analyzed individually on GC-MS using SIM mode, after going through the derivatization step.

Table 16: List of the 36 cathinone related compounds and their synonyms, in addition to the retention times of the separated two diasterioisomers for each compound analyzed on GC-MS using SIM mode

	Name	Abbreviations	Time (min)		Resolution	Selectivity Factor (α)
			t_{R1}	t_{R2}		
1	2-Methoxymethcathinone	2-MeOMC	48.98	49.98	9.59	1.03
2	3-Fluoroethcathinone	3-FEC	43	43.3	2.64	1.01
3	4-Fluoroethcathinone	4-FEC	42.7	43.2	3.47	1.01
4	2,3-Methylenedioxymethcathinone	2,3-MDMC	55.1	56.4	10.03	1.03
5	2-Methylmethcathinone	2-MMC	45.1	46.2	9.61	1.03
6	Nor-Mephedrone	-	44.9	47.2	17.07	1.06
7	4-Ethylethcathinone	4-EEC	51.6	52.5	7.03	1.02
8	3,4-Dimethylethcathinone	3,4-DMEC	52.8	53.6	6.56	1.02
9	2-Ethylmethcathinone	2-EMC	47.5	48.6	9.69	1.03
10	3-Methoxymethcathinone	3-MeOMC	51.4	51.7	2.97	1.01
11	2-Fluoromethcathinone	2-FMC	41.9	43	8.71	1.03
12	4-Ethylmethcathinone	4-EMC	50.5	51.7	11.61	1.03
13	3-Ethylethcathinone	3-EEC	50.4	51	4.72	1.01
14	4-Methylbuphedrone	-	48.96	49.4	3.42	1.01
15	2,3-Dimethylmethcathinone	2,3-DMMC	49.7	51.1	12.61	1.03
16	3-Ethylmethcathinone	3-EMC	49.8	50	1.55	1.00
17	3-Fluoromethcathinone	3-FMC	41.7	41.98	2.45	1.01
18	4-Fluoromethcathinone	4-FMC	41.5	41.96	3.08	1.01
19	2-Methylethcathinone	2-MEC	46.3	47.6	10.88	1.03
20	Buphedrone	-	45.2	45.4	1.48	1.01
21	4-Methyl-α-ethylaminobutiophenone	-	49.7	50.3	5.80	1.01
22	Pentedrone	-	47.6	47.7	1.07	1.00
23	Butylone	-	59.7	60.6	5.84	1.02
24	Pentylone	-	62.6	63.2	3.40	1.01
25	4-Methylethcathinone	4-MEC	48	49.2	11.70	1.03
26	Ethcathinone	-	44.2	44.9	6.16	1.02
27	3-Methylmethcathinone	3-MMC	46.3	47	5.33	1.02
28	4-Bromomethcathinone	4-BMC	53.96	54.3	2.93	1.01
29	3-Bromomethcathinone	3-BMC	42.9	43.6	4.72	1.02
30	2,4-Dimethylmethcathinone	2,4-DMMC	48.5	49.96	13.67	1.04

#	Name	Abbreviations	T1	T2	Resolution	α
31	2,4-Dimethylethcathinone	2,4-DMEC	49.8	51.2	12.15	1.03
32	3,4-Methylenedioxy-N-ethylcathinone	Ethylone	58.6	59.9	9.96	1.03
33	3-Methylbuphedrone	-	48.4	48.5	0.80	1.00
34	N-Ethylbuphedrone	NEB	45.9	46.1	1.93	1.01
35	2,3-Pentylone isomer	-	59.1	59.9	7.37	1.02
36	3-Methylethcathinone	3-MEC	47.4	48.1	6.66	1.02

Figures 6 and 7 show the total ion chromatogram of the fourteen synthetic cathinones spiked in urine and plasma, respectively.

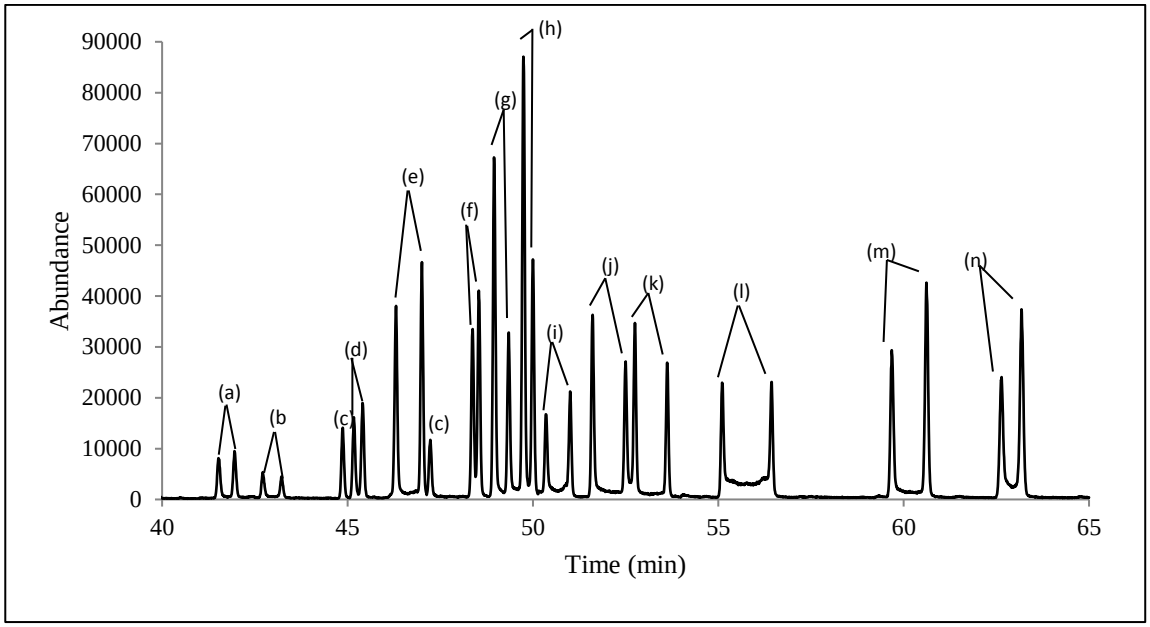

Figure 6: Total ion chromatogram (TIC) of the simultaneous chiral separation of 14 synthetic cathinone compounds spiked in urine and separated as L-TPC derivatives as the following: (a) 4-FMC, (b) 4-FEC, (c) Nor-mephedrone, (d) Buphendrone, (e) 3-MMC, (f) 3-Methylbuphedrone, (g) 4-Methylbuphedrone, (h) 3-EMC, (i) 3-EEC, (j) 4-EEC, (k) 3,4-DMEC, (l) 2,3-MDMC, (m) Butylone and (n)Pentylone

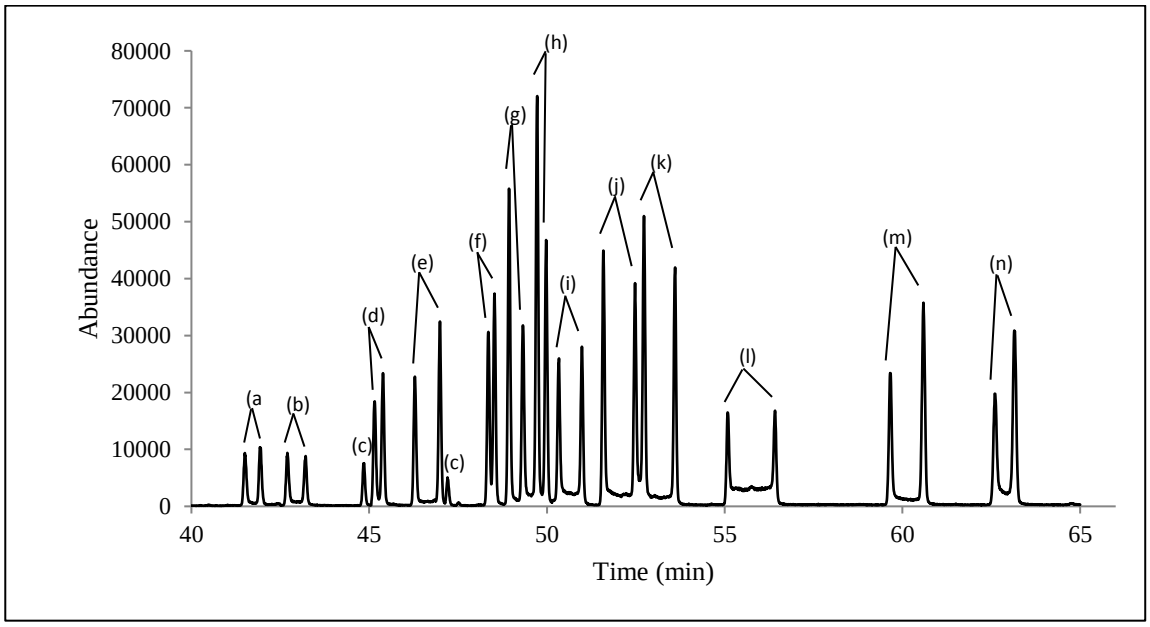

Figure 7: Total ion chromatogram (TIC) of the simultaneous chiral separation of 14 synthetic cathinone compounds spiked in plasma and separated as L-TPC derivatives as the following: (a) 4-FMC, (b) 4-FEC, (c) Nor-mephedrone, (d) Buphendrone, (e) 3-MMC, (f) 3-Methylbuphedrone, (g) 4-Methylbuphedrone, (h) 3-EMC, (i) 3-EEC, (j) 4-EEC, (k) 3,4-DMEC, (l) 2,3-MDMC, (m) Butylone and (n) Pentylone

The resulted enantiomer peaks were well separated with good peak resolution. To our knowledge, this is the first example in the literature that demonstrates the separation of fourteen pairs of L-TPC cathinone derivatives in one run analysis for these compounds in complex matrices of urine and plasma.

Validation of the developed method was performed on spiked mixtures successfully. Linearity of the calibration curves, limit of detection (LOD), limit of quantitation (LOQ), recoveries in addition to inter-day and intra-day reproducibilities were collected and summarized in Tables 17-22.

The calibration curves for the fourteen synthetic cathinones derivatives were found to be linear within the tested range of 1 to 100 ppb in urine and in plasma except some of them which had a range that extended from 5 to 100 ppb with mean regression coefficients (R^2; n = 3) higher than 0.99. Figure 8 shows the calibration graph of the formed diastereoisomers of nor-mephedrone in plasma and urine.

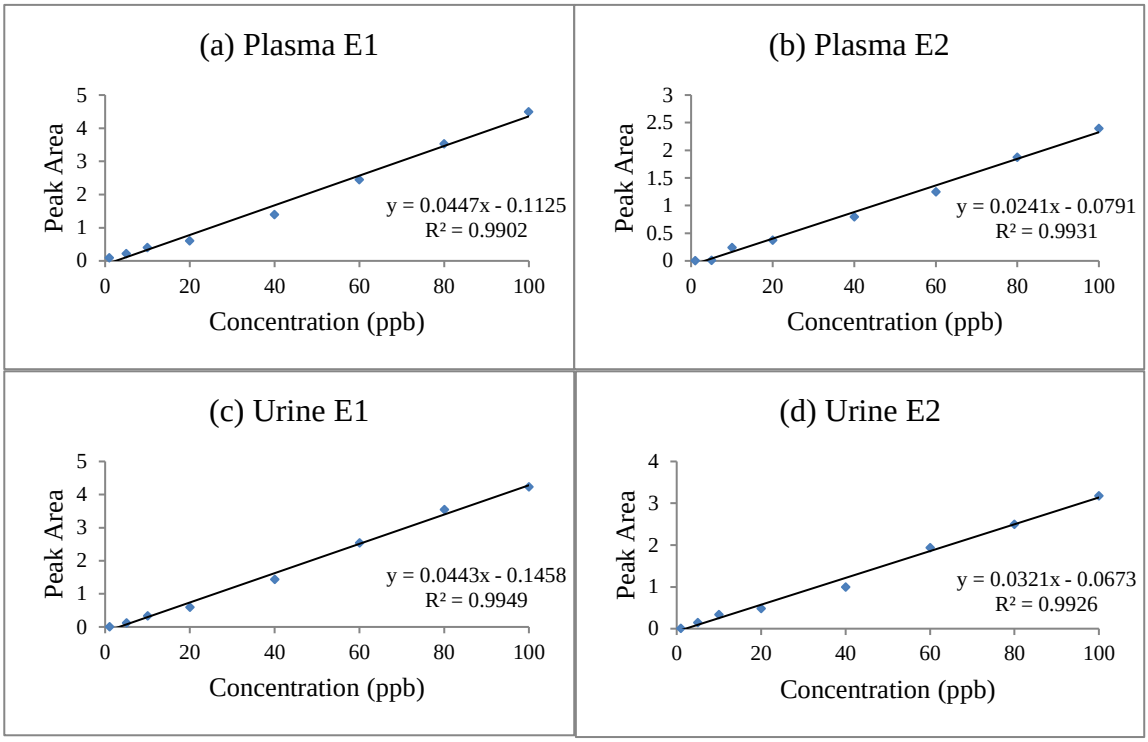

Figure 8: Calibration graphs of the two separated enantiomers of the Nor-mephedrone compound in (a & b) plasma, and (c & d) in urine. Calibration ranges was 1-100 ppb

The regression coefficients, the limit of detection (LOD) and limit of quantitation (LOQ) values for the two enantiomers of the synthetic cathinone compounds in the mixture that were spiked in urine and plasma are reported in Tables 17 and 18 respectively.

Table 17: Results for fourteen cathinone related compounds spiked in urine including linearity coefficient, R^2 values, limit of detection and limit of quantitations for the two enantiomers of each compound

		R2 ± SD		LOQ ± SD (ppb)		LOD ± SD (ppb)	
	Name	E1	E2	E1	E2	E1	E2
1	4-FMC	0.9912 ± 0.0017	0.9925 ± 0.0006	1.20 ± 0.0225	1.09 ± 0.0259	0.397 ± 0.0074	0.362 ± 0.0085
2	4-FEC	0.9960 ± 0.0005	0.9937 ± 0.0016	1.17 ± 0.0329	1.35 ± 0.0353	0.38 ± 0.0109	0.44 ± 0.0117
3	Nor-mephedrone	0.9943 ± 0.0028	0.992 ± 0.0019	0.89 ± 0.0292	1.366 ± 0.0054	0.294 ± 0.0096	0.451 ± 0.0018
4	Buphedrone	0.9944 ± 0.0025	0.9938 ± 0.0018	0.309 ± 0.0054	0.254 ± 0.0062	0.102 ± 0.0018	0.084 ± 0.0020
5	3-MMC	0.9943 ± 0.0048	0.9928 ± 0.0023	0.313 ± 0.0069	0.192 ± 0.0047	0.103 ± 0.0023	0.063 ± 0.0016
6	3-Methylbuphedrone	0.9937 ± 0.0039	0.9944 ± 0.0028	0.147 ± 0.0019	0.122 ± 0.0037	0.0485 ± 0.0006	0.040 ± 0.0012
7	4-Methylbuphedrone	0.9932 ± 0.0034	0.9911 ± 0.0036	0.238 ± 0.0036	0.382 ± 0.0076	0.078 ± 0.0012	0.126 ± 0.0025
8	3-EMC	0.9952 ± 0.0043	0.9909 ± 0.0009	0.180 ± 0.0046	0.326 ± 0.0089	0.059 ± 0.0015	0.108 ± 0.0030
9	3-EEC	0.994 ± 0.0028	0.9936 ± 0.0029	0.43 ± 0.0111	0.40 ± 0.0127	0.141 ± 0.0037	0.131 ± 0.0042
10	4-EEC	0.9954 ± 0.0014	0.9926 ± 0.0013	0.207 ± 0.0064	0.264 ± 0.0087	0.068 ± 0.0021	0.087 ± 0.0029
11	3,4-DMEC	0.9931 ± 0.0004	0.9925 ± 0.0013	0.192 ± 0.0054	0.218 ± 0.0071	0.063 ± 0.0017	0.072 ± 0.0024
12	2,3-MDMC	0.9925 ± 0.003	0.9918 ± 0.001	0.520 ± 0.0257	0.520 ± 0.0254	0.173 ± 0.0085	0.172 ± 0.0084
13	Butylone	0.9948 ± 0.0024	0.9922 ± 0.0046	0.326 ± 0.0058	0.214 ± 0.0042	0.107 ± 0.0019	0.070 ± 0.0014
14	Pentylone	0.9918 ± 0.0023	0.9941 ± 0.0024	0.465 ± 0.0067	0.3117 ± 0.0008	0.153 ± 0.0022	0.1028 ± 0.0002

Table 18: Results for fourteen cathinone related compounds spiked in plasma including linearity coefficient, R^2 values, limit of detection and limit of quantitations for the two enantiomers of each compound

		R^2 ± SD		LOQ ± SD (ppb)		LOD ± SD (ppb)	
	Name	E1	E2	E1	E2	E1	E2
1	4-FMC	0.9931 ± 0.0029	0.9939 ± 0.0048	1.200 ± 0.0225	1.09 ± 0.0259	0.398 ± 0.0074	0.362 ± 0.0085
2	4-FEC	0.9943 ± 0.0017	0.9940 ± 0.0009	1.510 ± 0.0426	1.75 ± 0.0456	0.500 ± 0.0141	0.580 ± 0.0151
3	Nor-mephedrone	0.9930 ± 0.0004	0.9942 ± 0.0029	0.910 ± 0.0299	1.397 ± 0.0056	0.301 ± 0.0099	0.461 ± 0.0018
4	Buphedrone	0.9941 ± 0.0036	0.9940 ± 0.0018	0.326 ± 0.0057	0.268 ± 0.0065	0.108 ± 0.0019	0.088 ± 0.0022
5	3-MMC	0.9934 ± 0.0015	0.9923 ± 0.0023	0.386 ± 0.0085	0.237 ± 0.0058	0.127 ± 0.0028	0.0781 ± 0.0019
6	3-Methyl buphedrone	0.9922 ± 0.0018	0.9934 ± 0.0033	0.160 ± 0.0020	0.133 ± 0.0040	0.0529 ± 0.0007	0.044 ± 0.0013
7	4-Methyl buphedrone	0.9916 ± 0.0013	0.9946 ± 0.0016	0.265 ± 0.0040	0.426 ± 0.0084	0.087 ± 0.0013	0.141 ± 0.0028
8	3-EMC	0.9920 ± 0.0010	0.9923 ± 0.0014	0.209 ± 0.0053	0.38 ± 0.0104	0.069 ± 0.0018	0.125 ± 0.0034
9	3-EEC	0.9931 ± 0.0035	0.9932 ± 0.0032	0.460 ± 0.0119	0.43 ± 0.0137	0.152 ± 0.0039	0.142 ± 0.0045
10	4-EEC	0.9930 ± 0.0007	0.9931 ± 0.0026	0.243 ± 0.0075	0.31 ± 0.0103	0.080 ± 0.0025	0.103 ± 0.0034
11	3,4-DMEC	0.9906 ± 0.0009	0.9929 ± 0.0015	0.229 ± 0.0064	0.260 ± 0.0085	0.076 ± 0.0021	0.086 ± 0.0028
12	2,3-MDMC	0.9918 ± 0.0022	0.9929 ± 0.0019	0.630 ± 0.0310	0.63 ± 0.0307	0.210 ± 0.0102	0.210 ± 0.0101
13	Butylone	0.9920 ± 0.002	0.9906 ± 0.0026	0.760 ± 0.0134	0.497 ± 0.0098	0.250 ± 0.0044	0.164 ± 0.0032
14	Pentylone	0.9909 ± 0.0011	0.9934 ± 0.0034	0.644 ± 0.0093	0.431 ± 0.0011	0.212 ± 0.0031	0.1422 ± 0.0004

Three different concentration levels were tested for each enantiomer of these compounds (20, 60 and 100 ppb) in order to ensure the reproducibility and to provide the recovery study of the new method. The interday and intraday reproducibilities of the cathinones mixture in urine and plasma matrices are shown in Tables 19 and 20 respectively.

Table 19: Interday and intraday reproducibility results in terms of coefficient of variance for fourteen cathinone related compounds spiked in urine at three different concentration levels for the two enantiomers of each compound

		CV% intraday						CV% interday					
		20 ppb		60 ppb		100 ppb		20 ppb		60 ppb		100 ppb	
		E1	E2	E1	E2	E1	E2	E1	E2	E1	E2	E1	E2
1	4-FMC	3.61	3.11	1.04	1.79	0.41	1.33	10.26	11.85	10.28	12.02	8.14	7.60
2	4-FEC	2.22	5.32	1.75	1.53	2.03	1.69	5.67	10.90	14.69	15.74	15.80	16.13
3	Nor-mephedrone	0.70	1.01	2.13	1.64	2.00	2.17	3.07	4.57	3.50	4.43	1.75	4.91
4	Buphedrone	1.42	1.60	1.89	2.28	2.12	1.17	5.60	14.08	15.31	16.91	16.62	15.29
5	3-MMC	3.68	2.03	0.93	1.66	0.39	1.34	12.27	9.02	1.72	2.41	0.82	1.29
6	3-Methyl buphedrone	1.36	3.07	2.06	4.48	0.93	1.09	5.32	14.73	6.73	11.96	10.04	9.44
7	4-Methyl buphedrone	1.25	2.16	0.35	0.75	0.68	1.14	3.73	11.28	9.25	2.04	10.22	9.93
8	3-EMC	2.38	2.57	0.63	2.10	0.74	1.69	14.53	14.81	13.18	3.51	7.62	10.98
9	3-EEC	3.22	6.13	1.13	3.60	1.71	2.13	13.29	15.44	8.42	10.94	3.27	4.10
10	4-EEC	3.45	1.85	0.93	2.17	0.84	0.82	14.48	11.31	9.31	12.68	7.19	1.80
11	3,4-DMEC	3.70	3.50	1.97	1.02	3.44	2.16	16.54	14.77	10.92	14.49	3.07	2.62
12	2,3-MDMC	2.07	3.24	3.16	1.43	4.11	5.56	5.50	4.43	13.57	14.03	5.74	6.60
13	Butylone	5.14	6.26	1.36	0.50	0.85	0.88	12.57	14.11	14.56	14.90	1.25	1.56
14	Pentylone	7.10	1.34	2.59	1.84	1.83	0.19	12.98	5.99	12.77	14.03	2.29	3.86

Table 20: Interday and intraday reproducibility results in terms of coefficient of variance for fourteen cathinone related compounds spiked in plasma at three different concentration levels for the two enantiomers of each compound

		CV% intraday						CV% interday					
		20 ppb		60 ppb		100 ppb		20 ppb		60 ppb		100 ppb	
		E1	E2	E1	E2	E1	E2	E1	E2	E1	E2	E1	E2
1	4-FMC	6.00	4.79	2.59	5.36	2.26	2.59	11.01	10.60	10.99	13.30	10.95	12.35
2	4-FEC	10.57	11.65	5.31	3.89	1.69	2.21	7.44	8.43	7.59	11.25	6.65	7.76
3	Nor-mephedrone	7.59	7.95	3.07	3.51	2.79	6.97	6.01	7.10	14.13	6.48	14.30	14.21
4	Buphedrone	11.13	10.88	3.37	6.27	1.32	3.14	8.04	8.49	13.39	14.26	5.00	8.32
5	3-MMC	9.74	12.68	4.55	6.19	2.51	3.69	8.42	9.85	4.03	4.78	16.30	16.97
6	3-Methyl buphedrone	10.58	11.42	5.04	5.44	1.19	3.58	7.00	7.90	10.55	15.34	13.67	14.31
7	4-Methyl buphedrone	9.77	11.67	5.41	4.49	2.42	2.82	9.25	11.85	19.55	6.83	18.03	19.59
8	3-EMC	11.36	8.27	5.41	4.55	3.01	3.16	11.35	9.79	19.65	7.13	19.04	17.92
9	3-EEC	8.81	12.64	4.30	5.28	3.15	3.71	6.62	9.27	10.19	12.67	14.15	14.82
10	4-EEC	11.48	10.53	6.12	4.48	4.24	3.59	8.31	9.46	19.81	19.90	10.97	15.42
11	3,4-DMEC	12.11	13.14	4.50	6.31	3.26	3.06	9.44	11.05	18.98	20.31	9.66	15.70
12	2,3-MDMC	10.94	7.12	2.74	4.02	7.24	7.13	9.20	5.11	3.41	4.46	19.77	19.35
13	Butylone	10.78	12.89	4.97	6.67	2.63	3.25	11.42	13.60	3.66	7.62	9.06	9.14
14	Pentylone	10.20	18.64	3.74	5.93	2.00	2.06	10.29	19.91	9.77	6.67	5.01	6.59

Moreover, percent error evaluation has been done for the spiked mixture to obtain the recovery study which is summarized in Tables 21 and 22.

Table 21: Recovery measurements expressed in percent errors for three different concentrations of the cathinone related compounds spiked in urine matrix

		Error %					
		20 ppb		60 ppb		100 ppb	
		E1	E2	E1	E2	E1	E2
1	4-FMC	0.80	10.57	9.49	8.47	1.24	0.68
2	4-FEC	9.28	5.31	2.38	9.21	0.10	0.61
3	Nor-mephedrone	8.67	7.48	1.82	4.48	1.71	0.69
4	Buphedrone	9.12	5.58	4.84	4.88	1.90	0.72
5	3-MMC	3.91	3.02	4.91	3.54	0.25	0.91
6	3-Methylbuphedrone	3.71	9.13	4.09	0.15	1.54	1.77
7	4-Methylbuphedrone	1.15	0.42	0.97	2.54	2.30	4.01
8	3-EMC	3.61	1.27	4.86	8.04	1.55	3.32
9	3-EEC	5.69	4.88	2.10	4.18	2.44	2.22
10	4-EEC	2.37	12.25	0.66	6.64	0.90	1.52
11	3,4-DMEC	9.61	7.83	7.35	8.05	2.07	1.64
12	2,3-MDMC	7.25	10.31	9.45	6.68	0.94	0.54
13	Butylone	2.93	3.78	8.95	8.38	0.83	0.24
14	Pentylone	9.54	0.05	0.14	3.25	2.52	3.14

Table 22: Recovery measurements expressed in percent errors for three different concentrations of the cathinone related compounds spiked in plasma matrix.

		Error %					
		20 ppb		60 ppb		100 ppb	
		E1	E2	E1	E2	E1	E2
1	4-FMC	2.63	5.32	2.48	0.62	2.45	0.26
2	4-FEC	0.17	4.89	5.80	3.10	2.19	1.60
3	Nor-mephedrone	5.64	1.94	3.25	7.64	1.69	2.64
4	Buphedrone	3.18	5.94	0.79	3.78	0.06	1.71
5	3-MMC	1.03	1.47	0.87	0.55	0.74	1.40
6	3-Methylbuphedrone	1.26	7.10	6.41	9.61	4.03	1.71
7	4-Methylbuphedrone	0.69	5.64	1.77	0.73	2.56	1.90
8	3-EMC	0.65	5.73	2.19	4.70	0.56	0.52
9	3-EEC	8.70	7.62	2.22	1.06	0.42	0.34
10	4-EEC	4.38	5.72	7.91	5.68	2.01	2.32
11	3,4-DMEC	4.36	3.85	2.20	2.46	1.89	2.93
12	2,3-MDMC	9.98	8.22	6.17	8.34	1.97	3.51
13	Butylone	1.41	10.98	2.05	5.97	1.62	1.98
14	Pentylone	5.80	10.43	1.07	1.47	1.68	0.22

3.4 Discussion

L –TPC is considered as a chiral derivatizing agent (CDA) which can react with the primary and secondary amine enantiomers of synthetic cathinones producing two corresponding diastereomers. As a result of the differences in stereochemistry and stability of the formed diastereoisomers, the enantioseparation can occur on an achiral stationary phase with different resolution of product compounds (Toyo'oka 2002, Płotka, Biziuk et al. 2011). In this study, chiral separation of 36 racemic mixtures of synthetic cathinone derivatives were carried out, fourteen of them were selected in the spiked mixtures; each enantiomer was quantitated in urine and plasma as shown in the example of Nor-mephedrone in Figure 5. However, the enantioseparations that were obtained showed that there are differences in peak areas for the most resulted diastereoisomers. Mohr *et al.* assumed that the reason of inequality in the formed peaks is due to (a) racemization of L-TPC during the derivatization reaction, (b) kinetic resolution of the two enantiomers and (c) the difference in diastereoisomers yields which are explained in terms of keto-enol tautomerization of the analytes. Moreover, the main reason for enantiomer peak inequality is related to the tested compounds themselves (Mohr, Weiß et al. 2012).

Interestingly, the fourteen spiked cathinone derivatives were separated simultaneously in one chromatogram since they have different retention times in the new developed method as shown in Figures 6 and 7 respectively. Moreover, enhancement of the enantiomers peaks resolution has been accomplished by using a slow heating rate of 2 ^{o}C/min in the chromatographic method. Also the use of Ultra inert column helped in minimizing the overlap of the two adjacent peaks of the enantiomers. Ultra inert of the stationary phase means the lower column bleeding

you get, and as a result of lowering column bleeding, signal-to-noise ratio will enhance leading to better and smooth chromatogram. Construction of calibration curves were done for the diastereoisomers based on the peak areas of the following concentration: 1, 5, 10, 20, 40, 60, 80, 100 ppb. Figure 8 shows the calibration graphs for Nor-mephdrone enantiomers in plasma and urine sample matrices. Regression values (R^2) confirm the good linearity of the four calibrations lines. In order to correct for the loss of analyte during sample inlet or sample preparation, (+)-cathinone has been used as internal standard (IS) as it has a similar structure to synthetic cathinones and shows a good stability. The correlation coefficient (R^2) values were calculated for the mixture components and they were found to be higher than 0.99 in all cases as shown in Tables 17 and 18. Additionally, the limits of detection (LOD's) and limits of quantitation (LOQ's) were calculated according to IUPAC method and are reported in Tables 17 and 18. The reported values of LOD's and LOQ's for the synthetic cathinones in this study were in the ppb range due to the high sensitivity of the analytical technique (GC-NCI-MS). The high sensitivity of NCI is due to the low mass and high mobility of the secondary or thermal electrons (low energy electrons) produced under the CI high pressure conditions in the presence of methane reagent gas, which is responsible for the enhancement factor by nearly 100 times in the sensitivity of NCI compared to that of positive CI for a suitably electrophilic compounds (Watson and Sparkman 2007). The LOD in urine was in the range of 0.02 -0.76 ppb and in plasma it was in the range of 0.02 - 0.34 ppb. While the LOQ in urine was in the range of 0.07 - 2.31 ppb and in plasma it was in the range of 0.07 – 1.03 ppb (as shown in Tables 17 and 18).

Three different concentration levels were chosen to test the inter-day and intra-day reproducibility measurements of the synthetic cathinone compounds

mixture in urine and plasma as shown in Tables 19 and 20. In fact, good reproducibility and repeatability were established using the new developed method since most of the coefficients of variance values were below 15 % in both urine and plasma matrices for measurements done on the same day or on two different days. A comparison between spiked urine and spiked plasma samples shows that urine samples were more reproducible than spiked plasma samples because of the competition between analyte and blood interferences unlike spiked urine samples where the urine was diluted with deionized water prior to the spiking step. Moreover, the presence of proteins and other interferences in plasma can cause difficulty in solid phase extraction processes and can also create competition between the targeted analyte and unneeded interferences which will lead to variation in spiked plasma results (Prabu and Suriyaprakash 2012).

Solid phase extraction (SPE) efficiencies were studied by percent error calculations for the spiked mixture at the following concentration levels: 20, 60 and 100 ppb. The calculated values in recovery studies were within the acceptable range.

By comparing the results of the GC-EI-MS method recently reported for some of these synthetic cathinones (Alrumaithi, Meetani et al. 2016), and the current study results using GC-NCI-MS, the latter has showed lower detection limit by a factor of 3.

3.5 Conclusion

Indirect chiral separation of synthetic cathinones after derivatization with trifluoroacetyl-l-prolyl chloride (L-TPC) was achieved using a new developed method of GC-NCI-MS that provided low detection limit and selectivity for the separation and quantitation of the targeted compounds. The use of 60m HP5-MS Ultra inert capillary column helps to separate more than thirty-six compounds of synthetic cathinones to their optical enantiomers. (+)-cathinone was used as internal standard in cathinones quantitation which has similar skeleton and chemical structure and showed good stability. A mixture of fourteen cathinone derivatives that were spiked in urine and plasma was separated in one chromatogram simultaneously. For each enantiomer peak in the cathinones mixture chromatogram, calibration curves were constructed using the following concentration: 1, 5, 10, 20, 40, 60, 80, 100 ppb. The developed method was validated in terms of linearities, limit of detection (LOD), limit of quantitation (LOQ), reproducibilities and recoveries for all the tested mixtures.

Chapter 4: Development and validation of an HPLC method for the determination of synthetic cathinones “bath salts” enantiomers in human samples

4.1 Introduction

In recent years, the abuse of novel psychoactive drugs (NPD) has grown up very fast which has put governments on alert (Kelly 2011, Katz, Bhattacharya et al. 2014).. The “bath salt” term which is used mainly in United States of America, is to hinder a kind of new designer drugs called “synthetic cathinones” (Zawilska and Wojcieszak 2013, German, Fleckenstein et al. 2014). It was agreed that the enantiomeric determination of these kinds of compounds is important and attractive for a group of researchers.

In general, chiral separation can be carried out by using one of the following techniques: directly on chiral stationary phase (CSP) (Mohr, Taschwer et al. 2012, Wolrab, Frühauf et al. 2016), or indirectly using derivatization with enantiomerically pure reagents that convert the enantiomers to diastereoisomers which will be separable on achiral stationary phases (Tao and Zeng 2002, Mohr, Weiß et al. 2012, Weiss, Mohr et al. 2015). CSP can be either immobilized on the stationary phase of the column (Mohr, Taschwer et al. 2012, Wolrab, Frühauf et al. 2016), or used as a chiral selector that can be added to the mobile phase composition (Mohr, Pilaj et al. 2012, Aturki, Schmid et al. 2014, Merola, Fu et al. 2014, TASCHWER, SEIDL et al. 2014, Li and Lurie 2015). Mostly, CSP is based on one of the following principles: host – guest inclusion reaction with cyclodextrins, hydrogen bonding on a chiral center, or coordination on chiral metal complexes (Schurig 2002).

In this work, we focused on chiral separation of synthetic cathinones that contain mainly tertiary amines by HPLC-UV system. In addition to tertiary amine

synthetic cathinones analysis, 43 compounds of primary and secondary amine cathinones have been analyzed by two commercially available columns as reported in this study. A comparison between two columns that contain different chiral separation phases in terms of resolution of separation and selectivity factor has been conducted. The two commercially available columns were Astec Cellulose DMP column, and CHIRALPAK AS-H Amylose column. Finally, quantitative analysis has been carried out for three tertiary cathinone derivatives after spiking and extracting them from urine and plasma sample matrices, Scheme 15 shows the structure of the compounds that were analyzed quantitatively in this study. 2,3-Methylenedioxy Pyrovalerone (2,3-MDPV) was used as the internal standard (IS). The analytical method was validated in terms of linearities, limits of detection (LOD), limits of quantitation (LOQ), recoveries, and reproducibilities for the compounds under investigation.

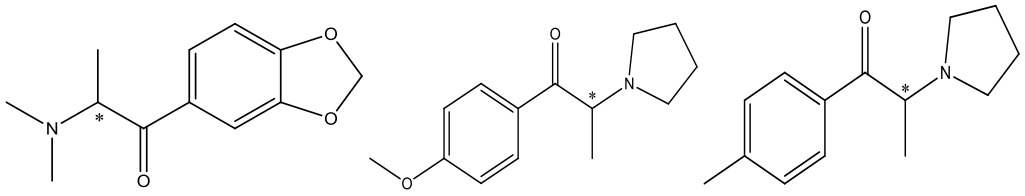

Scheme 15: Structures of tertiary amine synthetic cathinone derivatives that analyzed quantitatively

4.2 Materials and methods

4.2.1 Chromatographic condition

Separation of the enantiomers of cathinone related compounds has been performed on Agilant HP 1200 series HPLC system coupled with UV-VIS detector. λ_{max} for ultraviolet (UV) measurement was 270 nm in the collection range from 200 nm to 600 nm on the diode array detector. Mobile phase composition was: hexane, isopropanol (IPA) and triethylamine (TEA), (99 : 1.0 : 0.1), respectively. The flow rate was 0.5 mL/min in an isocratic condition. Two commercially available columns were used, namely Astec Cellulose DMP chiral column, 150 mm, 4.6 mm, in which dimethylphenyl carbamate-derivatized cellulose (DMPC) was coated on 5 µm silica-gel and CHIRALPAK AS-H Amylose column, 150 mm, 4.6 mm, in which Amylose tris [(S)-α-methylbenzylcarbamate] was coated on 5 µm silica gel. For both columns, the column temperature was set at 40 ^{o}C. Prior to injection, the needle was flushed with 100 µl of the mobile phase.

4.2.2 Chemicals

All solvents used in this study were of HPLC grade. Hexane, acetic acid, methanol, 2-propanol, triethylamine, ammonium hydroxide, dichloromethane and sodium phosphate were obtained from Sigma–Aldrich Chemicals (St. Louis, MO, USA). Water was of nanopure quality. All analytes in Table 16, were of standard grade (purity > 97%), and purchased from an official supplier, Cayman chemicals (Michigan, USA).

4.2.3 Sample preparation

4.2.3.1 Samples

This investigation conforms to the UAE community guidelines for the use of humans in experiments. The Human Ethics committee at the Dubai police approved the study. Blood and urine samples were collected at Dubai police with subjects' consent.

4.2.3.2 Urine and plasma spiking and SPE

SPE was carried out for the spiked urine and plasma samples as shown in extraction steps of section 2.2.3.2.

4.3 Results

Figure 9 shows the liquid chromatograms for separation of the R and S enantiomers of dimethylone drug on DMP cellulose and AS-H Amylose columns. It was noted that the calculated values of resolution and selectivity factor on the DMP column were 1.23 and 1.06 respectively, while on the A-ASH amylose column, the calculated values of resolution and selectivity factor were 2.54 and 1.25 respectively.

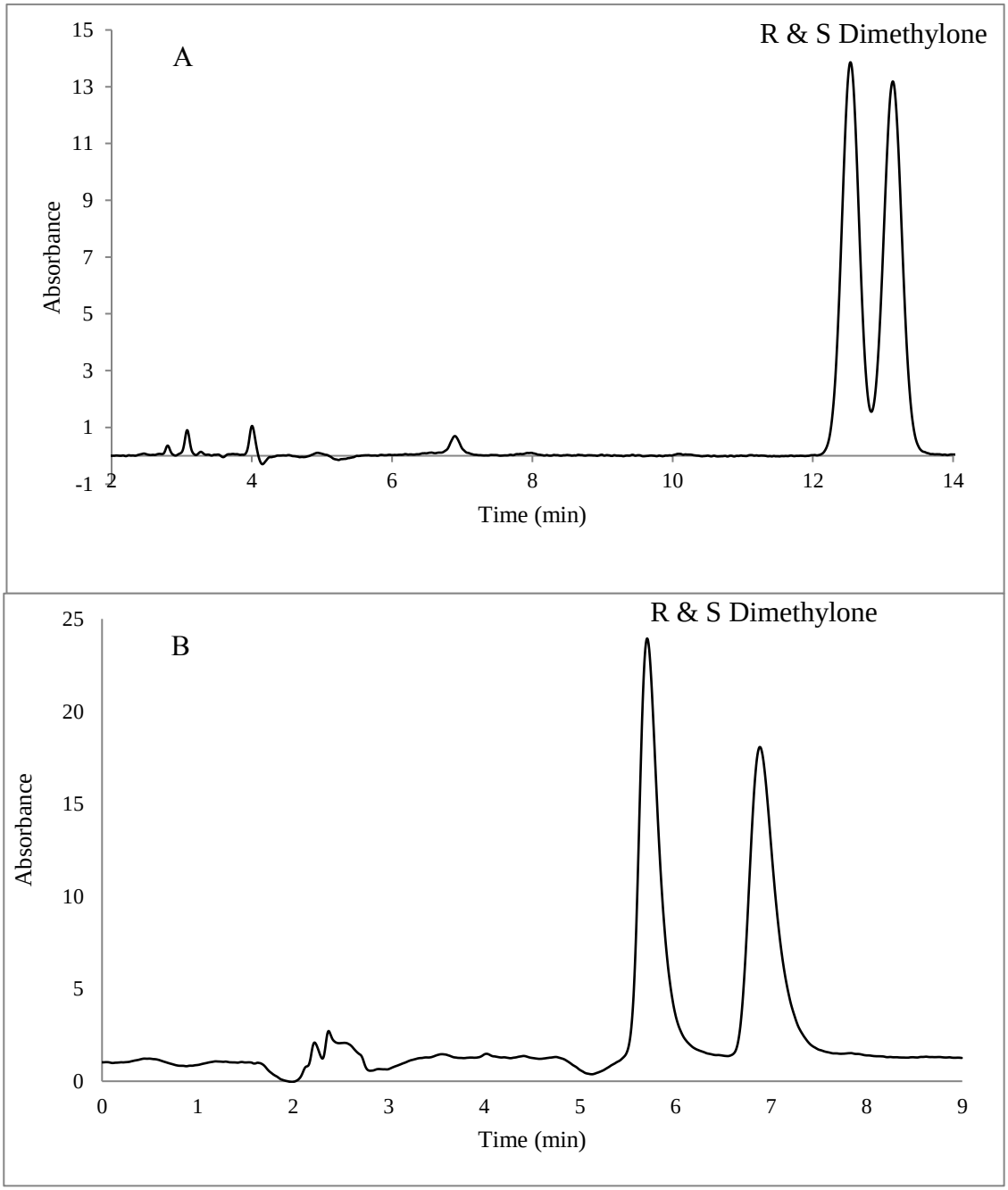

Figure 9: Liquid chromatogram for separation of the R and S enantiomers of 50 ppm of dimethylone drug using: a) on DMP cellulose column and (b) AS-H Amylose column

Tables 23 and 24 shows the list of the 22 tertiary amine cathinone related compounds and their retention times in addition to calculated resolution and selectivity factor for the separated two enantiomers for each compound analyzed on HPLC-UV by DMP cellulose and AS-H Amylose columns, respectively.

Table 23: List of the 22 tertiary amine cathinone related compounds and their synonyms, in addition to the retention times, resolutions (Rs) and selectivity factor (α) of the separated two diasterioisomers for each compound analyzed on HPLC-UV by DMP cellulose column

#	Compound Name	Abbreviation	t_{R1} (min)	t_{R2} (min)	Rs	α
1	Dibutylone	bk-DMBDB	No sep.			
2	Dimethylone	bk-MDDMA	12.54	13.14	1.23	1.057
3	α-Pyrrolidinopropiophenone	α-PPP	7.28	8.05	2.70	1.147
4	N,N-Dimethylcathinone	N,N-DMC	6.49	6.70	1.00	1.048
5	2,3-Methylenedioxy Pyrovalerone	2,3-MDPV	No sep.			
6	2-Methyl-α-Pyrrolidinopropiophenone	2-Methyl-α-PPP	7.06	10.65	10.55	1.708
7	4-Ethyl-N,N-Dimethylcathinone	4-Ethyl-N,N-DMC	5.94	6.17	1.09	1.059
8	3-Methyl-α-Pyrrolidinopropiophenone	3-Methyl-α-PPP	7.19	8.39	3.77	1.231
9	3,4-Methylenedioxy-α-Pyrrolidinopropiophenone	3,4-MD-α-PPP	14.50	15.41	1.45	1.073
10	4-Methyl-N-Methylbuphedrone		No sep.			
11	4'-Methoxy-α-Pyrrolidinopropiophenone	4'-MeO-α-PPP	13.98	15.74	2.89	1.147
12	4'-Methyl-α-Pyrrolidinohexanophenone	4'-Methyl-α-PHP	4.65	5.28	1.62	1.238
13	Diethylcathinone		4.54	5.08	3.37	1.212
14	4-Methyl-α-Pyrrolidinobutiophenone	4-Methyl PBP	5.33	5.51	0.99	1.055
15	α-Pyrrolidinopentiophenone	α-PVP	4.84	4.99	0.95	1.055
16	α-Pyrrolidinobutiophenone	α-PBP	5.48	5.78	1.48	1.086
17	4'-Methyl-α-Pyrrolidinopropiophenone	4'-Methyl-α-PPP	6.91	7.63	2.02	1.148
18	3-Methyl-α-Pyrrolidinobutiophenone	3-Methyl PBP	5.18	5.57	1.86	1.121
19	3,4-Methylenedioxy-α-Pyrrolidinobutiophenone	3,4-MDPBP	11.51	12.00	1.15	1.051
20	N-Ethyl-N-Methylcathinone		5.15	5.63	2.41	1.154
21	2-Methyl-α-Pyrrolidinobutiophenone	2-Methyl PBP	5.34	5.92	2.31	1.172
22	4-Methoxy-N,N-Dimethylcathinone	4-MeO-N,N-DMC	9.71	10.25	1.11	1.071

Table 24: List of the 22 tertiary amine cathinone related compounds and their synonyms, in addition to the retention times, resolution and selectivity factor of the separated two diasterioisomers for each compound analyzed on HPLC-UV by AS-H Amylose column

#	Compound Name	Abbreviation	t_{R1} (min)	t_{R2} (min)	Rs	α
1	Dibutylone	bk-DMBDB	No sep.			
2	Dimethylone	bk-MDDMA	5.70	6.88	2.54	1.251
3	α-Pyrrolidinopropiophenone	α-PPP	No sep.			
4	N,N-Dimethylcathinone	N,N-DMC	2.80	3.08	1.82	1.156
5	2,3-Methylenedioxy Pyrovalerone	2,3-MDPV	No sep.			
6	2-Methyl-α-Pyrrolidinopropiophenone	2-Methyl-α-PPP	2.00	2.64	2.46	1.642
7	4-Ethyl-N,N-Dimethylcathinone	4-Ethyl-N,N-DMC	2.71	2.92	1.50	1.120
8	3-Methyl-α-Pyrrolidinopropiophenone	3-Methyl-α-PPP	No sep.			
9	3,4-Methylenedioxy-α-Pyrrolidinopropiophenone	3,4-MD-α-PPP	No sep.			
10	4-Methyl-N-Methylbuphedrone		No sep.			
11	4'-Methoxy-α-Pyrrolidinopropiophenone	4'-MeO-α-PPP	4.70	5.24	2.27	1.145
12	4'-Methyl-α-Pyrrolidinohexanophenone	4'-Methyl-α-PHP	No sep.			
13	Diethylcathinone		No sep.			
14	4-Methyl-α-Pyrrolidinobutiophenone	4-Methyl PBP	No sep.			
15	α-Pyrrolidinopentiophenone	α-PVP	No sep.			
16	α-Pyrrolidinobutiophenone	α-PBP	No sep.			
17	4'-Methyl-α-Pyrrolidinopropiophenone	4'-Methyl-α-PPP	No sep.			
18	3-Methyl-α-Pyrrolidinobutiophenone	3-Methyl PBP	No sep.			
19	3,4-Methylenedioxy-α-Pyrrolidinobutiophenone	3,4-MDPBP	4.69	5.22	2.99	1.144
20	N-Ethyl-N-Methylcathinone		No sep.			
21	2-Methyl-α-Pyrrolidinobutiophenone	2-Methyl PBP	2.10	2.24	1.37	1.123
22	4-Methoxy-N,N-Dimethylcathinone	4-MeO-N,N-DMC	No sep.			

All the separated enantiomers have shown resolution values above 1 and the selectivity factors were above 1 as well. The DMP cellulose column was more efficient in separating the cathinone related drugs with tertiary amine functionality more than the AS-H amylose column. This is obvious from Table 23 where only three of the investigated 22 compounds were not separated while in Table 24, fifteen of the investigated compounds were not separated.

Tables 25 and 26 shows the list of the 43 primary and secondary amine cathinone related compounds and their retention times in addition to calculated resolution and selectivity factor for the separated two enantiomers for each compound analyzed on HPLC-UV by DMP cellulose and AS-H Amylose columns, respectively.

Table 25: List of the 43 primary and secondary amine cathinone related compounds and their synonyms, in addition to the retention times, resolutions (Rs) and selectivity factor (α) of the separated two diasterioisomers for each compound analyzed on HPLC-UV by DMP cellulose column

	Compound Name	Abbreviation	t_{R1} (min)	t_{R2} (min)	Rs	α
1	2-Methoxymethcathinone	2-MeOMC	37.61	46.12	4.77	1.239
2	3-Fluoroethcathinone	3-FEC	7.67	9.54	3.62	1.329
3	2-Fluoroethcathinone	2-FEC	5.36	6.67	5.12	1.390
4	4-Fluoroethcathinone	4-FEC	11.41	11.95	1.25	1.058
5	2,3-Methylenedioxymethcathinone	2,3-MDMC	7.38	19.45	18.15	3.244
6	2-Methylmethcathinone	2-MMC	8.81	9.18	1.06	1.055
7	Nor-Mephedrone	-	5.57	7.69	7.56	1.593
8	4-Ethylethcathinone	4-EEC	9.17	9.65	1.27	1.068
9	3,4-Dimethylethcathinone	3,4-DMEC	9.77	11.18	3.19	1.182
10	2-Ethylmethcathinone	2-EMC	7.27	12.56	11.73	2.005
11	3-Methoxymethcathinone	3-MeOMC	25.27	26.23	1.08	1.041
12	2-Ethylethcathinone	2-EEC	9.44	9.77	0.82	1.044
13	2-Fluoromethcathinone	2-FMC	10.16	12.90	4.25	1.336
14	4-Ethylmethcathinone	4-EMC	13.35	14.55	1.51	1.105
15	3-Ethylethcathinone	3-EEC	8.29	8.63	1.16	1.055
16	4-Methylbuphedrone	-	7.80	8.32	1.68	1.090
17	2,3-Dimethylmethcathinone	2,3-DMMC	15.06	17.55	4.31	1.191
18	3-Ethylmethcathinone	3-EMC	No sep.			
19	3-Fluoromethcathinone	3-FMC	13.66	14.17	0.60	1.044
20	Eutylone	-	14.16	14.81	1.10	1.054
21	4-Fluoromethcathinone	4-FMC	14.98	16.46	2.35	1.114
22	2-Methylethcathinone	2-MEC	10.77	11.09	0.79	1.036
23	Buphedrone	-	No sep.			
24	4-Methyl-α-ethylaminobutiophenone	-	7.08	7.28	0.66	1.039
25	Pentedrone	-	7.26	7.66	1.27	1.075
26	Butylone	-	23.84	24.37	0.62	1.024
27	Pentylone	-	20.07	20.48	0.55	1.023
28	4-Methylethcathinone	4-MEC	10.72	11.12	0.96	1.046

#	Compound Name	Abbreviations	t_{R1} (min)	t_{R2} (min)	Rs	α
29	3,4-Dimethylmethcathinone	3,4-DMMC	16.89	20.48	4.85	1.241
30	Ethcathinone	-	7.39	7.93	1.56	1.100
31	Methedrone	-	45.76	48.46	1.30	1.062
32	3-Methylmethcathinone	3-MMC	6.36	8.55	7.35	1.503
33	4-Bromomethcathinone	4-BMC	18.01	19.36	2.54	1.084
34	3-Bromomethcathinone	3-BMC	15.87	17.37	2.26	1.108
35	Benzedrone	4-MBC	12.52	12.99	1.02	1.045
36	2,4-Dimethylmethcathinone	2,4-DMMC	No sep.			
37	2,4-Dimethylethcathinone	2,4-DMEC	7.92	8.27	1.06	1.059
38	3,4-Methylenedioxy-N-benzylcathinone	BMDP	31.42	35.01	2.43	1.122
39	3,4-Methylenedioxy-N-ethylcathinone	Ethylone	25.22	25.99	0.87	1.033
40	3-Methylbuphedrone	3-methyl BP	9.70	10.11	1.12	1.053
41	N-Ethylbuphedrone	NEB	6.88	7.16	0.93	1.058
42	2,3-Pentylone isomer	-	14.07	15.03	1.78	1.080
43	3-Mehyethcathinone	3-MEC	9.77	10.16	1.08	1.049

Table 26: List of the 43 primary and secondary amine cathinone related compounds and their synonyms, in addition to the retention times, resolution (Rs) and selectivity factor (α) of the separated two diasterioisomers for each compound analyzed on HPLC-UV by AS-H Amylose column

	Compound Name	Abbreviation	t_{R1} (min)	t_{R2} (min)	Rs	α
1	2-Methoxymethcathinone	2-MeOMC	8.35	9.92	3.60	1.214
2	3-Fluoroethcathinone	3-FEC	2.94	3.07	1.07	1.067
3	2-Fluoroethcathinone	2-FEC	No sep.			
4	4-Fluoroethcathinone	4-FEC	3.28	3.55	1.62	1.119
5	2,3-Methylenedioxymethcathinone	2,3-MDMC	9.47	12.54	5.34	1.363
6	2-Methylmethcathinone	2-MMC	4.20	4.75	2.83	1.172
7	Nor-Mephedrone	-	15.30	16.78	1.81	1.103
8	4-Ethylethcathinone	4-EEC	3.05	3.26	1.40	1.104
9	3,4-Dimethylethcathinone	3,4-DMEC	3.45	4.06	3.03	1.247
10	2-Ethylmethcathinone	2-EMC	3.22	3.37	1.10	1.066
11	3-Methoxymethcathinone	3-MeOMC	6.91	8.24	3.72	1.225
12	2-Ethylethcathinone	2-EEC	2.98	3.16	0.87	1.089
13	2-Fluoromethcathinone	2-FMC	9.71	10.25	1.11	1.063
14	4-Ethylmethcathinone	4-EMC	4.42	5.02	2.68	1.177
15	3-Ethylethcathinone	3-EEC	2.88	3.10	1.57	1.117
16	4-Methylbuphedrone	-	3.63	4.36	3.68	1.280
17	2,3-Dimethylmethcathinone	2,3-DMMC	3.82	4.38	2.38	1.196
18	3-Ethylmethcathinone	3-EMC	4.28	5.31	4.87	1.312
19	3-Fluoromethcathinone	3-FMC	4.43	5.10	2.96	1.197
20	Eutylone	-	4.68	4.96	1.15	1.077
21	4-Fluoromethcathinone	4-FMC	5.42	6.42	3.77	1.228
22	2-Methylethcathinone	2-MEC	2.91	3.16	1.66	1.134
23	Buphedrone	-	3.51	4.08	3.31	1.230
24	4-Methyl-α-ethylaminobutiophenone	-	2.57	2.72	1.25	1.098
25	Pentedrone	-	2.98	3.31	2.22	1.169
26	Butylone	-	7.96	9.40	3.19	1.206
27	Pentylone	-	5.83	6.74	2.57	1.190
28	4-Methylethcathinone	4-MEC	3.56	4.00	2.29	1.174
29	3,4-Dimethylmethcathinone	3,4-DMMC	5.30	7.63	7.07	1.543
30	Ethcathinone	-	3.51	3.82	1.73	1.120
31	Methedrone	-	12.27	14.93	3.47	1.236
32	3-Methylmethcathinone	3-MMC	4.03	4.80	3.39	1.253
33	4-Bromomethcathinone	4-BMC	5.16	5.55	1.38	1.094
34	3-Bromomethcathinone	3-BMC	3.75	4.33	3.10	1.214
35	Benzedrone	4-MBC	4.17	5.01	3.10	1.265
36	2,4-Dimethylmethcathinone	2,4-DMMC	3.55	3.88	1.64	1.128
37	2,4-Dimethylethcathinone	2,4-DMEC	2.61	2.72	0.84	1.068

#	Compound Name	Abbreviation	t_{R1} (min)	t_{R2} (min)	Rs	α
38	3,4-Methylenedioxy-N-benzylcathinone	BMDP	13.21	14.43	1.05	1.100
39	3,4-Methylenedioxy-N-ethylcathinone	Ethylone	5.78	6.49	2.15	1.148
40	3-Methylbuphedrone	3-methyl BP	2.98	3.69	3.17	1.361
41	N-Ethylbuphedrone	NEB	2.68	2.82	1.17	1.085
42	2,3-Pentylone isomer	-	5.44	7.37	5.34	1.434
43	3-Mehyethcathinone	3-MEC	2.90	3.09	1.32	1.101

The simultaneous HPLC separations of the enantiomers of the three cathinone derivatives – namely, 4'-methyl-α-Pyrrolidinopropiophenone (4'-methyl-α-PPP), Dimethylone and 4'-methoxy-α-Pyrrolidinopropiophenone (4'-MeO-α-PPP) on the DMP cellulose column- after being spiked into urine and plasma are reported in Figures 10 and 11 respectively.

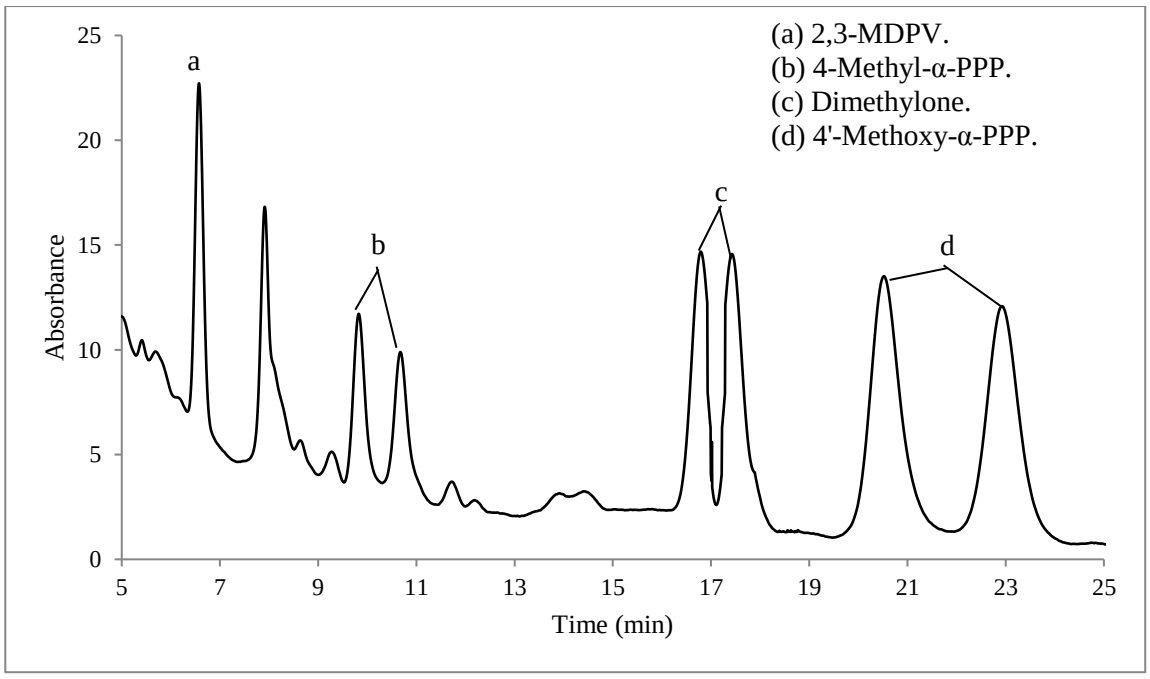

Figure 10: Total ion chromatogram (TIC) of the simultaneous chiral separation of 4'-methyl-α-PPP, Dimethylone and 4'-MeO-α-PPP in urine sample by HPLC-UV system

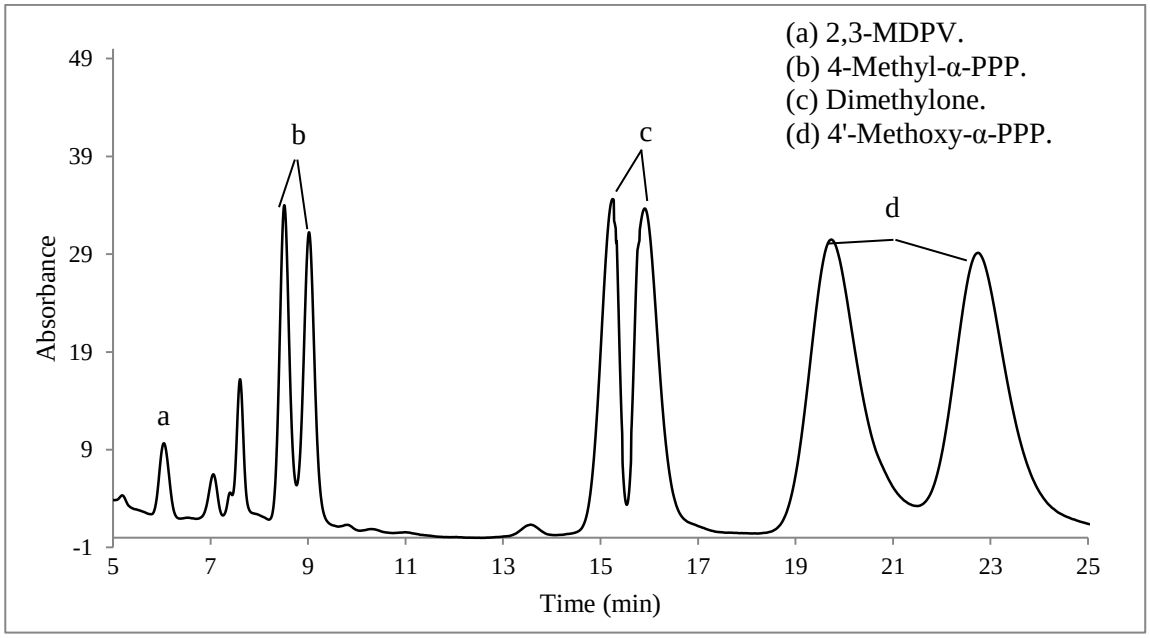

Figure 11: Total ion chromatogram (TIC) of the simultaneous chiral separation of 4'-methyl-α-PPP, Dimethylone and 4'-MeO-α-PPP in plasma sample by HPLC-UV system

Furthermore, the quantitative analysis method of these three cathinone derivatives has been reported in urine and plasma samples. For instance, Figure 12, shows the calibration graphs of the two separated enantiomers of the 4-Methoxy-a-PPP compound in urine (a & b), and in plasma (c & d). The calibration range was 5-250 ppm.

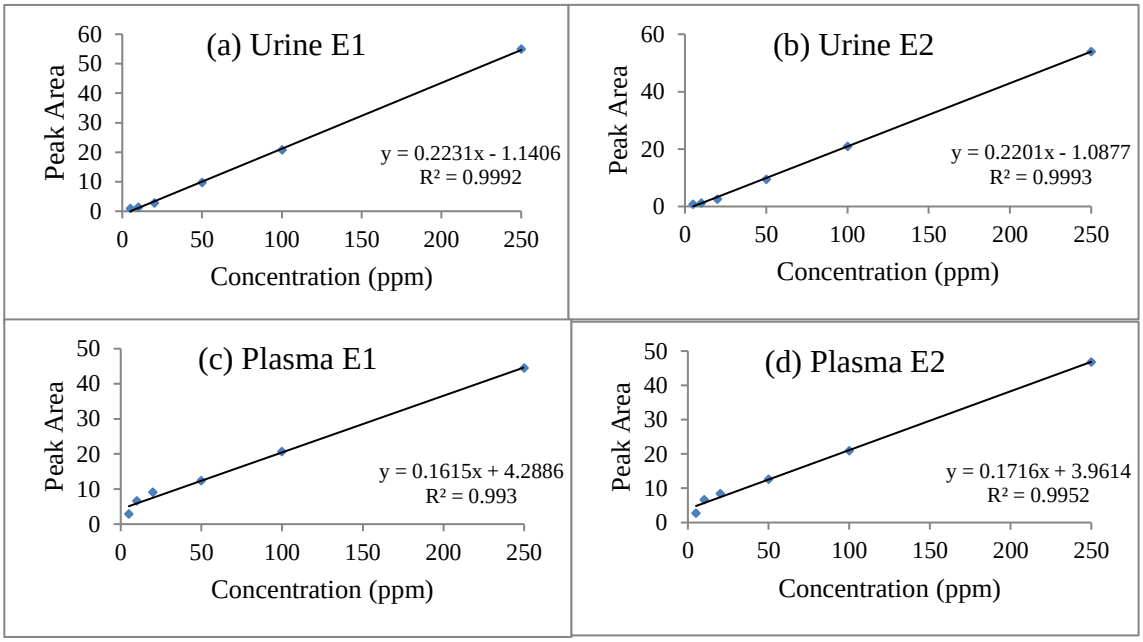

Figure 12: Calibration graphs of the two separated enantiomers of the 4-Methoxy-a-PPP compound in (a & b) urine, and (c & d) in plasma. Calibration ranges was 5-250 ppm

For method validation, the following parameters have been taken into consideration: linearity, limit of detection (LOD) and quantitation (LOQ), recovery studies and intra- and inter-day assay in terms of reproducibility. Linearity was tested by constructing of calibration curves for each enantiomer of the three cathinone derivatives in spiked urine and plasma ranging from 5 to 250 ppm for (4'-methyl-α-PPP), Dimethylone, and 4'-methoxy-α- (4'-MeO-α-PPP). Moreover, the LOD and LOQ have been reported in plasma and urine matrices in Tables 27 and 28, respectively.

Table 27: Results for three cathinone related compounds spiked in plasma including linearity coefficient, R^2 values, Limits of detection and limits of quantitations for the two enantiomers of each compound

		R^2 ± SD		LOQ ± SD (ppm)		LOD ± SD (ppm)	
	Name	E1	E2	E1	E2	E1	E2
1	4'-Methyl-α-PPP	0.9954 ± 0.0026	0.9958 ± 0.0029	3.8 ± 0.1061	4.3 ± 0.1318	1.28 ± 0.0350	1.43 ± 0.0435
2	Dimethylone	0.9932 ± 0.0038	0.9954 ± 0.0036	3.0 ± 0.1441	3.1 ± 0.1073	0.99 ± 0.0476	1.04 ± 0.0354
3	4'-MeO-α-PPP	0.9957 ± 0.0035	0.9965 ± 0.0025	3.6 ± 0.1860	3.9 ± 0.1648	1.18 ± 0.0614	1.31 ± 0.0544

Table 28: Results for three cathinone related compounds spiked in urine including linearity coefficient, R^2 values, Limits of detection and limits of quantitations for the two enantiomers of each compound

		R^2 ± SD		LOQ ± SD (ppm)		LOD ± SD (ppm)	
	Name	E1	E2	E1	E2	E1	E2
1	4'-Methyl-α-PPP	0.9943 ± 0.0030	0.9920 ± 0.0009	1.8 ± 0.1426	1.9 ± 0.1443	0.59 ± 0.0470	0.63 ± 0.0476
2	Dimethylone	0.9924 ± 0.0010	0.9917 ± 0.0027	0.52 ± 0.0644	0.55 ± 0.0694	0.17 ± 0.0213	0.17 ± 0.0229
3	4'-MeO-a-PPP	0.9922 ± 0.0008	0.9941 ± 0.0012	0.43 ± 0.0106	0.445 ± 0.0082	0.142 ± 0.0035	0.147 ± 0.0027

Reproducibility measured in terms of coefficients of variance at three different concentration levels (5, 20 and 100 ppm) within the same day and at two different days in plasma and urine matrices and they were reported in tables 29 and 30, respectively.

Table 29: Inter-day and intraday reproducibility results in terms of coefficient of variance for three cathinone related compounds spiked in plasma at three different concentration levels for the two enantiomers of each compound

		CV% intraday						CV% interday					
		5 ppm		20 ppm		100 ppm		5 ppm		20 ppm		100 ppm	
	Name	E1	E2	E1	E2	E1	E2	E1	E2	E1	E2	E1	E2
1	4'-Methyl-α-PPP	4.69	3.68	0.27	2.57	2.83	3.51	5.39	3.57	3.14	3.83	2.53	2.92
2	Dimethylone	2.48	0.78	0.74	2.45	1.92	3.04	3.32	3.91	1.43	1.75	2.36	2.61
3	4'-MeO- α -PPP	3.03	1.35	1.75	1.22	2.98	2.70	4.81	4.72	3.72	2.31	3.18	2.72

Table 30: Inter-day and intraday reproducibility results in terms of coefficient of variance for three cathinone related compounds spiked in urine at three different concentration levels for the two enantiomers of each compound

		CV% intraday						CV% interday					
		5 ppm		20 ppm		100 ppm		5 ppm		20 ppm		100 ppm	
	Name	E1	E2	E1	E2	E1	E2	E1	E2	E1	E2	E1	E2
1	4'-Methyl-α-PPP	1.38	2.87	1.95	0.47	0.27	0.36	1.74	2.30	1.47	1.41	1.30	1.31
2	Dimethylone	1.41	1.53	2.08	2.69	2.46	2.12	1.68	1.41	3.12	2.87	2.50	2.46
3	4'-MeO- α -PPP	0.79	1.68	1.58	1.63	1.54	1.79	0.86	2.26	1.43	1.48	1.58	1.60

Finally, the method accuracy was reported as percent error for three concentration levels, 50, 100 and 250 ppm in plasma and urine matrices, through recovery measurements for each enantiomer of the three cathinone compounds as shown in Tables 31 and 32, respectively.

Table 31: Recovery measurements expressed in percent errors for three different concentrations of the cathinone related compounds spiked in plasma matrix

		Error %					
		50 ppm		100 ppm		250 ppm	
	Cathinones	E1	E2	E1	E2	E1	E2
1	4'-Methyl-α-PPP	2.75	5.28	4.68	11.86	0.96	1.78
2	Dimethylone	3.55	4.65	1.89	1.00	0.10	0.59
3	4'-MeO- α -PPP	0.35	1.08	1.50	0.68	0.49	0.14

Table 32: Recovery measurements expressed in percent errors for three different concentrations of the cathinone related compounds spiked in urine matrix

		Error %					
		50 ppm		100 ppm		250 ppm	
	Cathinones	E1	E2	E1	E2	E1	E2
1	4'-Methyl-α-PPP	9.77	2.06	6.67	6.41	0.66	0.78
2	Dimethylone	2.59	6.96	8.60	2.13	1.26	0.02
3	4'-MeO- α -PPP	3.21	3.33	2.12	0.38	0.50	0.14

4.4 Discussion

In this work, chiral separation was based on the interaction between the analytes and the chiral stationary phase in the column in which one type of the polysaccharide enantiomers has been immobilized on the surface of a solid support. Formation of diastereomeric adsorbates of different stabilities is the reason for the chiral selectivity of the CSP (Płotka, Biziuk et al. 2011). During the elution process, if both enantiomers of analytes have the same interaction with CSP, it will not be able to separate them. Conversely, if they have different way of interaction with CSP, then they will reach the detector at different retention times which will lead to the chiral separation of the racemic mixture. The size of cavities of the poly-saccharides stationary phase plays a principal role in enantioseparation of the cathinone derivatives where the host – guest inclusion reaction takes place between the analytes and the cavity of the CSP. Figure 9, shows that the two columns were able to separate the two enantiomers of dimethylone drug well, however, the values of retention times, resolution and separation factor for each column were not the same. This indicates that the interaction of the dimethylone enantiomers with the cavity of the polysaccharide immobilized on the stationary phase surface was different and involved different interaction mechanisms. It is expected that the separation mechanism of these compounds on the DMP cellulose column depends more on the host – guest inclusion reaction in addition to (π-π) interaction and steric hindrance effect while in the case of the AS-H Amylose column, the inclusion reaction and other factors such as dipole – dipole interaction, hydrogen bonding, and (π-π) interaction (Mohr, Taschwer et al. 2012) are participating in the separation process.

Mohr et al. have reported the chiral separation of synthetic cathinone compounds on CHIRALPAK AS-H column using HPLC-UV system. Amongst the 24 compounds analyzed, there were 5 synthetic cathinone with tertiary amine functional group (Mohr, Taschwer et al. 2012). However, it was noticed that all of the synthetic cathinones in the previous study have been separated except 4 tertiary amine cathinones: MDPV, MPPP, α-PPP and naphyrone. They have explained this observation based on the fact that AS-H column, which consists of amylose tris [(S)-a-methylbenzylcarbamate] as CSP, was not suitable for enantioseparation of cathinones that has nitrogen atom included in a ring (Mohr, Taschwer et al. 2012). However, in this study, the focus was on the enantioseparation of tertiary amine synthetic cathinones by using dimethylphenyl carbamate-derivatized cellulose (DMPC) as CSP which shows good separation results for 19 compounds out of 22 as shown in Table 23, without an interfering peak at the same retention time of the analytes of interest. 2,3-MDPV was one of the compounds that did not get separated in this work and this can be explained on the basis of steric hindrance that prevent the host – guest inclusion reaction between the drug of interest and the DMPC immobilized molecule in CSP. Due to lack of interaction between 2,3-MDPV and CSP, it appears as one peak in the HPLC chromatogram which let us to decide to use it as an internal standard (IS) for the quantitative analysis in spiked biological sample. Interestingly, 13 compounds of the separable cathinone derivatives in Table 23 are compounds that have nitrogen atom included in the ring structure. Unlike AS-H column, Astec Cellulose DMP column is not affected by ring that contains the nitrogen group and it can differentiate between enantiomers of tertiary amine cathinones easily.

Figures 10 and 11, show the simultaneous chiral separation of a mixture of 4'-methyl-α-PPP, Dimethylone and 4'-MeO-α-PPP that has been spiked into samples of plasma and urine, respectively. Method linearity has been tested for the three cathinone derivatives that have been chosen for quantitative analysis in spiked urine and plasma and gave comparable results in the concentrations of: 5, 10, 20, 50, 100 and 250 ppm. Correlation coefficients for spiked cathinones are higher than 0.99 as shown in Figure 12 and Tables 27 & 28. Limit of detection (LOD) and limit of quantitation (LOQ) were also calculated for each enantiomer in spiked urine and plasma. It was found that the LODs of these cathinone derivatives in urine were in the range of 1 -1.47 ppm; while in plasma, the LODs were in the range of 0.14 -0.67 ppm. The LOQs in urine were in the range of 3.03- 4.46 ppm and in plasma they were in the range of 0.42 - 2.04 ppm. The results in Tables 29 and 30 show intra- and inter-assay precision reported at three different levels, 5, 100 and 200 ppm. The coefficient of variance were in the range of (0.27-5.39)% in plasma and (0.47-3.12)% in urine which lies in the acceptable range. Tables 31 and 32 show the method recovery and accuracy in terms of percent error and they are less than 10% which match the international criteria and tell us that that SPE process displayed good efficiency.

4.5 Conclusion

In conclusion, development of a sensitive and a selective method for detection and quantitation of tertiary amine cathinone related compounds using HPLC-UV system with Astec Cellulose DMP chiral column has been done successfully. To our knowledge, 18 compounds of tertiary amine synthetic cathinones were separated into their optical enantiomers successfully for the first time. 2,3-MDPV was used as an internal standard in cathinones quantitation which showed good stability. Three of the tertiary amine cathinones derivatives were separated in one chromatogram simultaneously after being spiked in urine and plasma samples. It was found that the LODs of these cathinone derivatives in urine were in the range of 0.1 -0.7 ppm; while in plasma, the LODs were in the range of 0.17 -1.33 ppm. The LOQs in urine were in the range of 0.29 - 2.14 ppm and in plasma they were in the range of 0.50 - 4.01 ppm. The method recoveries reported in percent error had an overall average value around 2.4% and 3.2% in plasma and urine respectively; while inter-day and intra-day reproducibilities reported at three different levels, 5, 100 and 200 ppm, in terms of coefficient of variance were in the range of (0.27-5.39) % in plasma and (0.47-3.12) % in urine which lies in the acceptable range.

Chapter 5: Determination of p-aminohippuric acid with β-Cyclodextrin sensitized fluorescence spectrometry

5.1 Introduction

The correct determination of effective renal plasma flow (ERPF) is crucial to evaluate kidney function in clinical or research settings. One of the commonly used markers for estimating ERPF is *para*-amino hippuric acid (PAH), since it is freely filtered at the glomerulus and undergoes extensive secretion and negligible reabsorption within renal tubules when it has low plasma concentration (Baccard, Hoizey et al. 1999). Many analytical methods have been established to measure PAH in plasma and urine, such as UV/Vis spectroscopy (Karabacak, Cinar et al. 2012), HPLC with UV detection (Decosterd, Karagiannis et al. 1997, Marsilio, Dall'Amico et al. 1997, Agarwal 1998, Dowling, Frye et al. 1998, Kos, Moser et al. 2000, Farthing, Sica et al. 2005), electrochemical detections (Guan, Wu et al. 2005) and tandem mass spectrometry (Han, Shaw et al. 2009, Fan, Lin et al. 2010). Although PAH shows fluorescence activity, few reports have studied the determination of PAH using HPLC – Fluorescence detection (Song and Hsu 1996).

In the last two decades, the macro cyclic oligosaccharides cyclodextrins, which consist of glucopyranose units attached together, were reported to form enormous host-guest inclusion complexes, enhancing the analytical signal of the guest molecules and therefore enhancing the sensitivity of their analytical detections in aqueous media. When the guest molecules are non-covalently encapsulated inside the cyclodextrin cavity, a modification of their chemical and physical properties always occurs due to the altered microenvironment, as well as confinement and isolation from the surrounding medium such as the enhancement in solubility and fluorescence emission (Manzoori and Amjadi 2003). As a result, the use of

cyclodextrins in improving drug solubility and stability and in particular in analytical sensing has increased in popularity.

In fact, the plan was to study the inclusion reaction between cyclodextrins as a host molecules and synthetic cathinones as a guest molecule, however, these kinds of experiments may need a large amount of the synthetic cathinones which is considered as an expensive and hard to get chemical. As a result of that, an alternative compound (PAH) has been chosen in this study due to the similarity in chemical structure of this compound to cathinone derivatives as shown in Scheme 16.

While aiming at the detection and determination of PAH utilizing the supramolecular approach of β-CD, a sensitive method was developed using two techniques, namely spectrofluorometry and liquid chromatography with fluorescence detection. Fluorescence signals were enhanced with the addition of β-CD in aqueous solutions. The experimental conditions that gave the best results were investigated in terms of cyclodextrin cavity size, concentration of PAH, concentration of cyclodextin, and pH effects. The interaction between PAH and cyclodextrin was investigated and considered as a host – guest inclusion which was evident by DFT calculations and found to be with 1:2 (host-guest) stoichiometry. A calibration curve was established from the spectrofluorometric data in the concentration range 0.05 - 100 μM and the detection limit was determined to be 0.015 μM. HPLC with fluorescence detection was investigated in the presence of β-CD in the mobile phase, during which the effect of concentration of β-CD in the mobile phase was also monitored. Finally, urine samples were spiked with 100 μM and 500 μM of PAH and recoveries were calculated.

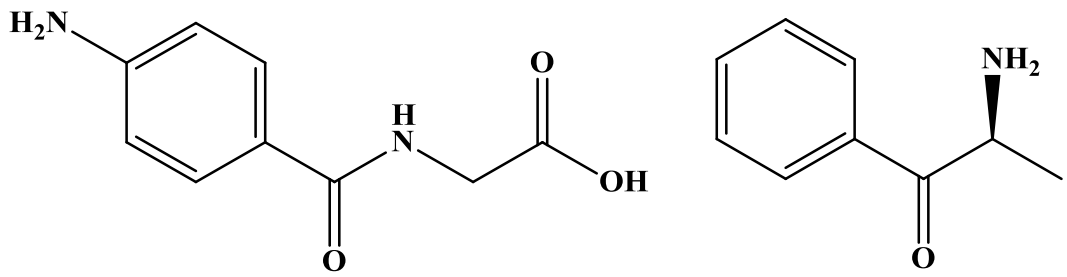

p-aminohippuric acid **Cathinone**

Scheme 16: Structures of cathinone and PAH

5.2 Experimental

para-aminohippuric acid, α-, β- and γ-cyclodextrins, acetic acid and acetonitrile (HPLC grade) were purchased from sigma Aldrich, USA. Doubly distilled water obtained from gradient Milli-Q system (millipore) was used to prepare stock and working solutions. Fluorescence and UV-Visible measurements were carried out using Agilent Cary Eclipse fluorescence spectrofluorometer and Agilent Cary 50/300 UV-visible spectrophotometer, respectively. HPLC data carried out by Agilent 1200 LC system with a fluorescence detector (Agilent, USA).

Liquid chromatographic separation was conducted on Waters Symmetry C18 column (250 mm, 4.6 mm, 5μm) at ambient temperature to achieve the chromatographic separations with isocratic elution. The mobile phase used was 90%, 0.1 M acetic acid in water, 10% acetonitrile and different concentrations of β-CD. The detection wavelengths were set at λ_{ex} = 275 nm and λ_{em} = 355 nm.

A 1 mM PAH solution was prepared in deionized water as a stock solution and it was kept inside a dark vial in the refrigerator. The experimental samples (working) solutions were prepared fresh daily from the stock solution.

UV-visible measurements were done in order to know the right excitation wavelength of PAH for fluorescence measurements.

For the fluorescence measurements, the concentration of PAH was fixed and cyclodextrin concentration was varied. Different variables were tested in order to reach the best detection conditions. Cyclodextrin type, cyclodextrin concentration and pH were varied. pH was adjusted by adding aliquot amounts of HCl and KOH solutions and then measured using a WTW 330i pH meter with SenTix Mic glass electrode. The mobile phase composition was the same except the concentration of β-CD which was varied from 0 – 15 mM. The sample PAH was pure and no internal standard was thus needed for the spectrofluorometric measurements. On the other hand, analysis of PAH in urine samples was performed after the urine samples was diluted 10 times without further sample processing.

Proton NMR measurements were carried out using Varian, 400 MHz instrument. NMR spectra were collected for the β-CD and PAH separately in D_2O solvent, then a mixture of 0.5 mM PAH and 10mM β-CD in D_2O was measured.

All Density Functional Theory (DFT) calculations were performed using the Gaussian 09 program (M. J. Frisch 2009). The structures of free β-cyclodextrin and para-aminohippuric acid were optimized using the B3LYP functional (D. 1993) and 6-31G(d) basis set. Initial structures of complexes between β-cyclodextrin and para-aminohippuric acid were optimized using the PM3 semiempirical method (Stewart 1989, Stewart 1989). Structures were optimized for binding of one PAH molecule outside and inside the β-CD ring. Additionally, a structure with two PAH molecules, aligned 'head-to-tail' within the β-cyclodextrin cavity was optimized. Resultant optimized structures were further optimized using B3LYP/3-21G followed by

BYLYP/6-31G(d) density functional calculations. Binding energies for PAH with β-CD were calculated with single-point energy calculations on optimized structures, corrected for basis-set-superposition-error using the counterpoise method (Boys and Bernardi 1970, Sílvia Simon 1996) in Gaussian 09.

5.3 Results

UV-visible spectral measurements of β-CD in water and PAH in aqueous solutions with and without β-CD are shown in Figure 13 and 14. While the absorption maximum was not shifted, it was enhanced slightly with the addition of the β-CD (the absorption maximum of guest – PAH - at 275 nm is close to the absorption maximum of host - β-CD – at 258 nm where the host-induced change is difficult to track).

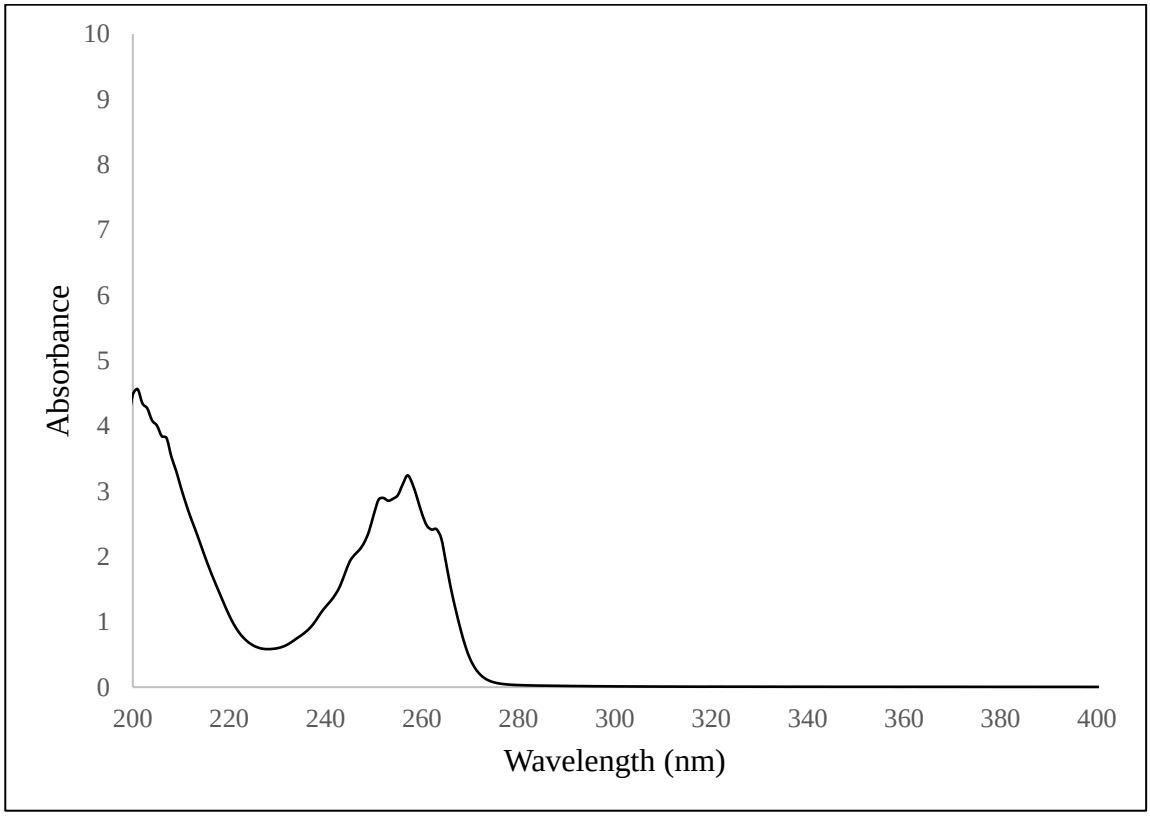

Figure 13: UV-visible absorption spectra of 10 mM β-CD aqueous solution

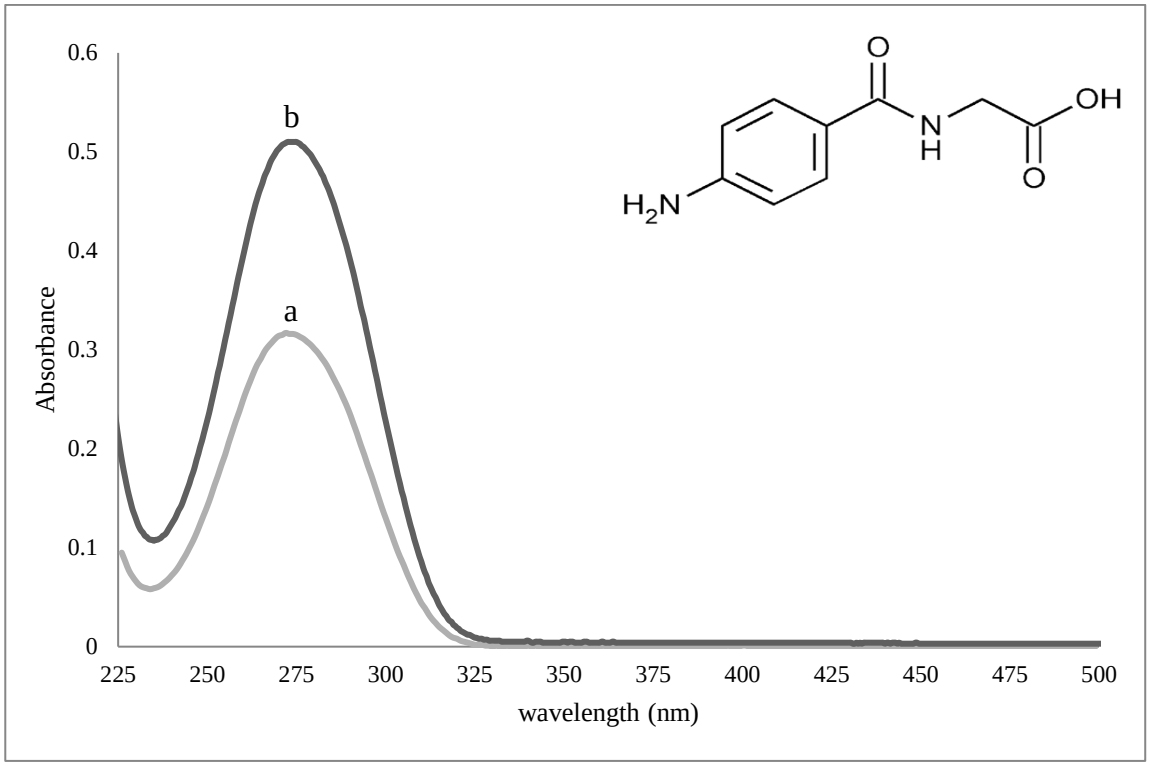

Figure 14: UV-visible absorption spectra of 20 µM PAH in (a) water and (b) β-CD aqueous solution 5.5 µM at pH 4.06

Fluorescence measurements of the PAH in aqueous solution revealed two fluorescence peaks at 305 nm and 355 nm, the first one with low intensity while the second one is of higher intensities as shown in Figure 15. Moreover, the fluorescence peak position of PAH in water was red-shifted when measured in hexane (from 305,355 nm to 395 nm), which indicates that the PAH fluorescence is affected by the surrounding environment such as solvent polarity in agreement with a previous report(Karabacak, Cinar et al. 2012).

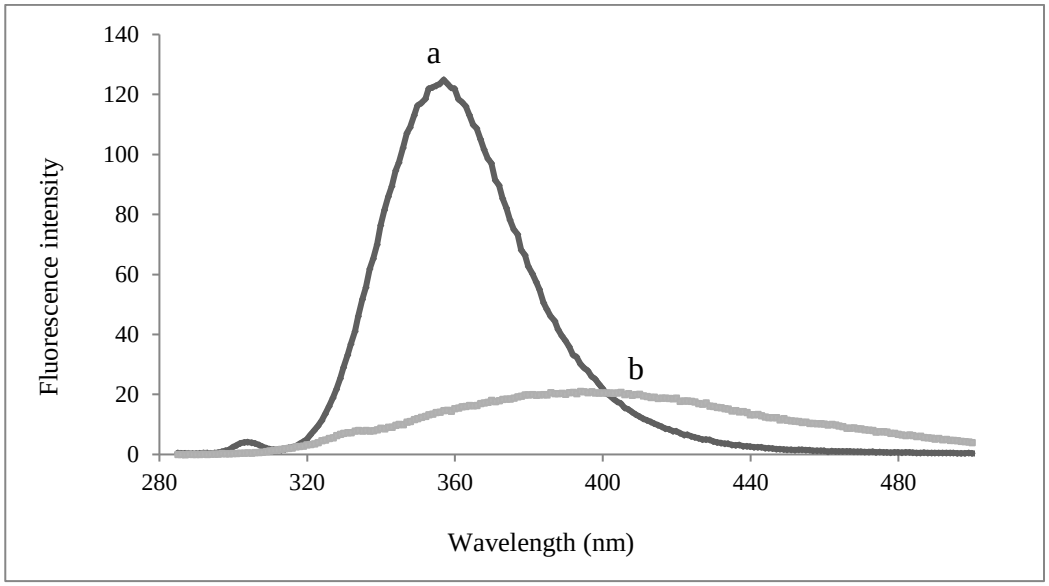

Figure 15: Fluorescence spectra of 100 µM of PAH in (a) water (pH 3.1 and (b) hexane

Figure 16a shows the effect of changing the PAH concentrations on the fluorescence signal of PAH in the absence of β-CD. At low concentration of PAH, around 0.1 µM, the fluorescence at 305 nm is dominant. In order to double check the source of 305 nm peak, and to make sure that it is not a peak that comes from Raman shift of water, a fluorescence measurement was done for a blank water with the same excitation and emission wavelength of the PAH experiment as shown in figure 18.

When the concentration of PAH is increased, the fluorescence at 355 nm increases until it becomes the major emission over that at 305 nm at concentration above 10 µM, (Figure 16a). Figure 16b shows the effect of altering the PAH concentration on the fluorescence profile of PAH at 305 nm and 355 nm in the presence of β-CD. Two scenarios are observed from the measured spectra at concentrations 1 µM and 10 µM; at concentration 1 µM, addition of β-CD has enhanced the emission at 305 nm more significantly than that at 355 nm (10 times vs. 2 times). On the contrary, the fluorescence at 355 nm at concentration 10 µM

overlaid the band at 305 nm with a concomitant double increase in its intensity in presence of the β-CD when compared to that intensity at 355 nm in water. A fluorescence measurement of 15 mM β-CD in water was carried out in figure 17 in order to assure that the enhancement of fluorescence intensity is not from the addition of β-CD.

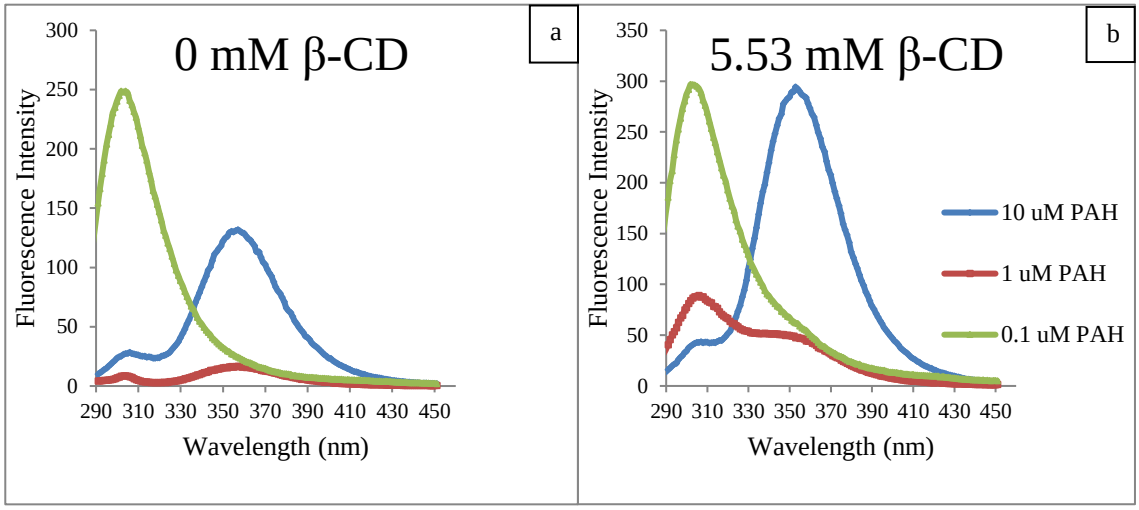

Figure 16: a) Fluorescence spectra of PAH in aqueous solution at concentrations of 0.1,1 and 10 uM, b) fluorescence spectra of PAH at concentrations of 0.1,1 and 10 uM in 5.53 mM β-CD solution

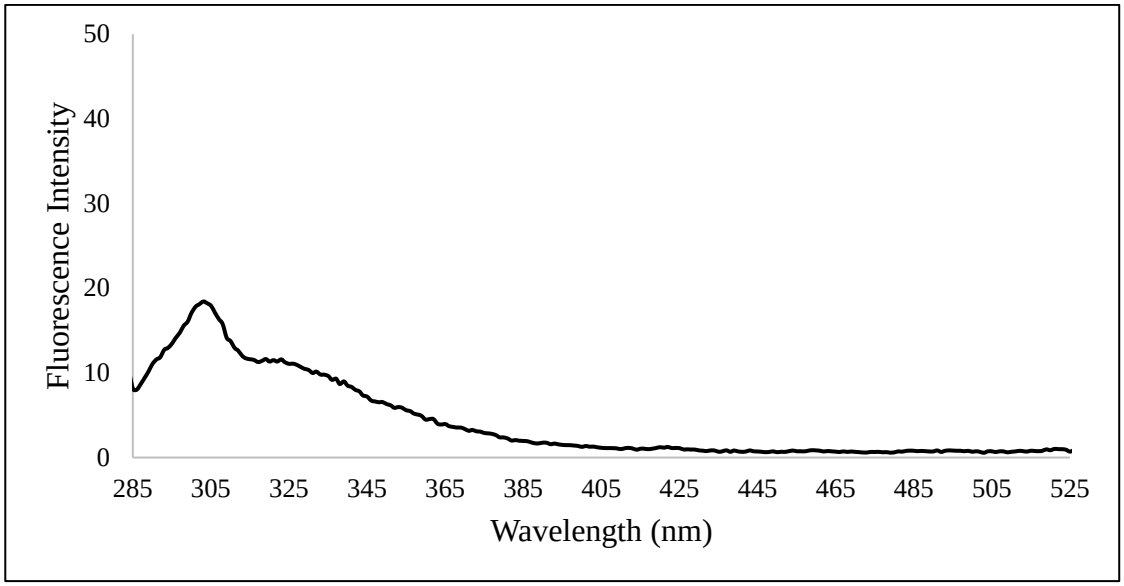

Figure 17: Fluorescence spectra of 15 mM β-CD solution at excitation of 275 nm

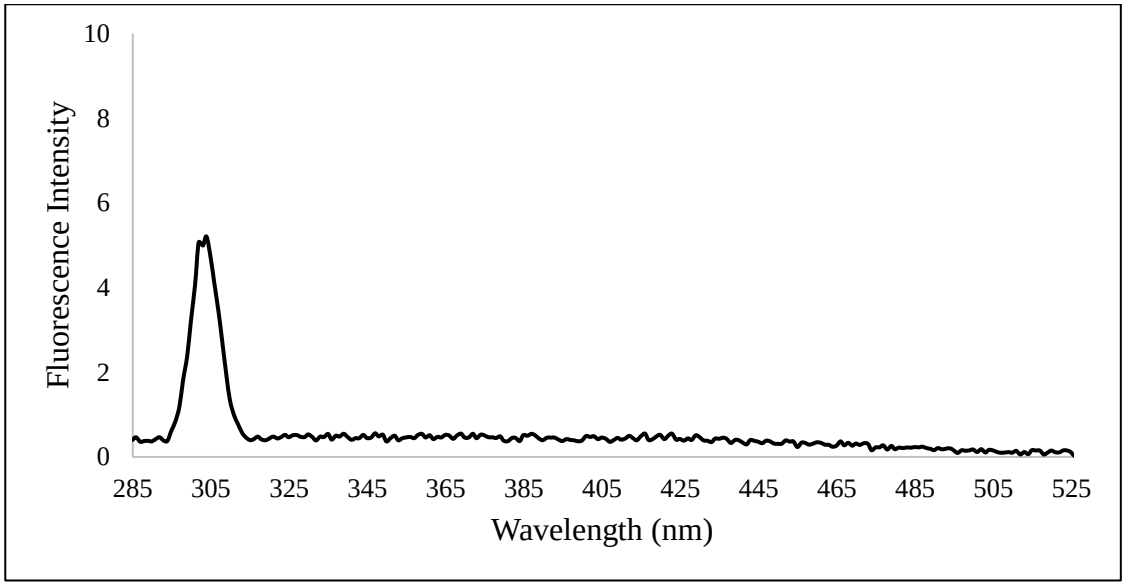

Figure 18: Fluorescence spectra of deionized water at excitation of 275 nm

Figure 19 shows the fluorescence titration measurements of 10 μM PAH in aqueous solution of 0-5.53 mM of α, γ, and β – CD at pH 7. A clear fluorescence enhancement was observed at 355 nm in the presence of β-CD. In contrast, addition of α- and γ-CD enhances the peak at 305 nm. The fluorescence measurements of α, γ, and β – CDs has been calculated individually without the presence of PAH to make sure that they will not interfere guest spectra.

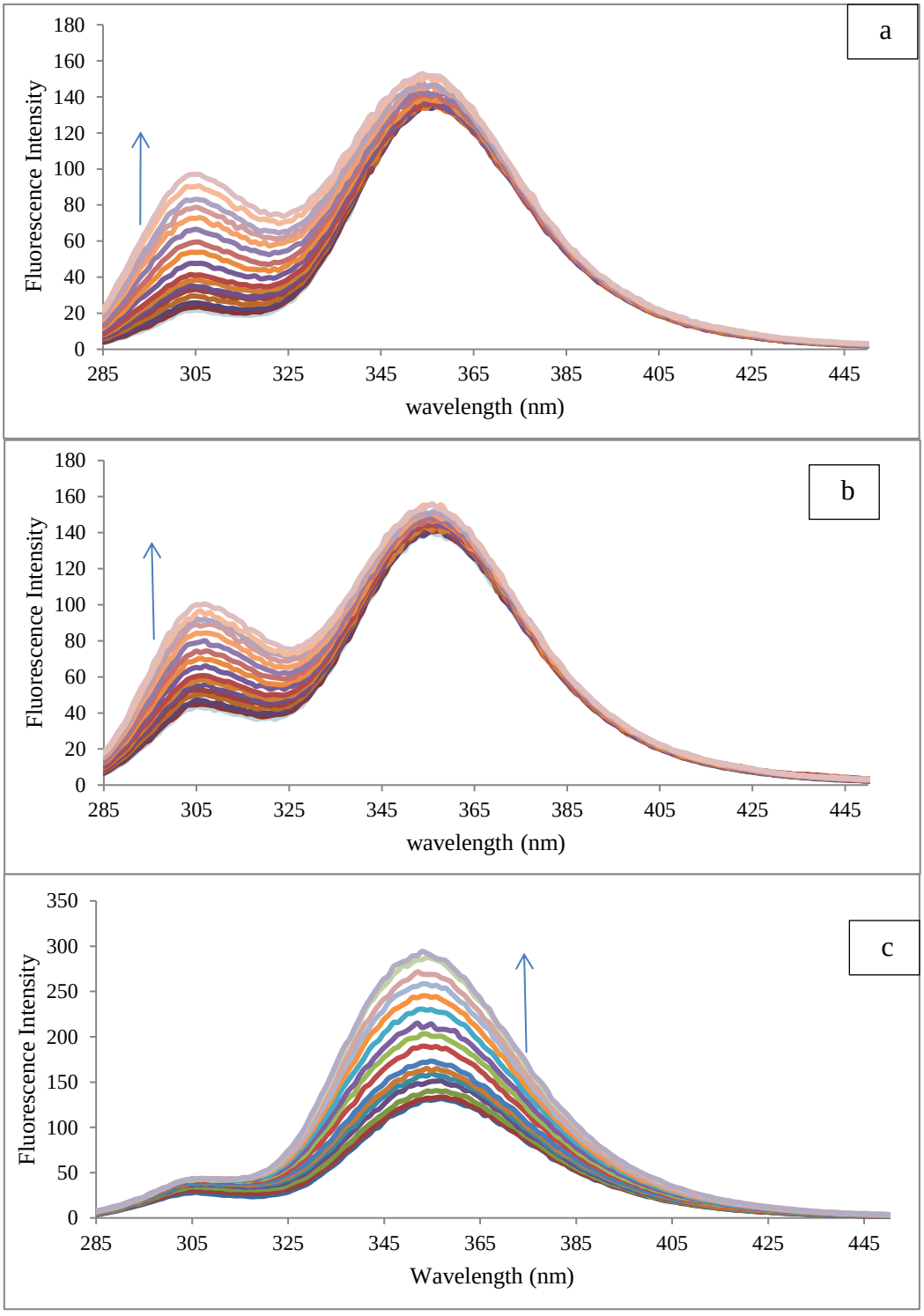

Figure 19: Titration of 10uM PAH and (0 – 5.53mM) of: (A) α-CD, (B) γ-CD and (C) β-CD at pH 6.8

The pH effect on the fluorescence behavior of PAH in β-CD solution was also investigated. Figure 20 shows the titration of 10 μM PAH with 4.09 mM β-CD

in acidic, basic and neutral solutions. After the addition of cyclodextrin, the fluorescence enhancement was more pronounced in acidic solution over that in neutral or basic solutions (three vs. two times).

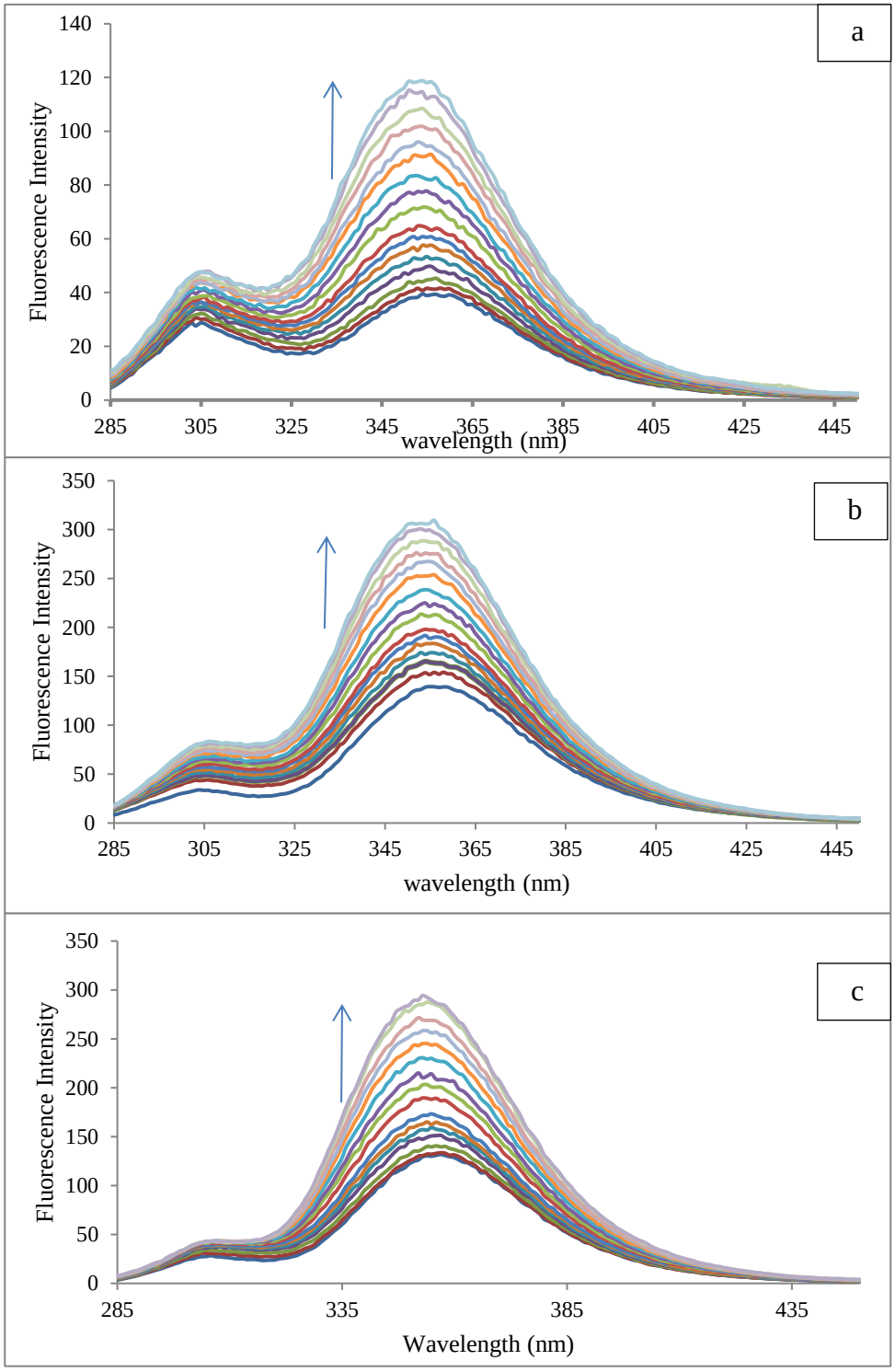

Figure 20: Titration of 10uM PAH and (0 - 5.53) mM β-CD at: (a) acidic, (b) basic and (c) neutral solutions

Theoretical calculations of the guest-host interaction between the PAH and β-CD were conducted using Gaussian 09. The optimized structure of binding of PAH to β-CD outside the β-CD cavity is shown in Scheme 18. Four hydrogen bonding interactions between β-CD and PAH are predicted with bond lengths varying from 1.89 to 2.16 A. The total binding energy after BSSE correction was calculated to be -18.2kcal/mole. The optimized structure for one PAH molecule encapsulated within the β-CD cavity is shown in Scheme 19. The encapsulated PAH molecule is predicted to arrange within the β-CD cavity to maximize hydrogen-bonding between the carboxylic acid group and β-CD. Consequently, two hydrogen-bonding interactions are observed, with bond lengths of 1.71 and 1.92 A. These interactions occur on opposite sides of the cyclodextrin ring. Due to the maximizing of these two interactions, the amino group of PAH appears to have little or no interaction with the β- β-CD ring. The calculated binding energy after Basis set superposition error (BSSE) correction is -15.3 kcal/mole. Although this structure is calculated to have lower binding energy than that with the PAH molecule outside of the cavity, it may be preferred in aqueous solutions due to the displacement of water molecules from within the β-CD cavity. The optimized structure for two PAH molecules encapsulated within β-CD is show in Scheme 17.

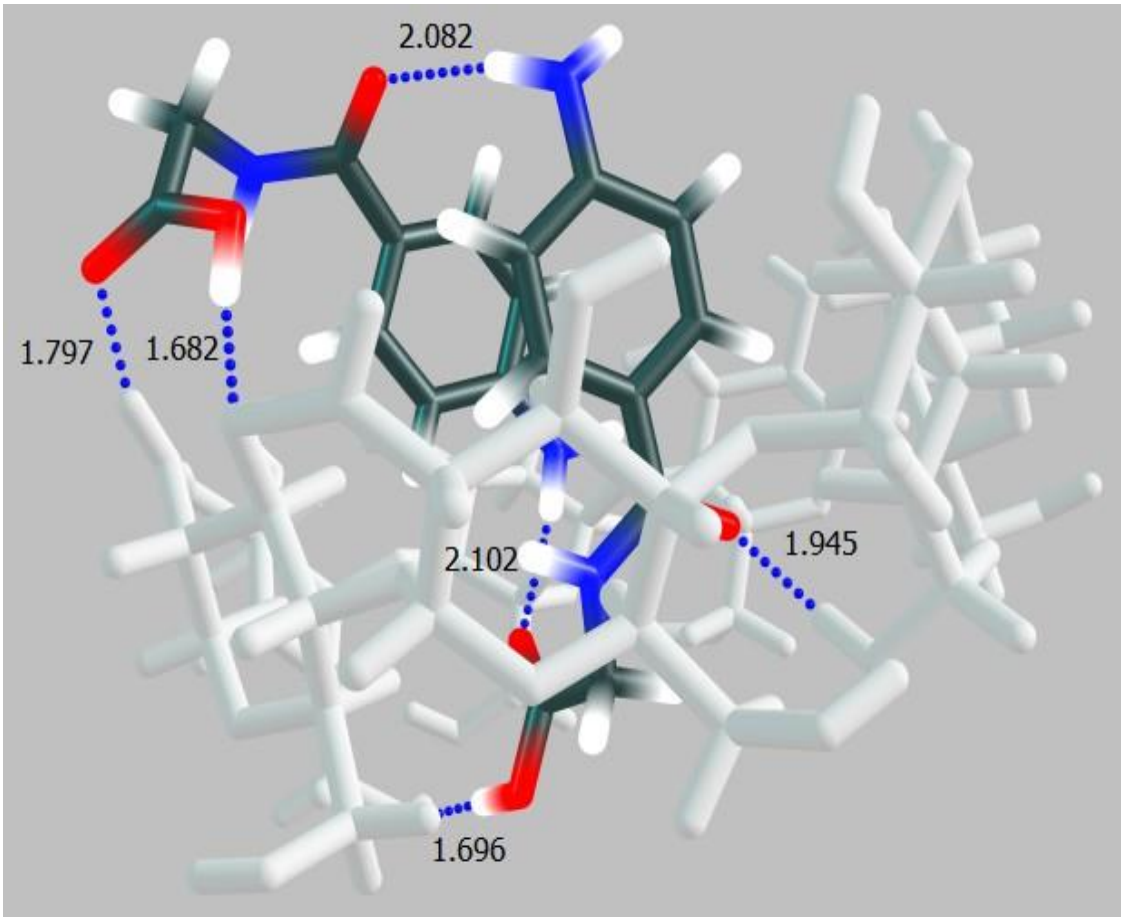

Scheme 17: Optimized gas-phase structure for two PAH molecules inside β-CD cavity

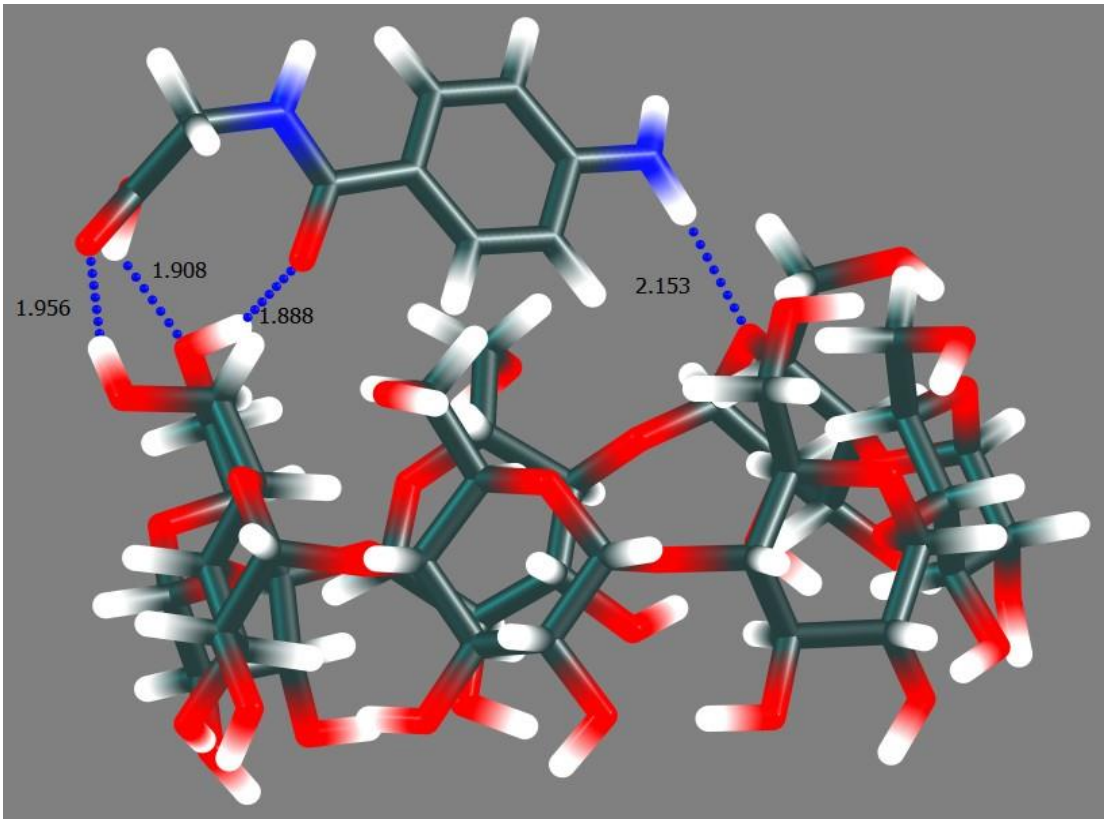

Scheme 18: Optimized gas-phase structure for interaction of PAH and β-CD with PAH outside β-CD cavity

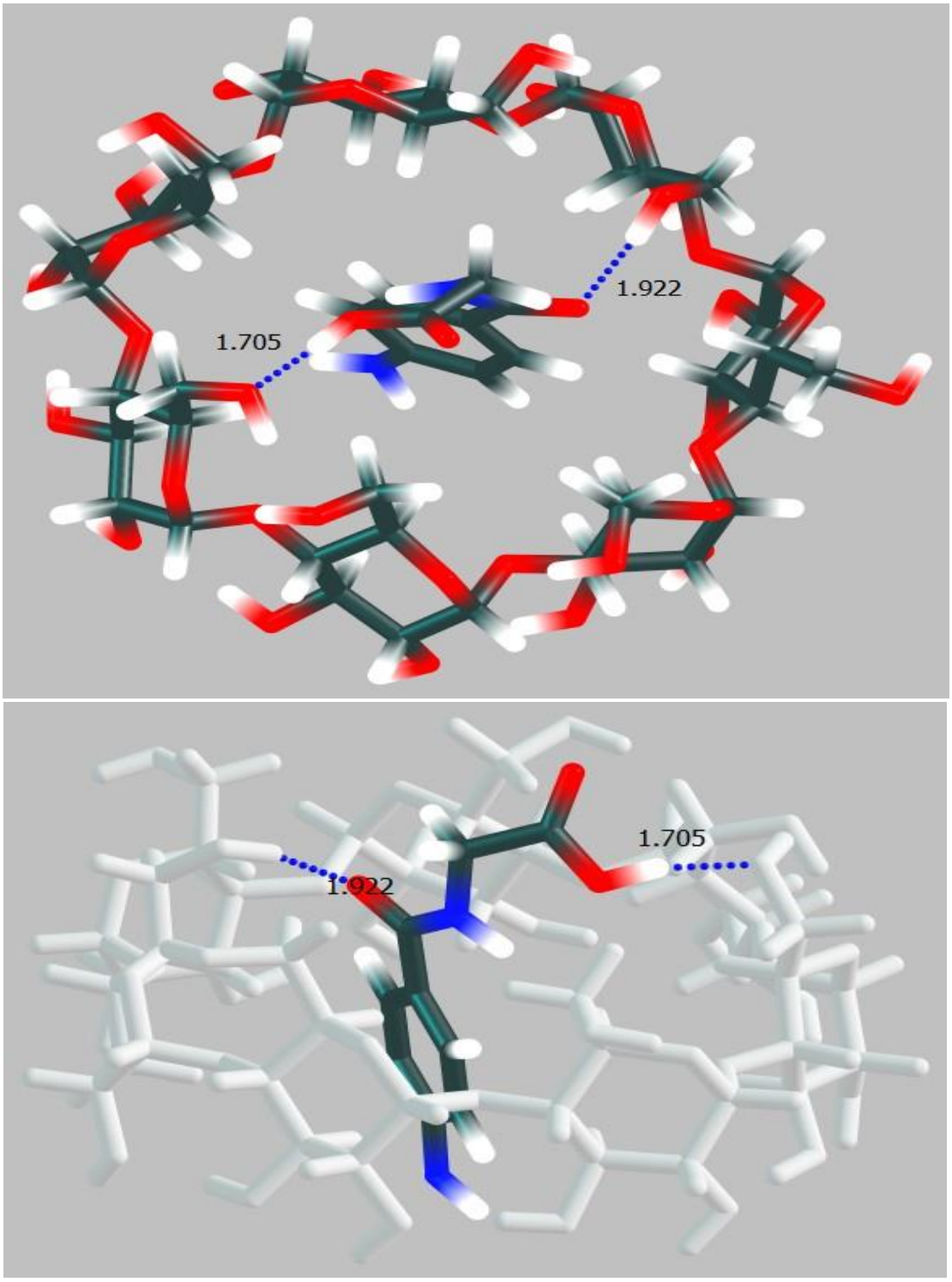

Scheme 19: Optimized gas-phase structure for interaction of PAH and β-CD with PAH inside β-CD cavity

Hydrogen bonding interactions are predicted between the two PAH molecules, and between the PAH molecules and β-CD ring. The optimized structure shows 6 hydrogen-bonding interactions; two between the PAH molecules and four between PAH and β-CD. Bond lengths vary from 1.69 to 2.10 A. The calculated binding energy is =-34.0kcal/mole after BSSE correction. Hence it appears that encapsulation of two PAH molecules is preferred over one, allowing for additional hydrogen-bonding interactions between the two PAH molecules, with subsequent enhancement in binding energy per molecule.

NMR measurements show that there was an inclusion of the PAH inside the cavity of the β-CD indicated by changes in the chemical shifts of the two protons on the ortho-poistion relative to amine group on the benzene ring, as shown in Figure 21.

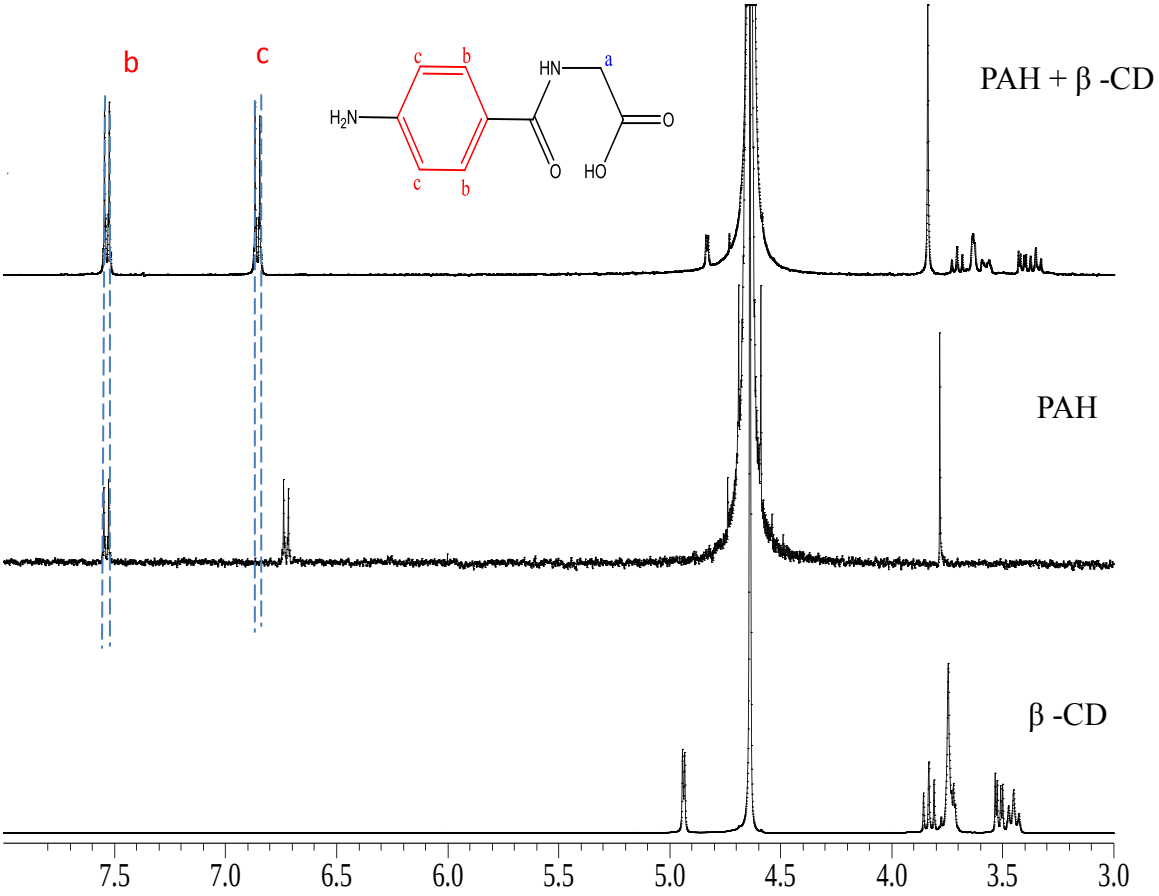

Figure 21: NMR spectra of β-CD (10 mM), PAH (0.5 mM) and mixture of (0.5 mM PAH and 10mM β-CD), all solutions were prepared in D2O Solvent

The observed enhancement in the fluorescence intensity at 355 nm could be used as a tool to develop a spectrofluorometric analytical method for detection and quantitation of PAH in aqueous media by the addition of β-CD. Figure 22 shows the calibration curve of 0.05-100 µM solutions of PAH in the presence of 5 mM β-CD. The correlation coefficient shows a very good linearity over the tested concentration range. Moreover the limit of detection was calculated and found to be 0.015 µM according to IUPAC definition for the limit of detection in analysis (Wilkinson 1997).

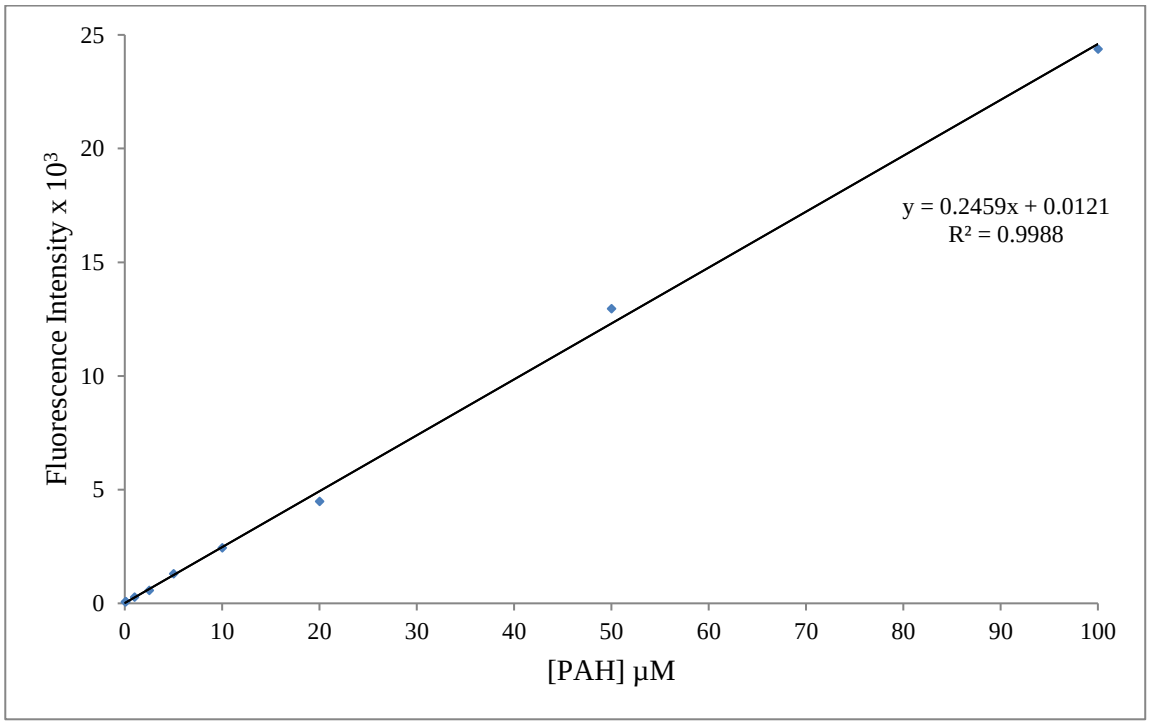

Figure 22: Calibration curve of (0.05 – 100 µM) PAH in aqueous solution containing 15mM β-CD

High performance liquid chromatography coupled with fluorescence detection was used to develop an analytical method for detection of PAH in urine samples. β-CD was added to the HPLC mobile phase at different concentrations in order to see its effect on the fluorescence detection of PAH compound. Figure 23

shows the HPLC-FLD chromatograms for 10uM PAH in the presence β-CD at different concentrations (0-15 mM) in the mobile phase (0.1 M acetic acid in 90:10 (water: acetonitrile). It was observed that the PAH peak area increased as the concentration of the β-CD is increased in the mobile phase.

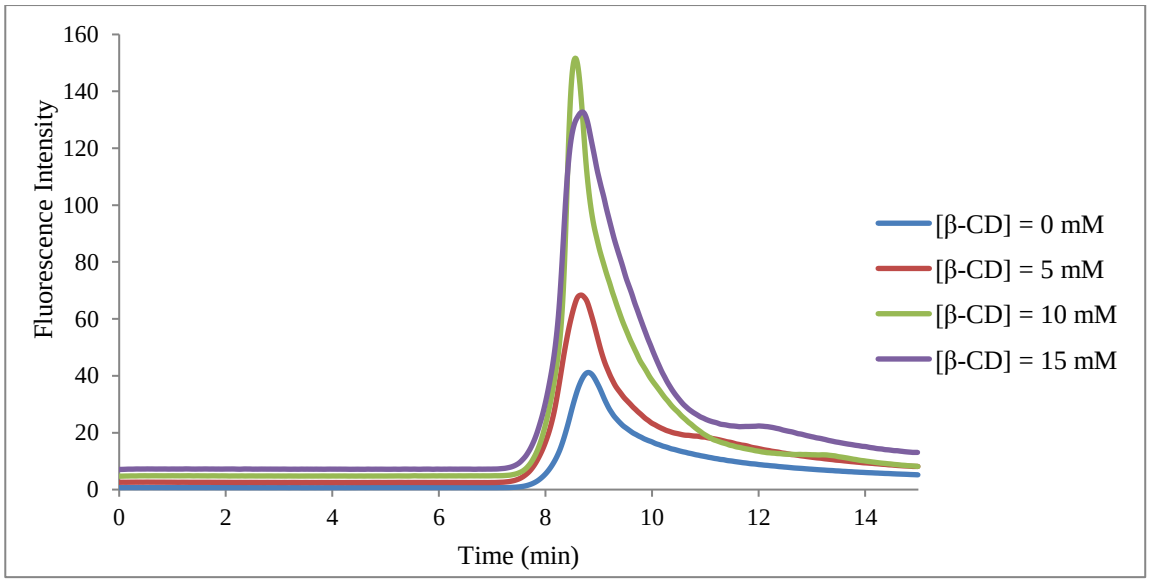

Figure 23: HPLC –FLD chromatograms for 10uM PAH in the presence of different concentrations of β-CD; Mobile phase is 90% 0.1 M acetic acid in water, 10% Acetonitrile

Figure 24 shows the calibration curves of PAH (concentrations range 0.025 - 500 µM) at different concentrations of β-CD in the mobile phase. The correlation coefficients (R^2) of these calibration curves show good linearity of the calibration results. Moreover, it was noted the slope of the calibration curves have shown an increase as the concentration of the β-CD increased which indicates its effect on the enhancement of the method sensitivity.

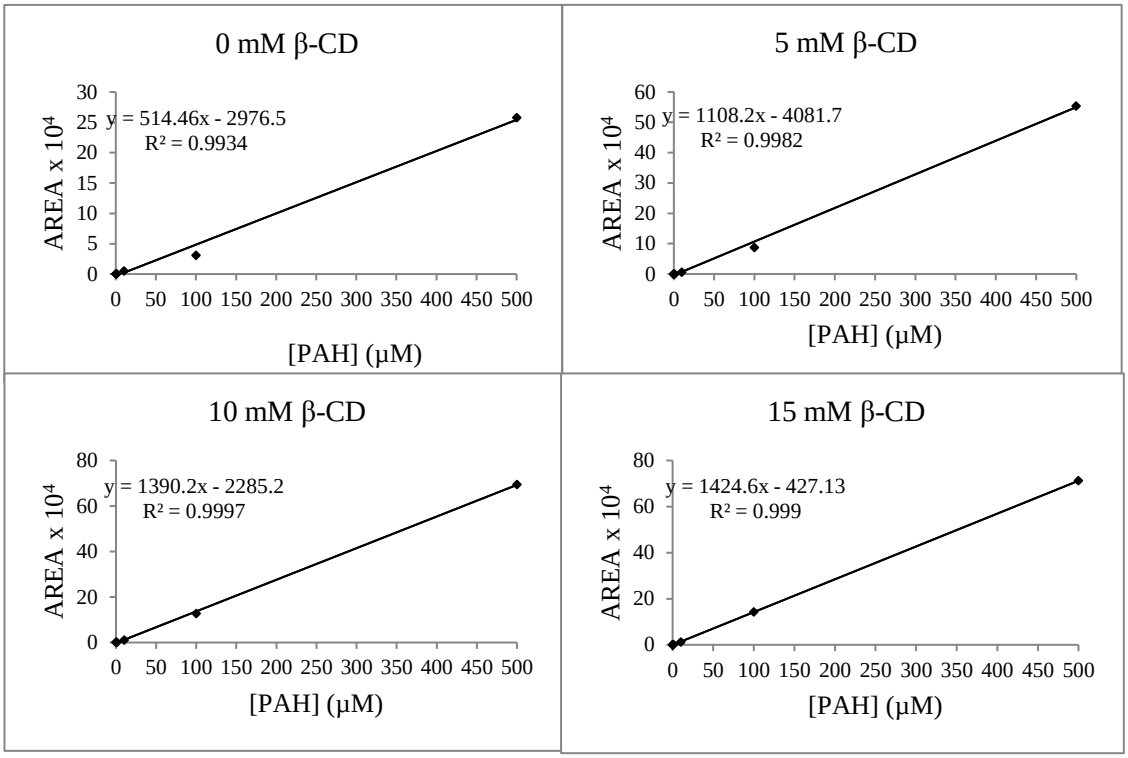

Figure 24: Calibration curves of PAH (Conc. Range 0.025-500 µM) at different concentrations of β-CD in the mobile phase

Figure 25 shows the calibration curve of the PAH in urine matrix in the presence of 4- aminobenzoic acid as an internal standard and β-CD was added to the mobile phase. The curve was established over the concentration range of 10 -500 µM. This curve was used to estimate the levels of PAH in urine after spiking it with two different concentrations of 100 µM and 500 µM.

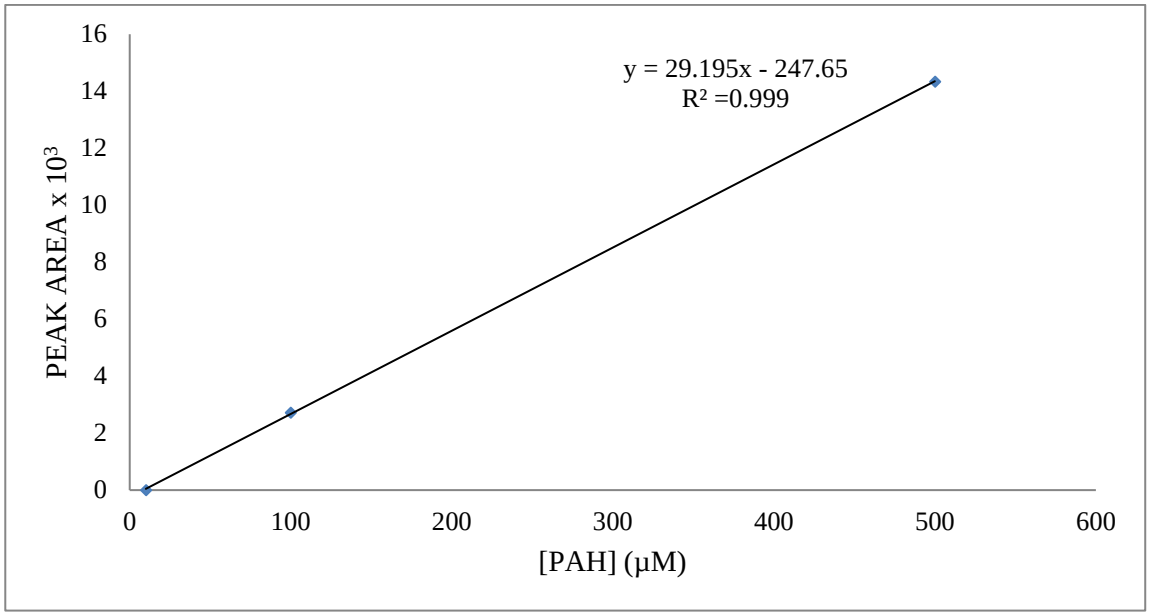

Figure 25: Calibration curves of the HPLC –FLD data of PAH after extraction from urine sample matrix in the presence of 15 mM β-CD in the mobile phase

5.4 Discussion

PAH has shown one absorption peak at 275 nm in aqueous solution at pH 4.06 without β-CD as shown in Figure 14, while the same absorption maximum was observed when β-CD was added to the aqueous solution. However, an increase in the intensity of the absorption was observed, indicating an interaction between the PAH and β-CD. It appears that no new structure such as a dimer or charge transfer complex is formed in the ground state.

Fluorescence measurements for PAH in aqueous and organic solutions are shown in Figure 15. Two fluorescence peaks were observed in aqueous solution at 305 nm and 355 nm, whereas one fluorescence peak at 395 nm was observed in hexane. These results indicate that the fluorescence behavior of PAH is affected by the solvent polarity in agreement with a previous report (Karabacak, Cinar et al. 2012). This primary result encouraged us to study the effects of microenvironment by adding CD to the aqueous solution of PAH and see whether the PAH's fluorescence behavior would be affected or not. The effect of PAH concentration on the intensities of the fluorescence peaks at 305 nm and 355 nm with and without β-CD was obvious. Figure 15 shows that the fluorescence intensity is affected by changing the guest concentrations in the absence and presence of β-CD, thus supporting the assignment of the peak at 355 nm to the formation of excited dimer (excimer) at high concentration of PAH while the peak at low concentration is attributed to the monomer species. β-CD facilitates the excimer formation (Willner, Eichen et al. 1989, Zhang, Deng et al. 2015) by sequestering two PAH molecules within its cavity (see theoretical modeling below). The results in Figure 16 can be also explained by two scenarios depending on PAH concentration: At low concentration of 1 μM, β-

CD prevents aggregation and enhances the intensity of the monomer species over the dimer whereas at higher concentration of 10 μM, host-guest complexation does not compete with excimer formation and the macrocycle binds the dimer as a whole, thus enhancing its fluorescence intensity.

It was noticed that among the three types of the cyclodextrins tested, β-CD has shown an opposite trend to that observed upon the addition of other hosts, (Figure 19). This observation can be explained by the fact that only the larger β-CD cavity is capable of encapsulating two guest units when compared to the smaller cavity of α-CD. Moreover, the cavity size for the γ-CD cavity is very large compared to the size of the PAH molecule, leading to a weaker hydrophobic interaction with a singly encapsulated PAH molecule with a concomitant enhancement in the relevant intensity at 305 nm. We have selectively pursued the use of β-CD in the rest of this study since it shows the optimum size and produces the maximum enhancement of the PAH fluorescence.

The PAH contains $–NH_2$ group that can be protonated or remain neutral depending on the pH values, thus pH effects on the fluorescence behavior of PAH in the absence and presence of β-CD solution in Figure 20 were expected. In the absence of β-CD, the peak at 305 nm is comparable to that at 355 nm at low pH, but decreased relatively with an increase in pH. This is true, since protonation diminishes the extent of dimerization (in principle the dimer is between two neutral units). Thus, in acidic media, the fluorescence intensity of the monomer is higher than that in basic and neutral solutions. The added β-CD thus enhanced the already lower intensity of the dimer band at 355 nm in acidic media as compared to that in neutral and basic media. It transpires that β-CD competes with the protonation of the $–NH_2$ group in

acidic media by virtue of the host-guest complexation, particularly when the concentration is above 10 μM (see Figure 16 above).

The theoretical calculations were performed in the gas phase and do not take into account interactions with solvent molecules. However, they do illustrate strong potential for binding of PAH to the rim of β-CD, and binding of PAH within β-CD. It is possible that binding within the β-CD ring is preferred, despite the lower calculated binding energy, due to the energetically favored displacement of water molecules from the β-CD cavity. The structure with two PAH molecules within the β-CD cavity appears to be even more favorable, introducing hydrogen-bonding between PAH molecules and between PAH and β-CD. The calculations indicate that such a complex is feasible with β-cyclodextrin and may promote the formation of an excimer upon excitation.

NMR data confirm the gust-host interaction where the chemical shifts of the two protons on the ortho-position relative to amine group on the benzene ring occurred.

The observed enhancement in the fluorescence intensity at 355 nm could be used as a tool to develop a spectrofluorometric analytical method for detection and quantitation of PAH in aqueous media containing β-CD. Figure 22 shows the calibration curve of 0.05-100 μM solutions of PAH in the presence of 5 mM β-CD. The correlation coefficient shows a very good linearity over the tested concentration range. Moreover, high performance liquid chromatography coupled with fluorescence detection was used to develop an analytical method for detection of PAH in urine samples. β-CD was added to the HPLC mobile phase at different concentrations in order to see its effect fluorescence detection of PAH compound.

Figure 23 shows the HPLC-FLD chromatograms for 10 µM PAH in the presence β-CD at different concentrations (0.0, 5.0, 10.0 and 15.0 mM) in the mobile phase which consist of 0.10 M acetic acid in 90:10 (water: acetonitrile). It was observed that the PAH peak area of the 10 µM concentration has been increased as the concentration of the β-CD is increased in the mobile phase. Higher concentration of β-CD will raise the probability of host – guest inclusion interaction between β-CD and PAH, thus the complex formation will cause the changes that have been observed in spectral properties of PAH. This result agrees with scientific literature where it was reported that unmodified cyclodextrins can be used as fluorescence enhancing agent in analytical measurements (Wagner and McManus 2003).

Analysis of the PAH in urine sample was conducted by spiking a diluted urine sample with a known concentration of the PAH, 100 and 500 µM. The calibration curve shown in Figure 25 was prepared in a urine matrix and was used to calculate the recovery of the spiked samples. Recovery ranges for 100 µM and 500 µM concentration were found to be in the ranges of 104%-119% and 99%-103%, respectively. It is possible to explain the high values of the recoveries above 100% by the fact that urine sample naturally contains some PAH that will show up even after the dilution that was used during the sample preparation.

5.5 Conclusion

It was possible to develop a sensitive spectrofluorometric method and liquid chromatography with fluorescence detection method for detection and determination of PAH in the presence of β-CD. The fluorescence signal at 355 nm, which is produced as a result of excimer emission, was enhanced upon the use of β-CD in sample preparation. The interaction between PAH and cyclodextrin was considered as host – guest inclusion which was evident by DFT calculations and showed 1:2 (host-guest) interaction. A calibration curve was established for the spectrofluorometric data of PAH with β-CD in the concentration range of 0.05 -100 µM of PAH and the detection limit was 0.015 µM. HPLC with fluorescence detection in the presence of β-CD in the mobile phase has shown an increase in fluorescence detection and the calibration curve slope increased as the concentration of β-CD increased. Finally, urine sample was spiked with 100 µM and 500 µM of PAH and showed recoveries in the range of 104%-118% and 99.2-103% respectively.

Chapter 6: Conclusion

Chirality is an inalienable part of drug research and pharmacology. Chiral compounds such as synthetic cathinone derivatives can differ in toxicity, potency and behavior in human being where each enantiomer has different effect on the chiral biological system. Therefore, enantioseparations of the chiral bioactive molecules have gained a lot of attention from researchers and pharmacologists in order to understand the bioactivity of these compounds.

Chiral separation can be achieved either by direct or indirect techniques. Indirect chiral analysis is about converting the inseparable racemic enantiomers to new products that have different physical and chemical properties which will be separable on achiral stationary phase column. The conversion of enantiomers to diastereoisomers can be done through the derivatization reaction with an optically pure derivatizing agent. In contrast, the use of chiral selector such as polysaccharides compounds can proceed to direct chiral separation. Chiral selector can be either immobilized on the stationary phase of the column or dissolved in the mobile phase of the system. Mostly, direct chiral separation is based on one of the following principles: host – guest inclusion reaction with polysaccharides as a host, hydrogen bonding on a chiral center, or coordination on chiral metal complexes.

In chapters 2 and 3 of this work, development of a sensitive and selective method for detection and quantitation of cathinone related compounds using GC-MS after indirect chiral derivatization with (S)-(–)-N- (trifluoroacetyl)pyrrolidine-2-carbonyl chloride (L-TPC) was possible. In the second chapter, Electron Impact (EI)

has been used as an ionization source while in the third chapter, Negative Chemical Ionization (NCI) source was used in order to enhance the detection sensitivity.

Using GC-EI-MS system in chapter two, the enantiomers of 31 synthetic cathiones were separated; 18 of them were separated as L-TPC derivatives for the first time. Moreover, pentedrone, which has been reported earlier as one of the difficult racemic mixture to separate after L-TPC derivatization, has been separated easily. Well resolved peaks have been observed for most of cathinone derivatives as a result of using 60m HP5-MS capillary column. In order to correct for analyte loss during sample preparation step and sample loss during injection process, nikethamide has been used as an internal standard. It showed good stability and reproducibility. Among the 31 synthetic cathinone compounds, 12 have been chosen to be spiked in urine and plasma as a mixture prior injection to GC-MS. Calibration curves of twelve selected cathinone derivatives in urine were constructed including the following concentrations: 5, 10, 20, 50, 100, 200 ppm. To our knowledge, it is the first time to perform quantitative analysis for synthetic cathinones enantiomers in the spiked biological samples. Validation of the developed method in terms of recoveries, reproducibilities, linearities, LOD, and LOQ for all the tested compounds was also performed. It was found that the LOD's of the 12 cathinone derivatives in urine were in the range of 0.1 -0.7 ppm and in plasma they were in the range of 0.17 -1.33 ppm. The LOQ's in urine was in the range of 0.29 - 2.14 ppm and in plasma it was in the range of 0.50 - 4.01 ppm. The correlation coefficient (R^2) value for each enantiomer for the mixture components was found to be higher than 0.99.

In chapter three, the use of newly developed method of GC-NCI-MS provided high sensitivity and selectivity for the chiral separation and quantitation of

the targeted synthetic cathinone compounds. After derivatization step with L-TPC, 60m HP5-MS Ultra inert capillary column was used to separate 36 compounds of synthetic cathinones to their optical enantiomers. (+)-cathinone was used as an internal standard for synthetic cathinones quantitation which has similar skeleton and chemical structure and showed good stability. A mixture of fourteen cathinone derivatives were spiked in urine and plasma and separated on one chromatogram simultaneously and to our knowledge, it is the highest number of cathinones L-TPC derivatives that have been run as a mixture in one chromatogram. Calibration curves were constructed for each enantiomer in the spiked mixture including the following concentration: 1, 5, 10, 20, 40, 60, 80 and 100 ppb. It was found that the LOD's of the 14 cathinones derivatives in urine were in the range of 0.02 -0.76 ppb and in plasma they were in the range of 0.02 - 0.34 ppb. While the LOQ's of the mixture in urine were in the range of 0.07 - 2.31 ppb and in plasma they were in the range of 0.07 – 1.03 ppb. The correlation coefficient (R^2) values for each enantiomer in the mixture by GC-NCI-MS also found to be higher than 0.99. The developed method has been validated in terms of linearities, limits of detection (LOD), limits of quantitation (LOQ), reproducibilities and recoveries for all tested mixture compounds.

By comparing the results for GC-MS analysis presented in chapter two, where electron ionization was used, with that presented in chapter three, where negative chemical ionization was used, it was found that the later technique has shown higher sensitivity by three orders of magnitudes. Moreover, in both cases, an enhancement in enantiomer peaks resolution was achieved due to the use of Ultra inert 60 m column while using slow heating rate (2 ^{o}C/min) on the GC oven.

Some of the drawbacks of the indirect chiral separation of synthetic cathinones are that it will consume some time in sample derivatization step and is only applicable for the primary and secondary amines synthetic cathinones and it was useless for tertiary amine cathinones since they do not have a derivatizable site i.e., there are no acidic hydrogen on them. As a result of that, an alternative technique that utilize direct chiral separation was investigated. It was found that there are a limited number of papers that discussed chiral separation of synthetic tertiary cathinone derivatives using chiral HPLC chiral column which means that it is not easy to separate these kinds of compounds.

In chapter four, we focused on chiral separation of synthetic cathinones that contain mainly tertiary amines by HPLC-UV system using two commercially available columns that has dimethylphenyl carbamate-derivatized cellulose (DMPC) namely Astec Cellulose DMP column and CHIRALPAK AS-H Amylose column (Amylose tris [(S)-α-methylbenzylcarbamate] coated on 5µm silica-gel), which were used as a chiral stationary phase (CSP). A comparison between the two chiral columns has been conducted in terms of separation resolutrion and selectivity factor. Sensitive and selective method has been established for detection and quantitation of tertiary amine cathinone related compounds using HPLC-UV system with Astec Cellulose DMP chiral column. To our knowledge, 18 compounds of tertiary amine synthetic cathinones were separated into their optical enantiomers for the first time. A stable internal standard (2,3-MDPV) was used in cathinones quantitation. A mixture of three tertiary amine cathinones derivatives were separated on one chromatogram simultaneously after spiking in urine and plasma sample. Construction of calibration curves have been obtained for the selected 3 cathinone derivatives including the following concentration: 5, 10, 20, 50, 100, 250 ppm.

Validation of the established method in terms of recoveries, reproducibilities, linearities, limits of detection (LOD), and limits of quantitation (LOQ) for all the tested compounds has been done in spiked urine and plasma samples. The linearity coefficient of the constructed calibration curves was higher than 0.99. It was found that the LOD's of the quantitated tertiary amines cathinone derivatives in urine was in the range of 0.1 -0.7 ppm; while, in plasma, the LOD's were in the range of 0.17 - 1.33 ppm. The LOQ's in urine was in the range of 0.29 - 2.14 ppm and in plasma it was in the range of 0.50 - 4.01 ppm.

The fifth chapter discussed the host-guest inclusion reaction and its effect in fluorescence enhancement of the targeted analyte. In fact, the plan was to study the inclusion reaction between cyclodextrins as a host molecules and synthetic cathinones as a guest molecule, however, these kinds of experiments may need a large amount of synthetic cathinones which are considered as an expensive chemical. As a result of that, an alternative compound were chosen in this study namely "para-amino hippuric acid", due to its similarity to cathinone derivatives.

It was possible to develop a sensitive spectroflourometric method and liquid chromatography with fluorescence detection method for detection and determination of PAH in the presence of β-CD. The fluorescence signal at 355 nm, which is produced as a result of excimer emission, enhanced upon the use of β-CD in sample preparation. It was found that the interaction between PAH and cyclodextrin was considered as host – guest inclusion as was evident by mass spectrometry and DFT calculations and showed 1:2 (host-guest) interaction. A calibration curve was established for the spectrofluorometric data of PAH with β-CD in the concentration range of 0.05 -100 µM of PAH and the detection limit was 0.015 µM. HPLC with

fluorescence detection in the presence of β-CD in the mobile phase has shown an increase in fluorescence detection and the slope of calibration line increased as the concentration of β-CD increased. Finally, urine sample was spiked with 100 µM and 500 µM of PAH and showed recoveries in the range of 104%-118% and 99.2-103% respectively.

6.1 Recommendations

The following recommendations are suggested as possible ways to extend this study:

- Indirect chiral separation of synthetic cathinones can be investigated by using another kind of derivatizing agents such as menthylchloroformate which available at very cheap price and it has not investigated yet with synthetic cathinones.

- The usage of chiral GC column instead of using chiral derivatizing agent (CDA) for primary and secondary synthetic cathinones analysis.

- Negative Chemical Ionization (NCI) could lower the detection limit for the analysis of synthetic cathinones by using Multi Reaction Monitoring (MRM) mode. In order to do that an intense molecular ion peak is implied. The use of isobutene in CI source instead of methane is an option to observe high molecular ion peak in MS which will make MRM analysis possible for these kinds of compounds.

- Comparison between different gases in the CI source is also possible by using methane, isobutene and argon and a mixture of methane + ammonia.

- Sulfated β-Cyclodextrin (S-β-CD) can be used for synthetic cathinones enantioseparation especially for those new derivatives that have not been investigated in CE/UV system.

- Fluorescent derivatizing agent can be used with primary and secondary cathinones in order to permit detection using fluorescence detector.

References

Adamowicz, P., D. Gil, A. Skulska and B. Tokarczyk (2013). "Analysis of MDPV in blood—determination and interpretation." Journal of analytical toxicology.

Adamowicz, P., B. Tokarczyk, R. Stanaszek and M. Slopianka (2013). "Fatal mephedrone intoxication—a case report." Journal of analytical toxicology **37**(1): 37-42.

Adebamiro, A. and M. A. Perazella (2012). "Recurrent acute kidney injury following bath salts intoxication." American journal of kidney diseases **59**(2): 273-275.

Agarwal, R. (1998). "Chromatographic estimation of iothalamate and p-aminohippuric acid to measure glomerular filtration rate and effective renal plasma flow in humans." Journal of Chromatography B: Biomedical Sciences and Applications **705**(1): 3-9.

Albals, D., Y. Vander Heyden, M. G. Schmid, B. Chankvetadze and D. Mangelings (2015). "Chiral separations of cathinone and amphetamine-derivatives: Comparative study between capillary electrochromatography, supercritical fluid chromatography and three liquid chromatographic modes." Journal of pharmaceutical and biomedical analysis.

Albals, D., Y. Vander Heyden, M. G. Schmid, B. Chankvetadze and D. Mangelings (2016). "Chiral separations of cathinone and amphetamine-derivatives: Comparative study between capillary electrochromatography, supercritical fluid chromatography and three liquid chromatographic modes." Journal of pharmaceutical and biomedical analysis **121**: 232-243.

Alem, A., D. Kebede and G. Kullgren (1999). "The prevalence and socio-demographic correlates of khat chewing in Butajira, Ethiopia." Acta Psychiatr Scand Suppl **397**: 84-91.

Alrumaithi, R. H., M. A. Meetani and S. A. Khalil (2016). "A validated gas chromatography mass spectrometry method for simultaneous determination of cathinone related drugs enantiomers of in urine and plasma." RSC Advances.

Anizan, S., K. Ellefsen, M. Concheiro, M. Suzuki, K. C. Rice, M. H. Baumann and M. A. Huestis (2014). "3, 4-Methylenedioxypyrovalerone (MDPV) and metabolites quantification in human and rat plasma by liquid chromatography–high resolution mass spectrometry." Analytica chimica acta **827**: 54-63.

Armstrong, E. G. (2008). "Research note: Crime, chemicals, and culture: on the complexity of khat." Journal of Drug Issues **38**(2): 631-648.

Aturki, Z., M. G. Schmid, B. Chankvetadze and S. Fanali (2014). "Enantiomeric separation of new cathinone derivatives designer drugs by capillary electrochromatography using a chiral stationary phase, based on amylose tris (5- chloro- 2- methylphenylcarbamate)." Electrophoresis **35**(21-22): 3242-3249.

Baccard, N., G. Hoizey, C. Frances, D. Lamiable, T. Trenque and H. Millart (1999). "Simultaneous determination of inulin and p-aminohippuric acid (PAH) in human plasma and urine by high-performance liquid chromatography." Analyst **124**(6): 833-836.

Bailey, W., M. Hernandez Martin, J. Jimenez, K. Ding, M. Holtsclaw, C. English, A. Carroll and W. Pearson (1995). "Alcohol, tobacco, and other drug use by Indiana children and adolescents: the Indiana Prevention Resource Center Survey-1995." Bloomington, IN: Indiana Prevention Resource Center.

Banjaw, M. Y., M. Fendt and W. J. Schmidt (2005). "Clozapine attenuates the locomotor sensitisation and the prepulse inhibition deficit induced by a repeated oral administration of Catha edulis extract and cathinone in rats." Behav Brain Res **160**(2): 365-373.

Banks, M. L., T. J. Worst, D. E. Rusyniak and J. E. Sprague (2014). "Synthetic Cathinones (“Bath Salts”)." The Journal of Emergency Medicine **46**(5): 632-642.

Bentur, Y., A. Bloom-Krasik and B. Raikhlin-Eisenkraft (2008). "Illicit cathinone ("Hagigat") poisoning." Clin Toxicol (Phila) **46**(3): 206-210.

Bertol, E., F. Mari, R. B. Berto, G. Mannaioni, F. Vaiano and D. Favretto (2014). "A mixed MDPV and benzodiazepine intoxication in a chronic drug abuser: determination of MDPV metabolites by LC–HRMS and discussion of the case." Forensic science international **243**: 149-155.

Björklund, A. and S. B. Dunnett (2007). "Dopamine neuron systems in the brain: an update." Trends in neurosciences **30**(5): 194-202.

Bossong, M., J. Van Dijk and R. Niesink (2005). "Methylone and mCPP, two new drugs of abuse?" Addiction biology **10**(4): 321-323.

Boulanger-Gobeil, C., M. St-Onge, M. Laliberte and P. L. Auger (2012). "Seizures and hyponatremia related to ethcathinone and methylone poisoning." J Med Toxicol **8**(1): 59-61.

Boys, S. F. and F. Bernardi (1970). "The calculation of small molecular interactions by the differences of separate total energies. Some procedures with reduced errors." Molecular Physics **19**(4): 553-566.

Cosbey, S. H., K. L. Peters, A. Quinn and A. Bentley (2013). "Mephedrone (methylmethcathinone) in toxicology casework: a Northern Ireland perspective." Journal of analytical toxicology: bks094.

D., B. A. (1993). "Density- functional thermochemistry. III. The role of exact exchange." *The Journal of Chemical Physics* **98**: 5648-5562

Dargan, P., S. Albert and D. Wood (2010). "Mephedrone use and associated adverse effects in school and college/university students before the UK legislation change." QJM **103**(11): 875-879.

Dargan, P. I., R. Sedefov, A. Gallegos and D. M. Wood (2011). "The pharmacology and toxicology of the synthetic cathinone mephedrone (4-methylmethcathinone)." Drug testing and analysis **3**(7- 8): 454-463.

Decosterd, L. A., A. Karagiannis, J. M. Roulet, N. Bélaz, M. Appenzeller, T. Buclin, P. Vogel and J. Biollaz (1997). "High-performance liquid chromatography of the renal blood flow marker p-aminohippuric acid (PAH) and its metabolite N-acetyl PAH improves PAH clearance measurements." Journal of Chromatography B: Biomedical Sciences and Applications **703**(1–2): 25-36.

DeLong, M. R. (1990). "Primate models of movement disorders of basal ganglia origin." Trends in neurosciences **13**(7): 281-285.

den Hollander, B. (2015). "Neuropharmacology and toxicology of novel amphetamine-type stimulants." Dissertationes Scholae Doctoralis Ad Sanitatem Investigandam Universitatis Helsinkiensis.

DeRuiter, J., L. Hayes, A. Valaer, C. R. Clark and F. Noggle (1994). "Methcathinone and designer analogues: Synthesis, stereochemical analysis, and analytical properties." Journal of chromatographic science **32**(12): 552-564.

Di Chiara, G. (1998). "A motivational learning hypothesis of the role of mesolimbic dopamine in compulsive drug use." Journal of psychopharmacology **12**(1): 54-67.

Dimba, E., B. Gjertsen, T. Bredholt, K. Fossan, D. Costea, G. Francis, A. Johannessen and O. Vintermyr (2004). "Khat (Catha edulis)-induced apoptosis is inhibited by antagonists of caspase-1 and-8 in human leukaemia cells." British Journal of Cancer **91**(9): 1726-1734.

Dowling, T. C., R. F. Frye and M. A. Zemaitis (1998). "Simultaneous determination of p-aminohippuric acid, acetyl-p-aminohippuric acid and iothalamate in human plasma and urine by high-performance liquid chromatography." Journal of Chromatography B: Biomedical Sciences and Applications **716**(1–2): 305-313.

Elmi, A. S. (1983). "The chewing of khat in Somalia." J Ethnopharmacol **8**(2): 163-176.

EMCfDaD, A. (2011). "Report on the risk assessment of mephedrone in the framework of the Council Decision on new psychoactive substances." Luxembourg: The Publications Office of the European Union **193**.

Fan, H.-Y., C.-C. Lin and L.-H. Pao (2010). "Determination of p-aminohippuric acid in rat plasma by liquid chromatography-tandem mass spectrometry." Journal of Chromatography B **878**(19): 1643-1646.

Fanali, S. (2000). "Enantioselective determination by capillary electrophoresis with cyclodextrins as chiral selectors." Journal of Chromatography A **875**(1): 89-122.

Farthing, D., D. A. Sica, I. Fakhry, T. Larus, S. Ghosh, C. Farthing, M. Vranian and T. Gehr (2005). "Simple HPLC–UV method for determination of iohexol, iothalamate, p-aminohippuric acid and n-acetyl-p-aminohippuric acid in human plasma and urine with ERPF, GFR and ERPF/GFR ratio determination using colorimetric analysis." Journal of Chromatography B **826**(1–2): 267-272.

Feyissa, A. M. and J. P. Kelly (2008). "A review of the neuropharmacological properties of khat." Progress in Neuro-Psychopharmacology and Biological Psychiatry **32**(5): 1147-1166.

Floresco, S. B. and O. Magyar (2006). "Mesocortical dopamine modulation of executive functions: beyond working memory." Psychopharmacology **188**(4): 567-585.

Forrester, M. B. (2012). "Synthetic cathinone exposures reported to Texas poison centers." The American journal of drug and alcohol abuse **38**(6): 609-615.

Gallo, R. (1983). "Electrokinetic separation of chiral compounds." Proc. Natd. Acad. Sci. USA **80**: 339.

German, C. L., A. E. Fleckenstein and G. R. Hanson (2014). "Bath salts and synthetic cathinones: An emerging designer drug phenomenon." Life Sciences **97**(1): 2-8.

Gil, D., P. Adamowicz, A. Skulska, B. Tokarczyk and R. Stanaszek (2013). "Analysis of 4-MEC in biological and non-biological material—three case reports." Forensic science international **228**(1): e11-e15.

Glennon, R. A., B. R. Martin, T. A. Dal Cason and R. Young (1995). "Methcathinone ("CAT"): An enantiomeric potency comparison." Pharmacology Biochemistry and Behavior **50**(4): 601-606.

Guan, Y., T. Wu and J. Ye (2005). "Determination of uric acid and p-aminohippuric acid in human saliva and urine using capillary electrophoresis with electrochemical detection: Potential application in fast diagnosis of renal disease." Journal of Chromatography B **821**(2): 229-234.

Han, P. Y., P. N. Shaw and C. M. J. Kirkpatrick (2009). "Determination of para-aminohippuric acid (PAH) in human plasma and urine by liquid chromatography–tandem mass spectrometry." Journal of Chromatography B **877**(27): 3215-3220.

Hasegawa, K., A. Wurita, K. Minakata, K. Gonmori, H. Nozawa, I. Yamagishi, O. Suzuki and K. Watanabe (2014). "Identification and quantitation of a new cathinone designer drug PV9 in an “aroma liquid” product, antemortem whole blood and urine specimens, and a postmortem whole blood specimen in a fatal poisoning case." Forensic Toxicology **32**(2): 243-250.

Hassan, N. A., A. A. Gunaid and I. M. Murray-Lyon (2007). "Khat (Catha edulis): health aspects of khat chewing." East Mediterr Health J **13**(3): 706-718.

Herraez-Hernandez, R., P. Campıns-Falcó and J. Verdu-Andres (2002). "Strategies for the enantiomeric determination of amphetamine and related compounds by liquid chromatography." Journal of biochemical and biophysical methods **54**(1): 147-167.

Hyde, J., E. Browning and R. Adams (1928). "Synthetic homologs of d, l-ephedrine." Journal of the American Chemical Society **50**(8): 2287-2292.

Ihunwo, A. O., F. I. Kayanja and U. B. Amadi-Ihunwo (2004). "Use and perception of the psychostimulant, khat (catha edulis) among three occupational groups in south western Uganda." East Afr Med J **81**(9): 468-473.

Ilisz, I., R. Berkecz and A. Péter (2008). "Application of chiral derivatizing agents in the high-performance liquid chromatographic separation of amino acid enantiomers: A review." Journal of pharmaceutical and biomedical analysis **47**(1): 1-15.

James, D., R. D. Adams, R. Spears, G. Cooper, D. Lupton, J. P. Thompson and S. H. Thomas (2011). "Clinical characteristics of mephedrone toxicity reported to the UK National Poisons Information Service." Emergency Medicine Journal **28**(8): 686-689.

Jirovský, D., K. Lemr, J. Ševčík, B. Smysl and Z. Stránský (1998).

"Methamphetamine—properties and analytical methods of enantiomer determination." Forensic science international **96**(1): 61-70.

Jirovský, D., K. Lemr, J. Ševčík, B. Smysl and Z. Stránský (1998). "Methamphetamine — properties and analytical methods of enantiomer determination." Forensic Science International **96**(1): 61-70.

Johnson, R. D. and S. R. Botch-Jones (2013). "The stability of four designer drugs: MDPV, mephedrone, BZP and TFMPP in three biological matrices under various storage conditions." Journal of analytical toxicology **37**(2): 51-55.

Karabacak, M., Z. Cinar and M. Cinar (2012). "A structural and spectroscopic study on para-aminohippuric acid with experimental and theoretical approaches." Spectrochimica Acta Part A: Molecular and Biomolecular Spectroscopy **85**(1): 241-250.

Katz, D. P., D. Bhattacharya, S. Bhattacharya, J. Deruiter, C. R. Clark, V. Suppiramaniam and M. Dhanasekaran (2014). "Synthetic cathinones: "A khat and mouse game"." Toxicology Letters **229**(2): 349-356.

Kavanagh, P., J. O'Brien, J. D. Power, B. Talbot and S. D. McDermott (2013). "'Smoking'mephedrone: The identification of the pyrolysis products of 4- methylmethcathinone hydrochloride." Drug testing and analysis **5**(5): 291-305.

Kelly, J. P. (2011). "Cathinone derivatives: a review of their chemistry, pharmacology and toxicology." Drug Testing and Analysis **3**(7- 8): 439-453.

Kos, T., P. Moser, N. Yilmatz, G. Mayer, R. Pacher and S. Hallström* (2000). "High-performance liquid chromatographic determination of p-aminohippuric acid and iothalamate in human serum and urine: comparison of two sample preparation methods." Journal of Chromatography B: Biomedical Sciences and Applications **740**(1): 81-85.

Kriikku, P., L. Wilhelm, O. Schwarz and J. Rintatalo (2011). "New designer drug of abuse: 3, 4-Methylenedioxypyrovalerone (MDPV). Findings from apprehended drivers in Finland." Forensic Science International **210**(1): 195-200.

Krikorian, A. D. (1984). "Kat and its use: An historical perspective." Journal of Ethnopharmacology **12**(2): 115-178.

LeBelle, M., G. Lauriault and A. Lavoie (1993). "Gas chromatographic-mass spectrometric identification of chiral derivatives of the alkaloids of khat." Forensic science international **61**(1): 53-64.

Li, B. and D. T. Haynie (2006). "Chiral drug separation." Encyclopedia of chemical processing **1**: 449-458.

Li, D.-X., L. Gan, A. Bronja and O. J. Schmitz (2015). "Gas chromatography coupled to atmospheric pressure ionization mass spectrometry (GC-API-MS): Review." Analytica Chimica Acta **891**: 43-61.

Li, L. and I. S. Lurie (2015). "Regioisomeric and enantiomeric analyses of 24 designer cathinones and phenethylamines using ultra high performance liquid chromatography and capillary electrophoresis with added cyclodextrins." Forensic science international **254**: 148-157.

Manzoori, J. L. and M. Amjadi (2003). "Spectrofluorimetric study of host–guest complexation of ibuprofen with β-cyclodextrin and its analytical application." Spectrochimica Acta Part A: Molecular and Biomolecular Spectroscopy **59**(5): 909-916.

Marinetti, L. J. and H. M. Antonides (2013). "Analysis of synthetic cathinones commonly found in bath salts in human performance and postmortem toxicology: method development, drug distribution and interpretation of results." Journal of analytical toxicology: bks136.

Marsilio, R., R. Dall'Amico, G. Montini, L. Murer, M. Ros, G. Zacchello and F. Zacchello (1997). "Rapid determination of p-aminohippuric acid in serum and urine by high-performance liquid chromatography." Journal of Chromatography B: Biomedical Sciences and Applications **704**(1–2): 359-364.

Maskell, P. D., G. De Paoli, C. Seneviratne and D. J. Pounder (2011). "Mephedrone (4-methylmethcathinone)-related deaths." Journal of analytical toxicology **35**(3): 188-191.

Merola, G., H. Fu, F. Tagliaro, T. Macchia and B. R. McCord (2014). "Chiral separation of 12 cathinone analogs by cyclodextrin- assisted capillary electrophoresis with UV and mass spectrometry detection." Electrophoresis **35**(21-22): 3231-3241.

Meyer, M. R., P. Du, F. Schuster and H. H. Maurer (2010). "Studies on the metabolism of the α- pyrrolidinophenone designer drug methylenedioxy- pyrovalerone (MDPV) in rat and human urine and human liver microsomes using GC–MS and LC–high- resolution MS and its detectability in urine by GC–MS." Journal of Mass Spectrometry **45**(12): 1426-1442.

Miotto, K., J. Striebel, A. K. Cho and C. Wang (2013). "Clinical and pharmacological aspects of bath salt use: A review of the literature and case reports." Drug and Alcohol Dependence **132**(1–2): 1-12.

Mohr, S., S. Pilaj and M. G. Schmid (2012). "Chiral separation of cathinone derivatives used as recreational drugs by cyclodextrin-modified capillary electrophoresis." Electrophoresis **33**(11): 1624-1630.

Mohr, S., M. Taschwer and M. G. Schmid (2012). "Chiral separation of cathinone derivatives used as recreational drugs by HPLC-UV using a CHIRALPAK(R) AS-H column as stationary phase." Chirality **24**(6): 486-492.

Mohr, S., J. A. Weiß, J. Spreitz and M. G. Schmid (2012). "Chiral separation of new cathinone- and amphetamine-related designer drugs by gas chromatography–mass spectrometry using trifluoroacetyl-l-prolyl chloride as chiral derivatization reagent." Journal of Chromatography A **1269**: 352-359.

Moini, M. and C. M. Rollman (2015). "Compatibility of highly sulfated cyclodextrin with electrospray ionization at low nanoliter/minute flow rates and its application to capillary electrophoresis/electrospray ionization mass spectrometric analysis of cathinone derivatives and their optical isomers." Rapid Commun. Mass Spectrom **29**: 304-310.

Morris, H. (2010). "Hamilton's Pharmacopeia. Mephedrone: the phantom menace." Vice Magazine. Retrieved: 07-04.

Namera, A., S. Urabe, T. Saito, A. Torikoshi-Hatano, H. Shiraishi, Y. Arima and M. Nagao (2013). "A fatal case of 3, 4-methylenedioxypyrovalerone poisoning: coexistence of α-pyrrolidinobutiophenone and α-pyrrolidinovalerophenone in blood and/or hair." Forensic Toxicology **31**(2): 338-343.

Nordal, A. (1980). "Khat: pharmacognostical aspects." Bull Narc **32**(3): 51-64.

Ojanperä, I. A., P. K. Heikman and I. J. Rasanen (2011). "Urine analysis of 3, 4-methylenedioxypyrovalerone in opioid-dependent patients by gas chromatography–mass spectrometry." Therapeutic drug monitoring **33**(2): 257-263.

Padivitage, N. L., E. Dodbiba, Z. S. Breitbach and D. W. Armstrong (2014). "Enantiomeric separations of illicit drugs and controlled substances using cyclofructan- based (LARIHC) and cyclobond I 2000 RSP HPLC chiral stationary phases." Drug testing and analysis **6**(6): 542-551.

Patel, N. B. (2000). "Mechanism of action of cathinone: the active ingredient of khat (Catha edulis)." East Afr Med J **77**(6): 329-332.

Pearson, J. M., T. L. Hargraves, L. S. Hair, C. J. Massucci, C. C. Frazee, U. Garg and B. R. Pietak (2012). "Case Report: Three Fatal Intoxications Due to Methylone." Journal of analytical toxicology: bks043.

Perera, R. W. H., I. Abraham, S. Gupta, P. Kowalska, D. Lightsey, C. Marathaki, N. S. Singh and W. J. Lough (2012). "Screening approach, optimisation and scale-up for chiral liquid chromatography of cathinones." Journal of Chromatography A **1269**: 189-197.

Płotka, J. M., M. Biziuk and C. Morrison (2011). "Common methods for the chiral determination of amphetamine and related compounds I. Gas, liquid and thin-layer chromatography." TrAC Trends in Analytical Chemistry **30**(7): 1139-1158.

Porter, J. C., W. Kedzierski, N. Aguila-Mansilla, B. A. Jorquera and H. A. González (1990). The tuberoinfundibular dopaminergic neurons of the brain: hormonal regulation. Circulating Regulatory Factors and Neuroendocrine Function, Springer**:** 1-23.

Prabu, S. L. and T. N. K. Suriyaprakash (2012). Extraction of Drug from the Biological Matrix: A Review, INTECH Open Access Publisher.

Rasmussen, L. B., K. H. Olsen and S. S. Johansen (2006). "Chiral separation and quantification of R/S-amphetamine, R/S-methamphetamine, R/S-MDA, R/S-MDMA, and R/S-MDEA in whole blood by GC-EI-MS." J Chromatogr B Analyt Technol Biomed Life Sci **842**(2): 136-141.

Rojek, S., M. Kłys, M. Strona, M. Maciów and K. Kula (2012). "“Legal highs”—Toxicity in the clinical and medico-legal aspect as exemplified by suicide with bk-MBDB administration." Forensic science international **222**(1): e1-e6.

Rust, K. Y., M. R. Baumgartner, A. M. Dally and T. Kraemer (2012). "Prevalence of new psychoactive substances: A retrospective study in hair." Drug testing and analysis **4**(6): 402-408.

Saito, T., A. Namera, M. Osawa, H. Aoki and S. Inokuchi (2013). "SPME–GC–MS analysis of α-pyrrolidinovaleorophenone in blood in a fatal poisoning case." Forensic toxicology **31**(2): 328-332.

Schurig, V. (2002). "Chiral separations using gas chromatography." TrAC Trends in Analytical Chemistry **21**(9–10): 647-661.

Shima, N., M. Katagi, H. Kamata, S. Matsuta, K. Nakanishi, K. Zaitsu, T. Kamata, H. Nishioka, A. Miki and M. Tatsuno (2013). "Urinary excretion and metabolism of the newly encountered designer drug 3, 4-dimethylmethcathinone in humans." Forensic Toxicology **31**(1): 101-112.

Shima, N., M. Katagi, H. Kamata, S. Matsuta, K. Sasaki, T. Kamata, H. Nishioka, A. Miki, M. Tatsuno and K. Zaitsu (2014). "Metabolism of the newly encountered designer drug α-pyrrolidinovalerophenone in humans: identification and quantitation of urinary metabolites." Forensic Toxicology **32**(1): 59-67.

Sikk, K. and P. Taba (2015). Chapter Twelve - Methcathinone “Kitchen Chemistry” and Permanent Neurological Damage. International Review of Neurobiology. A. L. Pille Taba and S. Katrin, Academic Press. **Volume 120:** 257-271.

Sílvia Simon, M. D., J. J. Dannenberg (1996). "How does basis set superposition error change the potential surfaces for hydrogen- bonded dimers?" The Journal of Chemical Physics **105**.

Song, D.-J. and K.-Y. Hsu (1996). "Determination ofp-aminobenzoic acid and its metabolites in rabbit plasma by high-performance liquid chromatography with fluorescence detection." Journal of Chromatography B: Biomedical Sciences and Applications **677**(1): 69-75.

Sørensen, L. K. (2011). "Determination of cathinones and related ephedrines in forensic whole-blood samples by liquid-chromatography–electrospray tandem mass spectrometry." Journal of Chromatography B **879**(11): 727-736.

Spiller, H. A., M. L. Ryan, R. G. Weston and J. Jansen (2011). "Clinical experience with and analytical confirmation of "bath salts" and "legal highs"(synthetic cathinones) in the United States." Clinical Toxicology **49**(6): 499-505.

Stewart, J. J. P. (1989). "Optimization of parameters for semiempirical methods I. Method." Journal of computational chemistry **10**(2): 209-220.

Stewart, J. J. P. (1989). "ptimization of parameters for semiempirical methods II. Applications." Journal of Computational Chemistry **10**(2): 221-264.

Strano- Rossi, S., A. B. Cadwallader, X. de la Torre and F. Botrè (2010). "Toxicological determination and in vitro metabolism of the designer drug methylenedioxypyrovalerone (MPDV) by gas chromatography/mass spectrometry and liquid chromatography/quadrupole time- of- flight mass spectrometry." Rapid Communications in Mass Spectrometry **24**(18): 2706-2714.

Švidrnoch, M., L. Lněníčková, I. Válka, P. Ondra and V. Maier (2014). "Utilization of micellar electrokinetic chromatography–tandem mass spectrometry employed volatile micellar phase in the analysis of cathinone designer drugs." Journal of Chromatography A **1356**: 258-265.

Tao, Q. F. and S. Zeng (2002). "Analysis of enantiomers of chiral phenethylamine drugs by capillary gas chromatography/mass spectrometry/flame-ionization detection and pre-column chiral derivatization." Journal of biochemical and biophysical methods **54**(1): 103-113.

Tao, Q. F. and S. Zeng (2002). "Analysis of enantiomers of chiral phenethylamine drugs by capillary gas chromatography/mass spectrometry/flame-ionization detection and pre-column chiral derivatization." Journal of Biochemical and Biophysical Methods **54**(1–3): 103-113.

Taschwer, M., M. G. Hofer and M. G. Schmid (2014). "Enantioseparation of benzofurys and other novel psychoactive compounds by CE and sulfobutylether β- cyclodextrin as chiral selector added to the BGE." Electrophoresis **35**(19): 2793-2799.

TASCHWER, M., Y. SEIDL, S. MOHR and M. G. SCHMID (2014). "Chiral Separation of Cathinone and Amphetamine Derivatives by HPLC/UV Using Sulfated ß-Cyclodextrin as Chiral Mobile Phase Additive." Chirality **26**: 411-418.

Taschwer, M., J. A. Weiß, O. Kunert and M. G. Schmid (2014). "Analysis and characterization of the novel psychoactive drug 4-chloromethcathinone (clephedrone)." Forensic science international **244**: e56-e59.

TesaŘOvÁ, E. and D. W. Armstrong (1998). Chapter 5 - Enantioselective Separations. Journal of Chromatography Library. I. M. F. T. Zdeněk Deyl and T. Eva, Elsevier. **Volume 60:** 197-256.

Toennes, S. W. and G. F. Kauert (2002). "Excretion and detection of cathinone, cathine, and phenylpropanolamine in urine after kath chewing." Clinical chemistry **48**(10): 1715-1719.

Toyo'oka, T. (2002). "Resolution of chiral drugs by liquid chromatography based upon diastereomer formation with chiral derivatization reagents." J Biochem Biophys Methods **54**(1-3): 25-56.

Uralets, V., S. Rana, S. Morgan and W. Ross (2014). "Testing for designer stimulants: metabolic profiles of 16 synthetic cathinones excreted free in human urine." Journal of analytical toxicology: bku021.

Usui, K., T. Aramaki, M. Hashiyada, Y. Hayashizaki and M. Funayama (2014). "Quantitative analysis of 3, 4-dimethylmethcathinone in blood and urine by liquid chromatography–tandem mass spectrometry in a fatal case." Legal Medicine **16**(4): 222-226.

Vouga, A., R. A. Gregg, M. Haidery, A. Ramnath, H. K. Al-Hassani, C. S. Tallarida, D. Grizzanti, R. B. Raffa, G. R. Smith and A. B. Reitz (2015). "Stereochemistry and neuropharmacology of a 'bath salt'cathinone: S-enantiomer of mephedrone reduces cocaine-induced reward and withdrawal in invertebrates." Neuropharmacology **91**: 109-116.

Wagner, B. D. and G. J. McManus (2003). "Enhancement of the fluorescence and stability of o-phthalaldehyde-derived isoindoles of amino acids using hydroxypropyl-β-cyclodextrin." Analytical Biochemistry **317**(2): 233-239.

Wang, S.-M., R. J. Lewis, D. Canfield, T.-L. Li, C.-Y. Chen and R. H. Liu (2005). "Enantiomeric determination of ephedrines and norephedrines by chiral derivatization gas chromatography–mass spectrometry approaches." Journal of Chromatography B **825**(1): 88-95.

Wang, S.-M., T.-C. Wang and Y.-S. Giang (2005). "Simultaneous determination of amphetamine and methamphetamine enantiomers in urine by simultaneous liquid–liquid extraction and diastereomeric derivatization

followed by gas chromatographic–isotope dilution mass spectrometry." Journal of Chromatography B **816**(1): 131-143.

Waters, B., N. Ikematsu, K. Hara, H. Fujii, T. Tokuyasu, M. Takayama, A. Matsusue, M. Kashiwagi and S.-i. Kubo (2016). "GC-PCI-MS/MS and LC-ESI-MS/MS databases for the detection of 104 psychotropic compounds (synthetic cannabinoids, synthetic cathinones, phenethylamine derivatives)." Legal Medicine **20**: 1-7.

Watson, J. T. and O. D. Sparkman (2007). Introduction to mass spectrometry: instrumentation, applications, and strategies for data interpretation, John Wiley & Sons.

Weiss, J. A., S. Mohr and M. G. Schmid (2015). "Indirect chiral separation of new recreational drugs by gas chromatography-mass spectrometry using trifluoroacetyl-L-prolyl chloride as chiral derivatization reagent." Chirality **27**(3): 211-215.

Weiss, J. A., M. Taschwer, O. Kunert and M. G. Schmid (2015). "Analysis of a new drug of abuse: cathinone derivative 1-(3,4-dimethoxyphenyl)-2-(ethylamino)pentan-1-one." J Sep Sci **38**(5): 825-828.

Wilkinson, A. D. M. a. A. (1997). IUPAC. Compendium of Chemical Terminology, Scientific Publications, Oxford

Willner, I., Y. Eichen and A. J. Frank (1989). "Tailored semiconductor-receptor colloids: Improved photosensitized H/sub 2/ evolution from water with TiO/sub 2/-/beta/-cyclodextrin colloids." Journal Name: J. Am. Chem. Soc.; (United States); Journal Volume: 111:5: Medium: X; Size: Pages: 1884-1886.

Wolrab, D., P. Frühauf, A. Moulisová, M. Kuchař, C. Gerner, W. Lindner and M. Kohout (2016). "Chiral separation of new designer drugs (Cathinones) on chiral ion-exchange type stationary phases." Journal of Pharmaceutical and Biomedical Analysis **120**: 306-315.

Wright, T. H., K. Cline- Parhamovich, D. Lajoie, L. Parsons, M. Dunn and K. E. Ferslew (2013). "Deaths involving methylenedioxypyrovalerone (MDPV) in upper east Tennessee." Journal of forensic sciences **58**(6): 1558-1562.

Wu, Y.-H., K.-l. Lin, S.-C. Chen and Y.-Z. Chang (2008). "Integration of GC/EI-MS and GC/NCI-MS for simultaneous quantitative determination of opiates, amphetamines, MDMA, ketamine, and metabolites in human hair." Journal of Chromatography B **870**(2): 192-202.

Wurita, A., K. Hasegawa, K. Minakata, K. Gonmori, H. Nozawa, I. Yamagishi, O. Suzuki and K. Watanabe (2014). "Postmortem distribution of α-

pyrrolidinobutiophenone in body fluids and solid tissues of a human cadaver." Legal Medicine **16**(5): 241-246.

Wyman, J. F., E. S. Lavins, D. Engelhart, E. J. Armstrong, K. D. Snell, P. D. Boggs, S. M. Taylor, R. N. Norris and F. P. Miller (2013). "Postmortem tissue distribution of MDPV following lethal intoxication by “bath salts”." Journal of analytical toxicology: bkt001.

Zawilska, J. B. and J. Wojcieszak (2013). "Designer cathinones—An emerging class of novel recreational drugs." Forensic Science International **231**(1–3): 42-53.

Zhang, Q., T. Deng, J. Li, W. Xu, G. Shen and R. Yu (2015). "Cyclodextrin supramolecular inclusion-enhanced pyrene excimer switching for time-resolved fluorescence detection of biothiols in serum." Biosensors and Bioelectronics **68**(0): 253-258.

Zhang, T., P. Franco, D. Nguyen, R. Hamasaki, S. Miyamoto, A. Ohnishi and T. Murakami (2012). "Complementary enantiorecognition patterns and specific method optimization aspects on immobilized polysaccharide-derived chiral stationary phases." Journal of Chromatography A **1269**: 178-188.

Zuba, D., P. Adamowicz and B. Byrska (2013). "Detection of buphedrone in biological and non-biological material–two case reports." Forensic science international **227**(1): 15-20.

Appendix A: Gas chromatogram, mass spectrum and calibration plots of 31 synthetic cathinones that analyzed in chapter 2

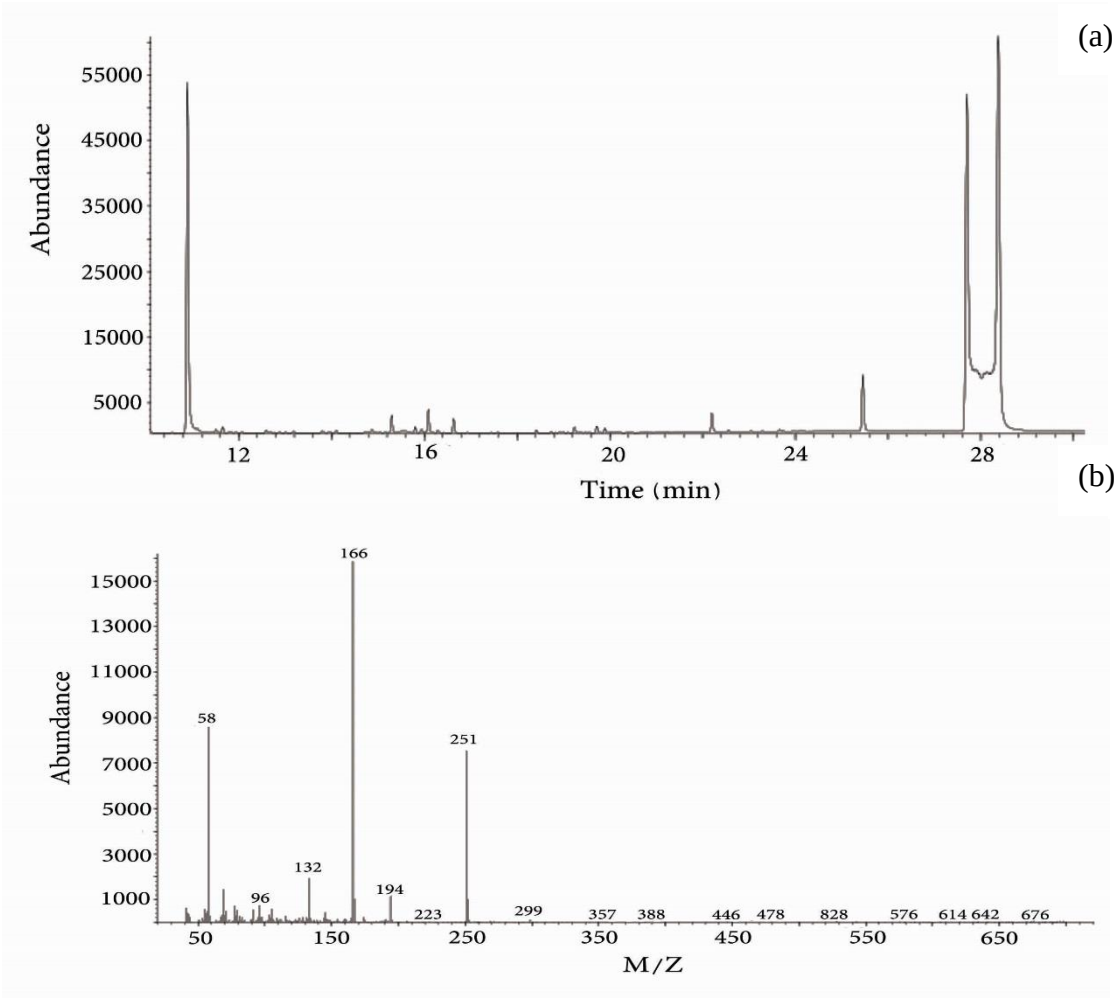

Figure 26: a) Gas chromatogram for separation of the R and S enantiomers of 2-Ethylmethcathinone (2-EMC) drug after derivatization with L-TPC in the presence of nikethamide internal standard and b) mass spectrum of the same compound analyzed by GC-EI-MS system

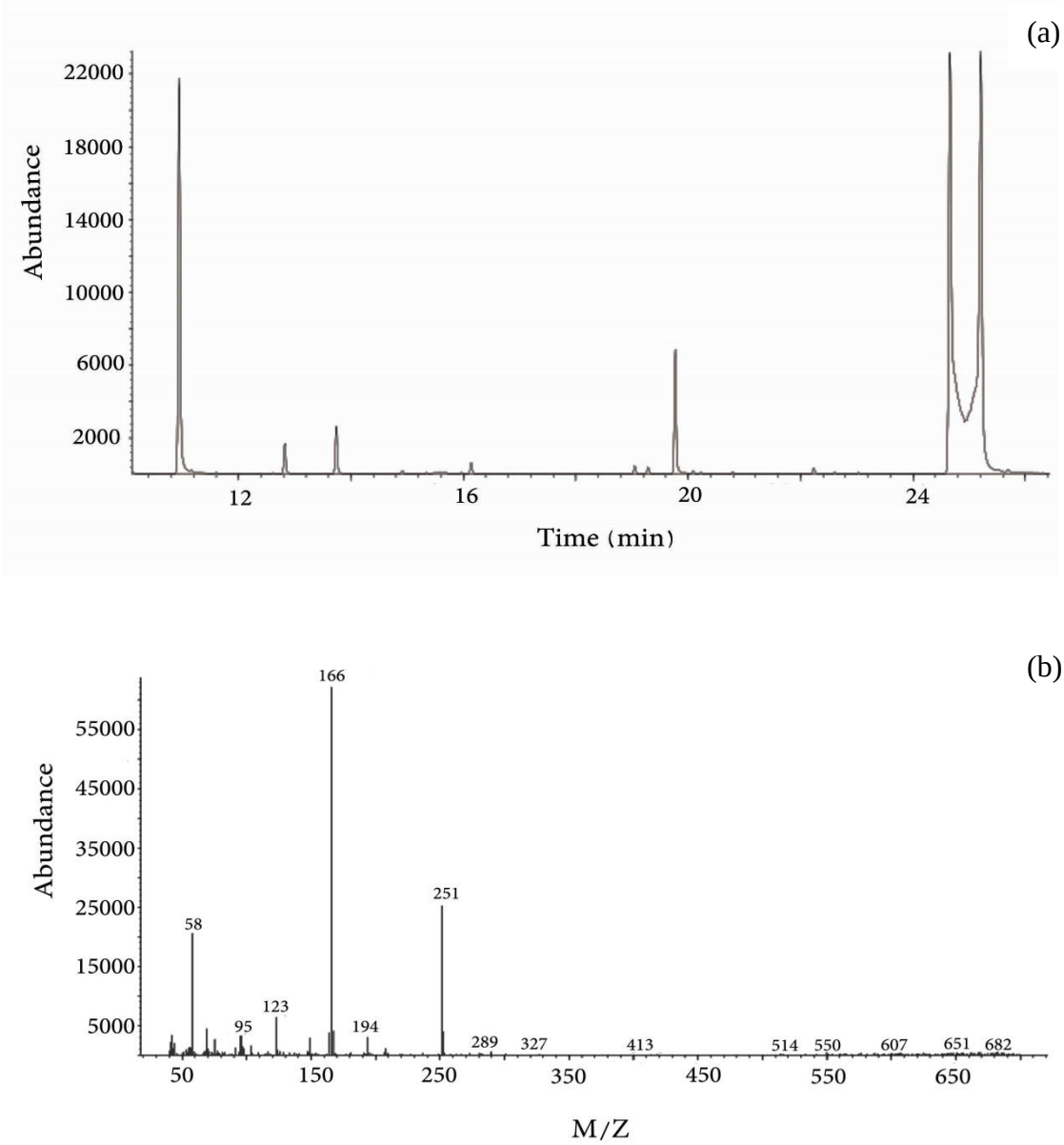

Figure 27: a) Gas chromatogram for separation of the R and S enantiomers of 2-Fluorolmethcathinone (2-FMC) drug after derivatization with L-TPC in the presence of nikethamide internal standard and b) mass spectrum of the same compound analyzed by GC-EI-MS system

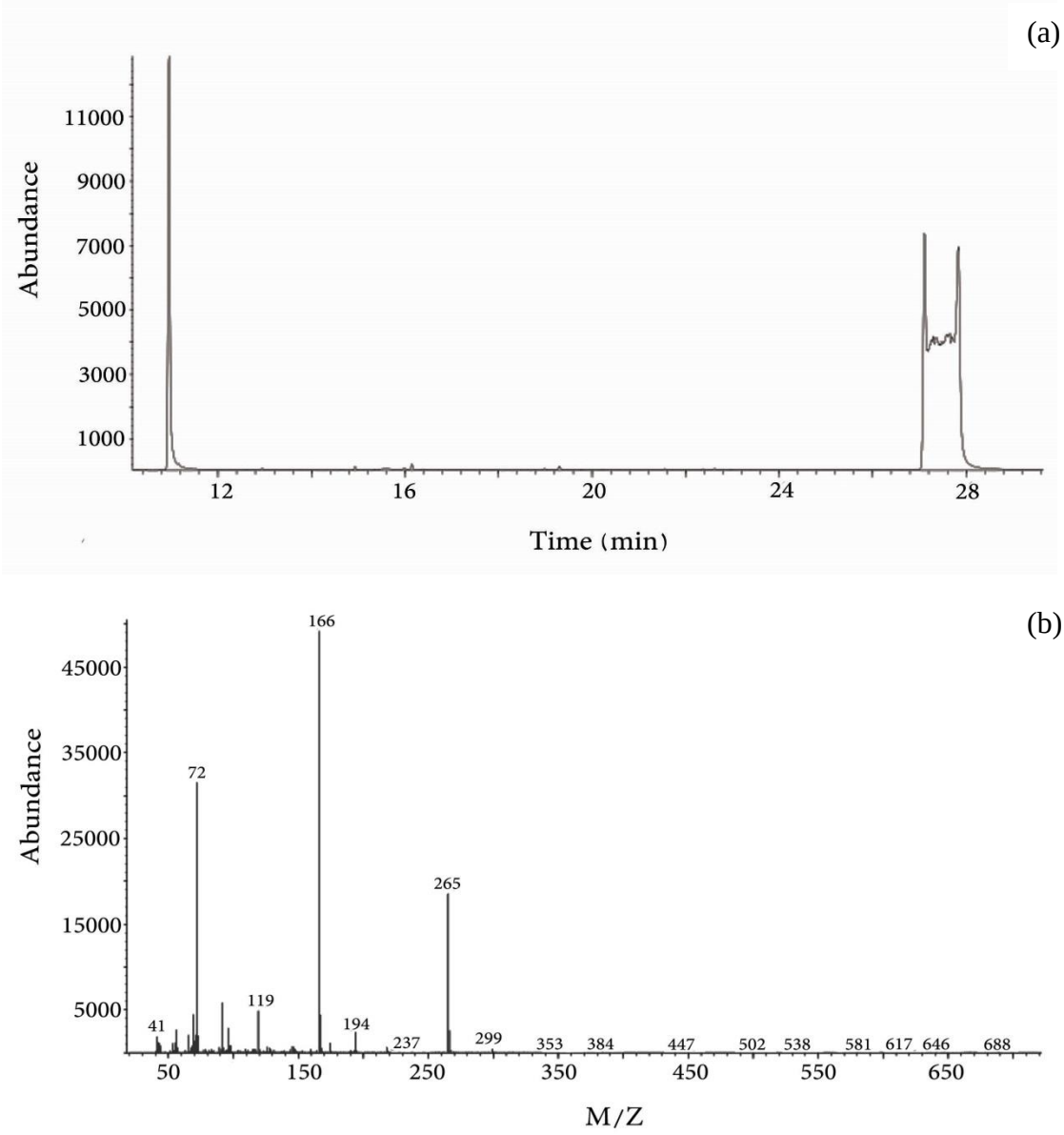

Figure 28: a) Gas chromatogram for separation of the R and S enantiomers of 2-Methylethcathinone (2-MEC) drug after derivatization with L-TPC in the presence of nikethamide internal standard and b) mass spectrum of the same compound analyzed by GC-EI-MS system

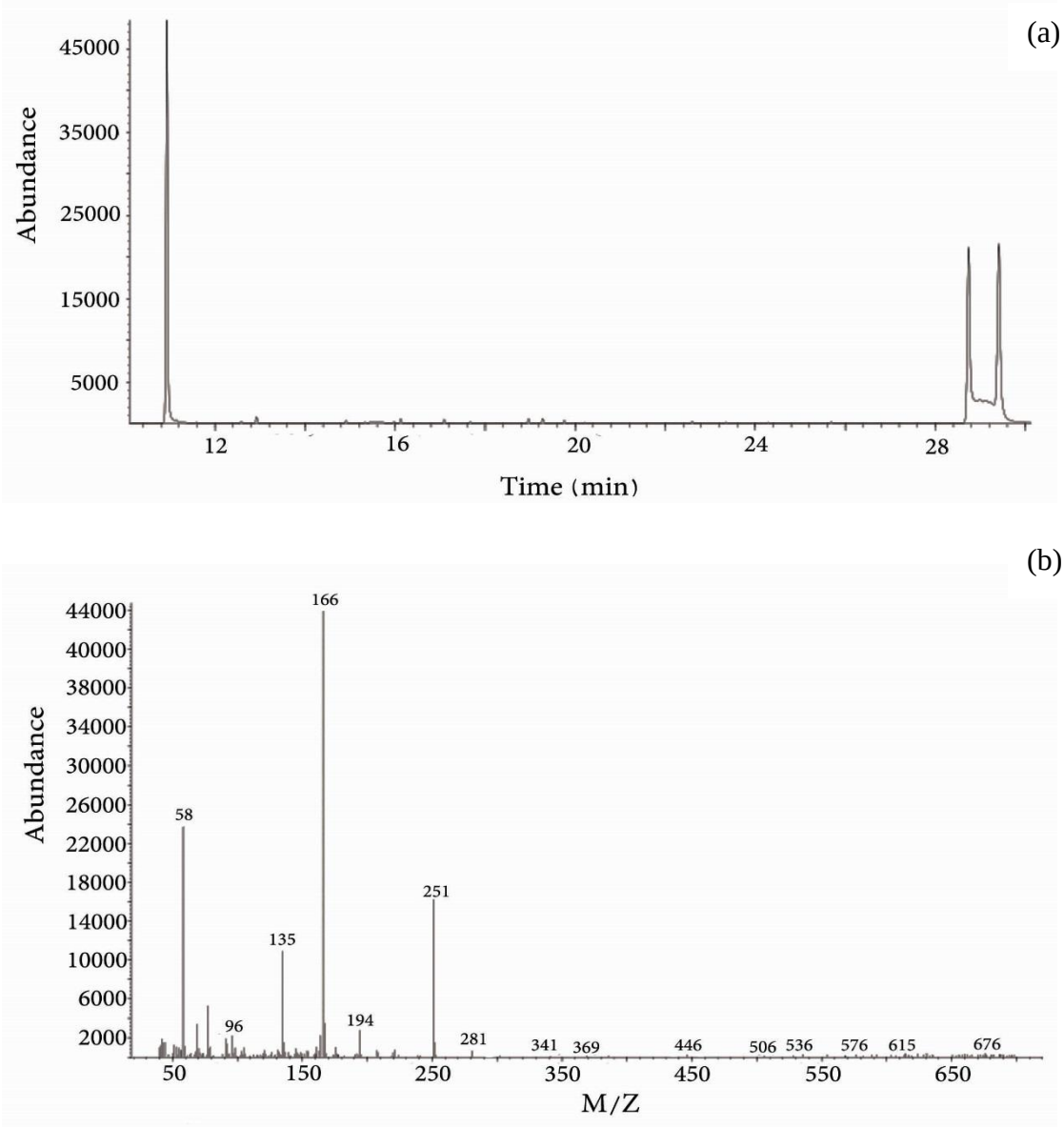

Figure 29: a) Gas chromatogram for separation of the R and S enantiomers of 2-Methoxymethcathinone (2-Me-O-MC) drug after derivatization with L-TPC in the presence of nikethamide internal standard and b) mass spectrum of the same compound analyzed by GC-EI-MS system

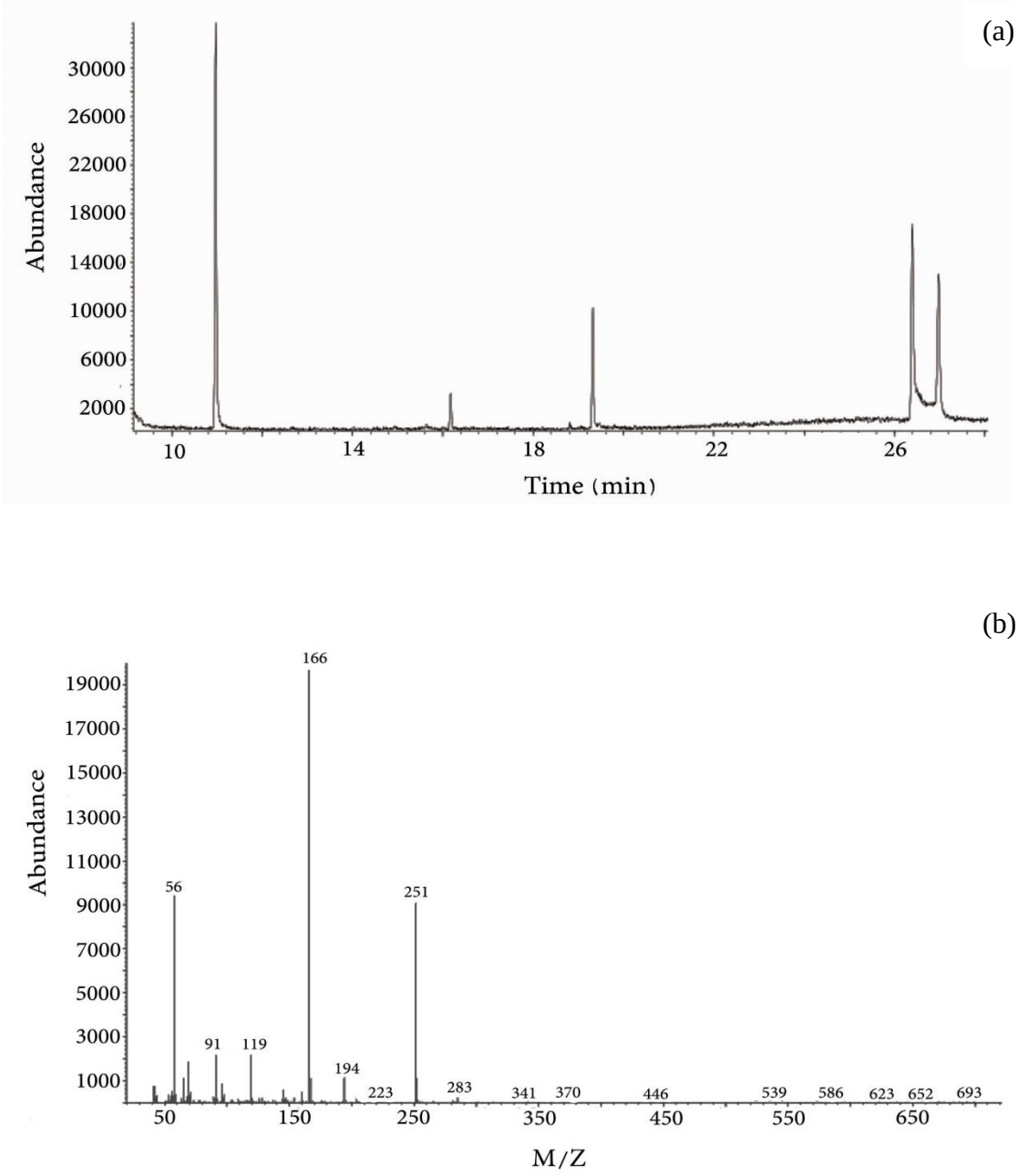

Figure 30: a) Gas chromatogram for separation of the R and S enantiomers of 2-Methylmethcathinone (2-MMC) drug after derivatization with L-TPC in the presence of nikethamide internal standard and b) mass spectrum of the same compound analyzed by GC-EI-MS system

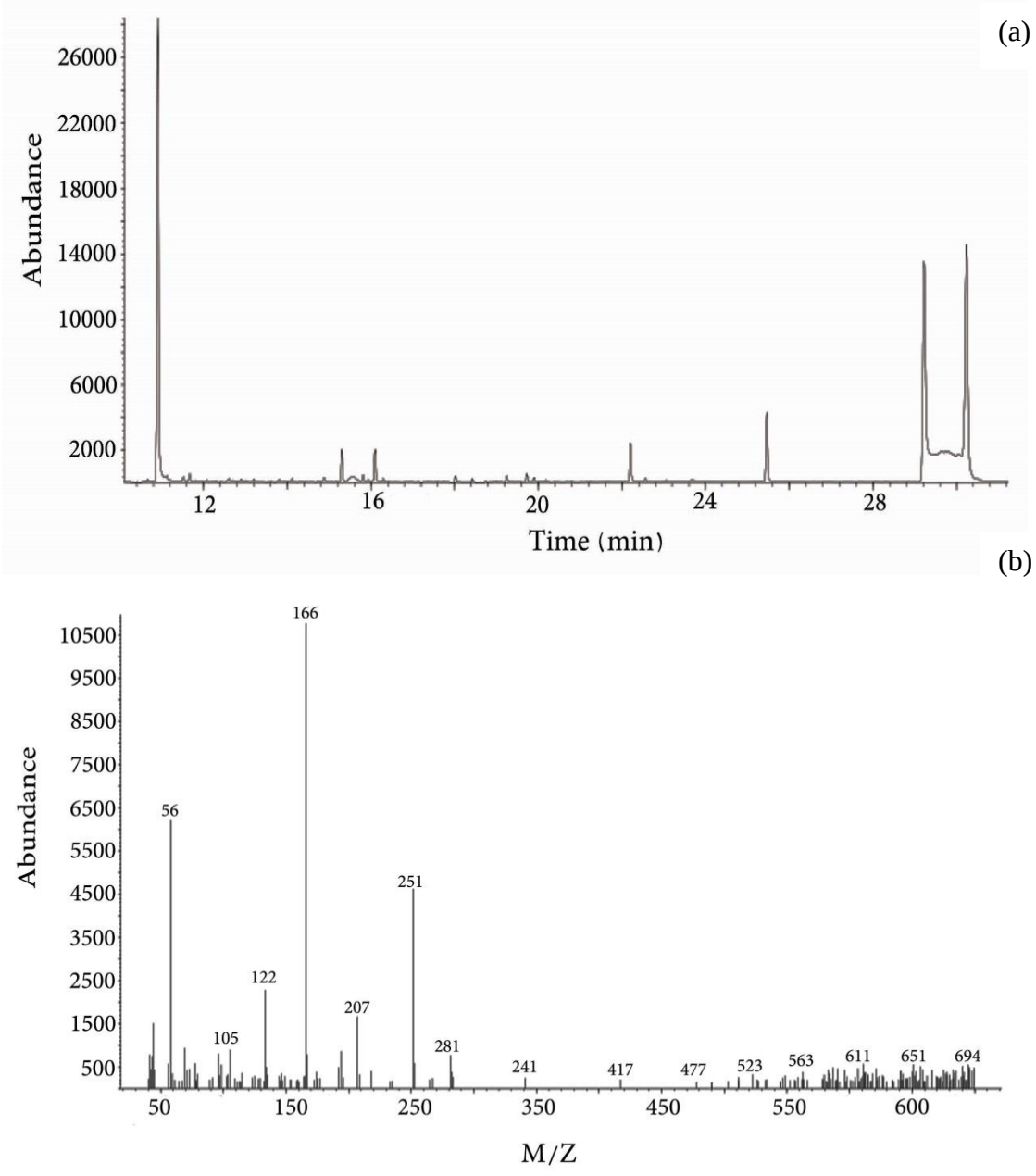

Figure 31: a) Gas chromatogram for separation of the R and S enantiomers of 2,3-Dimethylmethcathinone (2,3-DMMC) drug after derivatization with L-TPC in the presence of nikethamide internal standard and b) mass spectrum of the same compound analyzed by GC-EI-MS system

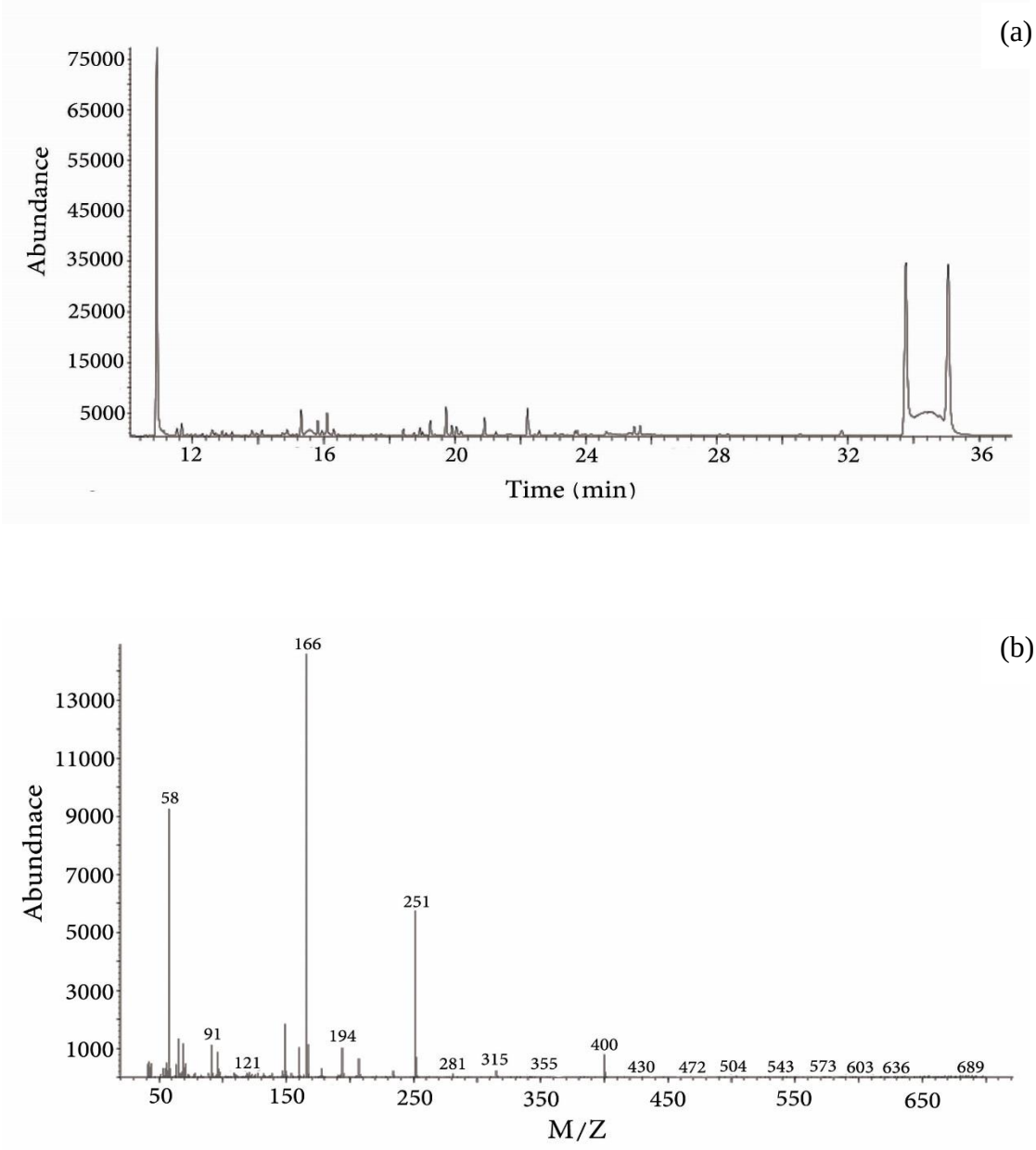

Figure 32: a) Gas chromatogram for separation of the R and S enantiomers of 2,3-Methelendioxymethcathinone (2,3-MDMC) drug after derivatization with L-TPC in the presence of nikethamide internal standard and b) mass spectrum of the same compound analyzed by GC-EI-MS system

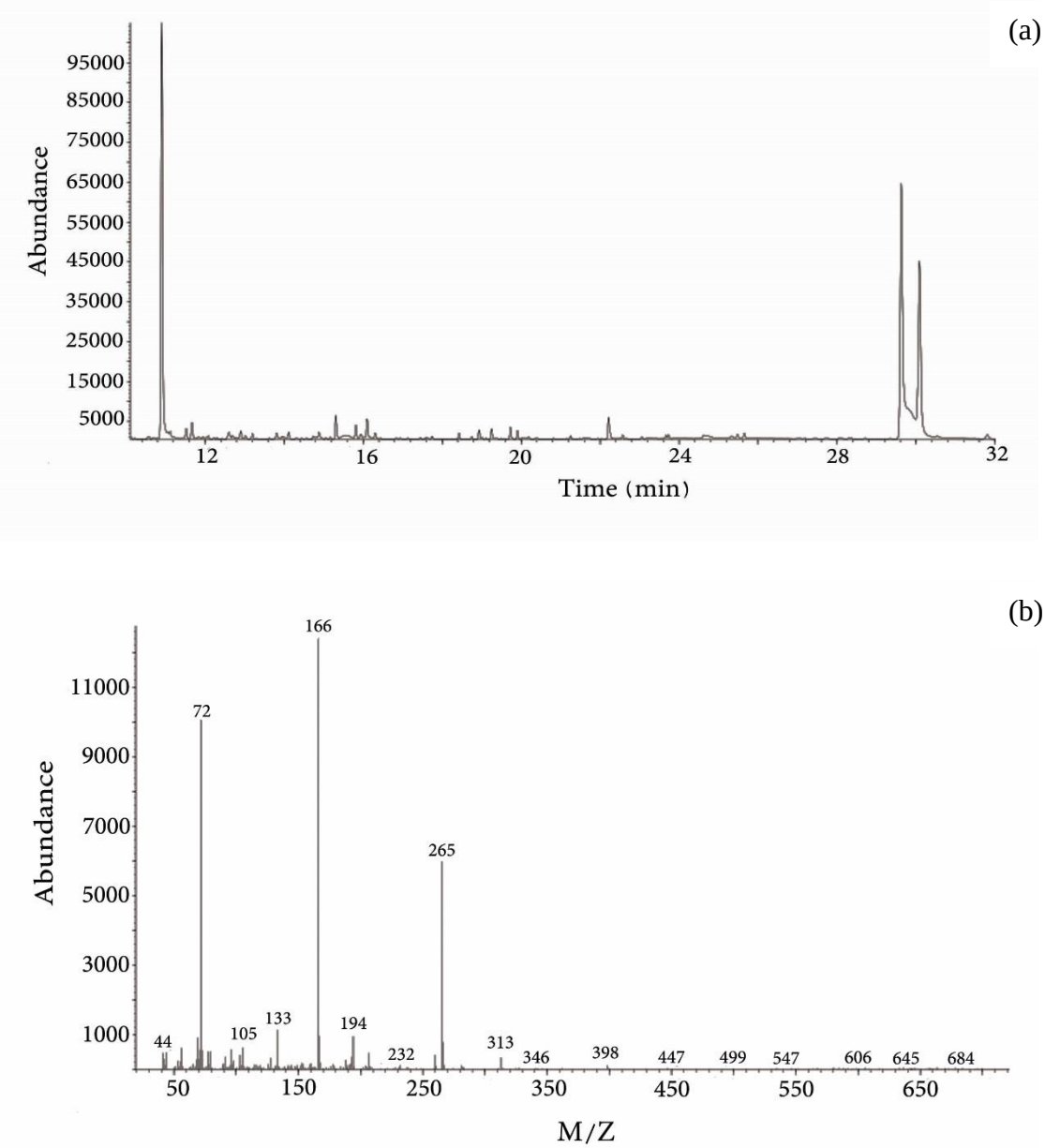

Figure 33: a) Gas chromatogram for separation of the R and S enantiomers of 3-Ethylethcathinone (3-EEC) drug after derivatization with L-TPC in the presence of nikethamide internal standard and b) mass spectrum of the same compound analyzed by GC-EI-MS system

(a)

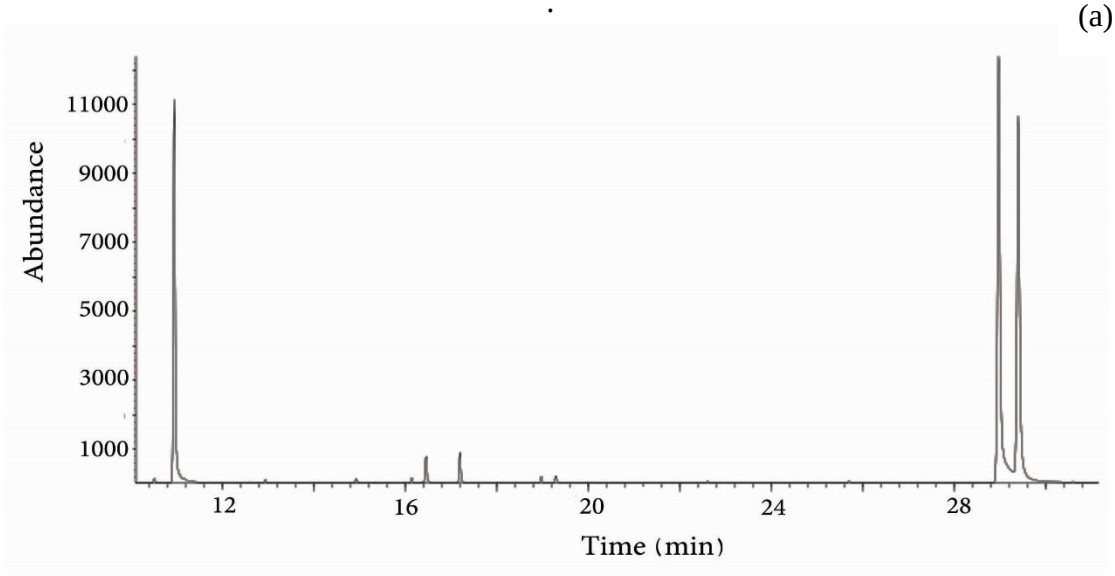

(b)

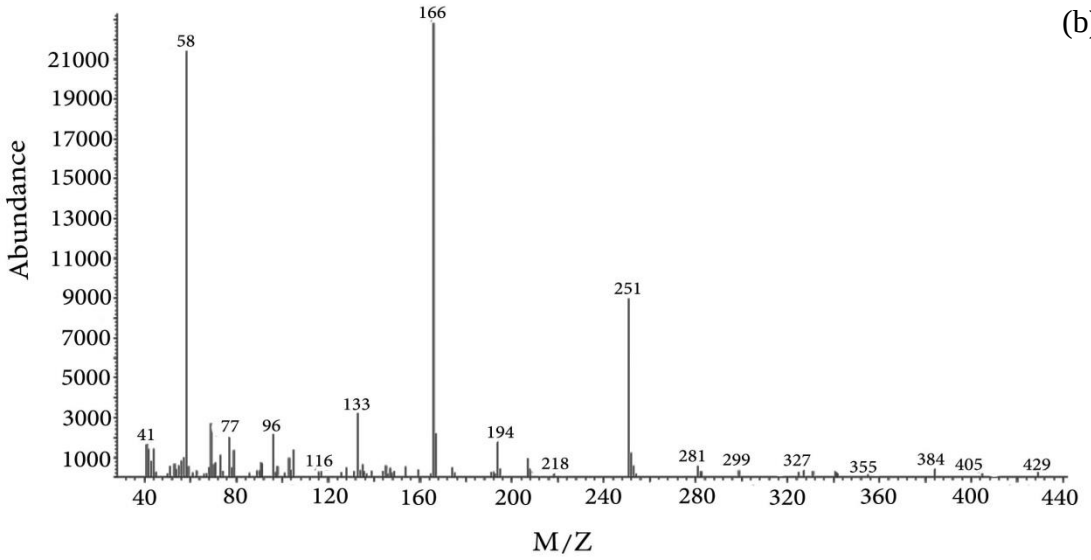

Figure 34: a) Gas chromatogram for separation of the R and S enantiomers of 3-Ethylmethcathinone (3-EMC) drug after derivatization with L-TPC in the presence of nikethamide internal standard and b) mass spectrum of the same compound analyzed by GC-EI-MS system

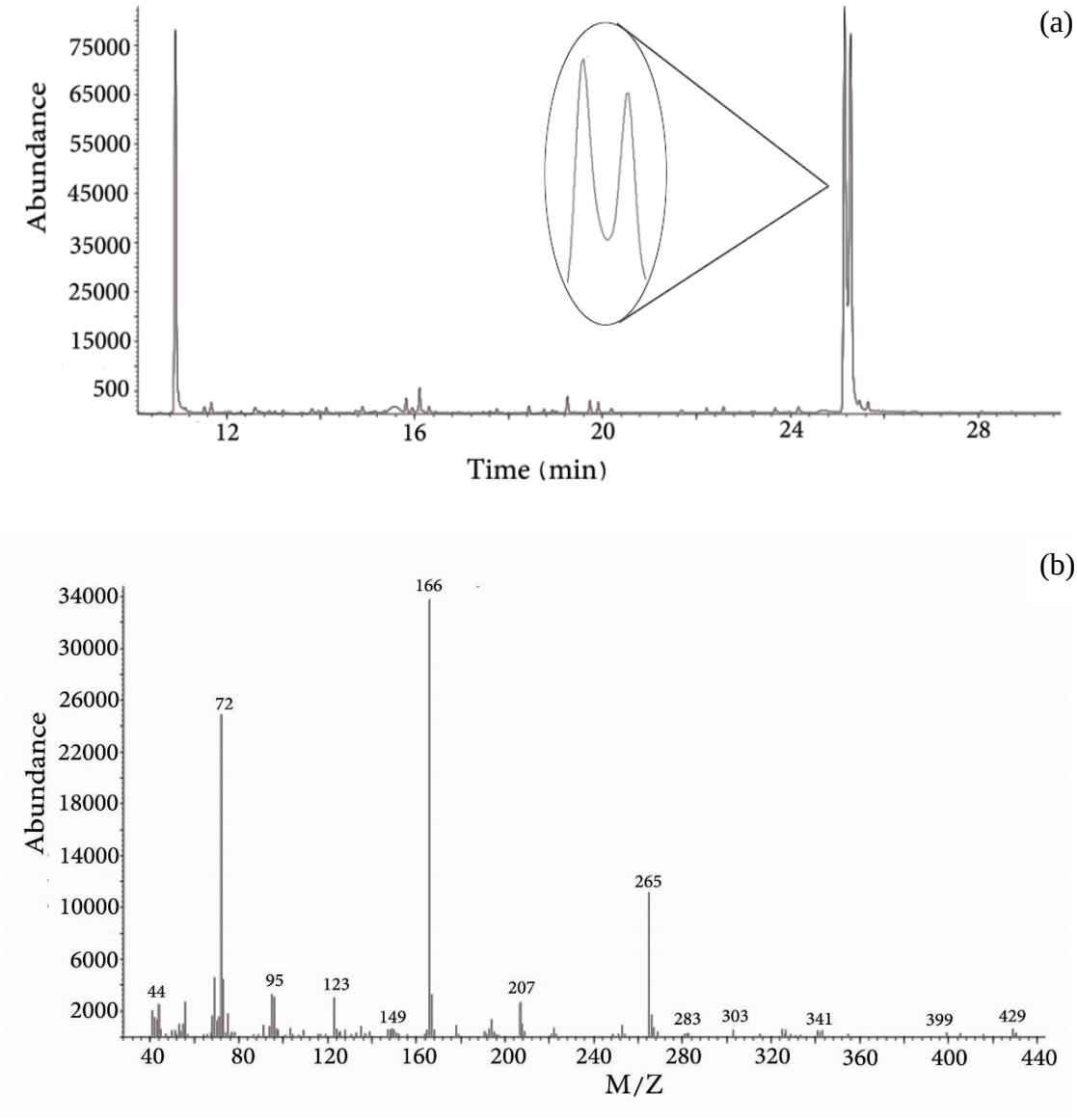

Figure 35: a) Gas chromatogram for separation of the R and S enantiomers of 3-Fluoroethcathinone (3-FEC) drug after derivatization with L-TPC in the presence of nikethamide internal standard and b) mass spectrum of the same compound analyzed by GC-EI-MS system

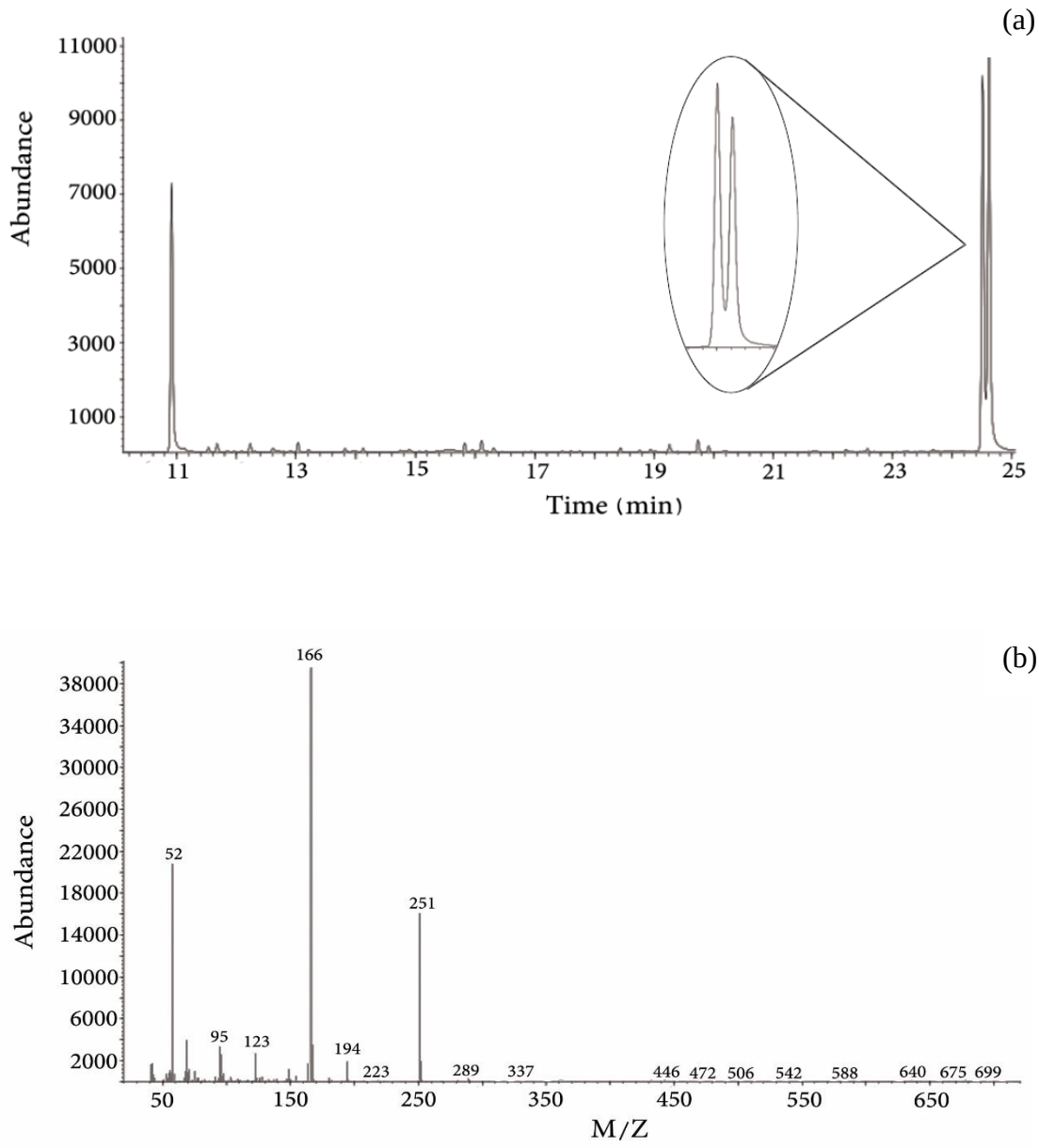

Figure 36: a) Gas chromatogram for separation of the R and S enantiomers of 3-Fluoromethcathinone (3-FMC) drug after derivatization with L-TPC in the presence of nikethamide internal standard and b) mass spectrum of the same compound analyzed by GC-EI-MS system

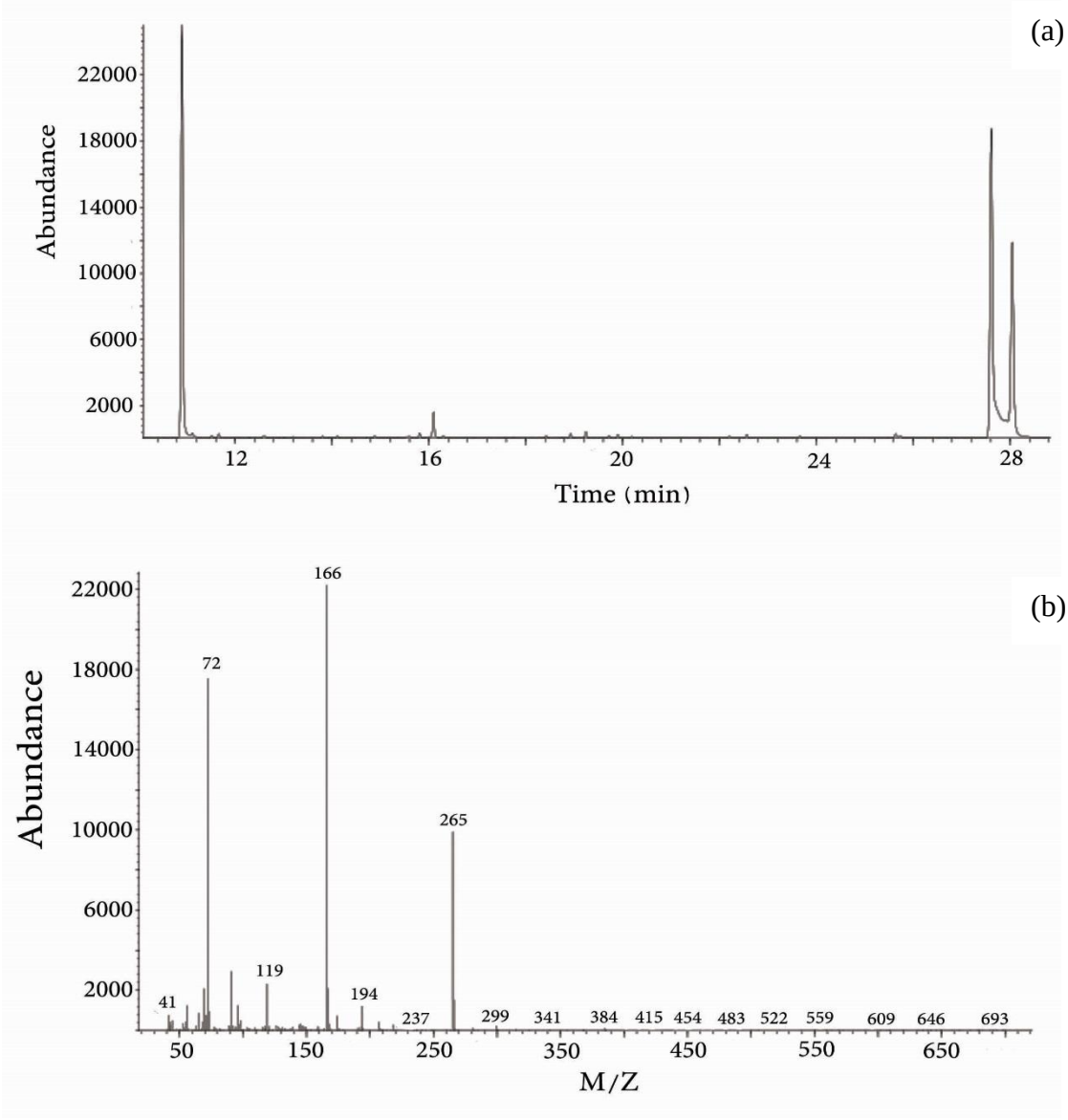

Figure 37: a) Gas chromatogram for separation of the R and S enantiomers of 3-Methylethcathinone (3-MEC) drug after derivatization with L-TPC in the presence of nikethamide internal standard and b) mass spectrum of the same compound analyzed by GC-EI-MS system

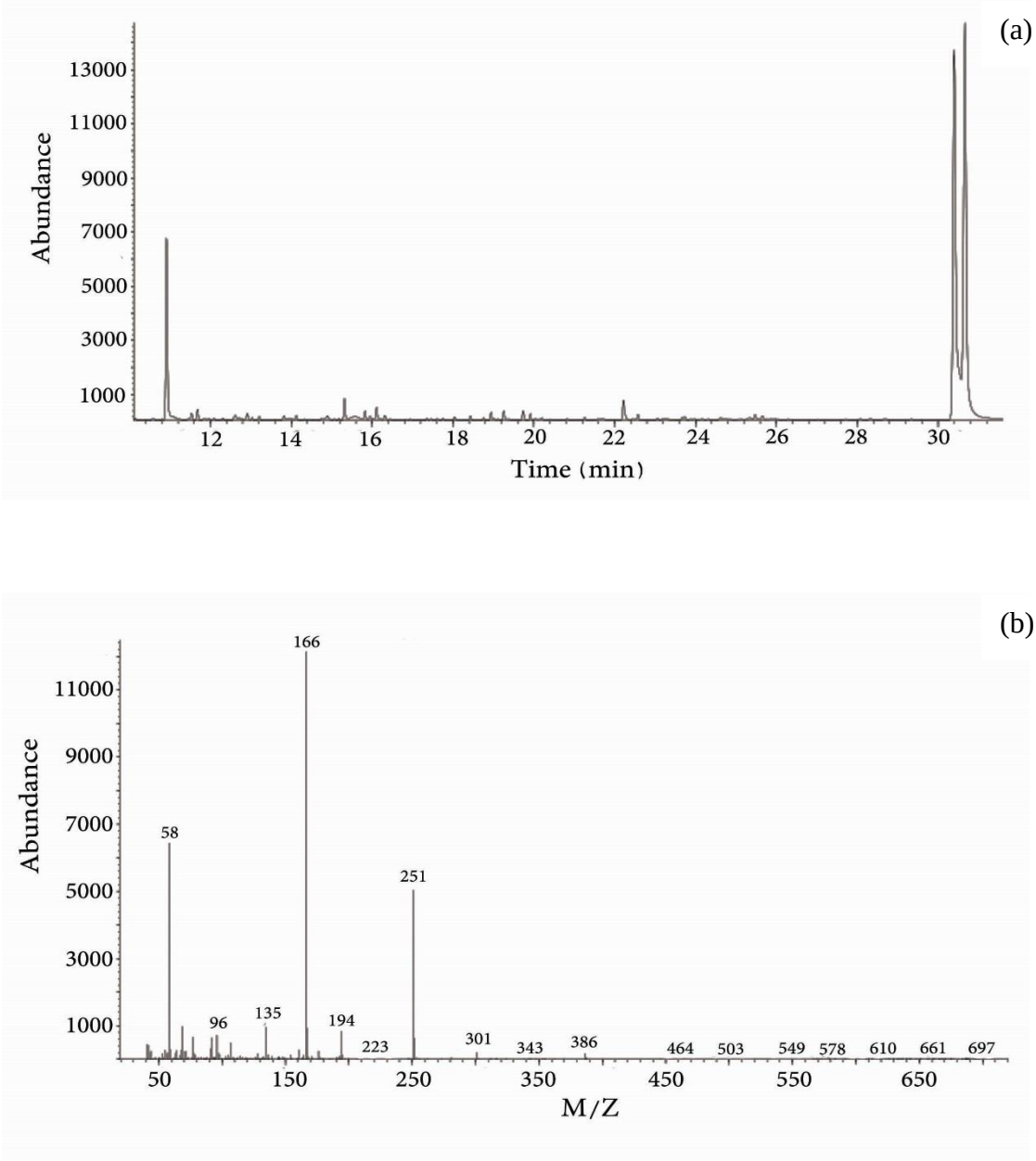

Figure 38: a) Gas chromatogram for separation of the R and S enantiomers of 3-Methoxymethcathinone (3-Me-O-MC) drug after derivatization with L-TPC in the presence of nikethamide internal standard and b) mass spectrum of the same compound analyzed by GC-EI-MS system

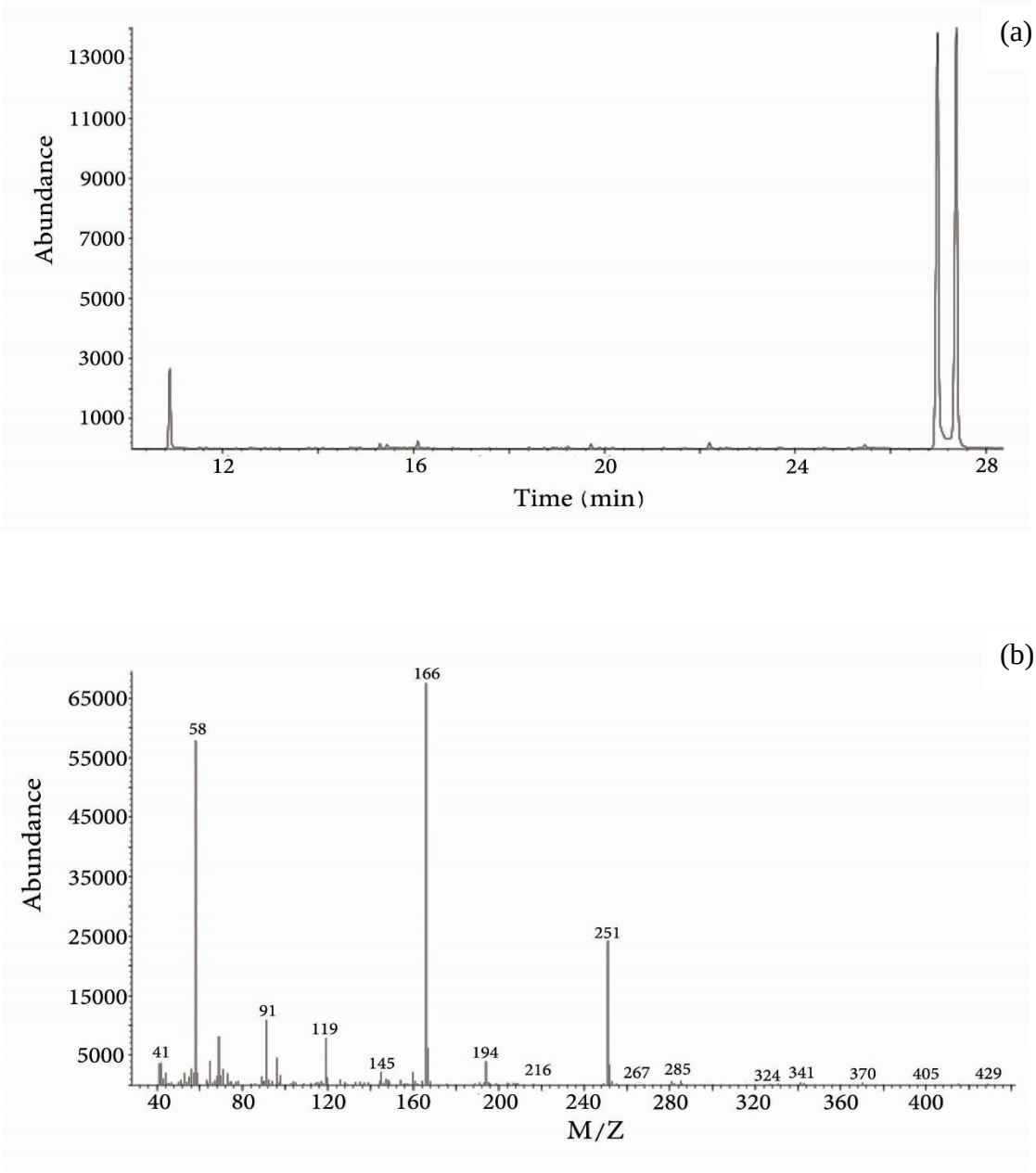

Figure 39: a) Gas chromatogram for separation of the R and S enantiomers of 3-Methylmethcathinone (3-MMC) drug after derivatization with L-TPC in the presence of nikethamide internal standard and b) mass spectrum of the same compound analyzed by GC-EI-MS system

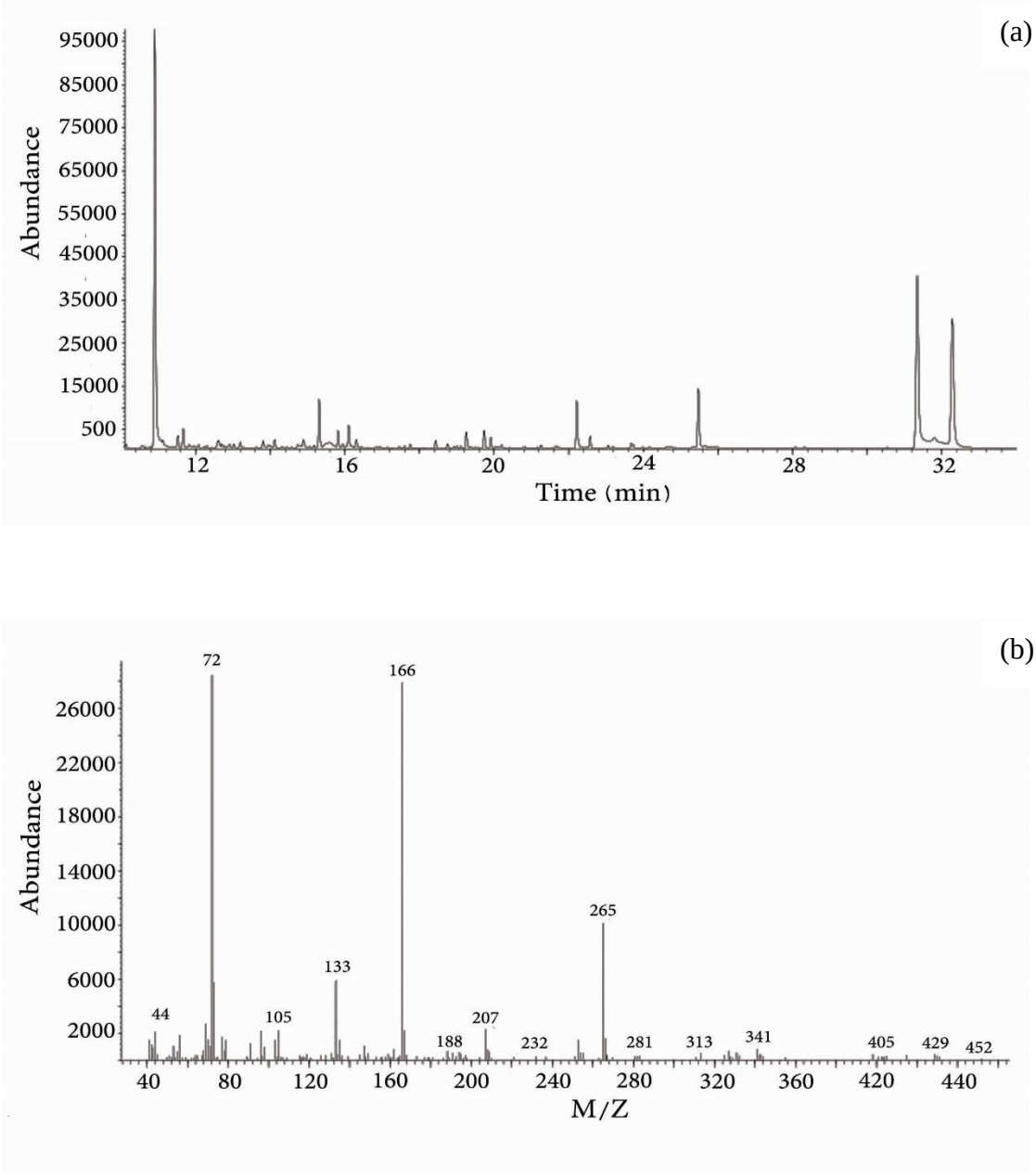

Figure 40: a) Gas chromatogram for separation of the R and S enantiomers of 3,4-Dimethylethcathinone (3,4-DMEC) drug after derivatization with L-TPC in the presence of nikethamide internal standard and b) mass spectrum of the same compound analyzed by GC-EI-MS system

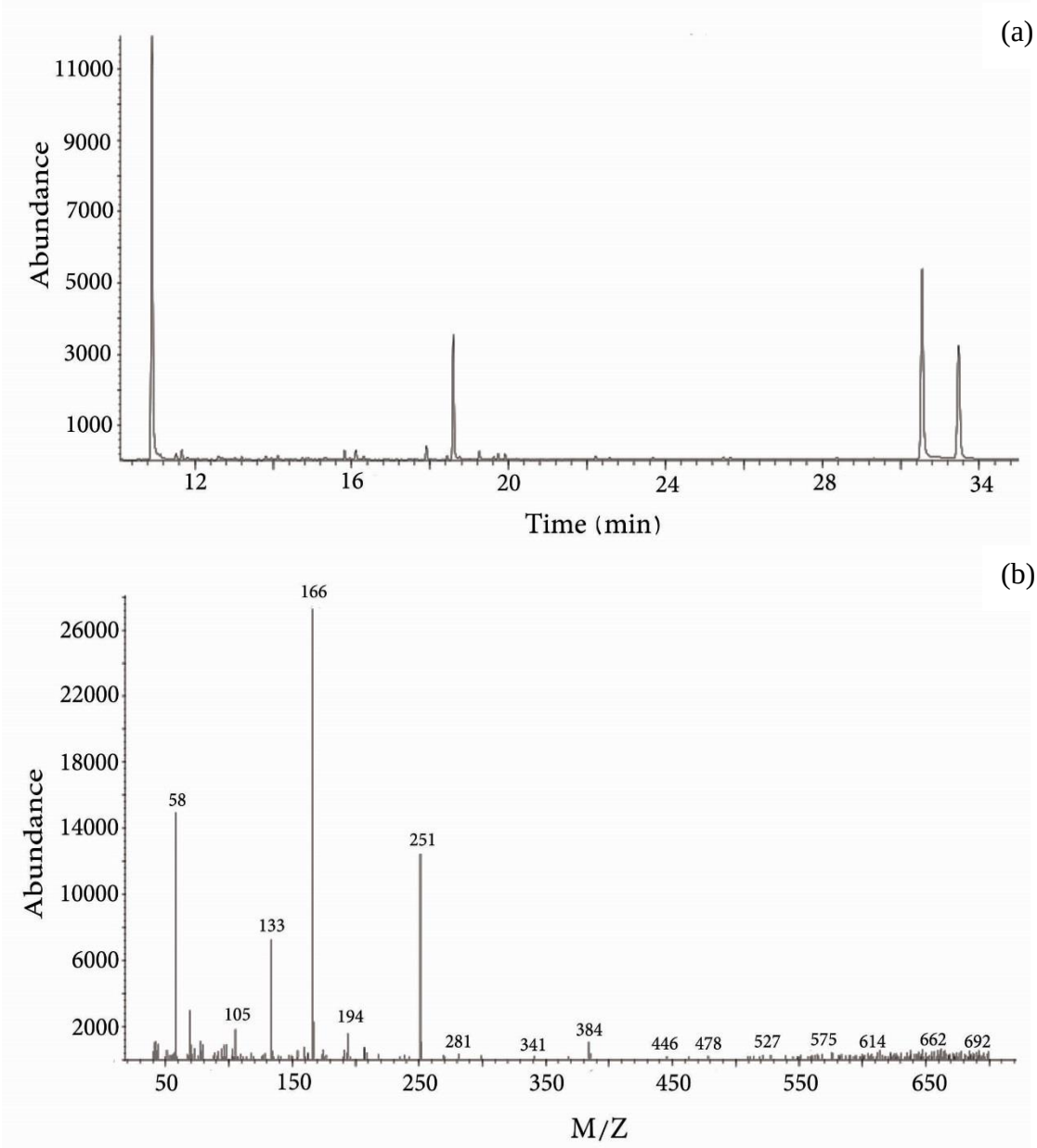

Figure 41: a) Gas chromatogram for separation of the R and S enantiomers of 3,4-Dimethylmethcathinone (3,4-DMMC) drug after derivatization with L-TPC in the presence of nikethamide internal standard and b) mass spectrum of the same compound analyzed by GC-EI-MS system

(a)

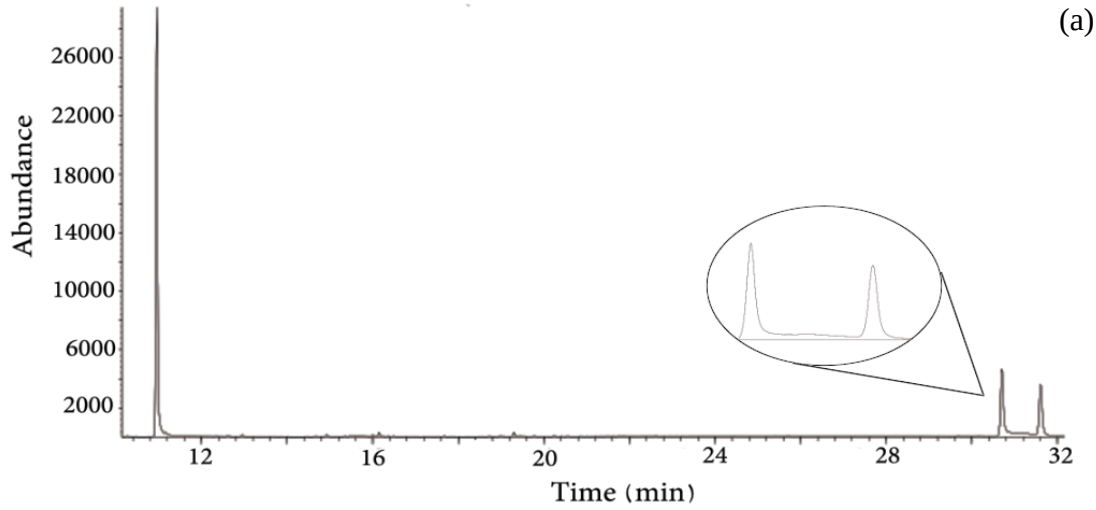

(b)

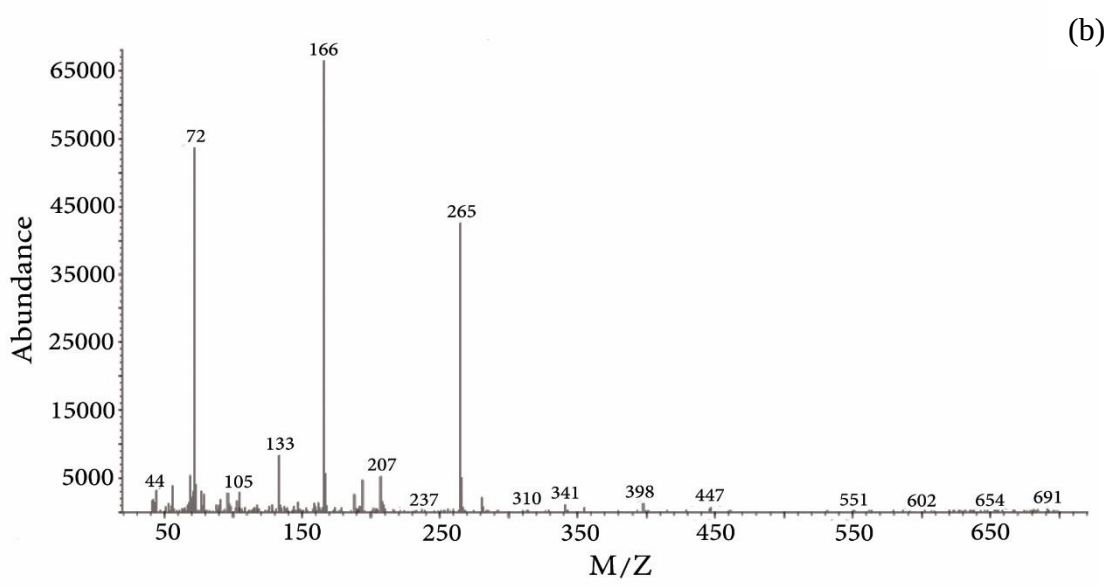

Figure 42: a) Gas chromatogram for separation of the R and S enantiomers of 4-Ethylethcathinone (4-EEC) drug after derivatization with L-TPC in the presence of nikethamide internal standard and b) mass spectrum of the same compound analyzed by GC-EI-MS system

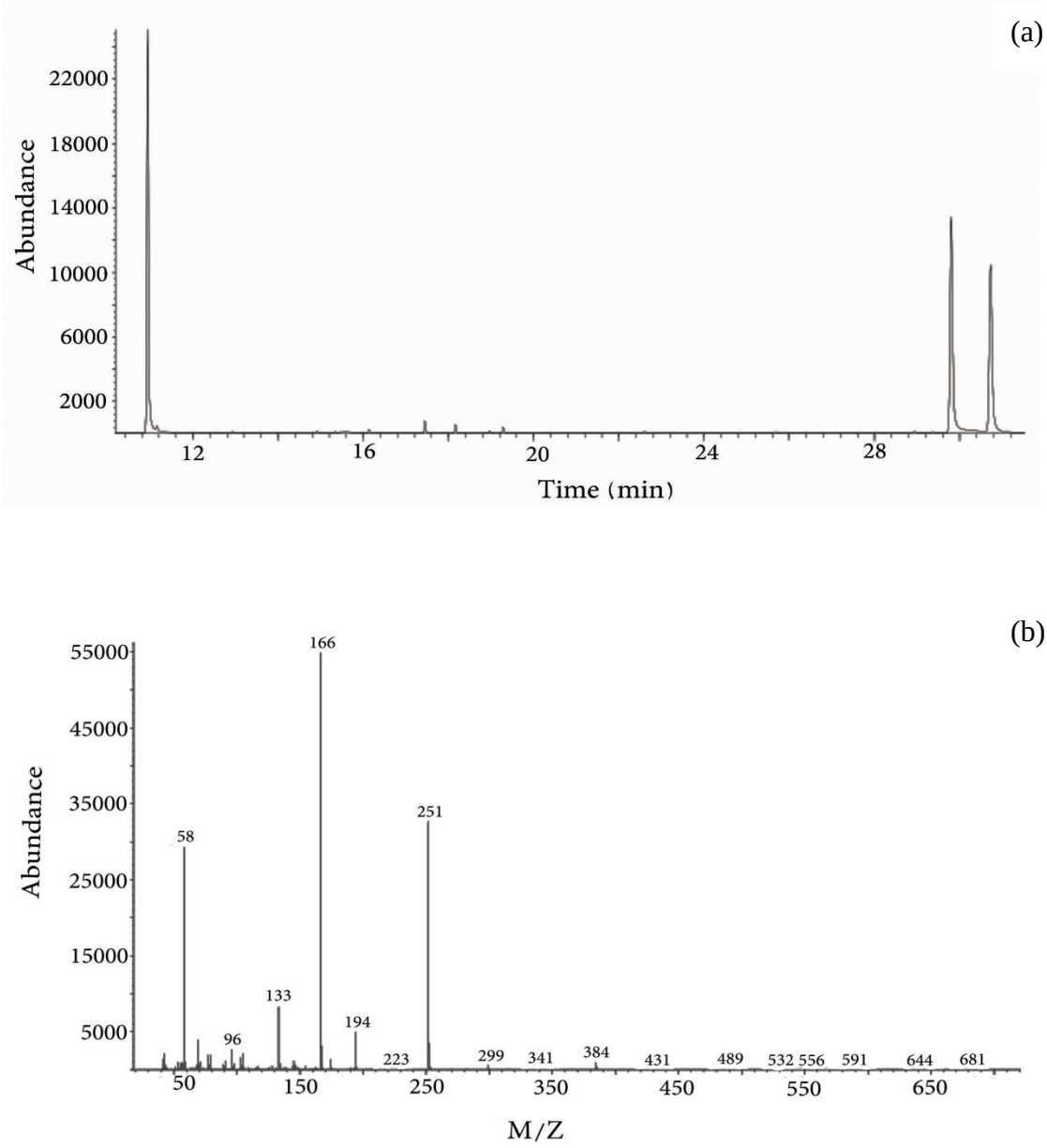

Figure 43: a) Gas chromatogram for separation of the R and S enantiomers of 4-Ethylmethcathinone (4-EMC) drug after derivatization with L-TPC in the presence of nikethamide internal standard and b) mass spectrum of the same compound analyzed by GC-EI-MS system

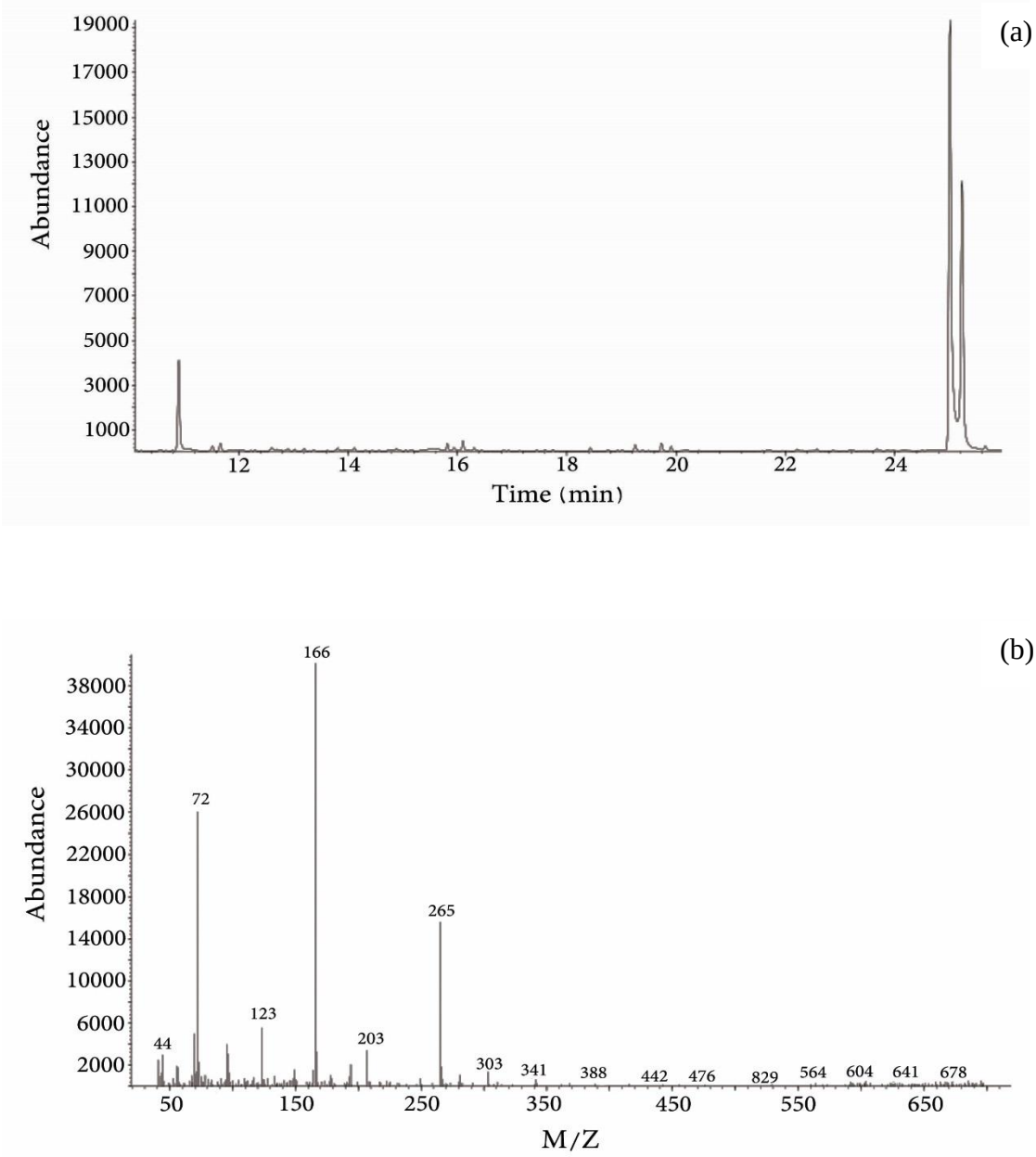

Figure 44: a) Gas chromatogram for separation of the R and S enantiomers of 4-Fluoroethcathinone (4-FEC) drug after derivatization with L-TPC in the presence of nikethamide internal standard and b) mass spectrum of the same compound analyzed by GC-EI-MS system

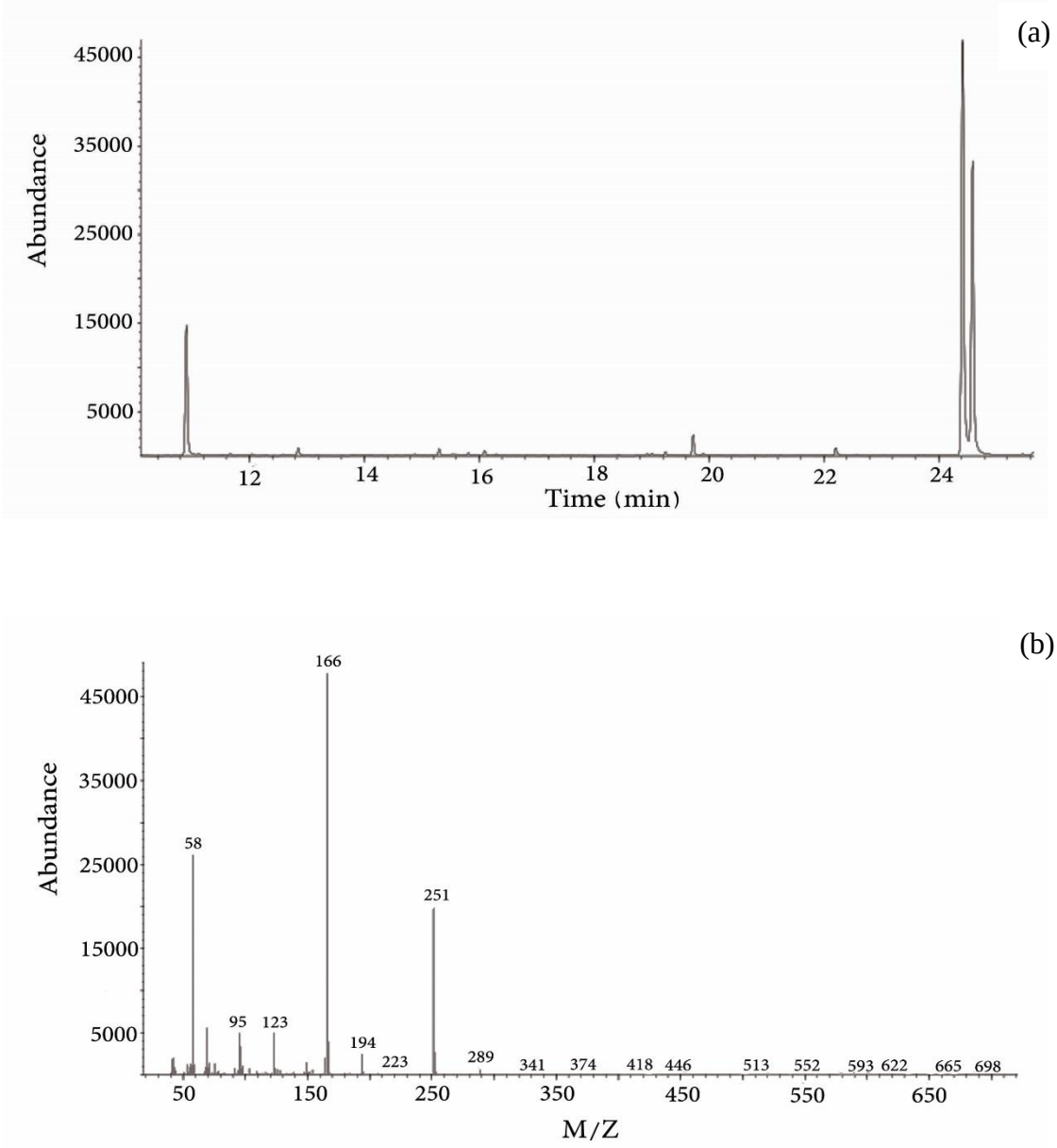

Figure 45: a) Gas chromatogram for separation of the R and S enantiomers of 4-Fluoromethcathinone (4-FMC) drug after derivatization with L-TPC in the presence of nikethamide internal standard and b) mass spectrum of the same compound analyzed by GC-EI-MS system

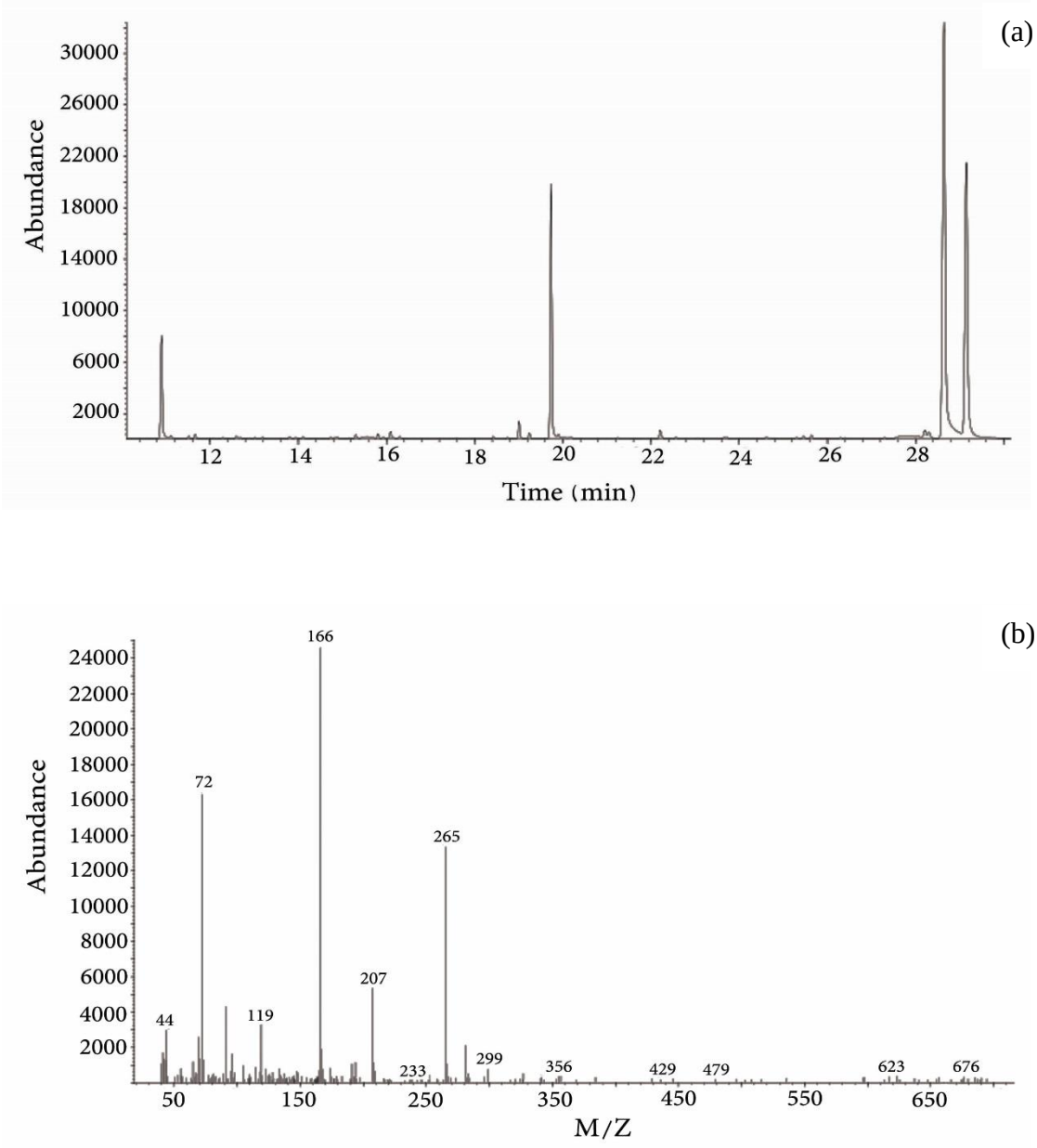

Figure 46: a) Gas chromatogram for separation of the R and S enantiomers of 4-Methylbuphedrone drug after derivatization with L-TPC in the presence of nikethamide internal standard and b) mass spectrum of the same compound analyzed by GC-EI-MS system

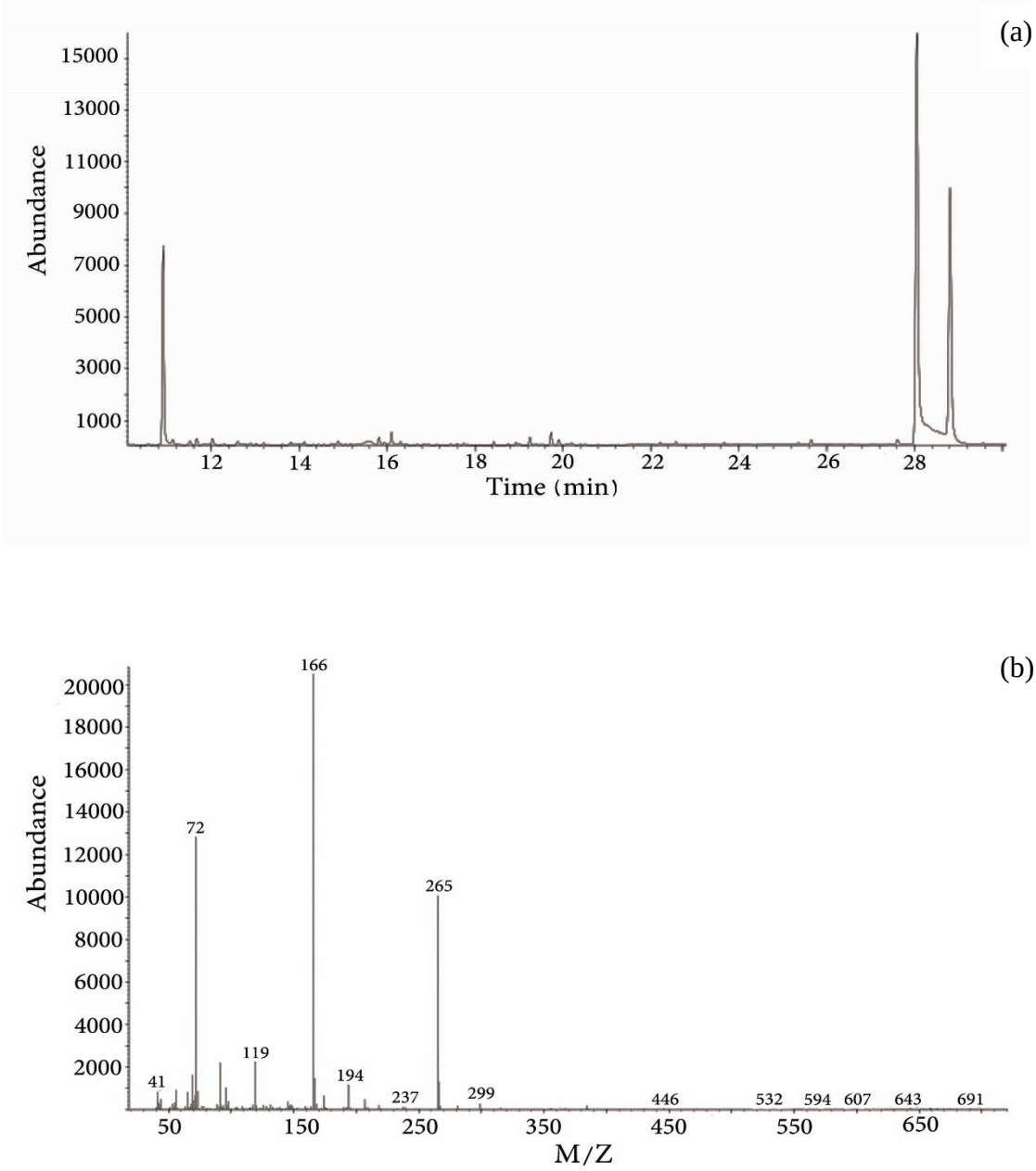

Figure 47: a) Gas chromatogram for separation of the R and S enantiomers of 4-Methylethcathinone (4-MEC) drug after derivatization with L-TPC in the presence of nikethamide internal standard and b) mass spectrum of the same compound analyzed by GC-EI-MS system

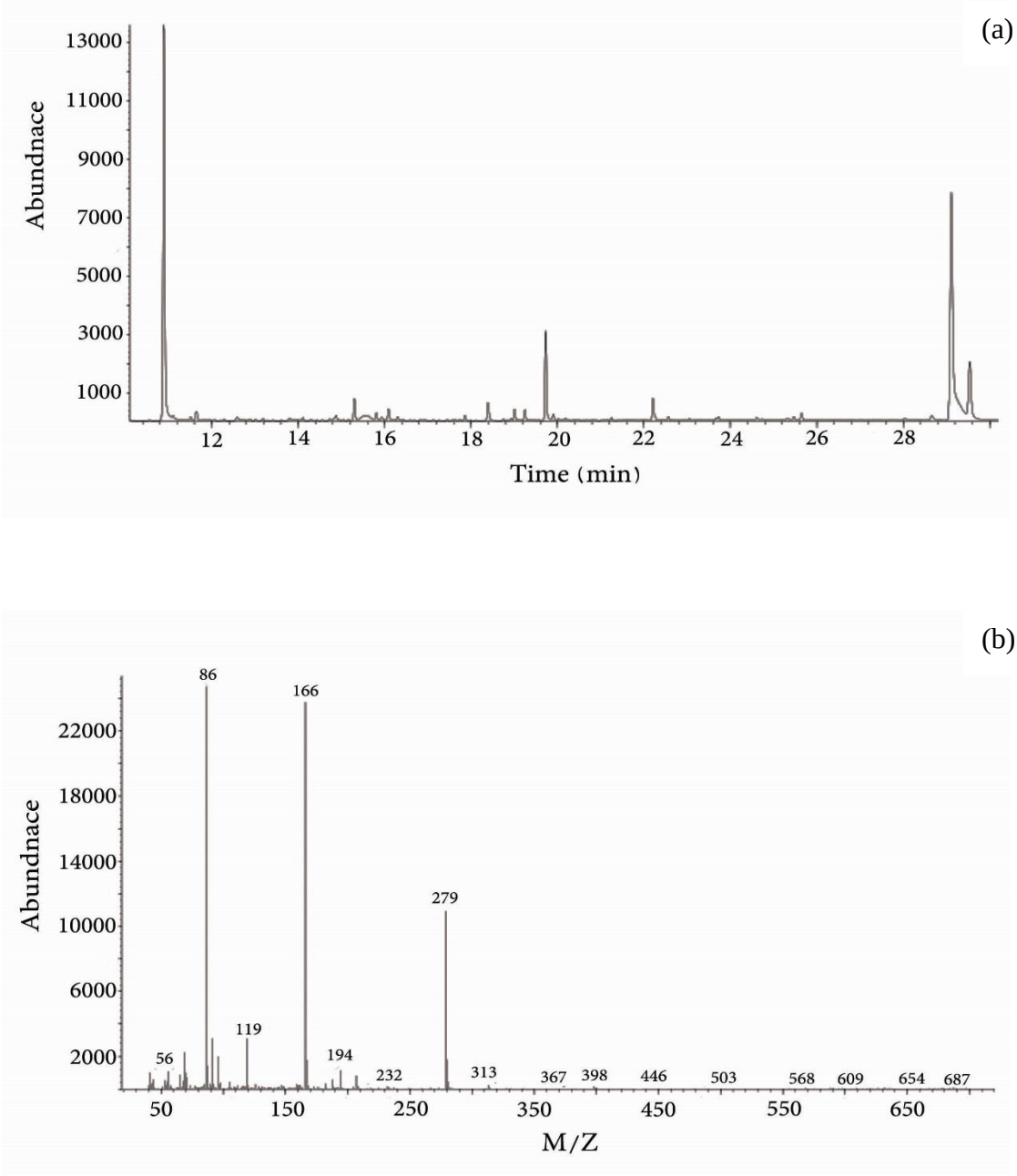

Figure 48: a) Gas chromatogram for separation of the R and S enantiomers of 4-Methyl-α-ethylaminobutiophenone drug after derivatization with L-TPC in the presence of nikethamide internal standard and b) mass spectrum of the same compound analyzed by GC-EI-MS system

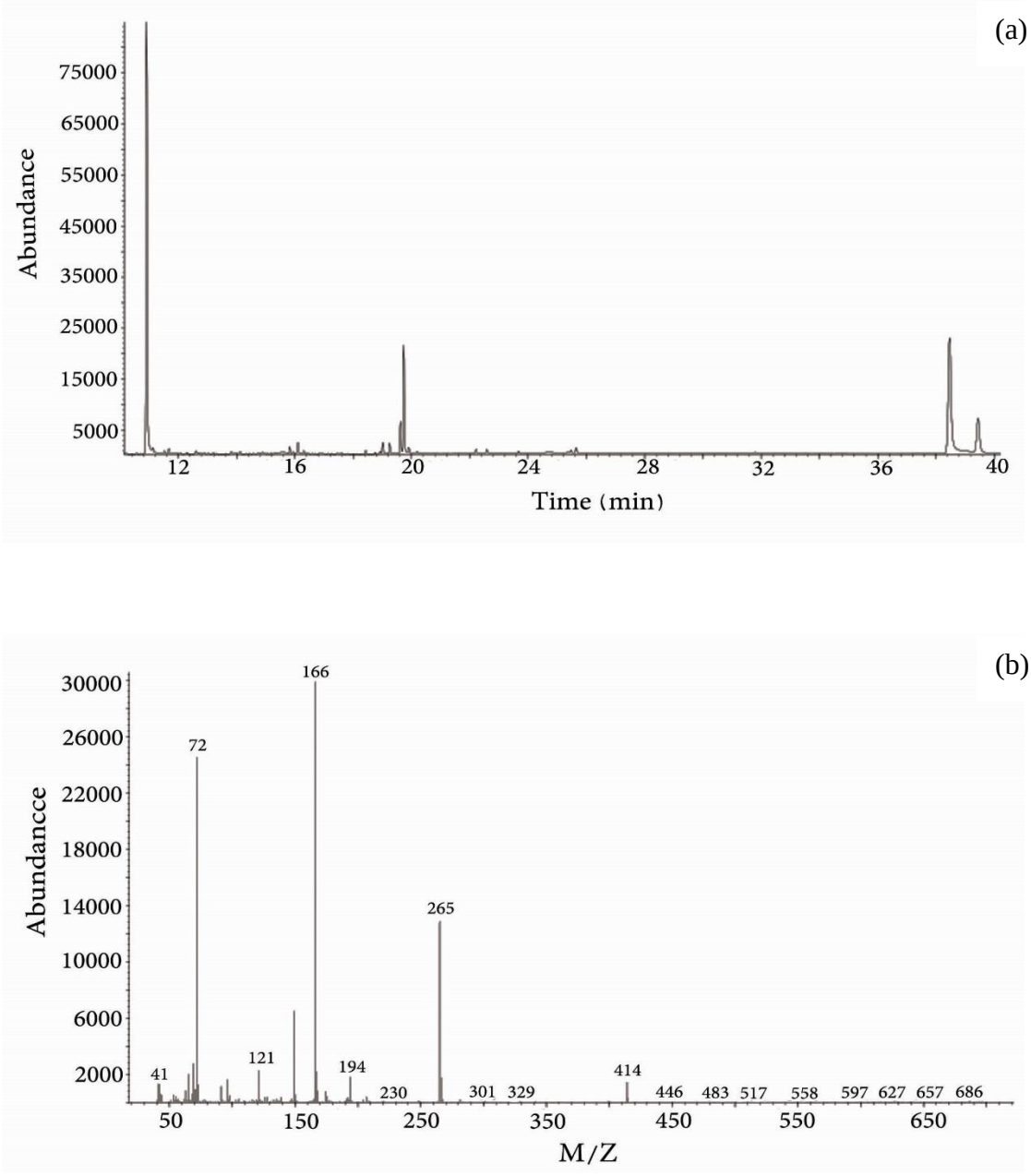

Figure 49: a) Gas chromatogram for separation of the R and S enantiomers of Butylone drug after derivatization with L-TPC in the presence of nikethamide internal standard and b) mass spectrum of the same compound analyzed by GC-EI-MS system

(a)

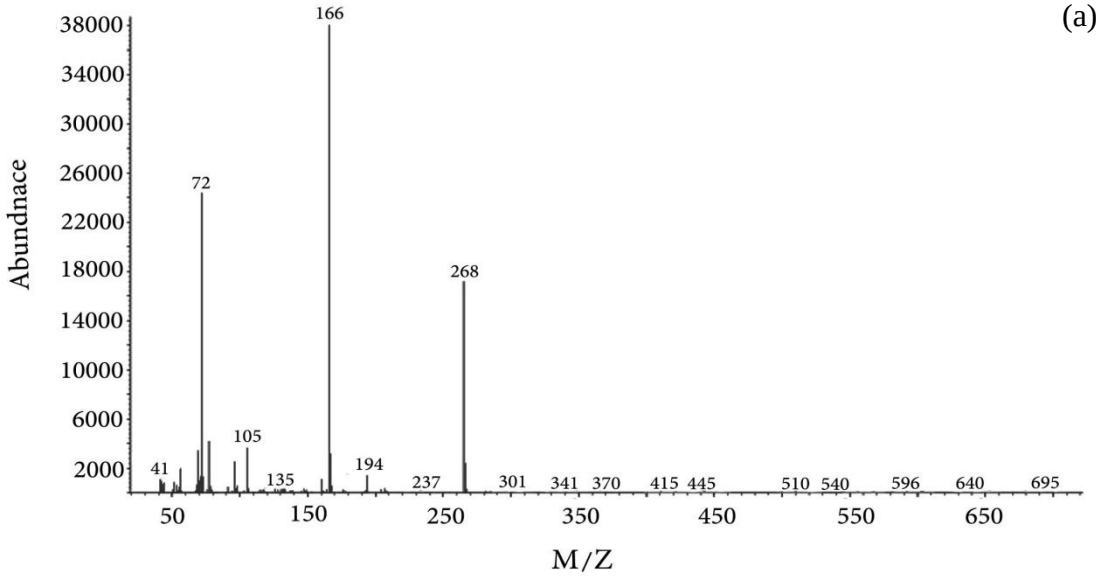

(b)

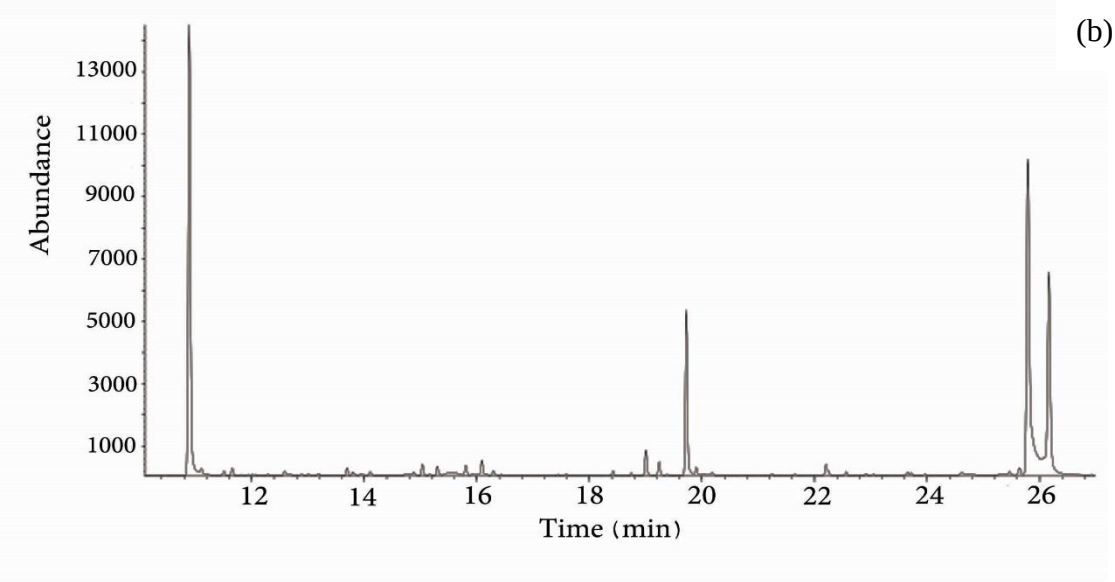

Figure 50: a) Gas chromatogram for separation of the R and S enantiomers of Ethcathinone drug after derivatization with L-TPC in the presence of nikethamide internal standard and b) mass spectrum of the same compound analyzed by GC-EI-MS system

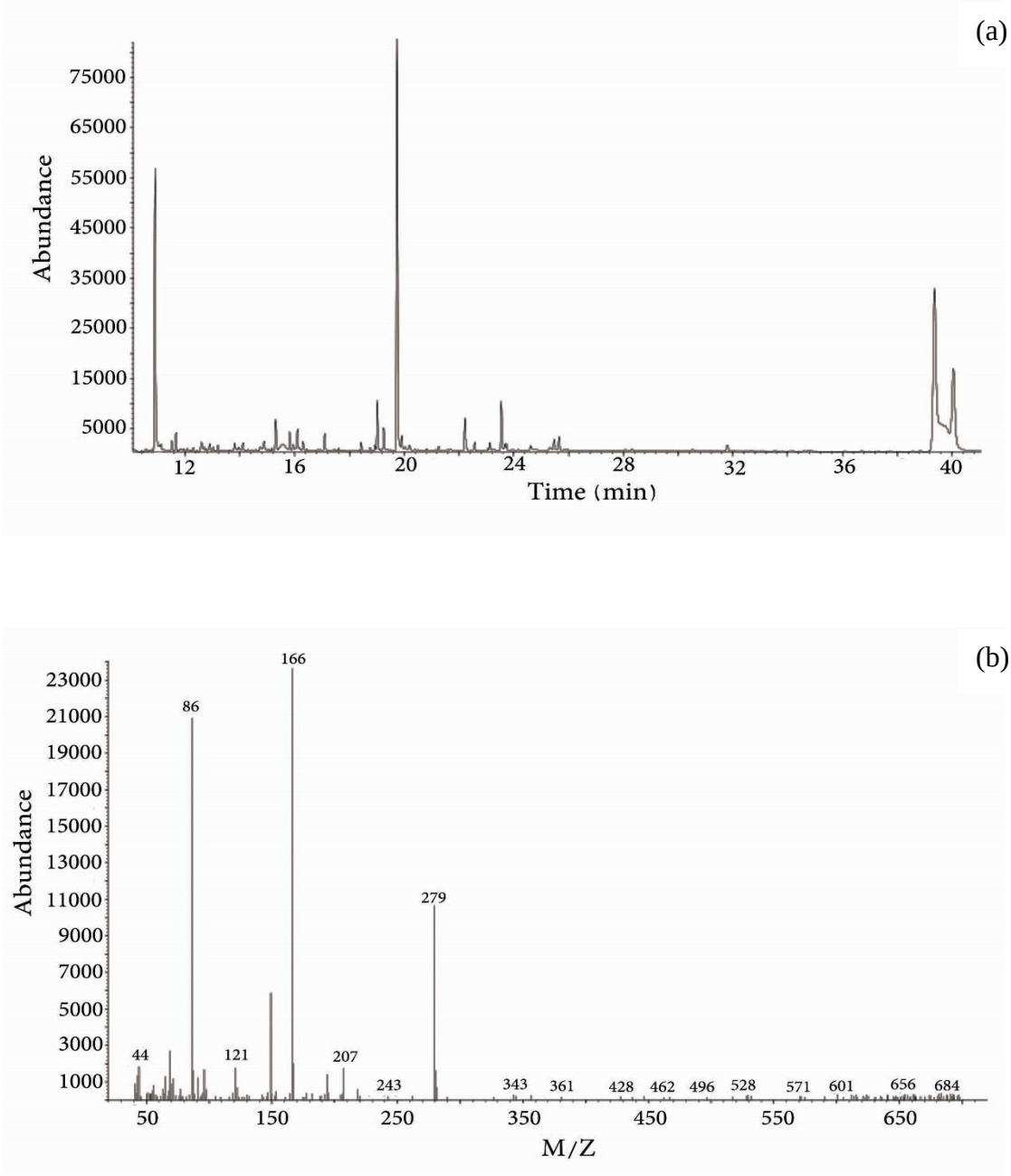

Figure 51: a) Gas chromatogram for separation of the R and S enantiomers of Eutylone drug after derivatization with L-TPC in the presence of nikethamide internal standard and b) mass spectrum of the same compound analyzed by GC-EI-MS system

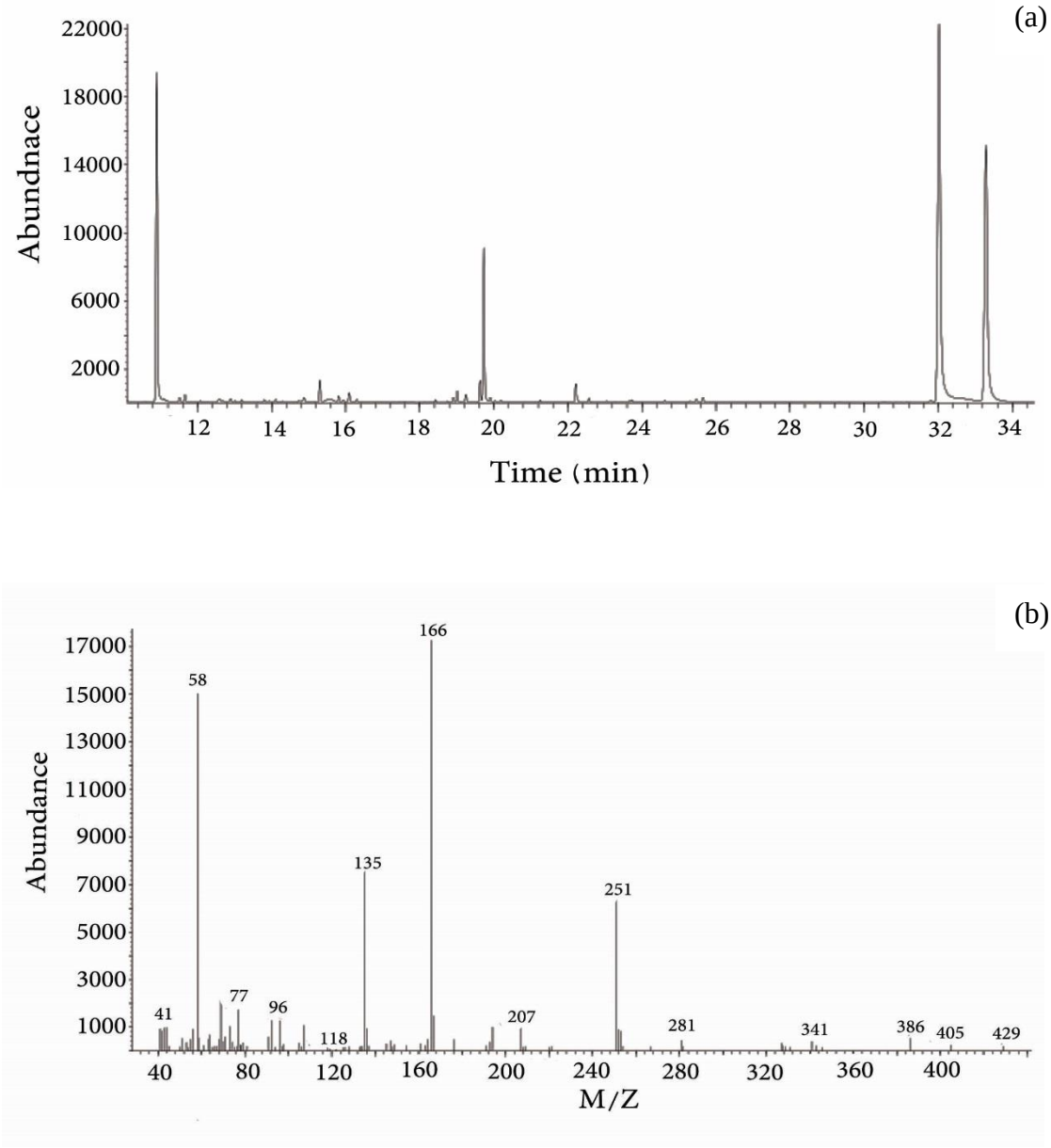

Figure 52: a) Gas chromatogram for separation of the R and S enantiomers of Methedrone drug after derivatization with L-TPC in the presence of nikethamide internal standard and b) mass spectrum of the same compound analyzed by GC-EI-MS system

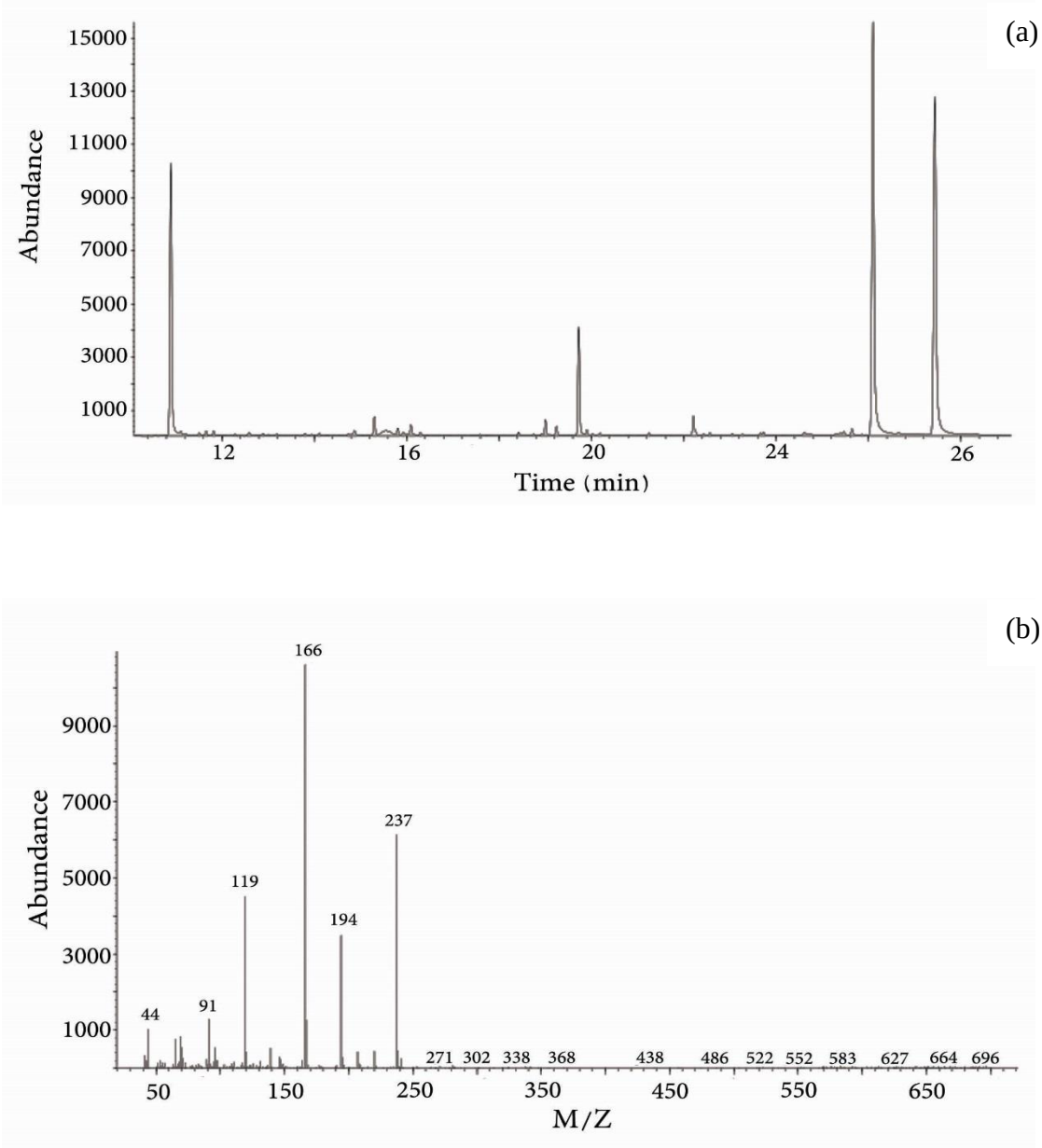

Figure 53: a) Gas chromatogram for separation of the R and S enantiomers of Nor-mephedrone drug after derivatization with L-TPC in the presence of nikethamide internal standard and b) mass spectrum of the same compound analyzed by GC-EI-MS system

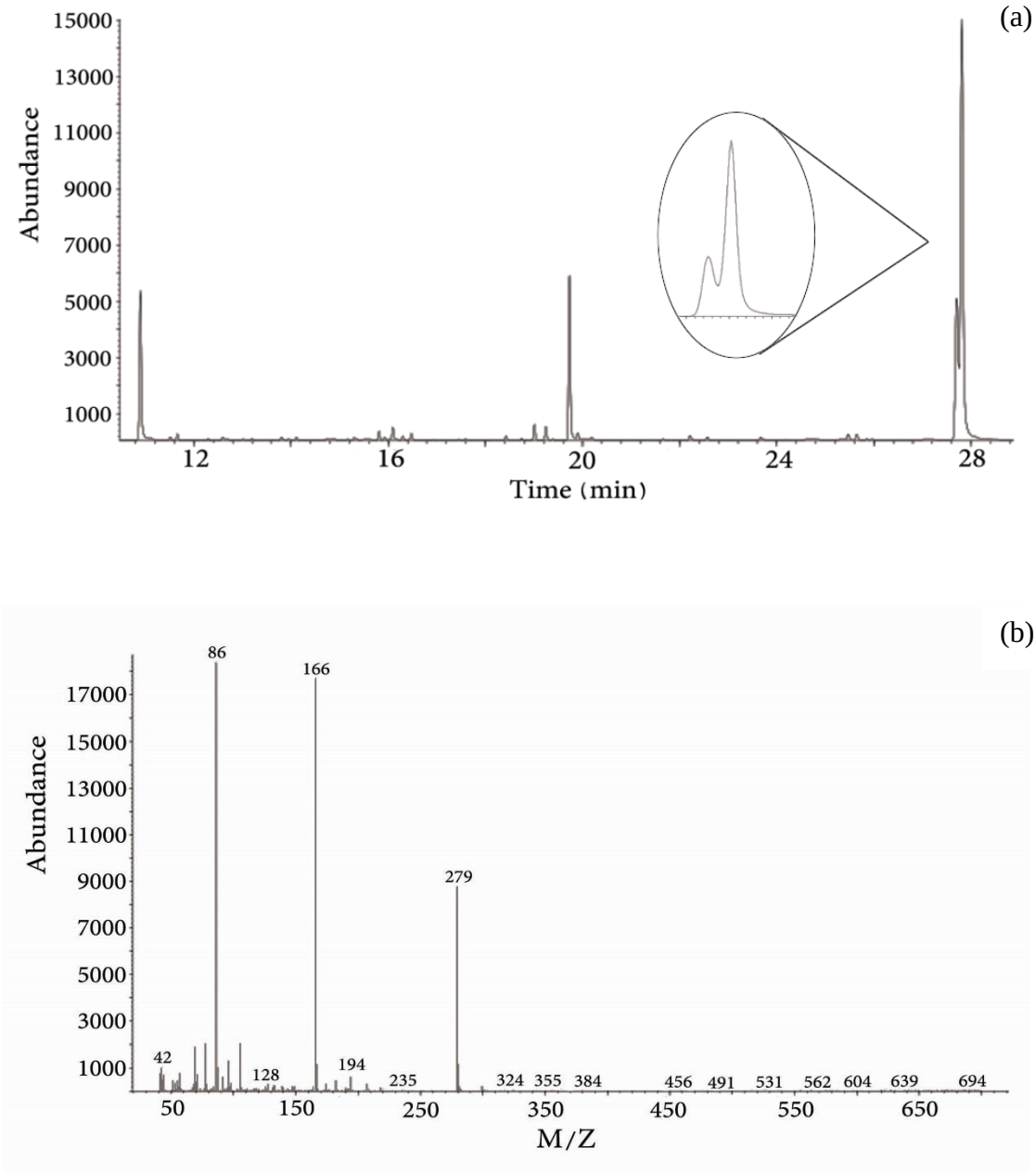

Figure 54: a) Gas chromatogram for separation of the R and S enantiomers of Pentedrone drug after derivatization with L-TPC in the presence of nikethamide internal standard and b) mass spectrum of the same compound analyzed by GC-EI-MS system

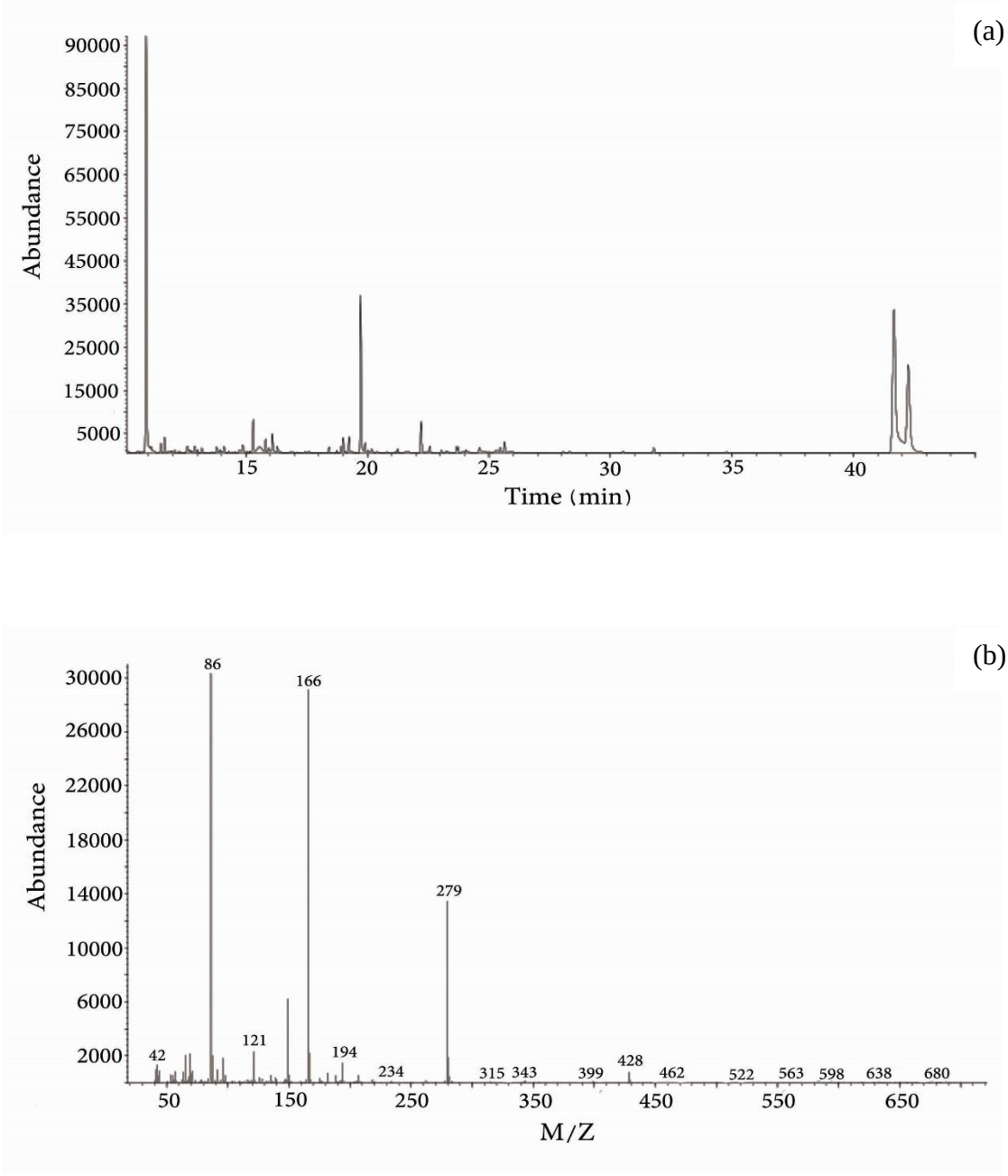

Figure 55: a) Gas chromatogram for separation of the R and S enantiomers of Pentylone drug after derivatization with L-TPC in the presence of nikethamide internal standard and b) mass spectrum of the same compound analyzed by GC-EI-MS system

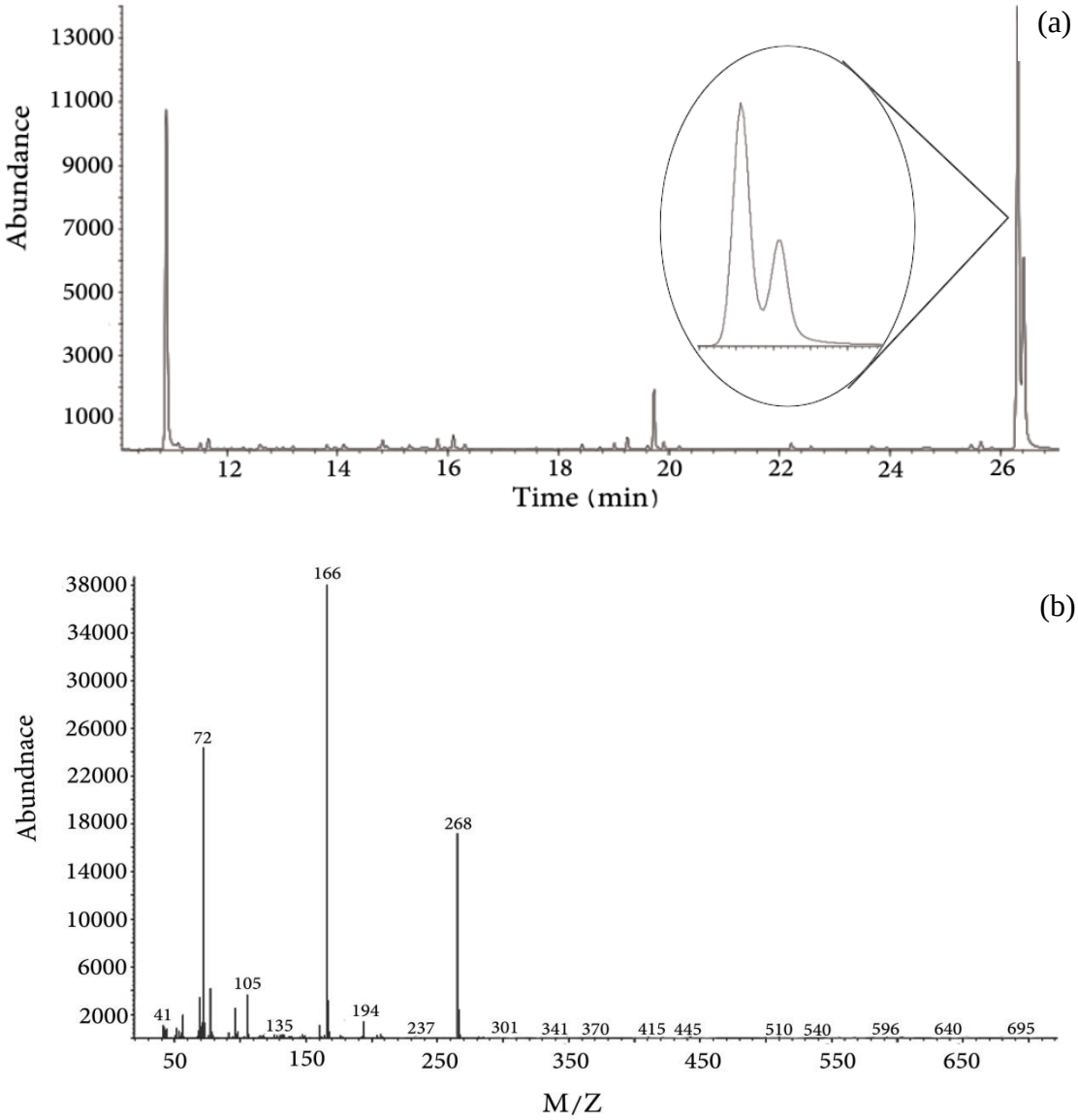

Figure 56: a) Gas chromatogram for separation of the R and S enantiomers of Buphedrone drug after derivatization with L-TPC in the presence of nikethamide internal standard and b) mass spectrum of the same compound analyzed by GC-EI-MS system

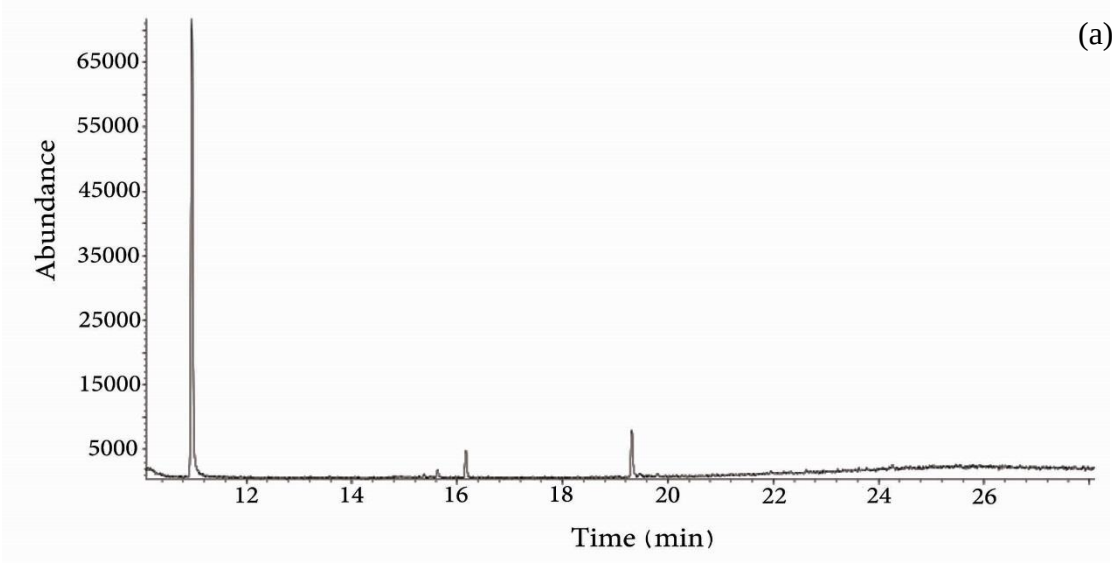

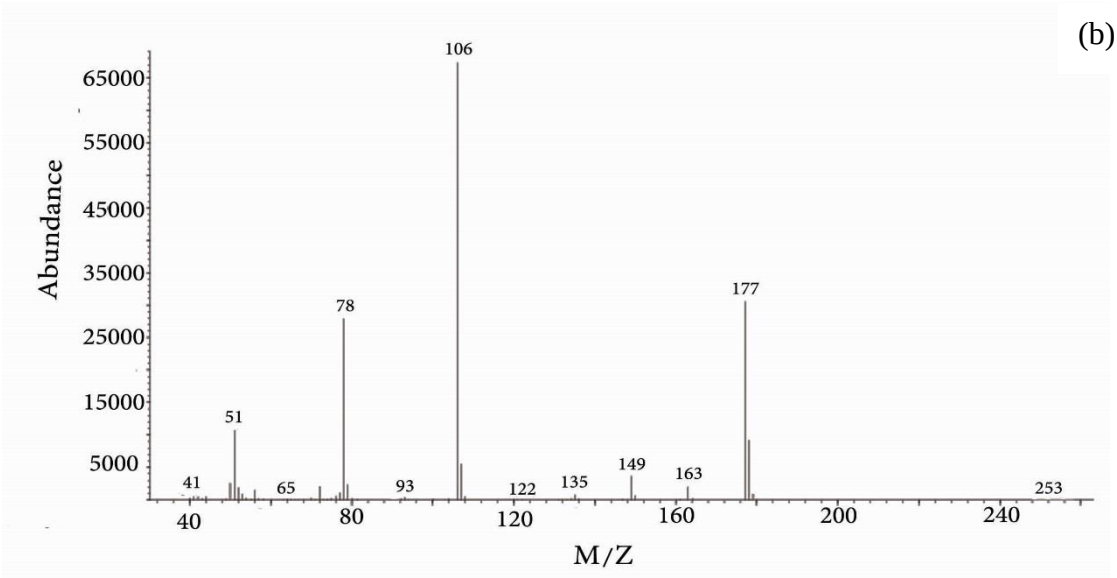

Figure 57: a) Gas chromatogram for the internal standard Nikethamide and b) mass spectrum of the same compound analyzed by GC-EI-MS system

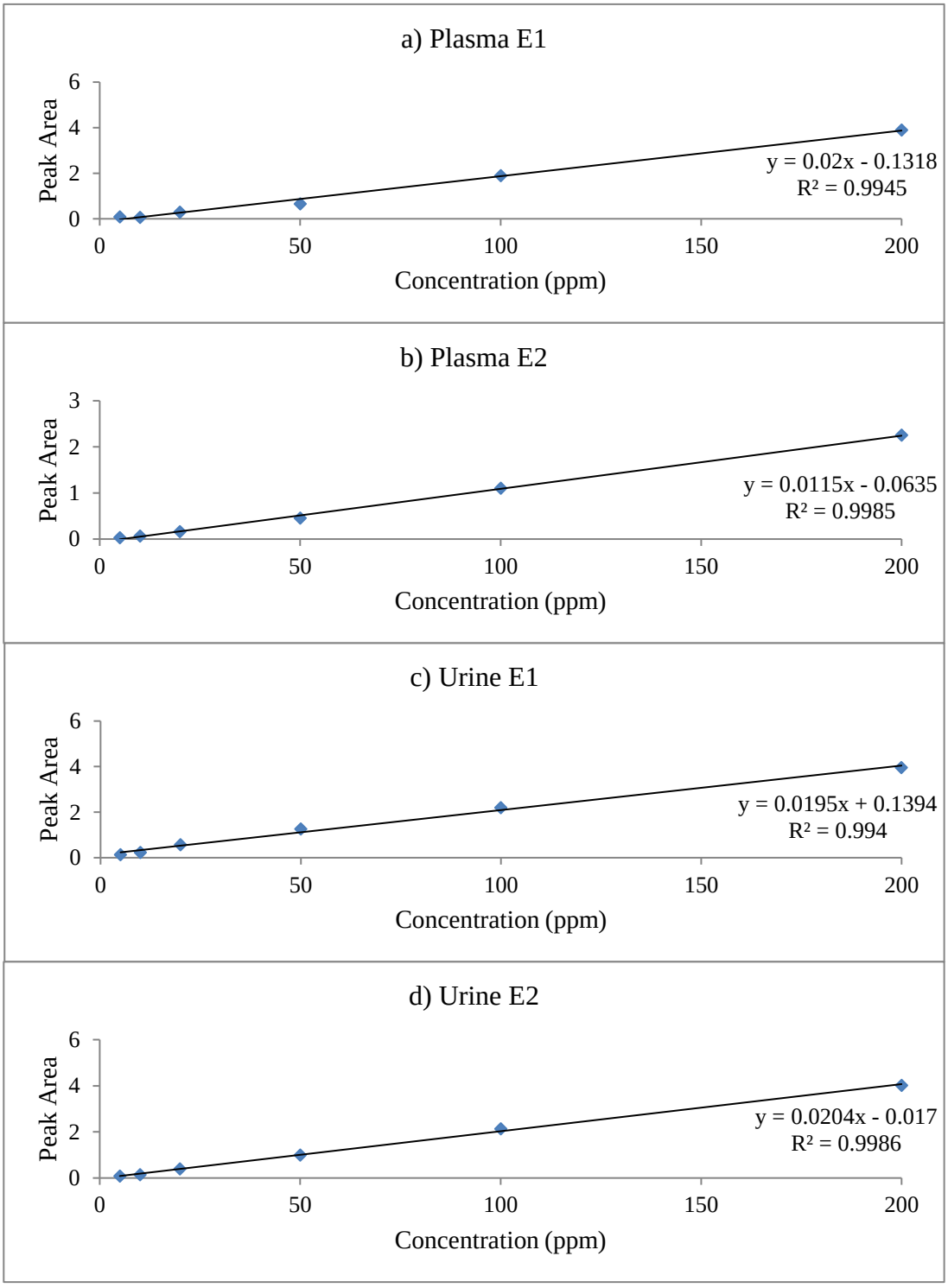

Figure 58: Calibration curves of 4-Methylbuphedrone enantiomers in plasma and urine

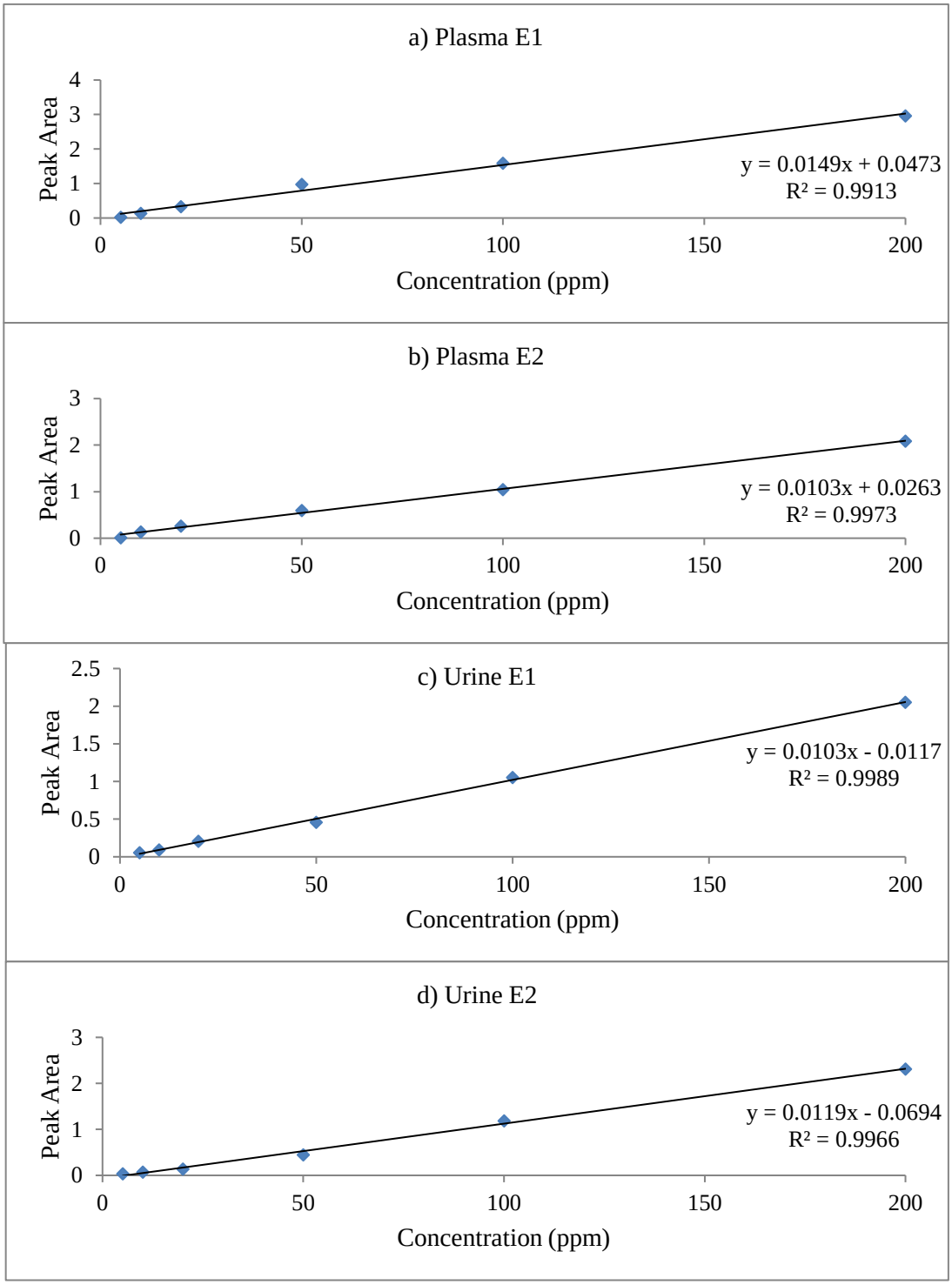

Figure 59: Calibration curves of Pentylone enantiomers in plasma and urine

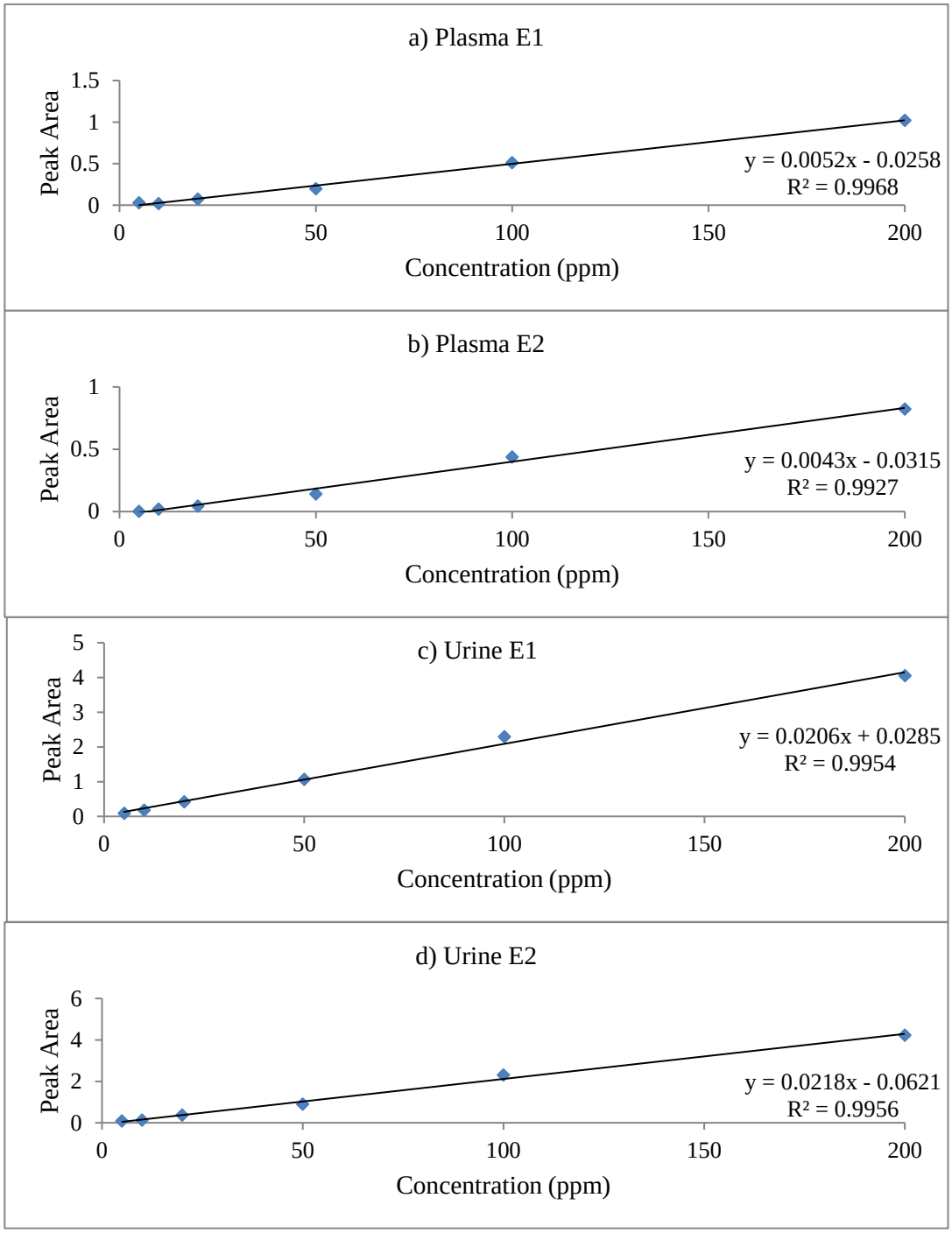

Figure 60: Calibration curves of Ethcathinone enantiomers in plasma and urine

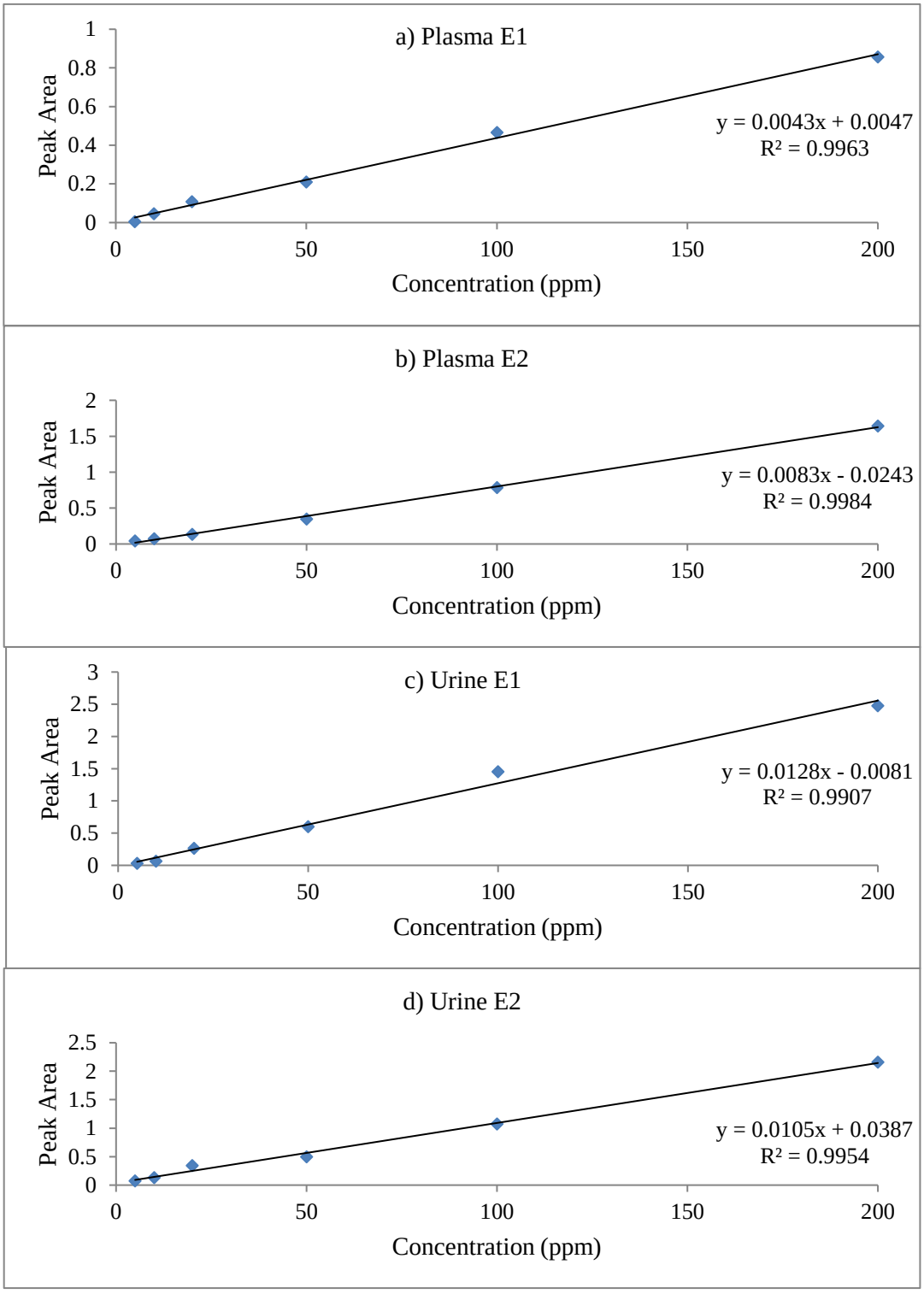

Figure 61: Calibration curves of Pentedrone enantiomers in plasma and urine

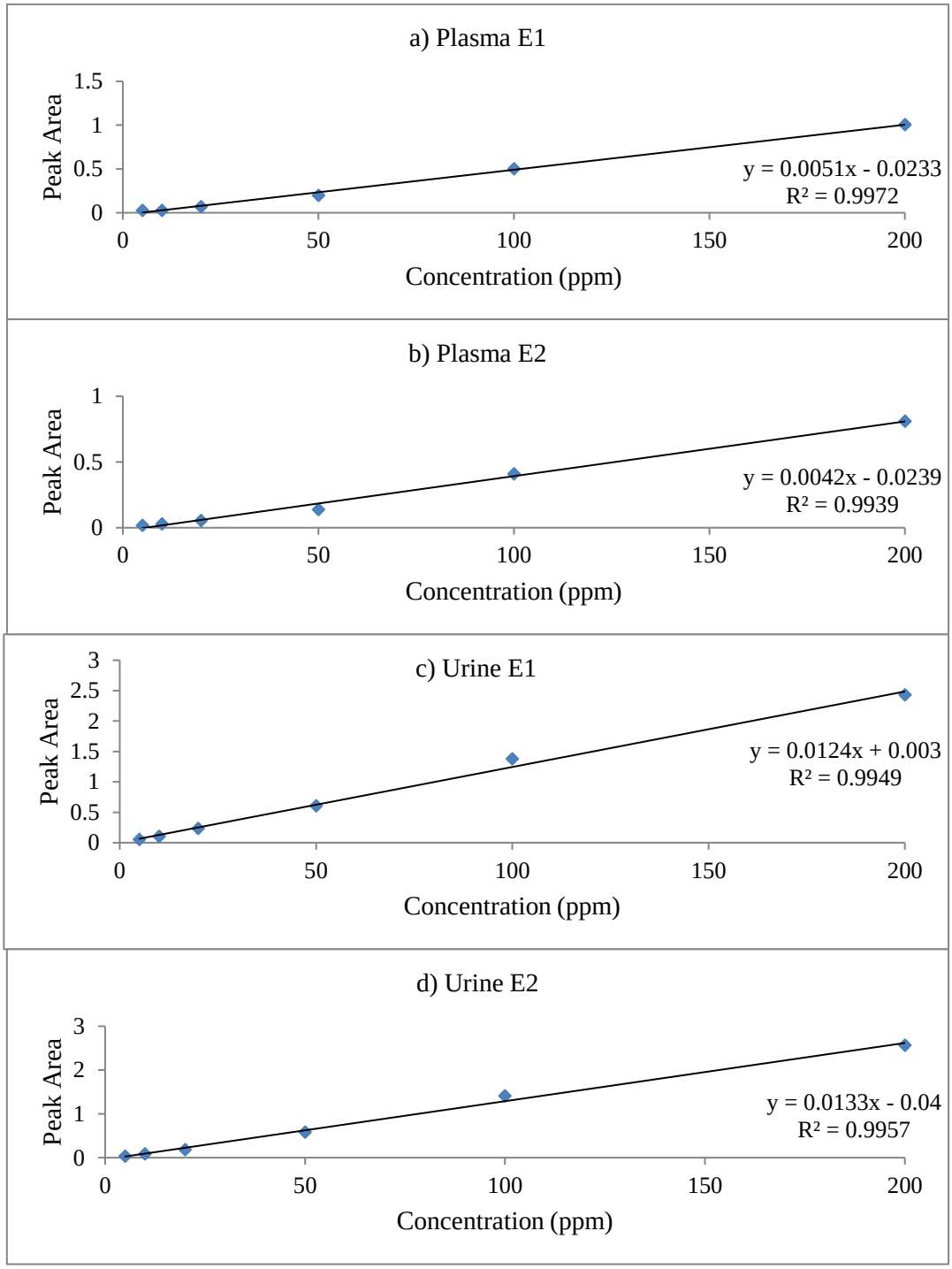

Figure 62: Calibration curves of 4-FEC enantiomers in plasma and urine

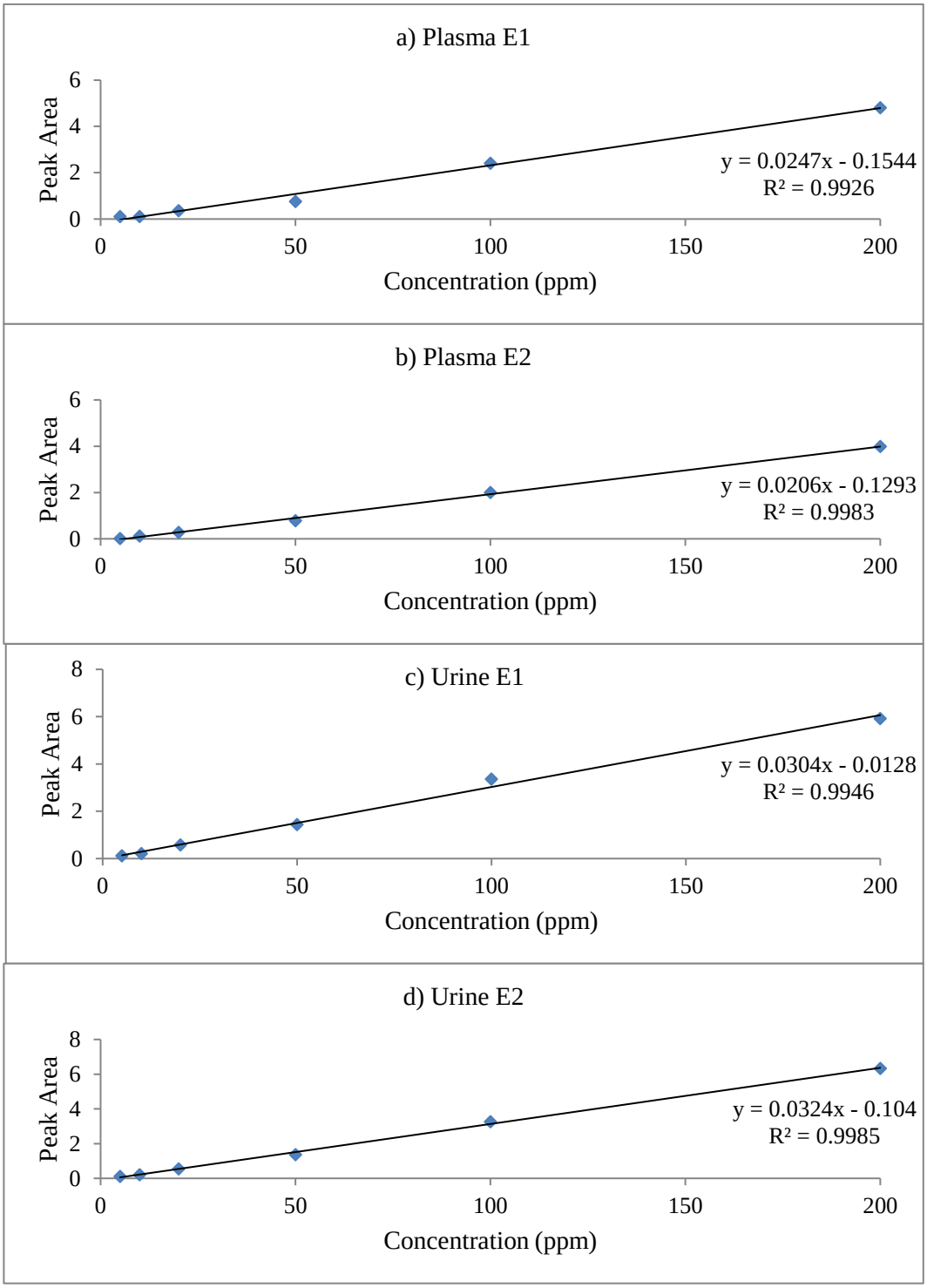

Figure 63: Calibration curves of 3-MMC enantiomers in plasma and urine

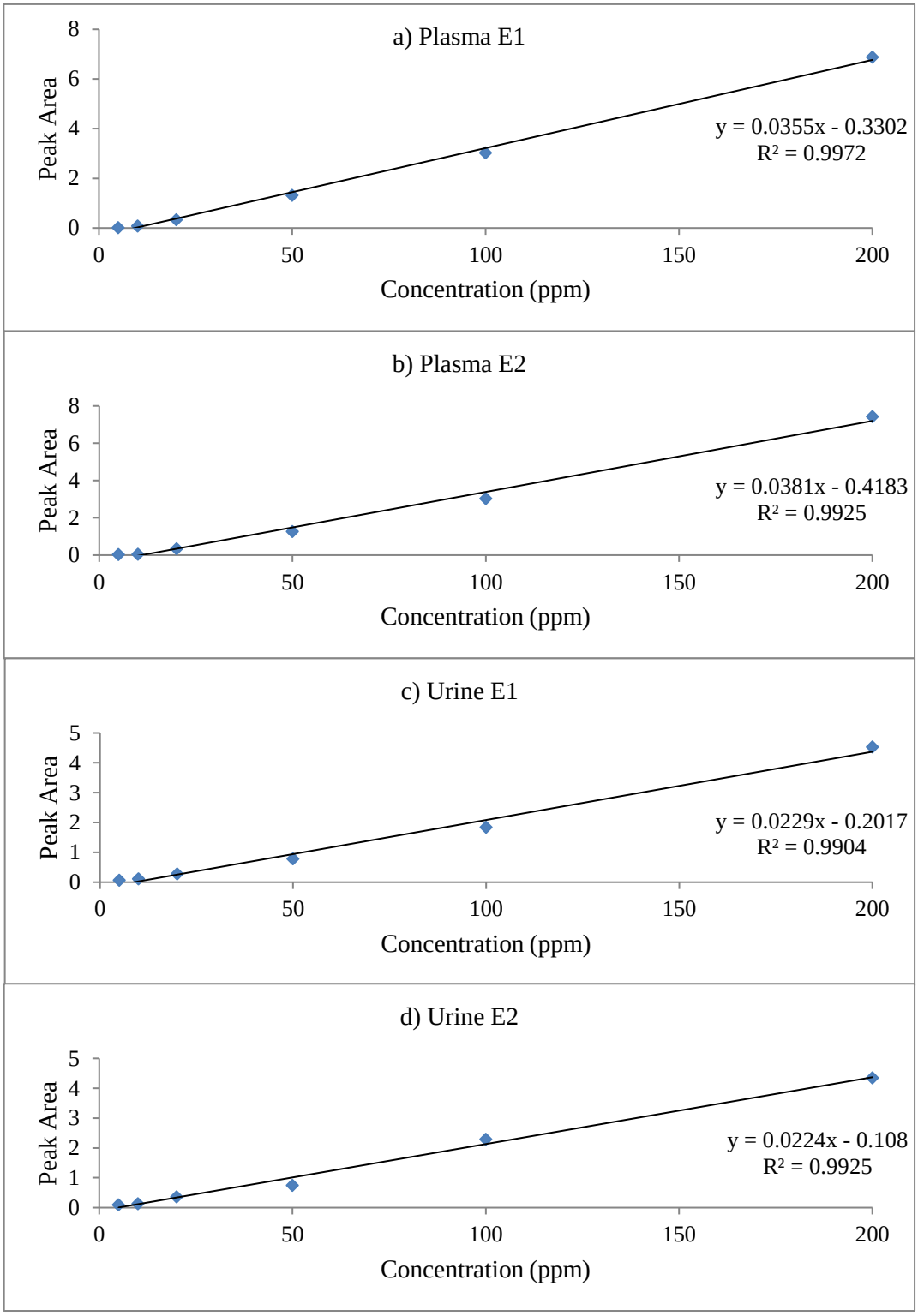

Figure 64: Calibration curves of 3-FMC enantiomers in plasma and urine

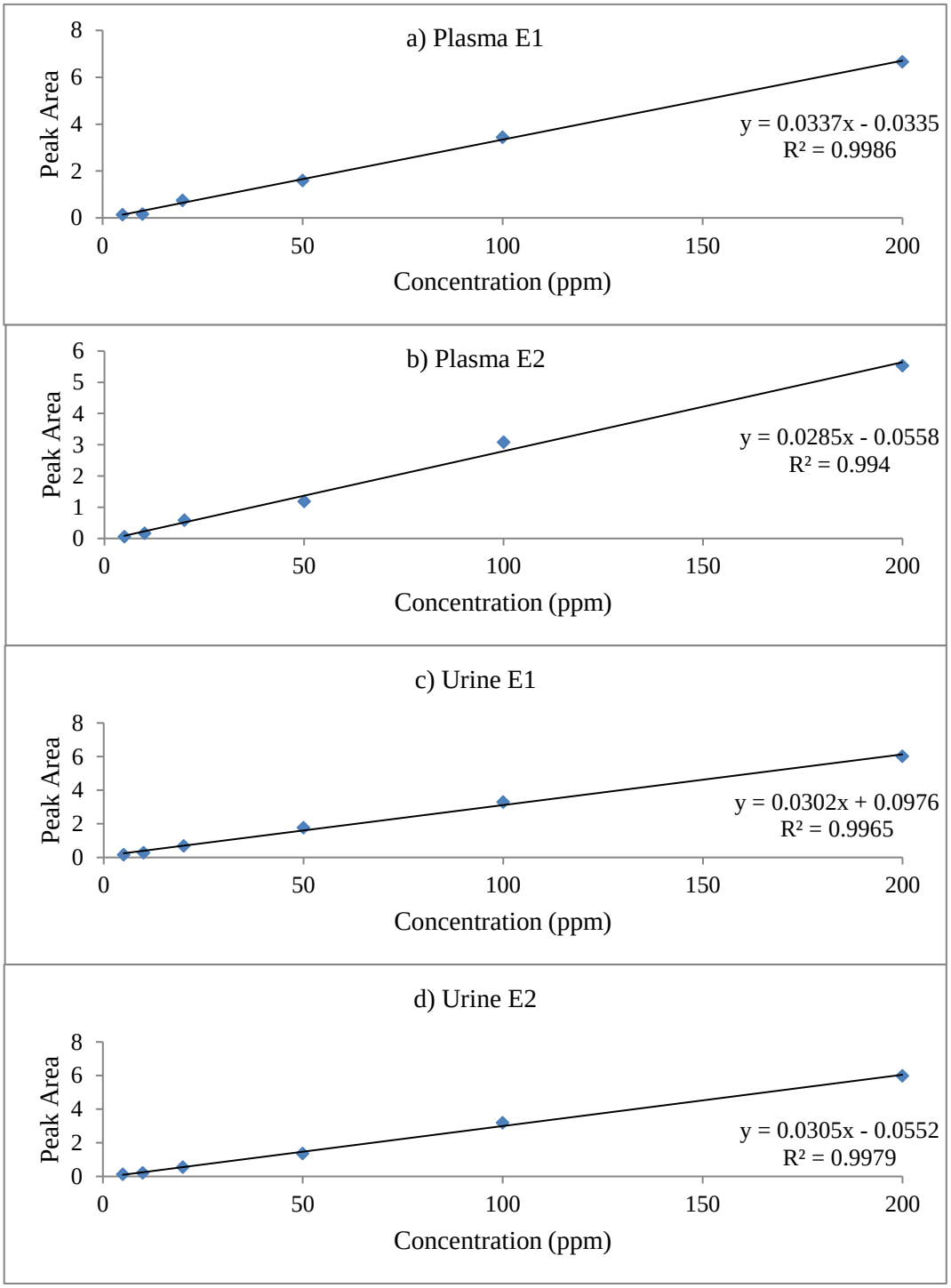

Figure 65: Calibration curves of 3,4-DMMC enantiomers in plasma and urine

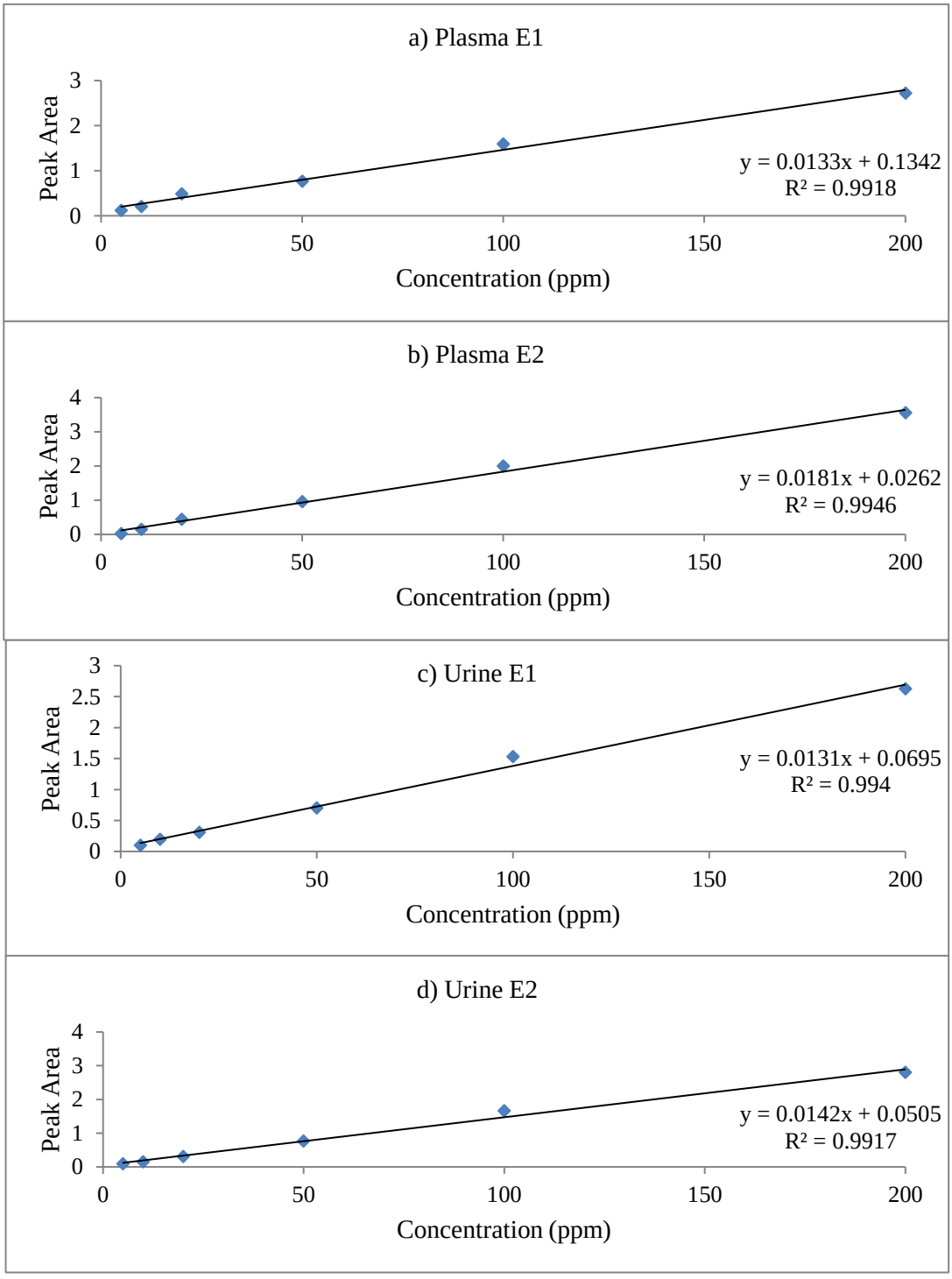

Figure 66: Calibration curves of 2,3-MDMC enantiomers in plasma and urine

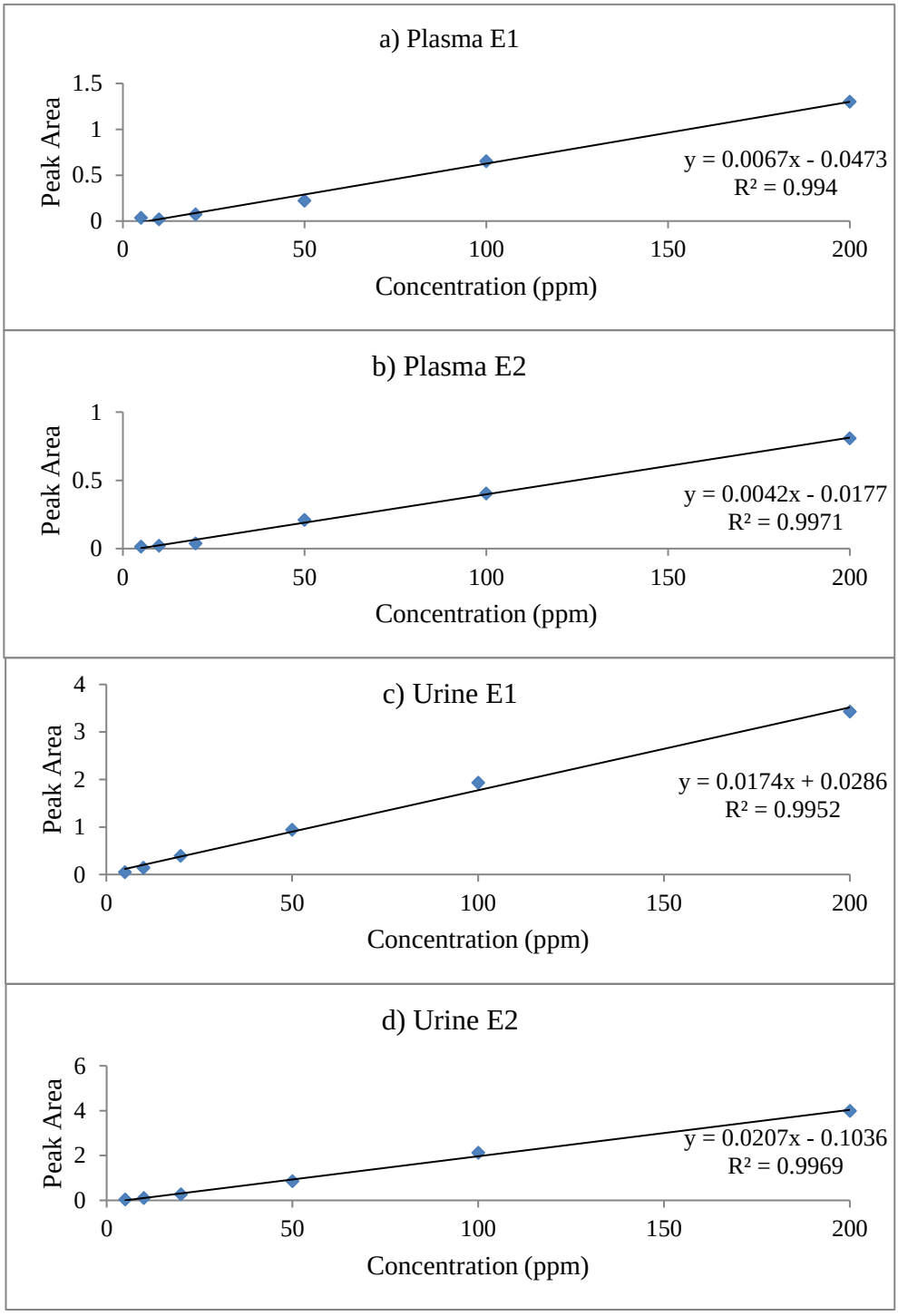

Figure 67: Calibration curves of Buphedrone enantiomers in plasma and urine

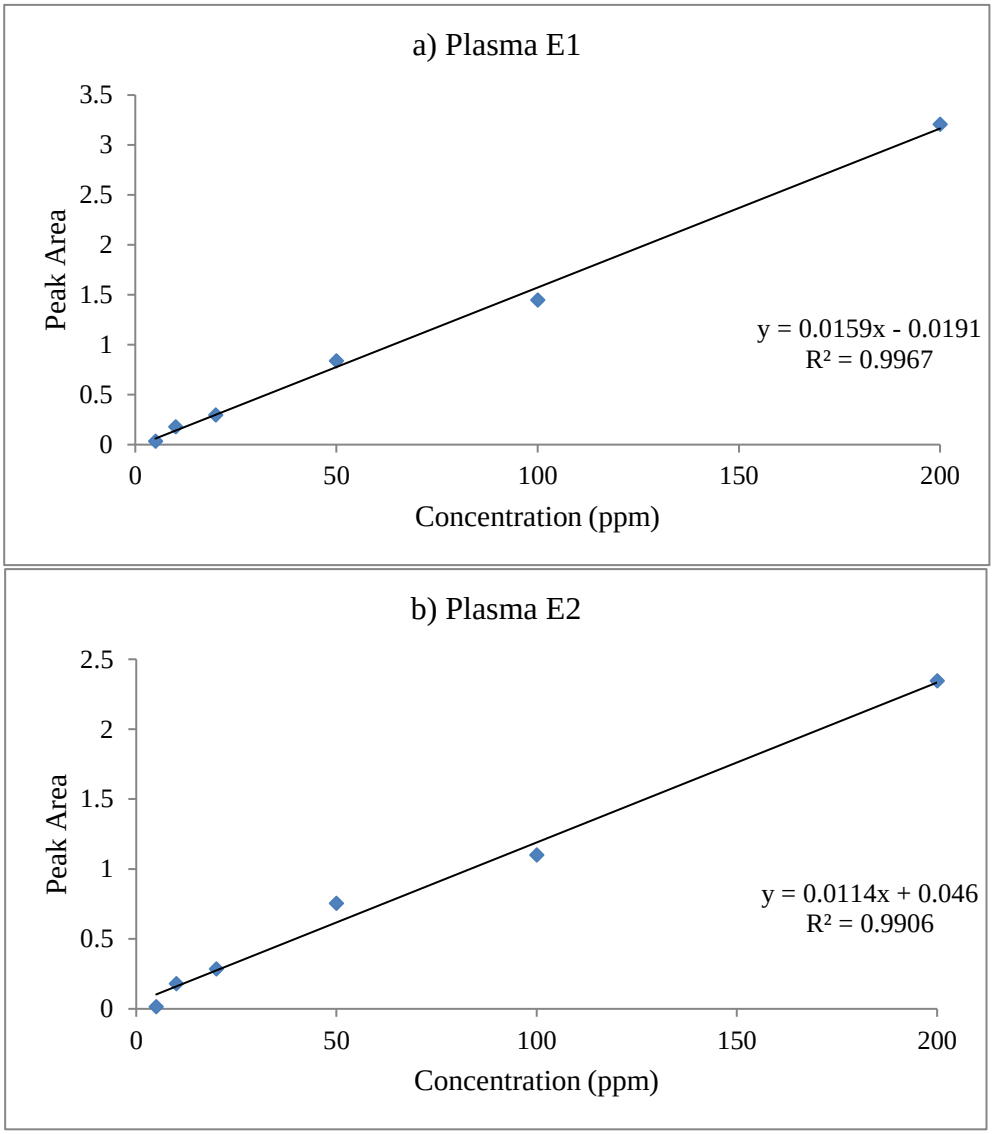

Figure 68: Calibration curves of Buphedrone enantiomers in plasma

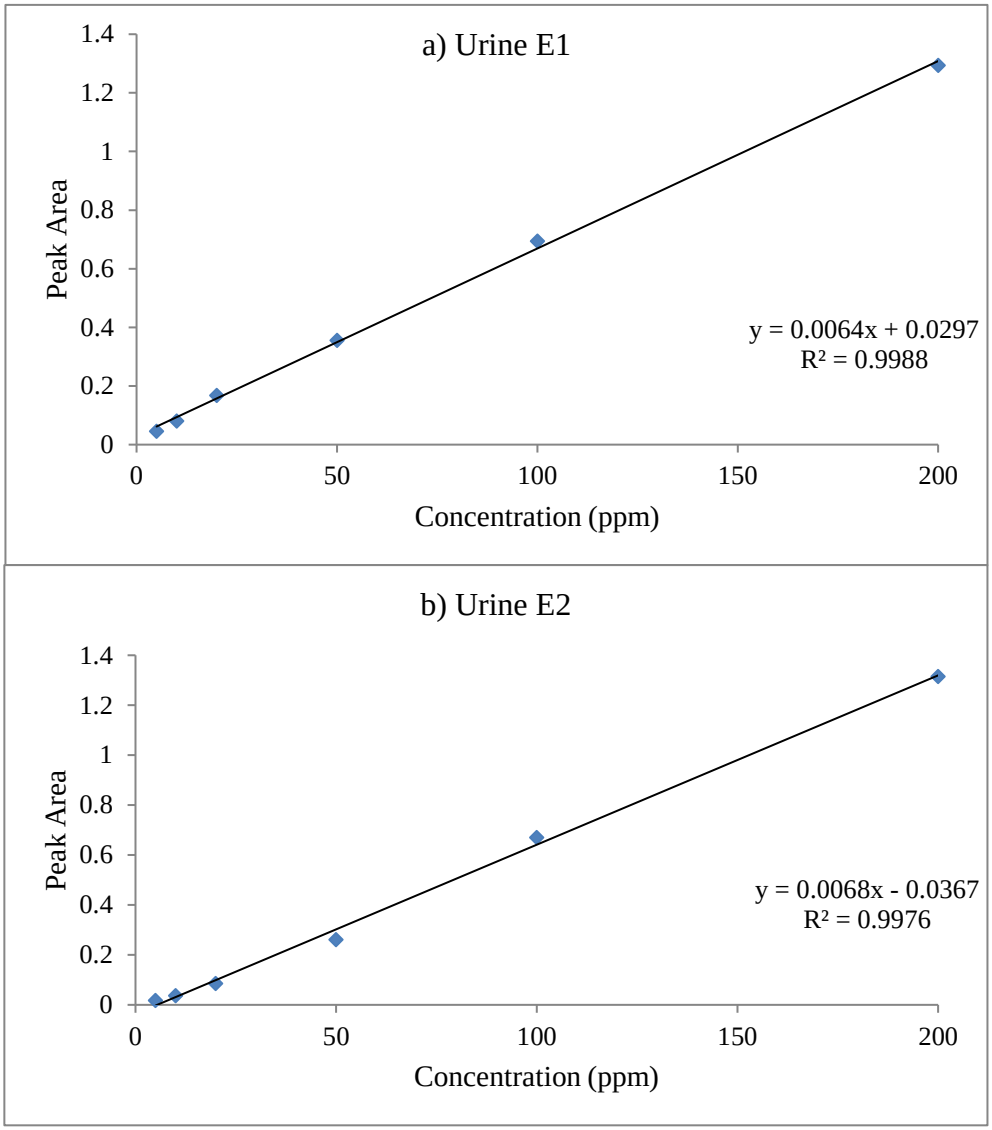

Figure 69: Calibration curves of Eutylone enantiomers in urine

Appendix B: Gas chromatogram, mass spectrum and calibration plots of 37 synthetic cathinones that analyzed in chapter 3

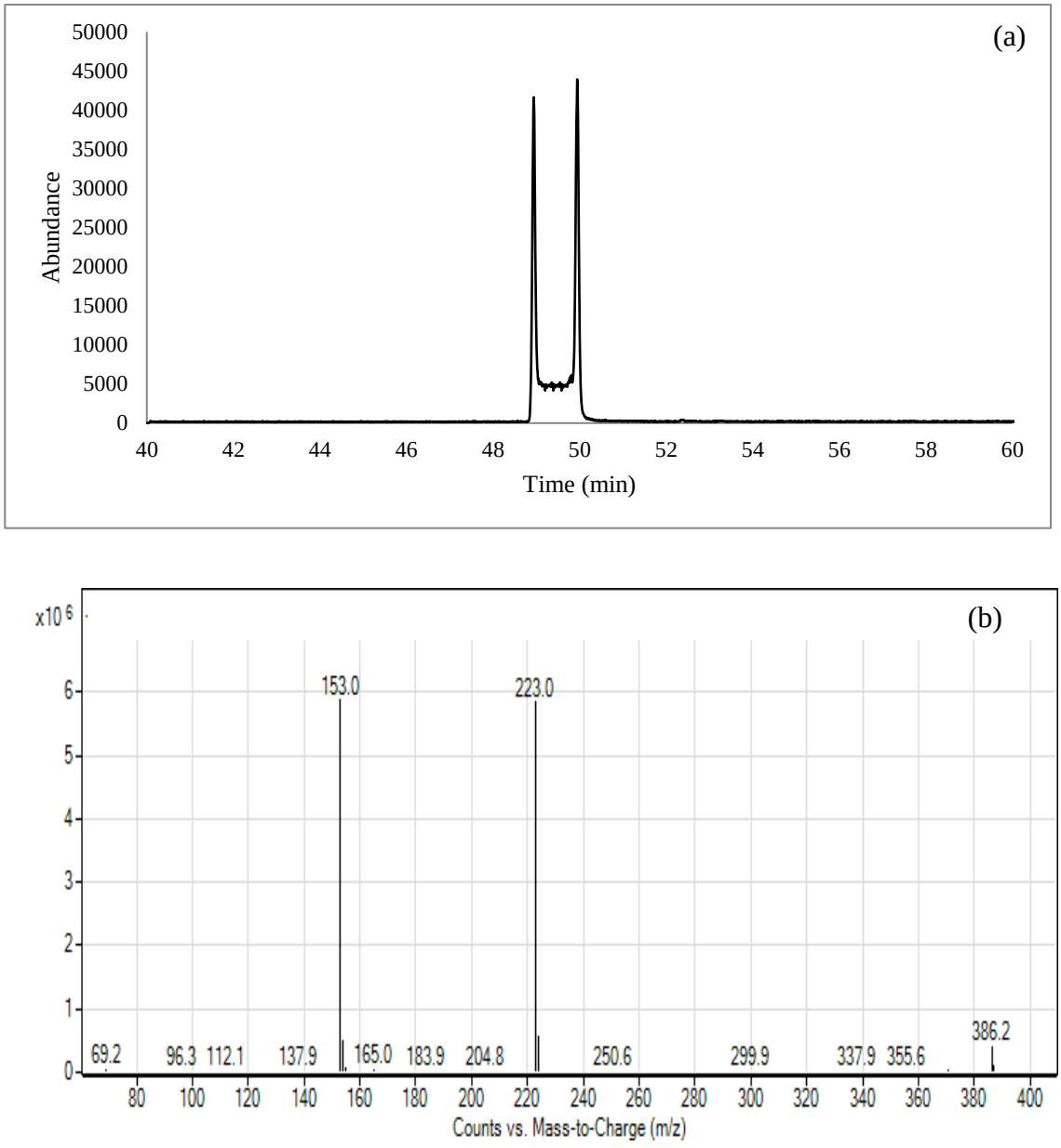

Figure 70: a) Gas chromatogram for separation of the R and S enantiomers of 2-Methoxymethcathinone (2-Me-O-MC) drug after derivatization with L-TPC and b) mass spectrum of the same compound analyzed by GC-NCI-MS system

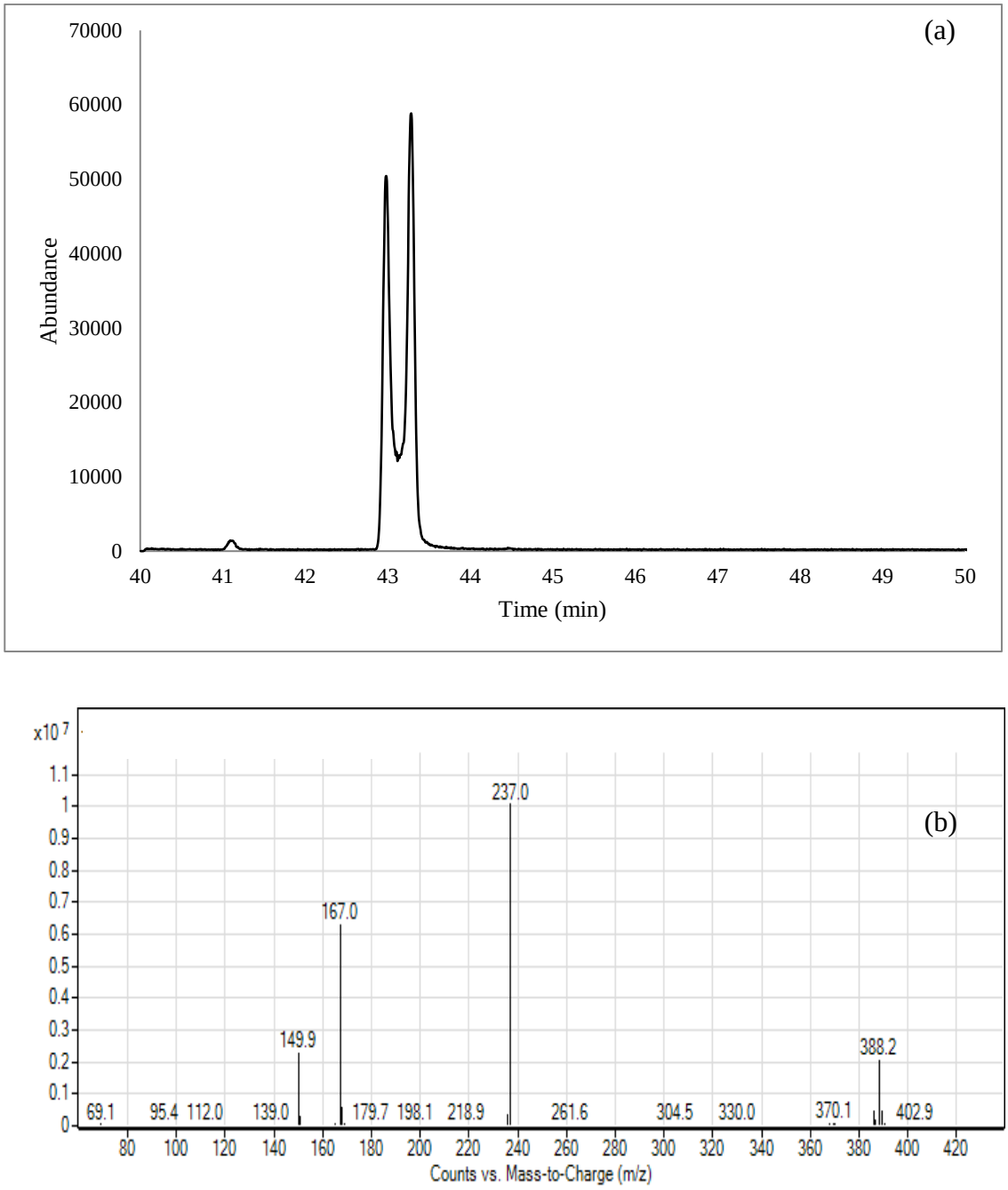

Figure 71: a) Gas chromatogram for separation of the R and S enantiomers of 3-Fluoroethcathinone (3-FEC) drug after derivatization with L-TPC and b) mass spectrum of the same compound analyzed by GC-NCI-MS system

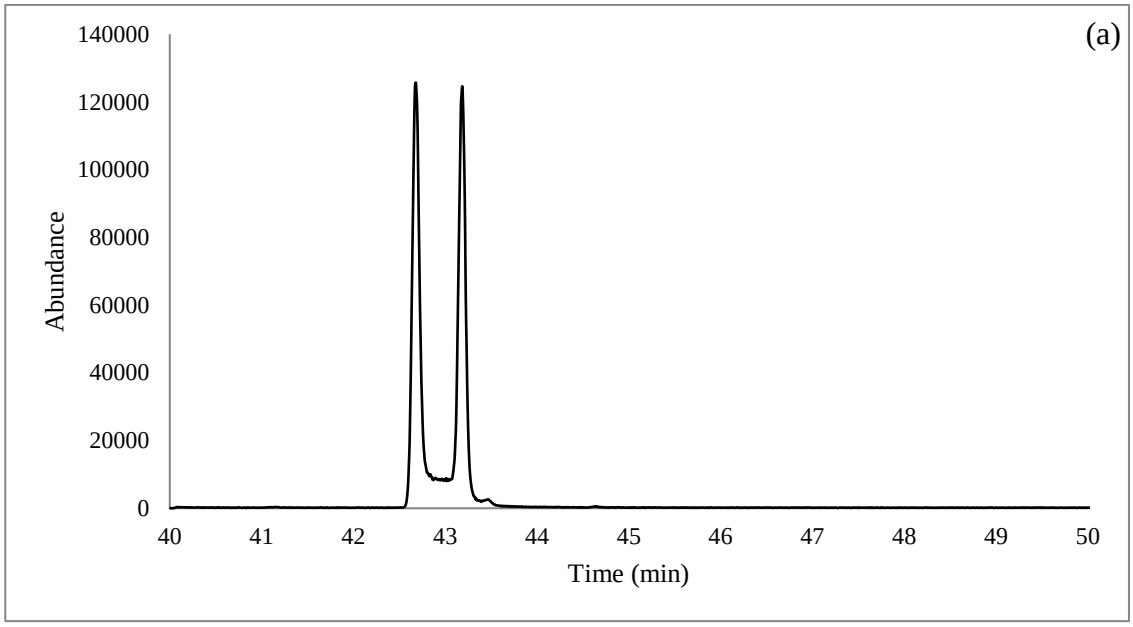

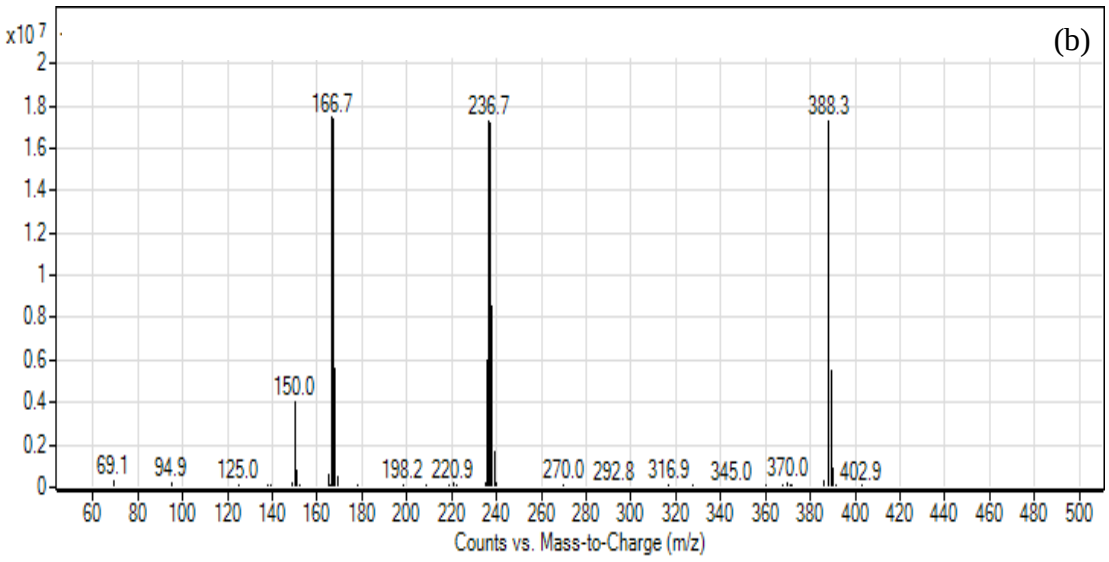

Figure 72: a) Gas chromatogram for separation of the R and S enantiomers of 4-Fluoroethcathinone (4-FEC) drug after derivatization with L-TPC and b) mass spectrum of the same compound analyzed by GC-NCI-MS system

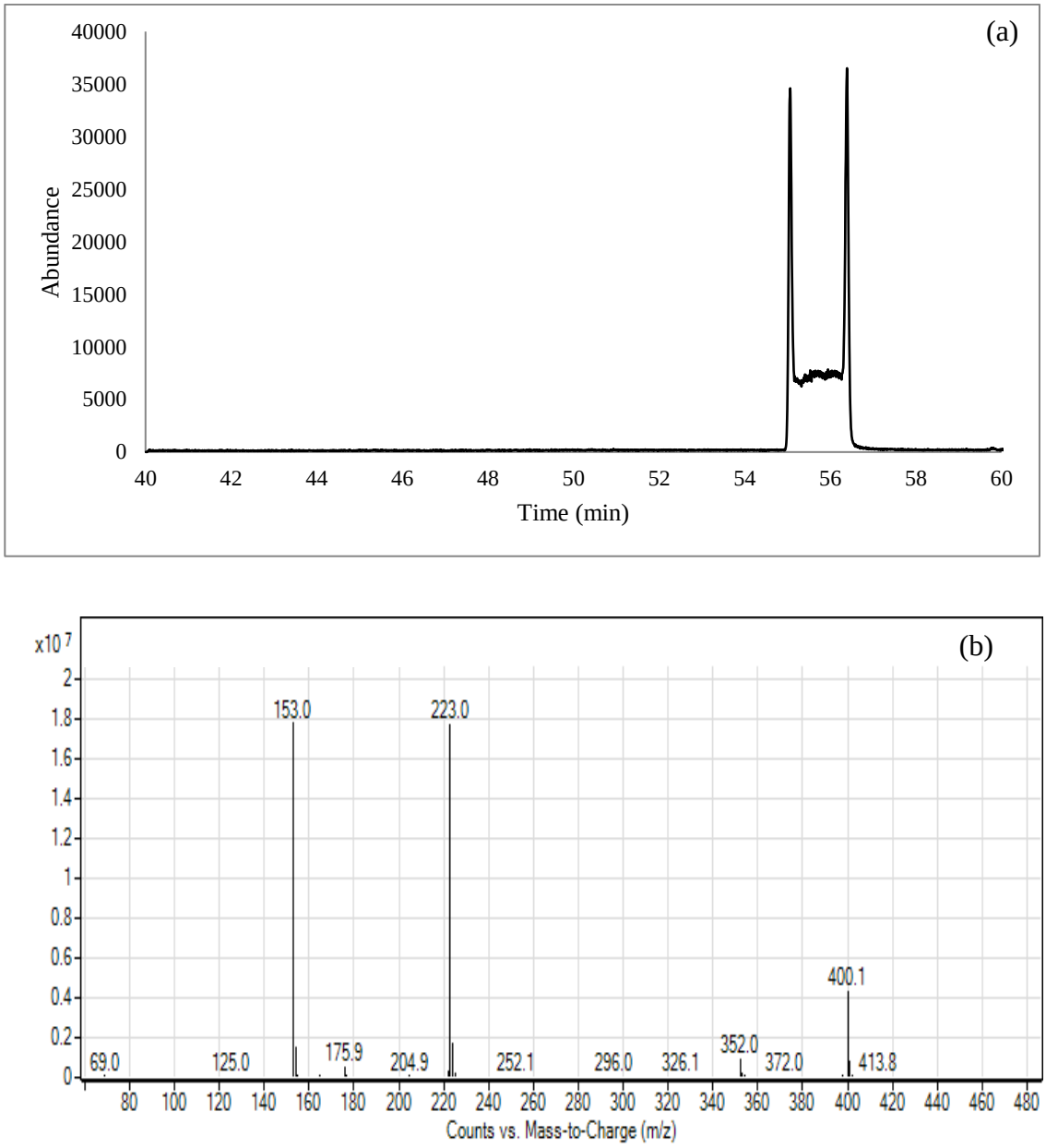

Figure 73: a) Gas chromatogram for separation of the R and S enantiomers of 2,3-Methylenedioxymethcathinone (2,3-MDMC) drug after derivatization with L-TPC and b) mass spectrum of the same compound analyzed by GC-NCI-MS system

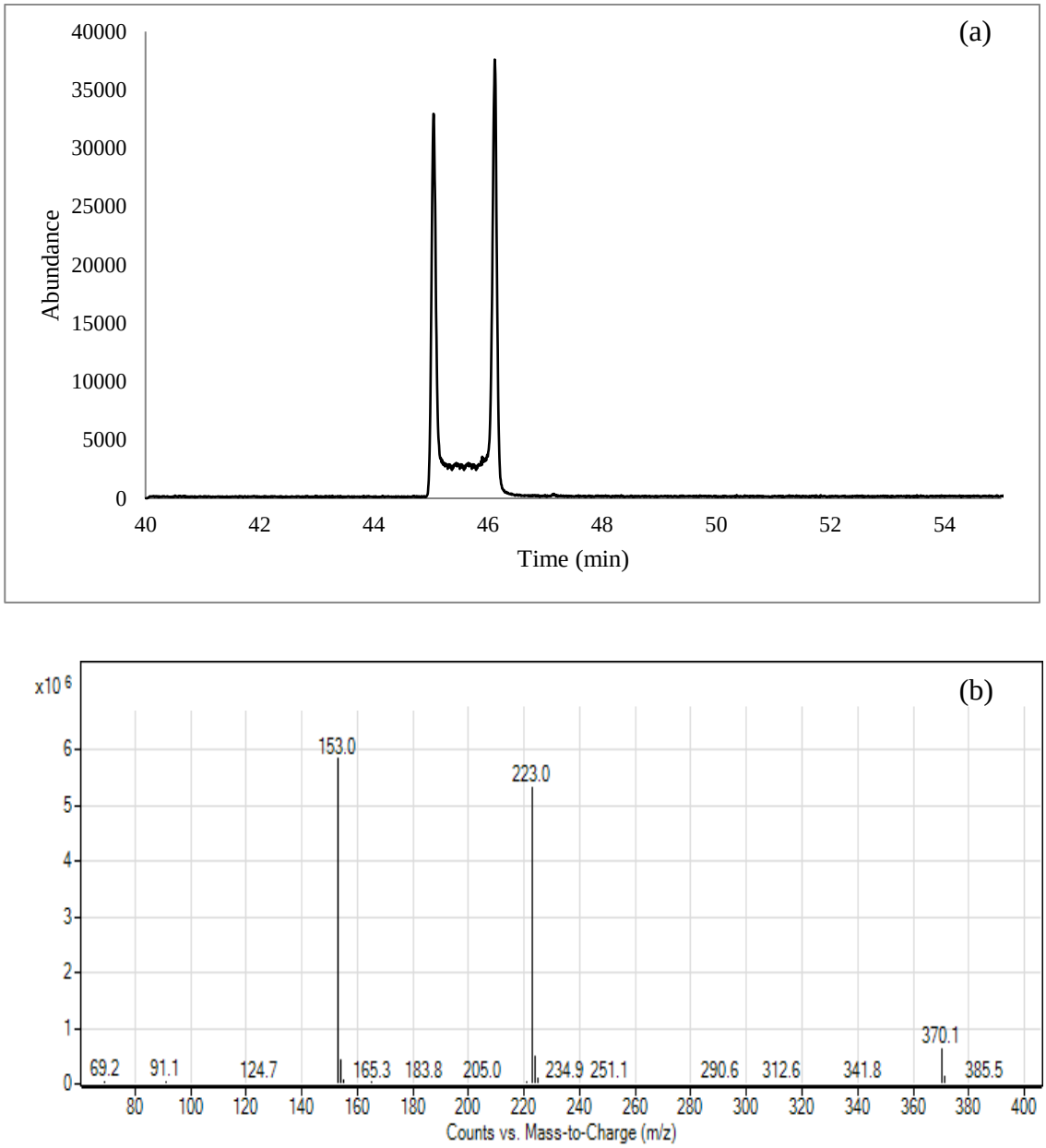

Figure 74: a) Gas chromatogram for separation of the R and S enantiomers of 2-Methylmethcathinone (2-MMC) drug after derivatization with L-TPC and b) mass spectrum of the same compound analyzed by GC-NCI-MS system

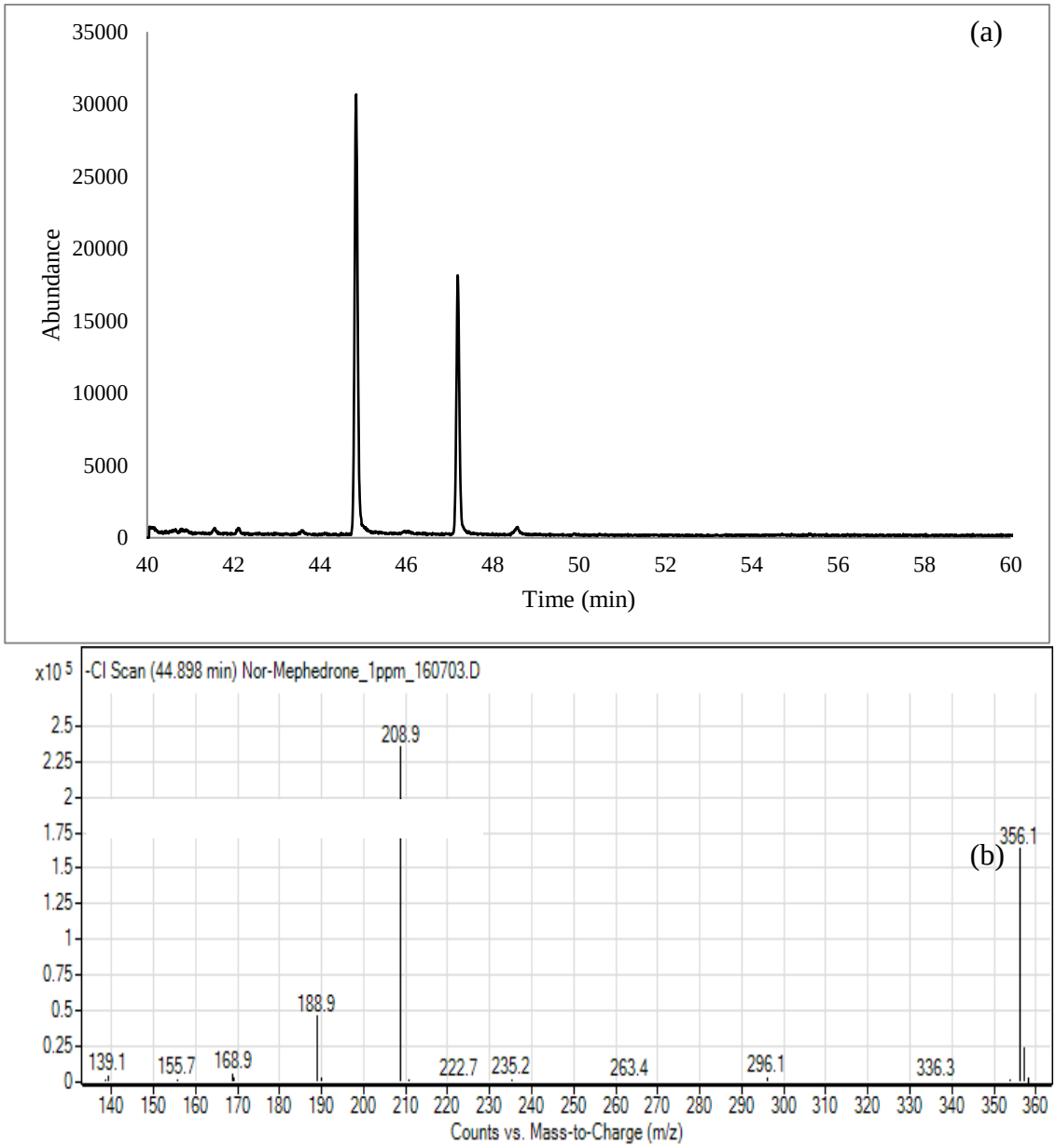

Figure 75: a) Gas chromatogram for separation of the R and S enantiomers of Nor-mephedrone drug after derivatization with L-TPC and b) mass spectrum of the same compound analyzed by GC-NCI-MS system

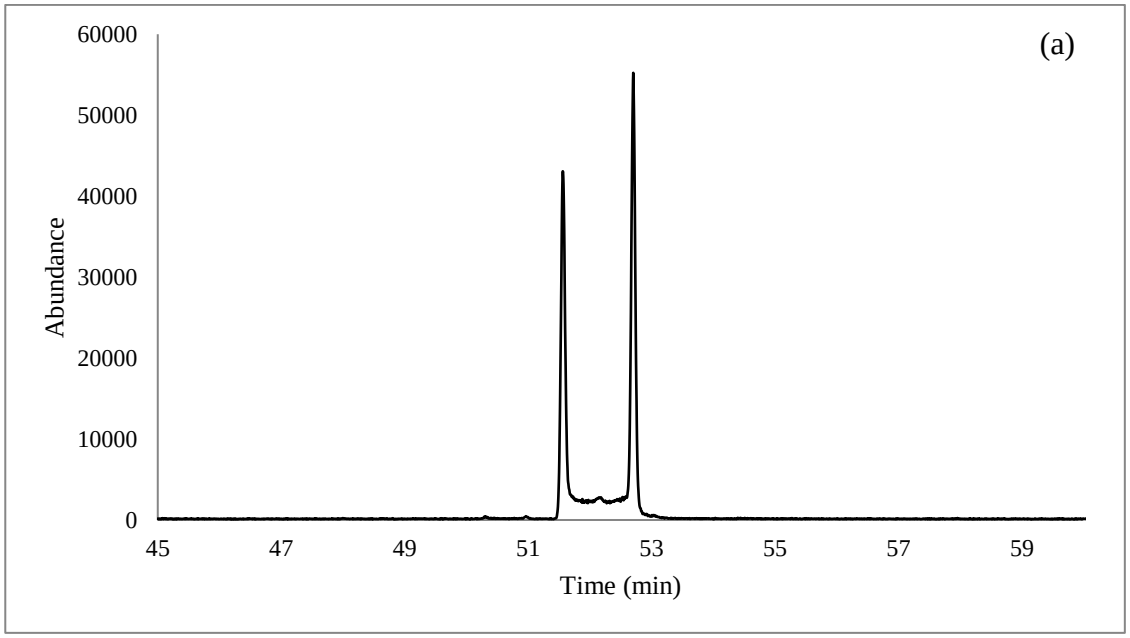

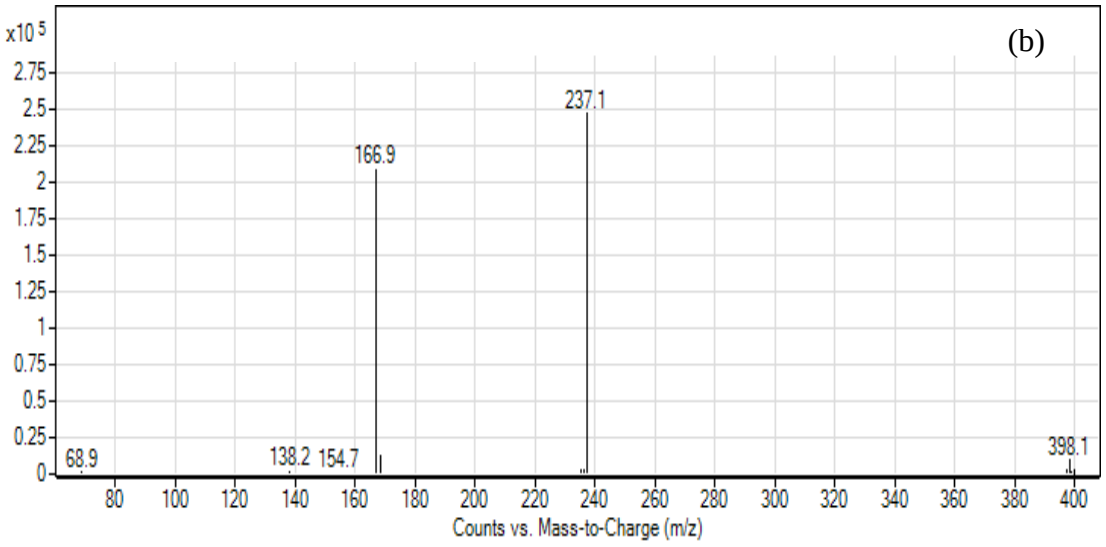

Figure 76: a) Gas chromatogram for separation of the R and S enantiomers of 4-Ethylethcathinone (4-EEC) drug after derivatization with L-TPC and b) mass spectrum of the same compound analyzed by GC-NCI-MS system

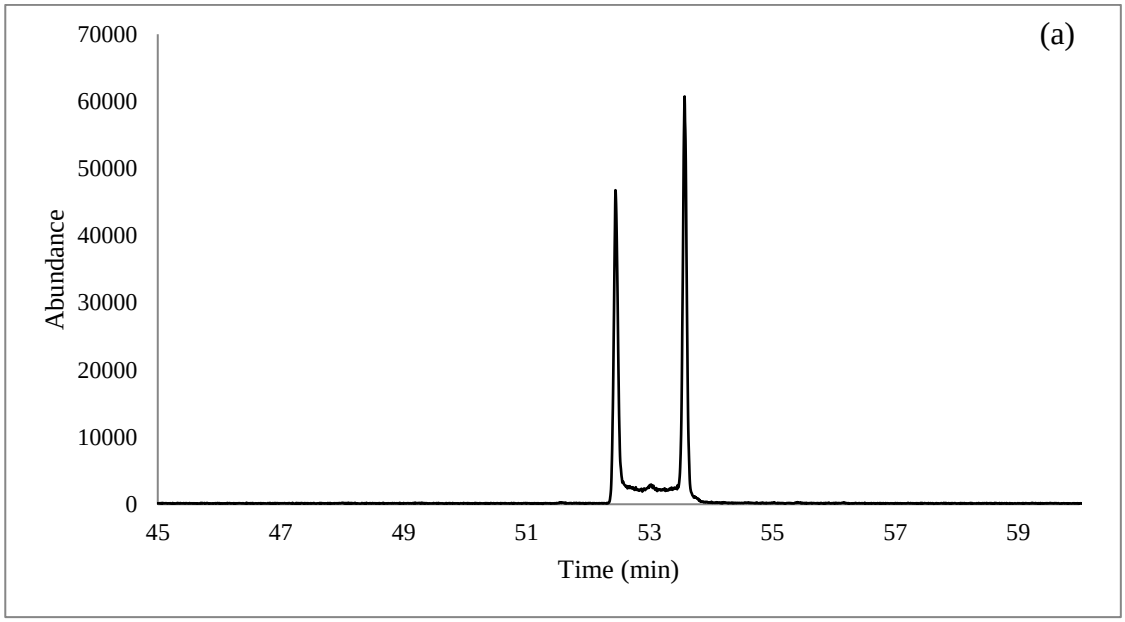

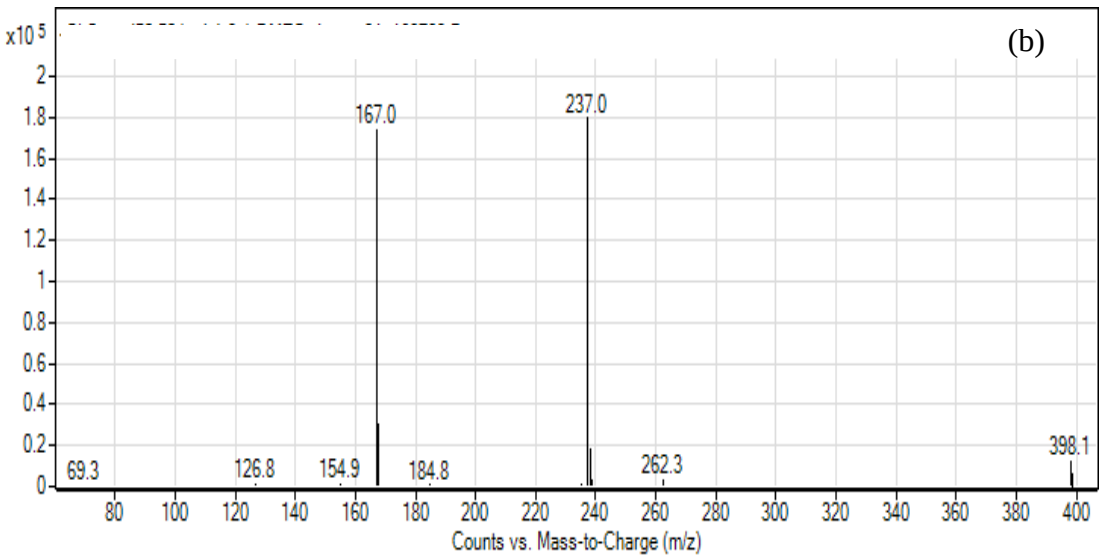

Figure 77: a) Gas chromatogram for separation of the R and S enantiomers of 3,4-Dimethylethcathinone (3,4-DMEC) drug after derivatization with L-TPC and b) mass spectrum of the same compound analyzed by GC-NCI-MS system

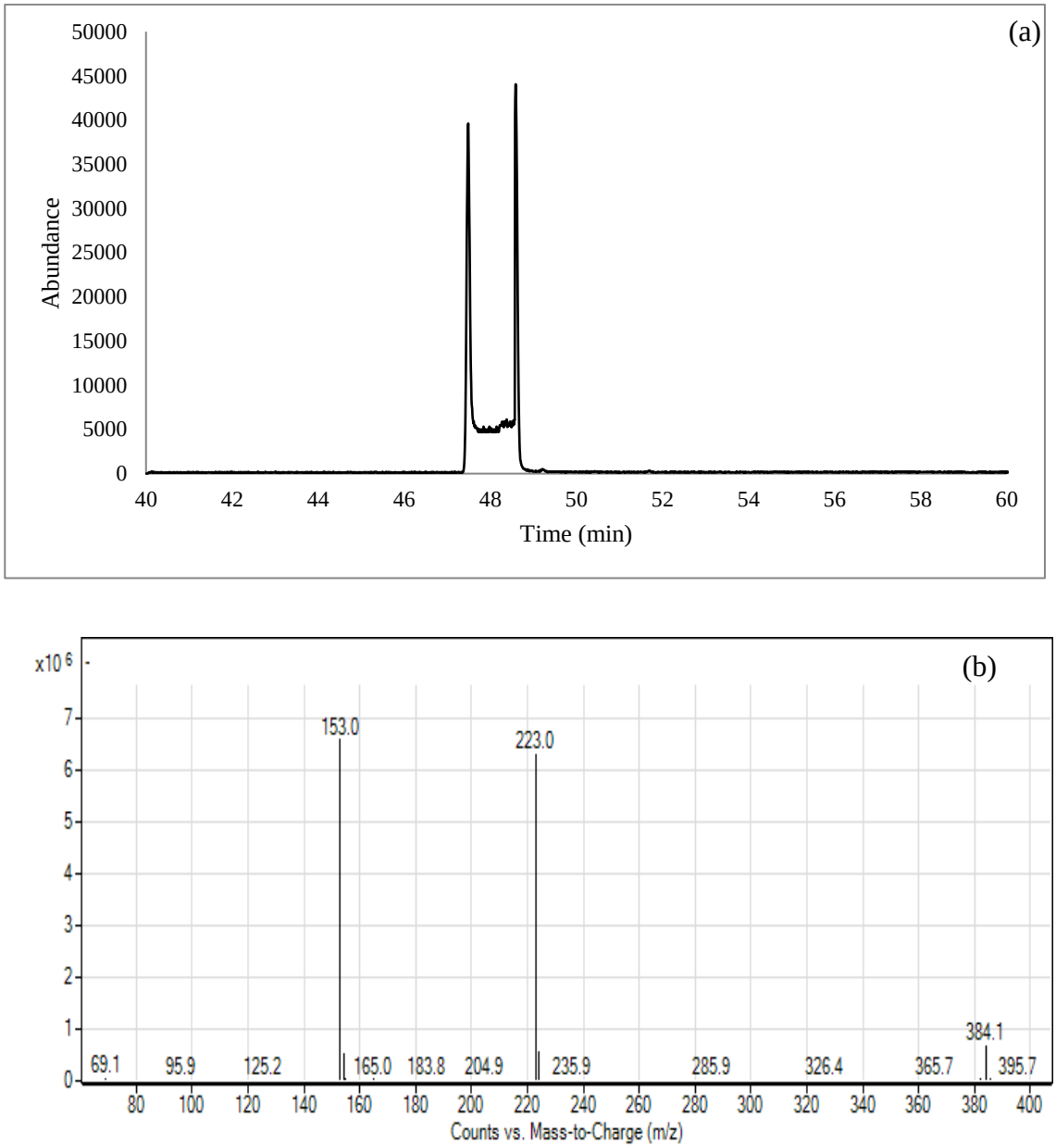

Figure 78: a) Gas chromatogram for separation of the R and S enantiomers of 2-Ethylmethcathinone (2-EMC) drug after derivatization with L-TPC and b) mass spectrum of the same compound analyzed by GC-NCI-MS system

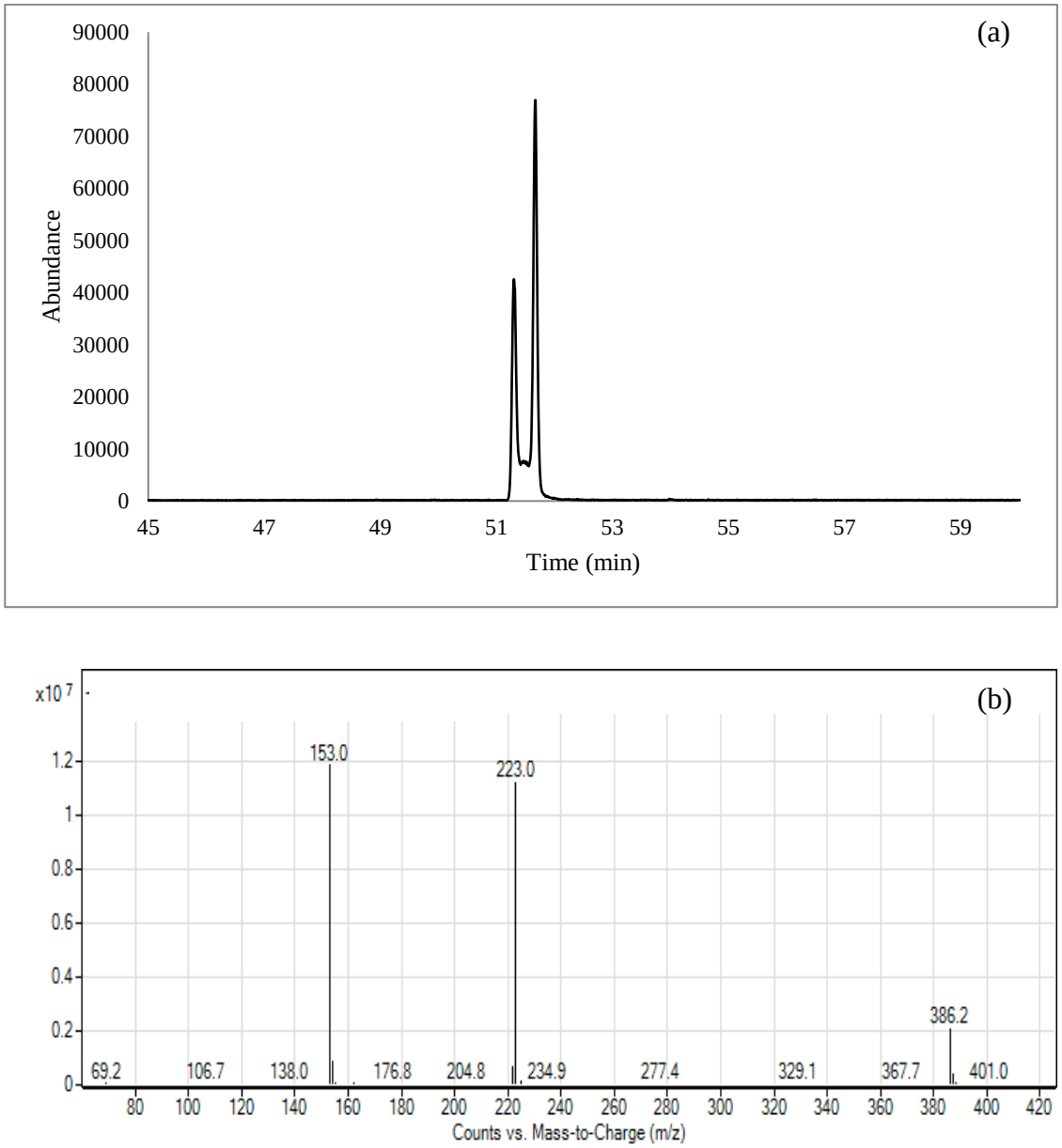

Figure 79: a) Gas chromatogram for separation of the R and S enantiomers of 3-Methoxymethcathinone (3-MeOMC) drug after derivatization with L-TPC and b) mass spectrum of the same compound analyzed by GC-NCI-MS system

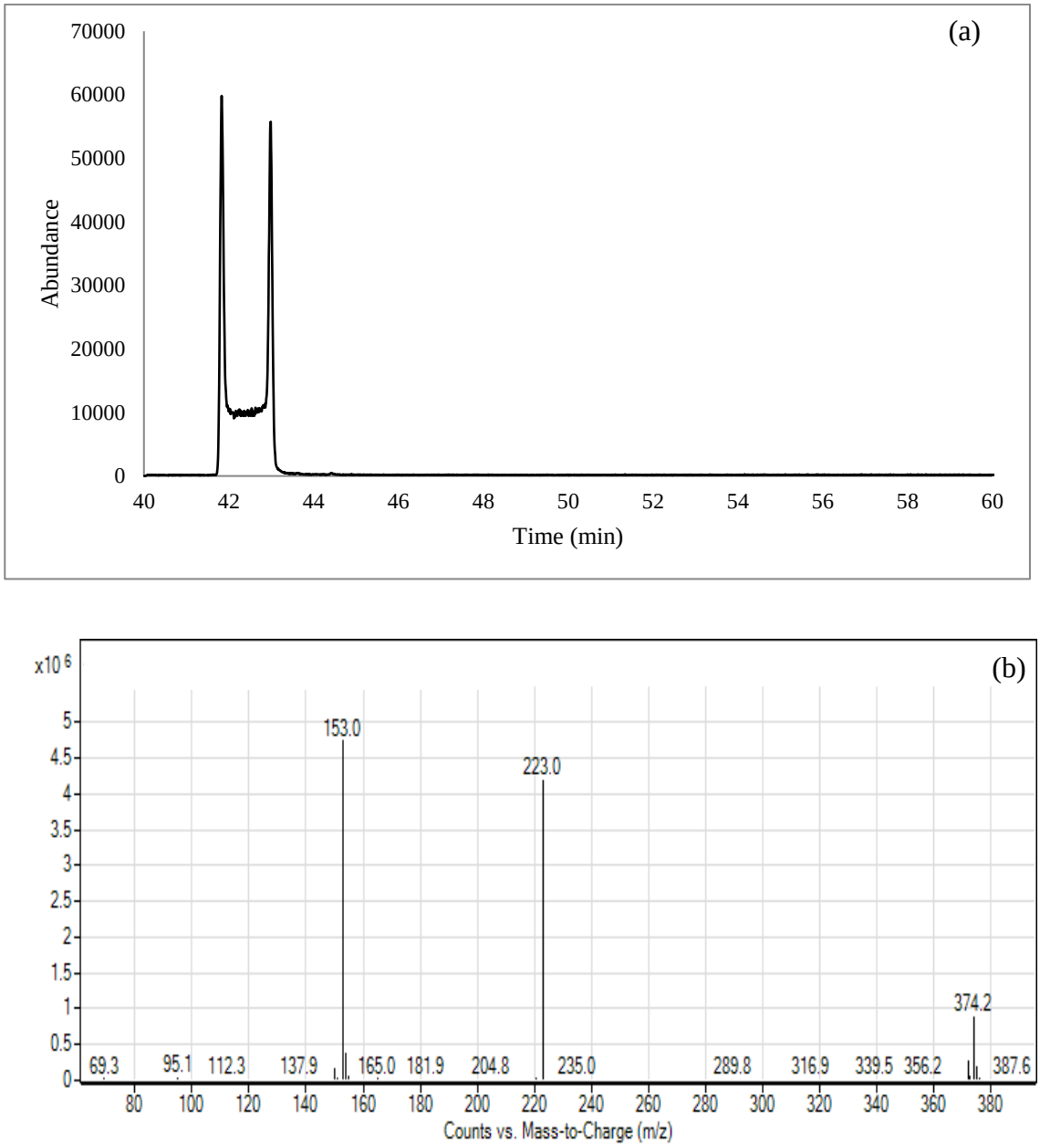

Figure 80: a) Gas chromatogram for separation of the R and S enantiomers of 2-Fluoromethcathinone (2-FMC) drug after derivatization with L-TPC and b) mass spectrum of the same compound analyzed by GC-NCI-MS system

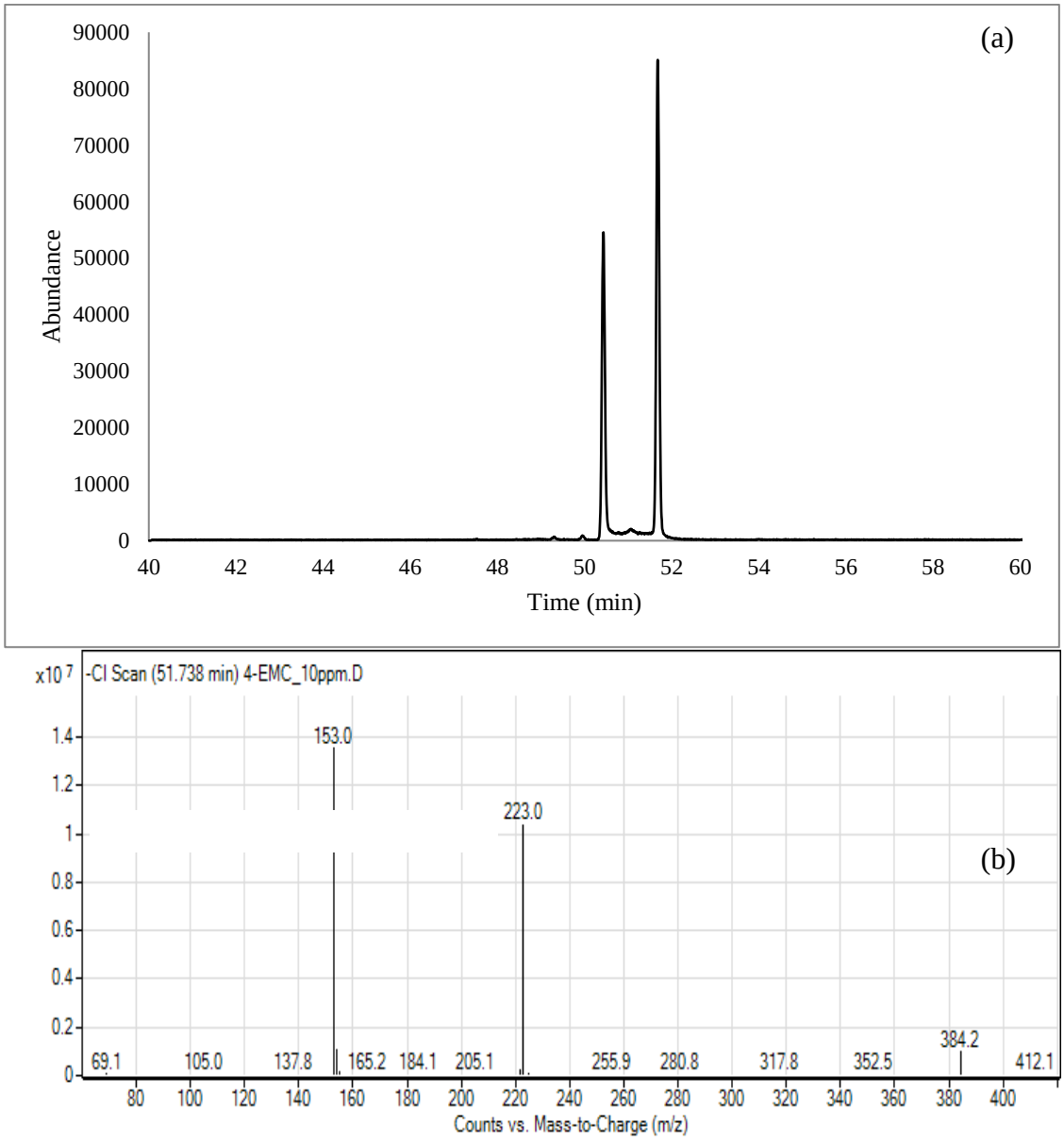

Figure 81: a) Gas chromatogram for separation of the R and S enantiomers of 4-Ethylmethcathinone (4-EMC) drug after derivatization with L-TPC and b) mass spectrum of the same compound analyzed by GC-NCI-MS system

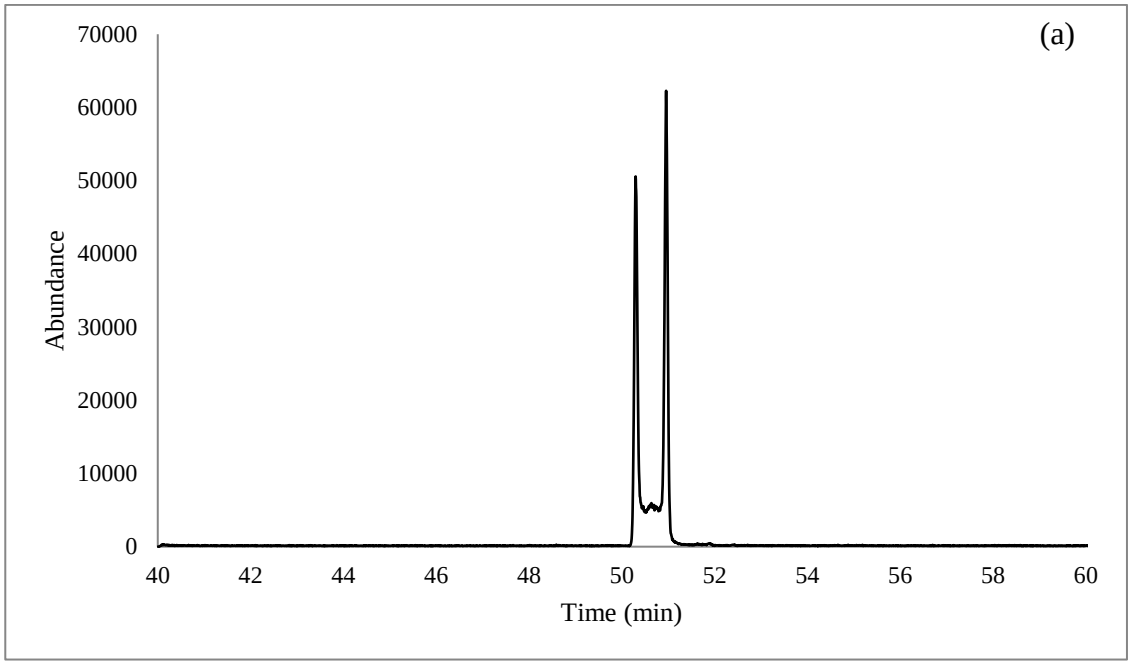

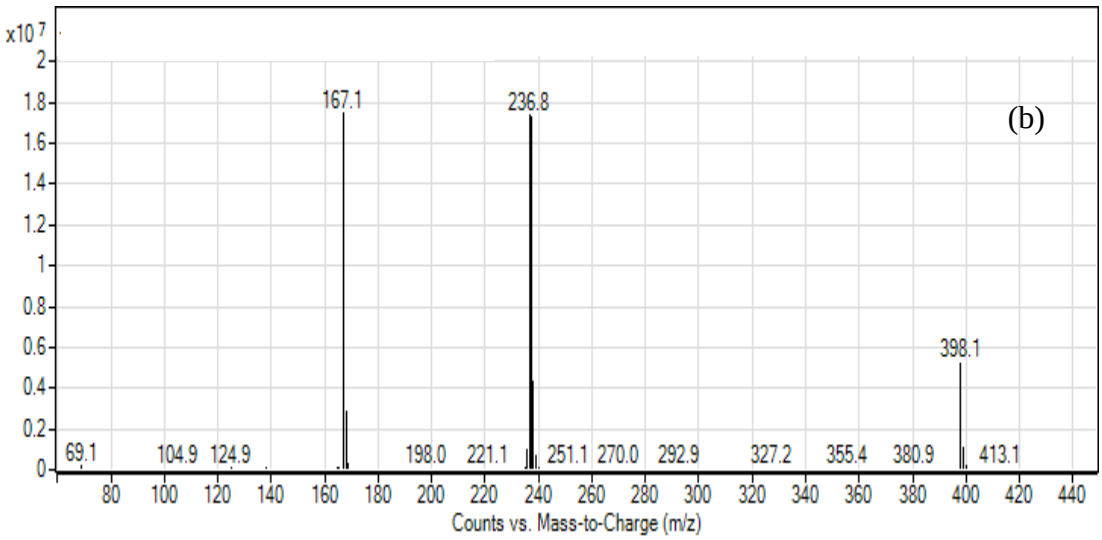

Figure 82: a) Gas chromatogram for separation of the R and S enantiomers of 3-Ethylethcathinone (3-EEC) drug after derivatization with L-TPC and b) mass spectrum of the same compound analyzed by GC-NCI-MS system

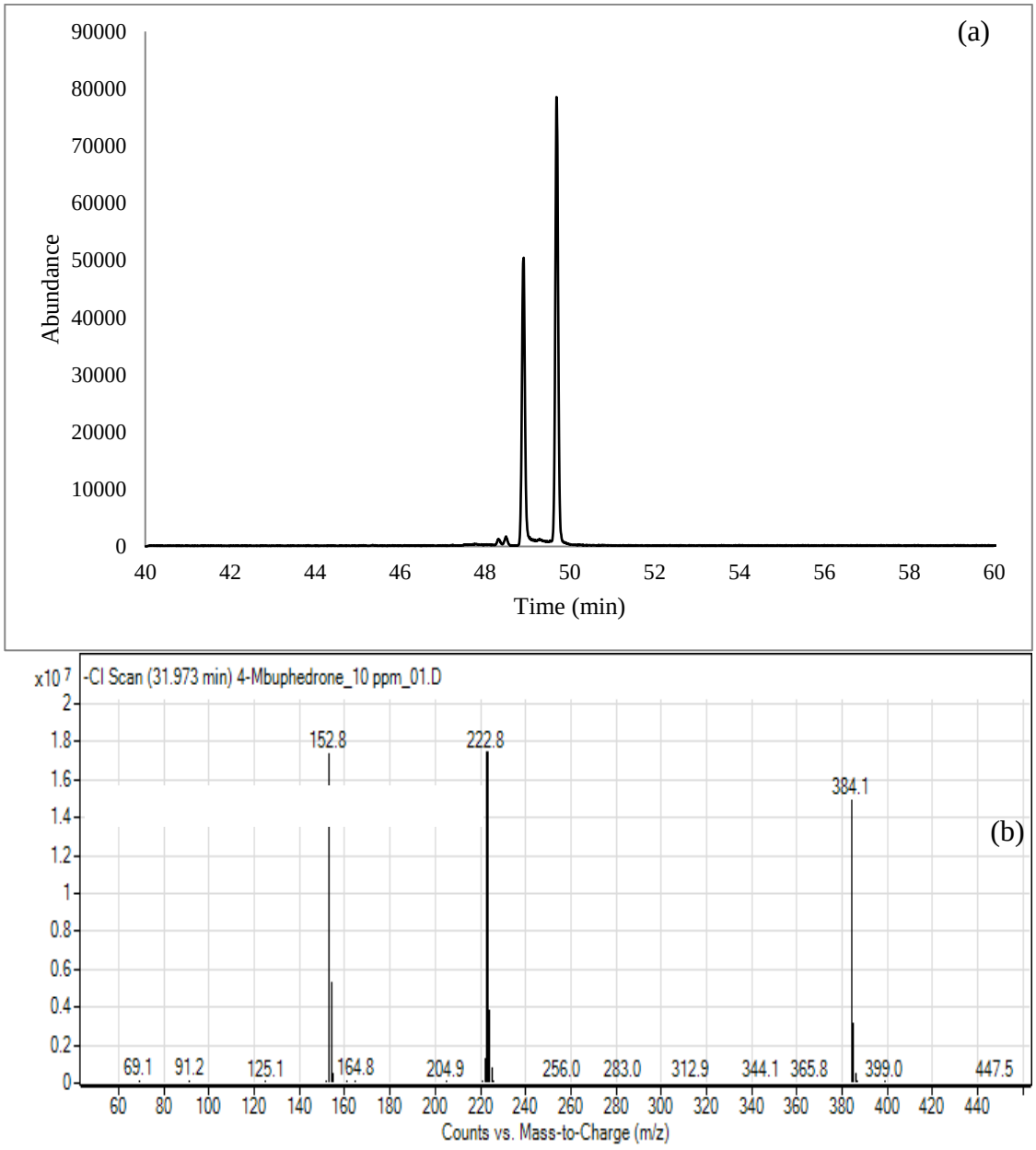

Figure 83: a) Gas chromatogram for separation of the R and S enantiomers of 4-Methylbuphedrone drug after derivatization with L-TPC and b) mass spectrum of the same compound analyzed by GC-NCI-MS system

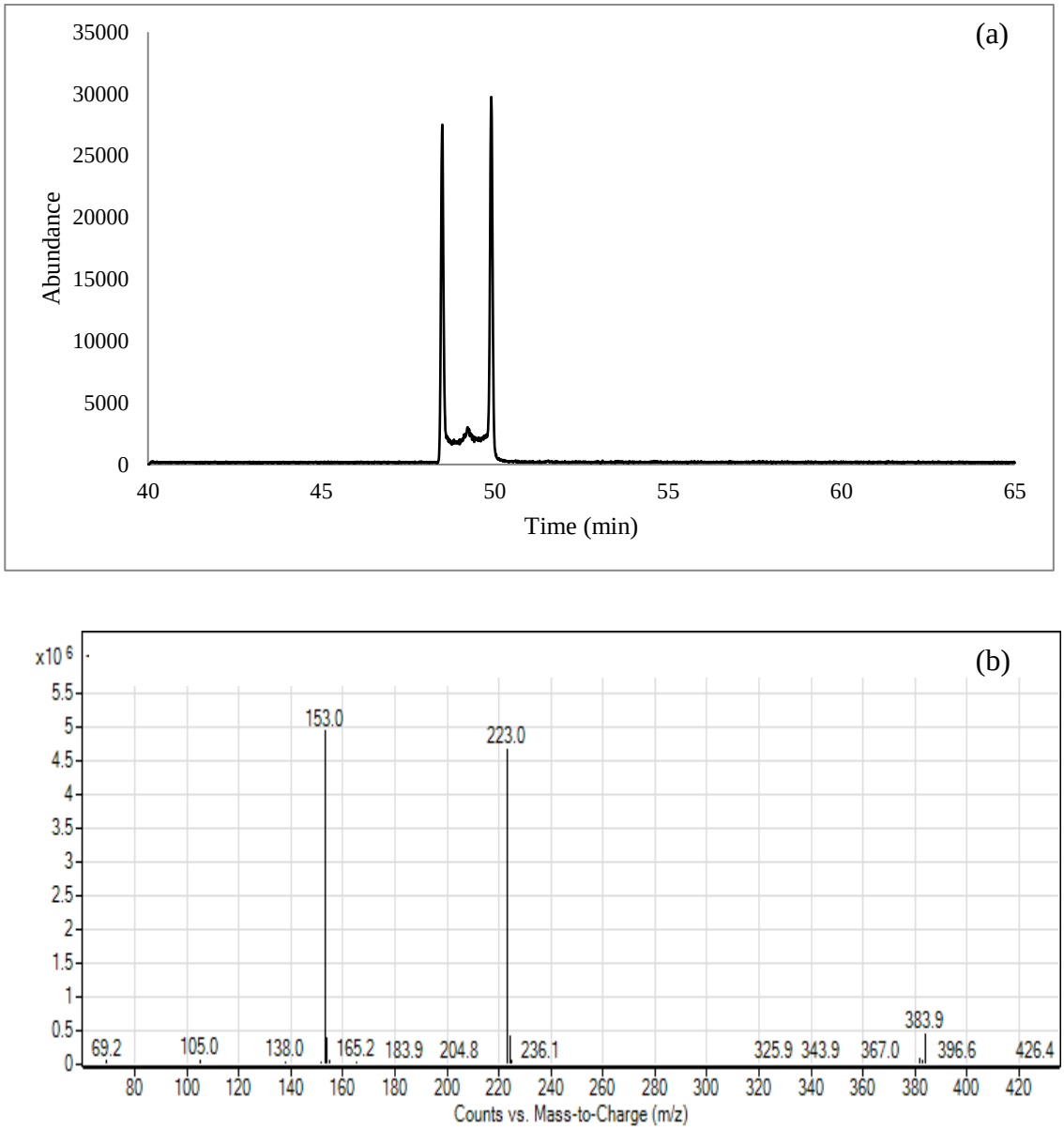

Figure 84: a) Gas chromatogram for separation of the R and S enantiomers of 2,3-Dimethylmethcathinone (2,3-DMMC) drug after derivatization with L-TPC and b) mass spectrum of the same compound analyzed by GC-NCI-MS system

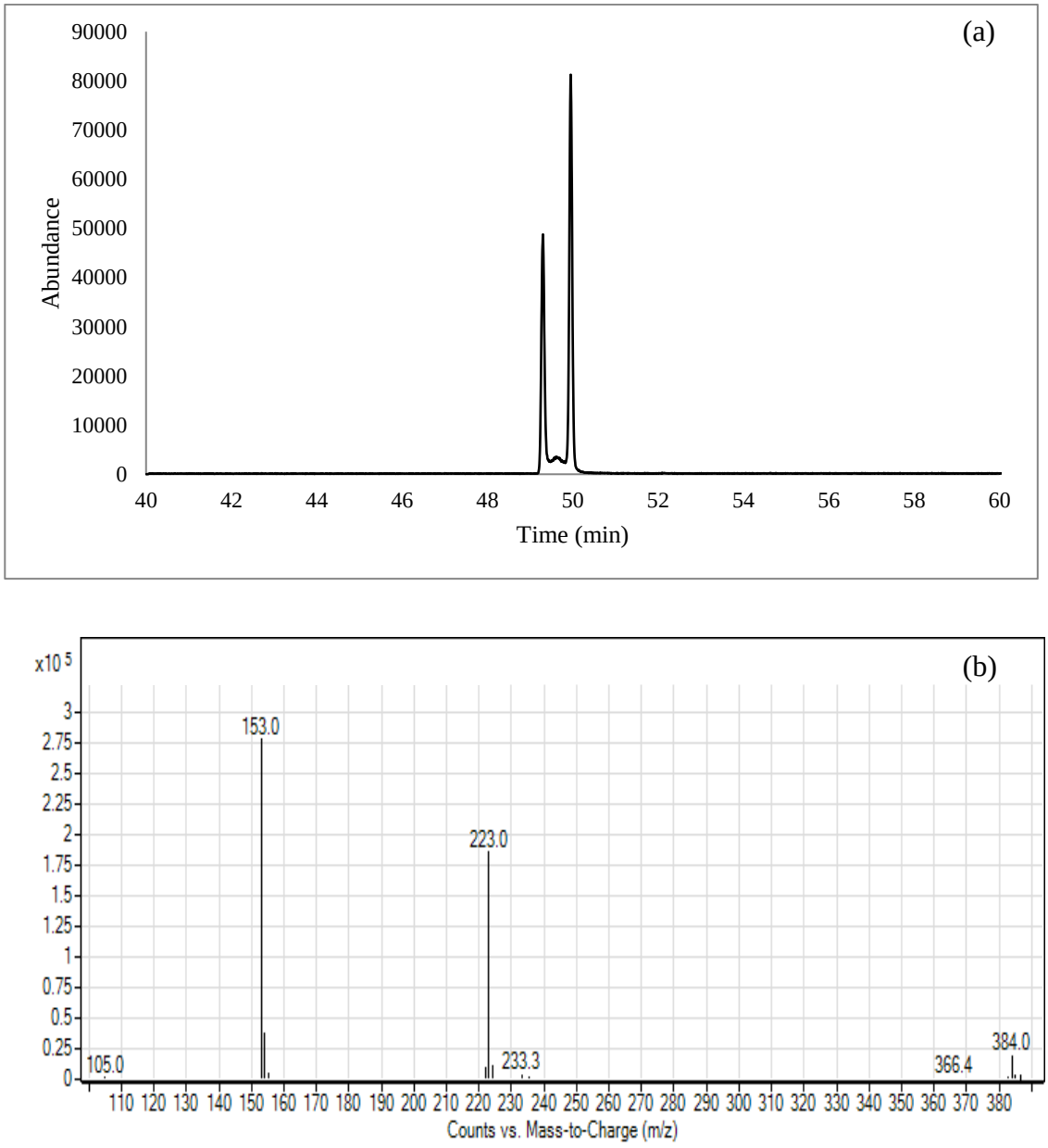

Figure 85: a) Gas chromatogram for separation of the R and S enantiomers of 3-Ethylmethcathinone (3-EMC) drug after derivatization with L-TPC and b) mass spectrum of the same compound analyzed by GC-NCI-MS system

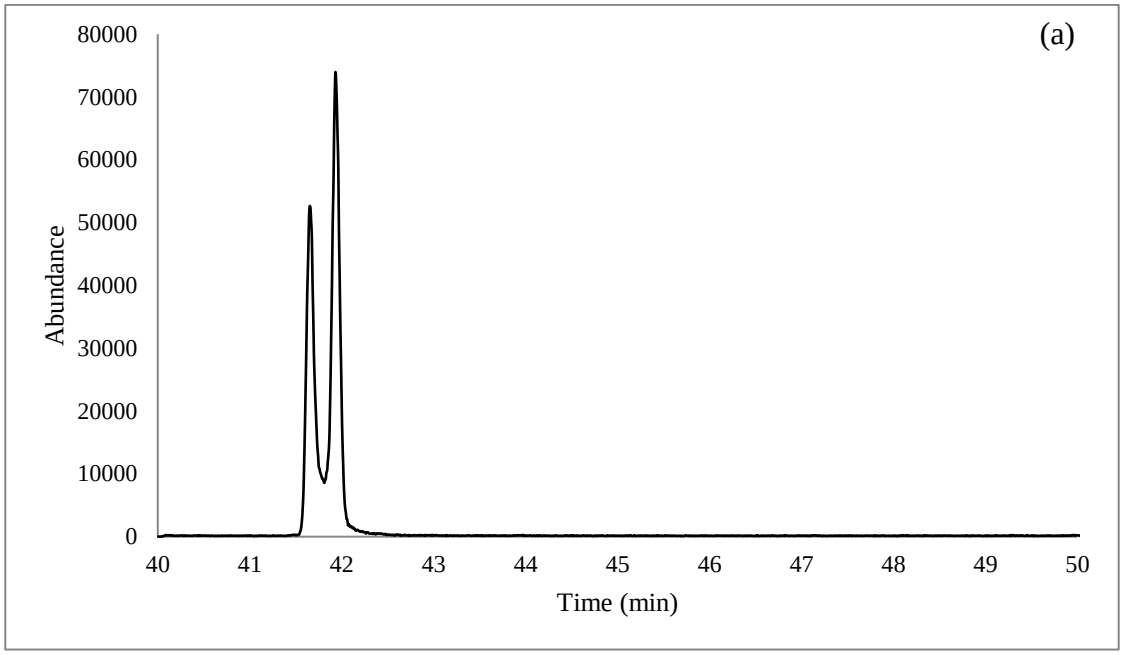

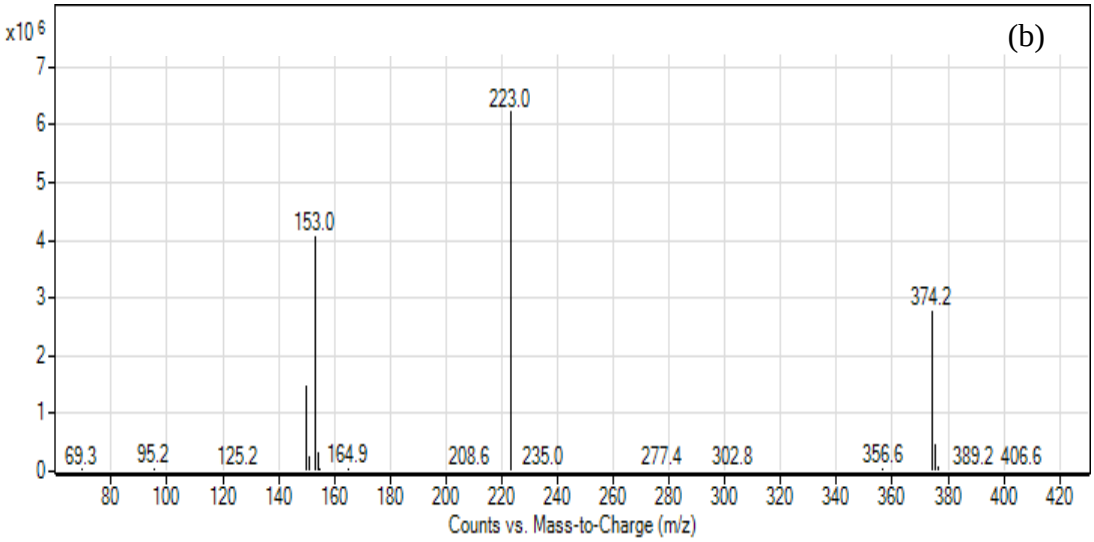

Figure 86: a) Gas chromatogram for separation of the R and S enantiomers of 3-Fluoromethcathinone (3-FMC) drug after derivatization with L-TPC and b) mass spectrum of the same compound analyzed by GC-NCI-MS system

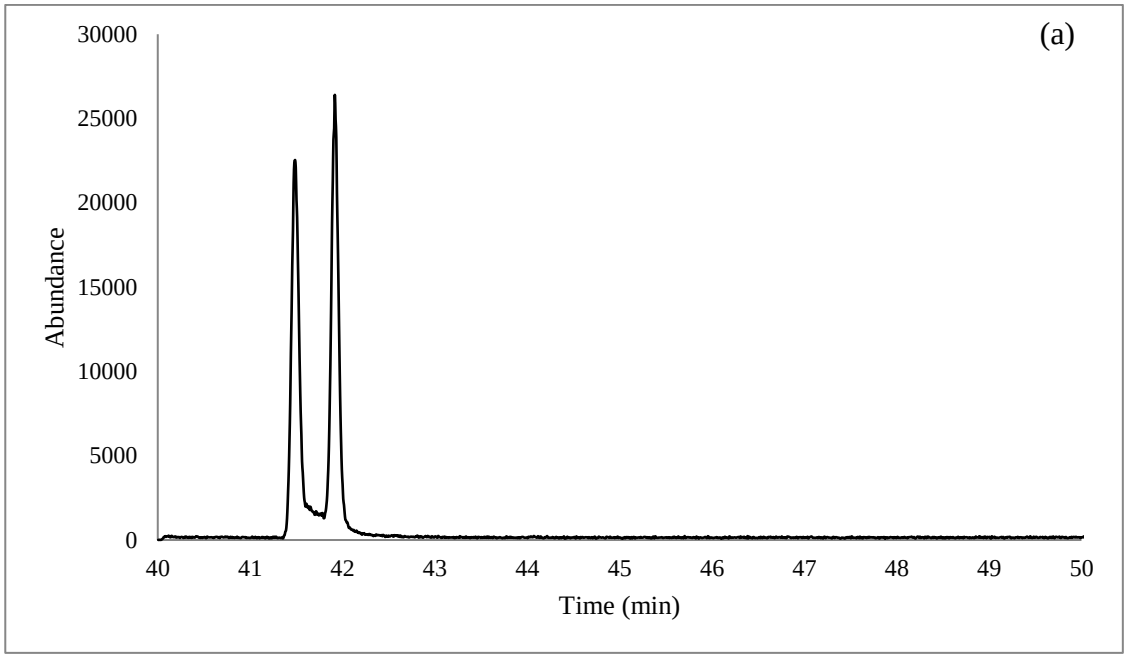

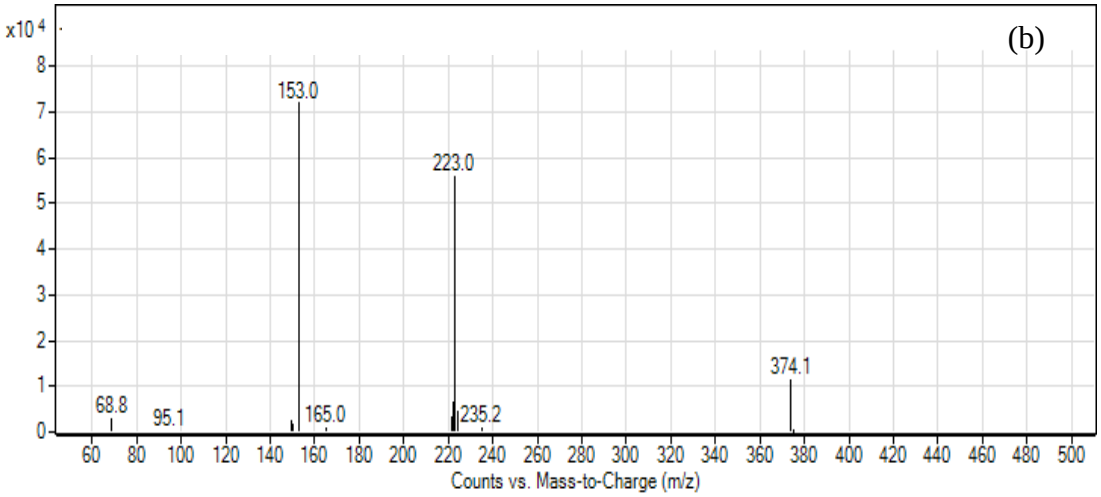

Figure 87: a) Gas chromatogram for separation of the R and S enantiomers of 4-Fluoromethcathinone (4-FMC) drug after derivatization with L-TPC and b) mass spectrum of the same compound analyzed by GC-NCI-MS system

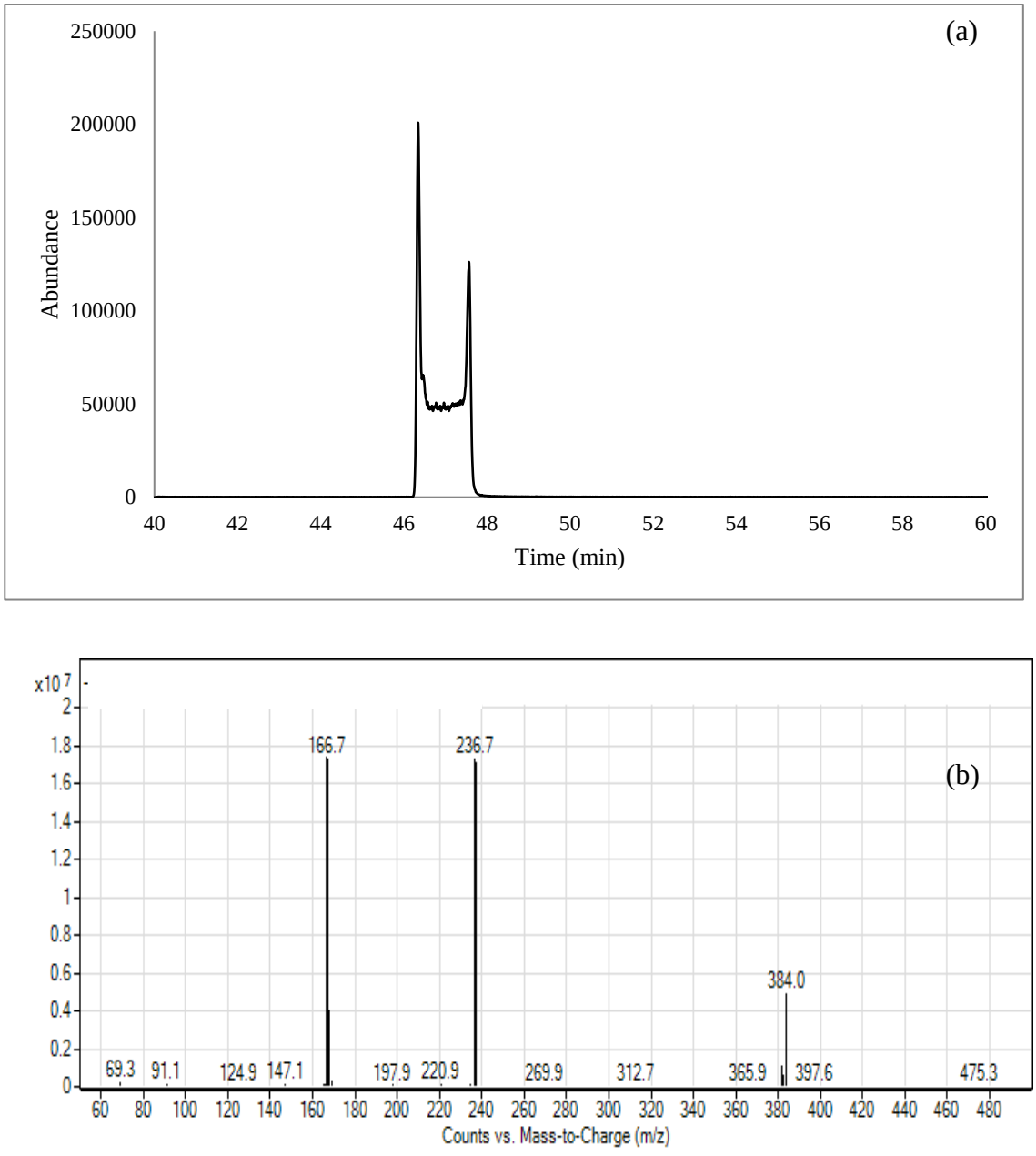

Figure 88: a) Gas chromatogram for separation of the R and S enantiomers of 2-Methylethcathinone (2-MEC) drug after derivatization with L-TPC and b) mass spectrum of the same compound analyzed by GC-NCI-MS system

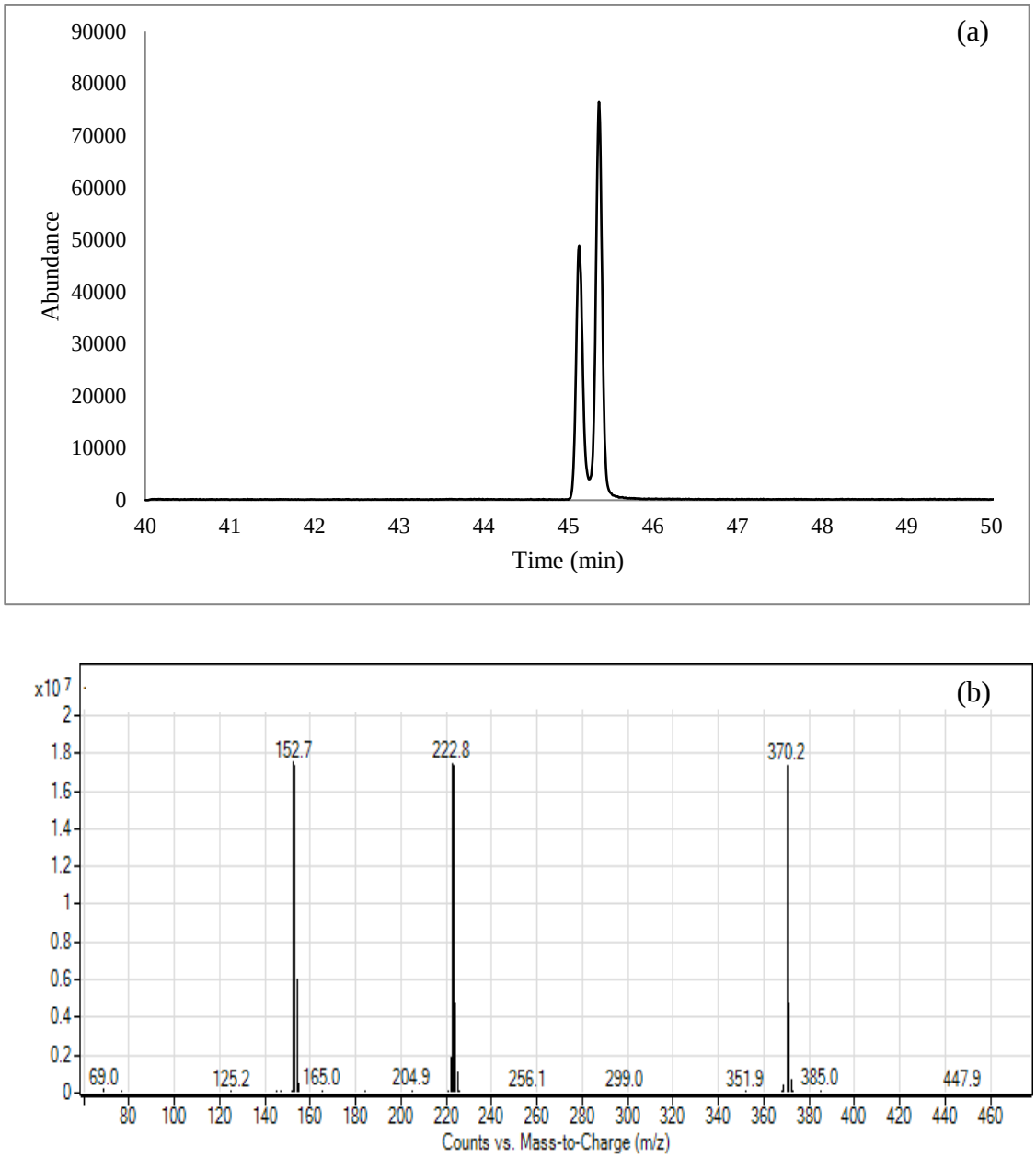

Figure 89: a) Gas chromatogram for separation of the R and S enantiomers of Buphedrone drug after derivatization with L-TPC and b) mass spectrum of the same compound analyzed by GC-NCI-MS system

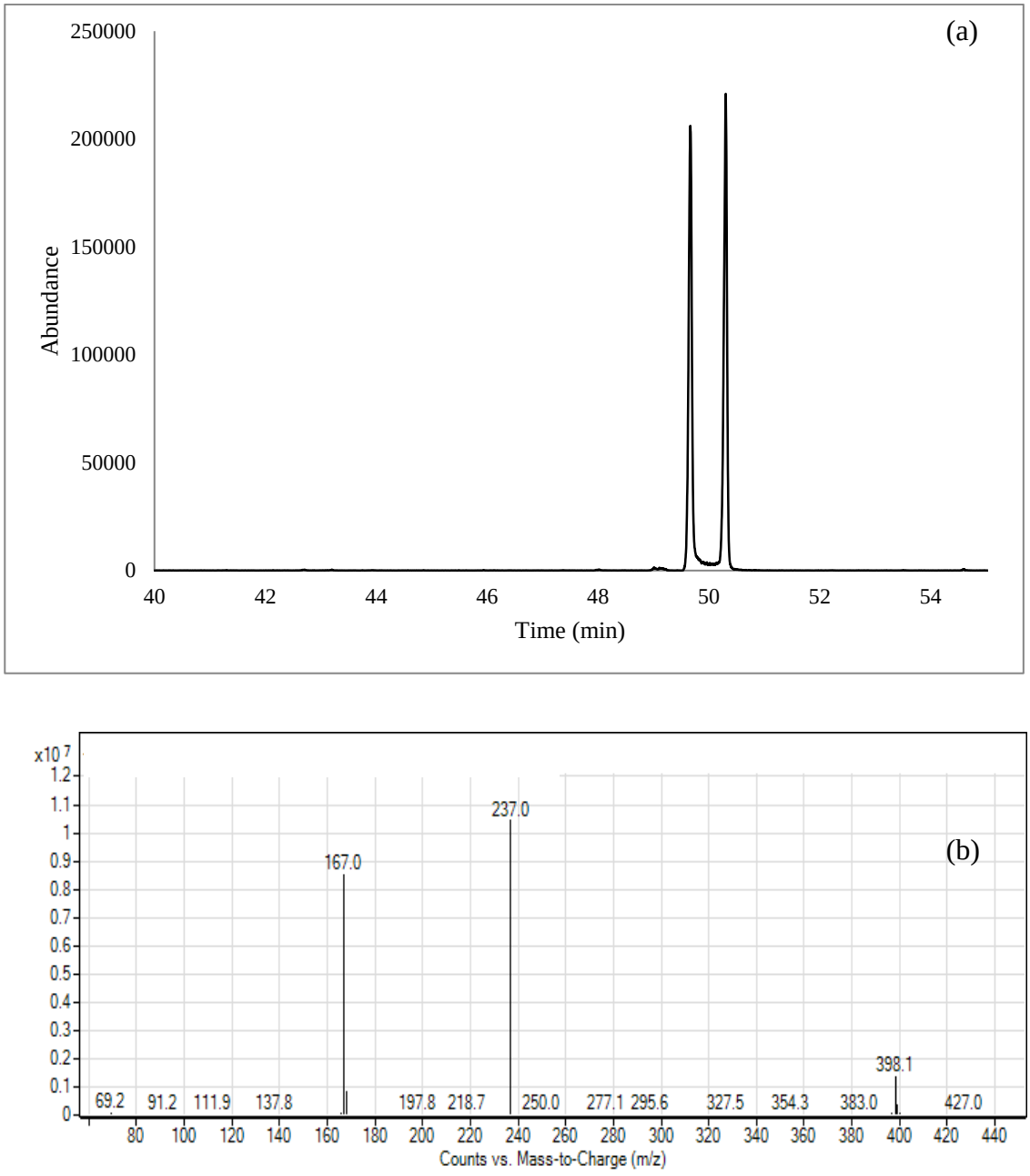

Figure 90: a) Gas chromatogram for separation of the R and S enantiomers of 4-Methyl-α-ethylaminobutiophenone drug after derivatization with L-TPC and b) mass spectrum of the same compound analyzed by GC-NCI-MS system

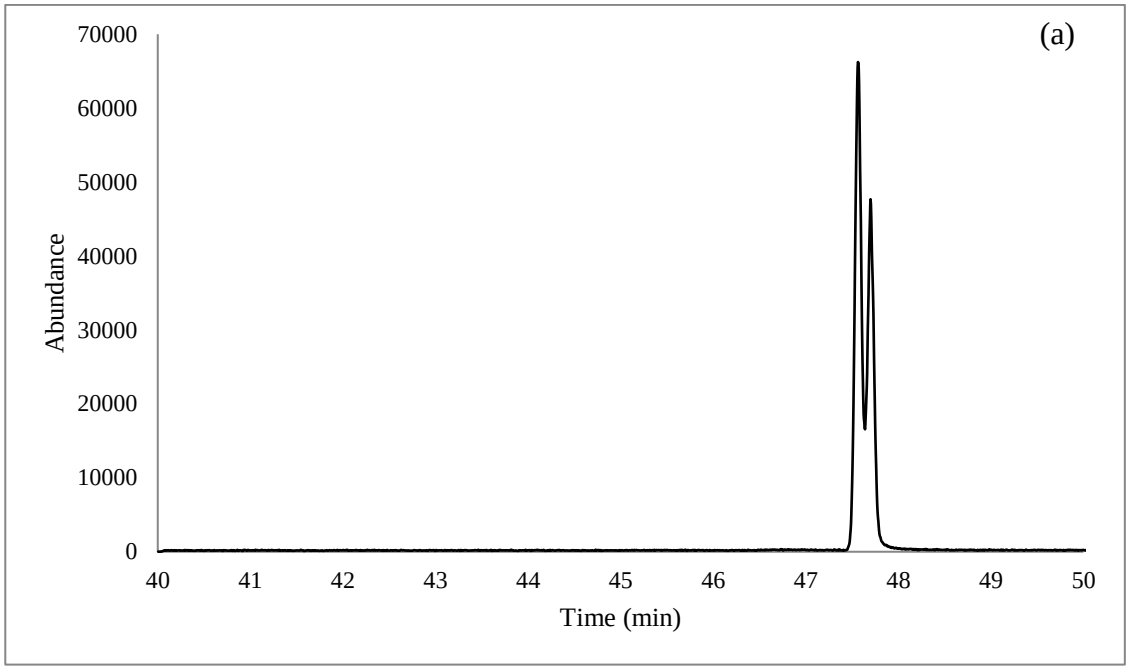

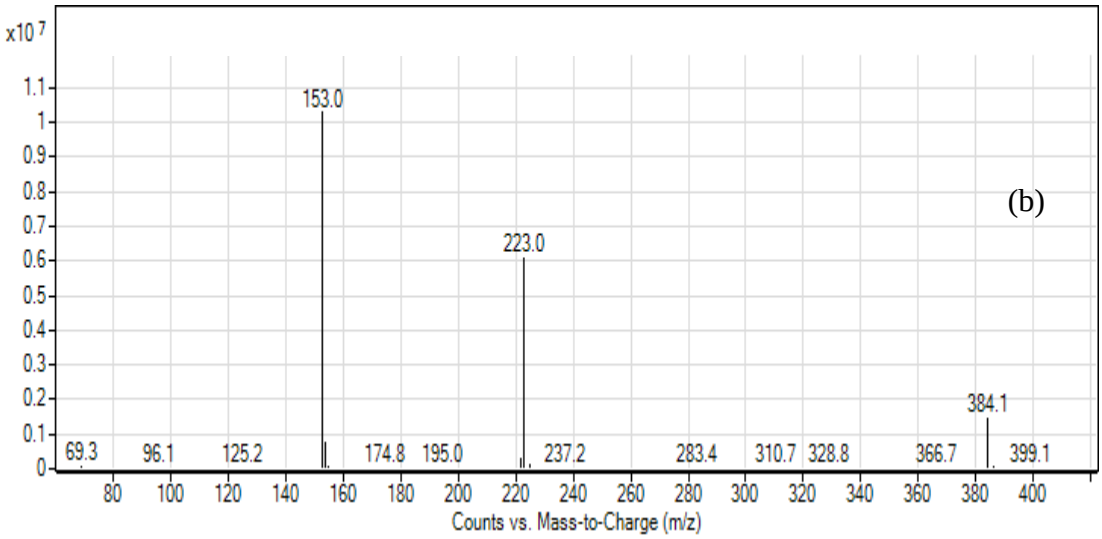

Figure 91: a) Gas chromatogram for separation of the R and S enantiomers of Pentedrone drug after derivatization with L-TPC and b) mass spectrum of the same compound analyzed by GC-NCI-MS system

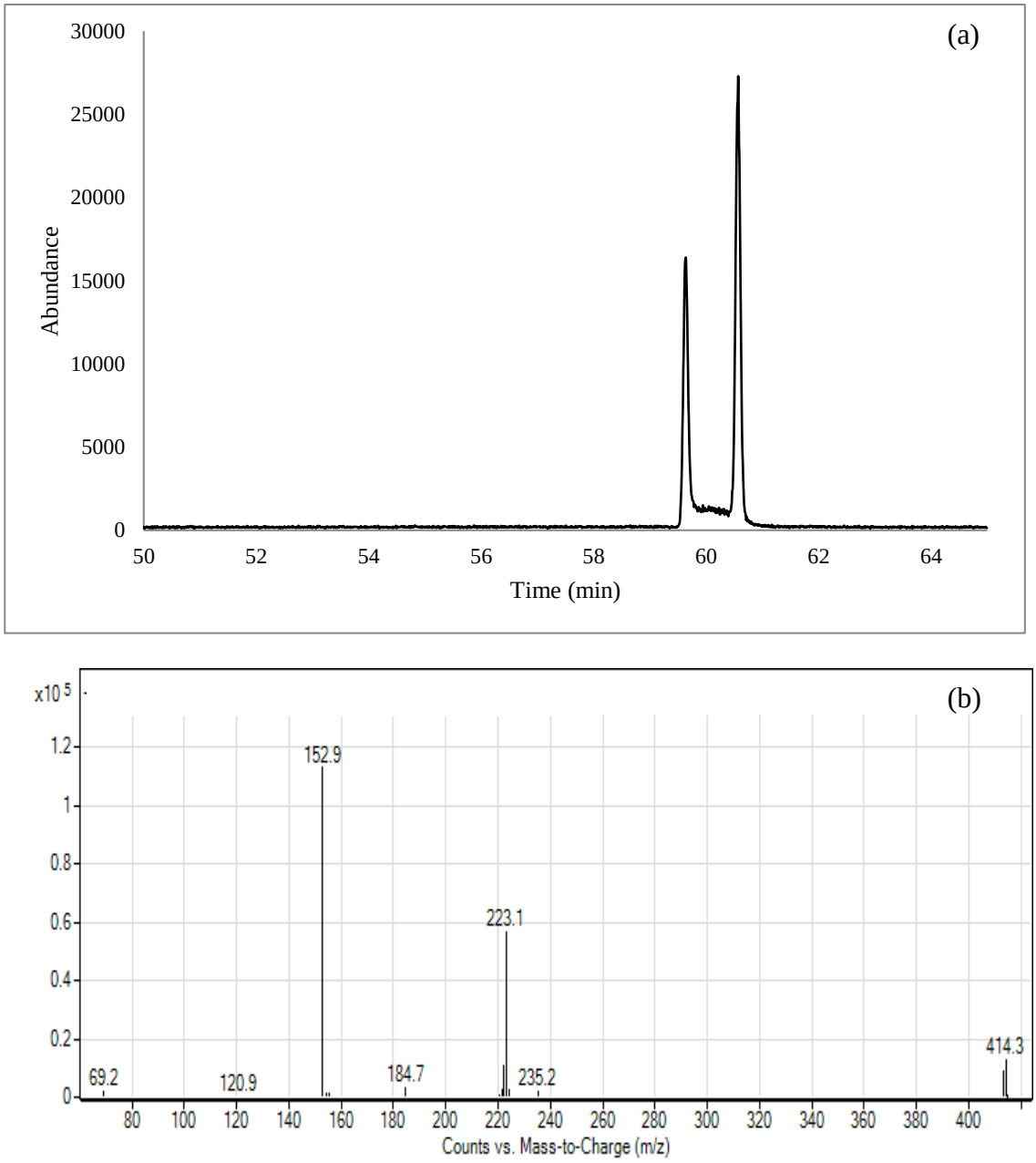

Figure 92: a) Gas chromatogram for separation of the R and S enantiomers of Butylone drug after derivatization with L-TPC and b) mass spectrum of the same compound analyzed by GC-NCI-MS system

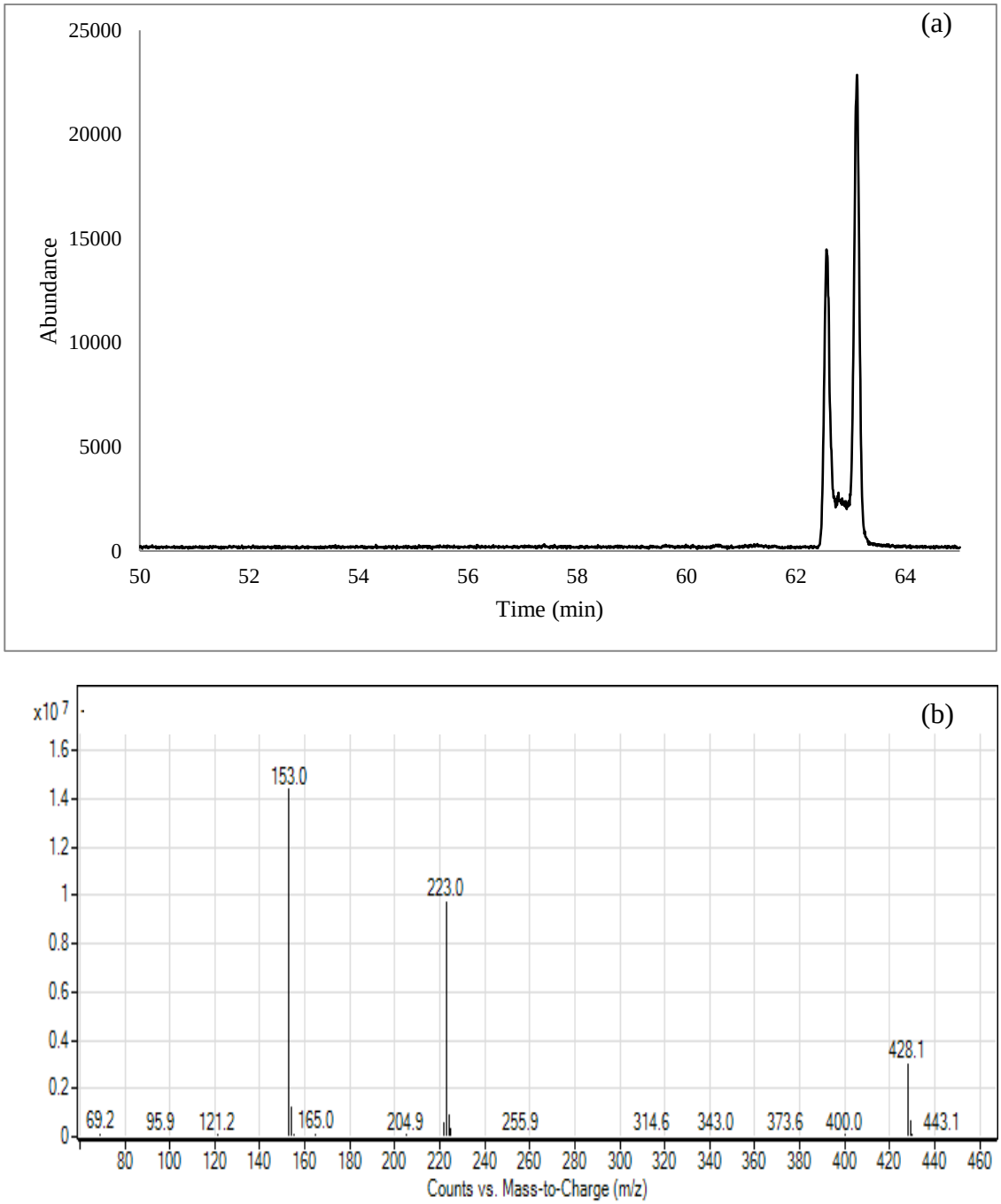

Figure 93: a) Gas chromatogram for separation of the R and S enantiomers of Pentylone drug after derivatization with L-TPC and b) mass spectrum of the same compound analyzed by GC-NCI-MS system

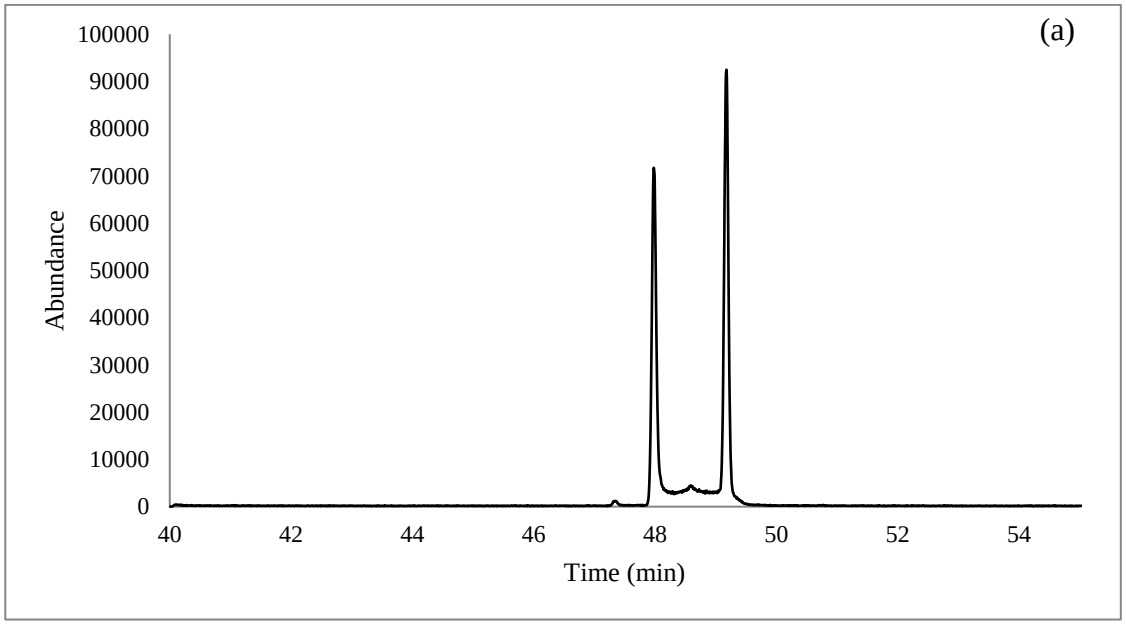

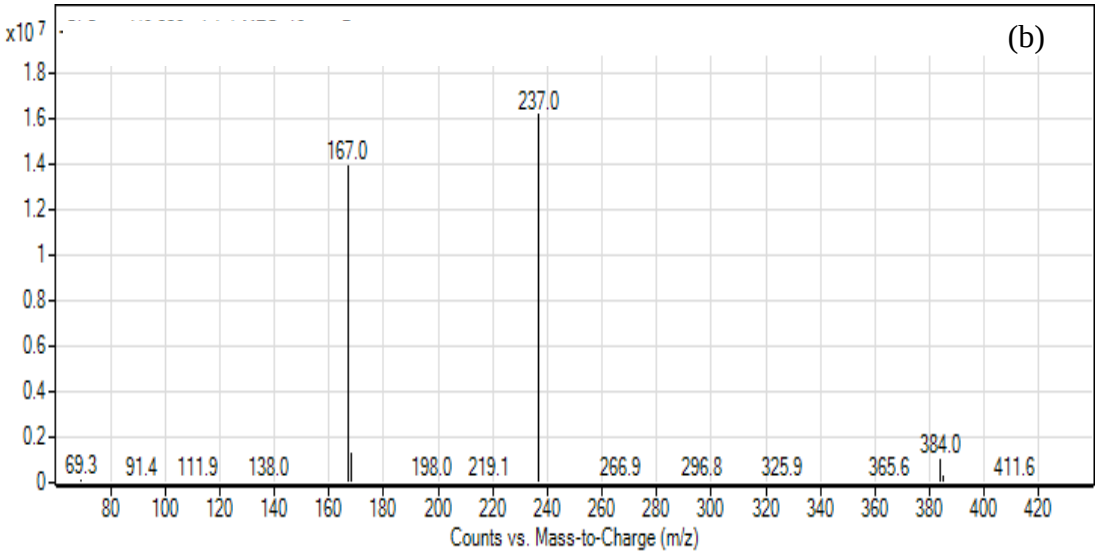

Figure 94: a) Gas chromatogram for separation of the R and S enantiomers of 4-Methylethcathinone (4-MEC) drug after derivatization with L-TPC and b) mass spectrum of the same compound analyzed by GC-NCI-MS system

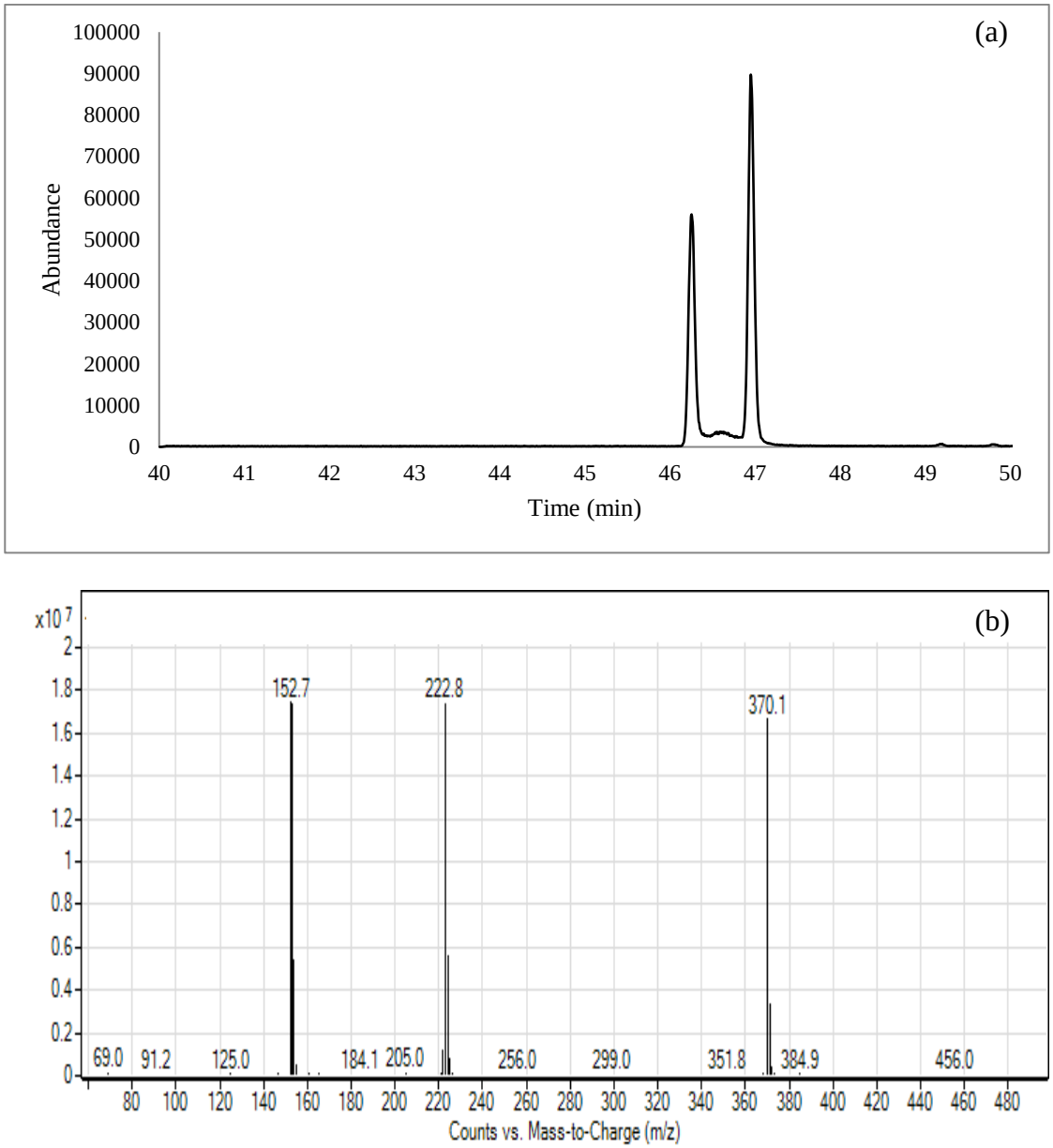

Figure 95: a) Gas chromatogram for separation of the R and S enantiomers of 3-Methylmethcathinone (3-MMC) drug after derivatization with L-TPC and b) mass spectrum of the same compound analyzed by GC-NCI-MS system

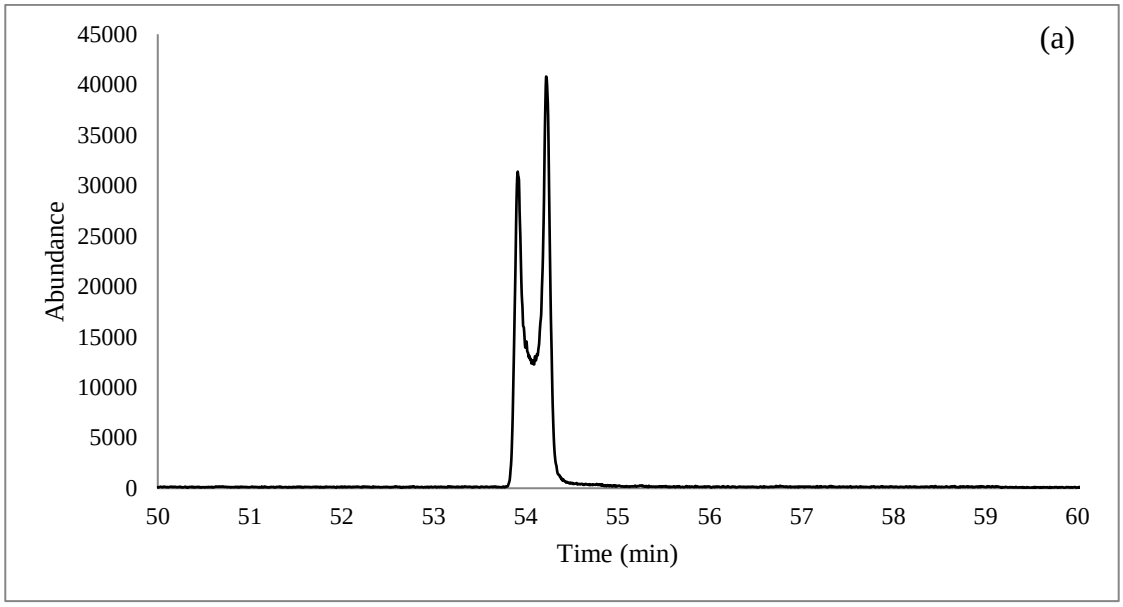

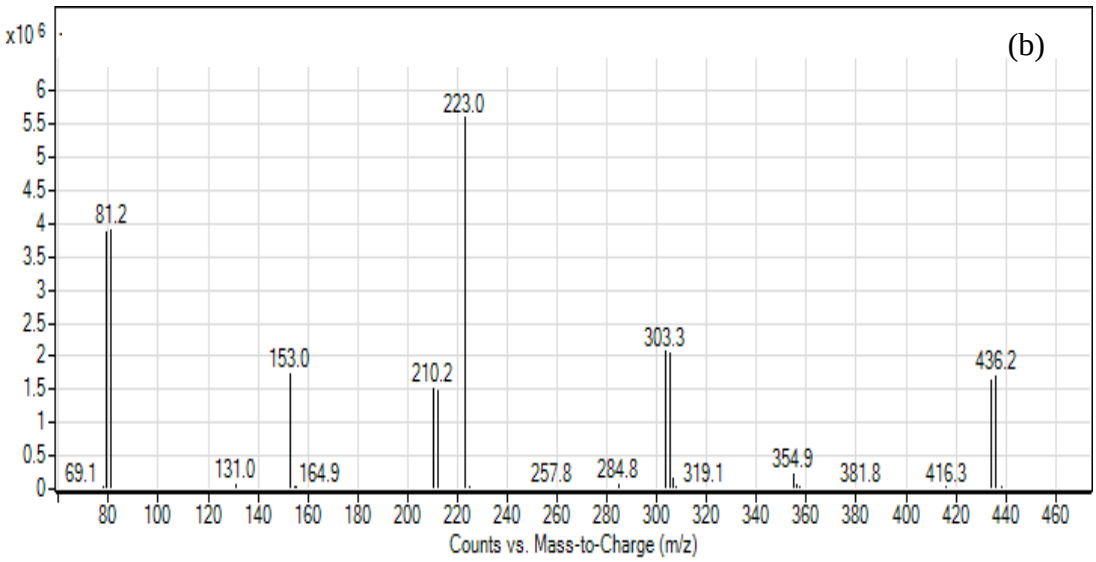

Figure 96: a) Gas chromatogram for separation of the R and S enantiomers of 4-Bromomethcathinone (4-BMC) drug after derivatization with L-TPC and b) mass spectrum of the same compound analyzed by GC-NCI-MS system

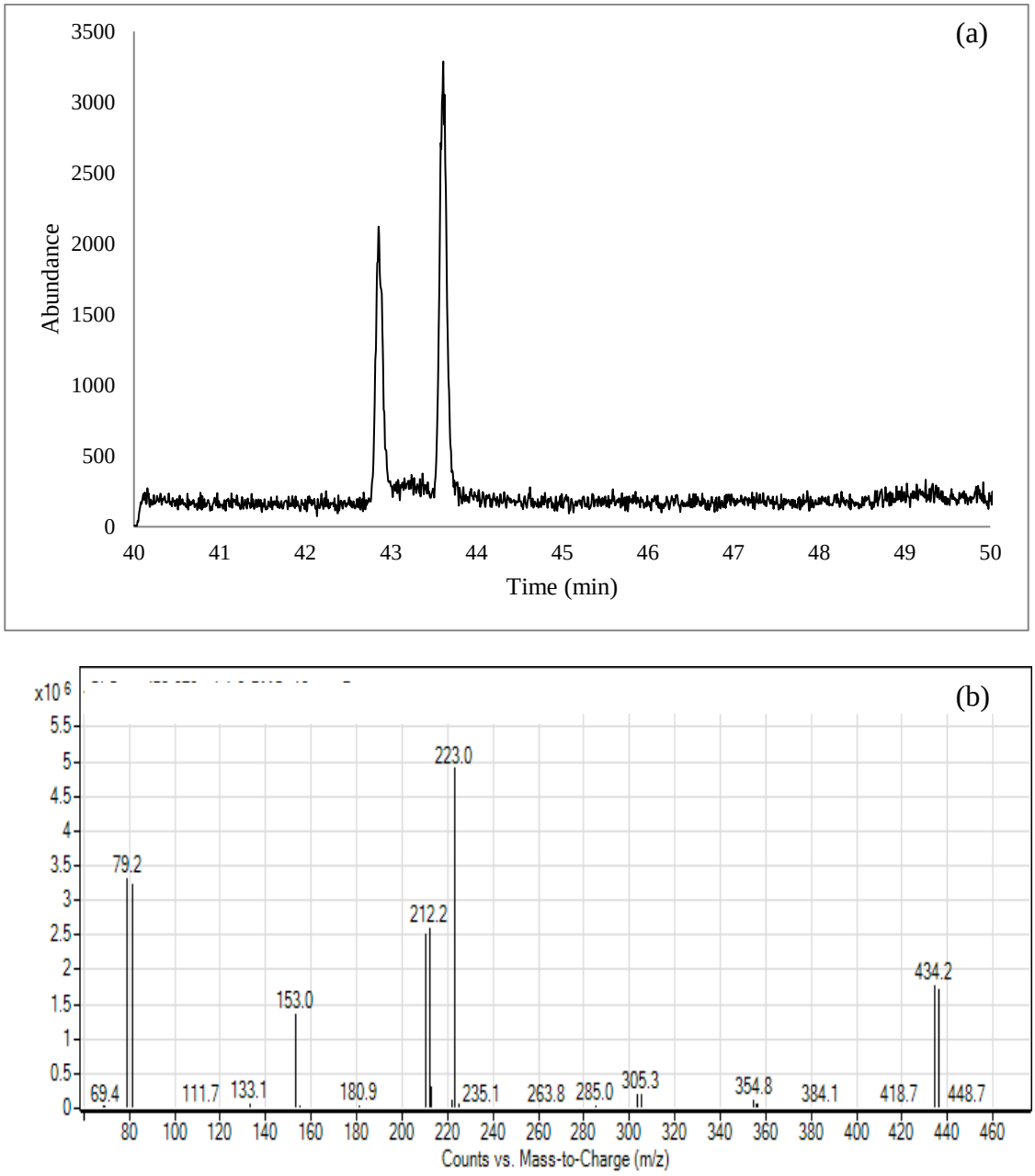

Figure 97: a) Gas chromatogram for separation of the R and S enantiomers of 3-Bromomethcathinone (3-BMC) drug after derivatization with L-TPC and b) mass spectrum of the same compound analyzed by GC-NCI-MS system

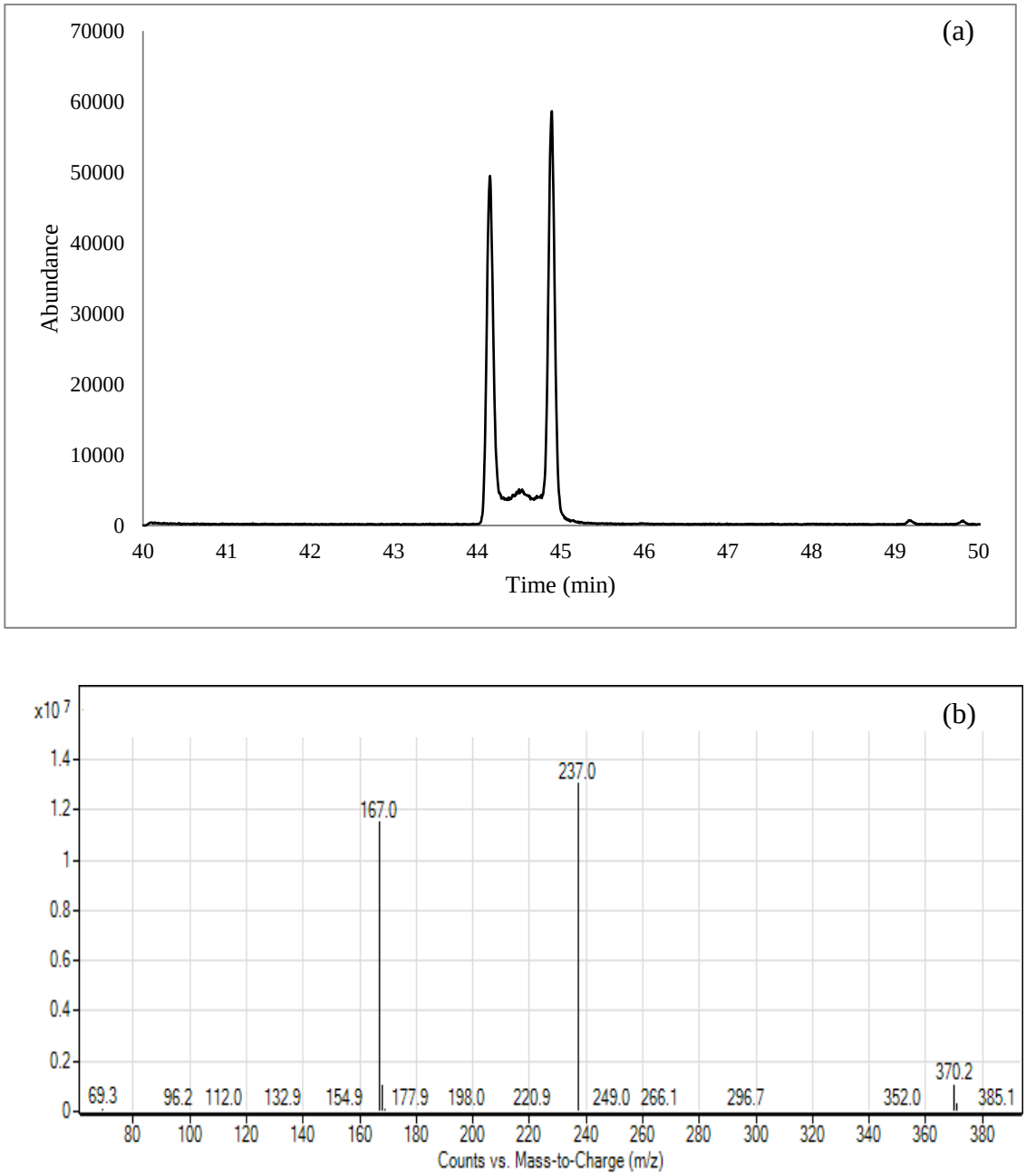

Figure 98: a) Gas chromatogram for separation of the R and S enantiomers of Ethcathinone drug after derivatization with L-TPC and b) mass spectrum of the same compound analyzed by GC-NCI-MS system

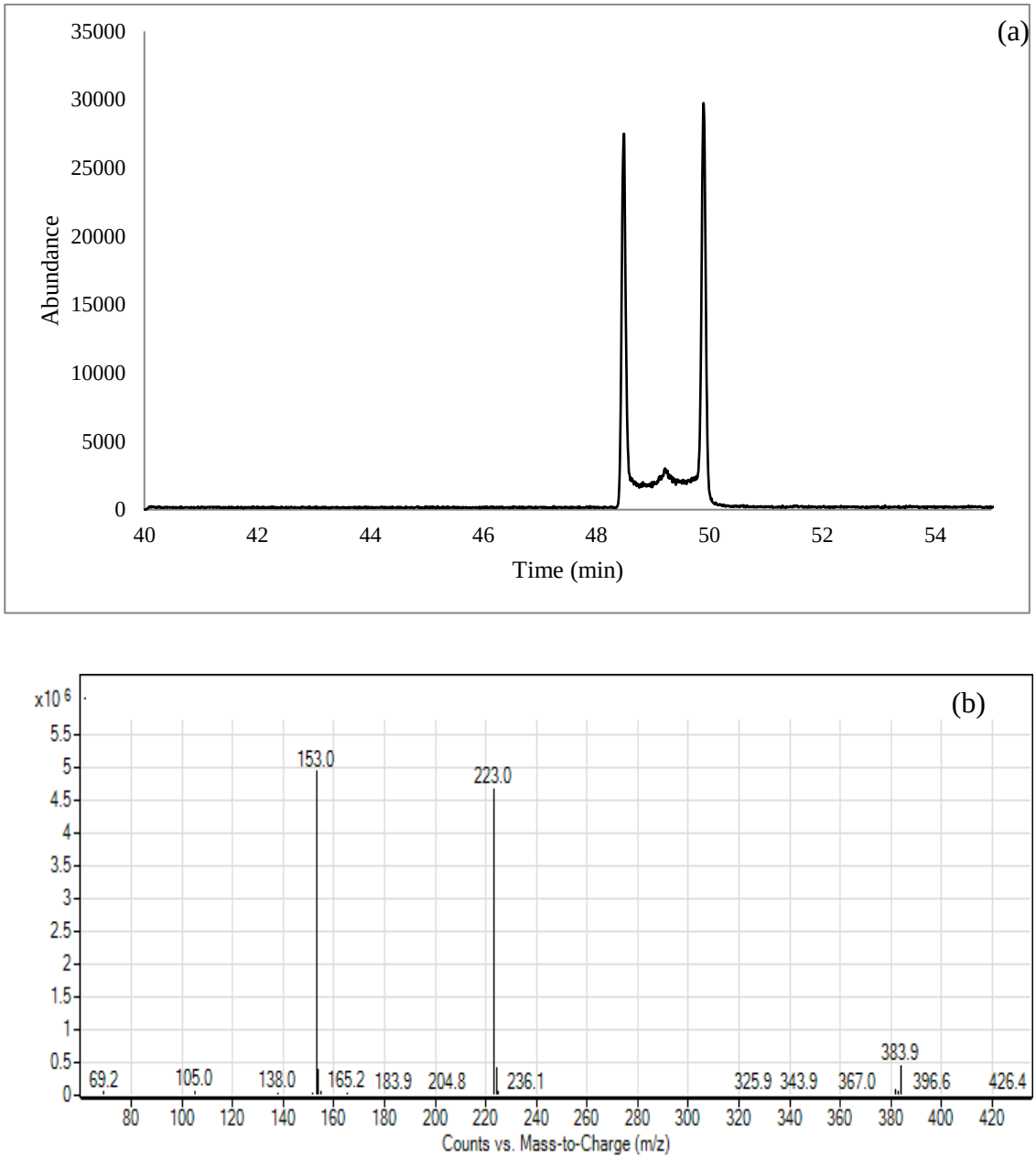

Figure 99: a) Gas chromatogram for separation of the R and S enantiomers of 2,4-Dimethylmethcathinone (2,4-DMMC) drug after derivatization with L-TPC and b) mass spectrum of the same compound analyzed by GC-NCI-MS system

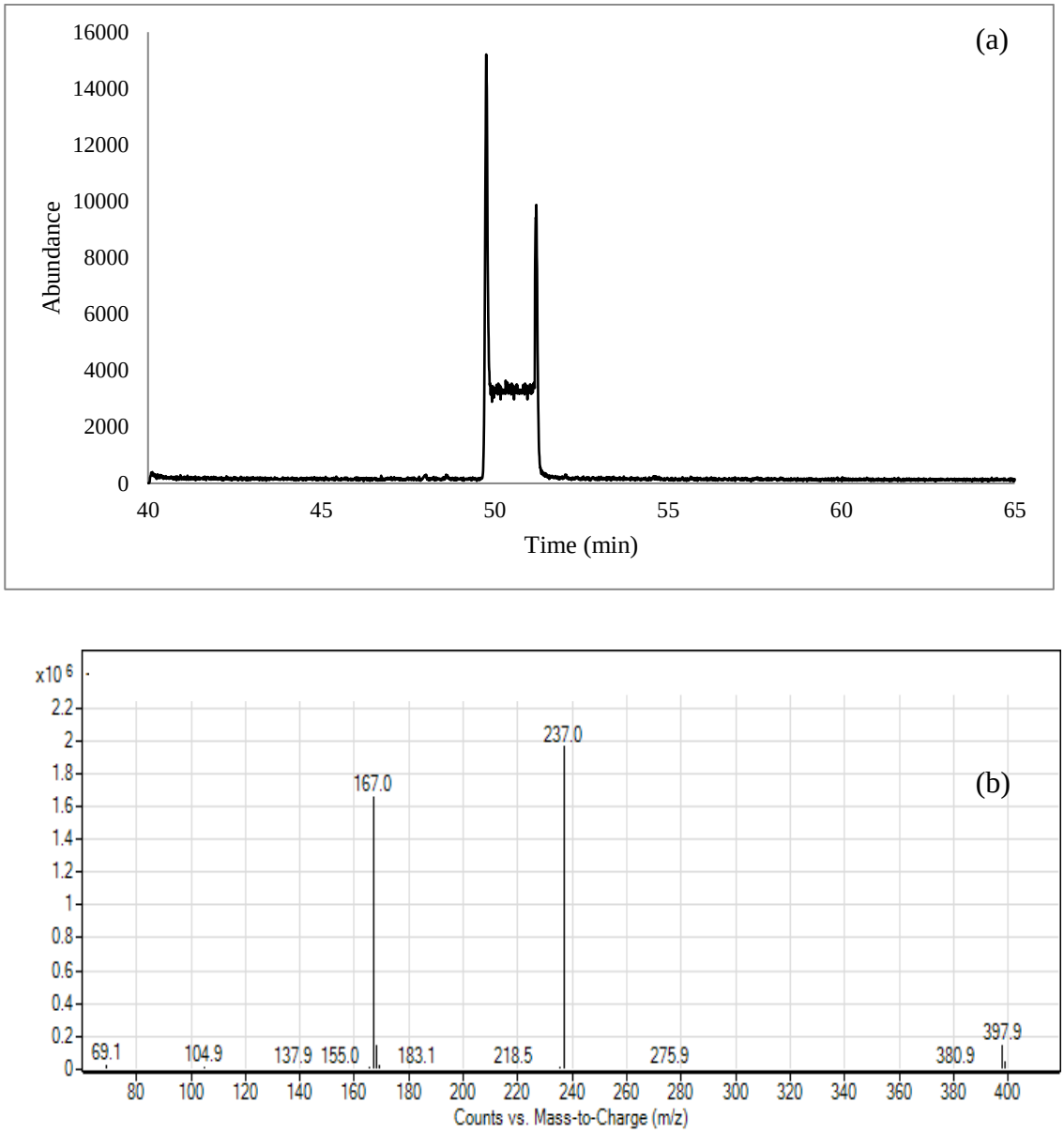

Figure 100: a) Gas chromatogram for separation of the R and S enantiomers of 2,4-Dimethylethcathinone (2,4-DMEC) drug after derivatization with L-TPC and b) mass spectrum of the same compound analyzed by GC-NCI-MS system

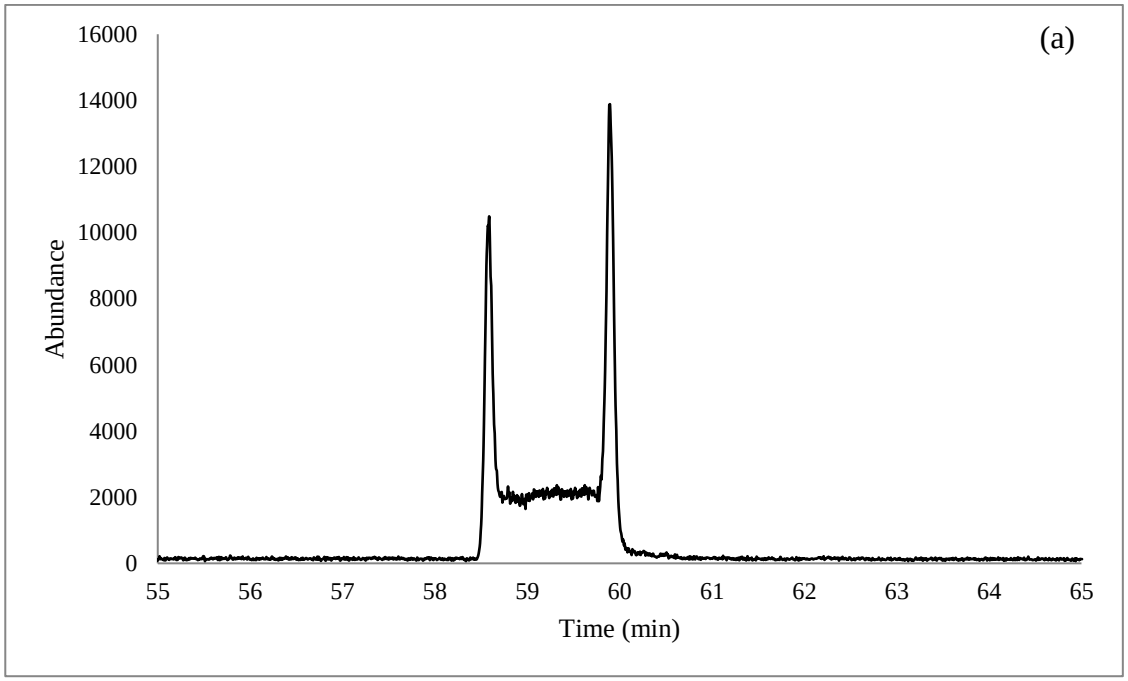

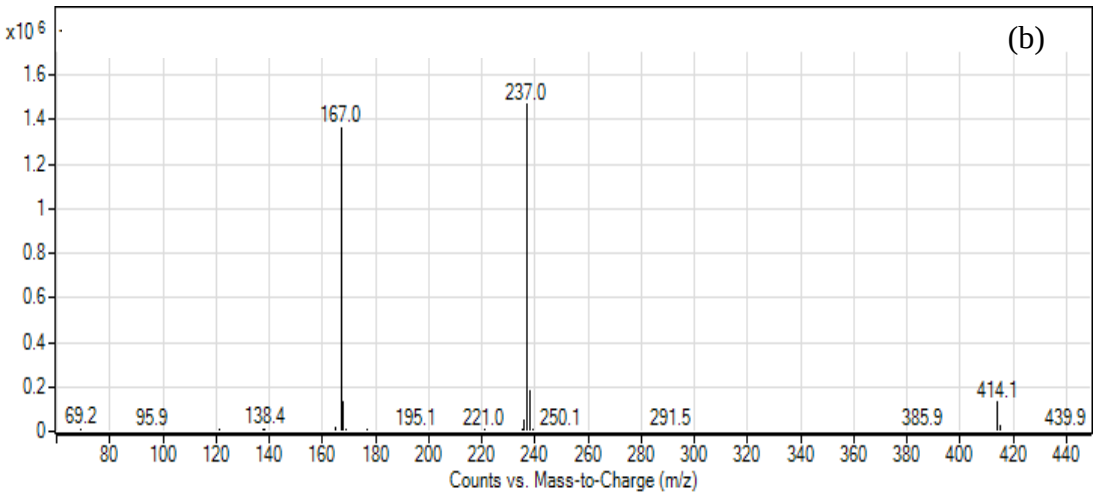

Figure 101: a) Gas chromatogram for separation of the R and S enantiomers of 3,4-Methylenedioxy-N-ethylcathinon (Ethylone) drug after derivatization with L-TPC and b) mass spectrum of the same compound analyzed by GC-NCI-MS system

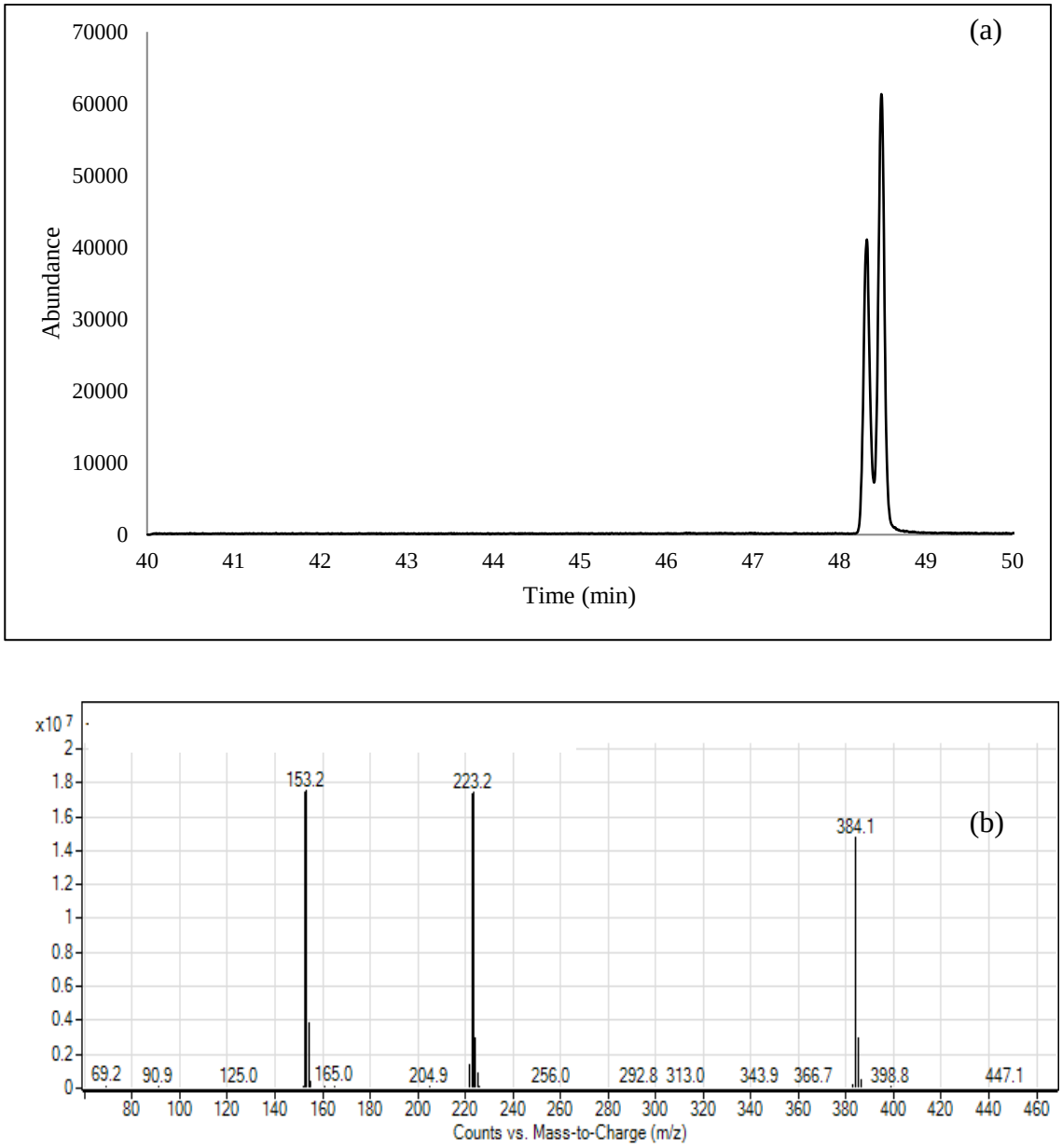

Figure 102: a) Gas chromatogram for separation of the R and S enantiomers of 3-Methylbuphedrone drug after derivatization with L-TPC and b) mass spectrum of the same compound analyzed by GC-NCI-MS system

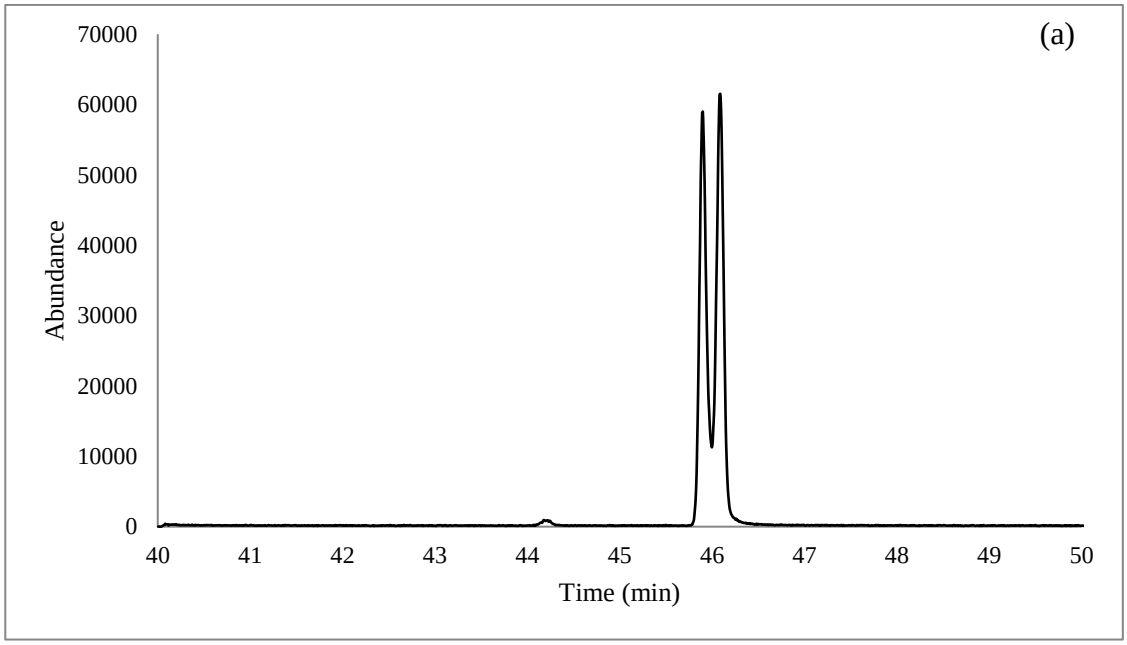

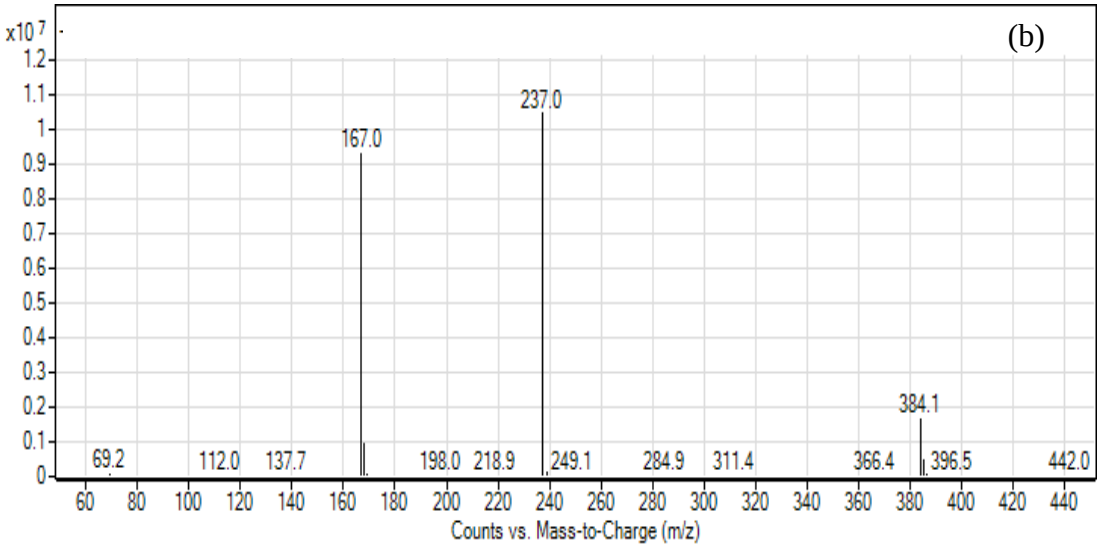

Figure 103: a) Gas chromatogram for separation of the R and S enantiomers of N-Ethylbuphedrone (NEB) drug after derivatization with L-TPC and b) mass spectrum of the same compound analyzed by GC-NCI-MS system

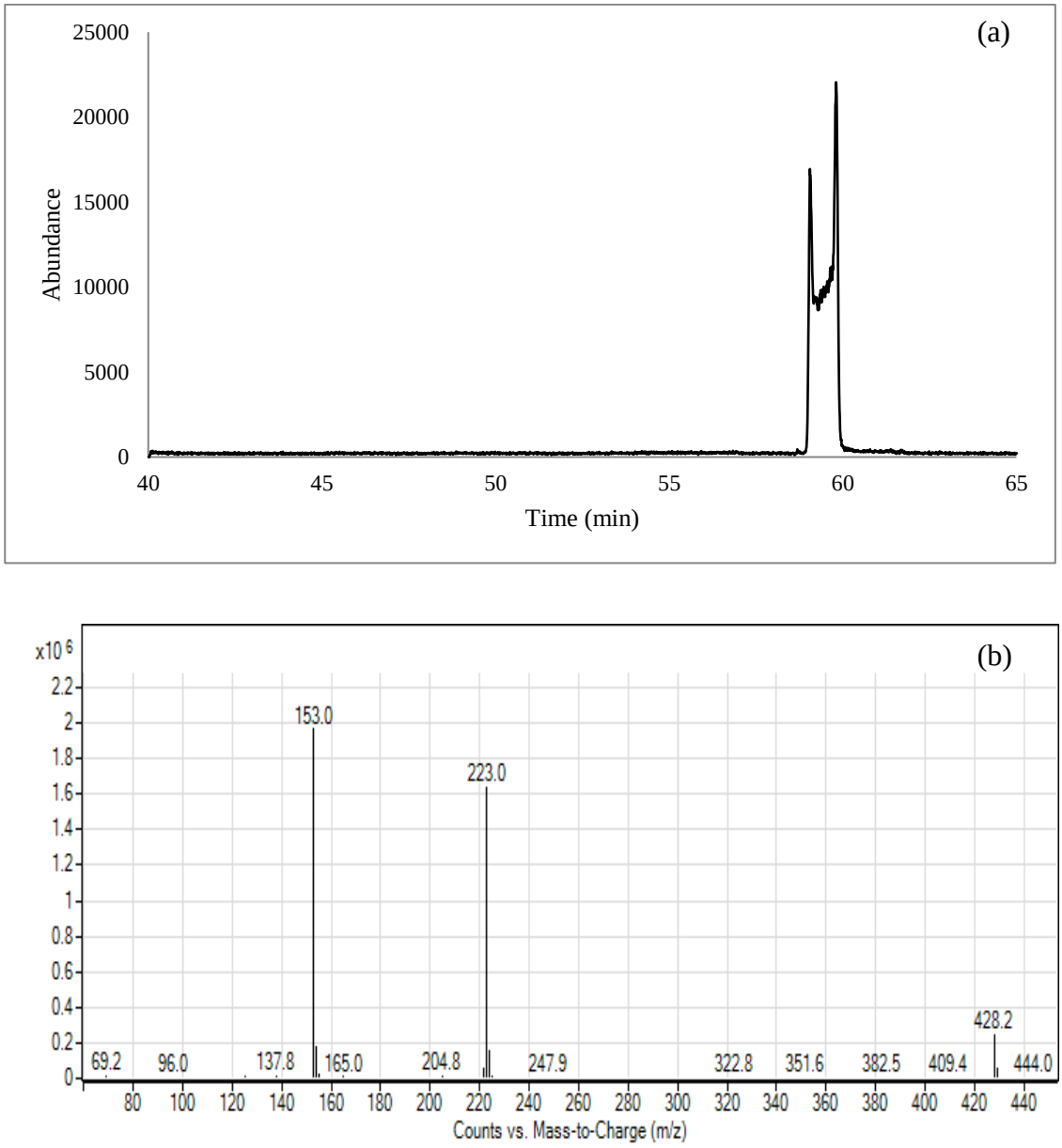

Figure 104: a) Gas chromatogram for separation of the R and S enantiomers of 2,3-Pentylone drug after derivatization with L-TPC and b) mass spectrum of the same compound analyzed by GC-NCI-MS system

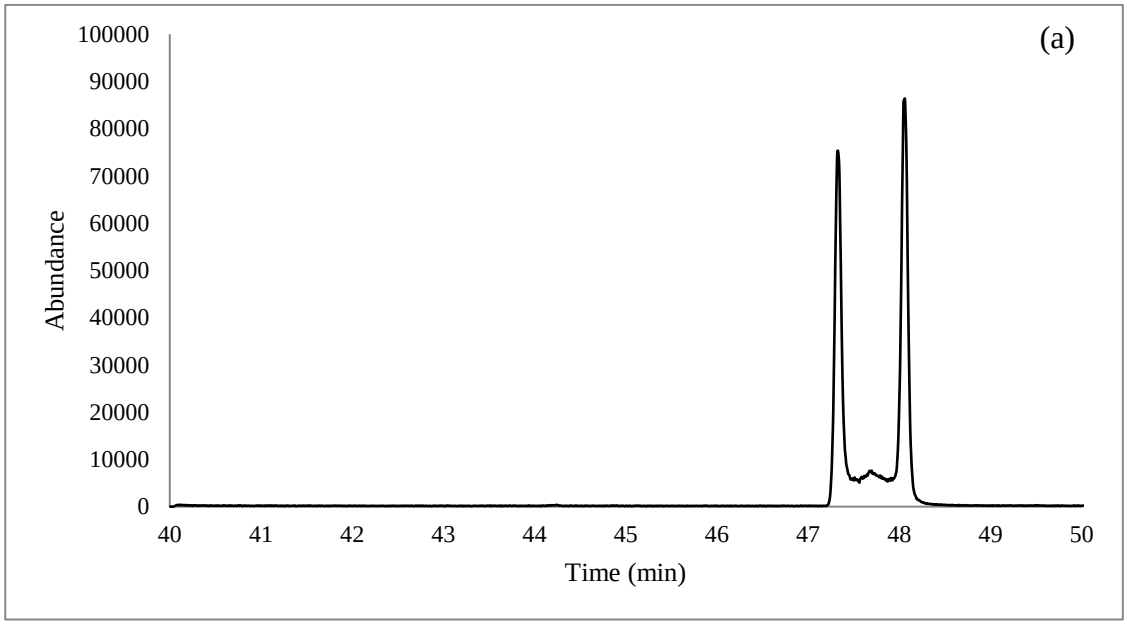

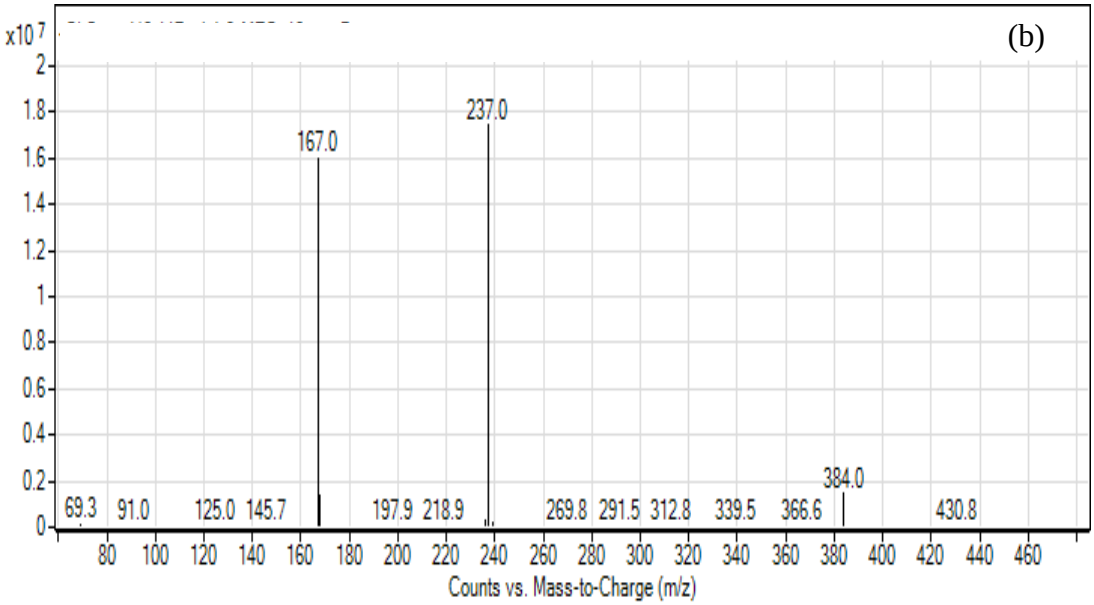

Figure 105: a) Gas chromatogram for separation of the R and S enantiomers of 3-Methylethcathinone (3-MEC) drug after derivatization with L-TPC and b) mass spectrum of the same compound analyzed by GC-NCI-MS system

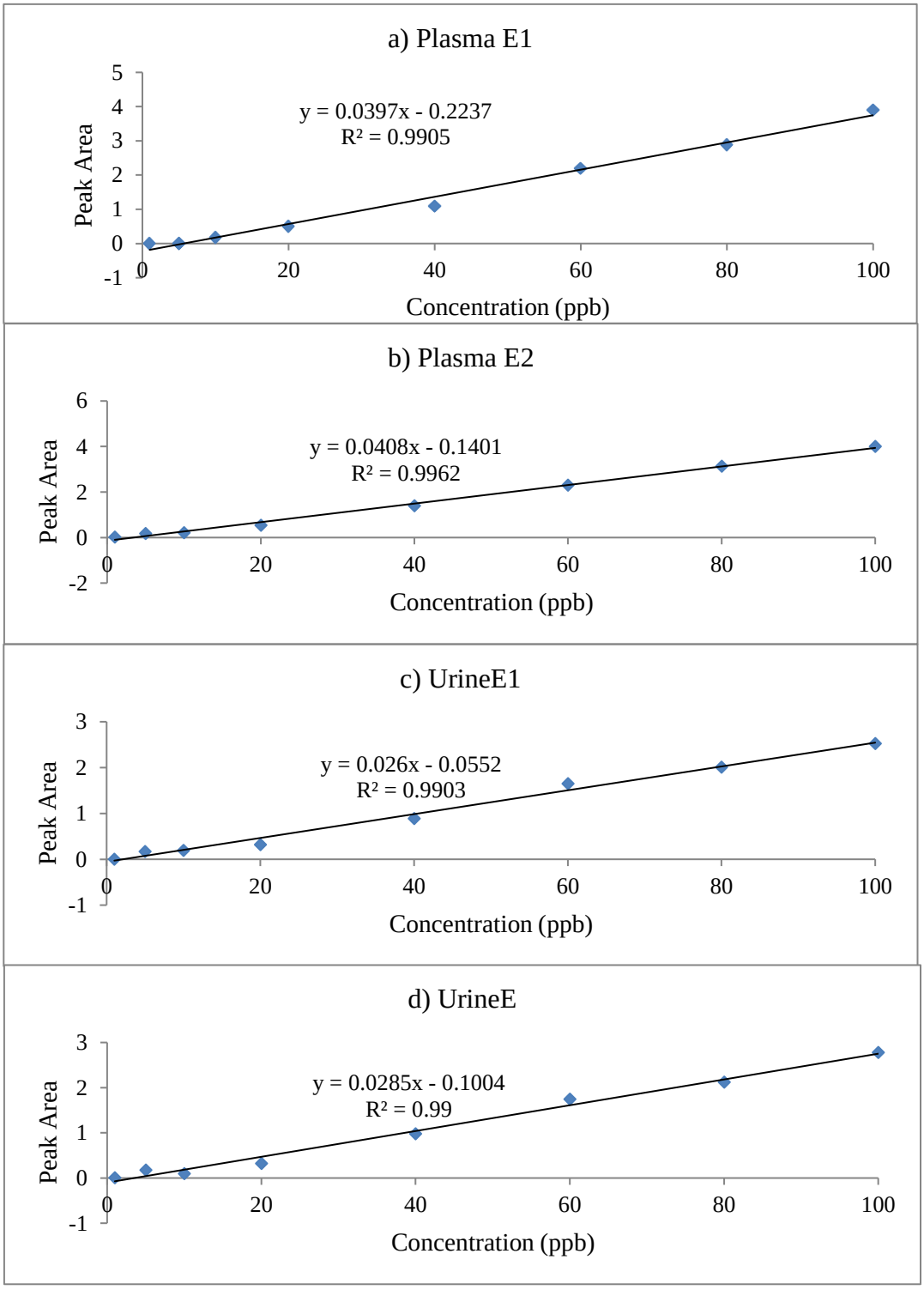

Figure 106: Calibration curves of 4-FMC enantiomers in plasma and urine

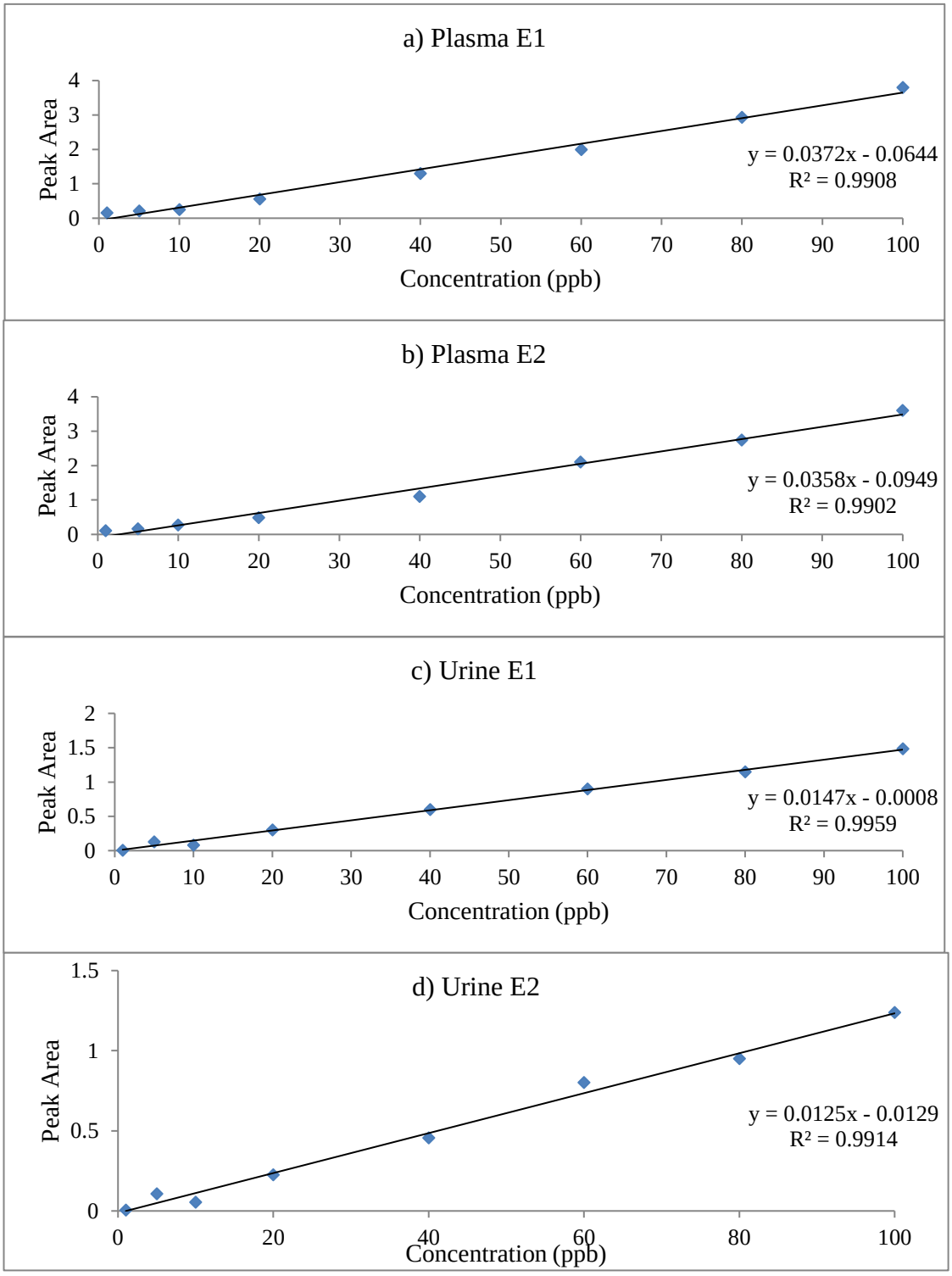

Figure 107: Calibration curves of 4-FEC enantiomers in plasma and urine

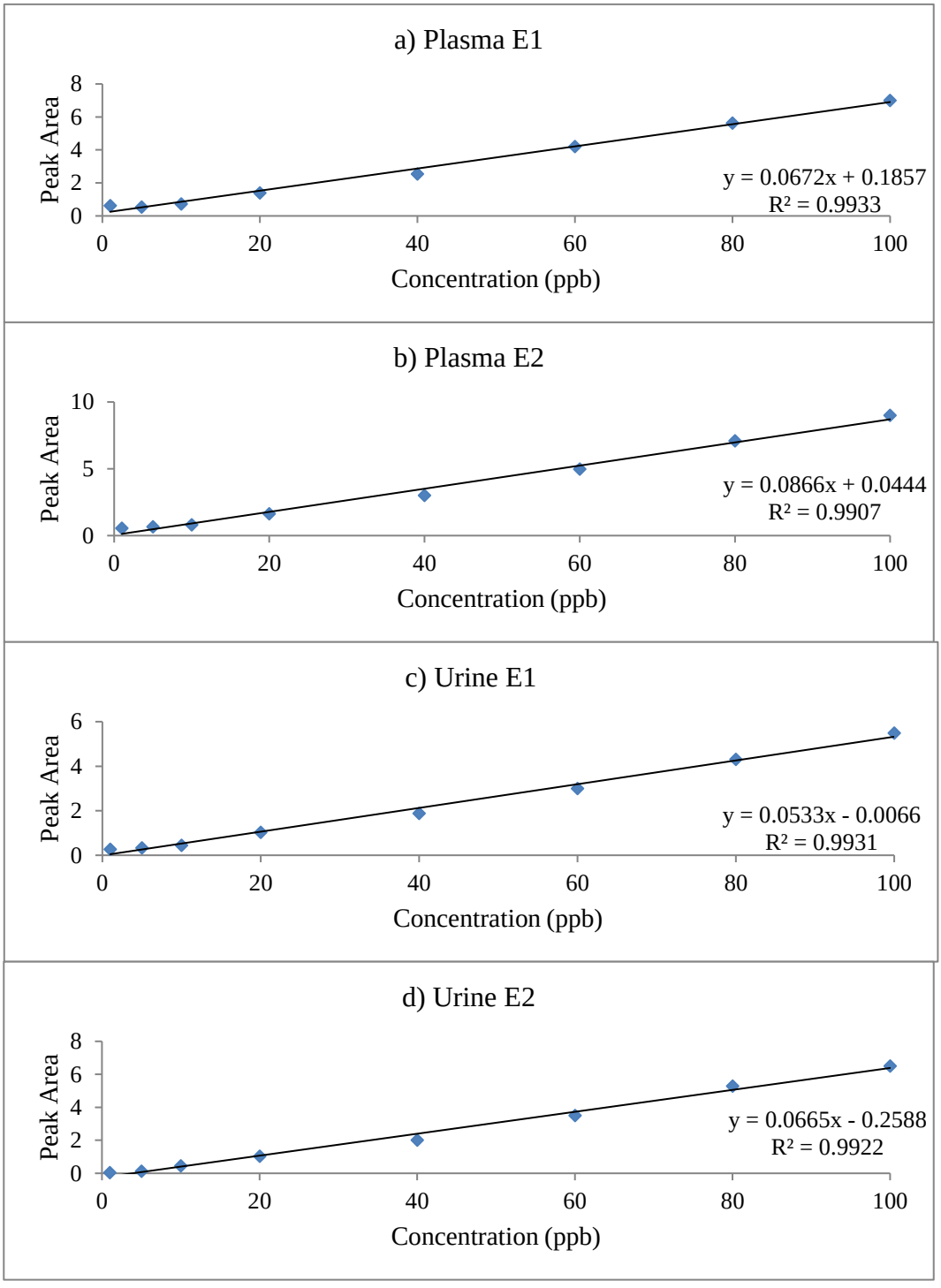

Figure 108: Calibration curves of Buphedrone enantiomers in plasma and urine

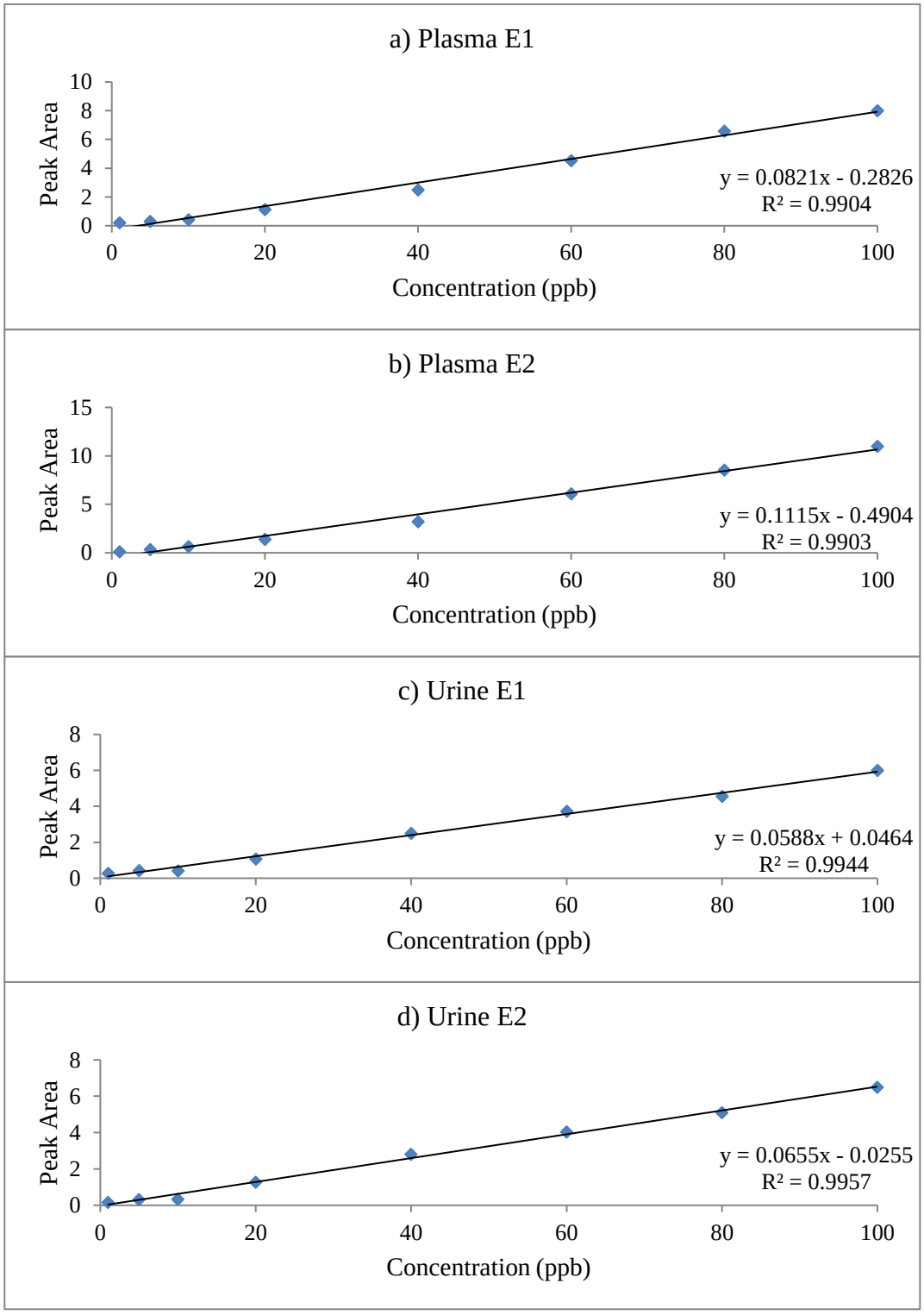

Figure 109: Calibration curves of 3-MMC enantiomers in plasma and urine

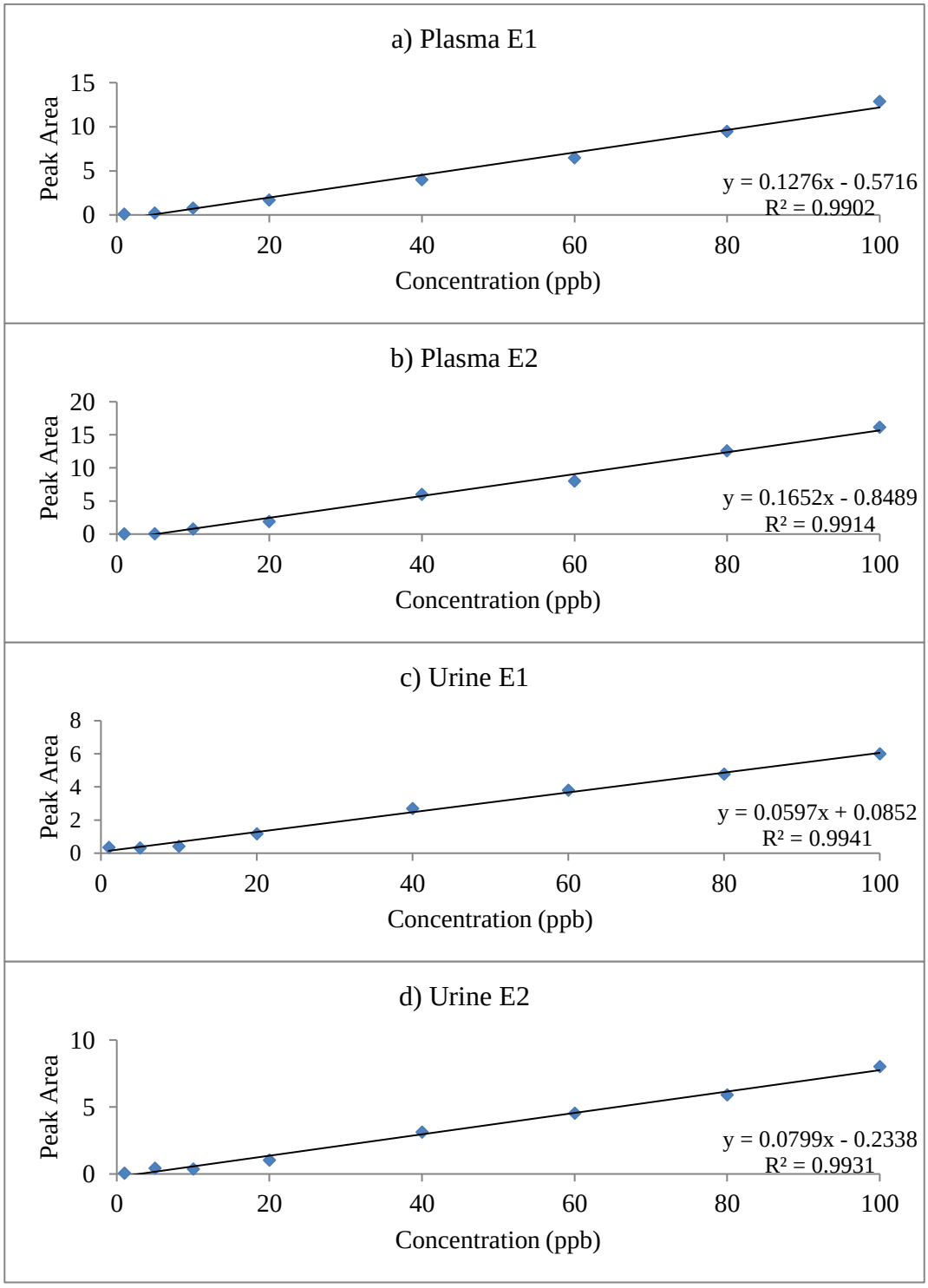

Figure 110: Calibration curves of 3-Methylbuphedrone enantiomers in plasma and urine

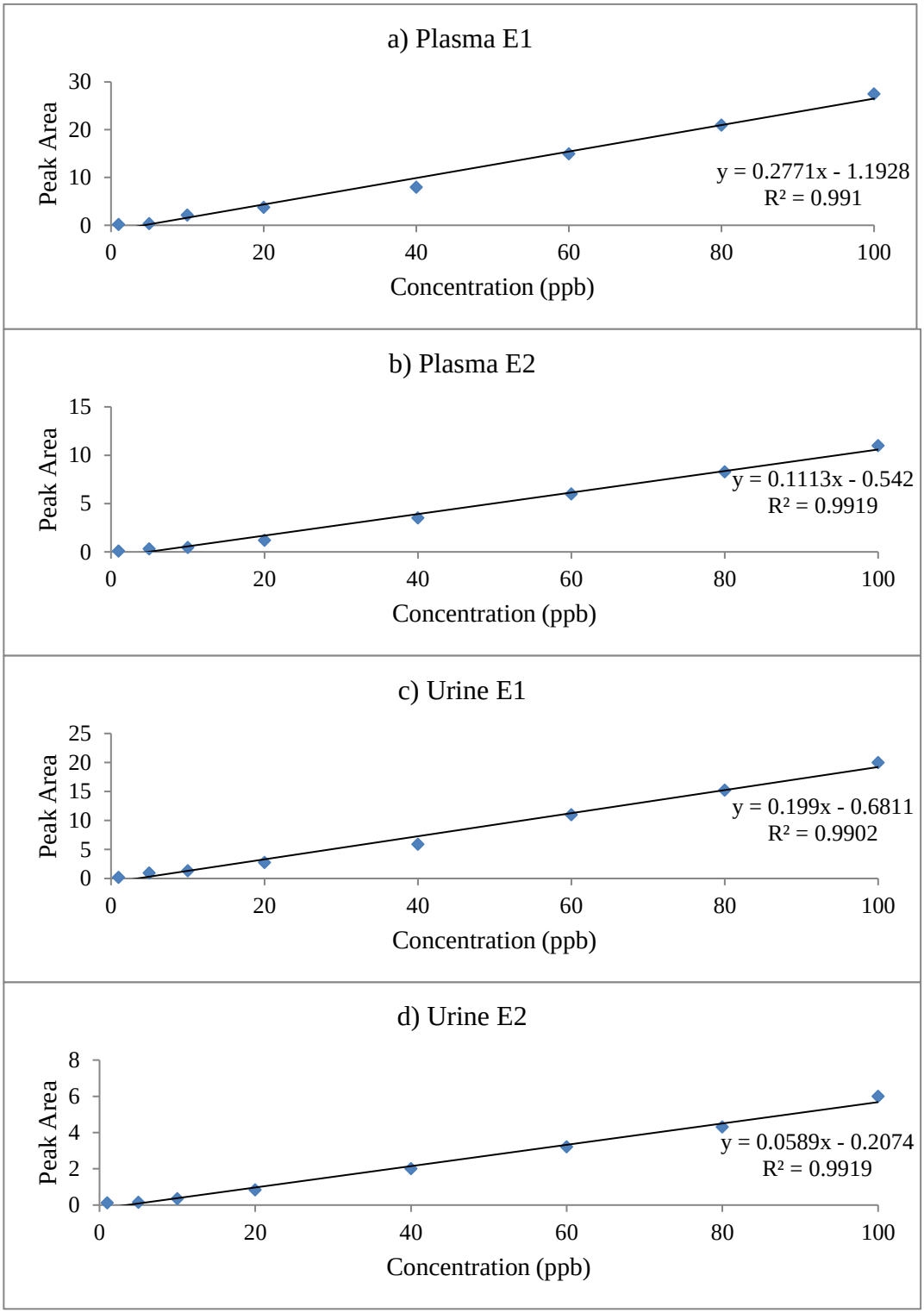

Figure 111: Calibration curves of 4-Methylbuphedrone enantiomers in plasma and urine

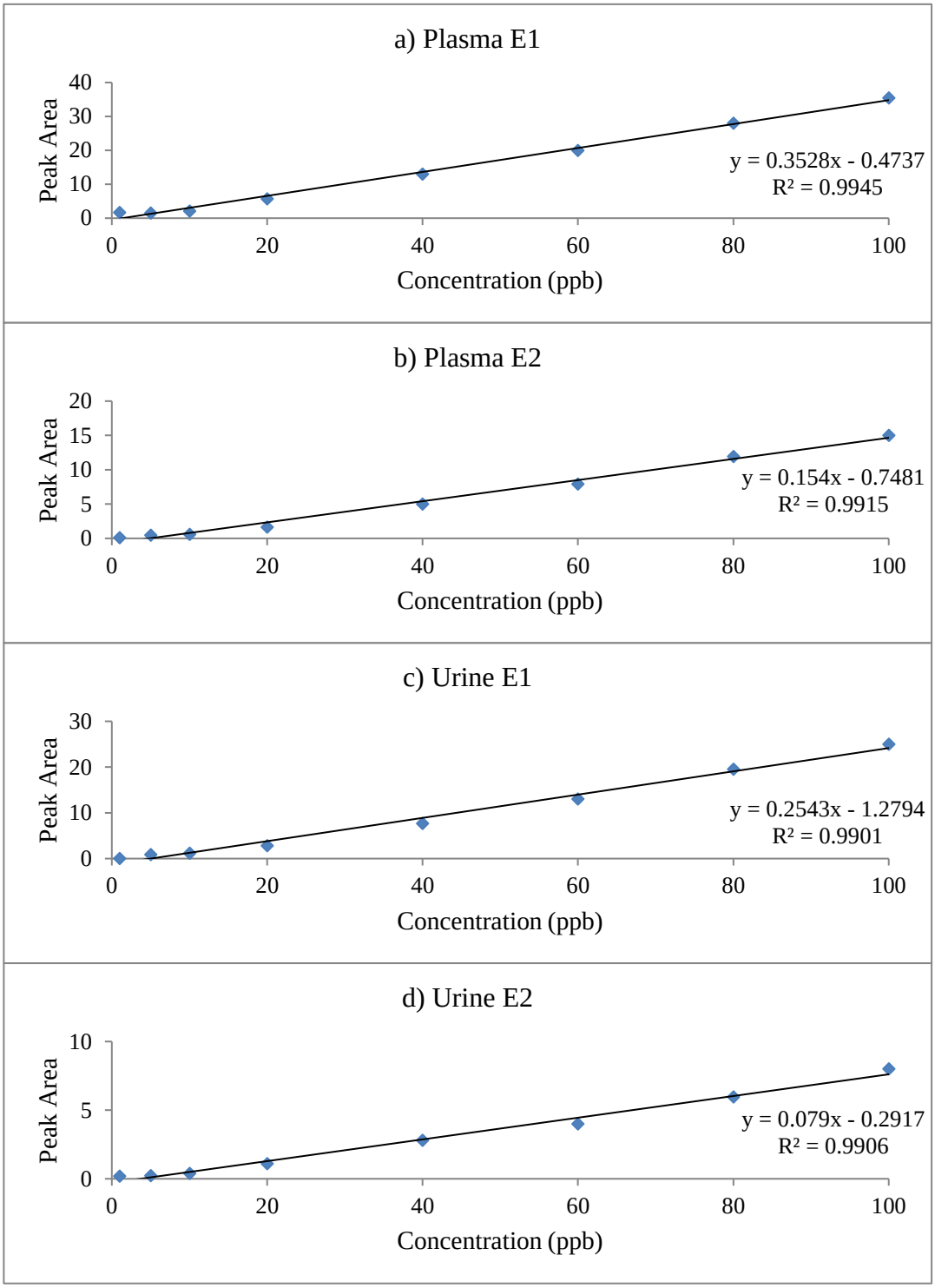

Figure 112: Calibration curves of 3-EMC enantiomers in plasma and urine

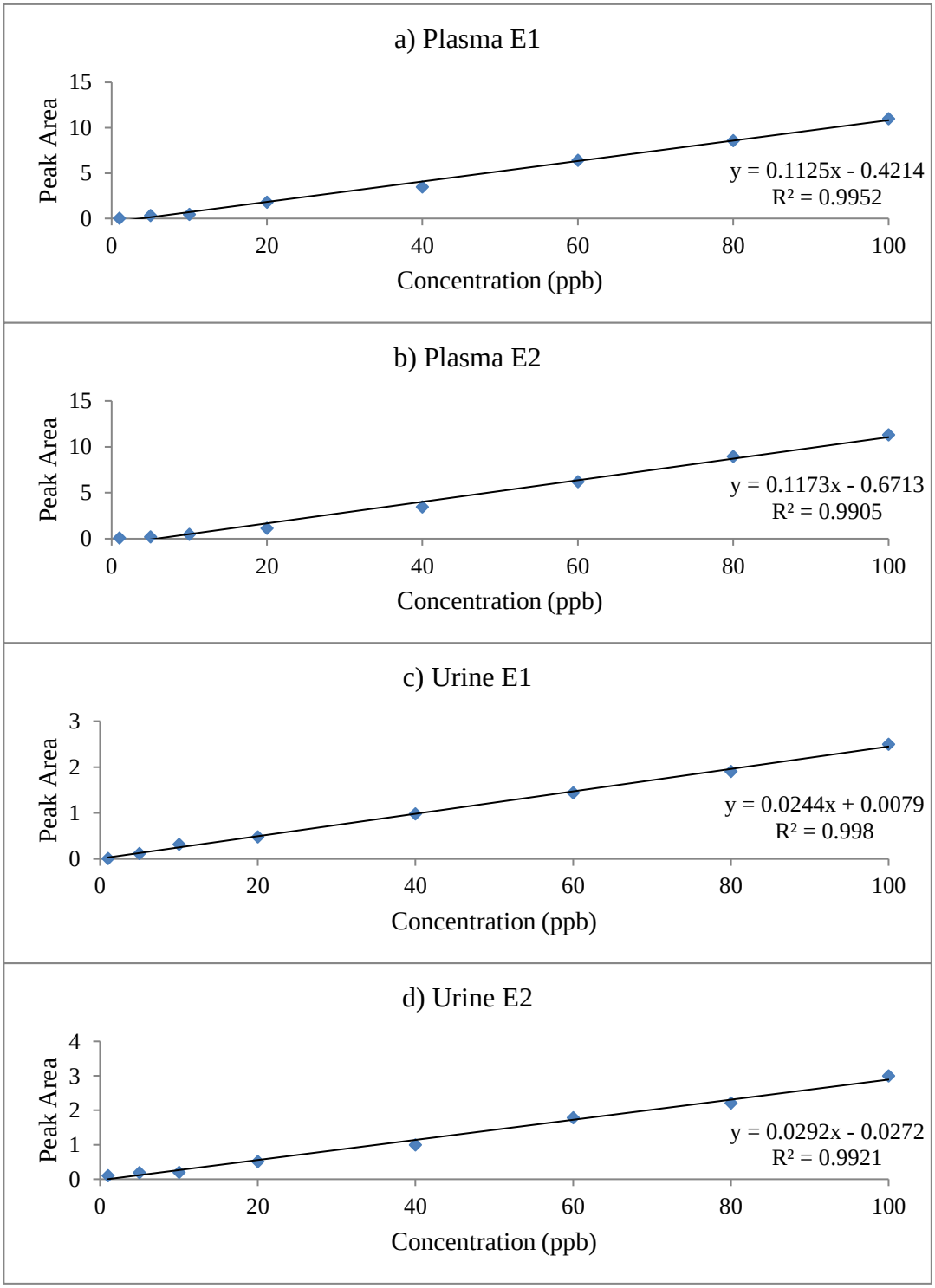

Figure 113: Calibration curves of 3-EEC enantiomers in plasma and urine

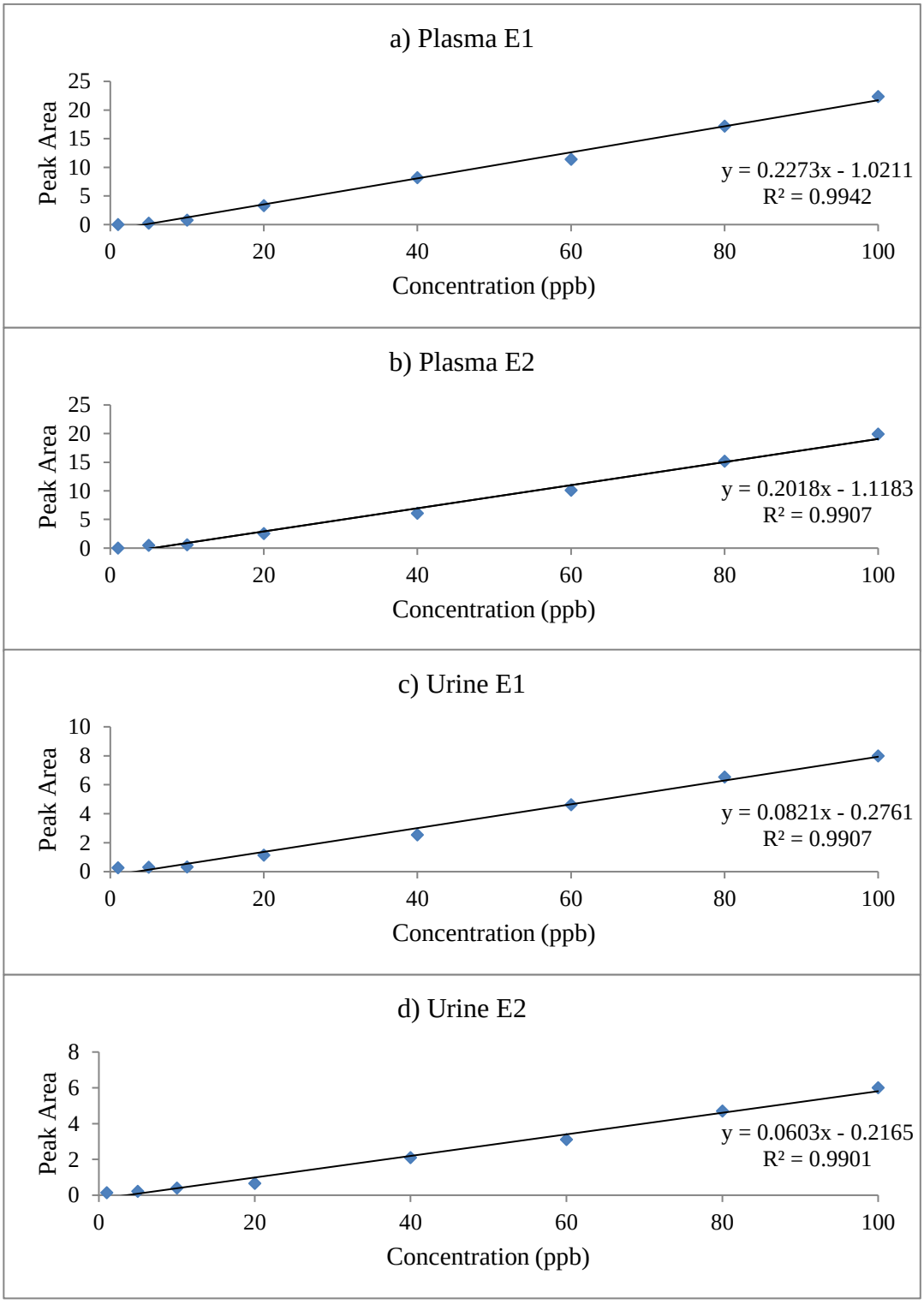

Figure 114: Calibration curves of 4-EEC enantiomers in plasma and urine

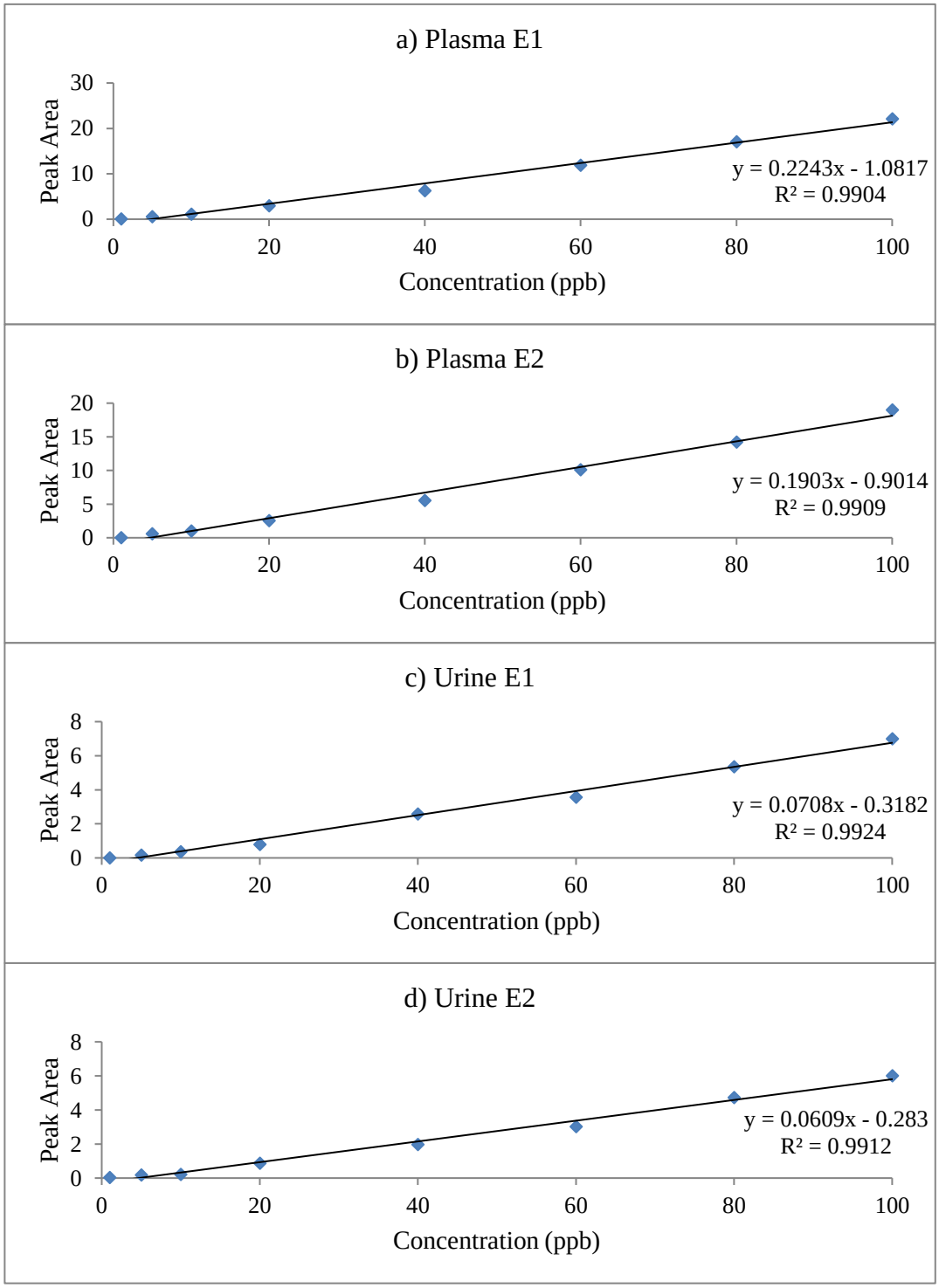

Figure 115: Calibration curves of 3,4-DMEC enantiomers in plasma and urine

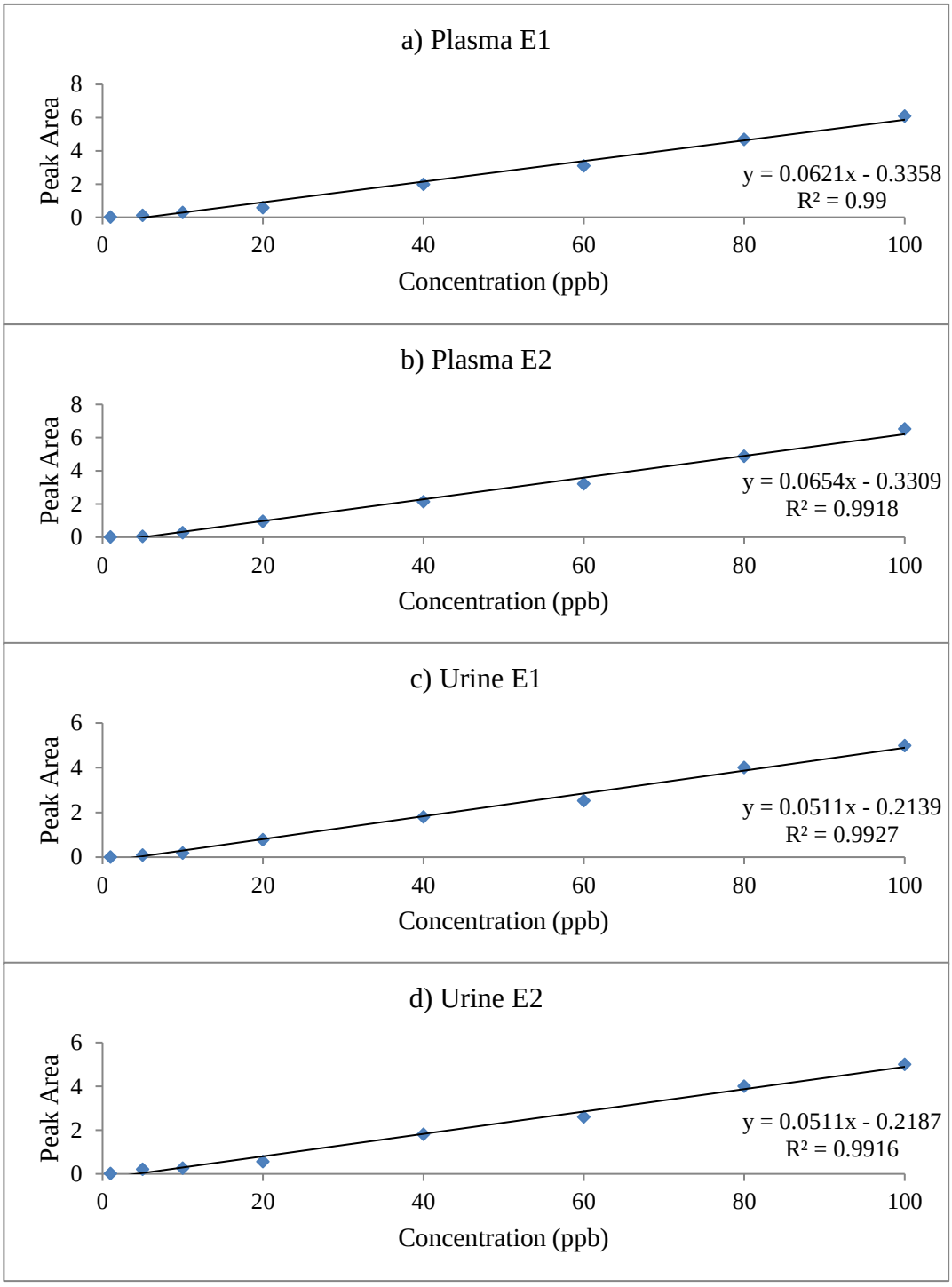

Figure 116: Calibration curves of 2,3--MDMC enantiomers in plasma and urine

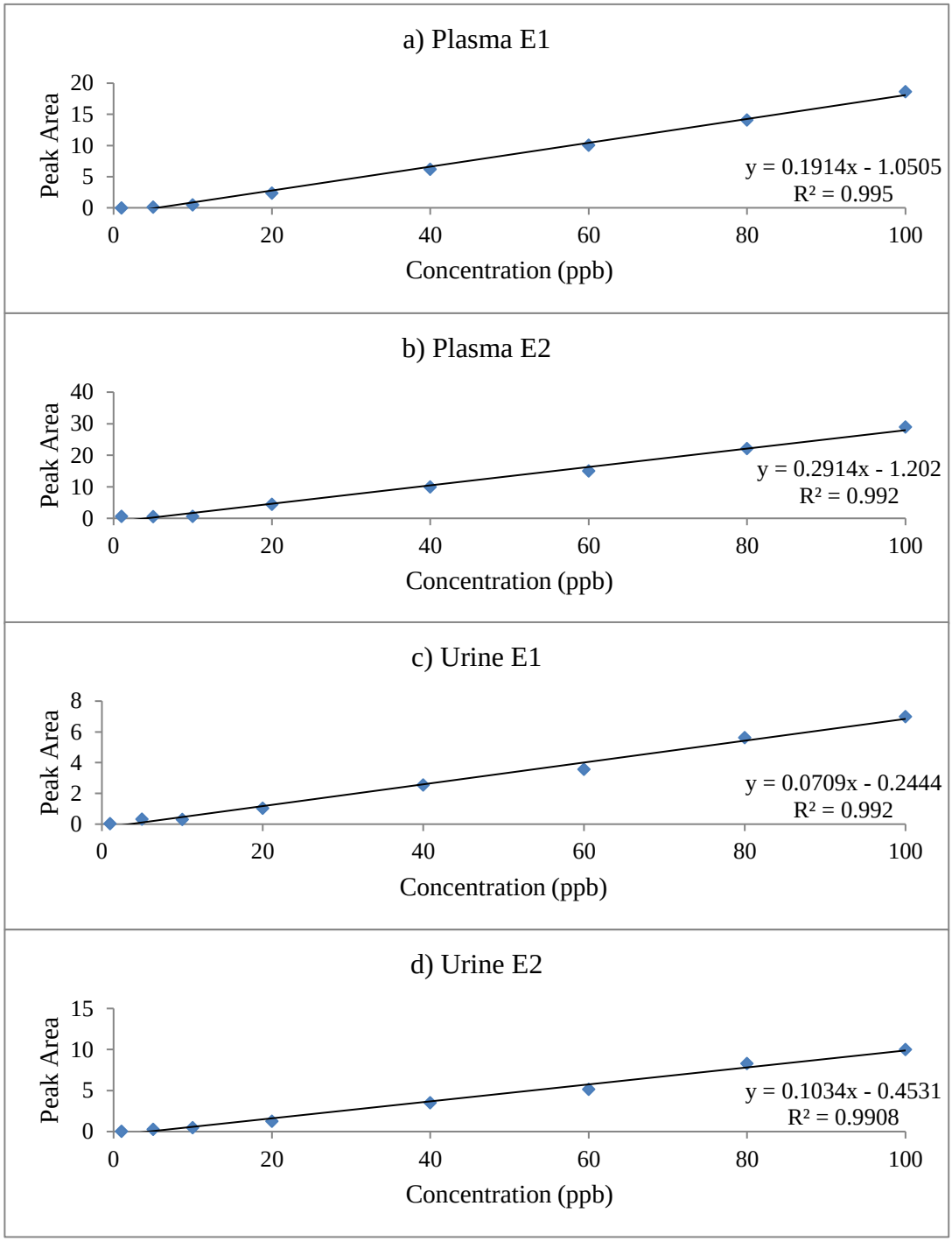

Figure 117: Calibration curves of Butylone enantiomers in plasma and urine

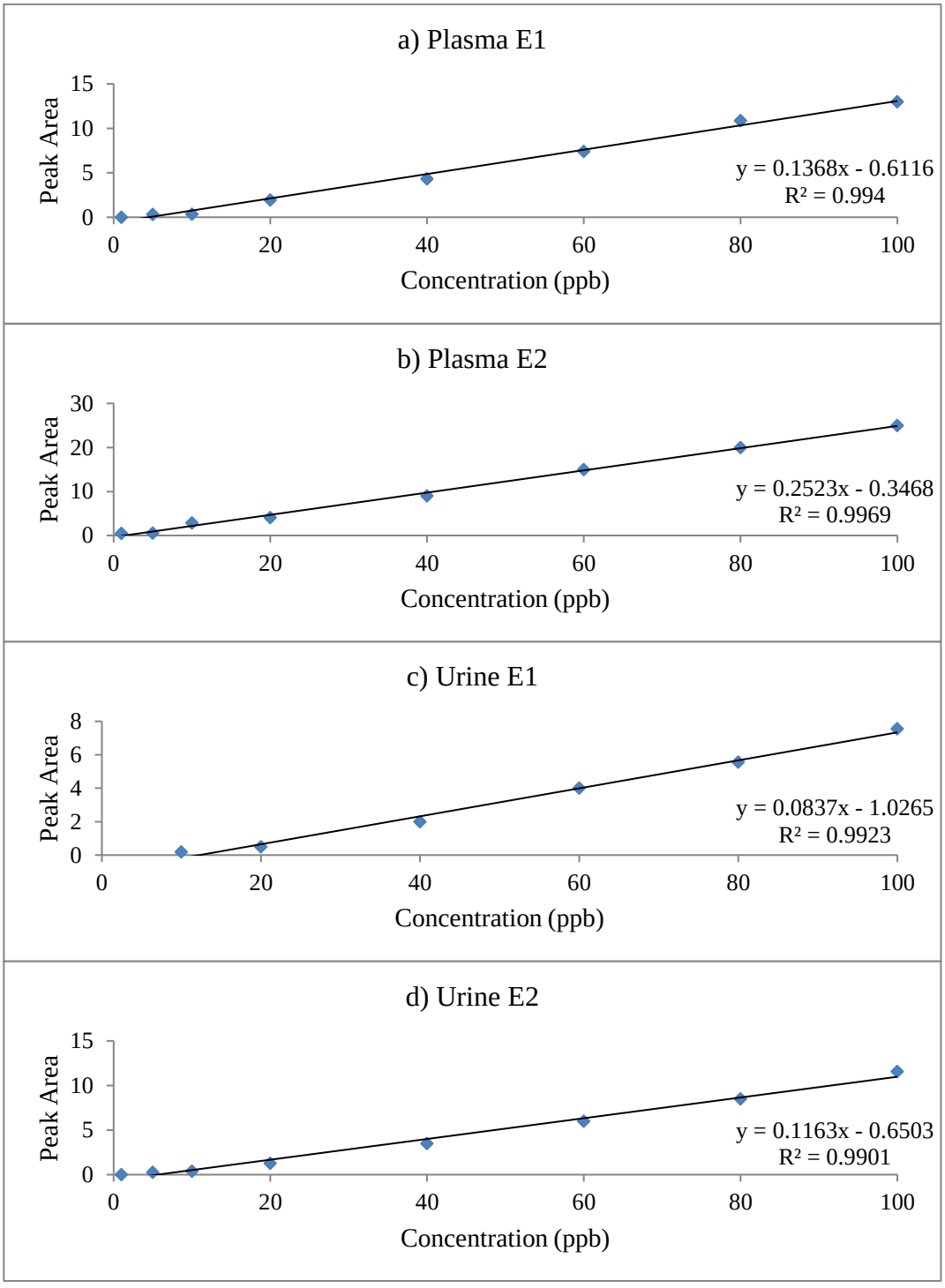

Figure 118: Calibration curves of Pentylone enantiomers in plasma and urine

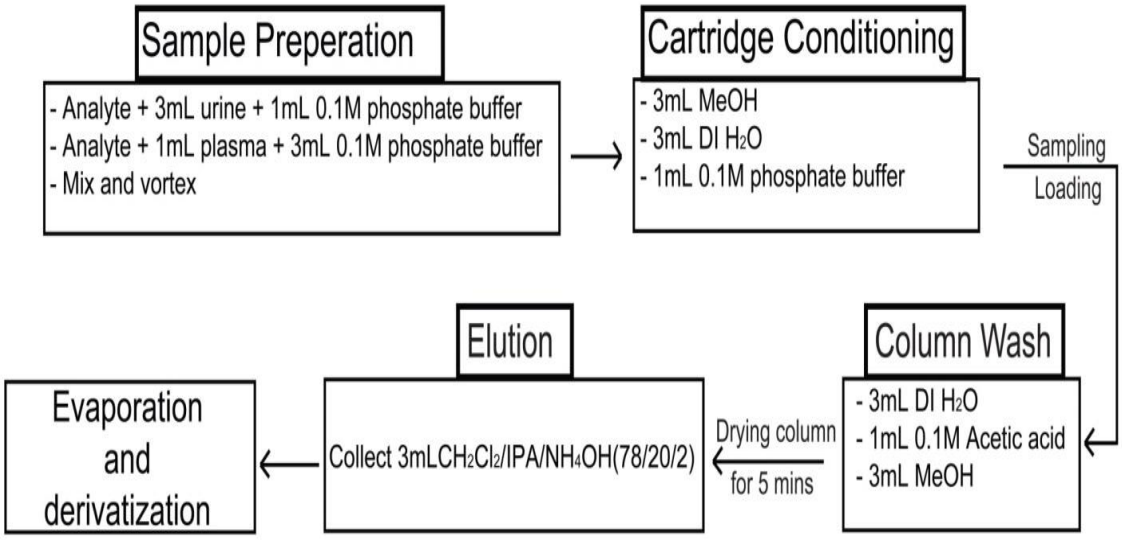

Scheme 20: Solid phase extraction (SPE) of spiked urine and plasma samples

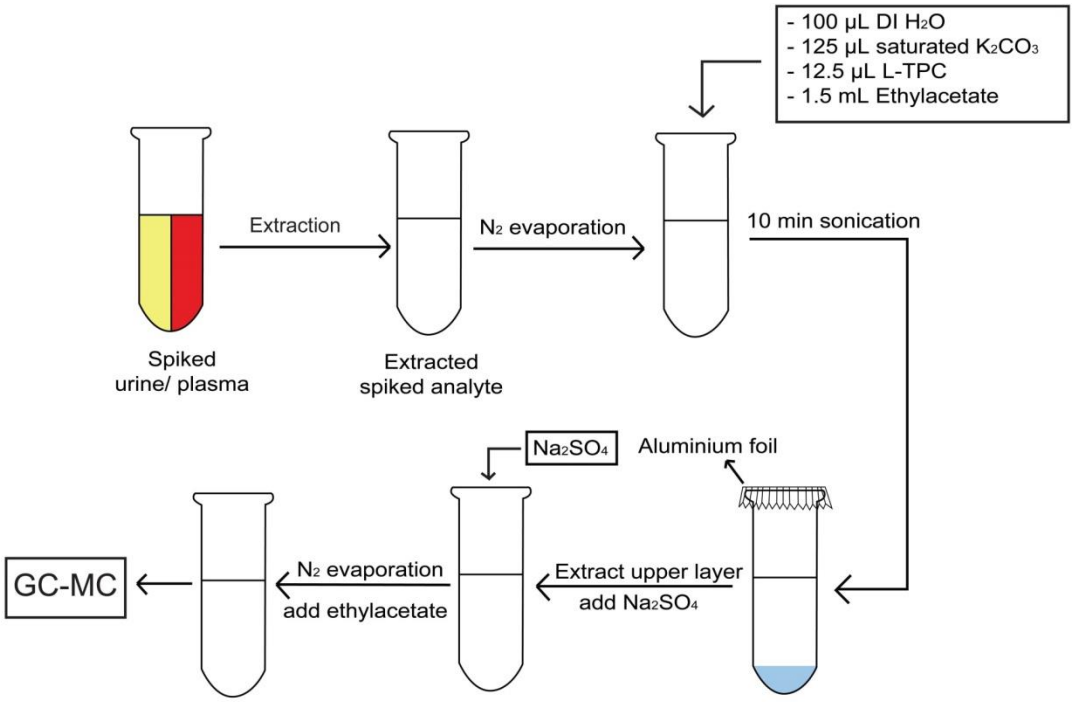

Scheme 21: Derivatization step of synthetic cathinones by L-TPC

Appendix C: Liquid chromatogram of 65 synthetic cathinones analyzed by HPLC-DAD using cellulose/amylose column (chapter 4)

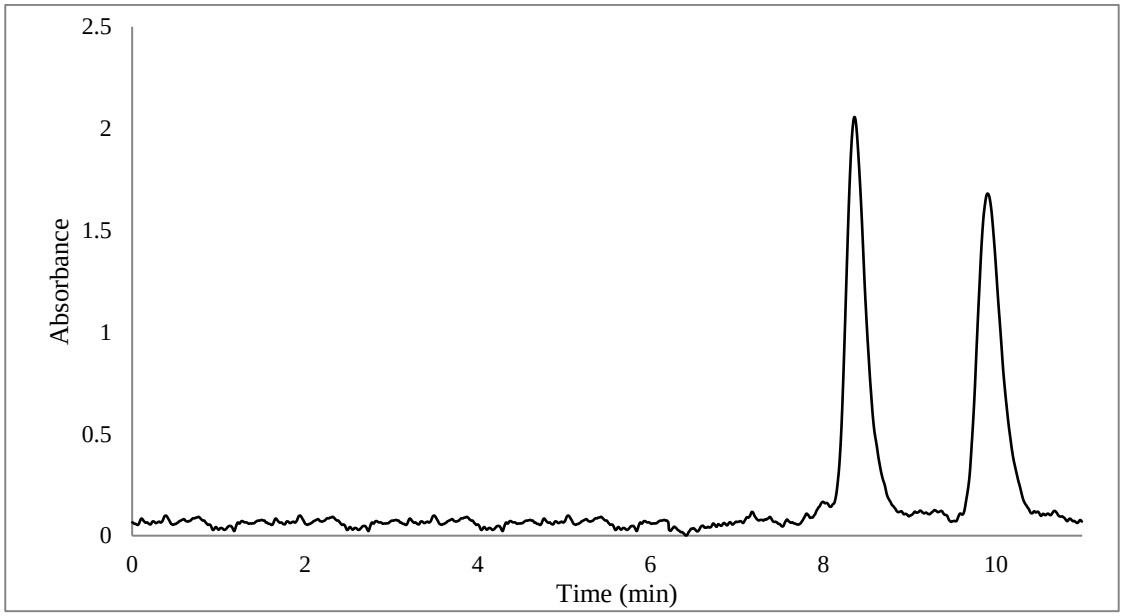

Figure 119: Liquid chromatogram for separation of the R and S enantiomers of 50 ppm of 2,3-Methylenedioxymethcathinone (2,3-MDMC) drug using AS-H Amylose column, λ_{max}. 254 nm

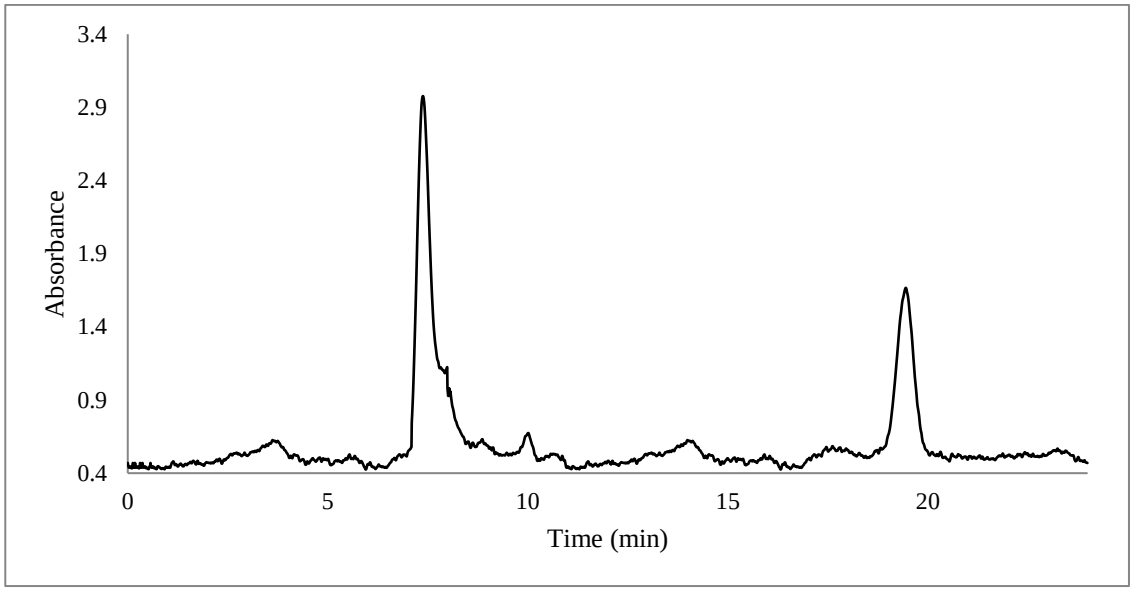

Figure 120: Liquid chromatogram for separation of the R and S enantiomers of 50 ppm of 2,3-Methylenedioxymethcathinone (2,3-MDMC) drug using DMP cellulose column, λ_{max}. 254 nm

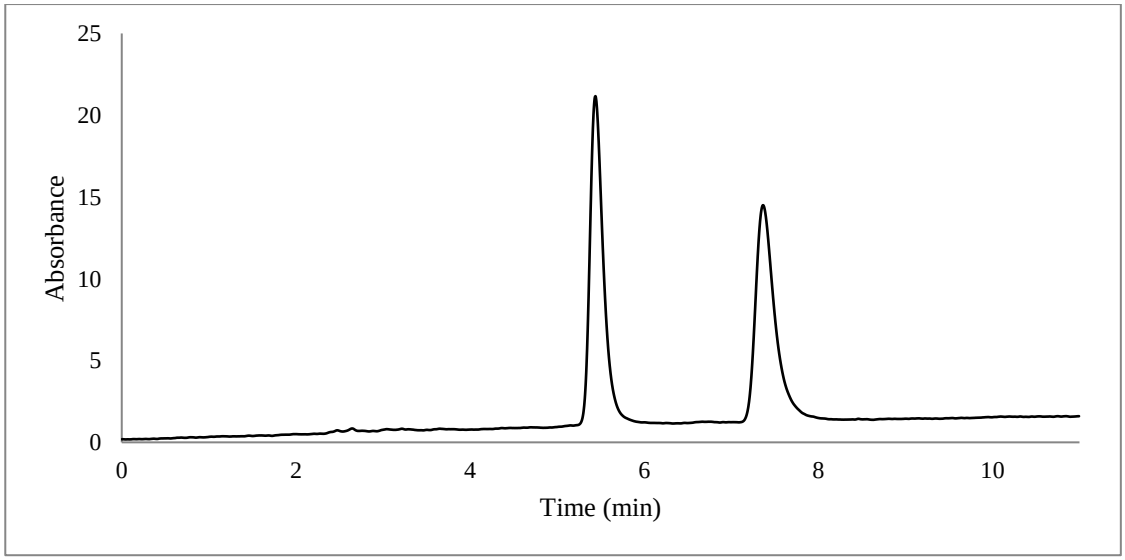

Figure 121: Liquid chromatogram for separation of the R and S enantiomers of 50 ppm of 2,3-Pentylone drug using AS-H Amylose column, λ_{max}. 300 nm

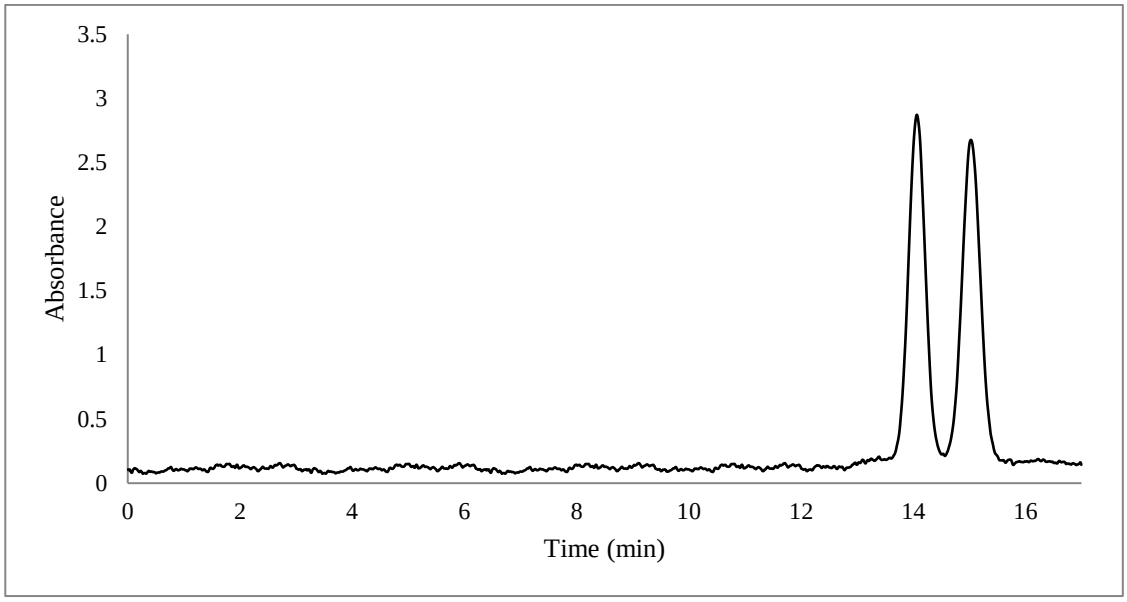

Figure 122: Liquid chromatogram for separation of the R and S enantiomers of 50 ppm of 2,3-Pentylone drug using DMP cellulose column, λ_{max}. 300 nm

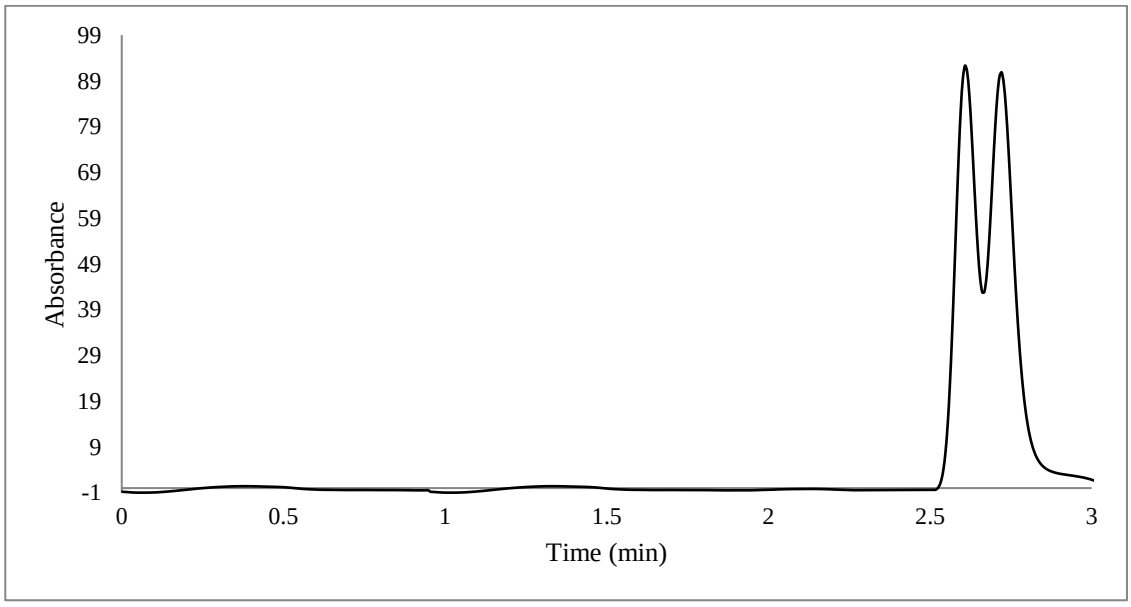

Figure 123: Liquid chromatogram for separation of the R and S enantiomers of 50 ppm of 2,4-Dimethylethcathinone (2,4-DMEC) drug using AS-H Amylose column, λ_{max}. 254 nm

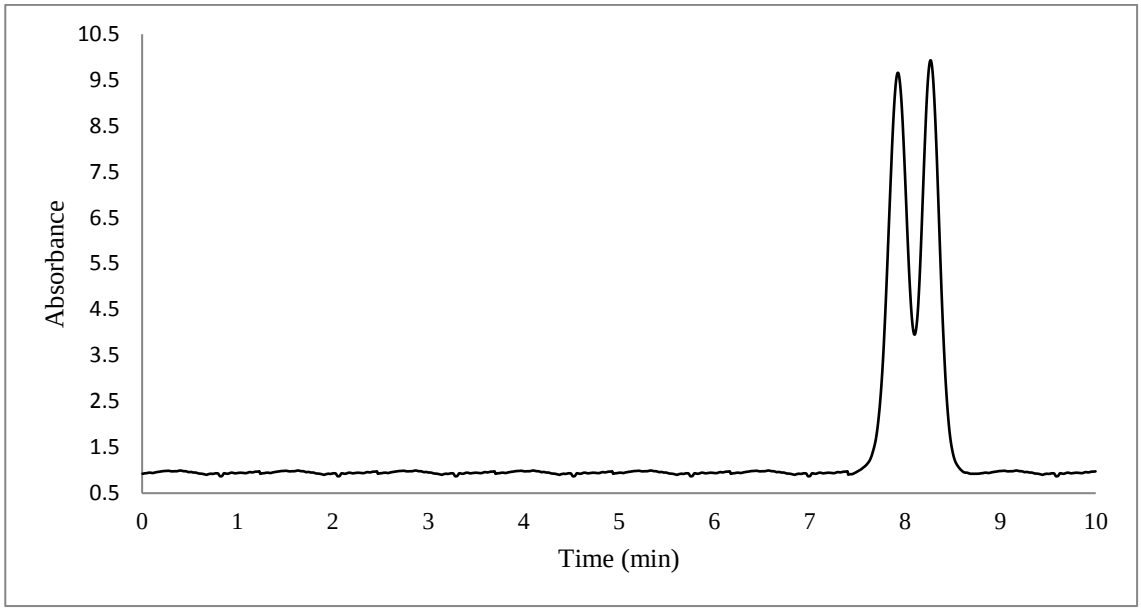

Figure 124: Liquid chromatogram for separation of the R and S enantiomers of 50 ppm of 2,4-Dimethylethcathinone (2,4-DMEC) drug using DMP cellulose column, λ_{max}. 254 nm

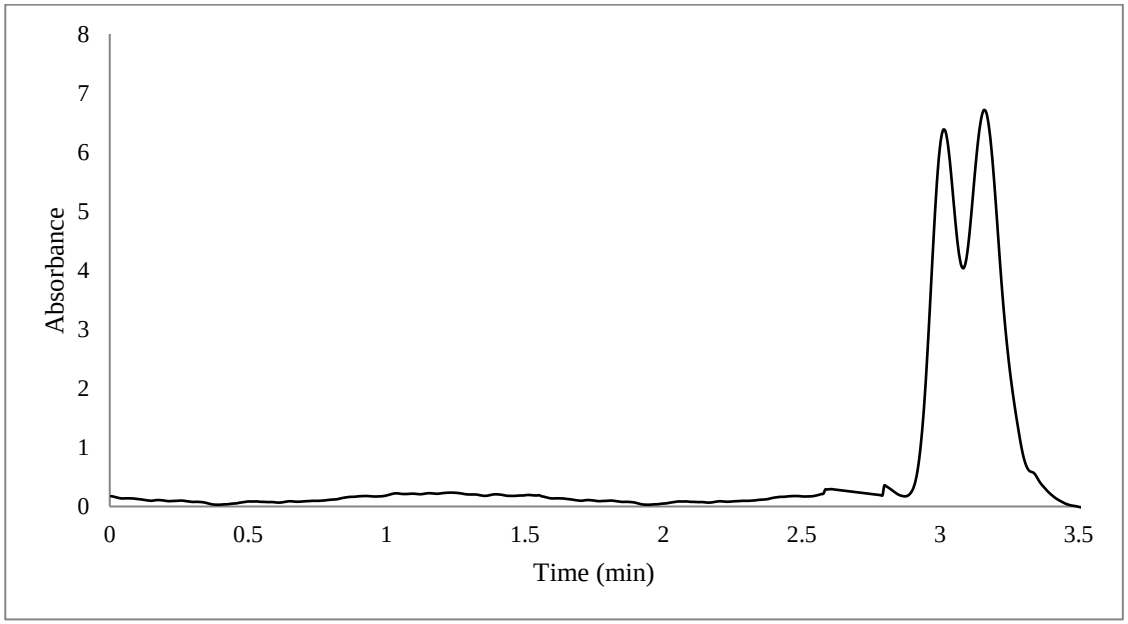

Figure 125: Liquid chromatogram for separation of the R and S enantiomers of 50 ppm of 2-Ethylethcathinone (2-EEC) drug using AS-H Amylose column, λ_{max}. 270 nm

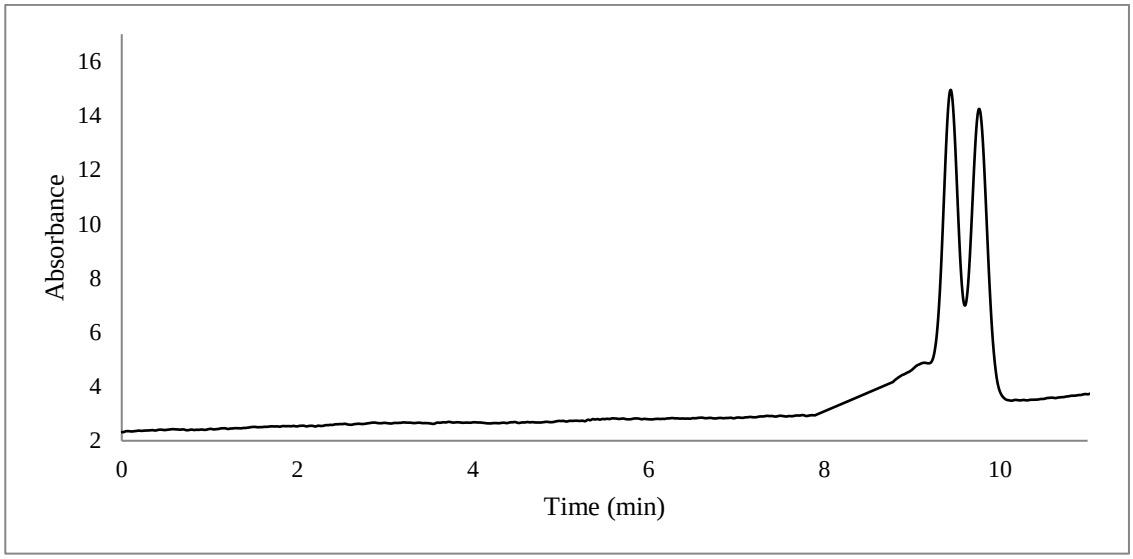

Figure 126: Liquid chromatogram for separation of the R and S enantiomers of 50 ppm of 2-Ethylethcathinone (2-EEC) drug using DMP cellulose column, λ_{max}. 270 nm

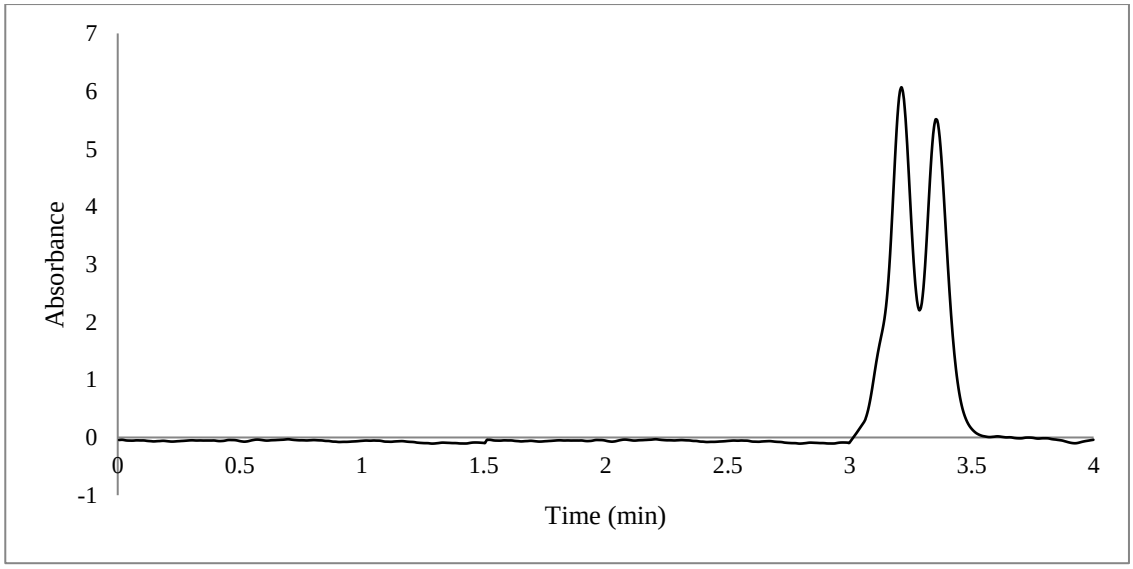

Figure 127: Liquid chromatogram for separation of the R and S enantiomers of 50 ppm of 2-Ethylmethcathinone (2-EMC) drug using AS-H Amylose column, λ_{max}. 270 nm

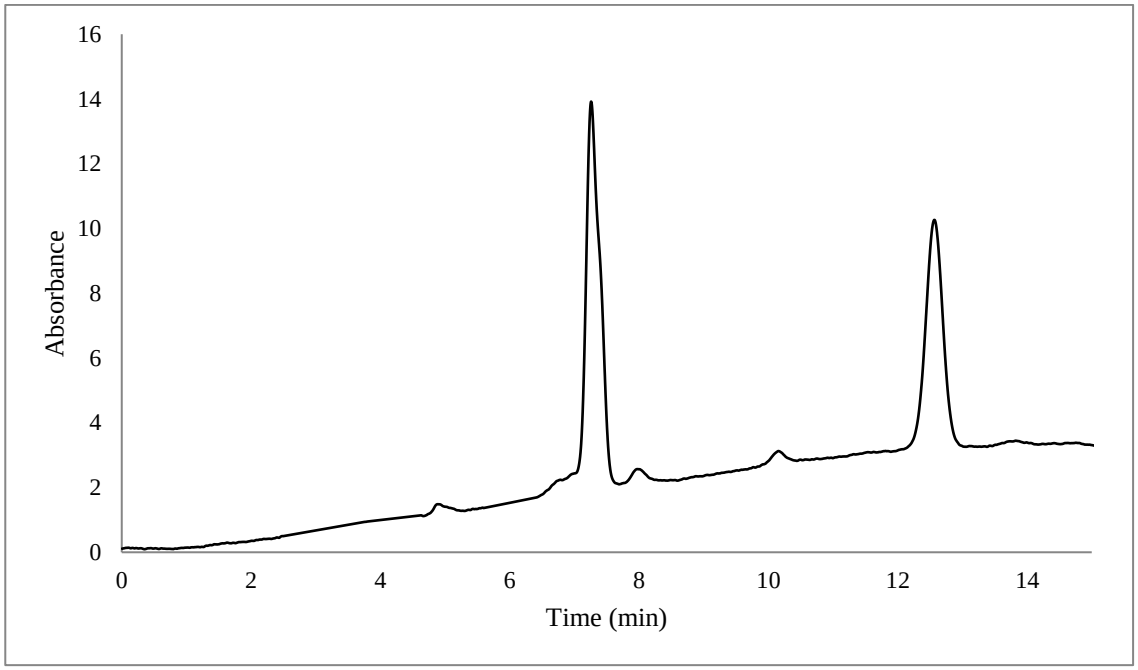

Figure 128: Liquid chromatogram for separation of the R and S enantiomers of 50 ppm of 2-Ethylmethcathinone (2-EMC) drug using DMP cellulose column, λ_{max}. 270 nm

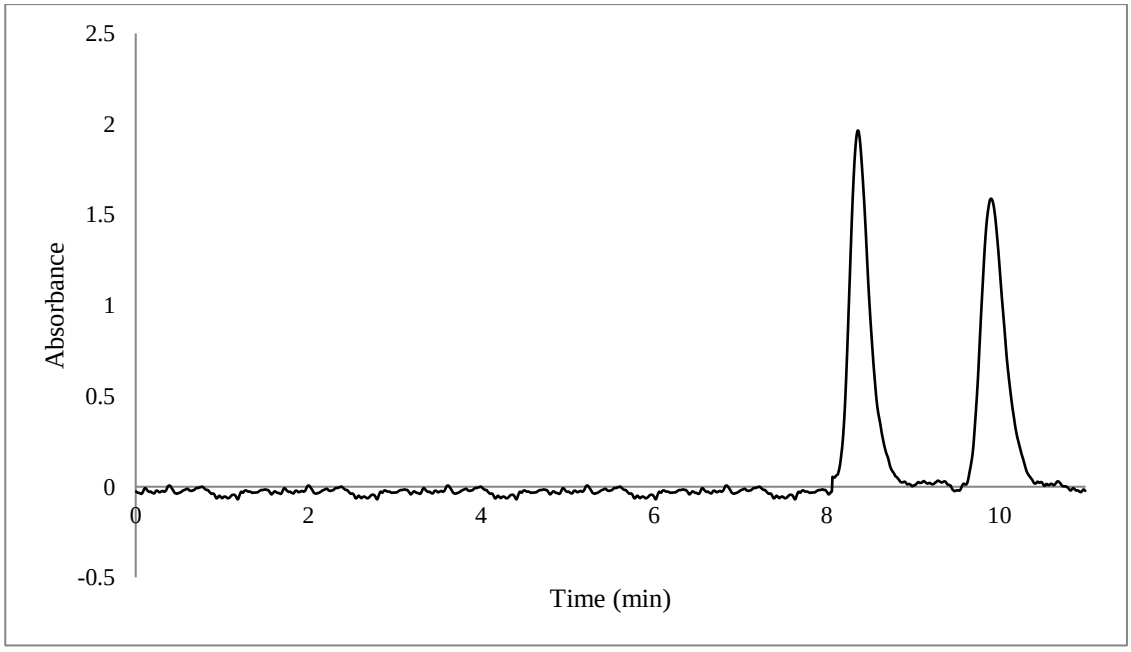

Figure 129: Liquid chromatogram for separation of the R and S enantiomers of 50 ppm of 2-Methoxymethcathinone drug using AS-H Amylose column, λ_{max}. 254 nm

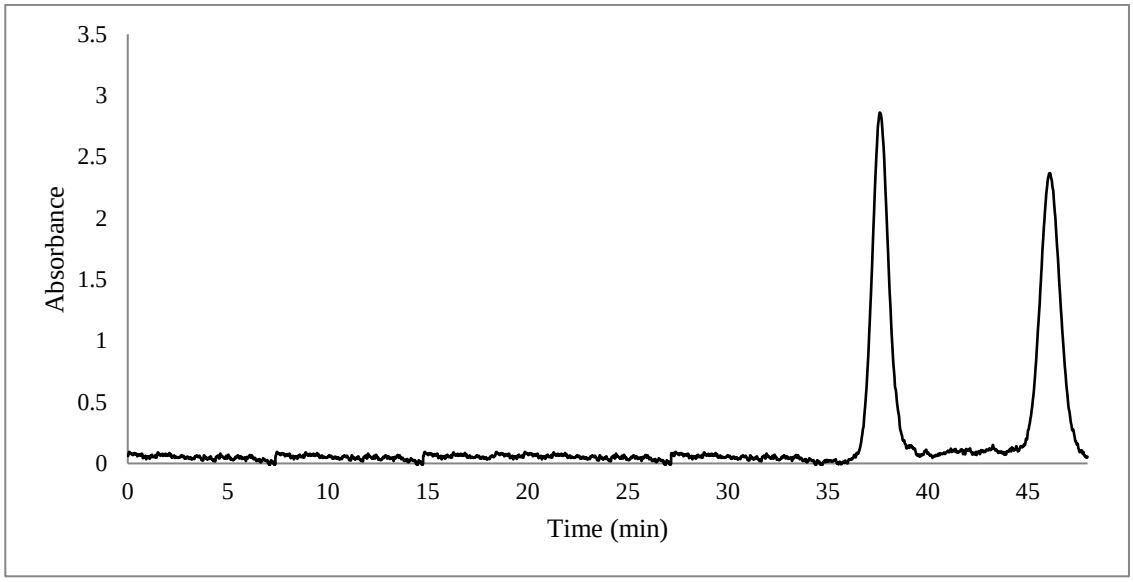

Figure 130: Liquid chromatogram for separation of the R and S enantiomers of 50 ppm of 2-Methoxymethcathinone drug using DMP cellulose column, λ_{max}. 270 nm

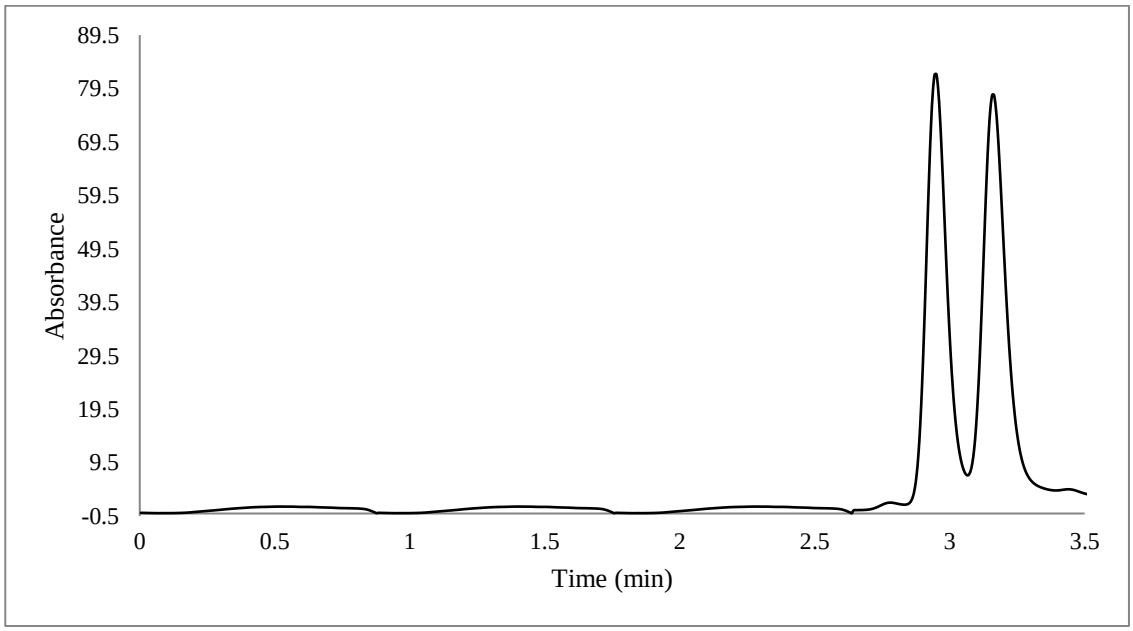

Figure 131: Liquid chromatogram for separation of the R and S enantiomers of 50 ppm of 2-Methylethcathinone (2-MEC) drug using AS-H Amylose column, λ_{max}. 254 nm

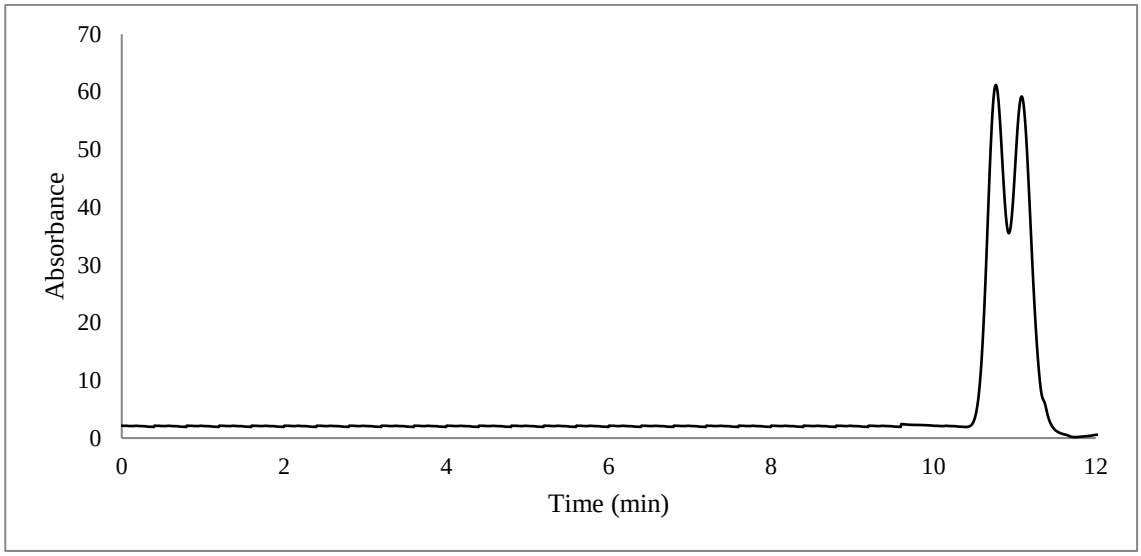

Figure 132: Liquid chromatogram for separation of the R and S enantiomers of 50 ppm of 2-Methylethcathinone (2-MEC) drug using DMP cellulose column, λ_{max}. 254 nm

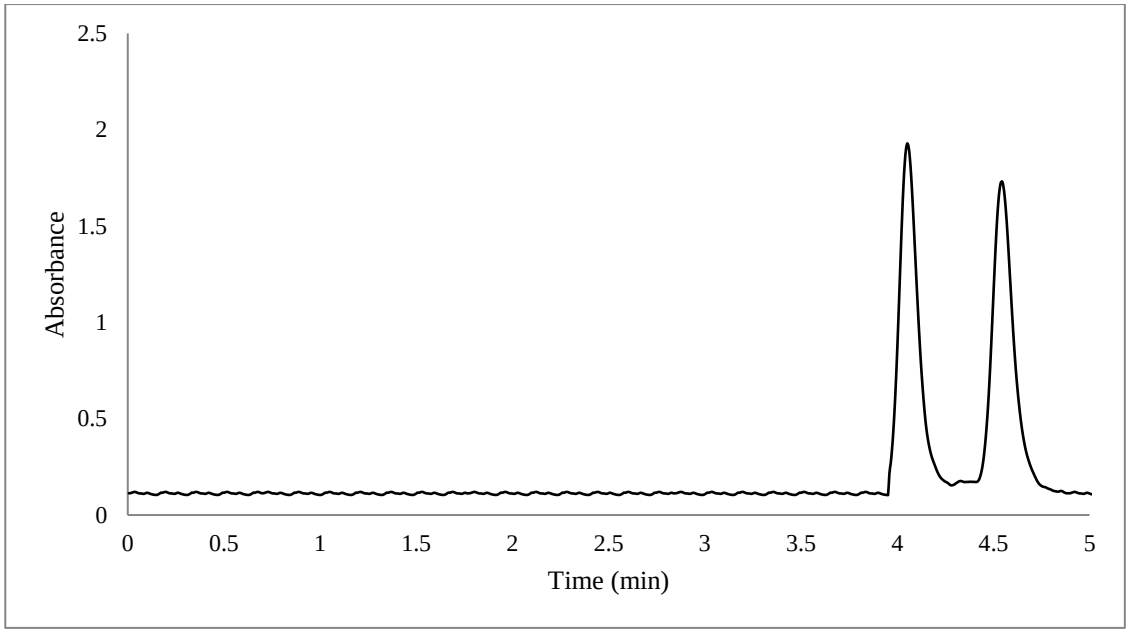

Figure 133: Liquid chromatogram for separation of the R and S enantiomers of 50 ppm of 2-Methylmethcathinone (2-MMC) drug using AS-H Amylose column, λ_{max}. 254 nm

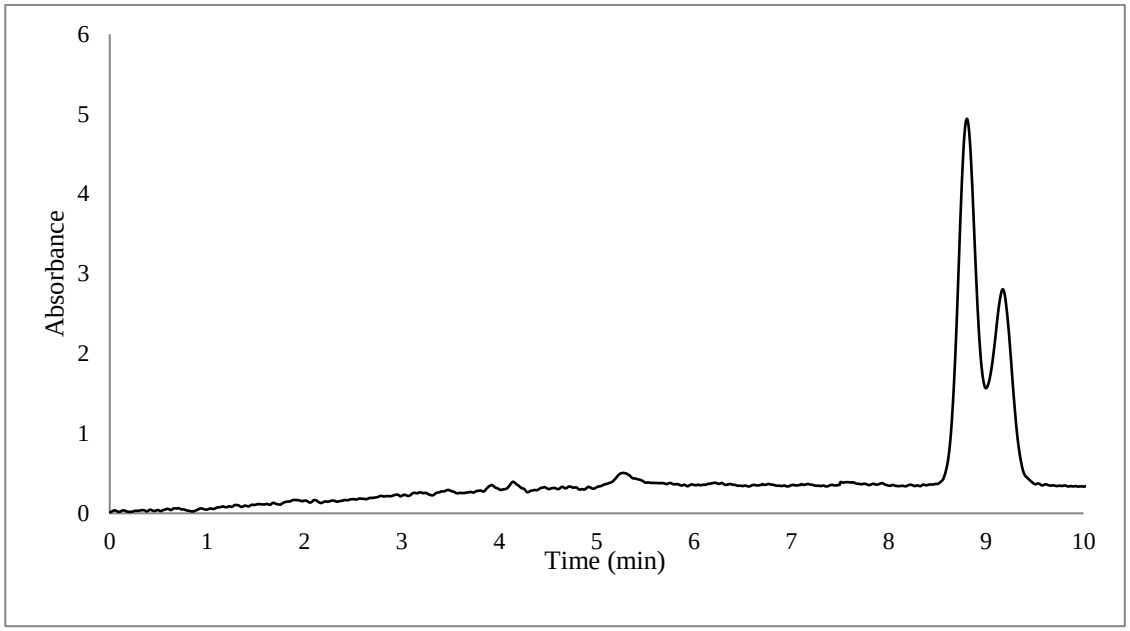

Figure 134: Liquid chromatogram for separation of the R and S enantiomers of 50 ppm of 2-Methylmethcathinone (2-MMC) drug using DMP cellulose column, λ_{max}. 254 nm

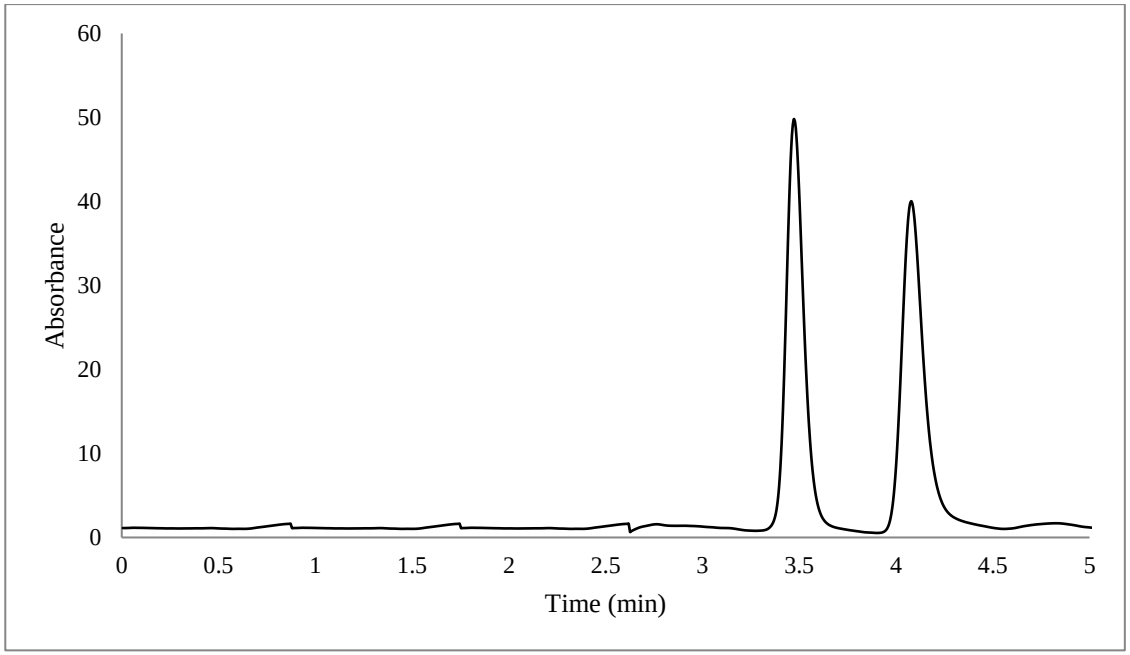

Figure 135: Liquid chromatogram for separation of the R and S enantiomers of 50 ppm of 3,4-Dimethylethcathinone (3,4-DMEC) drug using AS-H Amylose column, λ_{max}. 254 nm

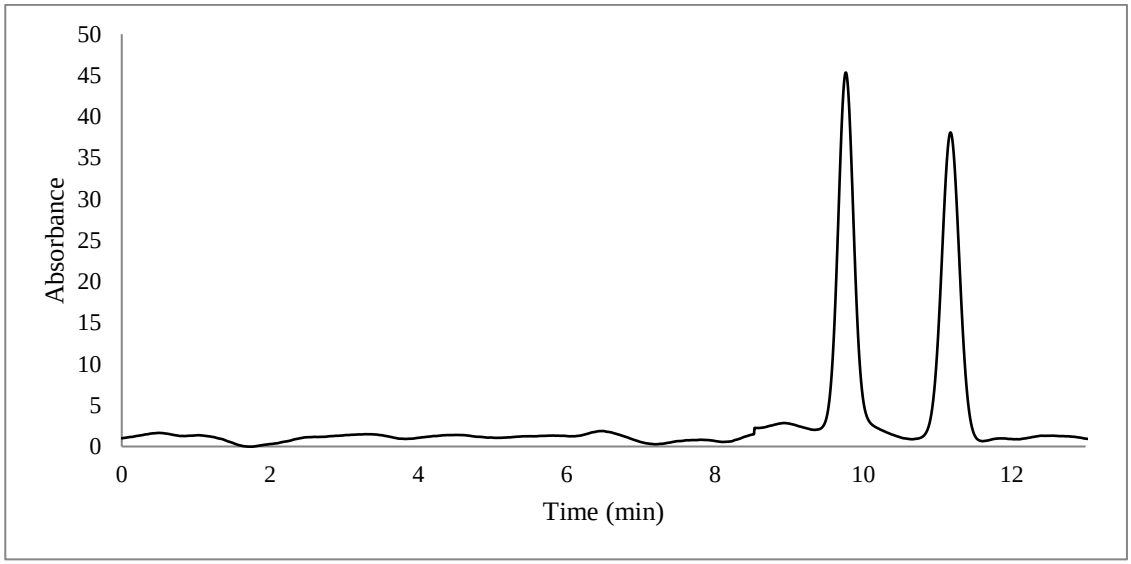

Figure 136: Liquid chromatogram for separation of the R and S enantiomers of 50 ppm of 3,4-Dimethylethcathinone (3,4-DMEC) drug using DMP cellulose column, λ_{max}. 254 nm

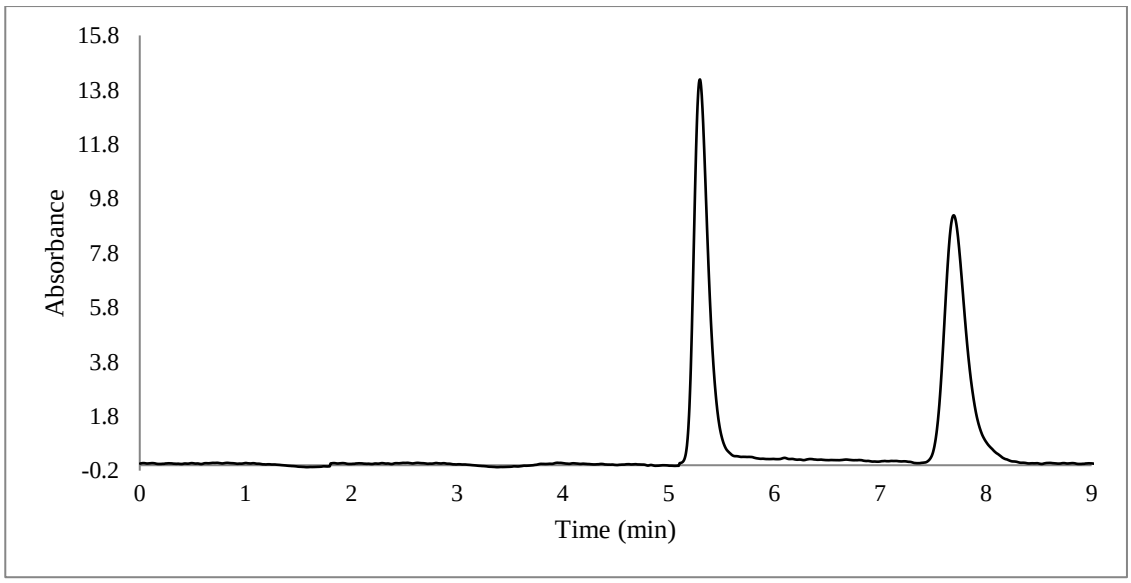

Figure 137: Liquid chromatogram for separation of the R and S enantiomers of 50 ppm of 3,4-Dimethylmethcathinone (3,4-DMMC) drug using AS-H Amylose column, λ_{max}. 270 nm

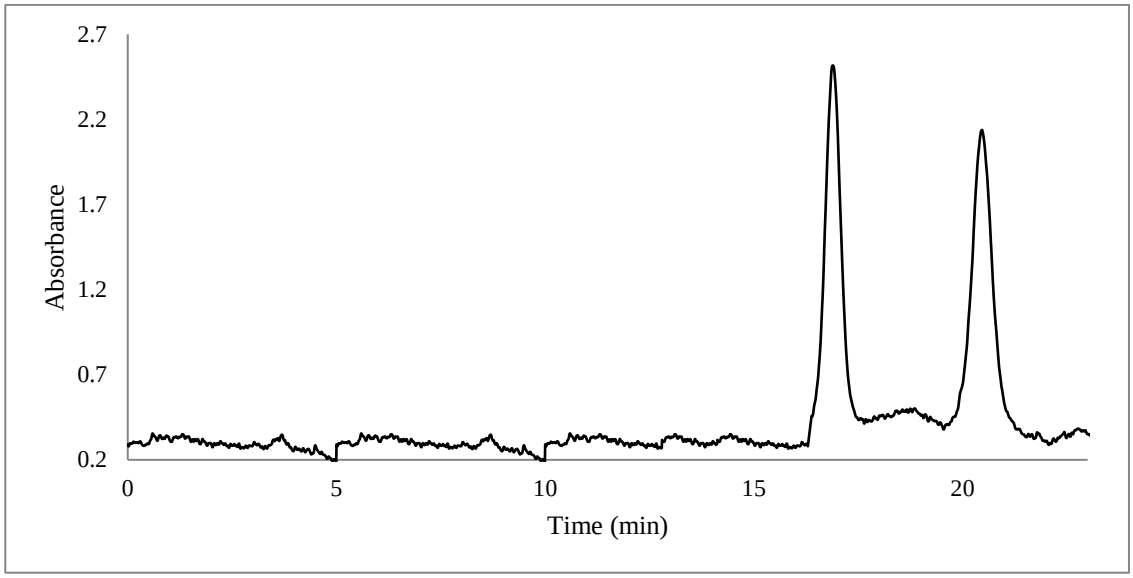

Figure 138: Liquid chromatogram for separation of the R and S enantiomers of 50 ppm of 3,4-Dimethylmethcathinone (3,4-DMMC) drug using DMP cellulose column, λ_{max}. 270 nm

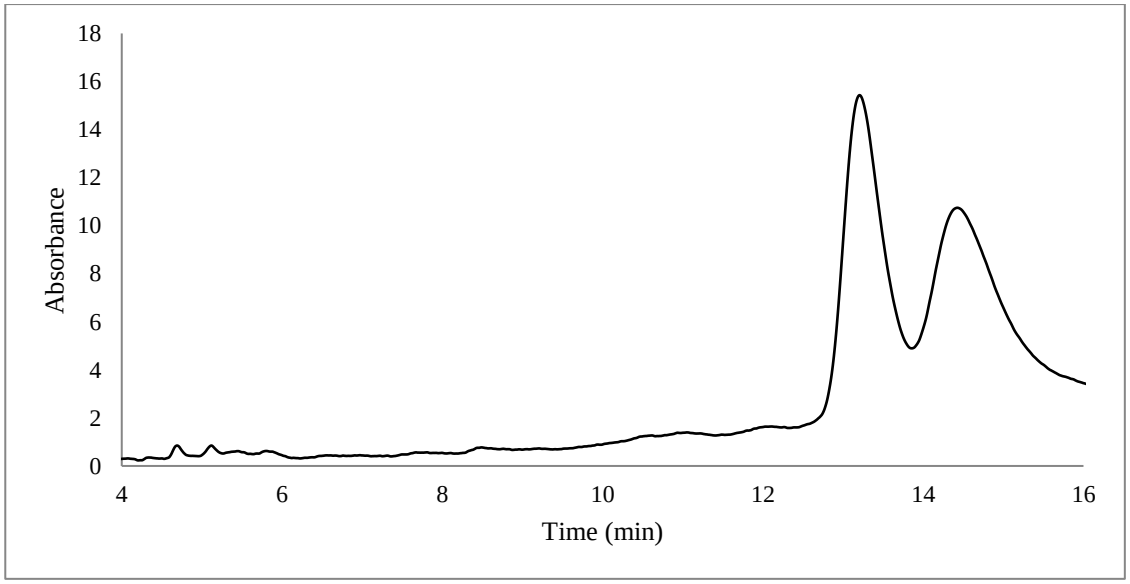

Figure 139: Liquid chromatogram for separation of the R and S enantiomers of 50 ppm of 3,4-Methylenedioxy-N-benzylcathinone drug using AS-H Amylose column, λ_{max}. 270 nm

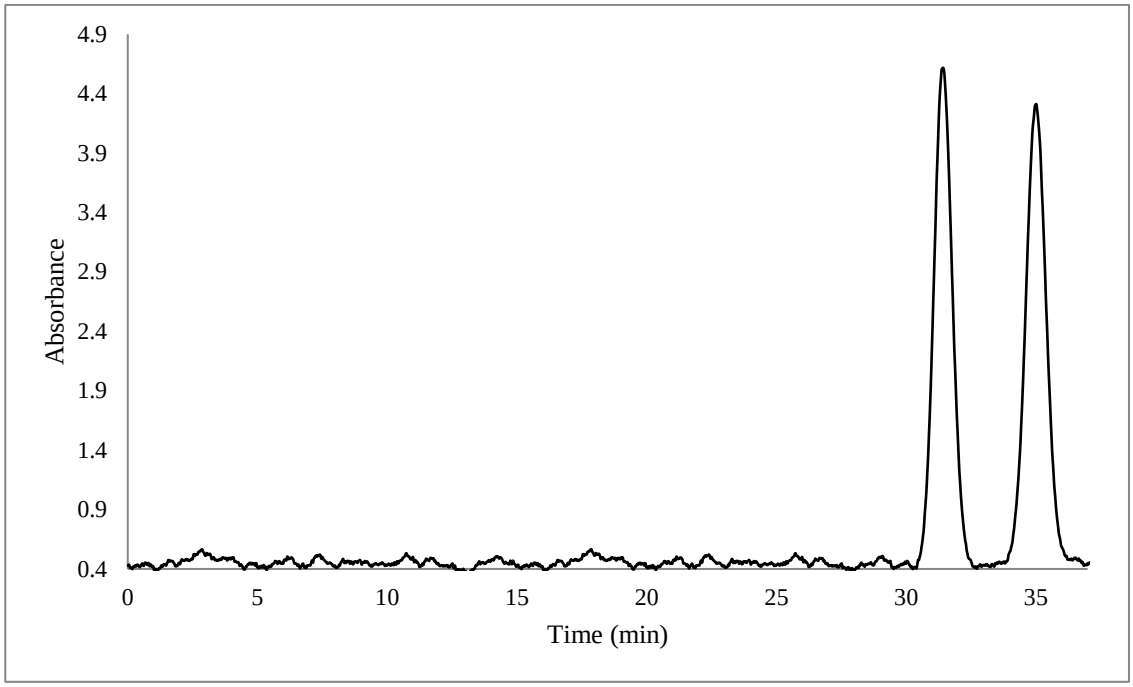

Figure 140: Liquid chromatogram for separation of the R and S enantiomers of 50 ppm of 3,4-Methylenedioxy-N-benzylcathinone drug using DMP cellulose column, λ_{max}. 270 nm

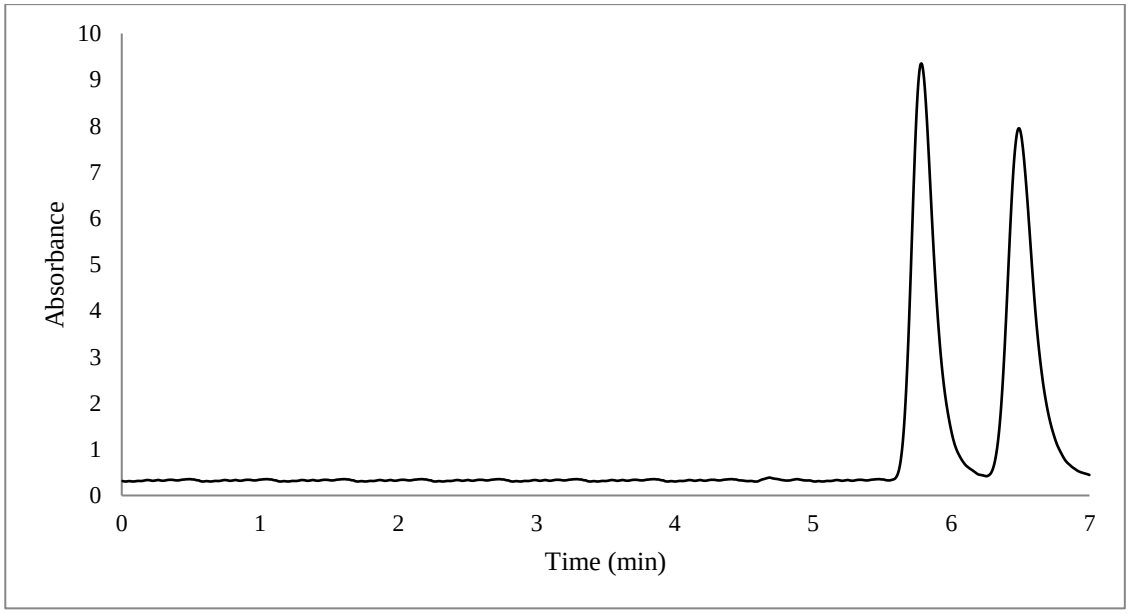

Figure 141: Liquid chromatogram for separation of the R and S enantiomers of 50 ppm of 3,4-Methylenedioxy-N-ethylcathinone drug using AS-H Amylose column, λ_{max}. 270 nm

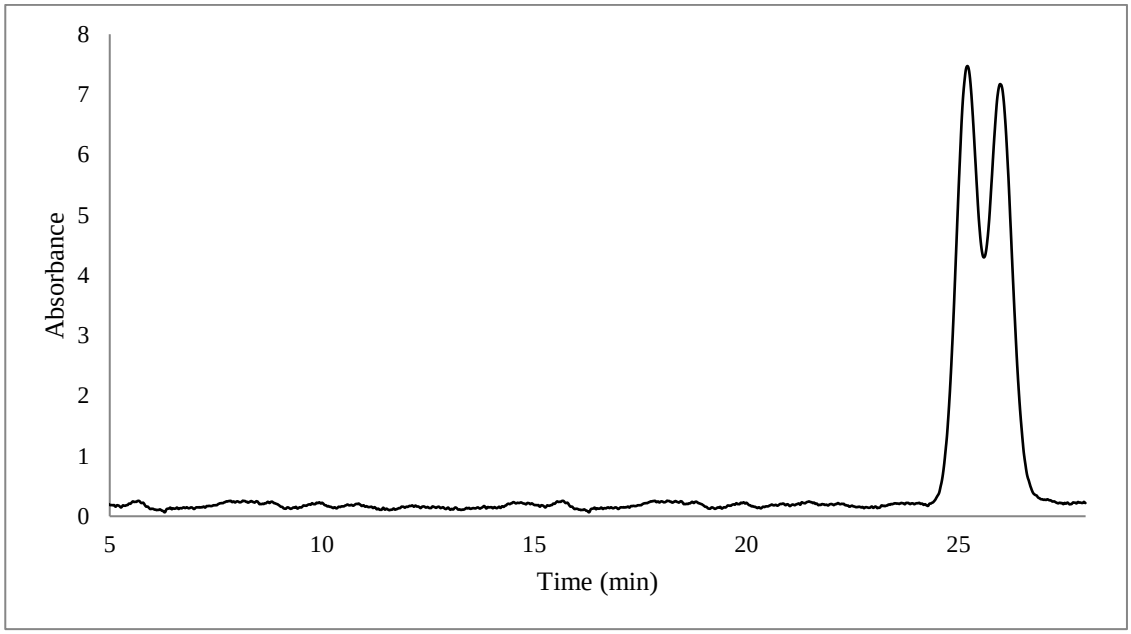

Figure 142: Liquid chromatogram for separation of the R and S enantiomers of 50 ppm of 3,4-Methylenedioxy-N-ethylcathinone drug using DMP cellulose column, λ_{max}. 270 nm

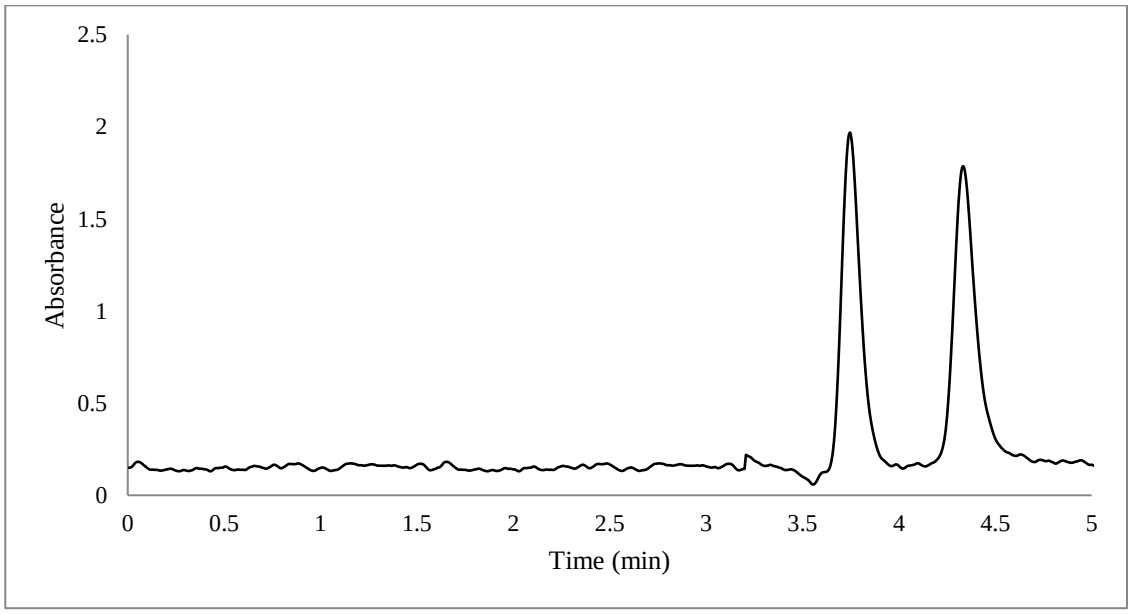

Figure 143: Liquid chromatogram for separation of the R and S enantiomers of 50 ppm of 3-Bromomethcathinone (3-BMC) drug using AS-H Amylose column, λ_{max}. 300 nm

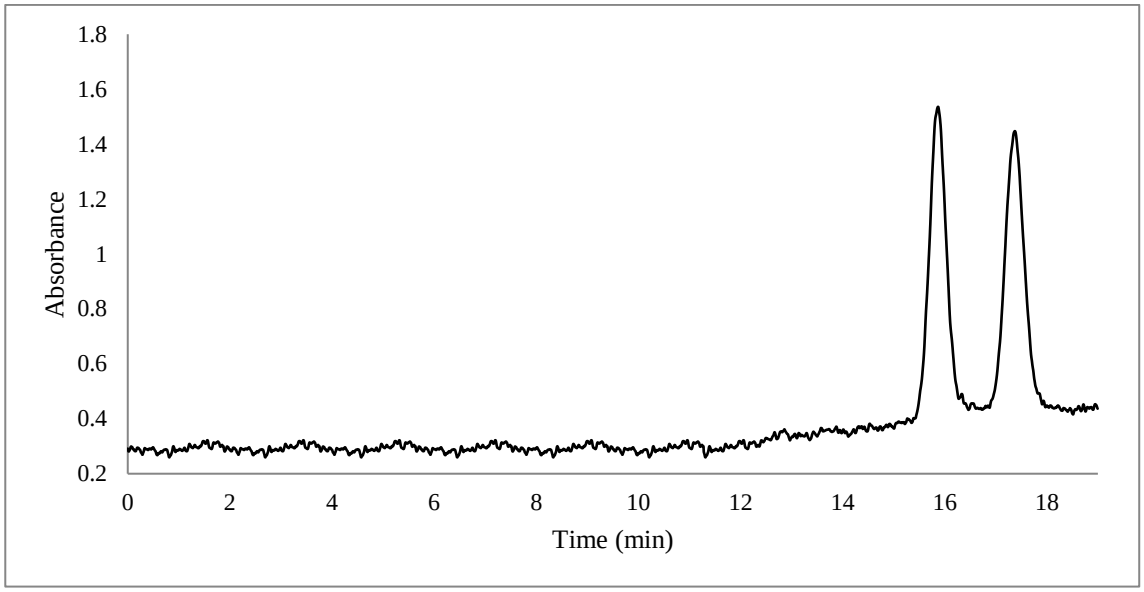

Figure 144: Liquid chromatogram for separation of the R and S enantiomers of 50 ppm of 3-Bromomethcathinone (3-BMC) drug using DMP cellulose column, λ_{max}. 300 nm

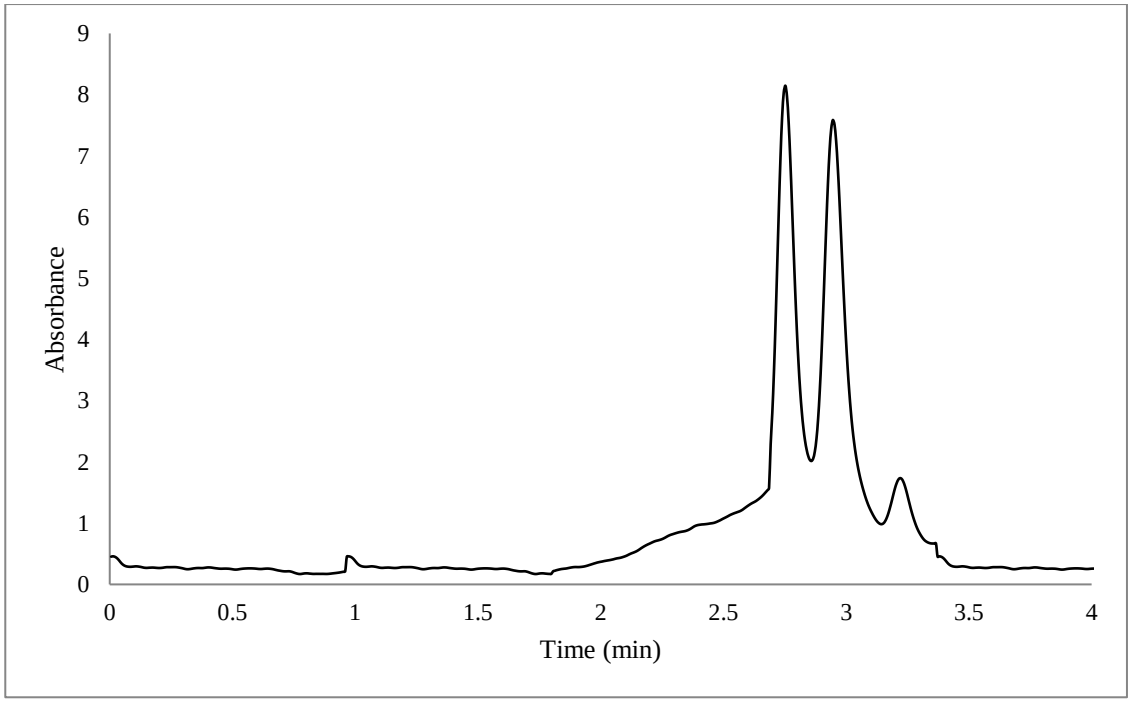

Figure 145: Liquid chromatogram for separation of the R and S enantiomers of 50 ppm of 3-Ethylethcathinone (3-EEC) drug using AS-H Amylose column, λ_{max}. 270 nm

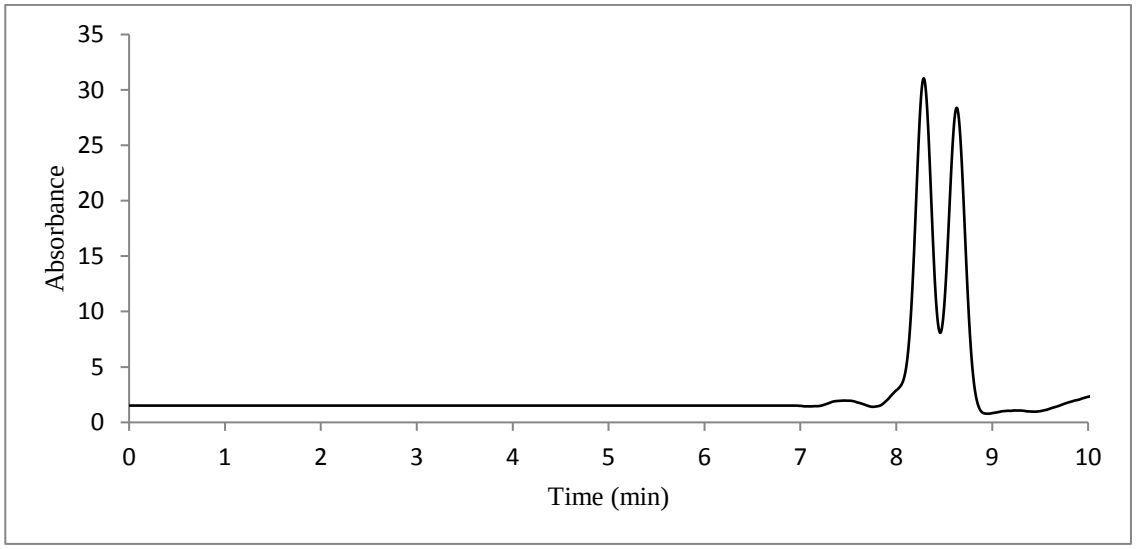

Figure 146: Liquid chromatogram for separation of the R and S enantiomers of 50 ppm of 3-Ethylethcathinone (3-EEC) drug using DMP cellulose column, λ_{max}. 300 nm

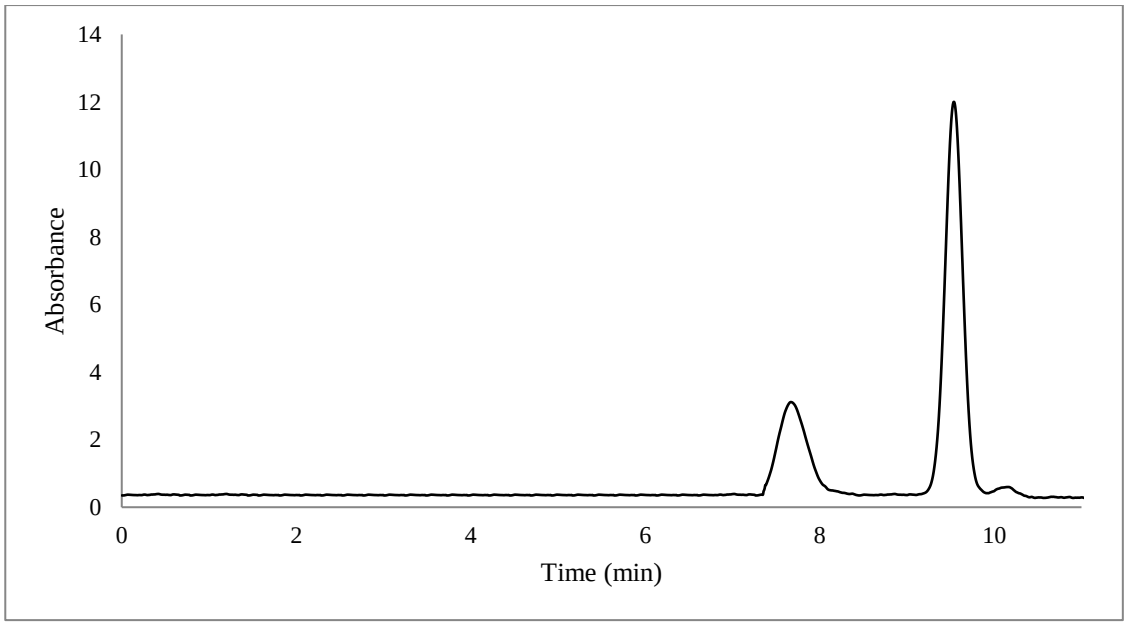

Figure 147: Liquid chromatogram for separation of the R and S enantiomers of 50 ppm of 3-Fluoroethcathinone (3-FEC) drug using DMP cellulose column, λ_{max}. 270 nm

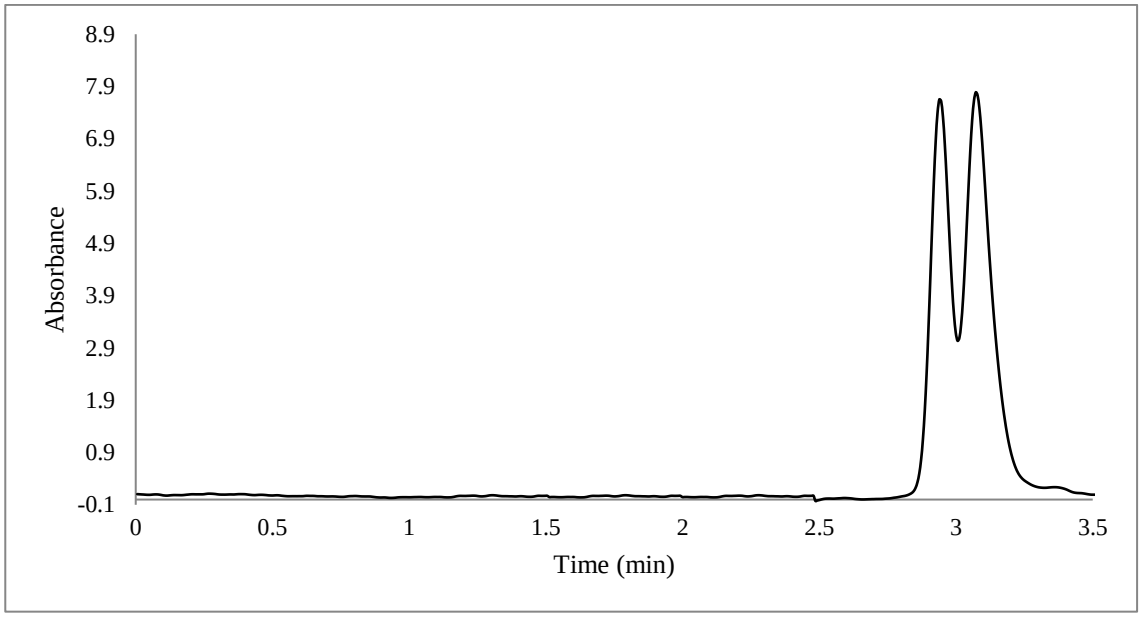

Figure 148: Liquid chromatogram for separation of the R and S enantiomers of 50 ppm of 3-Fluoroethcathinone (3-FEC) drug using AS-H Amylose column, λ_{max}. 270 nm

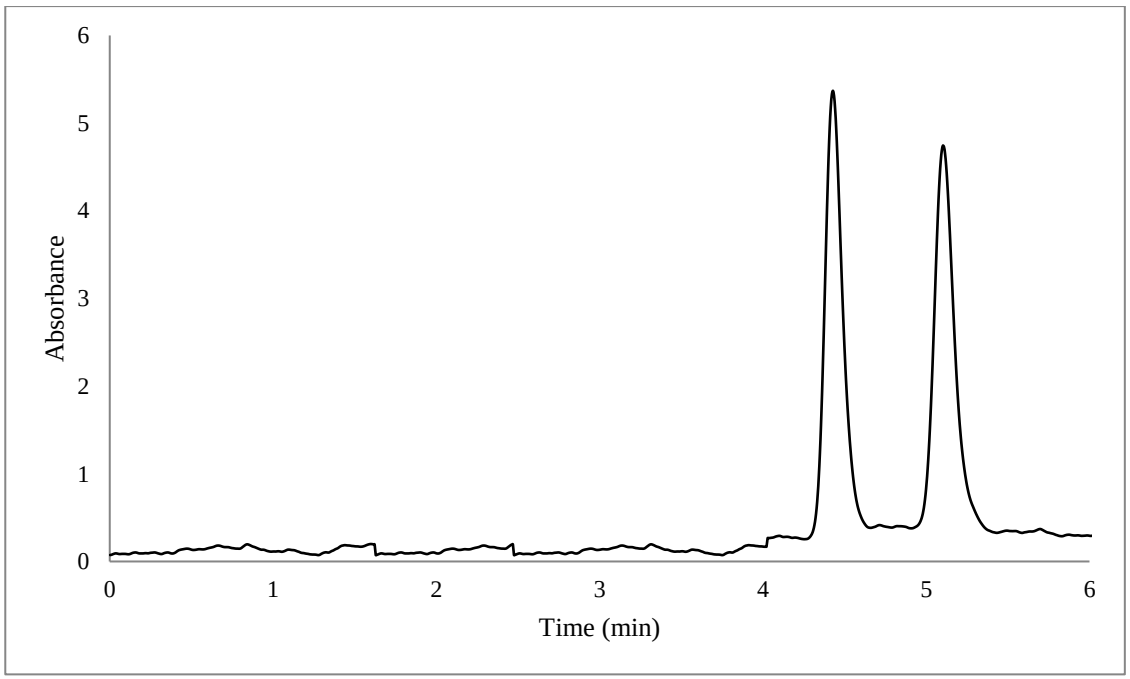

Figure 149: Liquid chromatogram for separation of the R and S enantiomers of 50 ppm of 3-Fluoromethcathinone (3-FMC) drug using AS-H Amylose column, λ_{max}. 270 nm

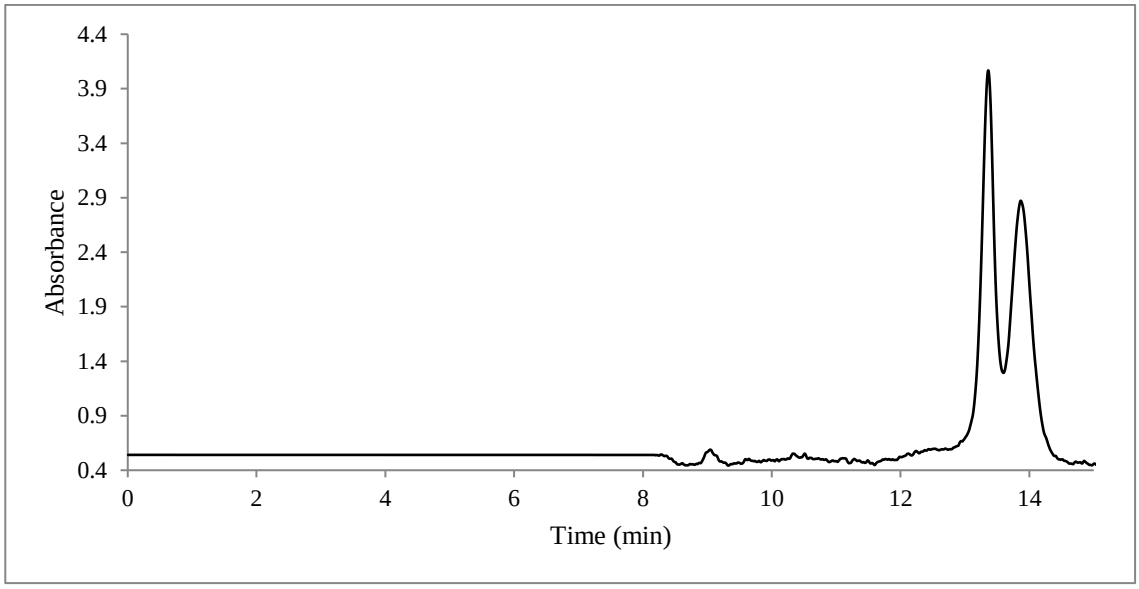

Figure 150: Liquid chromatogram for separation of the R and S enantiomers of 50 ppm of 3-Fluoromethcathinone (3-FMC) drug using DMP cellulose column, λ_{max}. 270 nm

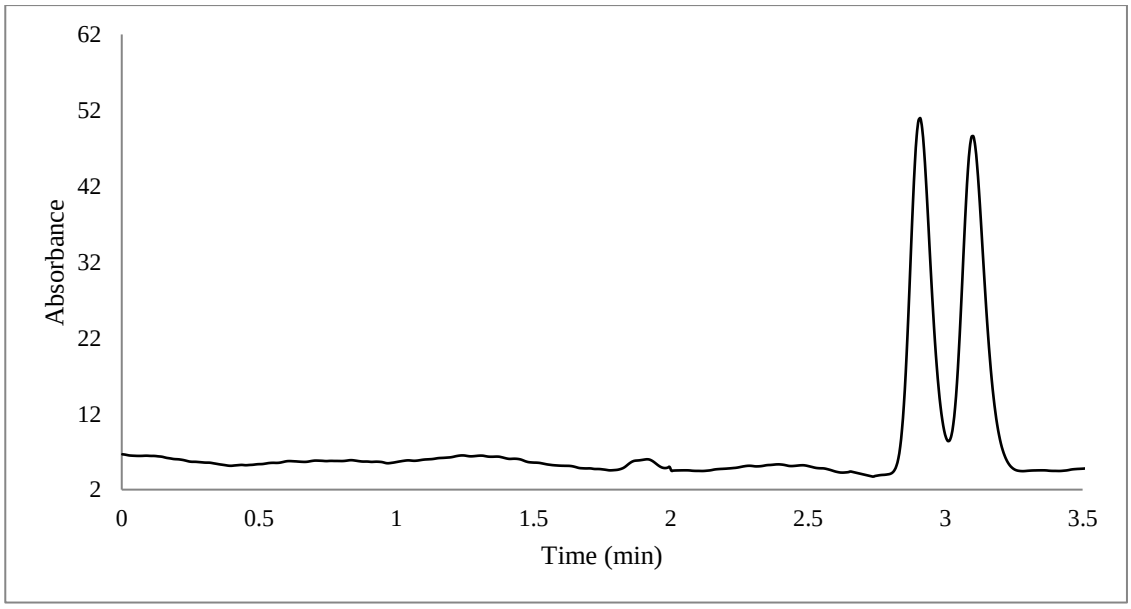

Figure 151: Liquid chromatogram for separation of the R and S enantiomers of 50 ppm of 3-Mehyethcathinone (3-MEC) drug using AS-H Amylose column, λ_{max}. 240 nm

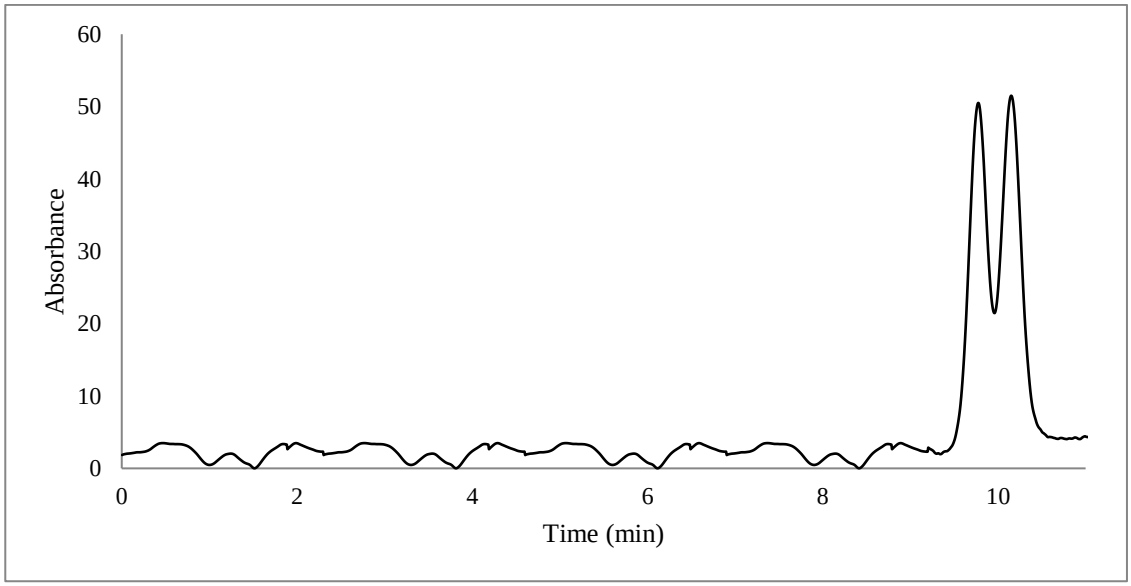

Figure 152: Liquid chromatogram for separation of the R and S enantiomers of 50 ppm of 3-Mehyethcathinone (3-MEC) drug using DMP cellulose column, λ_{max}. 240 nm

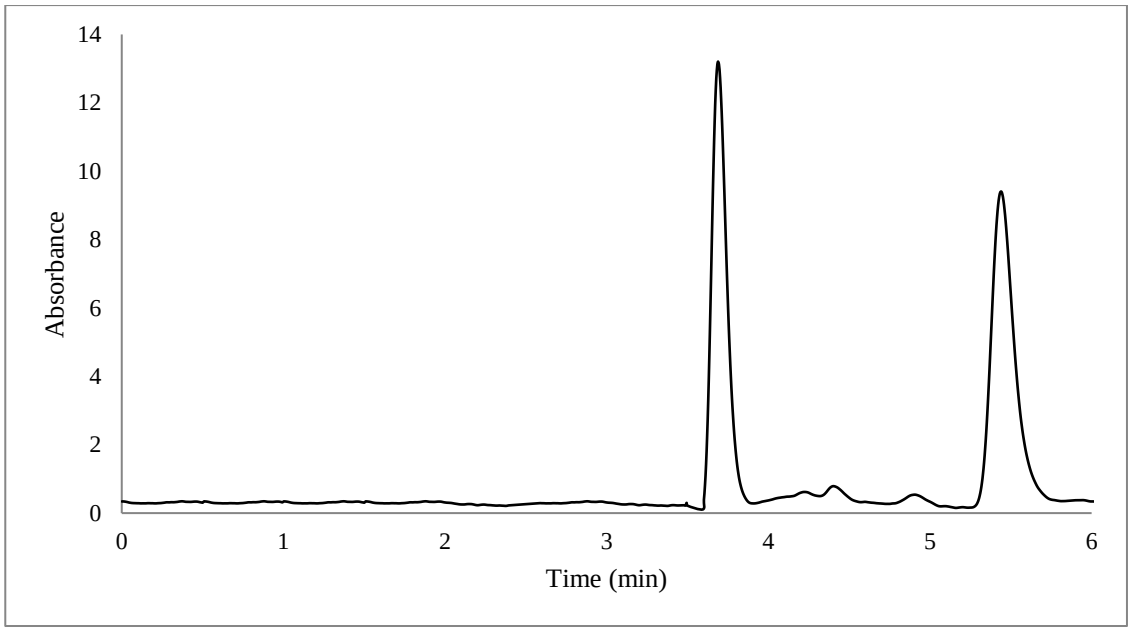

Figure 153: Liquid chromatogram for separation of the R and S enantiomers of 50 ppm of 3-Methylbuphedrone drug using AS-H Amylose column, λ_{max}. 270 nm

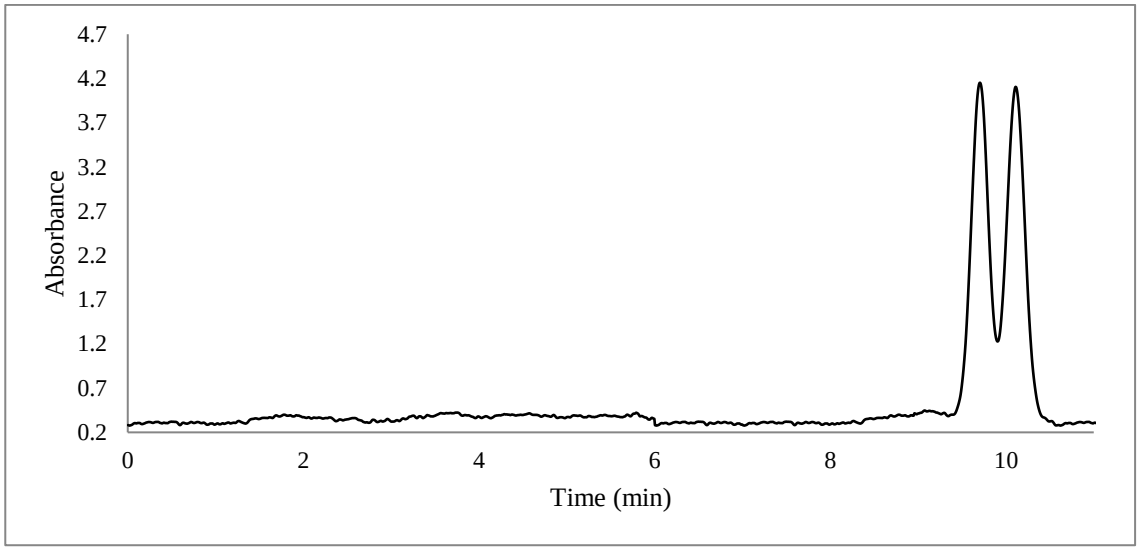

Figure 154: Liquid chromatogram for separation of the R and S enantiomers of 50 ppm of 3-Methylbuphedrone drug using DMP cellulose column, λ_{max}. 270 nm

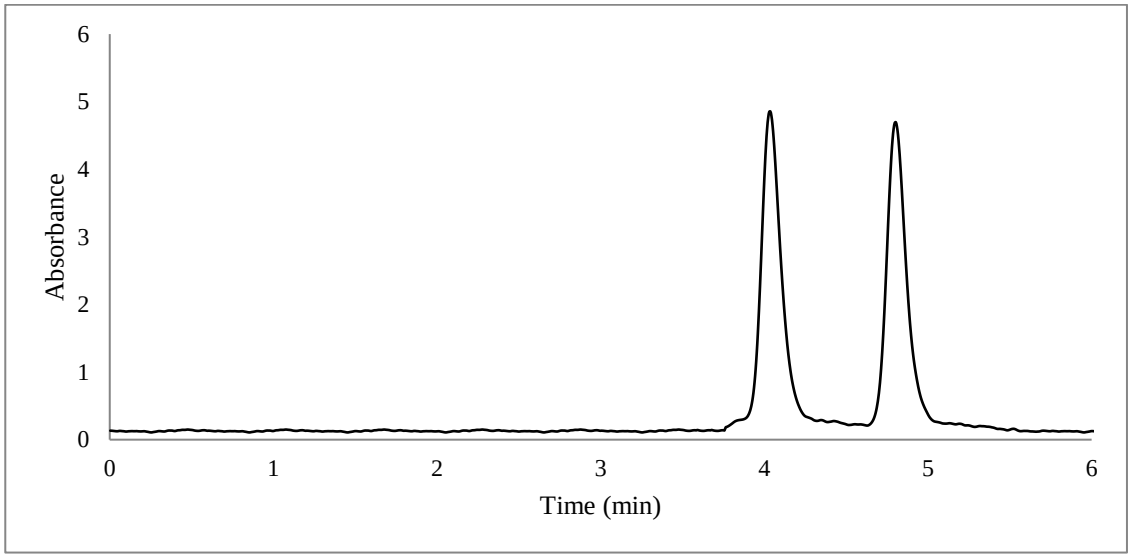

Figure 155: Liquid chromatogram for separation of the R and S enantiomers of 50 ppm of 3-Methylmethcathinone (3-MMC) drug using AS-H Amylose column, λ_{max}. 270 nm

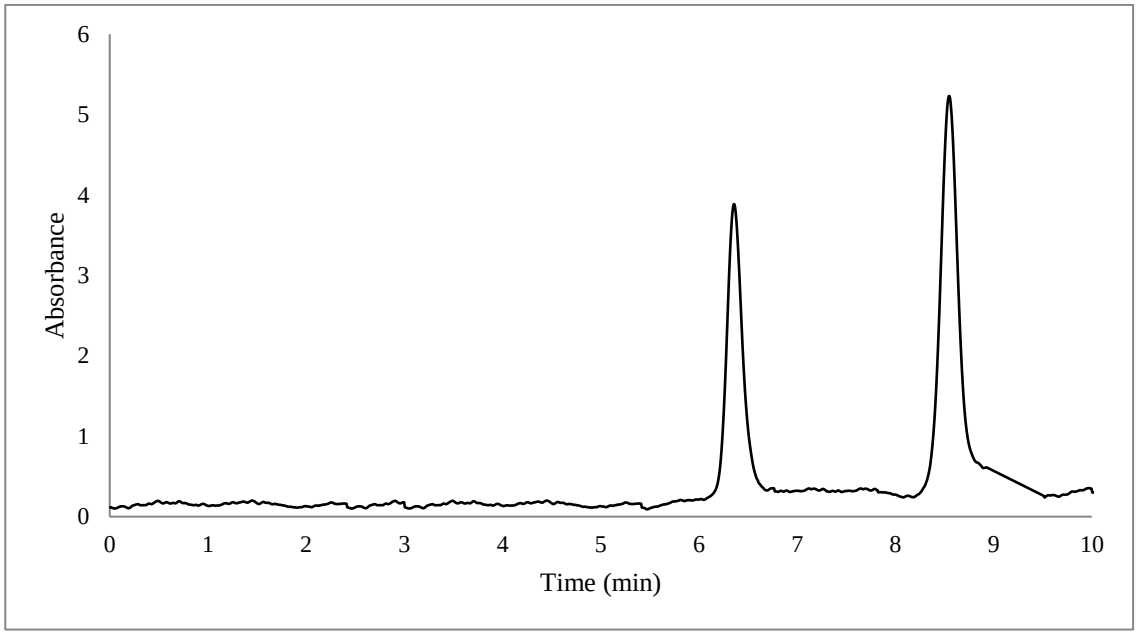

Figure 156: Liquid chromatogram for separation of the R and S enantiomers of 50 ppm of 3-Methylmethcathinone (3-MMC) drug using DMP cellulose column, λ_{max}. 270 nm

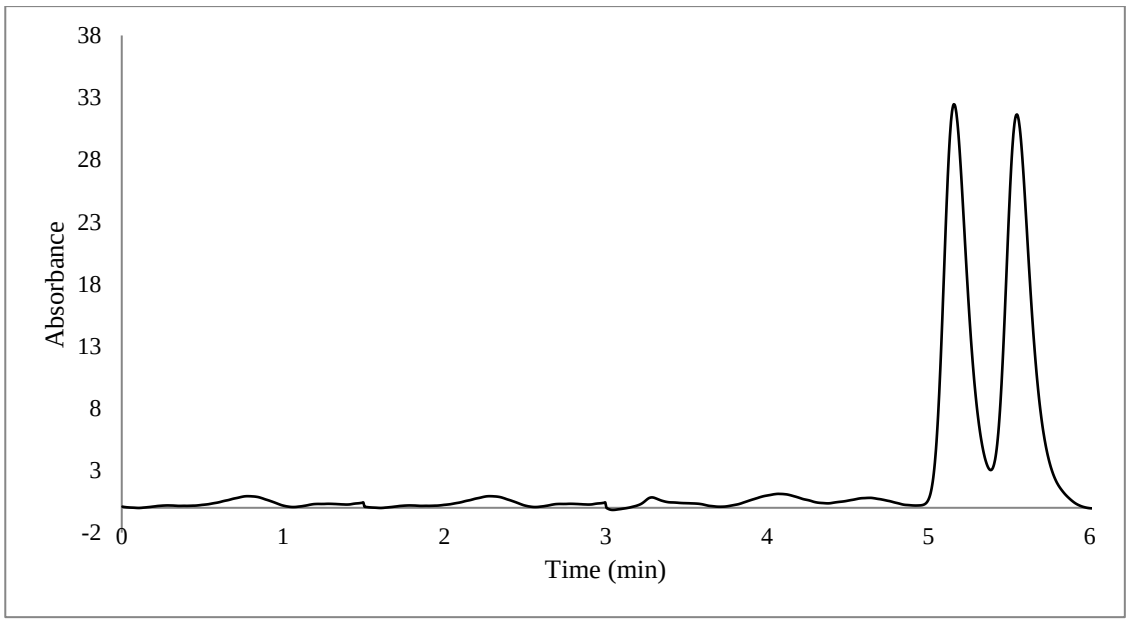

Figure 157: Liquid chromatogram for separation of the R and S enantiomers of 50 ppm of 4-Bromomethcathinone (4-BMC) drug using AS-H Amylose column, λ_{max}. 254 nm

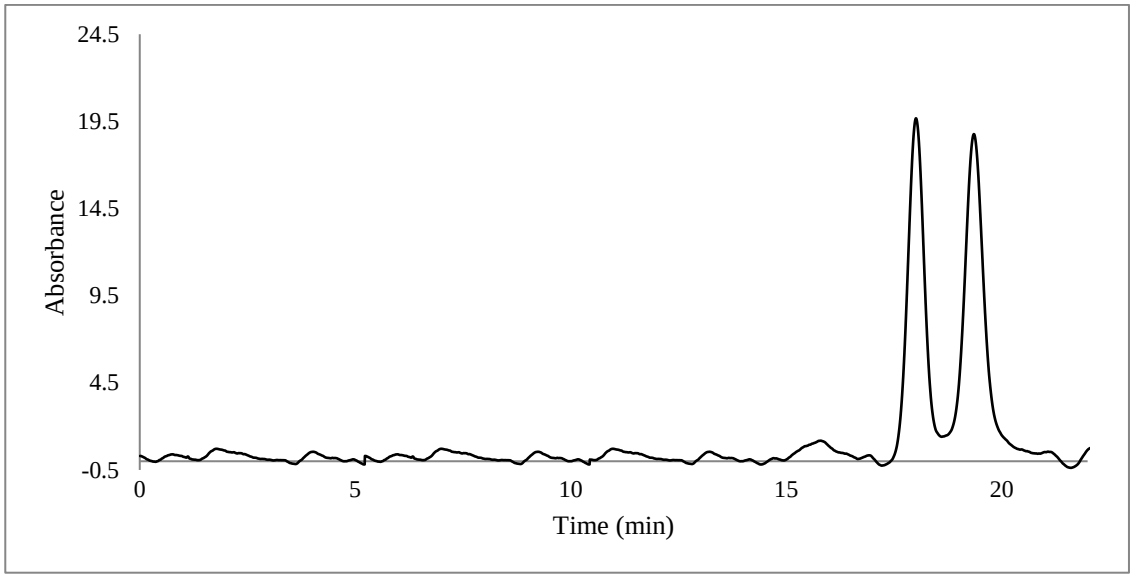

Figure 158: Liquid chromatogram for separation of the R and S enantiomers of 50 ppm of 4-Bromomethcathinone (4-BMC) drug using DMP cellulose column, λ_{max}. 254 nm

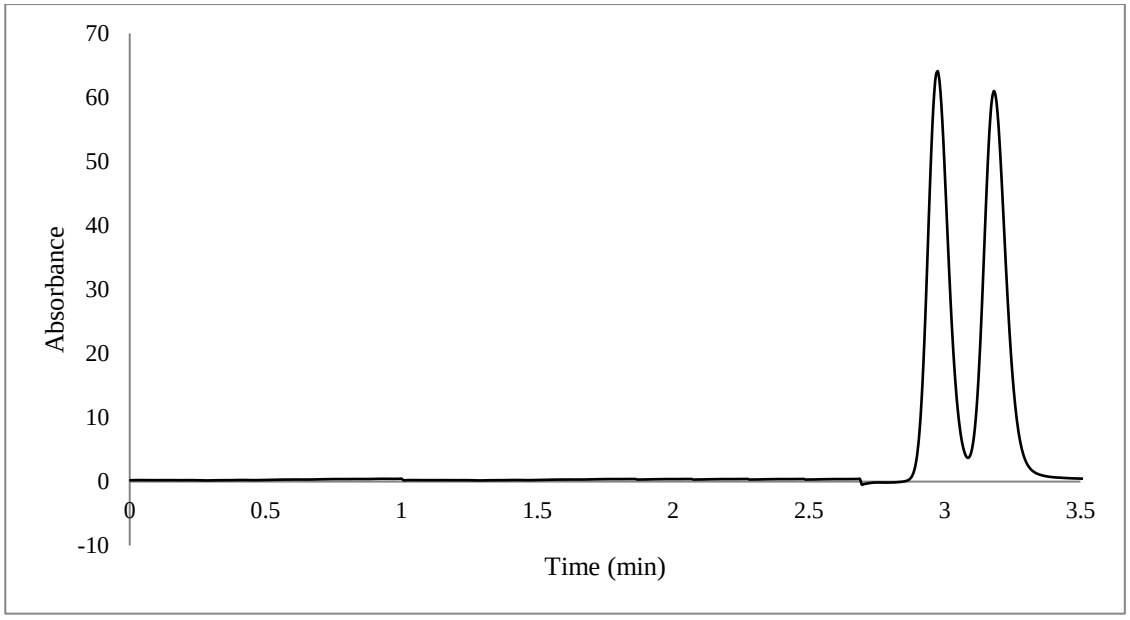

Figure 159: Liquid chromatogram for separation of the R and S enantiomers of 50 ppm of 4-Ethylethcathinone (4-EEC) drug using AS-H Amylose column, λ_{max}. 254 nm

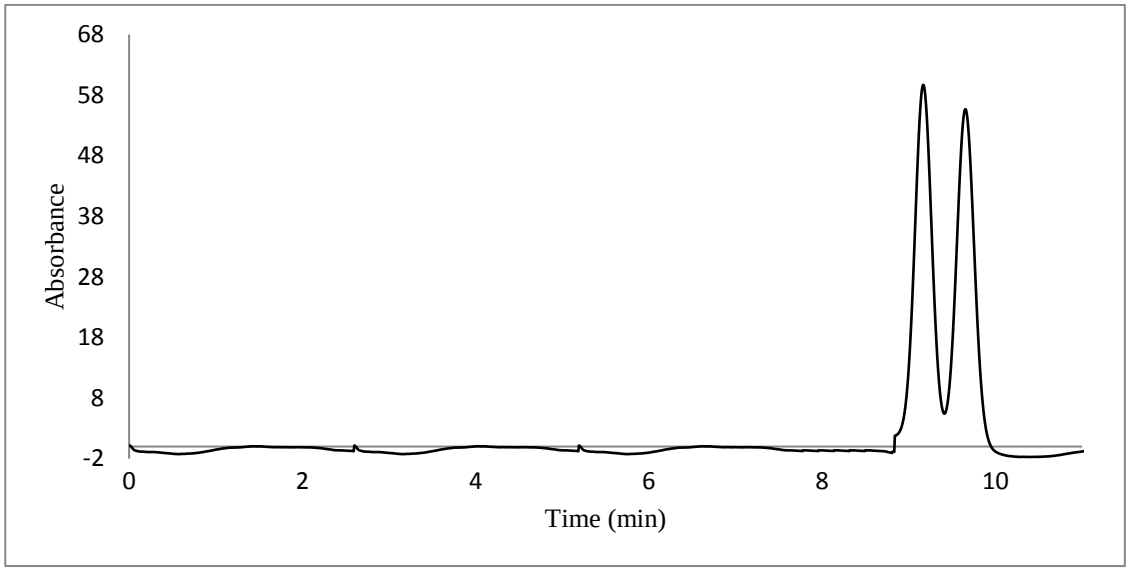

Figure 160: Liquid chromatogram for separation of the R and S enantiomers of 50 ppm of 4-Ethylethcathinone (4-EEC) drug using DMP cellulose column, λ_{max}. 254 nm

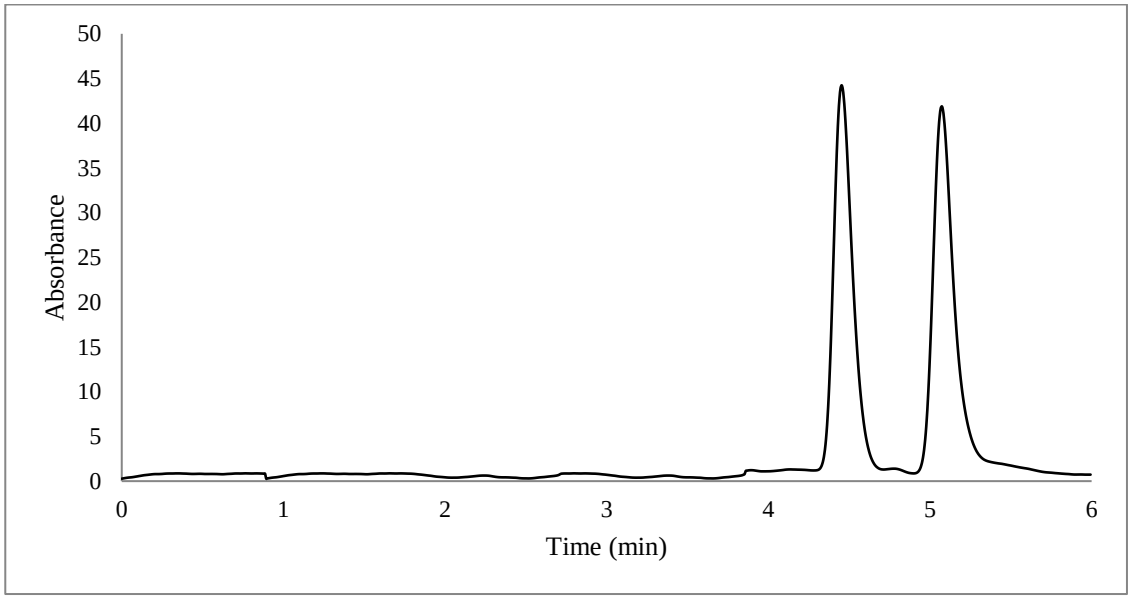

Figure 161: Liquid chromatogram for separation of the R and S enantiomers of 50 ppm of 4-Ethylmethcathinone (4-EMC) drug using AS-H Amylose column, λ_{max}. 254 nm

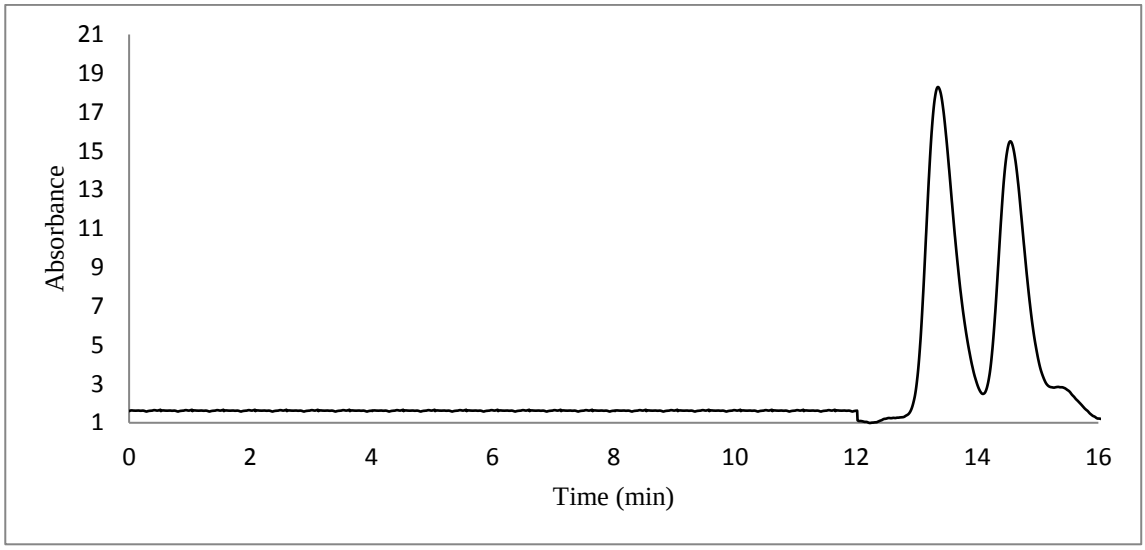

Figure 162: Liquid chromatogram for separation of the R and S enantiomers of 50 ppm of 4-Ethylmethcathinone (4-EMC) drug using DMP cellulose column, λ_{max}. 254 nm

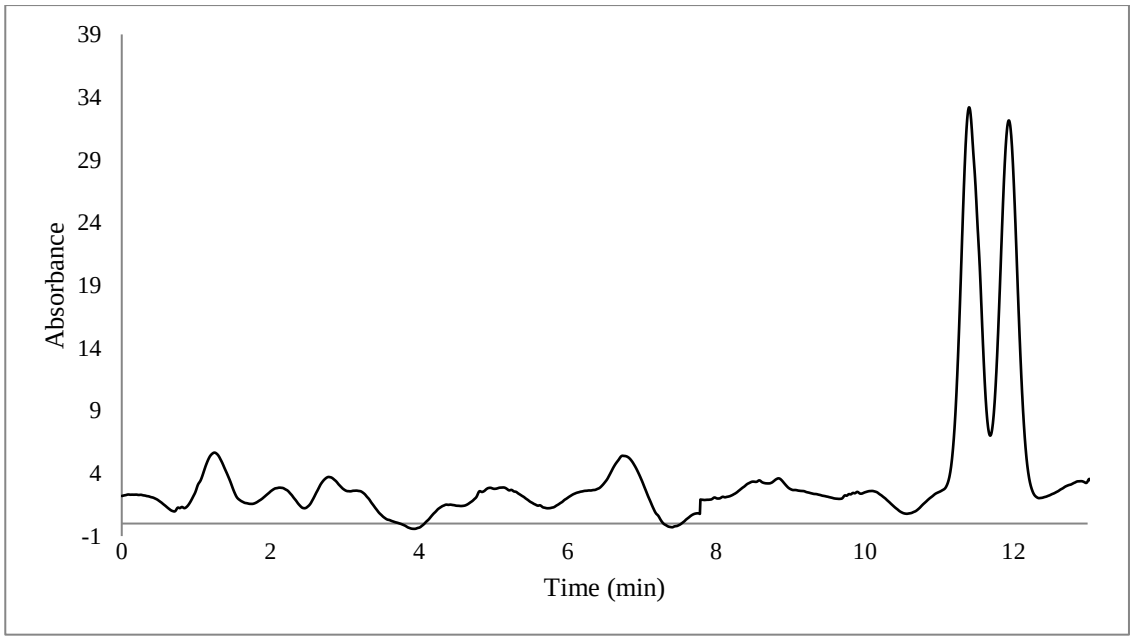

Figure 163: Liquid chromatogram for separation of the R and S enantiomers of 50 ppm of 4-Fluoroethcathinone (4-FEC) drug using AS-H Amylose column, λ_{max}. 254 nm

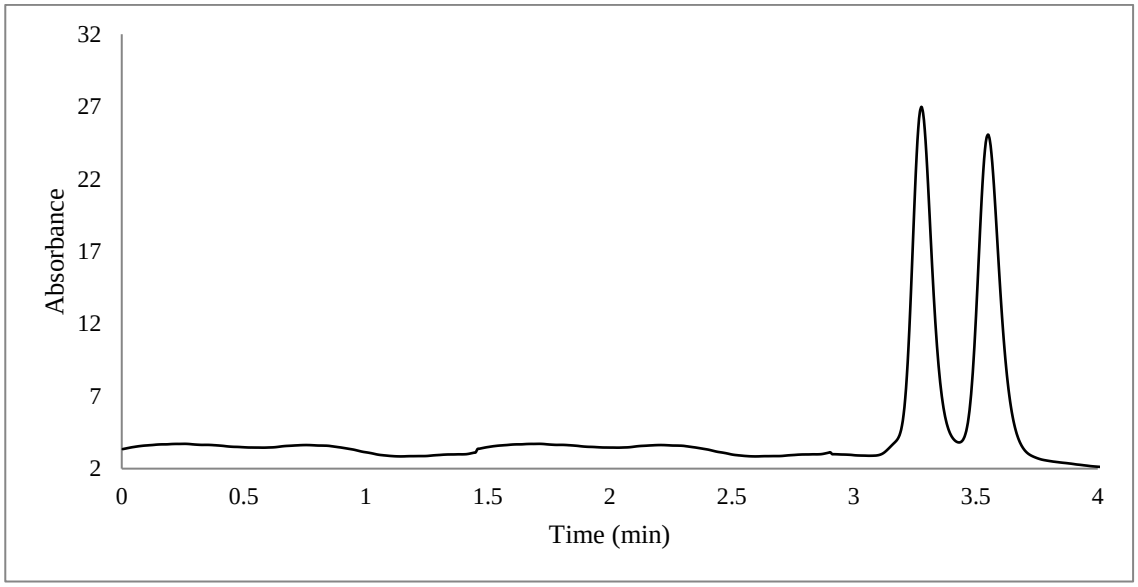

Figure 164: Liquid chromatogram for separation of the R and S enantiomers of 50 ppm of 4-Fluoroethcathinone (4-FEC) drug using DMP cellulose column, λ_{max}. 254 nm

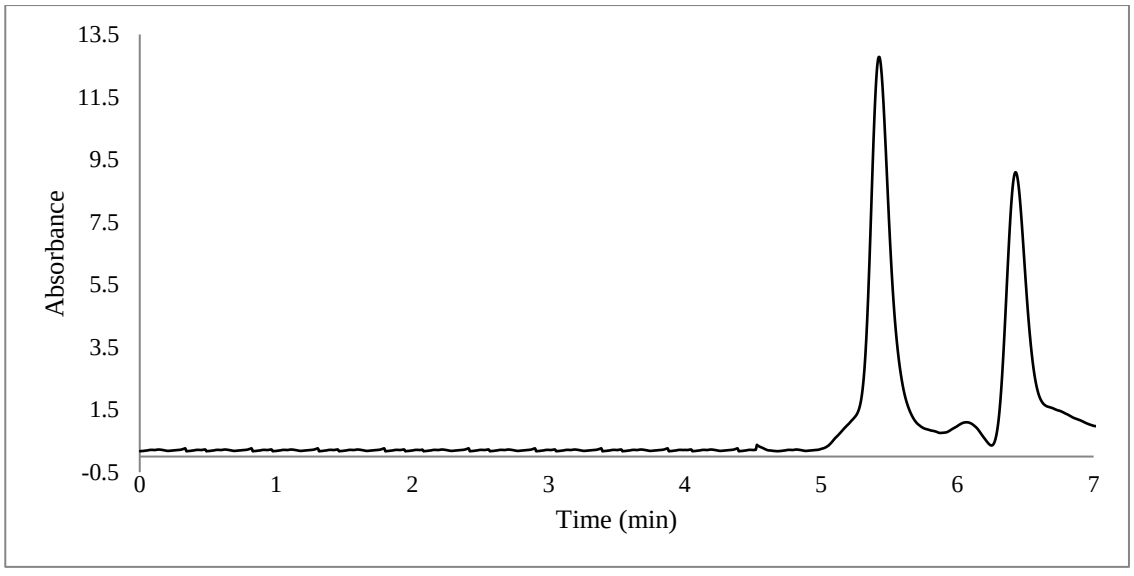

Figure 165: Liquid chromatogram for separation of the R and S enantiomers of 50 ppm of 4-Fluoromethcathinone (4-FMC) drug using AS-H Amylose column, λ_{max}. 254 nm

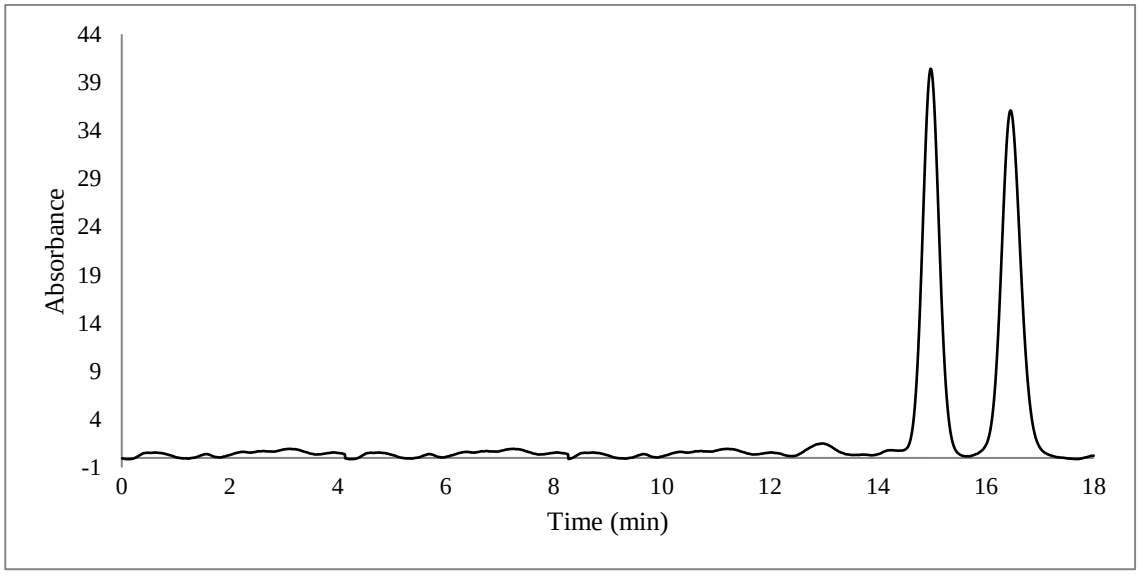

Figure 166: Liquid chromatogram for separation of the R and S enantiomers of 50 ppm of 4-Fluoromethcathinone (4-FMC) drug using DMP cellulose column, λ_{max}. 254 nm

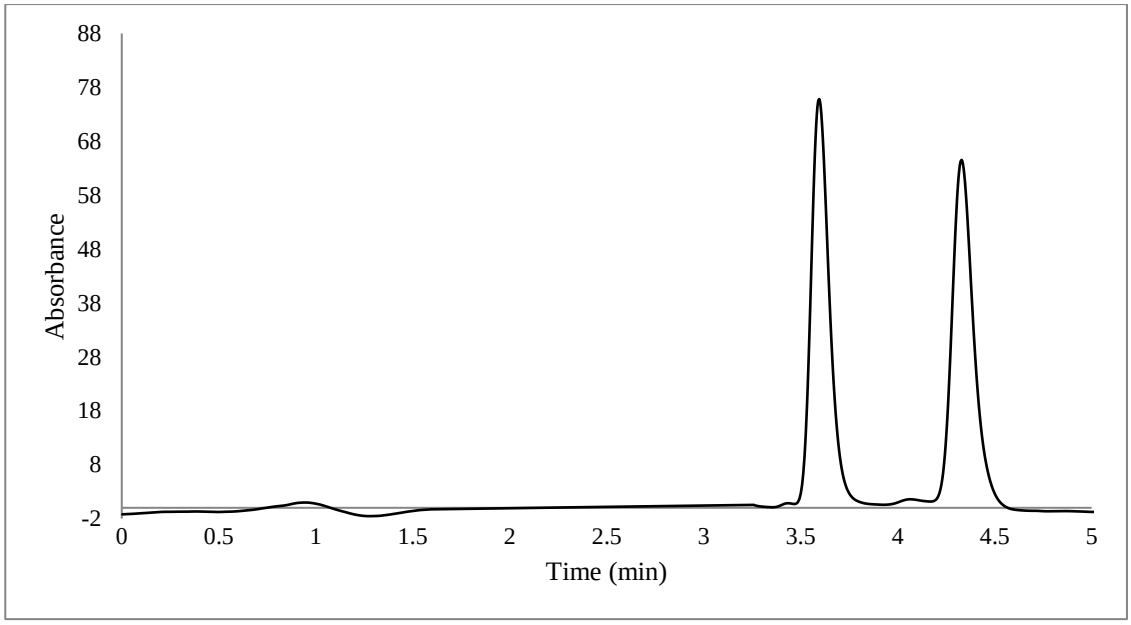

Figure 167: Liquid chromatogram for separation of the R and S enantiomers of 50 ppm of 4-Methylbuphedrone drug using AS-H Amylose column, λ_{max}. 254 nm

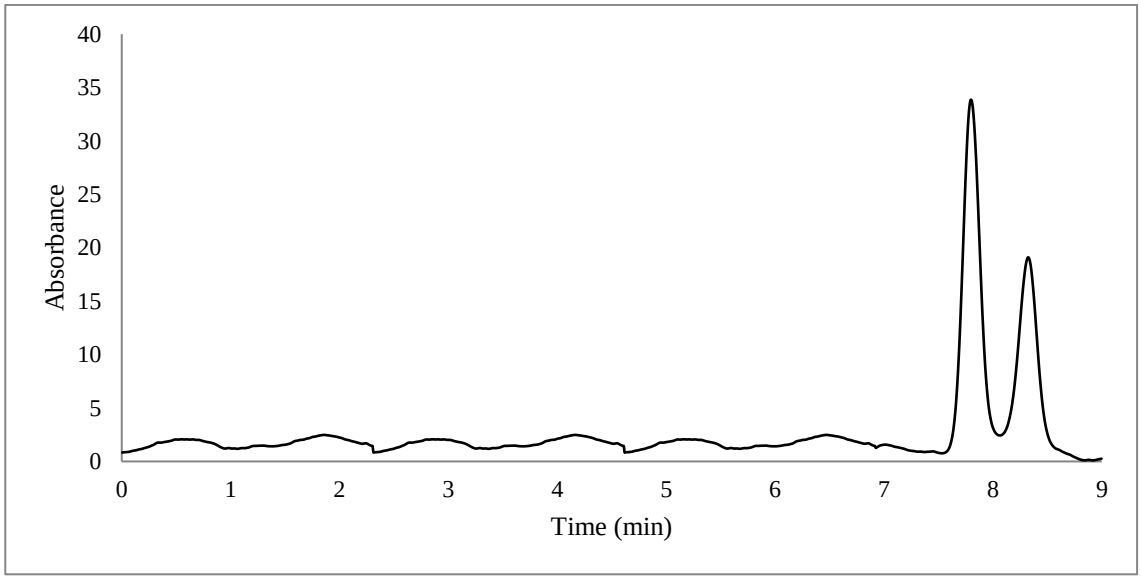

Figure 168: Liquid chromatogram for separation of the R and S enantiomers of 50 ppm of 4-Methylbuphedrone drug using DMP cellulose column, λ_{max}. 254 nm

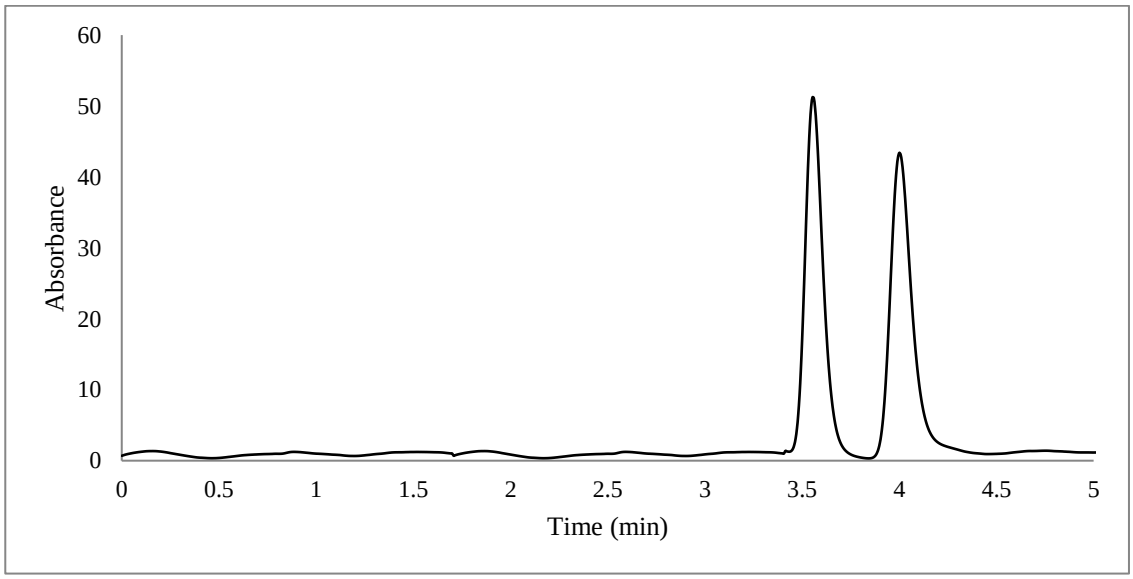

Figure 169: Liquid chromatogram for separation of the R and S enantiomers of 50 ppm of 4-Methylethcathinone (4-MEC) drug using AS-H Amylose column, λ_{max}. 254 nm

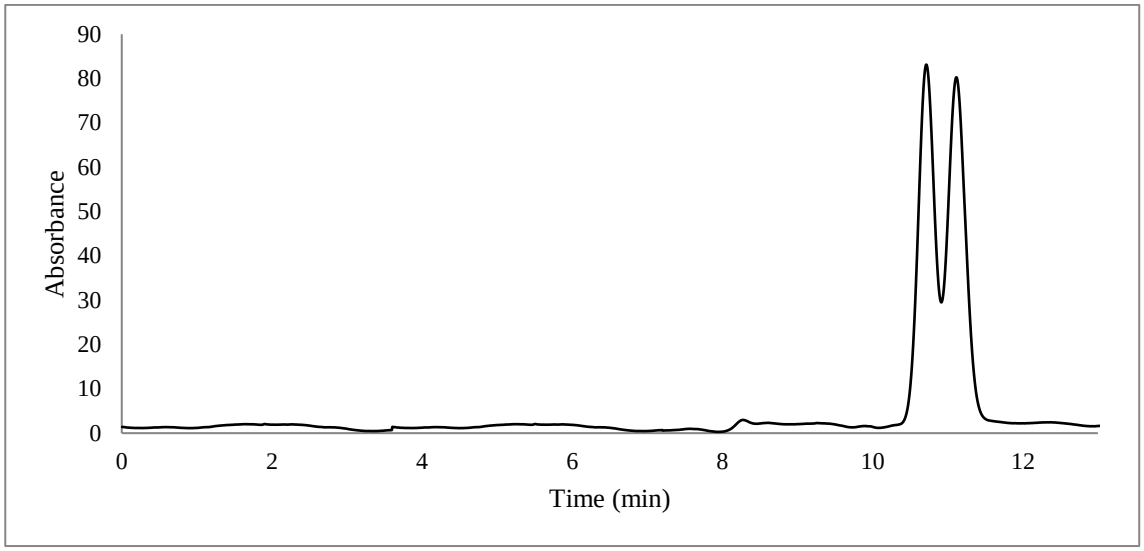

Figure 170: Liquid chromatogram for separation of the R and S enantiomers of 50 ppm of 4-Methylethcathinone (4-MEC) drug using DMP cellulose column, λ_{max}. 254 nm

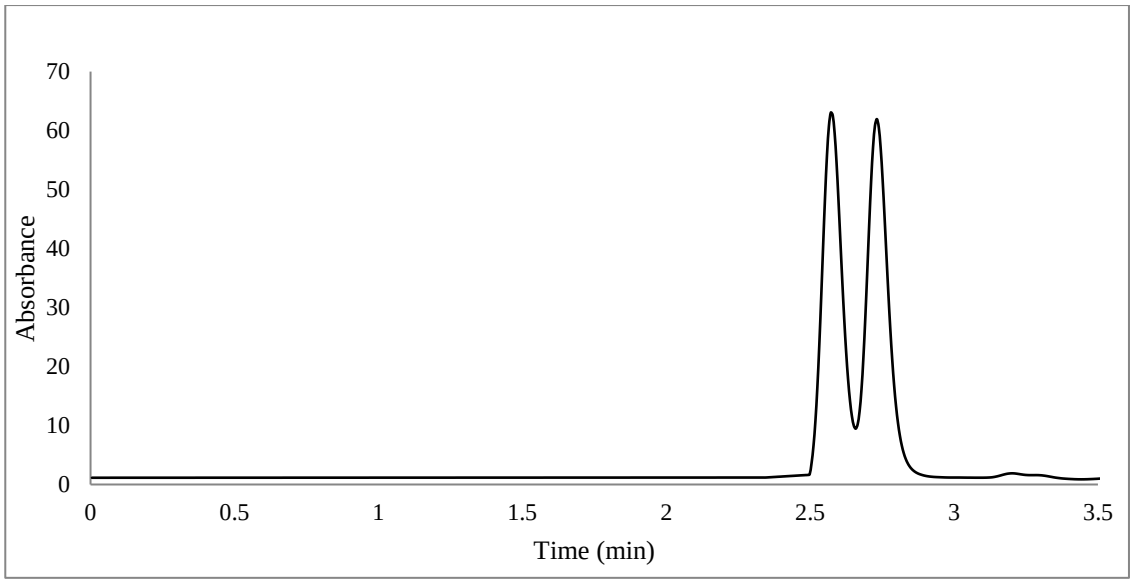

Figure 171: Liquid chromatogram for separation of the R and S enantiomers of 50 ppm of 4-Methyl-α-ethylaminobutiophenone drug using AS-H Amylose column, λ_{max}. 254 nm

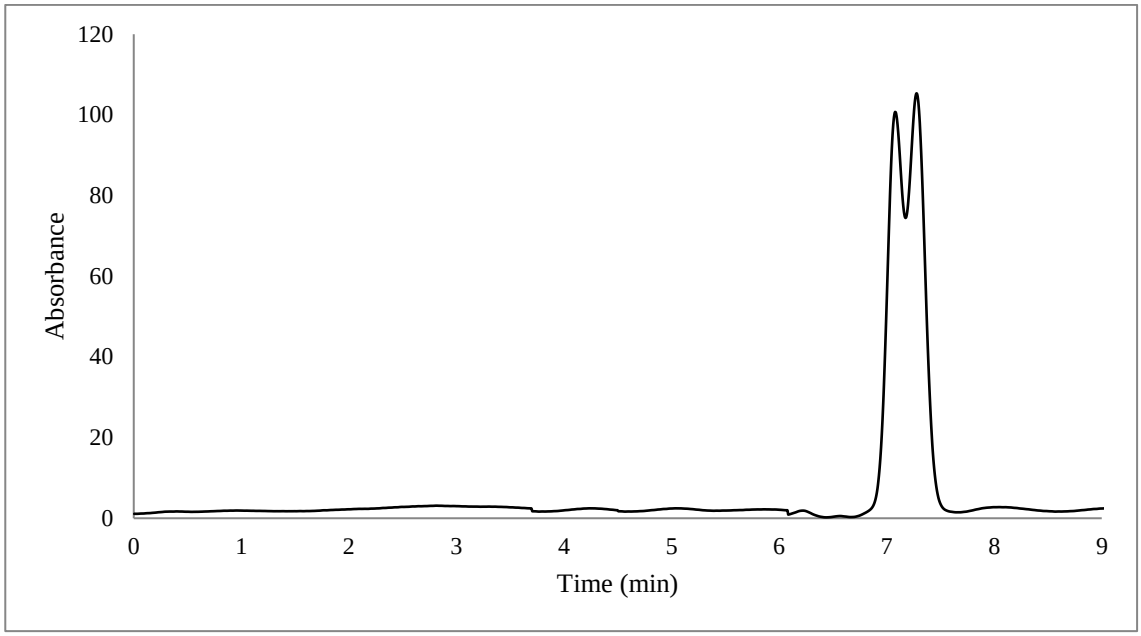

Figure 172: Liquid chromatogram for separation of the R and S enantiomers of 50 ppm of 4-Methyl-α-ethylaminobutiophenone drug using DMP cellulose column, λ_{max}. 254 nm

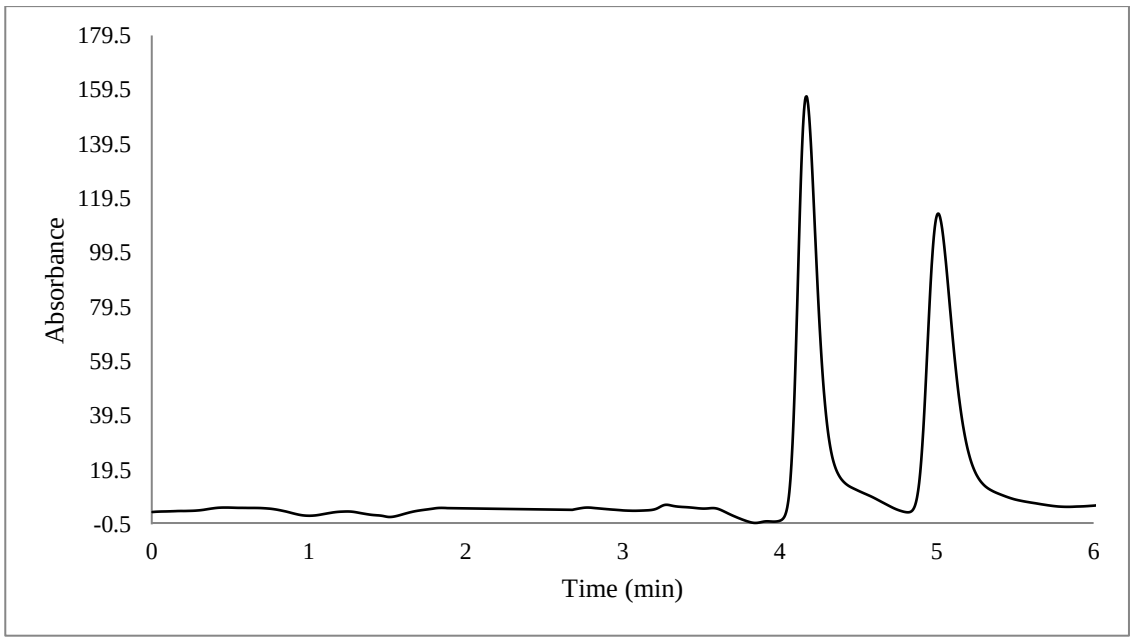

Figure 173: Liquid chromatogram for separation of the R and S enantiomers of 50 ppm of Benzedrone drug using AS-H Amylose column, λ_{max}. 254 nm

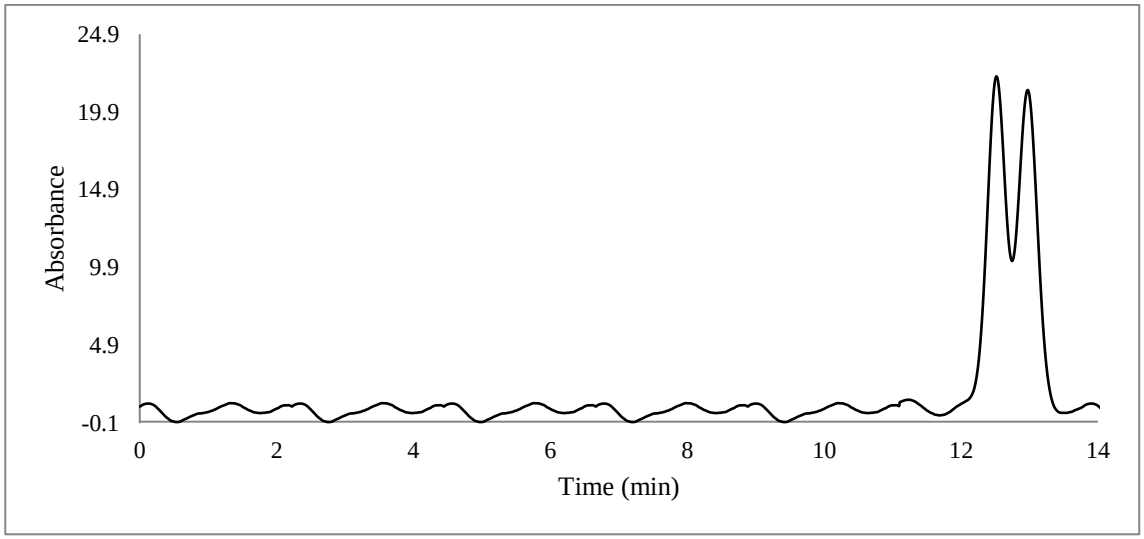

Figure 174: Liquid chromatogram for separation of the R and S enantiomers of 50 ppm of Benzedrone drug using DMP cellulose column, λ_{max}. 254 nm

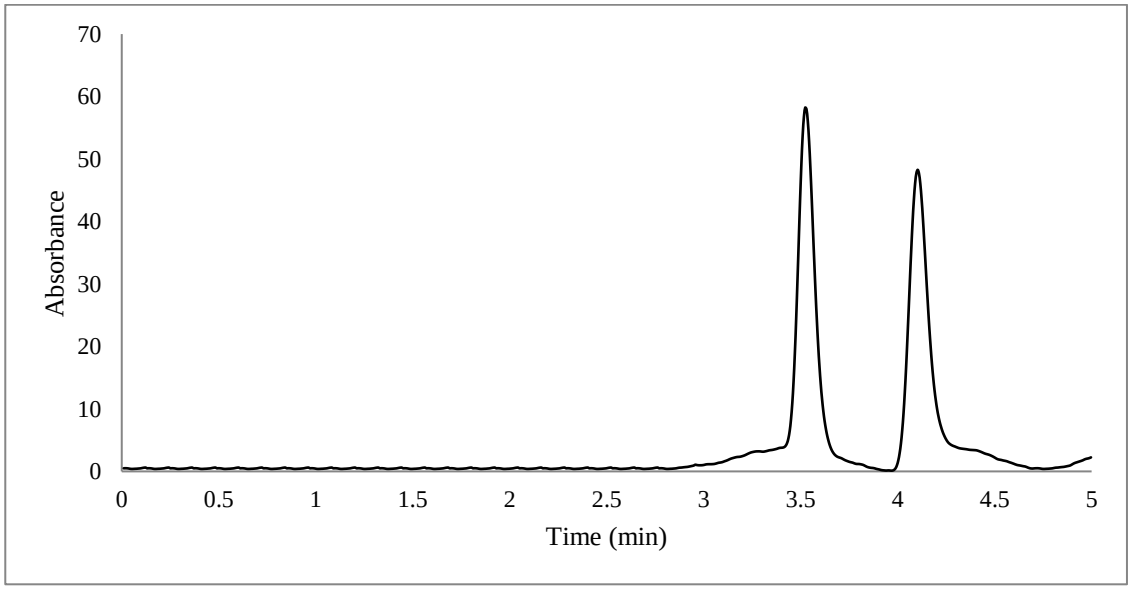

Figure 175: Liquid chromatogram for separation of the R and S enantiomers of 50 ppm of Buphedrone drug using AS-H Amylose column, λ_{max}. 240 nm

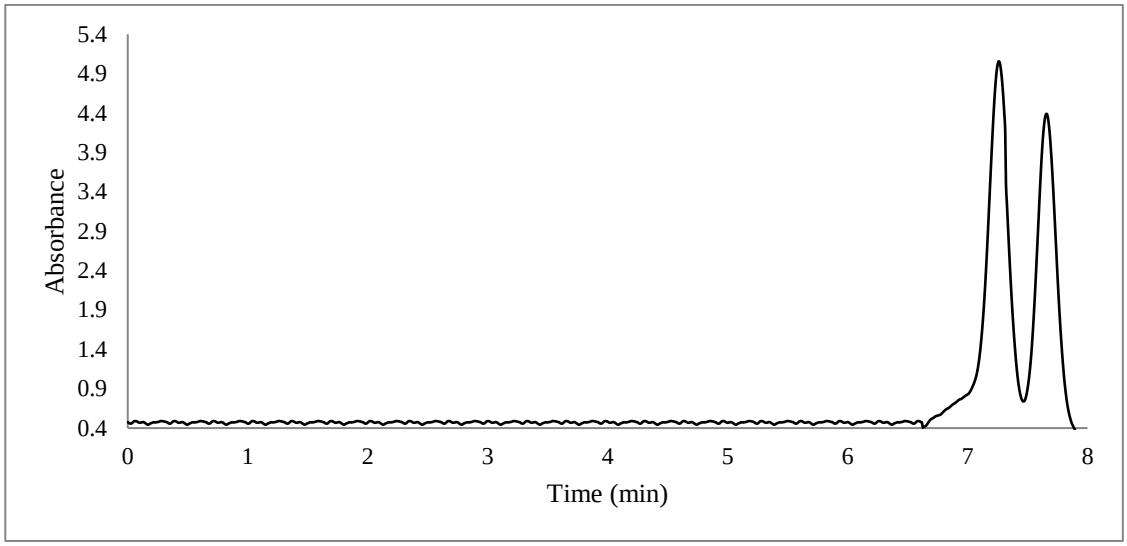

Figure 176: Liquid chromatogram for separation of the R and S enantiomers of 50 ppm of Buphedrone drug using DMP cellulose column, λ_{max}. 240 nm

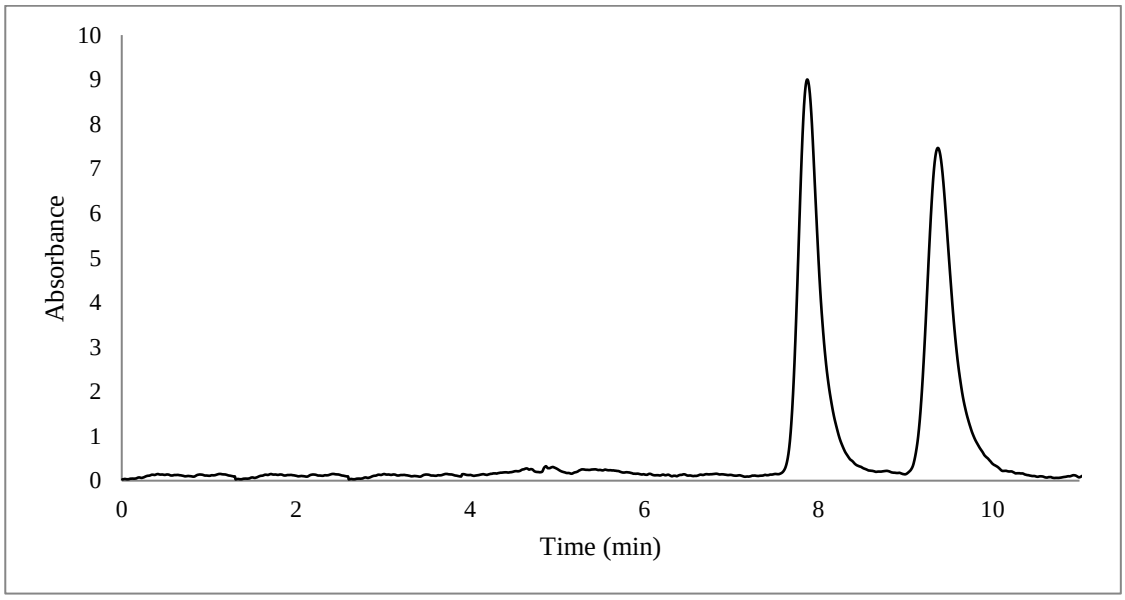

Figure 177: Liquid chromatogram for separation of the R and S enantiomers of 50 ppm of Butylone drug using AS-H Amylose column, λ_{max}. 300 nm

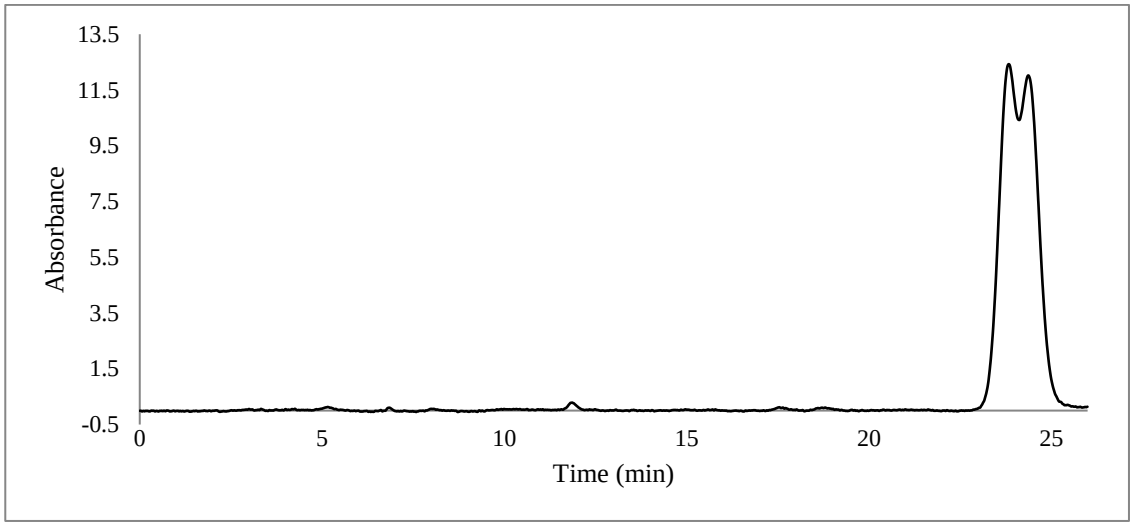

Figure 178: Liquid chromatogram for separation of the R and S enantiomers of 50 ppm of Butylone drug using DMP cellulose column, λ_{max}. 300 nm

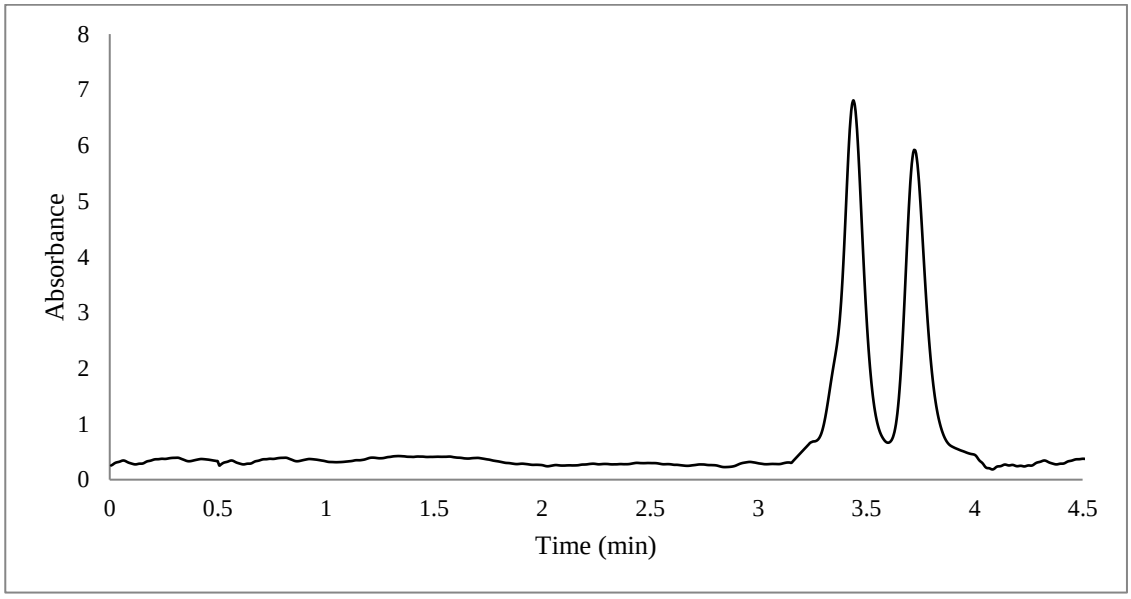

Figure 179: Liquid chromatogram for separation of the R and S enantiomers of 50 ppm of Ethcathinone drug using AS-H Amylose column, λ_{max}. 240 nm

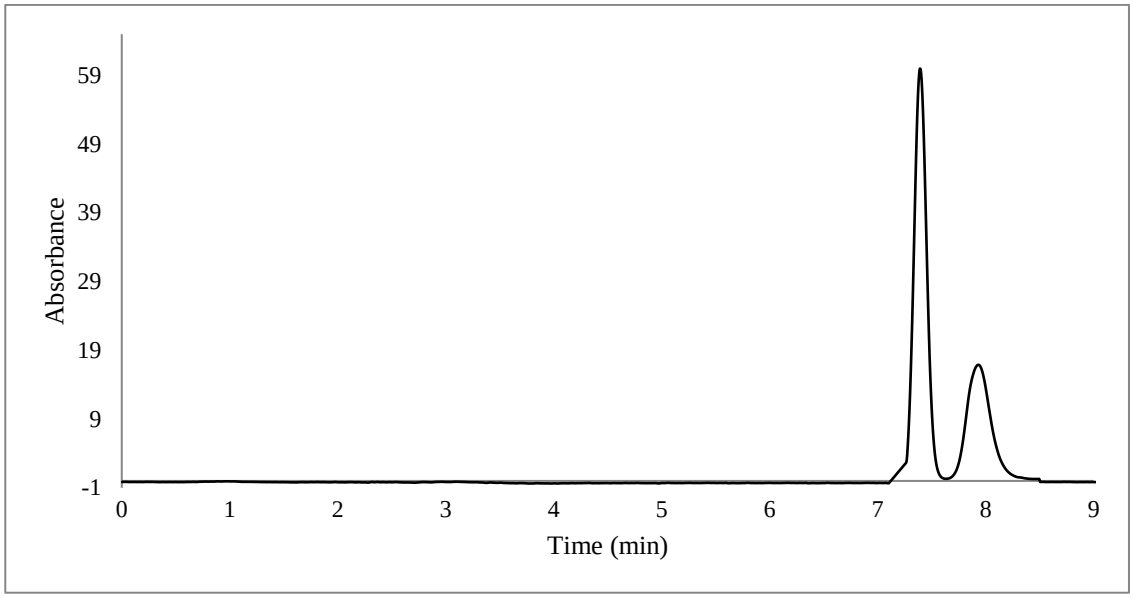

Figure 180: Liquid chromatogram for separation of the R and S enantiomers of 50 ppm of Ethcathinone drug using DMP cellulose column, λ_{max}. 240 nm

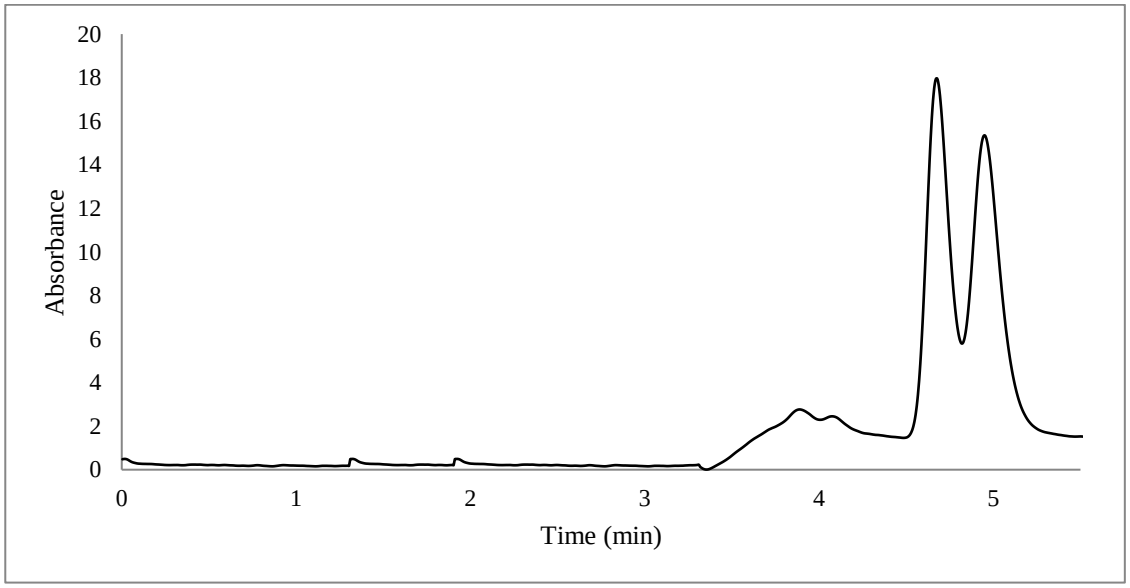

Figure 181: Liquid chromatogram for separation of the R and S enantiomers of 50 ppm of Eutylone drug using AS-H Amylose column, λ_{max}. 270 nm

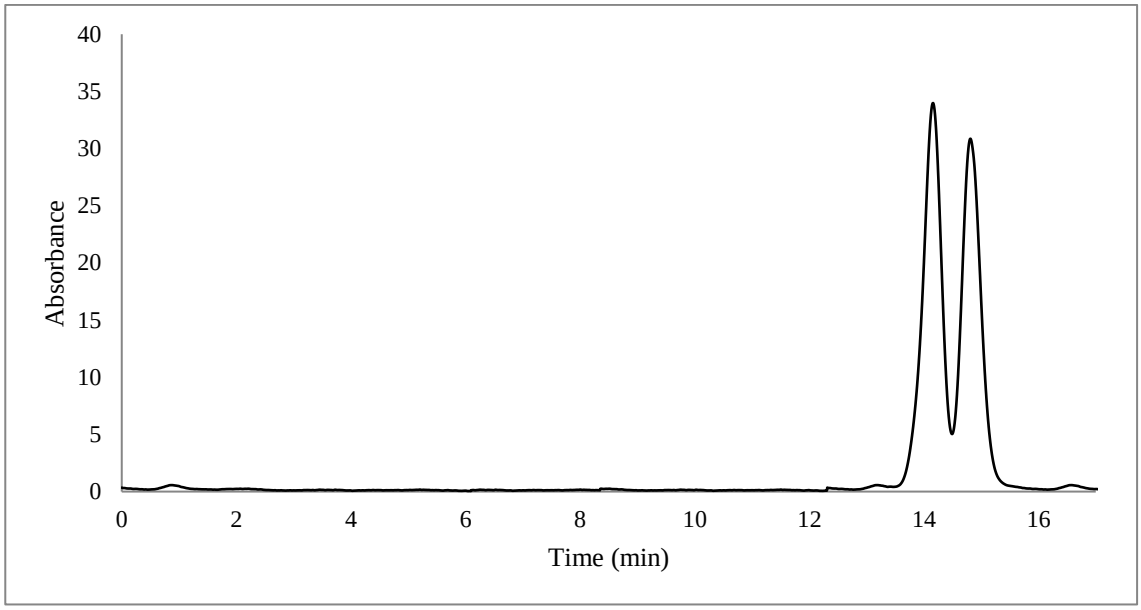

Figure 182: Liquid chromatogram for separation of the R and S enantiomers of 50 ppm of Eutylone drug using DMP cellulose column, λ_{max}. 270 nm

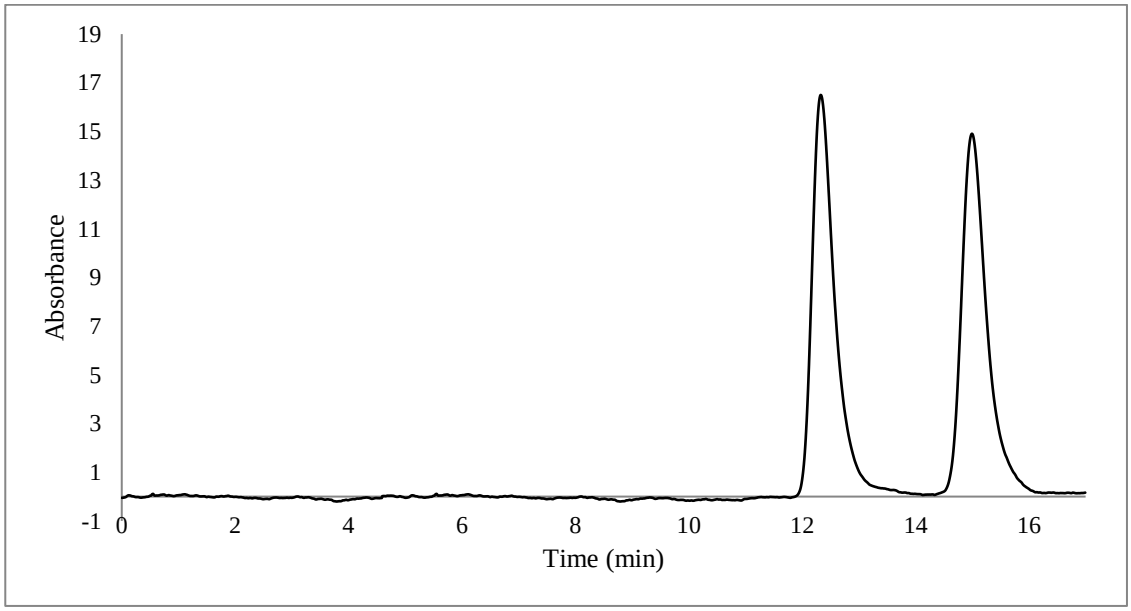

Figure 183: Liquid chromatogram for separation of the R and S enantiomers of 50 ppm of Methedrone drug using AS-H Amylose column, λ_{max}. 270 nm

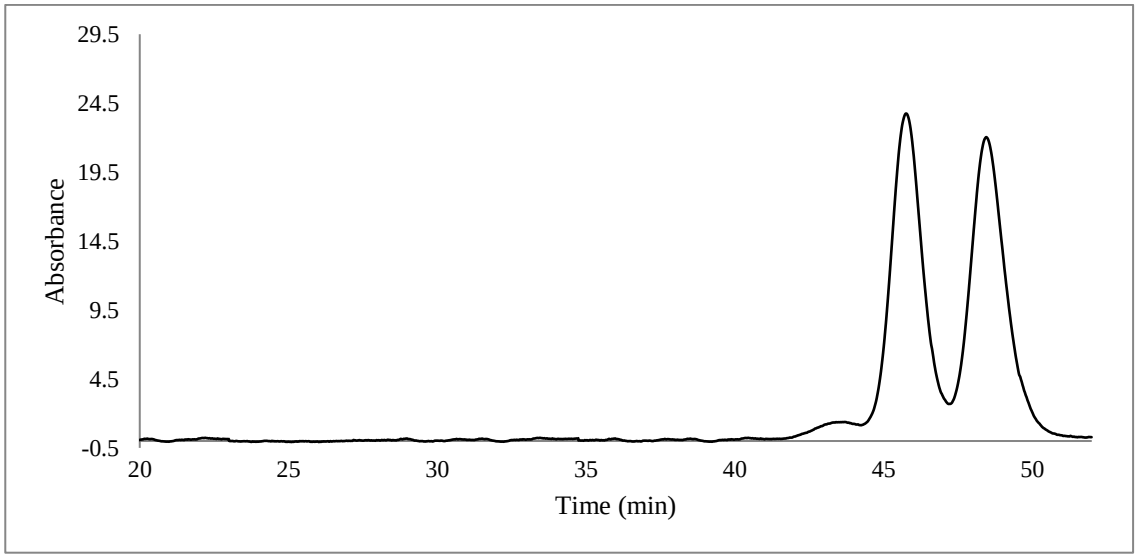

Figure 184: Liquid chromatogram for separation of the R and S enantiomers of 50 ppm of Methedrone drug using DMP cellulose column, λ_{max}. 270 nm

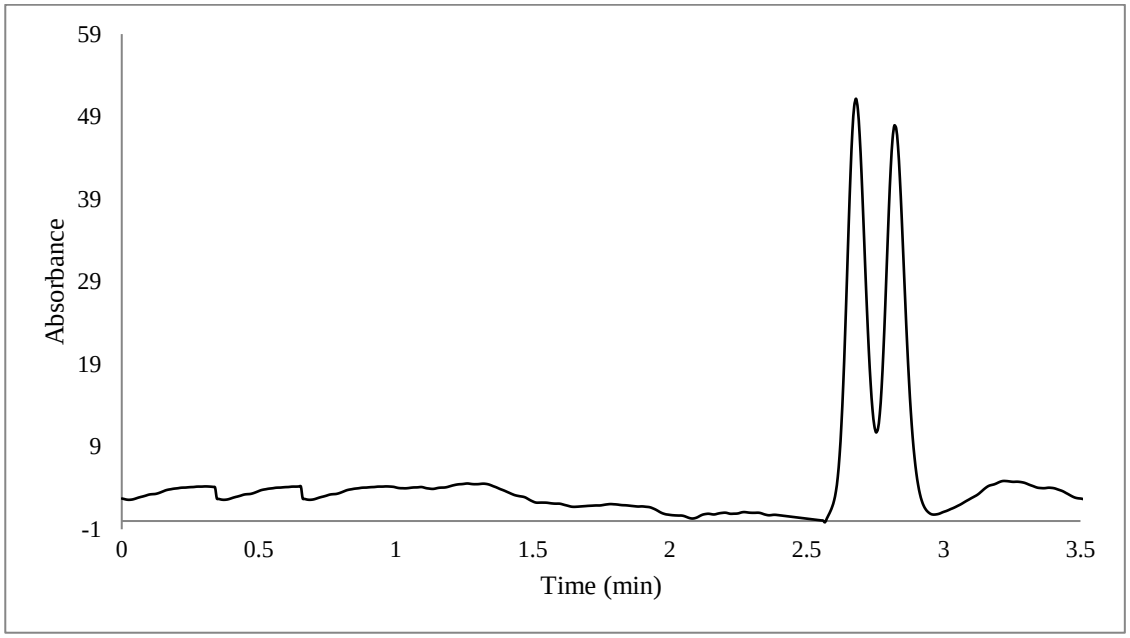

Figure 185: Liquid chromatogram for separation of the R and S enantiomers of 50 ppm of N-Ethylbuphedrone drug using AS-H Amylose column, λ_{max}. 240 nm

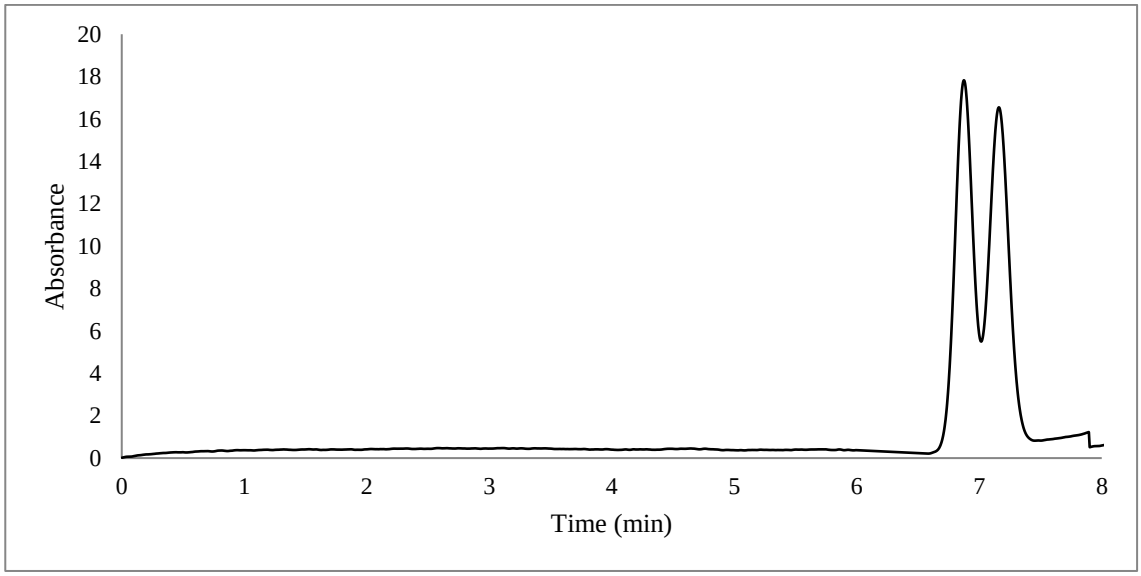

Figure 186: Liquid chromatogram for separation of the R and S enantiomers of 50 ppm of N-Ethylbuphedrone drug using DMP cellulose column, λ_{max}. 240 nm

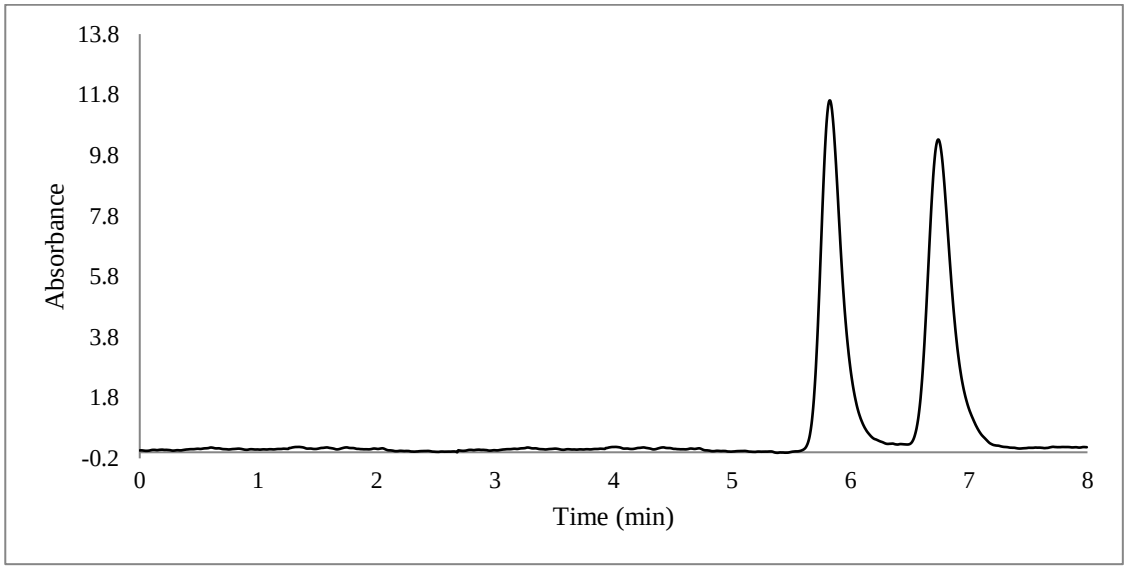

Figure 187: Liquid chromatogram for separation of the R and S enantiomers of 50 ppm of Pentylone drug using AS-H Amylose column, λ_{max}. 270 nm

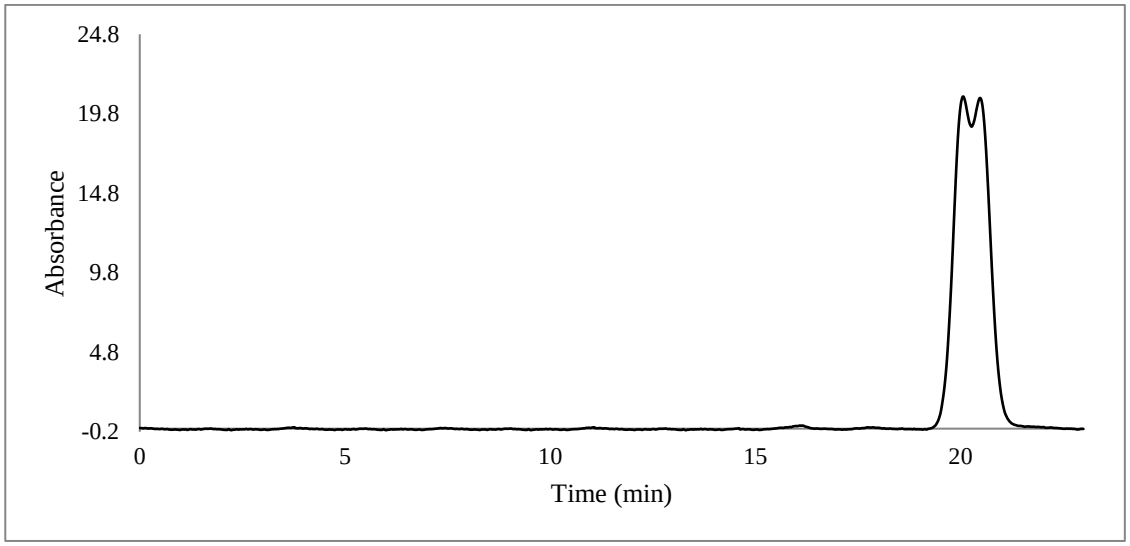

Figure 188: Liquid chromatogram for separation of the R and S enantiomers of 50 ppm of Pentylone drug using DMP cellulose column, λ_{max}. 270 nm

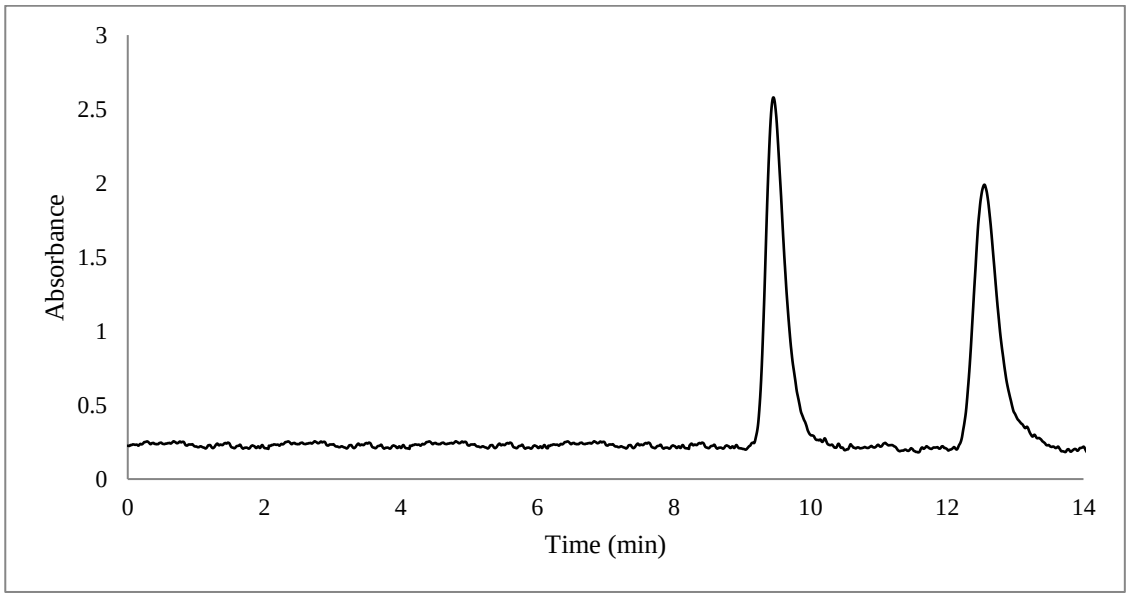

Figure 189: Liquid chromatogram for separation of the R and S enantiomers of 50 ppm of 2,3-Dimethylmethcathinone (2,3-DMMC) drug using AS-H Amylose column, λ_{max}. 300 nm

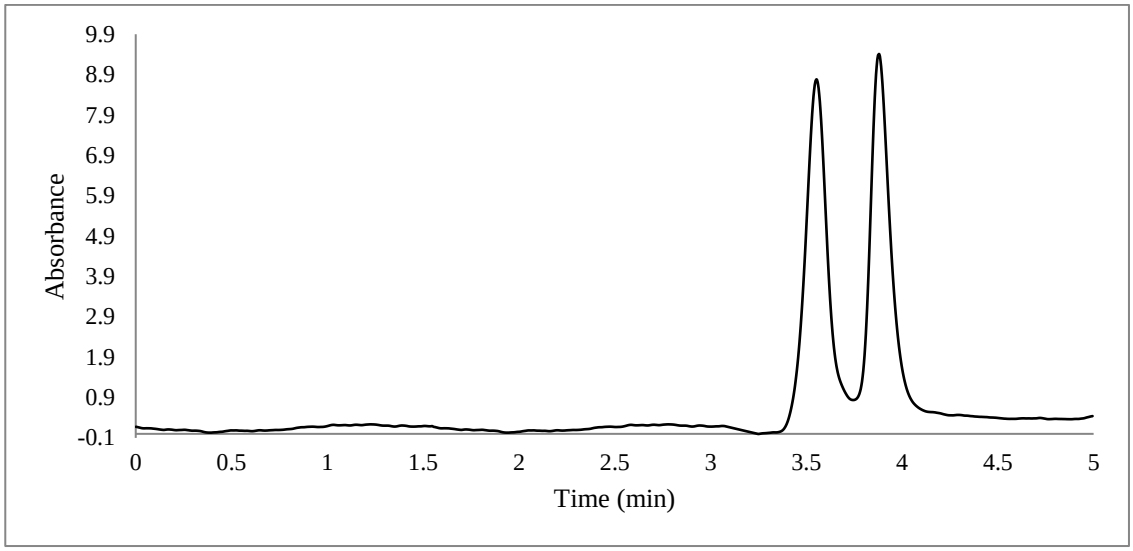

Figure 190: Liquid chromatogram for separation of the R and S enantiomers of 50 ppm of 2,4-Dimethylmethcathinone (2,4-DMMC) drug using AS-H Amylose column, λ_{max}. 270 nm

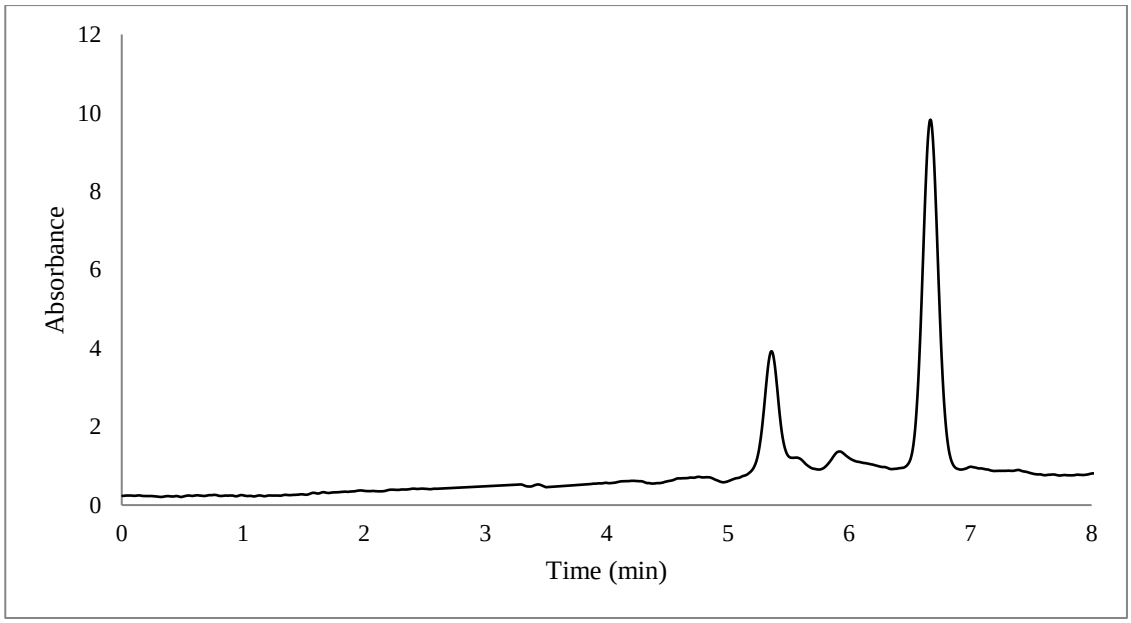

Figure 191: Liquid chromatogram for separation of the R and S enantiomers of 50 ppm of 2-Fluoroethcathinone (2-FEC) drug using DMP cellulose column, λ_{max}. 254 nm

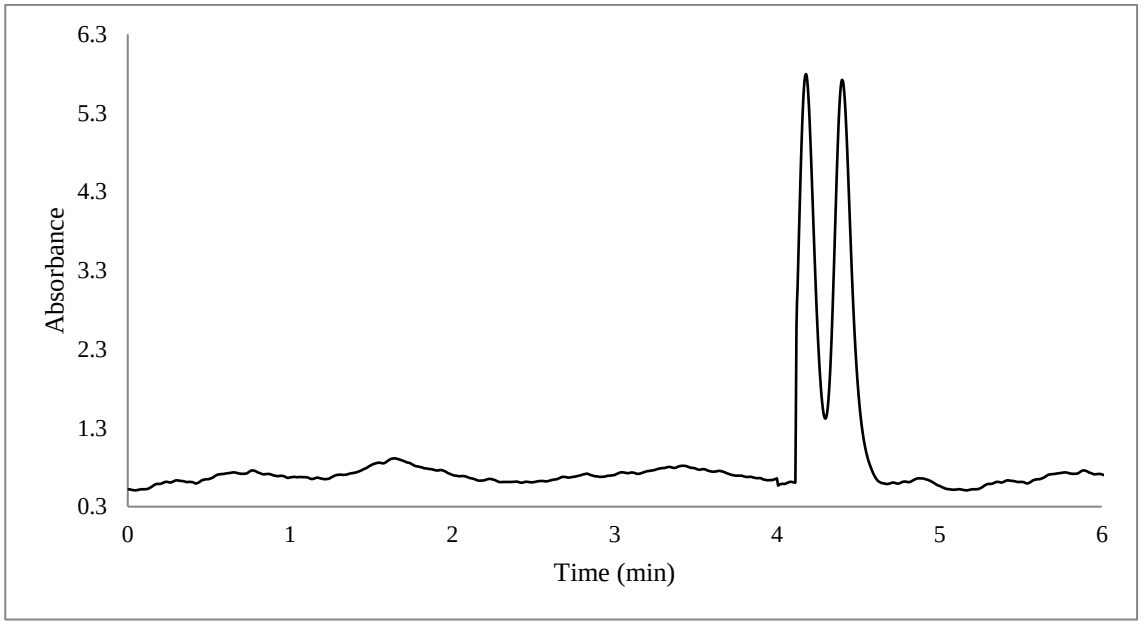

Figure 192: Liquid chromatogram for separation of the R and S enantiomers of 50 ppm of 2-Fluoromethcathinone (2-FMC) drug using AS-H Amylose column, λ_{max}. 270 nm

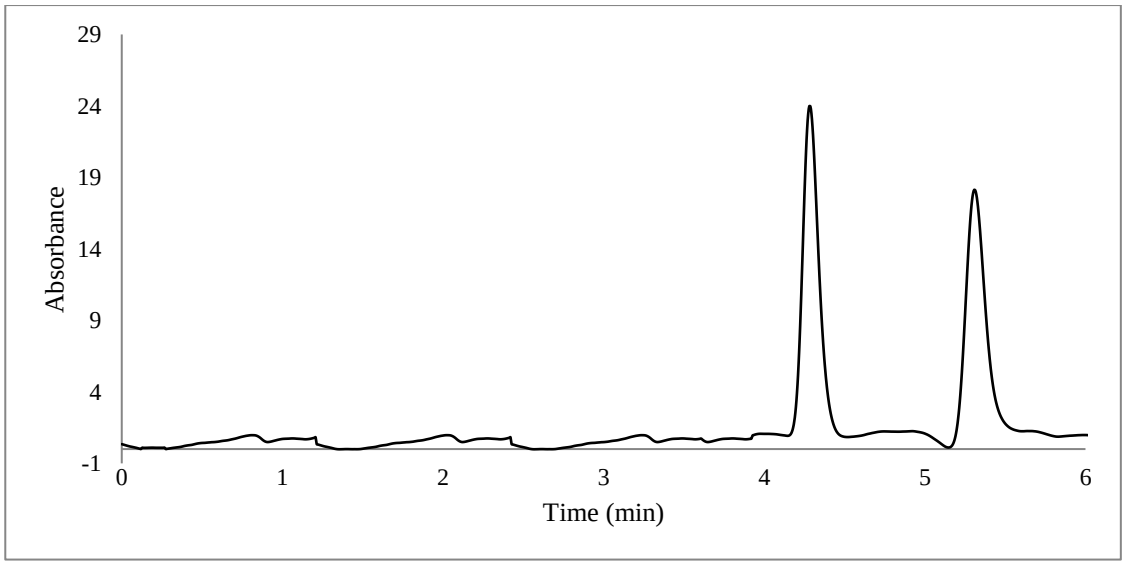

Figure 193: Liquid chromatogram for separation of the R and S enantiomers of 50 ppm of 3-Ethylmethcathinone (3-EMC) drug using AS-H Amylose column, λ_{max}. 254 nm

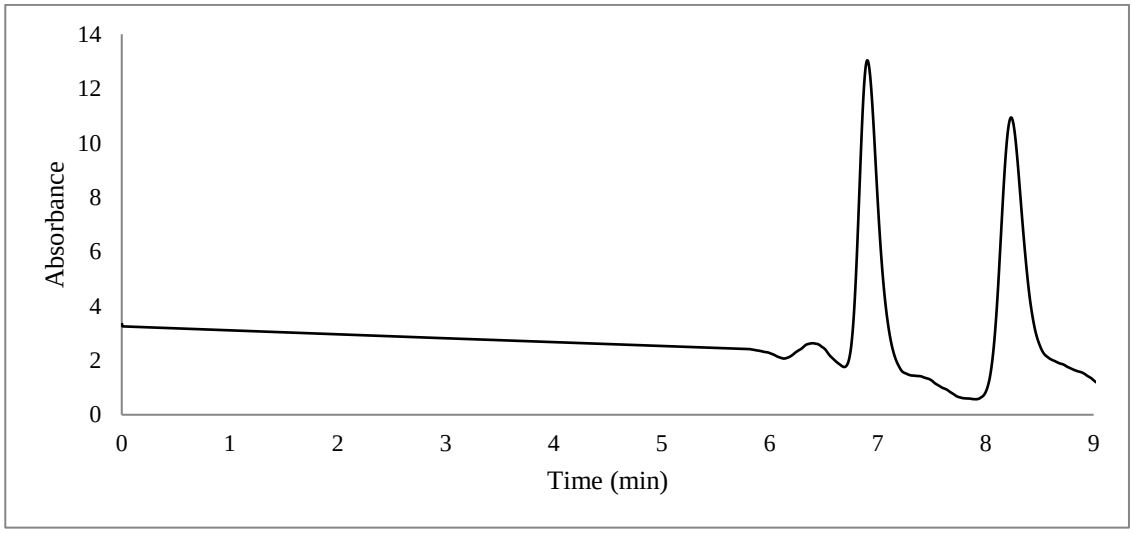

Figure 194: Liquid chromatogram for separation of the R and S enantiomers of 50 ppm of 3-Methoxymethcathinone drug using AS-H Amylose column, λ_{max}. 254 nm

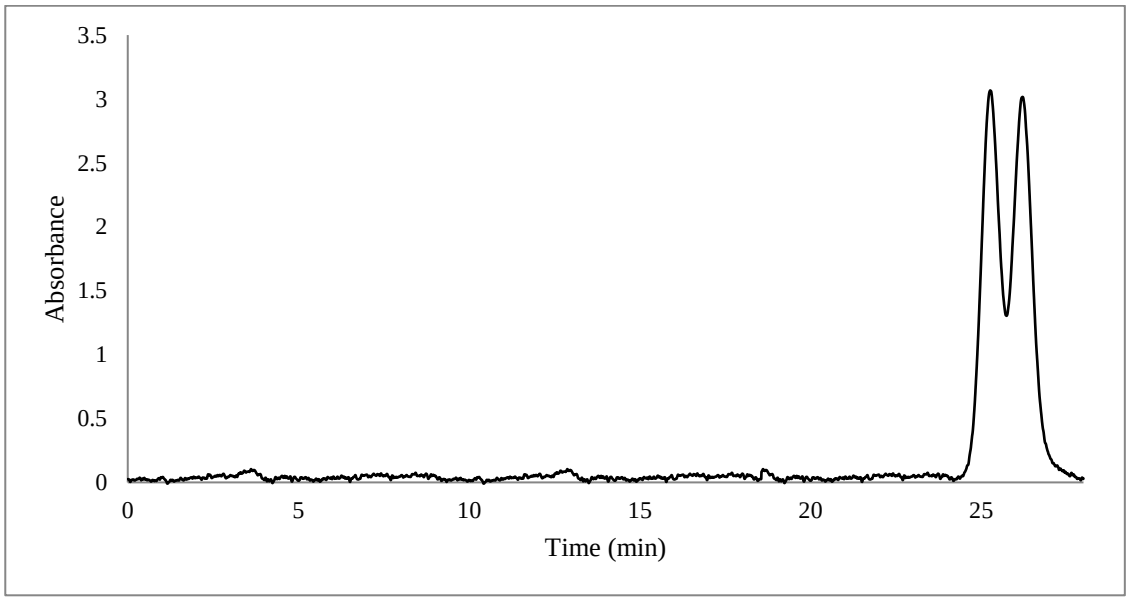

Figure 195: Liquid chromatogram for separation of the R and S enantiomers of 50 ppm of 3-Methoxymethcathinone drug using DMP cellulose column, λ_{max}. 254 nm

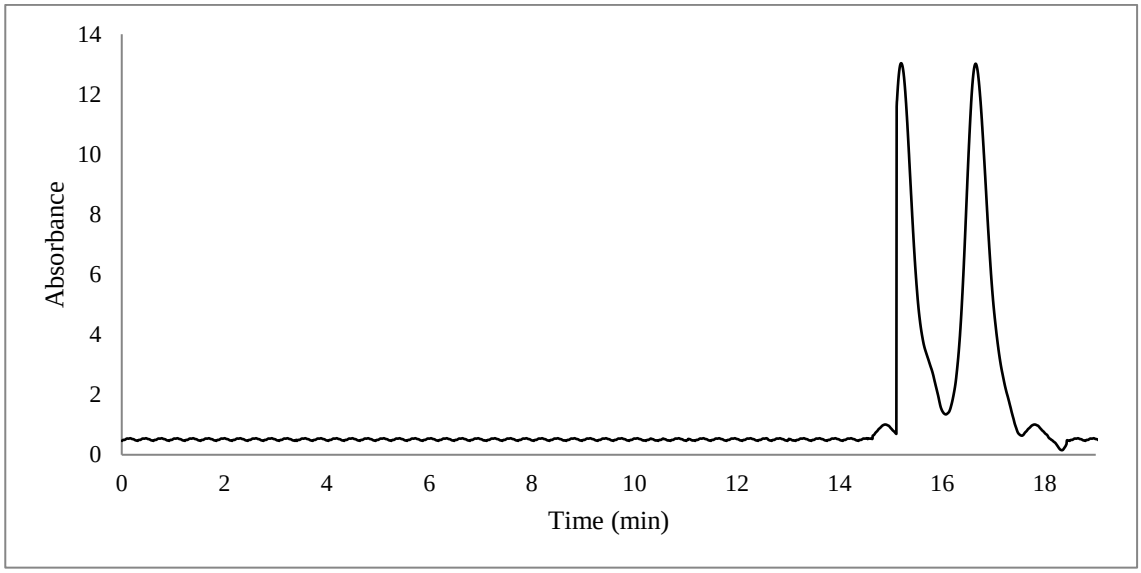

Figure 196: Liquid chromatogram for separation of the R and S enantiomers of 50 ppm of Nor-mephedrone drug using AS-H Amylose column, λ_{max}. 254 nm

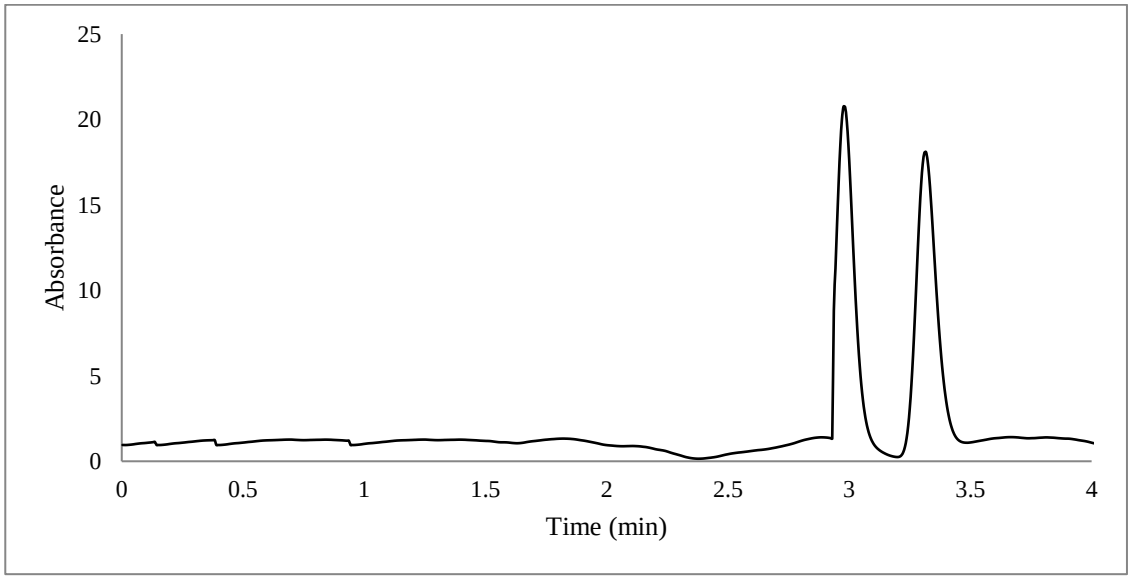

Figure 197: Liquid chromatogram for separation of the R and S enantiomers of 50 ppm of Pentedrone drug using AS-H Amylose column, λ_{max}. 254 nm

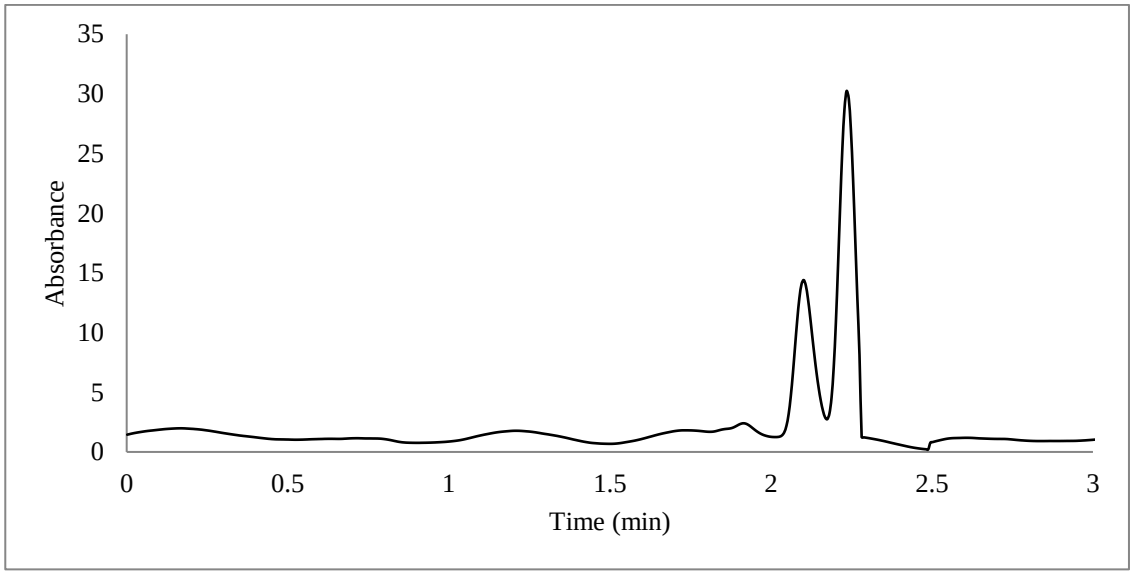

Figure 198: Liquid chromatogram for separation of the R and S enantiomers of 50 ppm of 2-Methyl-α-Pyrrolidinobutiophenone drug using AS-H Amylose column, λ_{max}. 270 nm

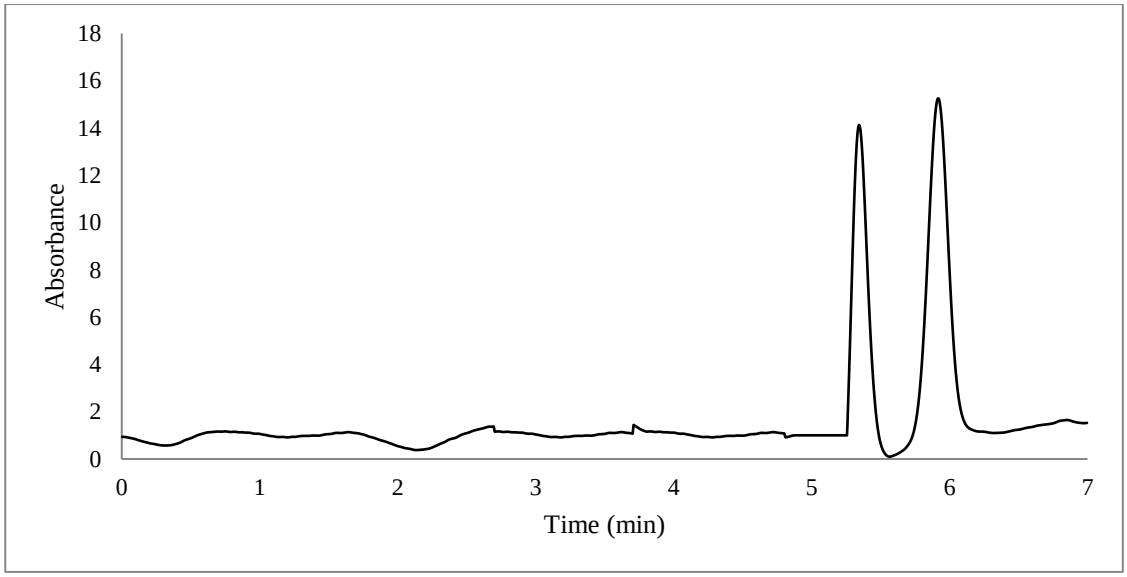

Figure 199: Liquid chromatogram for separation of the R and S enantiomers of 50 ppm of 2-Methyl-α-Pyrrolidinobutiophenone drug using DMP cellulose column, λ_{max}. 254 nm

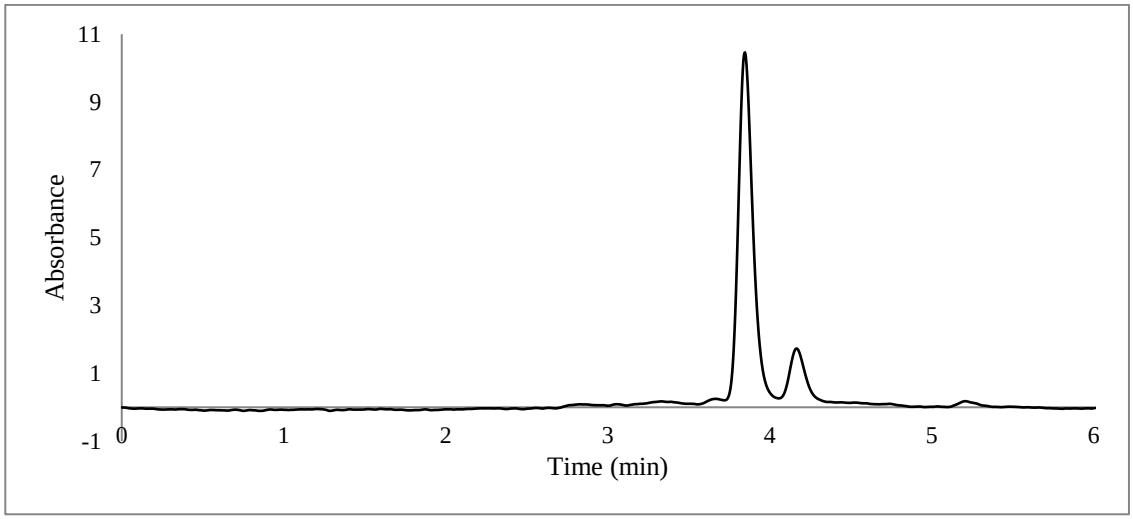

Figure 200: Liquid chromatogram for separation of the R and S enantiomers of 50 ppm of 2-Methyl-α-Pyrrolidinopropiophenone drug using AS-H Amylose column, λ_{max}. 300 nm

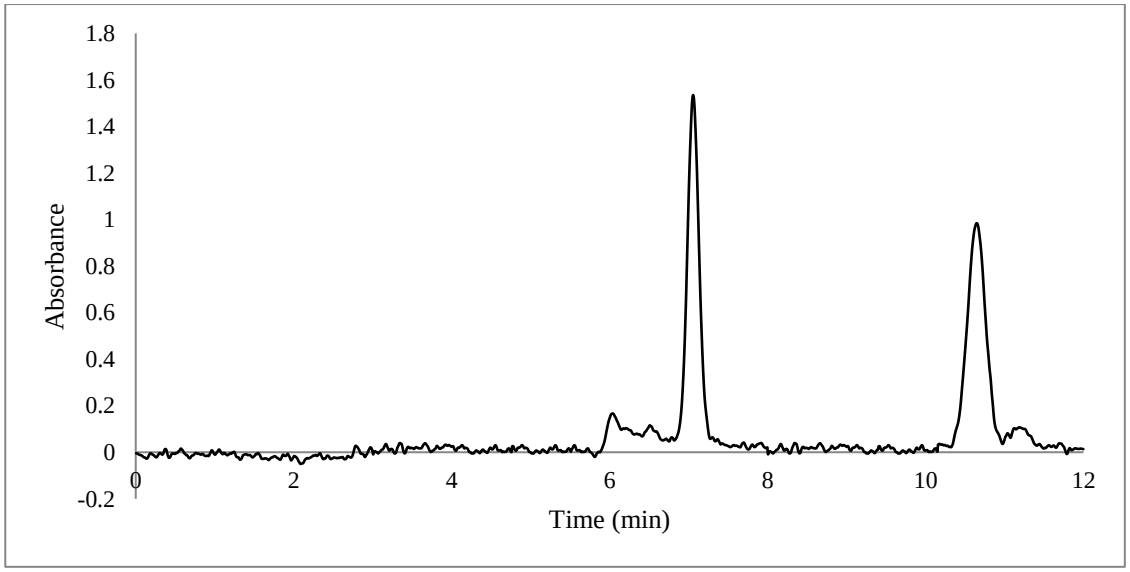

Figure 201: Liquid chromatogram for separation of the R and S enantiomers of 50 ppm of 2-Methyl-α-Pyrrolidinopropiophenone drug using DMP cellulose column, λ_{max}. 300 nm

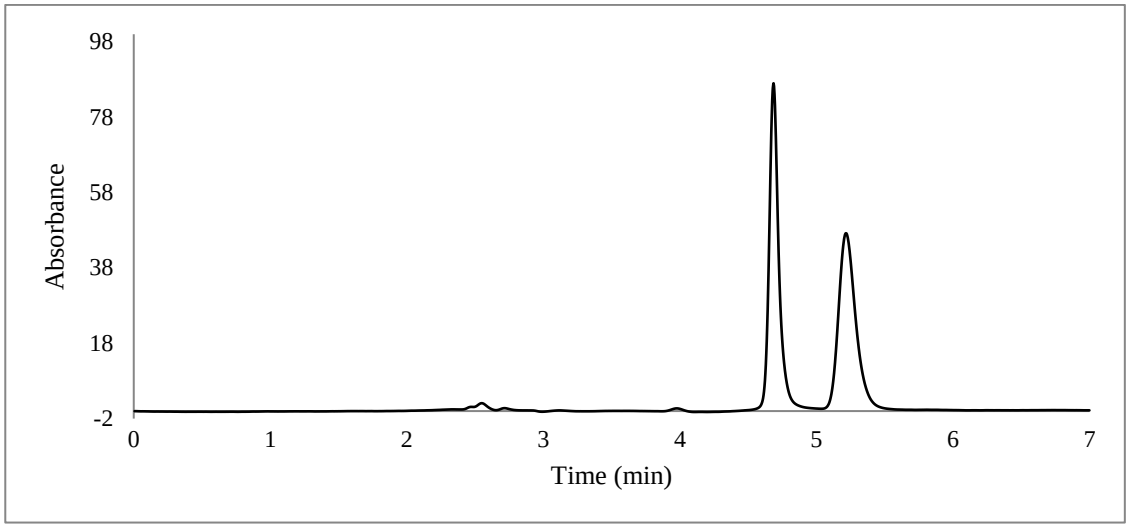

Figure 202: Liquid chromatogram for separation of the R and S enantiomers of 50 ppm of 3,4-Methylenedioxy-α-Pyrrolidinobutiophenone drug using AS-H Amylose column, λ_{max}. 270 nm

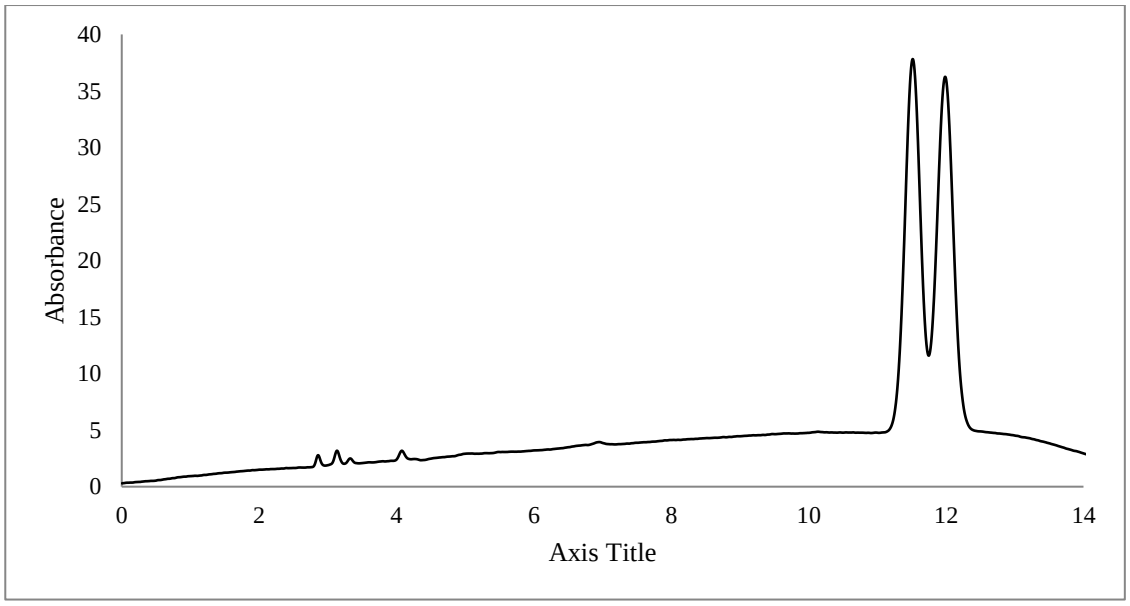

Figure 203: Liquid chromatogram for separation of the R and S enantiomers of 50 ppm of 3,4-Methylenedioxy-α-Pyrrolidinobutiophenone drug using DMP cellulose column, λ_{max}. 270 nm

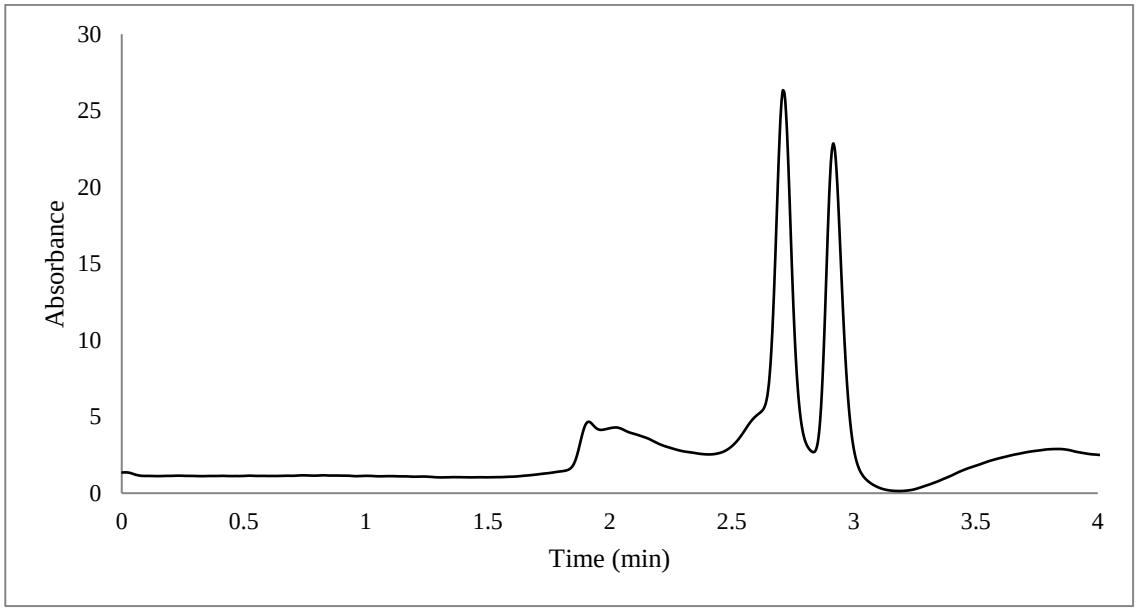

Figure 204: Liquid chromatogram for separation of the R and S enantiomers of 50 ppm of 4-Ethyl-N,N-Dimethylcathinone drug using AS-H Amylose column, λ_{max}. 270 nm

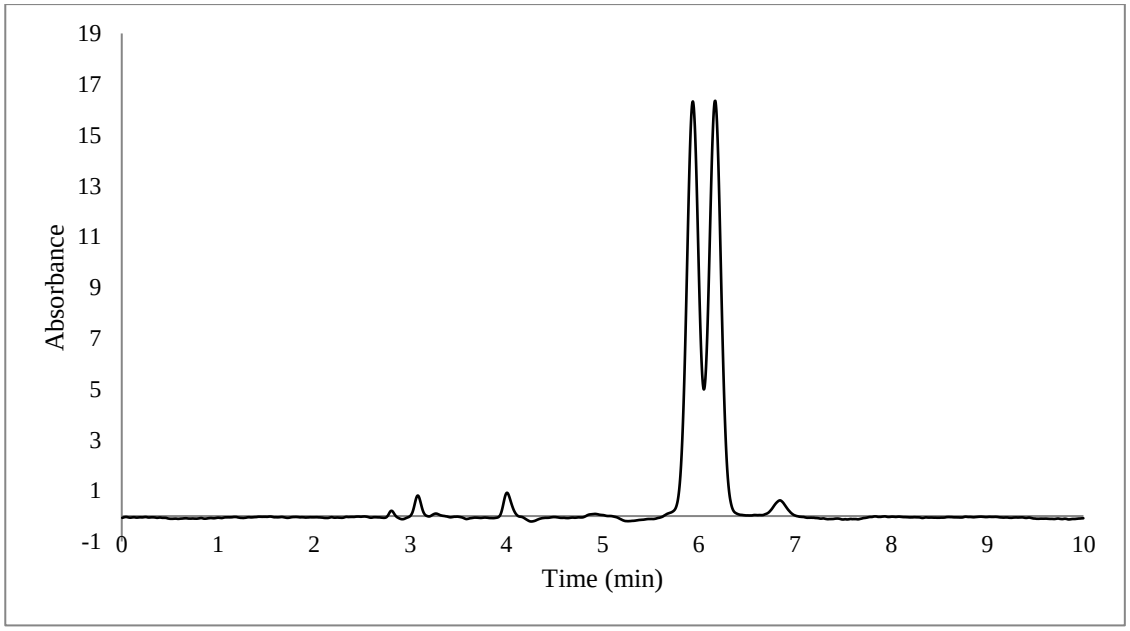

Figure 205: Liquid chromatogram for separation of the R and S enantiomers of 50 ppm of 4-Ethyl-N,N-Dimethylcathinone drug using DMP cellulose column, λ_{max}. 270 nm

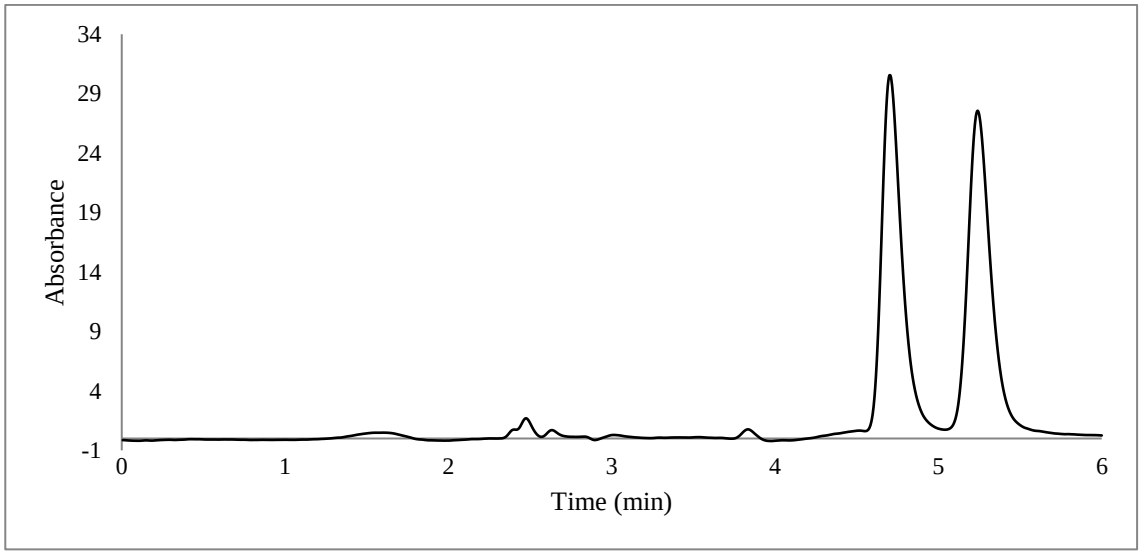

Figure 206: Liquid chromatogram for separation of the R and S enantiomers of 50 ppm of 4'-Methoxy-α-Pyrrolidinopropiophenone drug using AS-H Amylose column, λ_{max}. 270 nm

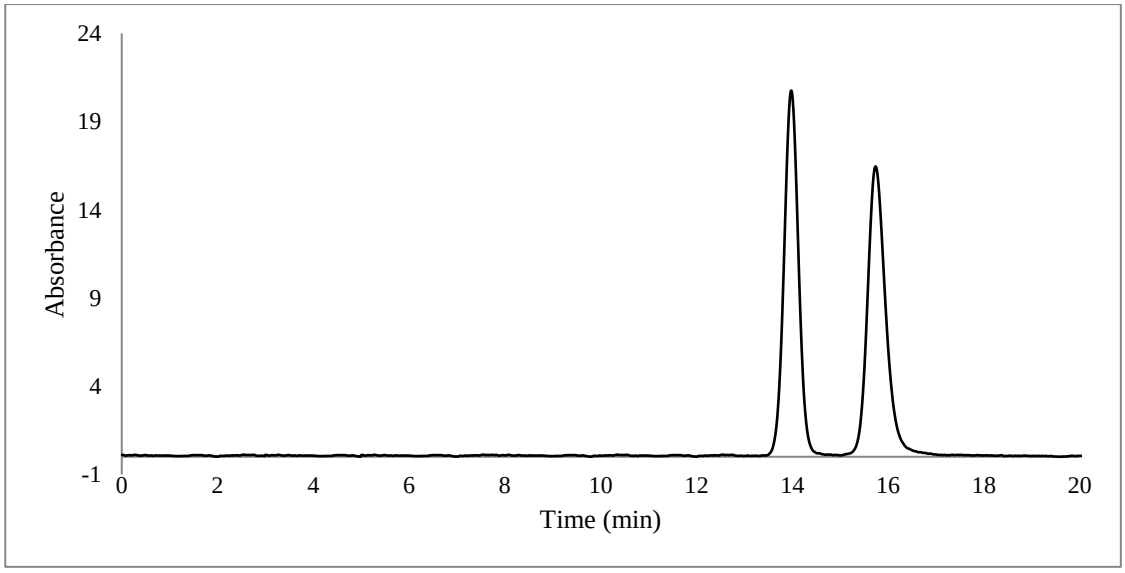

Figure 207: Liquid chromatogram for separation of the R and S enantiomers of 50 ppm of 4'-methoxy-α-Pyrrolidinopropiophenone drug using DMP cellulose column, λ_{max}. 270 nm

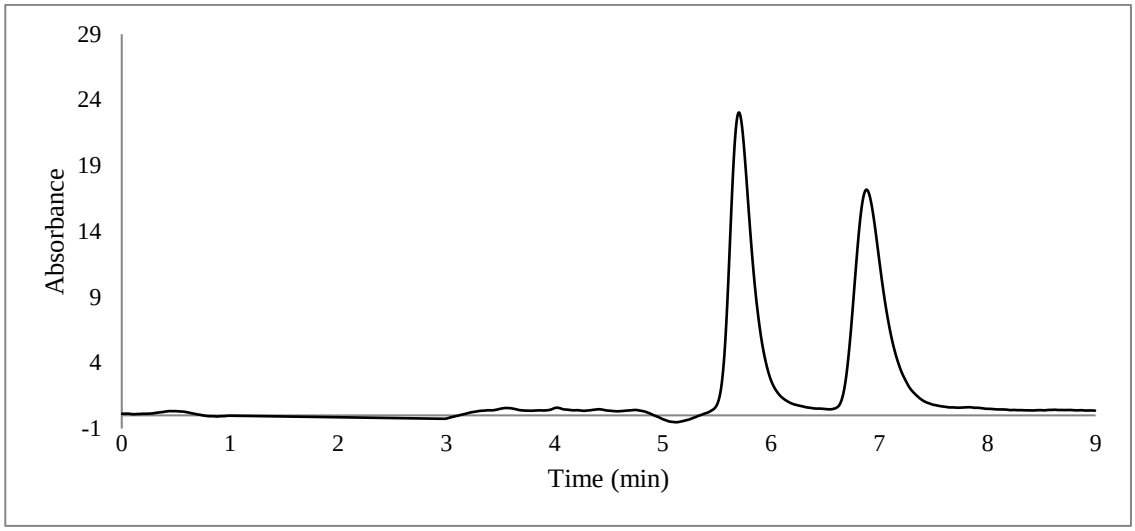

Figure 208: Liquid chromatogram for separation of the R and S enantiomers of 50 ppm of Dimethylone drug using AS-H Amylose column, λ_{max}. 270 nm

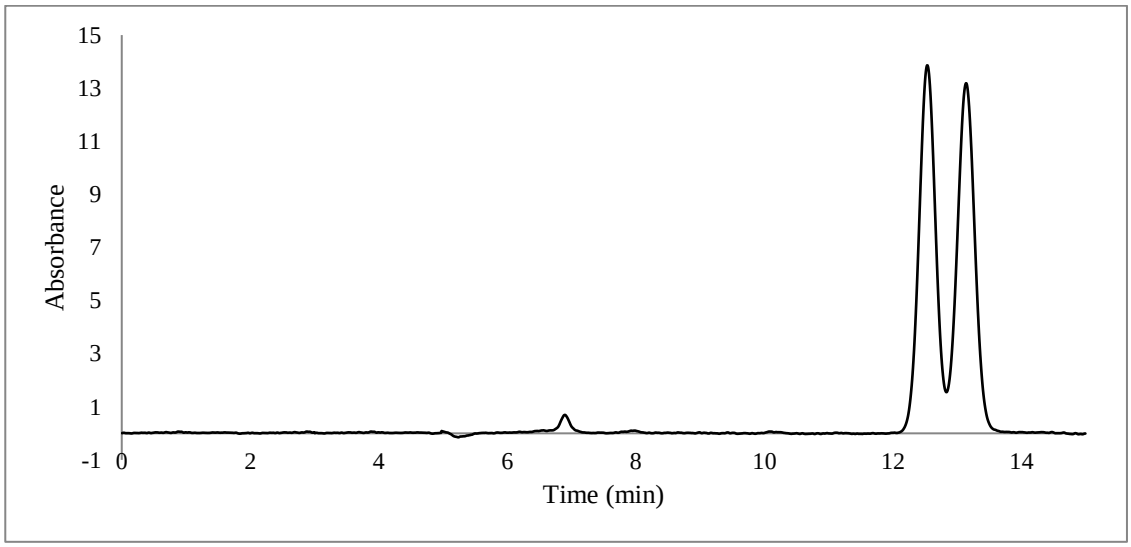

Figure 209: Liquid chromatogram for separation of the R and S enantiomers of 50 ppm of Dimethylone drug using DMP cellulose column, λ_{max}. 270 nm

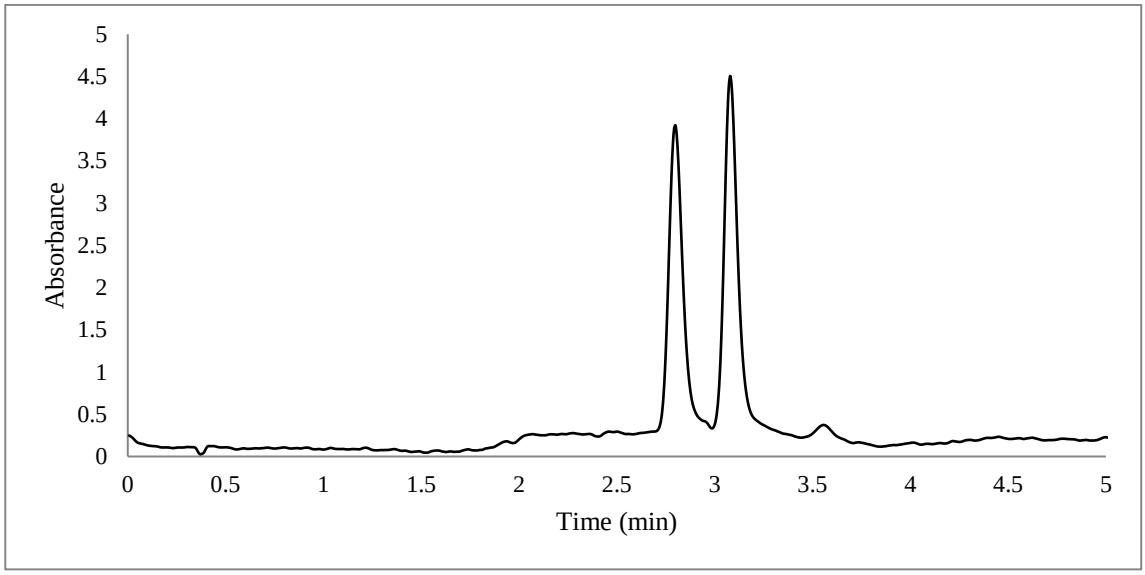

Figure 210: Liquid chromatogram for separation of the R and S enantiomers of 50 ppm of N,N-Dimethylcathinone drug using AS-H Amylose column, λ_{max}. 300 nm

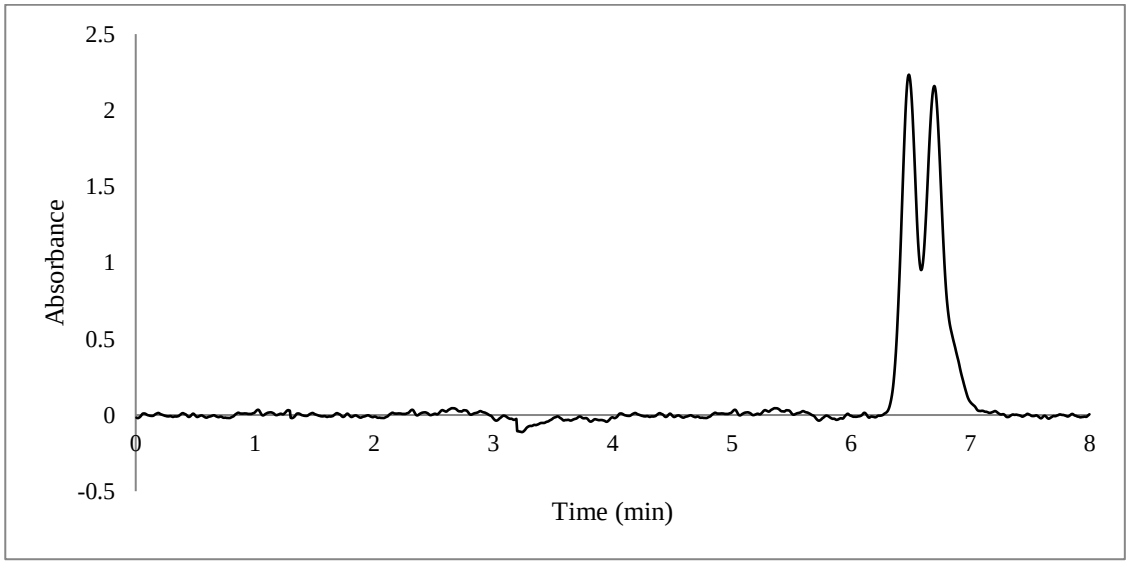

Figure 211: Liquid chromatogram for separation of the R and S enantiomers of 50 ppm of N,N-Dimethylcathinone drug using DMP cellulose column, λ_{max}. 300 nm

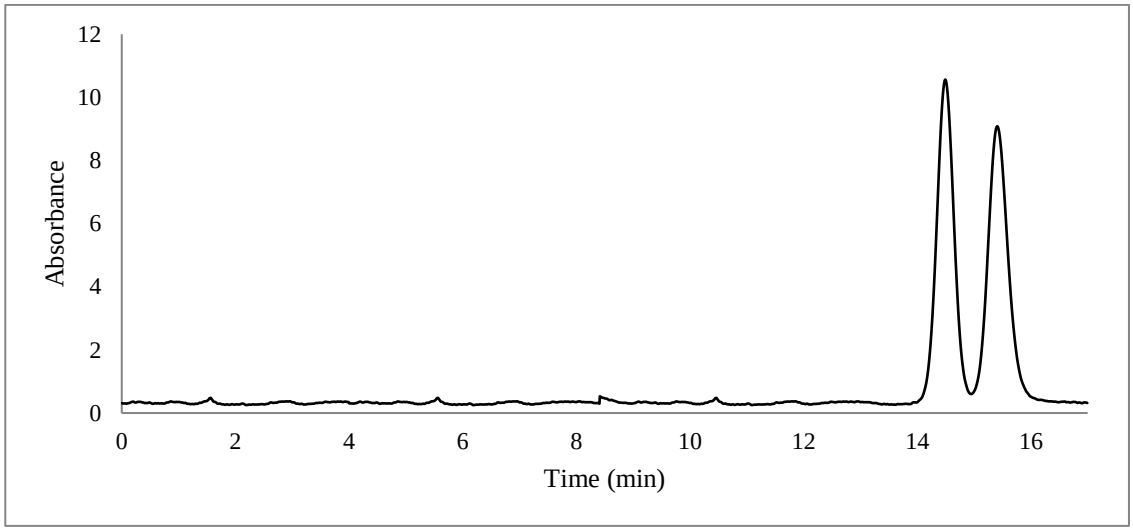

Figure 212: Liquid chromatogram for separation of the R and S enantiomers of 50 ppm of 3,4-Methylenedioxy-α-Pyrrolidinopropiophenone drug using DMP cellulose column, λ_{max}. 270 nm

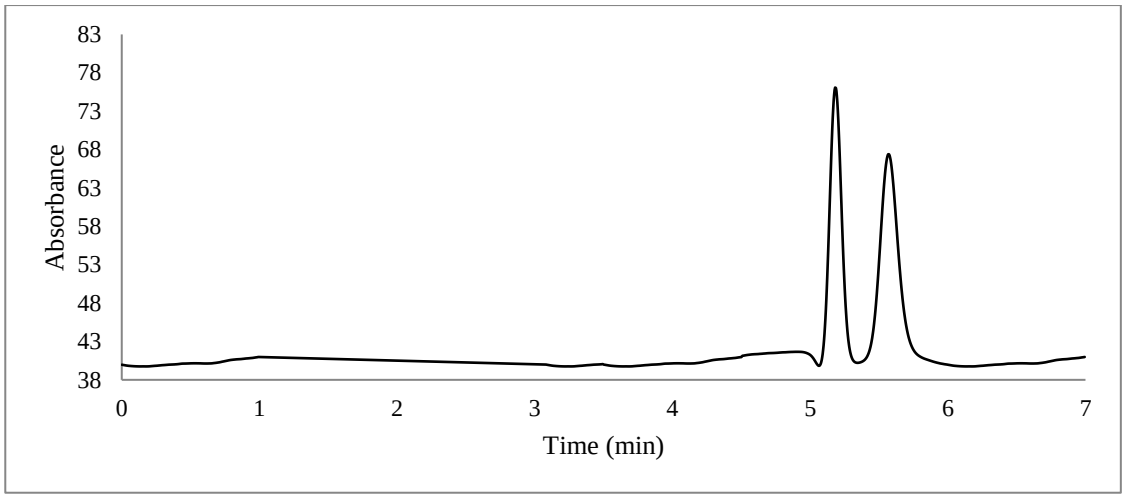

Figure 213: Liquid chromatogram for separation of the R and S enantiomers of 50 ppm of 3-Methyl-α-Pyrrolidinobutiophenone drug using DMP cellulose column, λ_{max}. 254 nm

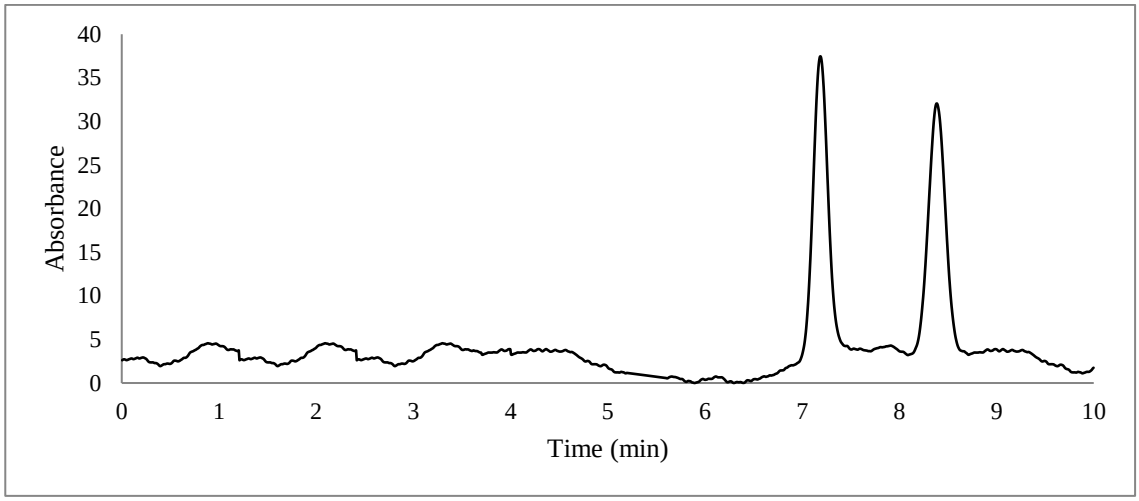

Figure 214: Liquid chromatogram for separation of the R and S enantiomers of 50 ppm of 3-Methyl-α-Pyrrolidinopropiophenone drug using DMP cellulose column, λ_{max}. 240 nm

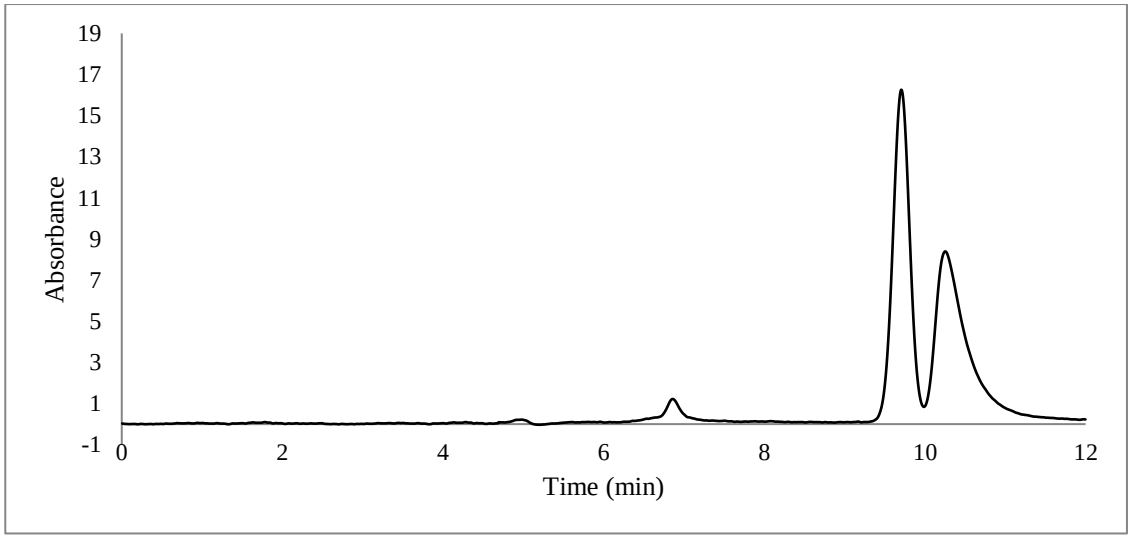

Figure 215: Liquid chromatogram for separation of the R and S enantiomers of 50 ppm of 4-Methoxy-N,N-Dimethylcathinone drug using DMP cellulose column, λ_{max}. 270 nm

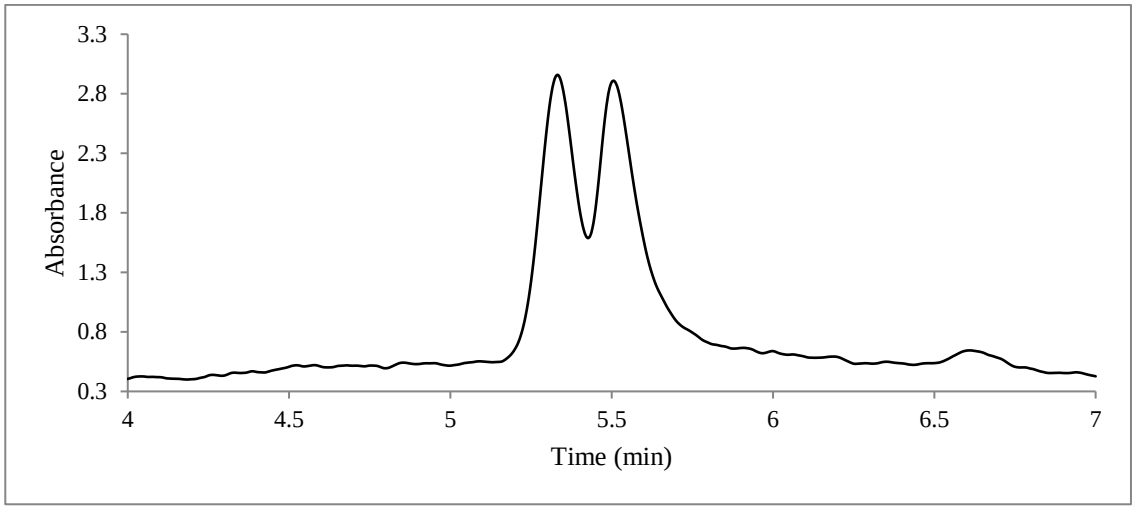

Figure 216: Liquid chromatogram for separation of the R and S enantiomers of 50 ppm of 4-Methyl-α-Pyrrolidinobutiophenone drug using DMP cellulose column, λ_{max}. 300 nm

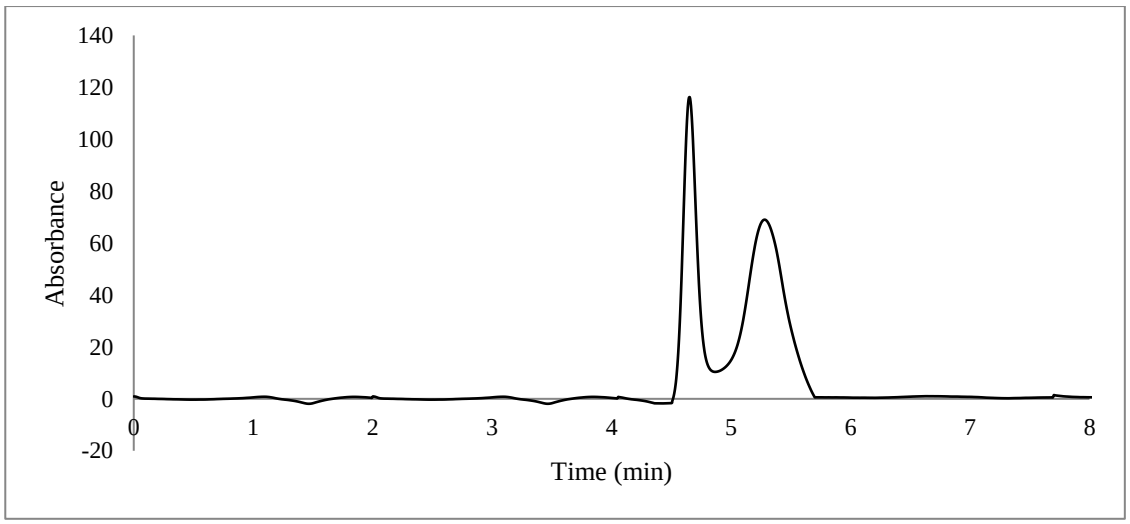

Figure 217: Liquid chromatogram for separation of the R and S enantiomers of 50 ppm of 4'-methyl-α-Pyrrolidinohexanophenone drug using DMP cellulose column, λ_{max}. 254 nm.

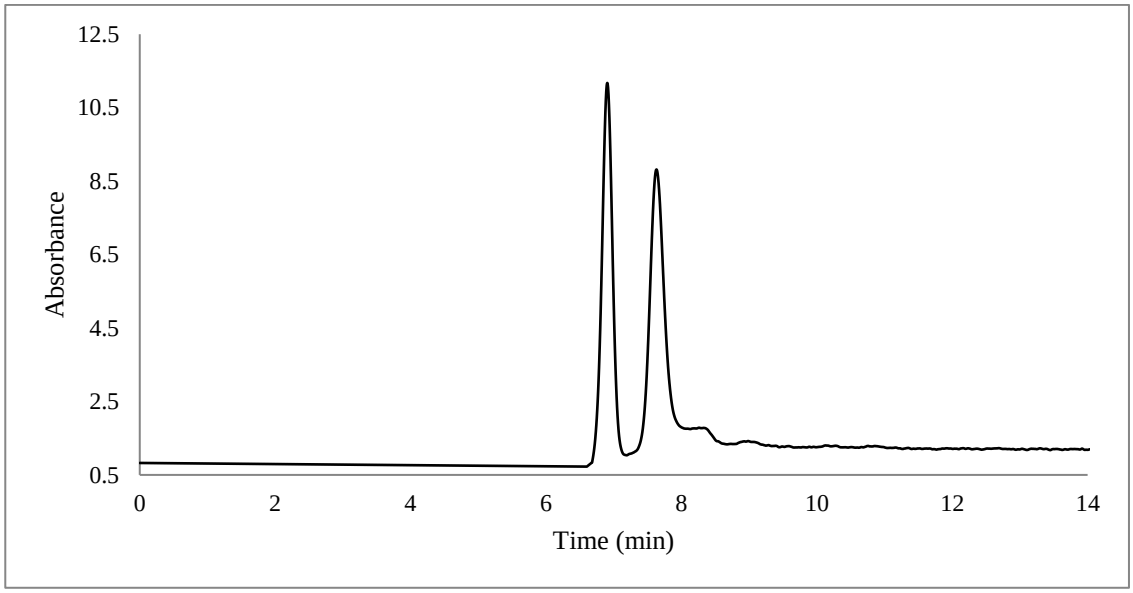

Figure 218: Liquid chromatogram for separation of the R and S enantiomers of 50 ppm of 4'-methyl-α-Pyrrolidinopropiophenone drug using DMP cellulose column, λ_{max}. 270 nm

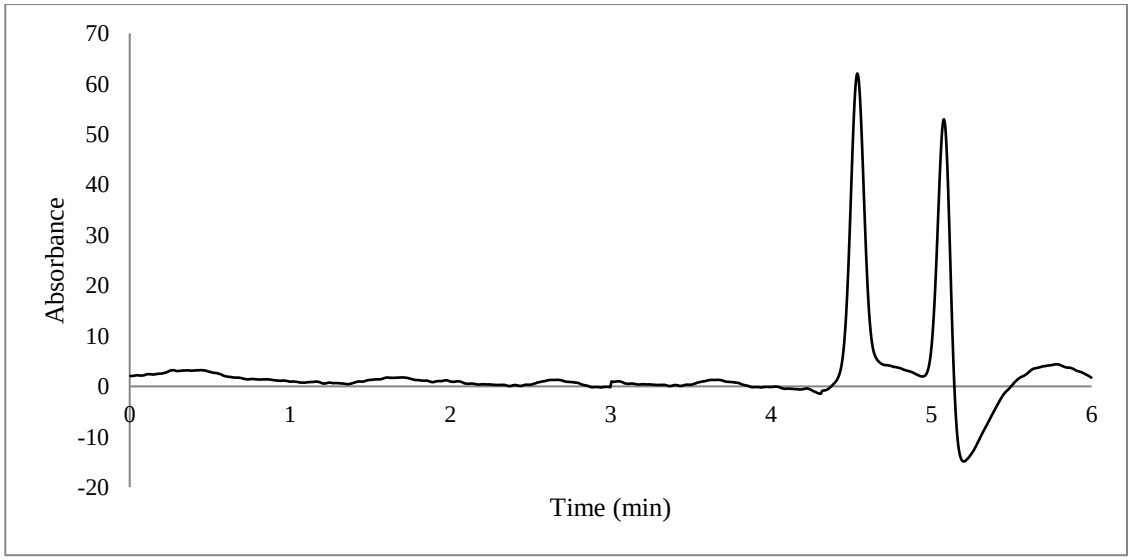

Figure 219: Liquid chromatogram for separation of the R and S enantiomers of 50 ppm of Diethylcathinone drug using DMP cellulose column, λ_{max}. 240 nm

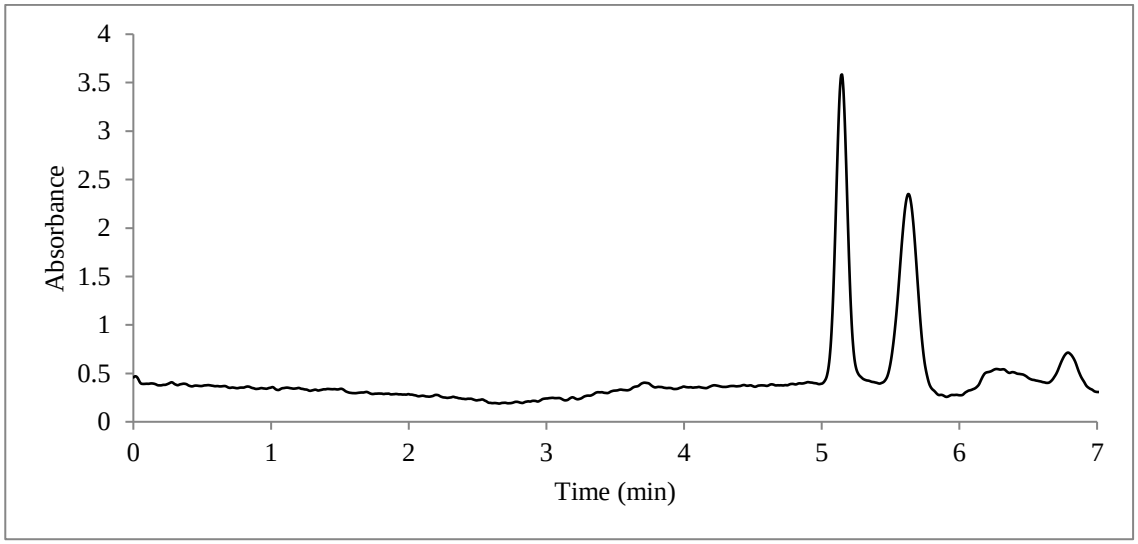

Figure 220: Liquid chromatogram for separation of the R and S enantiomers of 50 ppm of N-ethyl-N-methylcathinone drug using DMP cellulose column, λ_{max}. 300 nm

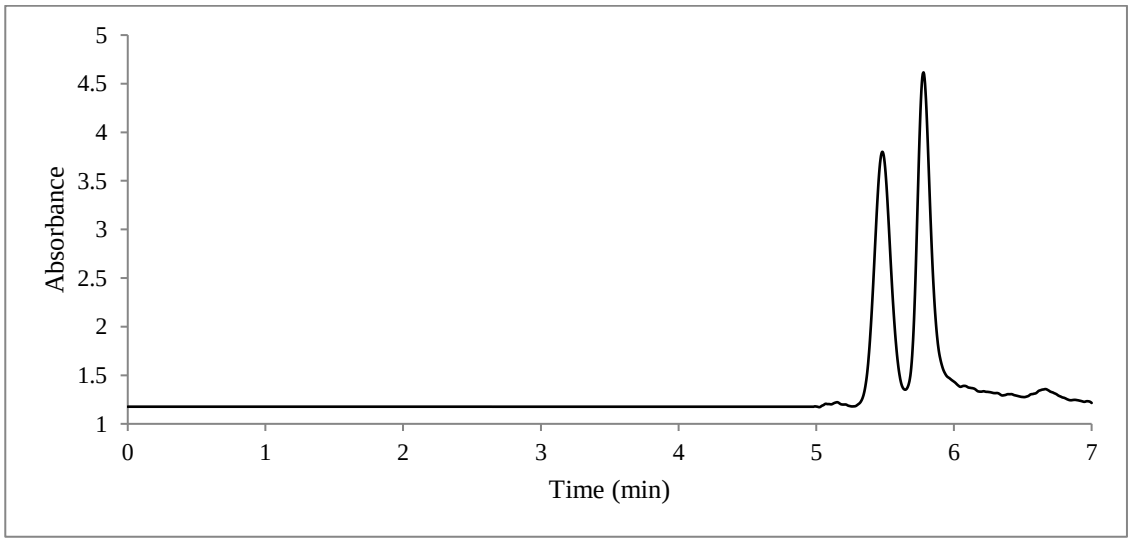

Figure 221: Liquid chromatogram for separation of the R and S enantiomers of 50 ppm of α-Pyrrolidinobutiophenone drug using DMP cellulose column, λ_{max}. 300 nm

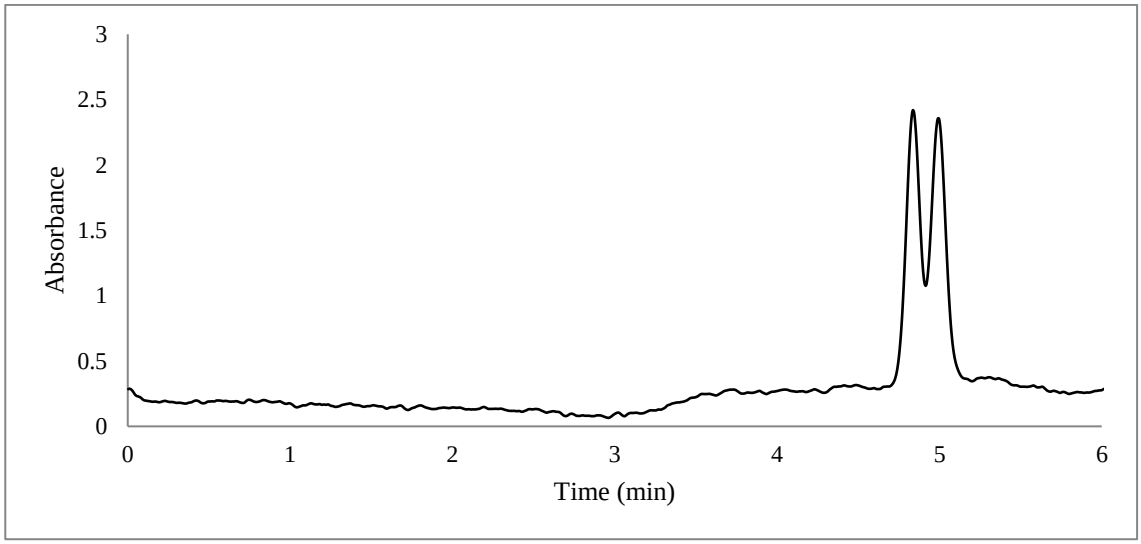

Figure 222: Liquid chromatogram for separation of the R and S enantiomers of 50 ppm of α-Pyrrolidinopentiophenone drug using DMP cellulose column, λ_{max}. 300 nm

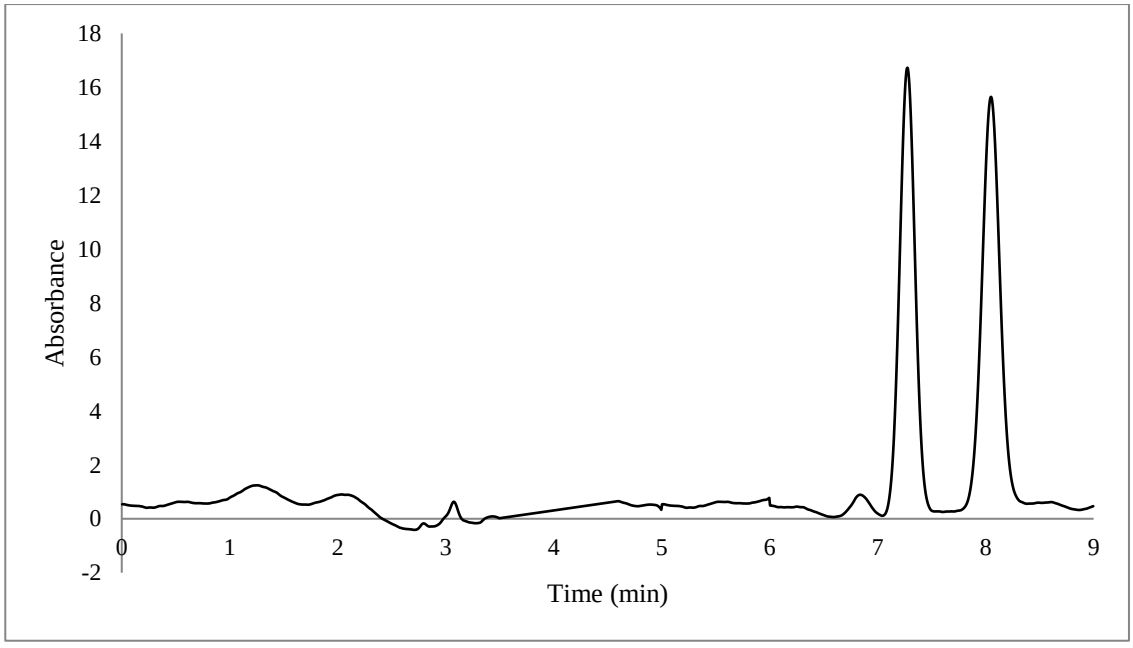

Figure 223: Liquid chromatogram for separation of the R and S enantiomers of 50 ppm of α-Pyrrolidinopropiophenone drug using DMP cellulose column, λ_{max}. 254 nm

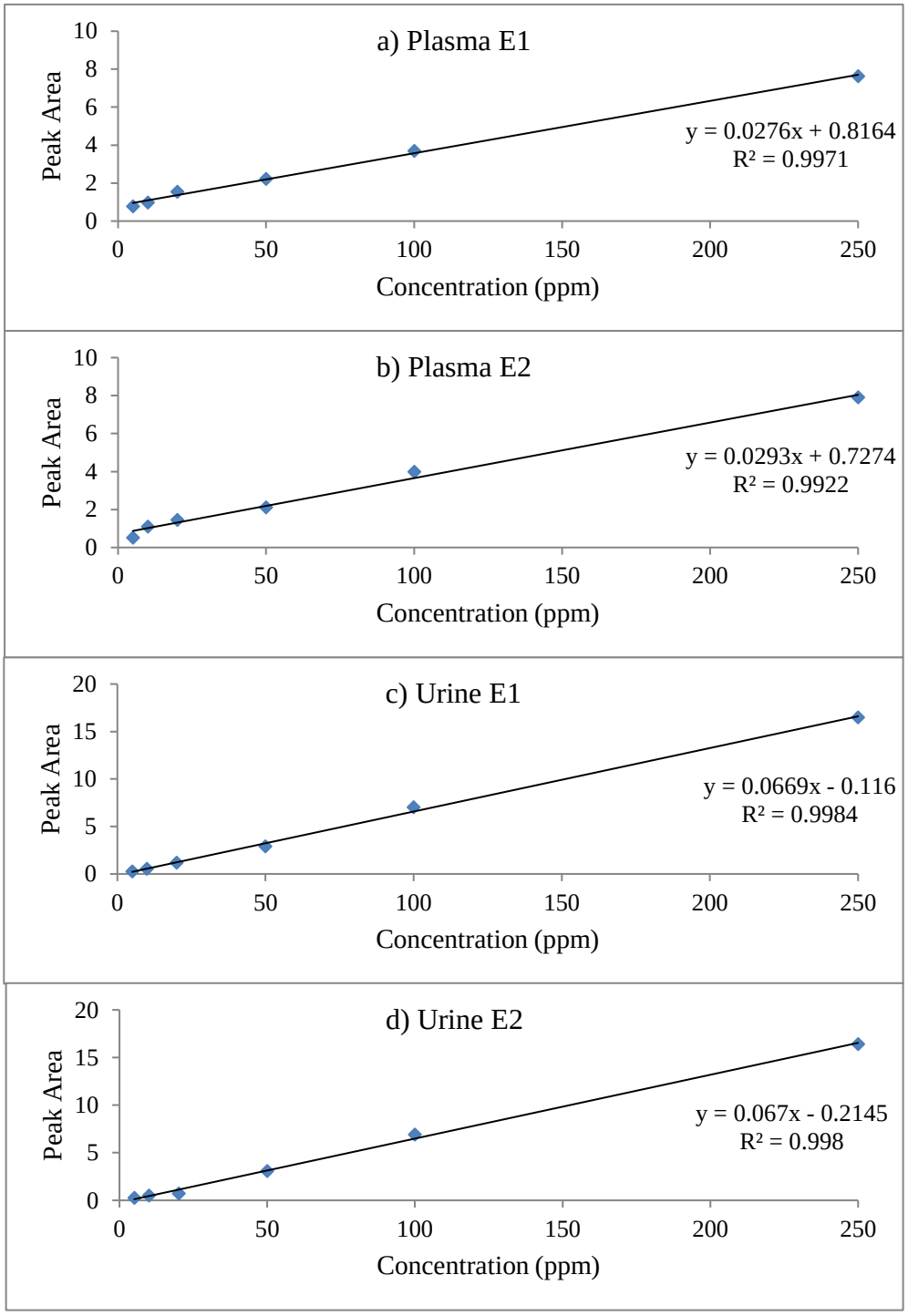

Figure 224: Calibration graphs of the two separated enantiomers of 4'-Methyl-α-ppp compound in urine and plasma

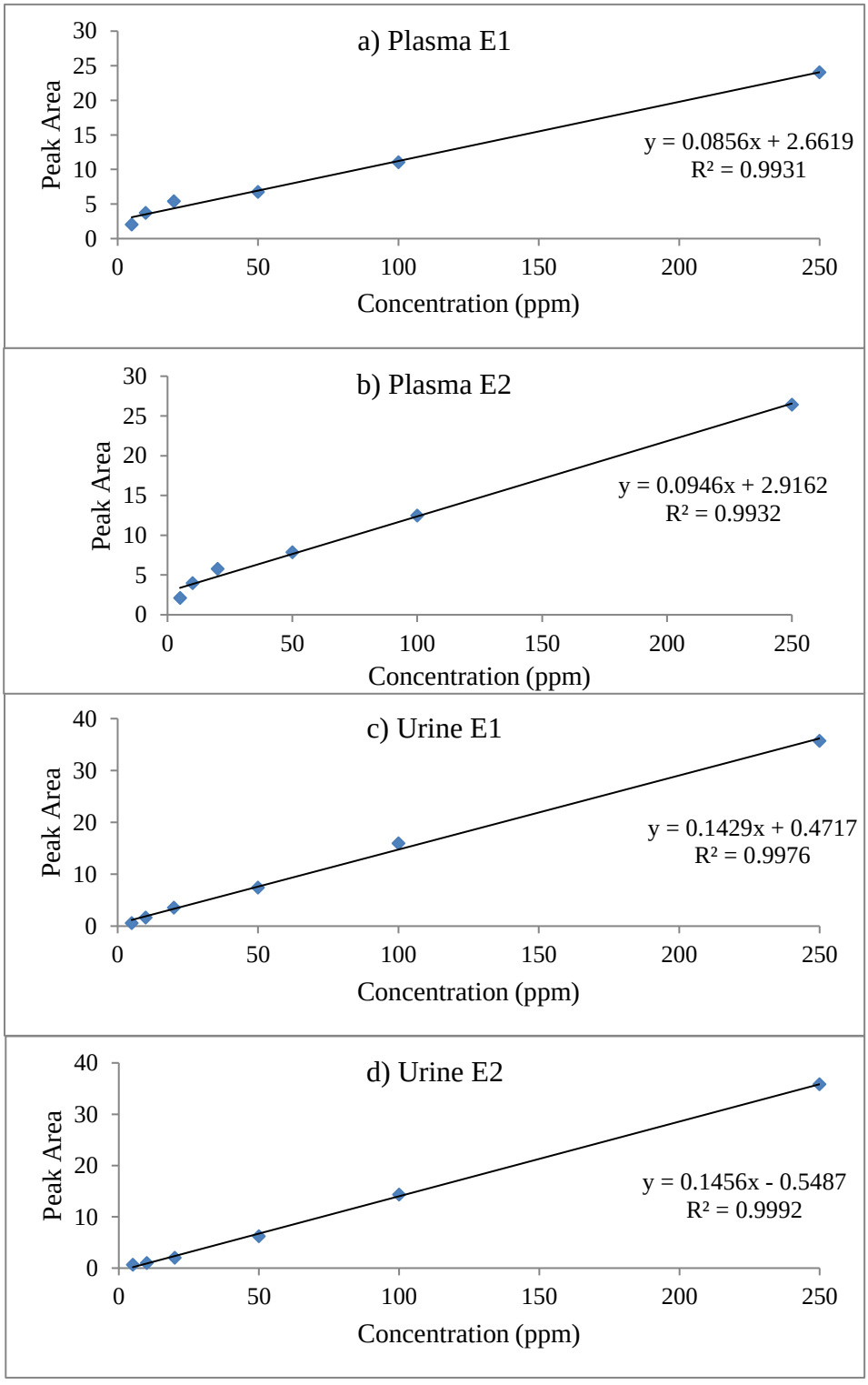

Figure 225: Calibration graphs of the two separated enantiomers of Dimethylone compound in urine and plasma

Shrieen
Digitally signed by Shrieen
DN: cn=Shrieen, o=UAEU, ou=Libraries Deanship, email=shrieen@uaeu.ac.ae, c=AE
Date: 2018.02.12 10:15:55 +04'00'